UNIVERSIDAD DE EXTREMADURA

TESIS DOCTORAL

IMPLICACIÓN DE LOS ESFINGOLIPIDOS EN EL PROCESO DE ABSCISIÓN DEL FRUTO EN OLIVO

BEATRIZ BRIEGAS CARRASCO

Conformidad del director/a y coodirector/a en su caso

Dra. Mª Carmen Gómez Jiménez (directora)

Dra. Juana Socorro Labrador Moreno (co-directora)

Dra. Mercedes Gallardo Medina (co-directora)

Esta tesis cuenta con la autorización del director/a y coodirector/a de la misma y de la Comisión Académica del programa. Dichas autorizaciones constan en el Servicio de la Escuela Internacional de Doctorado de la Universidad de Extremadura.

PROGRAMA DE DOCTORADO:

BIOLOGÍA MOLECULAR Y CELULAR, BIOMEDICINA Y BIOTECNOLOGÍA (R004)

2023

A mi padre

Por enseñarme el significado de la valentía, por hacer los problemas fugaces, las alegrías intensas y las verdades efímeras. Porque no se puede sentir más orgullo por una persona del que yo siento por él.

AGRADECIMIENTOS

Gracias a mi directora, la Catedrática María del Carmen Gómez Jiménez. Por ser inspiración, referente, compañera y amiga. Por enseñarme la pasión por la investigación, por confiar en mí y estar siempre, en las buenas y en las no tan buenas. Por creer en mí y apoyarme en todos los momentos de este largo camino. Por su dedicación y paciencia. Gracias, por su comprensión en todo momento, por apoyarme en los momentos de frustración y por alegrarse conmigo en cada momento de celebración. Mientras me ayudabas a formarme, me enseñaste a admirarte. GRACIAS.

Gracias a mis Co-directoras, Mercedes Gallardo y Juana Labrador, por su apoyo, por su gran labor y paciencia en mis correcciones.

Gracias a Antonio Cordeiro y Carla Inês, por ayudar a formarme durante mi estancia. Por su paciencia, por su alegría y por su apoyo.

Gracias al Profesor Miguel A. Paredes, porque, aunque lamentablemente ya no está con nosotros, su ayuda durante el principio de esta aventura fue indispensable, en la recogida de material, en el laboratorio, siempre tuvo una sonrisa de ánimo para mí.

Gracias a mi madre. Porque sin ella nada de esto sería posible, por estar siempre y apoyarme en cada paso. Por apostar más por mí que yo misma, por desvivirse acompañando y animando en cada parte del camino, siempre.

Gracias a mi hermana, por engrandecer cada paso que doy. Por hacerme sentir orgullosa cada día, y recordarme que los objetivos están para cumplirlos. Que no hay metas pequeñas y que mientras llegamos, ella siempre camina a mi lado. Que las risas ayudan y la constancia no es un deber, sino un placer. Gracias a mi cuñado, Fran, por comprenderme y apoyarme. Por saber estar y ayudar.

Gracias a Diego, sin lugar a duda. Por su apoyo incondicional, por estar al lado en cada loca decisión y por ayudarme a caminar en esta aventura. Por sufrir los desvelos, las alegrías y los nervios a mi lado. Por ser una parte indispensable de todo esto.

Gracias a mis abuelos, Agustín, José, Andrea y Juana. Porque ellos me acompañan siempre. De forma especial, gracias a mi abuela Juana por ser la que ha aguantado esta etapa a mi lado, apoyando hasta sin comprender, esperando paciente, hablando en tono bajo y animando como solo ella lo puede hacer.

Gracias a mis tíos, por aguantar esas charlas casi a diario donde mis incertidumbres con las investigaciones y resultados no cobraban coherencia, pero ellos no dudaban en animar y motivar. Gracias por formar parte siempre.

Gracias a mis primos, por interesarse, por preguntar y por alegrar. Porque cuando una conversación termina con risas a carcajadas, todo es mejor. Por saber elegir el momento, por no faltar nunca y por motivar siempre.

Gracias a mis amigas, por las hipótesis, por los finales y por el recorrido. Porque siempre están.

Gracias a mi compañera Mamen, por recorrer este largo camino conmigo. Por ser sufridora a mi lado y ayudar siempre en todo lo necesario.

Gracias a mis lunares, por estar siempre hasta sin estar. Por darme fuerza y energía hasta sin saberlo. Por motivarme hasta sin pretenderlo. Por ser fundamental en mis momentos de desconexión y relax. Y por ser primordial en mis momentos de nervios y bienestar. Porque no es fácil conseguir poner mi mente en blanco y reiniciarme tantas veces como sea necesario.

Gracias a Julia Trejo, porque cuando comenzó esta aventura, ella no dudó en ningún momento. Me animó, me motivó y me ayudó. Por que sin su ayuda esto no hubiera sido posible. Gracias por creer en mí.

Gracias a todos los que han formado parte de este camino.

ÍNDICE GENERAL

ÍNDICE GENERAL……i

ÍNDICE DE FIGURAS……iii

ÍNDICE DE TABLAS……iv

ABREVIATURAS……v

RESUMEN/SUMMARY……1

1. INTRODUCCIÓN GENERAL……5

1.1 Los esfingolípidos en plantas……7

1.1.1 Descubrimiento……7

1.1.2 Estructura de los esfingolípidos……8

1.1.3 Síntesis y catabolismo de esfingolípidos……10

1.1.4 Distribución de esfingolípidos en plantas……17

1.1.5 Tráfico de los esfingolípidos a nivel celular……21

1.1.6 Funciones de los esfingolípidos en las plantas……22

1.2. El proceso de abscisión……31

1.2.1 El proceso de abscisión en la agricultura……37

1.2.2. Control hormonal del proceso de abscisión……40

1.3 El Olivo……44

1.3.1 Importancia económica……45

1.3.2 La abscisión del fruto en el olivo……48

2. OBJETIVOS……55

3. RESULTADOS Y DISCUSIÓN……59

3.I. Transcriptome and hormone analyses revealed insights into hormonal and vesicle trafficking regulation among *Olea europaea* fruit tissues in late development……63

3.I.1. Abstract……63

3.I.2. Introduction……..…..63

3.I.3. Results and Discussion……...…..….65

3.I.4.Materials and Method……..85

3.I.5. Conclusions…….88

3.II The major plant sphingolipid long chain base sphinganine stimulates fruit abscission in olive…….…...…89

3.II.1. Abstract……...……...….91

3.II.2. Introduction……...…….….. 92

3.II.3. Results and Discussion…….94

3.II.4. Materials and Methods ……...……126

3.II.5. Conclusions……...……...129

4. CONCLUSIONES……...…….131

5. REFERENCIAS……...…141

6. ANEXOS…….……179

INDICE DE FIGURAS

Figura 1.1. Tipos de esfingolípidos en plantas……...……10

Figura 1.2. Biosíntesis de esfingolípidos vegetales……...…….12

Figura 1.3. Modelo fisiológico de la abscisión……...…33

Figura 1.4. Representación de las diferentes ubicaciones de las AZs de la fruta……..…..39

Figura 1.5. Modelo de implicación del etileno en el proceso de abscisión……..……42

Figura 1.6. Olivos cultivados de la variedad 'Arbequina'……..……46

Figura 1.7. Producción de aceite de oliva mundial……47

Figura 1.8. Inflorescencia y fruto de la variedad de olivo 'Picual'……..49

Figure 3.I.1. Differentially expressed cell wall-related genes ……..……66

Figure 3.I.2. Profiles of IAA, GA_1, GA_4, ABA, JA and SA levels……...….68

Figure 3I.3. Tissues of olive (*Olea europaea* L. cv Picual) used for this study……...……..71

Figure 3.I.4. Differentially expressed hormone-related genes……72

Figure 3.I.5. Schematic representation of the hormone metabolism and signaling……...75

Figure 3.I.6. Expression of *OeERF3*, *OeERF4*, *OeSNRK2.4*, *OeNPR1*, and *OeJAR1*…...…78

Figure 3.I.7. Schematic representation of the pathways……...…80

Figure 3.I.8. Expression profiling of fruit- or AZ- enriched genes……...……..84

Figure 3.II.1. Plant material used for the experiments……...…… 95

Figure 3.II.2 Distribution of genes differentially expressed…….... 96

Figure 3.II.3. The Top 10 enrichment analysis of GO……...…….100

Figure 3.II.4. The Top 10 enrichment analysis of GO……...……..101

Figure 3.II.5. The Top 10 enrichment analysis of GO……102

Figure 3.II. 6. Representations of the pathways of sphingolipids…….....….103

Figure 3.II.7. Expression profile of family genes……..…….…..106

Figure 3.II.8. Expression profile of transport – related genes……108

Figure 3.II.9. Expression profile of vesicle trafficking-related genes……..……110

Figure 3.II. 10. Profiles of levels of AZs from olive fruit and leaf treated……..112

Figure 3.II.11. Expression profile of auxin- and ethylene-related genes……115

Figure 3.II.12. Expression profile of hormone-related genes……..…120

Figure 3.II.13. Differential gene expression of protease and LRR-RKs genes……..……123

Figure 3.II. 14. Summary of the number of significant changes in olive TF……...…125

ÍNDICE DE TABLAS

Tabla 1.1. Balance del sector del olivar en España en la campaña 2022/2023……..…47

Table 3.II.1. Specific genes……98

ABREVIATURAS

AAL	Alternaria alternata lycopersici
ABA	Ácido abscísico
ABC	ATP-binding cassette transporter
ACC	1-Aminocyclopropane-1-carboxylic acid
ACD5	ACCELERATED CELL DEATH 5
ACD11	ACCELERATED CELL DEATH 11
ACER	Ceramidasa alcalina
ACO	Aminocyclopropane-1-carboxylic acid oxidase
ACS	Aminocyclopropane-1-carboxylic acid synthase
ADC	arginine decarboxylase
AED	APOPLASTIC, ***EDS1***-DEPENDENT
AGP	Arabinogalactano
AOase	acetylornithine deacetylase
ARF	Factor de respuesta auxina
ARF-GAP	Proteína activadora de factor de ribosilación de ADP-GTPasa
ATH1	Arabidopsis thaliana homeobox 1 gene
Aux/IAA	Auxin/Indole-3 acetic acid
AZ	Zona de abscisión
BOP	blade-on-petiole
BG	Beta-glucosidasa
BR	Brasinosteroide
BRI1	BR insensitive 1
BAK1	BRI1-associated kinase1
BIN2	BR insensitive 2

BZR	Brassinazole resistant
cDNA	Complementary deoxyribonucleic acid
CEL	Celulosa
Cer	Ceramida
CerK	Ceramida quinasa
CerS	Ceramida sintasa
CES	Celulosa sintasa
CHI	Quitinasa
CK	Citoquinina
CLE	CLAVATA3/ESR
COI	Consejo Oleícola Internacional
coi1	coronatine insensitive 1
CPK	Proteína quinasa Ser/Thr dependiente de calcio
CPS	ent-copalyl diphosphate synthase
CST	CAST AWAY
CTR	CONSTITUTIVE TRIPLE RESPONSE
CYP51	Obtusifoliol 14α-desmetilasa
C1P	Ceramida 1-fosfato
DEGs	Genes diferencialmente expresados
DES1	sphingolipid delta(4)-desaturase
DGDG	Digalactosildiacilglicerol
DHZ	dihydrozeatin
DP	Transcription factor Dimerization Partner
DPA	Dias post-antesis
DPL	LONG-CHAIN BASE PHOSPHATE LYASE
DPL1	Fito-S1P liasa

DRM	Membranas resistentes a detergentes
CLV3	*CLAVATA3*
ECM	Equivalent to the cell wall or apoplast
EIL	ETHYLENE INSENSITIVE
ERF	Ethylene response factor
ERS	ETHYLENE RESPONSE SENSOR
ET	Etileno
EXP	Expansina
EXT	Extensina
EVR	EVERSHED
FAE	Complejo de elongación de ácidos grasos microsomales
FAH	Hidroxilasa de ácido graso
FB1	Fumosina B1
FDF	Fuerza de desprendimiento de la fruta
FYF	FOREVER YOUNG FLOWER
FUL2	*FRUITFULL 2*
GA	Giberalina
GCS	Glucosilceramida sintasa
GGPS	geranylgeranyl pyrophosphate synthase
GID1	Gibberellin-insensitive dwarf1
GINT1	Glucosamina inositol fosforilceramida transferasa 1
GIPC	Glicosilinositolfosfoceramidas
GIPC-PLD	Fosfolipasa D específica de GIPC
GlcA	Resto de ácido glucurónico
GlcCers	Glucosilceramidas
GlcCerase	Glucosilceramidasa

GlcN	Glucosamina
GlcNAc	N-acetil-glucosamina
GLTP1	Proteína de transferencia de glicolípidos
GMT1	GIPC manosil transferasa 1
GPI	Glicosilfosfatidilinositol
GO	Ontología genética
GONST1	Transportador de azúcar de nucleótidos de Golgi 1
GONST2	Transportador de azúcar de nucleótidos de Golgi 2
GWAS	Genome-Wide Association Studies
HAE	Receptor quinasas HAESA
HB	Homeobox
hCers	Hidroxiceramidas
HexCers	Hexosilceramidas
HG	Homogalacturonano
HSF	Heat Stress transcription Factor
HSL2	Receptor quinasa HAE-like 2
H_2O_2	Peróxido de hidrógeno
IAA	Ácido indol-3-acético
IDA	INFLORESCENCE DEFICIENT IN ABSCISSION
IP	N6-isopentenyladenine
IPC	Inositolfosfoceramidas
IPCS	Inositolfosforilceramida sintasa
IPUT	Inositol fosforilceramida glucuronosiltransferasa
IS	ISOCHORISMATE SYNTHASE
JA	Ácido jasmónico
JA-Ile	Jasmonil-isoleucina
JAR1	JASMONATE-RESISTANT1

KCS	3-cetoacil-CoA sintasa
KD1	*KNOX-LIKE HOMEDOMAIN PROTEIN1*
KNAT	KNOTTED-like from Arabidopsis thaliana
KNOX	KNOTTED1- LIKE HOMEOBOX
KO	ent-kaurene oxidase
LAC	Lacasa
LCB	Base esfingoide o base de cadena larga
LCBK	LCB quinasas
LCB-Ps	LCB 1-fosfatos
LCB-PP1	LONG-CHAIN BASE PHOSPHATE PHOSPHATASEs 1
LCB-PP2	LONG-CHAIN BASE PHOSPHATE PHOSPHATASEs 2
LCFA	Ácido graso de cadena larga
LOH	Ceramida sintasa LAG
LPP	lipid phosphate phosphatase delta
LRR-RK	Leucine-rich repeat receptor-like kinase
MACC	Malonil-ACC
MAN	Manosa
MAP	mitogen-activated protein
MAPA	Ministerio de Agricultura, Pesca y Alimentación
MC	Macrocalyx
MeJA	methyljasmonate
MGDG	Monogalactosildiacilglicerol
MP	Membrana Plasmática
MPK	Proteínas quinasa activada por mitógeno
NCER	Ceramidasas neutral
NECD	epoxycarotenoid dioxygenase
NEV	NEVERSHED

NGS	Secuenciación de nueva generación
NLP	Proteínas similares al péptido 1
NO	Óxido nítrico
NPC4	Fosfolipasa C4 no específica
NR	Nitrato reductasa
ORM	Orosomucoides
OTCase	ornithine carbamoyltransferase
PA	Poliamina
PAO	polyamine oxidase
PI	Fosfatidilinositol
PCA	principal-component analysis
PCD	Muerte celular programada
PC1P	Fitoceramida 1-fosfato
PG	Poligalacturonasa
PDMP	1-fenil-2-decanoilamino-3-morfolino-1-propanol
PM	Membrana plasmática
PME	Pectina metilesterasa
PSK	Fitosulfocina
Pst	Pseudomonas syringae pv. Tomate
PUT	polyamine uptake transporter
qRT-PCR	Quantitative real-time polymerase chain reaction
RALF	Factor de alcalinización rápida/ rapid alkalinization factor
ROS	Especies reactivas de oxígeno
RPKM	Reads per kilobase of exon per million mapped reads
SA	Ácido salicílico
SAMDC	S-adenosilmetionina descarboxilasa

SAUR	Small auxin up RNA
SBT	Subtilasa
SCF	Skp1-Cullin1-F-box-type
SERK	SOMATIC EMBRYOGENESIS RECEPTOR-LIKE KINASE
SHT	spermidine hydroxycinnamoyl transferase
SL	Estrigolactonas
SLD	LCB desaturasa esfingoide
SMT2	C-24 esterol metiltransferasa2
SMXL	SUPPRESSOR OF MAX2 LIKE
SPDS	spermidine synthase
Sph	Esfingosina
SPHK1	SPHINGOSINE KINASE 1
SPHK2	SPHINGOSINE KINASE 2
SPPASE	Fito-S1P fosfatasa
SPT	Serina palmitoil transferasa
ssSPTs	Subunidades pequeñas de serina palmitoil transferase
SvLes1	Less Shattering1
TAG	Triacilgliceroles
TAR2	tryptophan aminotransferase protein 2
TE	Elemento transponible
TF	Factor de transcripción
TGN/EE	The trans-Golgi network and early endosomal compartments
TIR1	Transport inhibitor response 1
tZ	Trans-Zeatin
UGNT1	UDP-N-acetil-D-glucosamina transportador 1
VLCFA	Ácido graso de cadena muy larga

WUS	*WUSCHEL*
XTH	Xiloglucano endotransglicosilasa/hidrolasa
ZEP	ZEAXANTHIN EPOXIDASE
ZNT	Transportardor de Zinq

RESUMEN/ SUMMARY

RESUMEN

La abscisión de los órganos de las plantas está regulada por redes de señalización complejas que median respuestas del desarrollo y ambientales. En olivo (*Olea europaea* L.), la abscisión del fruto se asocia con cambios en las bases de cadena larga de esfingolípidos (LCB) en la zona de abscisión (AZ), mostrando una asociación específica entre la esfinganina LCB dihidroxilada (d18:0) y la abscisión del fruto. El objetivo general de este trabajo es profundizar en los mecanismos moleculares implicados en la abscisión del fruto y ampliar nuestra investigación sobre el papel de los esfingolípidos utilizando enfoques farmacológicos y transcriptómicos. En primer lugar, se mostraron los cambios hormonales y en el transcriptoma del fruto con respecto a su AZ en la última etapa de maduración cuando ocurre la abscisión natural del fruto. Estos datos transcriptómicos permitieron la identificación de transcritos únicos y comunes relacionados con modificación de la pared celular, metabolismo y la señalización de hormonas, tráfico vesicular, y flujos de iones entre los tejidos. Posteriormente, para comprender la señalización diferencial implicada en la abscisión del fruto y la hoja, se mostró la caracterización transcripcional de las AZs del fruto y de la hoja en respuesta al tratamiento d18:0, identificando nuevos reguladores de la señalización de la abscisión del fruto. Nuestros resultados aportan nuevos conocimientos sobre la biología de la abscisión del fruto en olivo y permitirán desarrollar nuevas estrategias para el control selectivo de la abscisión del fruto, facilitando la recolección mecánica del cultivo y reduciendo costes sin defoliación del árbol.

SUMMARY

Plant organs abscission is regulated by complex signalling networks that mediate development and environmental responses. In olive (*Olea europaea* L.), fruit abscission is associated with changes in sphingolipid long-chain bases (LCB) in the abscission zone (AZ), showing a specific association between the dihydroxylated LCB sphinganine (d18:0) and the olive fruit abscission. The main goal of this work is to help elucidate the molecular mechanisms involved in the fruit abscission in olive, broadening our research into the role of sphingolipids using pharmacological and transcriptomic approaches. Here, we firstly report hormonal and transcriptome changes in olive fruit with respect to their AZ at the last stage of ripening, when natural fruit abscission occurs. These transcriptomic data allowed for the identification of unique and common transcriptional signatures related to cell wall modification, plant hormone metabolism and signalling, vesicle trafficking, and ion fluxes between the fruit tissues. Subsequently, to understand the differential signalling involved in fruit and leaf abscission in olive, we undertake a transcriptional characterization of the olive AZs of fruit and leaf in response to d18:0 treatment. Also, we identify specific markes of the fruit AZ and novel regulators of olive fruit abscission signalling. Our results provide fresh insight into the biology of olive fruit abscission and enabling the development of new strategies for the selective control of the fruit abscission in olive, and thereby facilitating the mechanical harvest of the crop and reducing farming costs without tree defoliation.

1.INTRODUCCIÓN

1.INTRODUCCIÓN GENERAL

1.1 Los esfingolípidos en plantas

La identidad y funcionalidad de las membranas biológicas están determinadas por la composición y cantidad de proteínas, carbohidratos, así como de los lípidos que forman parte de las mismas. Los lípidos son constituyentes de vital importancia en las membranas, ya que su solubilidad, carga, volumen, tamaño y reactividad contribuyen a definir las propiedades biofísicas de las membranas. En este sentido, propiedades como el grosor, la estabilidad, la permeabilidad, la curvatura, la fluidez, la difusión lateral, la asimetría y la interdigitación, influyen decisivamente en el papel fisiológico de la membrana durante los procesos de desarrollo de la planta y ante condiciones de estrés ambiental (Niemelä et al., 2009; Marquês et al., 2015; Maula et al., 2015; Cacas et al., 2016; Fanani & Maggio, 2017; Fujimoto & Parmryd, 2017; Gronnier et al., 2017; Grosjean et al., 2018).

Las tres familias de lípidos más comunes y abundantes en las membranas vegetales son los glicerofosfolípidos, los esteroles y los **esfingolípidos**. El desarrollo relativamente reciente de técnicas y procedimientos selectivos de extracción e identificación de estas moléculas, han permitido situar a los esfingolípidos como un grupo de lípidos vasto, abundante y diverso en las plantas en las que además presentan importantes funciones (Markham et al., 2006; Cacas et al., 2013). En este sentido, recientes investigaciones atribuyen un número cada vez mayor de funciones para los esfingolípidos, demostrándose que influyen de manera importante en la biología celular (Ali et al., 2018; Huby et al., 2020), participando en la integridad de la membrana plasmática, la señalización, la polaridad celular, la muerte celular programada (PCD), así como en las respuestas celulares a los factores bióticos y abióticos (Chen et al., 2009; Pata et al., 2010; Cacas et al., 2012; Markham et al., 2013; Michaelson et al., 2016; Luttgeharm et al., 2016; Haslam & Feussner, 2022).

1.1.1 Descubrimiento

Los esfingolípidos constituyen una clase de lípidos con estructura y funciones muy diversificadas que aparecen de forma ubicua en todos los reinos de eucariotas, así como en algunas bacterias (Pata et al., 2010). Presentan una similitud estructural con los glicerolípidos, que son los componentes más comunes de las membranas biológicas, pero

tienen una química, un metabolismo y unas funciones distintas. Fueron descubiertos por el bioquímico y médico Johann Ludvig Thudichum en 1874 por cristalización de tejidos cerebrales animales. La estructura y naturaleza de estos componentes cerebrales fue considerada tan enigmática e inusual que Thudichum la denominó como 'sphingo-' en referencia al enigma de la esfinge en la mitología griega antigua (Thudichum, 1874). Se han estudiado ampliamente en sistemas animales debido a la multitud de funciones esenciales que llevan a cabo en el sistema nervioso, así como por las enfermedades asociadas a defectos en el metabolismo de los esfingolípidos (Hannun & Obeid, 2018). En plantas, desde su descubrimiento en 1874, se han elucidado cientos de estructuras de esfingolípidos, así como las características básicas de su metabolismo (Merrill et al., 1993; Markham et al., 2006; Markham & Jaworski, 2007; Buré et al., 2011, 2014, 2016; Cacas et al., 2012, 2013, 2016; Tarazona et al., 2015; Ishikawa et al., 2016).

En las células vegetales, los esfingolípidos representan el 40 % del contenido de lípidos de la membrana plasmática, contribuyendo de forma importante a las actividades de la superficie celular (Simons & Sampaio, 2011; Huby et al., 2020; Gömann et al., 2021). Asimismo, los esfingolípidos ayudan a definir las propiedades de las membranas y lipoproteínas, participan en la interacción célula-sustrato y en la comunicación célula-célula, incluyendo el reconocimiento de células por algunos microorganismos, virus y anticuerpos; interactúan con receptores para afectar las respuestas celulares a factores de crecimiento y otros agonistas, influyen en sistemas de transducción de señales y sirven como anclaje para algunas proteínas de membrana (Merrill et al., 1993; Tjellström et al., 2010; Cacas et al., 2016; Luttgeharm et al., 2016).

1.1.2 Estructura de los esfingolípidos

El término esfingolípido hace referencia a una clase de lípidos cuyo esqueleto es una base esfingoide o base de cadena larga (LCB). Esta LCB es el esfingolípido más simple, generalmente compuesto por 18 o 20 carbonos (Warnecke & Heinz, 2003), los cuales difieren entre sí en el número o la posición de los grupos hidroxilo y los dobles enlaces o en la conformación de las moléculas (Figura 1.1). Los principales esfingolípidos LCB de las plantas son las LCB de 18 carbonos: t18:1(Z), t18:1(E), t18:0, d18:1(Z), d18:1(E), y d18:0 (Chen et al., 2006). Las plantas también contienen trazas de otras cuatro LCB de 18 carbonos (d18:2(4E,8E), d18:2 (4E,8Z), t18:2 y una única d18:1 (con un doble C10=C11 enlace), además de una LCB de 20 carbonos (t20:0) y otras LCB especiales

d21:1 o d22:1 (contienen un doble enlace C7=C8) (Kimberlin et al., 2013; Ngo et al., 2020; Panzenboeck et al., 2020; Wang et al., 2020a).

En las plantas, los esfingolípidos complejos se clasifican en cuatro clases: ceramidas (Cers), hidroxiceramidas (hCers), glucosilceramidas (GlcCers) y glicosilinositolfosfoceramidas (GIPC), que constituyen aproximadamente el 4 %, 3 %, 37 % y 56 %, respectivamente, de los esfingolípidos totales extraídos de las hojas de Arabidopsis (*Arabidopsis thaliana*) (Sperling et al., 2005; Markham et al., 2006; Markham & Jaworski, 2007; Luttgeharm et al., 2016; Mamode Cassim et al., 2019).

A nivel estructural, los esfingolípidos están formados por una LCB unida por un enlace amida a un ácido graso para formar la Cer, que es la unidad estructural de los esfingolípidos más complejos (Cacas et al., 2012; Guillas et al., 2013) (Figura 1.1). Una LCB de 18C y un ácido graso con 16-26C constituyen el resto hidrofóbico de los esfingolípidos. A su vez, las LCB pueden estar dihidroxiladas en C1 y C3 o trihidroxiladas con un tercer OH en la posición C4 y pueden contener un doble enlace en C4 (configuración *trans*) y en C8 (configuración *cis* o *trans*). El ácido graso a su vez puede tener un doble enlace en C9 (configuración *cis*). Cuando la posición C2 de ácido graso se hidroxila, se forma una columna vertebral hCers. Asimismo, si el grupo hidroxilo del C1 del LCB forma un enlace glucosídico 1,4 con una unidad de glucosa, la estructura resultante se denomina GlcCer y si se esterifica con un grupo fosfoinositol unido a varias unidades de carbohidratos, da lugar a una glicosilinositolfosfoceramida (GIPC). A nivel estructural, el grupo OH de Cers y hCers, el residuo de glucosa de GlcCers y el fosfoinositol unido a los otros residuos de azúcar forman la cabeza polar de los esfingolípidos.

En los esfingolípidos complejos, el ácido graso suele ser de cadena muy larga (VLCFA), saturado o monoinsaturado, de 18 a 26 carbonos de longitud, lo que puede facilitar la hidrofobicidad, y la transición a la fase de gel. En particular, los esfingolípidos que contienen VLCFA, son conocidos por su papel crítico para el transporte polar de auxinas y el crecimiento vegetal en Arabidopsis (Pike, 2006).

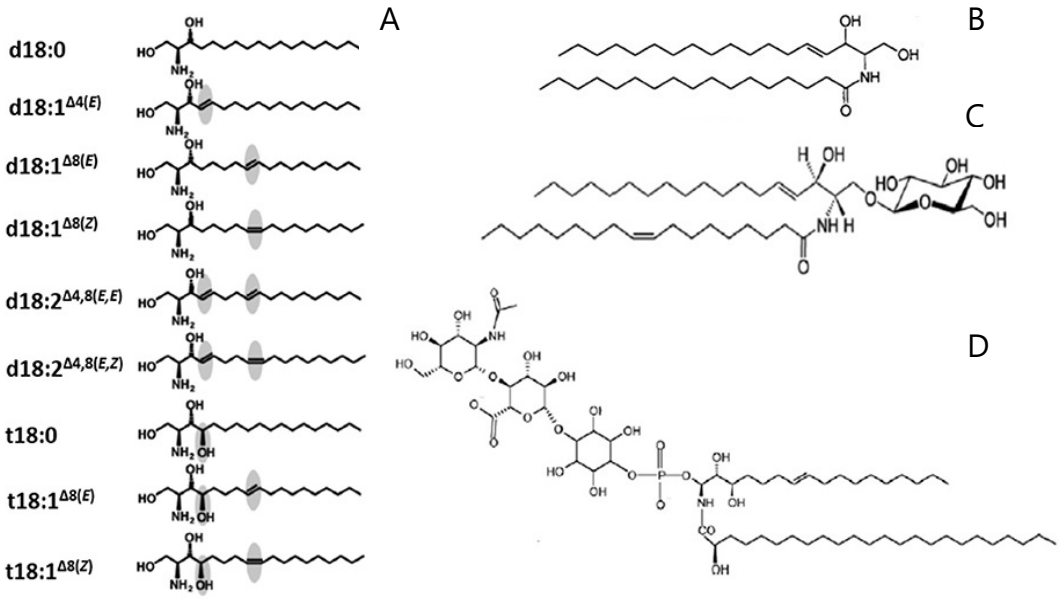

Figura 1.1. Tipos de esfingolípidos en plantas. **(A)** LCBs. Las nueve especies moleculares son esfinganina/dihidroesfingosina,d18:0; esfingosina/sphing-4(*trans*)-enina, d18:1 $^{\Delta 4(E)}$; sphing-8(*trans*)-enina, d18:1 $^{\Delta 8(E)}$; sphing-8(*cis*)-enina, d18:1 $^{\Delta 8(Z)}$; esfinga-4,8(*trans*, *trans*)-dienina, d18:1 $^{\Delta 4,8(E,E)}$; esfinga-4,8(*trans*, *cis*)-dienina, d18:1 $^{\Delta 4,8(E,Z)}$; fitoesfingosina/4-hidroxiesfinganina, t18:0; 4-hidroxiesfino-8(*trans*)-enina, t18:1 $^{\Delta 8(E)}$; 4-hidroxiesfino-8(*cis*)-enina, t18:1 $^{\Delta 8(Z)}$. (**B)** Cer (acido esfing-4(*trans*)-anina- *N*-octadecanoico). (**C)** GlcCer (Glucosil-O-β-ceramida (ácido esfing-4(*trans*)-enina- *N*-octadec-9(*cis*)- enoico)). (**D)** GIPC (N-acetilglucosamina-ácido glucurónico-inositolfosforil-ceramida (4-hidroxisphing-8(*cis*)-enina- *N*-ácido tetracosanoico). Figura adaptada de Cacas et al. (2012).

El número de formas posibles de LCB (hidroxilados, insaturados), ácidos grasos (hidroxilados, insaturados, con diferente número de carbonos) y carbohidratos (diversos tipos y números de azúcares) pueden dar lugar a una inmensa cantidad de combinaciones ensambladas o especies de esfingolípidos, lo que a su vez multiplica su variedad de funciones (Luttgeharm et al., 2016).

1.1.3. Síntesis y catabolismo de esfingolípidos.

La biosíntesis *de novo* de esfingolípidos se lleva a cabo en el retículo endoplasmático y se inicia por condensación de palmitoil-CoA y serina para generar 3-cetoesfinganina, en una reacción catalizada por la serina palmitoil transferasa (SPT), la cual funciona como heterodímero de las subunidades LCB1 y LCB2 interactuando con subunidades pequeñas serina palmitoiltransferasa (ssSPTs) que pueden aumentar la actividad SPT

(Mandon et al., 1992; Chen et al., 2006). La SPT es una enzima dependiente de pirodoxal 5' fosfato y está regulada por una ssSPT encargada de su estabilización (Kimberlin et al., 2013) y por las proteínas orosomucoides (ORM), que regulan negativamente la actividad de la SPT (Chueasiri et al., 2014; Li et al., 2016).

El paso siguiente en la biosíntesis de esfingolípidos consiste en la reducción del grupo *ceto* de la 3-cetoesfinganina a un hidroxilo para generar 1,3-dihidroesfingosina o esfinganina (d18:0), la cual constituye la forma más simple de LCB. Dicha reducción se lleva a cabo por la 3-cetodihidroesfingosina reductasa (Chen et al., 2006; Chao et al., 2011). Si bien en mamíferos la LCB predominante es la esfingosina, en plantas las formas de LCB más abundantes son la 4-hidroxi-esfinganina (fitoesfingosina, t18:0) y la 4-hidroxi-esfingosina (t18:1) (Cacas et al., 2012). Esta diferencia entre mamíferos y plantas se debe principalmente a que en la ruta de síntesis de plantas están implicadas desaturasas (delta-(4)- y delta(8)-desaturasas) e hidroxilasas (C4-hidroxilasas) que provocan modificaciones estructurales de la esfinaganina (Miller et al., 2010).

Una vez formadas las LCB en su gran mayoría se convierten en Cers mediante la unión con un ácido graso a través de un enlace amida. Dicha unión está catalizada por la ceramida sintasa LAG (LOH) (Markham et al., 2011). En Arabidopsis, las enzimas LOH1 y LOH3 participan preferentemente en la síntesis de las Cers con VLCFA, mientras que la enzima LOH2 es la principal responsable de la producción de las Cers portadores de LCFA (Markham et al., 2011; Luttgeharm et al., 2016). El ácido graso puede hidroxilarse en la posición C2, y de nuevo, la posición C1 del resto LCB puede a su vez fosforilarse, formando una P-Cer. Tanto la LCB como los restos de ácido graso de las Cers pueden también desaturarse, produciendo así una amplia variedad de estructuras diferentes (Melser et al., 2010).

La síntesis de Cer mediada por ceramida sintasa (CerS) es el centro de la ruta de síntesis de esfingolípidos (Figura 1.2). La CerS cataliza la combinación de esfingosina (Sph) y FA (VLCFA o LCFA) para formar Cer. La Cer puede generar además dos tipos de esfingolípidos, GluCer y GIPC, y posteriormente fosforilarse para formar Cer-1-P, y modificarse en las cadenas FA y LCB para formar diferentes moléculas de esfingolípidos (Liu et al., 2021). La biosíntesis de estas Cers, especialmente las Cers t18:0/t18:1 y C24:0/C24:1, también puede verse afectada por una enzima llamada modulador de descarga del floema (Yan et al., 2019).

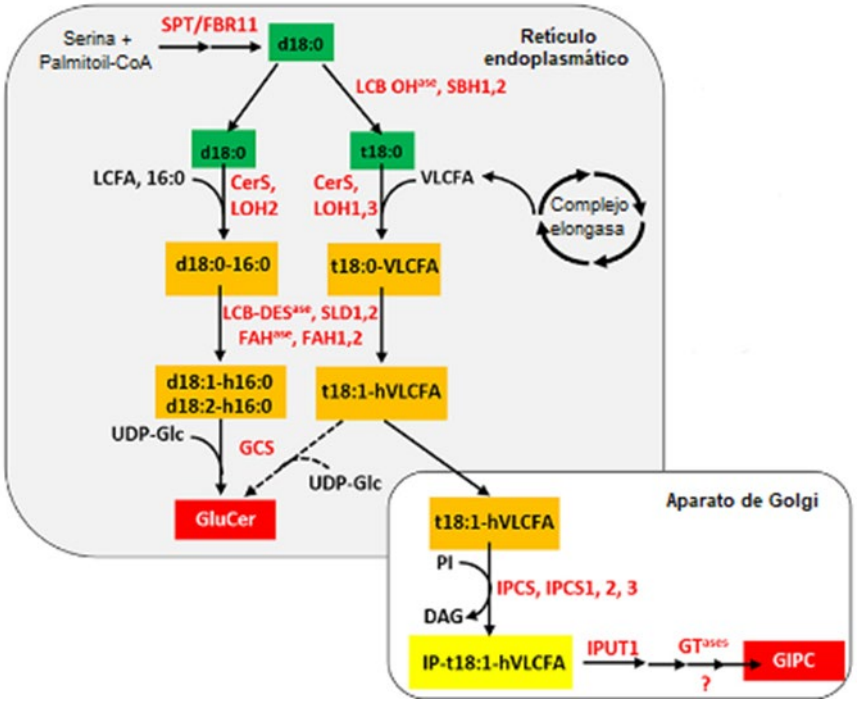

Figura 1.2. Biosíntesis de esfingolípidos vegetales. A excepción de los precursores de serina y palmitoil-CoA, los metabolitos de esfingolípidos aparecen en rectángulos de colores: verde para bases de cadena larga, naranja para ceramidas y rojo para productos finales como glucosilceramidas (GluCer) y glicosil-inositolfosforil-ceramidas (GIPC). La nomenclatura de la ceramida es la siguiente: por ejemplo, d18:0-16:0 indica que la base de cadena larga corresponde a la esfinganina y el ácido graso es un resto de palmitoilo, respectivamente. Las enzimas se escriben en rojo. Abreviaturas: CerS, ceramida sintasa; DAG, diacilglicerol; FAHasa , hidroxilasa de ácido graso; GCS, glucosilceramida sintasa; GT ase, glicosiltransferasa; IPCS, inositolfosforil-ceramida sintasa; IPUT1, INOSITOLFOSFORIL-CERAMIDA GLUCURONOSIL-TRANSFERASA 1; LCB, base de cadena larga; LCB DESasa , LCB desaturasa; LCB OHasa , LCB hidroxilasa; LCFA, ácido graso de cadena larga; LOH, LAG ONE HOMOLOG; PI, fosfatidilinositol; SPT/FBR11, serina palmitoil-CoA transferasa/RESISTENTE A FUMONISINA 11; SLD1,2, ESFINGOLÍPIDO LCB Δ8 DESAUTRASA 1,2; UDP-Glc, uridina difosfato-glucosa; VLCFA, ácido graso de cadena muy larga. Figura adaptada de De Bigault Du Granrut & Cacas, (2016).

Los LCB saturados pueden ser desaturados a través de LCB desaturasas esfingoideas (SLD) en C-8 o a través de esfingolípido δ-4-desaturasa en C-4 para generar Cers basadas en d18:1, t18:1 o d18:2 (Michaelson et al., 2009; Chen et al., 2012). Las Cers sufren una α-hidroxilación en la cadena del ácido graso por parte de la hidroxilasa de ácido graso C-2 (FAH) antes de la modificación de su grupo principal (Dunn et al., 2004; Markham & Jaworski, 2007; König et al., 2012; Nagano et al., 2012). Los VLCFA se biosintetizan mediante la elongación de dos carbonos de acil-CoAs grasos de cadena larga C16-C18 (Paul et al., 2006). Este proceso se lleva a cabo por la β- 3-cetoacil-CoA sintasa (KCS), una enzima clave en la elongación de VLCFA. Esta enzima es una proteína

de membrana integral que forma parte del complejo de elongación de ácidos grasos microsomales (FAE). El complejo FAE consta de cuatro enzimas centrales, cada una de las cuales cataliza uno de los cuatro pasos en la elongación de VLCFA (Haslam & Kunst, 2013). En primer lugar, la KCS condensa un acil-CoA graso con malonil-CoA para generar un 3-cetoacil-CoA. La reducción posterior del carbonilo por la cetoacil-CoA reductasa, la deshidratación del grupo hidroxilo por la hidroxiacil-CoA deshidratasa y la reducción del doble enlace por la enoil-CoA reductasa, producen un acil-CoA graso ampliado en dos carbonos. Este VLCFA puede usarse para otra ronda de elongación; sin embargo, ello depende de la especificidad de sustrato de la enzima de condensación (Fehling & Mukherjee, 1991). Los VLCFA cuticulares de las plantas, y sus derivados, generalmente contienen alrededor de 30 átomos de carbono, mientras que se ha demostrado que los tricomas de las hojas y las células del pavimento producen VLCFA con hasta 38 átomos de carbono (Hegebarth et al., 2016).

La glicosilación de Cers en el grupo hidroxilo C-1 produce GlcCers o GIPC (Luttgeharm et al., 2016). En esta reacción la glucosilceramida sintasa (GCS) transfiere un residuo de glucosa de la UDP-glucosa a una hCer para producir GlcCer mediante un enlace beta-glucosídico (Leipelt et al., 2001; Melser et al., 2010). La síntesis de GIPC se lleva a cabo en al aparato de Golgi, por lo que las Cers o hCers deben ser transportadas desde el retículo endoplasmático hasta el aparato de Golgi. En este orgánulo, las Cers y hCers son modificadas en primer lugar por la inositolfosforilceramida sintasa (IPCS) que agrega un grupo de cabeza derivado de fosfatidilinositol (PI) para formar inositolfosfoceramidas (IPC) (Mina et al., 2010). Seguidamente, se incorpora un resto de ácido glucurónico (GlcA) mediante un enlace α(1,4) y la participación de la inositol fosforilceramida glucuronosiltransferasa1 (IPUT1) (Rennie et al., 2014). La glicosilación adicional del grupo de cabeza está mediada por la GIPC manosil transferasa 1 (GMT1) o por la glucosamina inositol fosforilceramida transferasa 1 (GINT1) y requiere además del transportador de azúcar de nucleótidos de Golgi 1 y 2 (GONST1 y GONST2) o UDP-N-acetil-D-glucosamina transportador 1 (UGNT1) (Mortimer et al., 2013; Fang et al., 2016; Ebert et al., 2018; Ishikawa et al., 2018; Jing et al., 2021). Se ha demostrado que la GMT1 produce GIPC unidos a manosa o hexosa-manosa, mientras que la GINT1 transfiere principalmente glucosamina (GlcN) o N-acetil-glucosamina (GlcNAc) a las GlcA-IPC (Ishikawa et al., 2018). El Arabidopsis, *gonst1* muestra un contenido reducido de manosa-GIPC y

acumula más GlcA-IPC (Mortimer et al., 2013), mientras que la pérdida del transportador UDP-GlcNAc da como resultado una deficiencia significativa de GlcN(Ac)-GIPC (Ebert et al., 2018).

La fosforilación es una forma importante de modificación de los esfingolípidos y está estrechamente relacionada con la función de estos. La fosforilación puede ocurrir en la posición C-1 OH de los LCB mediante la acción de LCB quinasas (LCBK) para formar LCB 1-fosfatos (LCB-Ps) (Nishiura et al., 2000; Imai & Nishiura, 2005) o en la posición C-1 OH de Cers, la cual se lleva a cabo por Cer quinasas dando lugar a Cer 1-fosfatos (C1Ps) (Liang et al., 2003). En estas reacciones de fosforliación participan las fosfatasas vegetales LCB-1-P, siendo principalmente las encargadas de esta fosforilación la fito-S1P fosfatasa (SPPASE) y la fito-S1P liasa (DPL1) (Liang et al., 2003; Guo & Wang, 2012; Nakagawa et al., 2012; Luttgeharm et al., 2016; Qin et al., 2017). Las quinasas responsables de fosforilar las LCB, SPHINGOSINE KINASE 1 (SPHK1) y SPHINGOSINE KINASE 2 (SPHK2), han sido principalmente estudiadas en *A. thaliana* (Coursol et al., 2005; Worrall et al., 2008; Alden et al., 2011; Guo et al., 2011). A su vez, las LCB-P (derivados fosforilados de LCB) pueden agotarse por desfosforilación por LONG-CHAIN BASE PHOSPHATE PHOSPHATASEs (LCB-PP1 and LCB-PP2) (Worrall et al., 2008) o por escisión de la columna vertebral de LCB para producir hexadecanal y fosfoetanolamina por LONG-CHAIN BASE PHOSPHATE LYASE (DPL) (Tsegaye et al., 2007).

Los LCBs y LCB-Ps son reguladores críticos de muchos procesos fisiológicos y respuestas al estrés (Shi et al., 2007; Chen et al., 2008; Worrall et al., 2008; Teng et al., 2008; Islam et al., 2012; Dutilleul et al., 2012, 2015; Markham et al., 2013; Wu et al., 2014; Haslam & Feussner, 2022). La fosforilación de LCB en su grupo hidroxilo C-1 es catalizada por la LCBK, a menudo denominadas también como SPHK. Se han identificado cuatro genes (LCBK1, LCBK2, SPHK1 y SPHK2) que codifican estas enzimas en Arabidopsis (Chen et al., 2009). Los SPHK funcionan como transductores de señales importantes en las respuestas al estrés (Imai & Nishiura, 2005; Worrall et al., 2008; Dutilleul et al., 2012; Guo et al., 2012; Saucedo-García et al., 2011). En este sentido, se ha demostrado que en Arabidopsis, el ácido abscísico (ABA) estimula la actividad enzimática de SPHK1 y SPHK2 durante el cierre estomático (Ng et al., 2001; Coursol et al., 2003, 2005). Asimismo, se ha asociado una función para LCBK1 actuando como un regulador positivo de la tolerancia a la congelación (Huang et al., 2017).

Además, estudios recientes indican un papel de SPHK1 en la modulación de la muerte celular provocada por la fumonisina B1 (FB1) a través de las interacciones de las rutas del ácido salicílico (SA) y el ácido jasmónico (JA) (Qin et al., 2017). En plantas de arroz también se ha indicado que tanto OsLCBK1 como OsLCBK2 modulan la resistencia a enfermedades de las plantas y la muerte celular (Zhang et al., 2013). Por otra parte, agentes como el frío se ha observado que estimulan la actividad de la quinasa LCBK2 para catalizar la producción de fitosfingosina-1-fosfato (t18:0-P) (Dutilleul et al., 2012). Por su parte, las fosfatasas LCB-P y las liasas LCB-P (SPL) desfosforilan LCB-P y afectan la respuesta de deshidratación en Arabidopsis (Tsegaye et al., 2007; Nishikawa et al., 2008; Nakagawa et al., 2012). Asimismo, los mutantes de Arabidopsis que carecen de SPL (AtDPL1) acumulan trihidroxi-18:1 LCB-P (Tsegaye et al., 2007; Nakagawa et al., 2012). Estas plantas no muestran fenotipos de crecimiento, pero son hipersensibles a la FB1, lo que probablemente se deba a niveles más altos de acumulación de LCB-Ps en el mutante en respuesta a la micotoxina en relación con las plantas de tipo silvestre (Tsegaye et al., 2007).

Las Cers pueden sufrir posteriores modificacionesmediante la adición de varios grupos polares, y estos esfingolípidos más complejos se pueden clasificar por su enlace con la Cer. Los glicoesfingolípidos contienen un enlace glucosídico, y en las plantas generalmente están presentes como una sola forma y con un solo grupo principal, la glucosa, para producir GlcCer (Warnecke & Heinz, 2003). Por lo tanto, la Cer es el precursor de los esfingolípidos complejos y la modificación más común de las Cers vegetales es la adición de glucosa para generar GlcCer. No obstante, existen excepciones; por ejemplo, se han detectado diglicosilceramidas en la diatomea *Thalassiosira pseudonana* (Hunter et al., 2018), hojas de espinaca (Ohnishi et al., 1983) y semillas de guisantes (Ito et al., 1985). Estos a veces contienen azúcares distintos de la glucosa, por lo que esta clase de esfingolípidos se denomina con mayor precisión hexosilceramidas (HexCers). Los fosfoesfingolípidos tienen un grupo principal unido a la Cer a través de un enlace fosfodiéster (Miller et al., 2010). En las plantas, estos están presentes como un grupo diverso de lípidos de membrana, GIPC, que pueden modificarse ampliamente con una variedad de azúcares (Mamode Cassim et al., 2019). GlcCers y GIPC constituyen ~34 % y 64 % del conjunto total de esfingolípidos, respectivamente (Markham et al., 2006), aunque esta proporción varía sustancialmente entre especies y tejidos. Los esfingolípidos complejos son componentes principales de las membranas de las células vegetales (Miller et al., 2010), y los GIPC por sí solos

pueden constituir hasta el 45 % de los lípidos de la membrana plasmática (Cacas et al., 2016). Dada su abundancia, no sorprende que recientemente se haya demostrado que los GIPC actúen como una fuente importante de fosfato en ausencia del mismo (Yang et al., 2021).

Si bien la gran mayoría de los esfingolípidos sintetizados en *A.* thaliana están destinados a convertirse en esfingolípidos complejos, las formas más simples, LCB y Cers libres, son también destinos metabólicos con funciones fisiológicas propias que dependen de su estado de fosforilación (Berkey et al., 2012; Luttgeharm et al., 2016). Las LCB libres y las Cers se acumulan en niveles bajos en los tejidos de las plantas, presentando juntos <3 % de la reserva total de esfingolípidos (Markham & Jaworski, 2007). Ambas son moléculas de señalización que afectan fuertemente los niveles de fitohormonas y cumplen funciones clave en la señalización de la PCD (Berkey et al., 2012). En términos generales, se considera que las LCB y LCB-P tienen actividad antagónica en la señalización de la muerte celular, así, mientras que los LCB desencadenan la muerte celular, se ha demostrado que los LCB-P mitigan o regulan a la baja este proceso (Berkey et al., 2012). La fosforilación de la Cer está catalizada por una Cer quinasa, ACCELERATED CELL DEATH5 (ACD5) (Greenberg et al., 2000; Liang et al., 2003; Wang et al., 2008). Sin embargo. no se conoce en plantas ninguna fosfatasa que catalice la desfosforilación de fosfatos de la Cer.

La síntesis de esfingolípidos en las plantas también está equilibrada por rutas catabólicas que no solo proporcionan un mecanismo para la renovación de los esfingolípidos, sino que también pueden generar moléculas bioactivas que regulan diversos procesos celulares (Ng et al., 2001; Coursol et al., 2003; Liang et al., 2003). En este sentido, las enzimas denominadas ceramidasas convierten las Cers en LCB y ácidos grasos libres. Las ceramidasas se clasifican en tres formas distintas según sus preferencias óptimas de pH en ensayos *in vitro*: ceramidasas ácidas, neutras y alcalinas (Mao & Obeid, 2008). Hasta la fecha, solo se han identificado y caracterizado en plantas ceramidasas neutras (NCER) y alcalinas (ACER) (Wu et al., 2015a; Haslam & Feussner, 2022). Sus actividades están estrechamente asociadas tanto con la señalización similar a la PCD desencadenada por patógenos, como con la PCD controlada por el programa de desarrollo, la autofagia y la presión de turgencia celular (Chen et al., 2015; Li et al., 2015a; Wu et al., 2015a; Zheng et al., 2018; Zienkiewicz et al., 2020). La glucosilceramidasa (GlcCerase) descompone esfingolípidos complejos como GlcCer en

mamíferos, pero no se ha detectado tal homólogo en Arabidopsis. Sin embargo, en arroz se ha encontrado una OsCDasa con un pH óptimo entre 5,7–6,0 que hidroliza preferentemente d18:1Δ4-Cer sobre t18:0-Cer, de acuerdo con las propiedades de las CDasas neutras (Mao & Obeid, 2008; Pata et al., 2008).

Las flipasas también juegan un papel importante en el catabolismo de GlcCer, donde una combinación de flipasas ALA transportan GlcCers a la superficie de la membrana citosólica para ser degradadas por GlcCerase. Las GlcCerases eliminan el grupo principal de glucosa de los GlcCers para producir una molécula de Cer, que puede degradarse aún más hasta las propias bases esfingoides como fitosfingosina y ácidos grasos. En ausencia de flipasas transportadoras de GlcCer, éstas se aumulan en membranas extracitoplasmáticas o luminales (Davis et al., 2020). En Arabidopsis, se ha demostrado que una (AtACER hidroliza las Cers t18:0, y varias AtNCER pueden degradar las hCers en Sph y ácidos grasos (Li et al., 2015a; Wu et al., 2015a). Asimismo también se ha visto en enArabidopsis que la GlcCerase, AtGCD3, hidroliza preferentemente las GlcCers que contienen largas cadenas de acilo (Dai et al., 2020). Por su parte, estudios llevados a cabo en hojas de col, han determinado que una fosfolipasa D específica de GIPC (GIPC-PLD) provocaba una escisión en la posición D del enlace éster entre el inositol y el fosfato para producir fitoceramida 1-fosfato (PC1P) (Hasi et al., 2019). Esta enzima exhibe una preferencia de sustrato por las GIPC que contienen dos azúcares (Hasi et al., 2019). Además, recientemente se informó que una fosfolipasa C4 no específica (NPC4) hidroliza las GIPC durante la deficiencia de fosfato en Arabidopsis (Yang et al., 2021).

1.1.4. Distribución de esfingolípidos en plantas

Se han encontrado esfingolípidos en animales, plantas y hongos y se estima que existen de 300 a 400 diferentes especies moleculares de estos lípidos. Las GlcCers y los esfingolípidos relacionados son componentes minoritarios en extractos lipídicos de plantas, contribuyendo con 5 % o menos a la fracción lipídica. Sin embargo, en las membranas celulares, las GlcCers son un componente cuantitativamente importante, que comprende del 7 al 26 % en mol de los lípidos de la membrana plasmática, dependiendo de la concentración del tejido vegetal en estudio. A su vez, la GlcCer también es un componente importante de los lípidos del tonoplasto. Cabe mencionar que, a nivel celular, los esfingolípidos se concentran en la cara externa de la membrana,

expuestos en la superficie celular (Lynch, 1993; Bohn et al., 2001; Michaelson et al., 2016; Mamode Cassim et al., 2020; Haslam & Feussner, 2022). Todas estas observaciones son consistentes con los datos disponibles en mamíferos, donde diversos esfingolípidos se localizan principalmente en la membrana plasmática y endomembranas relacionadas.

Los esfingolípidos más comunes en plantas son aminoalcoholes C18 e incluyen a las bases dihidroxiladas, esfinganina (d18:0), 8-esfingenina (d18:1$^{8cis\ o\ trans}$), 4,8-esfingadienina (d18:2 $^{4trans,8trans\ o\ 4trans,8cis}$) y las bases trihidroxiladas 4-hidroxiesfinganina o Sph (t18:0) y 4-hidroxi-8-esfingenina (t18:1$^{8cis\ o\ trans}$) (Figura 1.1), mientras que la LCB predominante en animales es la esfingosina (Worrall et al., 2003). En vegetales existen además y, como constituyentes minoritarios, otras bases LCB que difieren en la longitud de la cadena, número de grupos hidroxilo, y en la posición y configuración estereoquímica de los dobles enlaces. Los ácidos grasos presentes en los esfingolípidos de plantas son casi exclusivamente 2-hidroxilados. A su vez, las cadenas acilo más abundantes tienen entre 16 a 24 C y son saturadas, aunque en algunas plantas se pueden encontrar cadenas C14 y C26. Por otra parte, la glucosa es por excelencia el monsacárido unido a la Cer en casi todos los glicoesfingolípidos vegetales, la cual se une por un enlace glicosídico al grupo hidroxilo de C-1 del aminoalcohol (Lynch, 1993; Sperling & Heinz, 2003; Michaelson et al., 2016; Mamode Cassim et al., 2020).

Cabe mencionar que la cantidad relativa de los diferentes esfingolípidos no es constante, sino que sufre cambios derivados dela propia regulación de la síntesis, el catabolismo o mediante fosforilación/desfosforilación lo que conduce a niveles diferenciales y específicos de esfingolípidos (Kihara et al., 2007; Merrill et al., 2009; Markham et al., 2013; Pata et al., 2010). A su vez, existen grandes diferencias entre las GlcCers en los diversos tejidos de plantas con respecto a la composición de su LCB y/o del ácido graso que forma parte de la molécula. Así, las GlcCers de tejidos de semillas generalmente están enriquecidas en LCFA hidroxilados (C_{16}-C_{20}), mientras que las GlcCers presentes en las hojas de dicotiledóneas y cereales están enriquecidas en LCBs trihidroxiladas y VLCFAs saturados e insaturados (>C_{20}). Por otra parte, la composición de GlcCers en raíces se ha visto que es similar a la de las hojas en un gran número de plantas estudiadas (Lynch, 1993; Michaelson et al., 2016). Otros esfingolípidos complejos encontrados en plantas son los que contienen inositol, derivados de la IPC. Estos se encuentran en muchos tejidos vegetales y tienen una amplia diversidad estructural. Su estructura principal está compuesta por Cers e inositolfosfato, así como oligosacáridos polares, tales

como la GlcNAc, GlcN, GlcA, galactosa, manosa, arabinosa y fucosa. En tabaco se han encontrado más de 20 especies moleculares diferentes de IPC con variaciones en el oligosacárido. Estos compuestos forman parte de las membranas plasmáticas y el tonoplasto. Sin embargo, su localización celular y su función aún no se ha determinado, aunque se ha demostrado que algunas proteínas ancladas a glicosilfosfatidilinositol (GPI), contienen esfingolípidos con fosfoinositol (Bromley et al., 2003; Mamode Cassim et al., 2020).

En las plantas, los GIPC están presentes como un grupo muy diverso de lípidos de membrana, los cuales pueden modificarse ampliamente por unión a una gran variedad de azúcares (Cassim et al., 2019). Ambos, GlcCers y GIPC constituyen ~34 % y 64 % de la reserva total de esfingolípidos, respectivamente (Markham et al., 2006), aunque esta proporción puede variar sustancialmente entre especies y tejidos.

La composición de los esfingolípidos en las células vegetales también varía según el tipo de célula y de especie vegetal. Una comparación de los esfingolipidomas indica una diferencia llamativa entre los esfingolípidos de la hoja de Arabidopsis y los del polen. Así, los LCB de esfingolípidos en las hojas son principalmente t18:1, t18:0, d18:1 y d18:0, mientras que en polen incluyen un gran porcentaje de d18:2 (Chen et al., 2006; Markham et al., 2006; Luttgeharm et al., 2016). Además, también se ha demostrado que hay más LCB y Cers libres en el polen que en las hojas (Markham & Jaworski, 2007). Mientras tanto, los esfingolípidos más abundantes en las hojas son los GIPC, mientras que en el caso del polen ganan abundancia los GlcCers (Luttgeharm et al., 2016). Los GIPC de la hoja son principalmente Hex(OH)-HexA-IPC (serie A), con una pequeña cantidad de Hex-Hex(OH)-HexA-IPC (serie B), mientras que los GIPC del polen contienen principalmente Hex(NAc)-HexA- IPC (serie A), $(Pen)_3$-Hex-Hex(NAc)-HexA-IPC (serie E), $(Pen)_2$-Hex-Hex(NAc)-HexA-IPC (serie D), y trazas de Hex-Hex(OH)-HexA-IPC (serie B) (Luttgeharm et al., 2016). Diferentes estudios destacan que las diferencias en la cantidad de residuos de azúcar vinculados a las IPC las cuales pueden contribuir a la susceptibilidad de las plantas a los patógenos que producen necrosis y proteínas similares al péptido 1 (NLP) inductoras de etileno (Lenarčič et al., 2017). A su vez la composición y distribución de los esfingolípidos (LCB libres, Cers/hCers, GlcCers y GIPC) también difieren entre las distintas especies de plantas. Por ejemplo, los esfingolípidos de la hoja de arroz tienen una relación LCB *cis/trans* y una relación de

ácidos grasos no hidroxi más altas que los esfingolípidos de la hoja de Arabidopsis (Ishikawa et al., 2016; Markham et al., 2006).

GlcCers y GIPC constituyen aproximadamente el 40 % de los lípidos de la membrana plasmática de las plantas (Sperling et al., 2005; Vu et al., 2014; Grison et al., 2015; Tarazona et al., 2015). Los esfingolípidos también son relativamente abundantes en el tonoplasto, el ER y el aparato de Golgi de las plantas, y representan hasta el 20 % de los lípidos totales en estas membranas (Verhoek et al., 1983; Warnecke & Heinz, 2003; Fouillen et al., 2018). Asimismo, se ha demostrado que los esfingolípidos están altamente enriquecidos en plasmodesmos y vesículas extracelulares, lo que representa más del 40 % de los lípidos de membrana en estas estructuras (Grison et al., 2015; Liu et al., 2020a). Sin embargo, a nivel celular, no se han detectado esfingolípidos en el cloroplasto y la mitocondria (Verhoek et al., 1983).

Además, la composición de esfingolípidos no es uniforme en los sistemas de membrana celular. Así, en un estudio reciente comparando el plasma de hoja de Arabidopsis y los esfingolipidomas de membrana vacuolar ha puesto de manifiesto variaciones importantes en la composición de esfingolípidos en las membranas microsomales (población heterogénea de vesículas de membrana de diferentes orgánulos y la membrana plasmática), membranas vacuolares, membrana plasmática y membranas resistentes a detergentes (DRM) derivadas de la membrana plasmática. En todas ellas las Cers aparecen en la proporción más baja, mientras que los GIPC son los más abundantes (excepto en las membranas vacuolares). A su vez, los DRM son los que poseen una mayor cantidad de esfingolípidos, mientras que las membranas microsomales presentan un contenido de esfingolípidos más bajo en relación con los niveles de proteinas (Carmona-Salazar et al., 2021). De forma general, las endomembranas (como las membranas vacuolares) prefieren los GlcCers de esfingolípidos glicosilados simples a los GIPC complejos. Sin embargo, la membrana plasmática, plasmodemos y vesículas extracelulares presentan un porcentaje mayor de GIPC (Warnecke & Heinz, 2003; Grison et al., 2015; Liu et al. , 2020b). Asimismo, las estructuras de membrana se caracterizan por presentar esfingolípidos con distintas cadenas laterales. Los esfingolípidos que contienen LCB saturados y cadenas de acilo graso son más abundantes en los plasmodesmos que en las membranas plasmáticas (Liu et al., 2020a). Recientemente, también se ha reportado que las DRM en la membrana plasmática pueden funcionar en el reclutamiento de proteínas específicas (Carmona-

Salazar et al., 2021). Así, en plantas, se ha demostrado que estos DRM contienen abundantes esfingolípidos (especialmente GIPC) y esteroles, así como una acumulación de ciertas proteínas (Simon-Plas et al., 2011). Sin embargo, las propiedades de los detergentes también han generado fuertes críticas al concepto DRM, como la afirmación de que el Triton X-100 en realidad promueve la condensación de lípidos en la membrana plasmática (Munro, 2003; Tanner et al., 2011). Aun así, los DRM todavía se consideran un punto de partida para el análisis de microdominios de membrana enriquecidos con esfingolípidos y esteroles de plantas.

Los DRM derivados de Golgi y los DRM derivados de la membrana plasmática presentan composiciones de GlcCer similares (Laloi et al., 2007). Sin embargo, dependiendo de la especie vegetal, los DRM derivados de la membrana plasmática muestran niveles de esfingolípidos (principalmente GIPC) de aproximadamente 2 a 7 veces más altos que las regiones que no son DRM en la membrana plasmática (Simon-Plas et al., 2011). En este sentido, estudios en *Nicotiana tabacum* han mostrado que los DMR están más enriquecidos en GIPC con VLCFA 2-hidroxilados y GIPC poliglicosilados, en comparación con el resto de la membrana plasmática (Cacas et al., 2016). La membrana plasmática, vacuolar, microsomal y DRM contienen el mismo conjunto de especies de esfingolípidos, pero cada tipo de membrana presenta una variedad específica propia de estos componentes que está basada en la proporción de clases de esfingolípidos y en el predominio de especies individuales (Carmona-Salazar et al., 2021).

1.1.5. Tráfico de los esfingolípidos a nivel celular

El tráfico de los esfingolípidos es necesario desde el momento de su propia biosíntesis ya que las Cers se sintetizan en el retículo endoplasmático y los principales esfingolípidos en las plantas, como los GIPC, se generan en el aparato de Golgi. Además, estas biomoléculas llevan a cabo movimientos de translocación, clasificación o transporte hasta localizarse en las membranas deseadas (Riboni et al., 2010; Hurlock et al., 2014; Haslam & Feussner, 2022).

El movimiento de los esfingolípidos entre las membranas generalmente ocurre de dos formas: transporte no vesicular (o mediado por proteínas) y vesicular. La Cer quinasa ACD11 (ACCELERATED CELL DEATH 11) y una proteína de transferencia

de glicolípidos (GLTP1) se consideran posibles candidatos para los transportadores de los esfingolípidos (Brodersen et al., 2002; West et al., 2008).

El transporte vesicular es la forma predominante de translocación intermembrana de los esfingolípidos. En este sentido, se ha demostrado que las Cers se asocian con vesículas derivadas del retículo endoplasmático (Kajiwara et al., 2008; Giussani et al., 2009), y los esfingolípidos complejos sintetizados en la luz de Golgi también se empaquetan en las vesículas por mecanismos aún desconocidos (Holthuis & Levine, 2005).

1.1.6. Funciones de los esfingolípidos en las plantas

Como moléculas anfifílicas, los esfingolípidos se encuentran enlas membranas celulares constituyendo un soporte estructural y dinámico de la bicapalipídica (Tapken & Murphy, 2015; Michaelson et al., 2016; Mamode Cassim et al., 2020). Presentan múltiples funciones, actuando como mediadores fisiológicos del cierre de estomas, en la PCD, en las interacciones planta-patógeno, en las respuestas frente al estrés abiótico, así como en el desarrollo de polen, frutos y semillas (Dietrich et al., 2008; Luttgeharm et al., 2016; Ali et al., 2018; Inês et al., 2018; Mamode Cassim et al., 2019; Gonzalez-Solis et al., 2020).

Las LCBs, las Cers y las hCers, que son los esfingolípidos menos abundantes, se consideran intermediarios metabólicos o fuentes de moléculas de señalización. En este sentido, las Cers han estado implicadas en las respuestas al estrés por frío, así como en la respuesta inmune de la planta (Liang et al., 2003; Dutilleul et al., 2015), mientras que las hCers actúan como transductores de señalización en situaciones de estrés por hipoxia (Xie et al., 2015). Por otra parte, los esfingolípidos de mayor abundancia, como los los GlcCers y GIPC se han identificado como componentes estructurales de las membranas plasmáticas y sistema de endomembranas como el tonoplasto, plasmodesmos, Golgi y retículo endoplasmático (Gronnier et al., 2019). Además, Cers y GIPC muestran roles de señalización relacionados con su asignación como componentes estructurales de la membrana. Así, por ejemplo, se ha visto que los GlcCers participan en el desarrollo de gametofitos, en la propia morfología y secreción de las membranas de Golgi, así como en otras funciones fisiológicas como la organogénesis y la diferenciación celular (Dietrich et al., 2008; Melser et al., 2010; Chen et al., 2012; Msanne et al., 2015). Asimismo, los GIPCs se han postulado como conectores de señalización estructural entre la membrana plasmática y la pared celular (Mamode Cassim et al., 2020), pero

también se le han atribuido funciones actuando como elementos que participan en la defensa contra patógenos, en la viabilidad del grano de polen y en la percepción de altos niveles de sal, participando en la respuesta al estrés salino (Wang et al., 2008; Mortimer et al., 2013; Rennie et al., 2014; Fang et al., 2016; Jiang et al., 2019). Esta diversidad de funciones explica el carácter esencial que se ha asignado a los esfingolípidos en las plantas.

Asimismo, de cara a conocer las funciones de estas biomoléculas, resulta muy interesante perfilar el contenido de esfingolípidos en diversas especies modelo y no modelo y combinarlo con la aplicación de inhibidores del ensamblaje de esfingolípidos. Los inhibidores son herramientas valiosas en estos sistemas menos manejables por manipulación genética, que sin embargo ofrecen ventajas específicas con respecto a su desarrollo y fisiología. Los inhibidores a menudo causan defectos de crecimiento y desarrollo que imitan a mutantes defectuosos en el ensamblaje de esfingolípidos. En este sentido, se han identificado diferentes productos químicos que afectan el metabolismo de los esfingolípidos, incluidas varias micotoxinas que inhiben la síntesis de Cer (Chen et al., 2020), 1-fenil-2-decanoilamino-3-morfolino-1-propanol (PDMP), que inhibe la síntesis de GlcCer (Msanne et al., 2015), y miriocina, que inhibe la síntesis de LCB (Miyake et al., 1995; Chen et al., 2021), entre otros. Asimismo, los inhibidores de Cer FB1 de Fusarium y la toxina de *Alternaria alternata* lycopersici (AAL) también han sido particularmente útiles para la investigación de las funciones de los esfingolípidos en plantas. Así, la aplicación de toxina FB1 o AAL a discos de hojas de *Solanum lycopersicum*, lenteja de agua (*Lemna pausicostata*), o callos de *Nicotiana tabacum* provocó la acumulación de LCB d18:0 y t18:0 en todos los casos (Abbas et al., 1994). Asimismo, el tratamiento directo de cultivos de *L. pausicostata* con LCB d18:0, t18:0 y d18:1Δ4 produjo defectos de crecimiento similares a los de las micotoxinas, lo que respalda la idea de que FB1 y AAL realmente actúan como inhibidores de la CerS y que sus efectos tóxicos estén mediados por una acumulación excesiva de sustrato LCB tras la inhibición de la CerS (Tanaka et al., 1993).

Asimismo, la inhibición de la síntesis de Cer por parte de FB1 puede ocasionar desde el desmantelamiento de estructuras vesiculares hasta la fusión de vesículas, pudiendo ello afectar a la ubicación de las proteínas transportadoras de auxina y con ello al crecimiento normal de la planta (Markham et al., 2011). Otros estudios llevados a cabo en polen de Arabidopsis también ha permitido dilucidar que la represión de la subunidad LCB2

del SPT conduce a la destrucción de las membranas del aparato de golgi y del retículo endoplasmático (Dietrich et al., 2008). En este sentido también se ha observado que el bloqueo de la biosíntesis de GlcCer por PDMP puede inducir la heteromorfosis del Golgi con vesículas circundantes inflamadas y, como resultado, provocar la rotura de la proteína dependiente de Golgi, vía secretora (Melser et al., 2010).

Recientemente, se ha demostrado que las Cers sintasas están implicadas en la regulación del crecimiento y desarrollo de plantas (Li et al., 2022). Así, estudios realizados en plantas de algodón han indicado que la aplicación exógena de FB1 reduce significativamente el contenido de GluCer, GIPC y Cers, mientras que aumenta significativamente el contenido de Sph, inhibiendo el crecimiento de las fibras (Wang et al., 2020b). Asimismo, tratamientos con miriocina (inhibidor de la síntesis de esfingolípidos a nivel de la STP), inhiben la síntesis de esfingolípidos y el crecimiento del embrión de algodón (Wang et al., 2021). Por su parte, en experimentos con Arabidopsis la sobreexpresión de LOH1 y LOH3 promueve la división celular y el crecimiento de las plantas, mientras que el doble mutante loh1loh3 provoca esterilidad, indicando que la CerS es importante para el desarrollo de las plantas. Por otro lado, también se ha observado que la sobreexpresión de LOH2 conduce al aumento de Cer que contiene en su estructura un ácido graso C16 y un grupo dihidroxilo Sph, lo que indujo la PCD y la acumulación de SA, dando lugar a plantas más pequeñas (Luttgeharm et al., 2015). Asimismo, las plantas que sobreexpresan LOH2 y LOH3 tienen una mayor resistencia a FB1, lo que no ocurre con las que sobreexpresan LOH1 (Luttgeharm et al., 2015). Recientemente otro estudio en *Physcomitrium patens* ha mostrado que la pérdida de LCB insaturados no afecta la viabilidad de la planta, mientras que el bloqueo de la síntesis de GlcCer en plantas gcs-1 provoca defectos graves en su crecimiento y desarrollo (Gömann et al., 2021).

El efecto de estas micotoxinas sobre el contenido de esfingolípidos también puede ayudar a revelar el orden de las reacciones durante el ensamblaje de la Cer; la acumulación de solo d18:0 y t18:0 tras el tratamiento con FB1 o AAL sugiere que la hidroxilación se produce en sustratos LCB y que la desaturación, en la posición Δ4 o Δ8, utiliza sustratos de Cer.

Este modelo también fue respaldado en estudios llevados a cabo con mutantes en *A. thaliana*. Así, en el mutante de hidroxilasa *sbh1 sbh2*, aparece una acumulación

exponencial de LCB libres dihidroxilados y de todos los esfingolípidos que incorporan restos LCB dihidroxilados, así como un agotamiento total de LCB trihidroxilados y esfingolípidos que contienen restos LCB trihidroxilados (Chen et al., 2008). Por el contrario, en el mutante sld1 sld2 que carece de la desaturasa Δ8 (SLD/SΔ8D), las Cers, GlcCers y GIPC con restos LCB t18:0 se acumulan exponencialmente, a expensas de t18:1, mientras que los LCB saturados libres muestran un aumento más modesto (Chen et al., 2012). El análisis global de estos datos proporciona un modelo lógico y consistente para el ensamblaje y modificación de la Cer.

Esfingolípidos en la PCD

La PCD juega un papel esencial en las plantas. Forma parte de su propio desarrollo al promover la diferenciación de células y tejidos, pero también resulta de la activación del sistema de defensa inmune en vegetales (Coll et al., 2011; Huysmans et al., 2017). Trabajos recientes con plantas expuestas a inhibidores de la biosíntesis de esfingolípidos o con aquellas alteradas genéticamente, han revelado que los esfingolípidos son reguladores de la PCD que se produce durante el desarrollo o durante la inmunidad de la planta (Ali et al., 2018; Huby et al., 2020; Zienkiewicz et al., 2020; Groux et al., 2022). Así, los esfingolípidos están implicados en el control de la PCD, ya sea como componentes estructurales de las membranas, o como iniciadores de la ruta reguladora de la muerte celular (Ali et al., 2018). En este sentido, y al igual que ocurre en células animales, se ha propuesto la existencia de un regulador en plantas entre las Cers/LCB y sus formas fosforiladas, que controlaría el destino celular. Según este modelo, las Cers y los LCB pueden desencadenar la muerte celular, mientras que los fosfatos de Cer y los LCB-P promueven la supervivencia celular (Shi et al., 2007; Alden et al., 2011). La inducción de PCD por LCBs se basa en la activación de proteínas quinasas activadas por mitógeno (MPK) como es la MPK6 (Saucedo-García et al., 2011) o proteínas quinasas Ser/Thr dependientes de calcio (CPK) como la CPK3 (Lachaud et al., 2013). Por otra parte, en el mutante acd5, el cual es defectuoso en Cer quinasa y, por tanto, con niveles elevados de Cers, se produce la PCD espontánea, la cual, se debe a una fuerte acumulación en la mitocondria de especies reactivas de oxígeno (ROS) (Bi et al., 2014). Este hallazgo sugiere que las ROS son un componente de la PCD inducida por esfingolípidos. Recientemente, también se ha demostrado que el JA modula el metabolismo de los esfingolípidos y acelera la muerte celular en el mutante acd5 para la ceramida quinasa (Huang et al. 2021). Además, se demostró que el metabolismo de los

esfingolípidos tiene conexiones no solo con las rutas de JA y SA, sino también con la señalización de etileno. En este senetido, el etileno o su precursor (ácido 1-aminociclopropano carboxílico) inhiben la biosíntesis de esfingolípidos de tal manera que los mutantes de la biosíntesis o señalización de etileno mostraron modificaciones constitutivas en el contenido de esfingolípidos (Wu et al., 2015b). Por ejemplo, los mutantes CONSTITUTIVE TRIPLE RESPONSE*1-1 (ctr1-1)*, que tienen una señalización de etileno inducida, contenían niveles más bajos de Cers y hCers en comparación con el fenotipo silvestre. Además, algunos mutantes de respuesta constitutiva a etileno mostraron una mayor tolerancia a la micotoxina FB1, mientras que los mutantes deficientes en la señalización de etileno presentaron más sensibilidad a FB1, lo que demuestra que la señalización inducida de etileno rescata de la muerte celular provocada por FB1 (Wu et al., 2015b; Huby et al., 2020).

Esfingolípidos como componentes estructurales y mensajeros de señalización en respuestas a estrés abióticos.

Como componente principal de las membranas plasmáticas, los esfingolípidos juegan un papel importante reduciendo los efectos del estrés abiótico, con respuestas tanto a nivel de la propia remodelación de la membrana plasmática como participando en la transducción de señales (Ali et al., 2018). En particular, son numerosos los estudios que demuestran un papel para los esfingolípidos en la respuesta al estrés por bajas temperaturas. En este sentido, la capacidad de aclimatación en plantas sometidas a estrés por frío se ha correlacionado con cambios en el contenido de TAG (triacilgliceroles), MGDG (monogalactosildiacilglicerol), DGDG (digalactosildiacilglicerol) y GlcCer (Degenkolbe et al., 2012). A su vez el análisis de los perfiles de lípidos en plantas de avena, centeno y Arabidopsis durante la aclimatación al frío, demostraron que el contenido de GlcCer disminuye en la membrana plasmática, mientras que sus niveles no cambiaron en los microdominios (Minami et al., 2009; Takahashi et al., 2016). Estos cambios podrían contribuir a una mayor hidratación de la membrana plasmática que podría, a su vez, aumentar la estabilidad de la membrana durante el estrés por frío.

En la misma línea, en un estudio llevado a cabo en hojas de vid, se observó una correlación entre niveles elevados de t18:1 (8Z) en los esfingolípidos complejos y la tolerancia a la congelación (Kawaguchi et al., 2000). Asimismo, también se ha observado que la SLD, que desatura el LCB en la posición Δ8 para ambas orientaciones cis y trans,

parecen desempeñar un papel en la tolerancia al frío en Arabidopsis (Chen et al., 2012) y tomate (Zhou et al., 2016). Además, también se ha descrito que, en respuesta al enfriamiento, las plantas de Arabidopsis incrementan el contenido de GIPC y disminuyen el de GlcCers (Nagano et al., 2014). Asimismo, la insaturación de los esfingolípidos puede estar implicada en la fluidez de la membrana y el mantenimiento de la función H+-ATPasa en la membrana plasmática (Chen et al., 2012).

Esfingolípidos como componentes estructurales y de señalización en respuestas a estrés biótico

La respuesta inmunitaria innata depende de la capacidad de la planta para reconocer a su invasor y luego traducir los diferentes estímulos a una respuesta adaptativa. Como componentes estructurales de la membrana plasmática, los esfingolípidos son moléculas importantes en la primera línea de reconocimiento de patógenos. La disrupción de los esfingolípidos también tiene un impacto sobre la PCD y la acumulación de diferentes moléculas que participan en la defensa de plantas (ROS, MAPK y/o hormonas), además de los propios esfingolípidos, que, por lo tanto, pueden actuar como mediadores en la cascada de señalización de defensa. En Arabidopsis, el análisis de su perfil metabolómico permitió identificar cambios en el contenido de esfingolípidos después de la exposición a estrés biótico. Asimismo, también se observó que la infección de *Brassica oleracea* por *Xantomonas campestris* pv. campestris desencadenó cambios dinámicos en el metabolismo de los esfingolípidos, incluida una reducción en los niveles de la ceramida N-palmitoilesfinganina (Tortosa et al., 2018).

Además, varios estudios han descrito que los mutantes de Arabidopsis con contenido anormal de esfingolípidos muestran una elevación constitutiva del contenido de SA y una mayor resistencia a los patógenos, lo que sugiere un papel de los esfingolípidos como moduladores moleculares de la defensa de las plantas (Berkey et al., 2012; Magnin-Robert et al., 2015; Zienkiewicz et al., 2020). Asimismo, en plantas de arroz se ha demostrado que los 2-hidroxi-esfingolípidos son fundamentales en la formación de microdominios y que la falta de la actividad de OsFAH1/2 altera la organización de proteínas de defensa localizadas en los mismos, como la NADPHoxidasa RbohB, requerida para la producción de ROS, el cual está implicado en la inmunidad del arroz (Nagano et al., 2016). Estos estudios sugirieron que el estrés biótico podría afectar al metabolismo de los esfingolípidos.

En Arabidopis, los mutantes de los genes GONST1, IPUT1 y GMT1 (Mortimer et al., 2013; Fang et al., 2016; Tartaglio et al., 2017) que están implicados en la glicosilación de GIPC, presentan niveles altos de SA y ROS durante la respuesta hipersensible, así como la inducción de genes de defensa, lo que sugiere una respuesta esencial al estrés por parte de estos esfingolípidos. Curiosamente, *gmt1* también presentó una disminución del contenido de celulosa acompañada de un aumento en los niveles de lignina, un proceso bien conocido en la resistencia a enfermedades. En su conjunto estos estudios demuestran que la glicosilación de GIPC y la identidad del grupo principal de glicanos son importantes para la respuesta inmune de las plantas.

Interacción de esfingolípidos con el metabolismo de los fosfolípidos

Al igual que los esfingolípidos, el ácido fosfatídico también se considera un mensajero lipídico implicado en la respuesta de la planta tanto a estreses bióticos como abióticos. Así, en Arabidopsis se ha observado que el ácido fosfatídico interactúa con la MPK6 durante la respuesta al estrés salino (Yu et al., 2010) y con la NADPH oxidasa para modular la producción de ROS durante la regulación del cierre estomático inducido por ABA (Zhang et al., 2009). Se ha demostrado también que la ruta biosintética del ácido fosfatídico es sensible a la temperatura y al estrés salino e interactúa con SPHK (Guo et al., 2011). A su vez la aplicación de ácido fosfatídico exógena induce la síntesis de LCB-P, mientras que los niveles de LCB-P aparecendisminuidos en pldα1 (gen codificante de PLD en Arabidopsis) en respuesta al ABA (Guo et al., 2012), y que la sobreexpresión de la SPHK aumenta la acumulación de ácido fosfatídico. Por lo tanto, la relación entre ácido fosfatídico y esfingolípidos puede ser un punto crítico para coordinar la respuesta celular y de la planta frente a situaciones de estrés (Guo & Wang, 2012; Ng & Coursol, 2012).

Interacción de esfingolípidos con las rutas de señalización hormonales

El contenido de LCB-P regulado por LCBK y fosfatasas juega un papel clave en la ruta de señalización del ABA en plantas. Un trabajo pionero sobre esfingolípidos ha puesto de manifiesto que d18: 1-P y t18: 0-P eran rápidamente inducidos por la sequía y estaban implicados en la ruta de señalización de ABA para controlar la turgencia de las células protectoras y, por lo tanto, la apertura estomática (Ng et al., 2001; Coursol et al., 2003, 2005). Esta ruta de señalización de los esfingolípidos implicó la movilización de Ca^{2+}, la modificación de la actividad del canal iónico y la proteína G heterotrimérica. De acuerdo

con ello, la AtLCBK1 podría ser inducida por condiciones de baja humedad o tratamientos con ABA (Imai & Nishiura, 2005). Es más, el ABA también induce la acumulación de varios LCB-P (Guo et al., 2012). SPHK1 es una enzima que fosforila d18:1 y t18:0. En este sentido, los estomas del mutante Atspp1 y de SPHK1-OE (que acumula d18:1-P) mostraron una mayor sensibilidad a ABA que el fenotipo solvestre (Worrall et al., 2008; Nakagawa et al., 2012).

Asimismo, a partir de los datos genéticos y bioquímicos disponibles se ha sugerido que el metabolismo de los esfingolípidos tiene conexiones no solo con las rutas de señalización del ABA, sino también con la señalización del SA, JA y etileno. Así, varios mutantes que muestran un metabolismo alterado para los esfingolípidos presentaron también un mayor contenido de SA y la activación de las respuestas dependientes de SA. Por el contrario, tanto la aplicación de SA como de su análogo benzotiadiazol afectaron al metabolismo de los esfingolípidos (Shi et al., 2015). En estudios llevados a cabo con el mutante de Arabidopsis fah1/2 se observó una acumulación de SA además de un aumento de Cers, aunque los cambios en la acumulación de LCB fueron moderados (König et al., 2012). Ello sugiere que los niveles elevados de Cers conducen a un aumento en el contenido de SA. Por el contrario, el mutante loh1 de Arabidopsis presenta una acumulación de Cers C16, aunque sin cambios en los niveles de SA (Ternes et al., 2011). Por tanto, la inducción de SA podría deberse a alteraciones en las distintas clases de esfingolípidos de LCB o ceramidas.

Varios estudios han revelado que además de la activación de la ruta de SA por esfingolípidos, aquellas plantas en las que se bloquea la biosíntesis de esfingolípidos también tienen afectada su capacidad para tolerar a patógenos biotróficos. Además, mientras que el SA se considera esencial para la resistencia a biotróficos y patógenos hemibiotróficos, también se ha demostrado en Arabidopsis que las rutas de señalización de JA y etileno igualmente son importantes para la resistencia a patógenos necrotróficos (Thomma et al., 2001; Glazebrook, 2005). En Arabidopsis, también se reconoce que el SA tiene un efecto antagónico de forma recíproca en la señalización de JA (Glazebrook, 2005). Usando plantas orm1 amiR-ORM2, el equipo de Li et al. (2016) han demostrado que la pérdida de la función ORM desencadenó una inducción constitutiva del gen dependiente de SA y una tolerancia a *Pseudomonas syringae* cepa DG3 en comparación con las plantas *silvestres*. Los mutantes acd5, erh1 (mejora de la muerte celular similar a HR mediada por RPW8) y fah1/2 también han mostrado una activación constitutiva de

la ruta de SA y una mayor resistencia al oídio, aunque mostraron un fenotipo similar a las plantas silvestres después de la infección con los patógenos P. syringae pv. maculicola o *Verticillium longisporum* (Wang et al., 2008; König et al., 2012). Del mismo modo, en tabaco la sobreexpresión de OsSPL1 redujo drásticamente el gen de expresión dependiente de SA y aumentó la susceptibilidad a *P. syringae* pv. tabaco.

Sin embargo, hasta la fecha, pocos estudios han analizado el papel de los esfingolípidos durante la interacción planta con patógenos necrotróficos. En plantas de tabaco donde la SPT fue silenciada se acumuló SA, provocando una expresión constitutiva de genes inducidos por SA y mostrando una mayor susceptibilidad al hongo *Alternaria alternata* f. sp. lycopersici (Rivas-San Vicente et al., 2013). De manera similar, la acumulación de SA acd5 mostró un aumento de la susceptibilidad a *B. cinerea* (Bi et al., 2014).

Otros estudios han demostrado también una relación entre los esfingolípidos y la ruta del JA. Así, el mutante Atdpl1 de tomate mostró sensibilidad hacia la bacteria *Pseudomonas syringae* pv. tomate, y tolerancia cuando es infectado por el hongo *Botrytis cinérea* (Magnin-Robert et al., 2015). Sin embargo, los niveles de SA fueron similares o incluso menores en comparación con la planta silvestre, mientras que los niveles de JA y la expresión génica dependiente de JA fueron mayores en el mutante Atdpl1 infectado. Esta situación sugiere una relación entre los esfingolípidos y la ruta del JA. Mediante el uso de plantas que sobreexpresan SPHK1, la producción de SA aumentó en respuesta al tratamiento con FB1. Por el contrario, las plantas SPHK1-KD mostraron un aumento en las transcripciones y los metabolitos relacionados con JA (Qin et al., 2017). Por lo tanto, se sugirió que el equilibrio entre LCBs y LCB-Ps modulados por la actividad de SPHK1 actúa como una señal para las rutas de señalización SA/JA durante la muerte celular inducida por FB1 (Qin et al., 2017).

Por último, Da Silva et al. (2011) demostraron que los tratamientos exógenos con LCB inducen la formación del óxido nítrico (NO) en células de tabaco. Por el contrario el NO regula aspectos específicos del metabolismo de esfingolípidos en las plantas (Guillas et al., 2013). En particular, el NO participa en el equilibrio entre la LCB/Cer y LCB-P/Cer-P (Cantrel et al, 2011; Dutilleul et al, 2012). En este contexto, el NO funciona como un regulador negativo de la formación del fosfoesfingolípidos (Cantrel et al., 2011), aunque se desconoce su mecanismo de regulación.

1.2. El proceso de abscisión

La abscisión es un proceso de separación celular activo, organizado, altamente coordinado y esencial para el desarrollo vegetativo y reproductivo (Addicott, 1982; Sexton & Roberts, 1982; Leslie et al., 2007; Roberts & Gonzalez-Carranza, 2007; Estornell et al., 2013; Tucker & Kim., 2015; Patterson et al., 2016; Patharkar & Walker, 2018, 2019; Kim et al., 2019; Tranbarger & Tadeo, 2020; Liu et al., 2022).

La activación del proceso de abscisión permite el desprendimiento de órganos vegetativos y reproductivos completos, mediante la modificación de la adhesión celular y la desintegración de las paredes celulares en lugares específicos del cuerpo de la planta, conocidos como zonas de abscisión (AZs). Los primeros estudios sobre el proceso de abscisión se centraron en la caracterización anatómica y fisiológica de la AZ (Addicott, 1982; Sexton & Roberts, 1982). Estos estudios han demostrado que la AZ consiste en pocas o múltiples capas de células queson frecuentemente más pequeñas que las otras células que no se separan, presentando además un citoplasma más denso. Durante el proceso de abscisión, es en esta AZ donde se lleva a cabo la disolución de la pared celular entre las células adyacentes para permitir la separación del órgano (Addicot, 1982; Leslie et al., 2007; Niederhuth et al., 2013a; Kim, 2014; Roongsattham et al., 2016; Merelo et al., 2017; Meir et al., 2019). Las primeras investigaciones también se centraron en dilucidar el papel de las enzimas que degradan y modifican la pared celular, incluyendo las poligalacturonasas y las celulasas (Meir et al., 2019).

Durante años, la investigación del proceso de abscisión en plantas utilizadas como modelos (arroz, maíz, Arabidopsis y tomate), han proporcionado información genética muy valiosa y han servido para comprender este proceso tanto a nivel genético como molecular (Kim et al., 2015, 2019; Patterson et al., 2016; Patharkar & Walker, 2018, 2019; Meir et al., 2019; Tranbarger & Tadeo, 2020). Sin embargo, el conocimiento de estos mecanismos moleculares en especies no modelo aún es limitado. Algunos elementos parecen ser comunes a muchos procesos de abscisión, incluyendo el transporte basipétalo de auxinas, la biosíntesis y la percepción de etileno, la actividad de las especies reactivas del oxígeno (ROS), la acción de otras hormonas, la participación del péptido INFLORESCENCE DEFICIENT IN ABSCISSION (IDA) y los receptores quinasas HAESA (HAE) y HAE-like 2 (HSL2) que conforman el módulo señalizador de la abscisión IDA-HAE-HSL2, el cual fue inicalmente definido en Arabidopsis (Patharkar

& Walker, 2018; Shi et al., 2019). No obstante, tanto en monocotiledóneas como en dicotiledóneas existen diferencias en la posición y estructura de las AZ y en las rutas genéticas que controlan el proceso de abscisión, (Addicott, 1982; Estornell et al., 2013; Kim et al. 2019; Yu et al., 2020). Además, la separación celular puede implicar no solamente diferencias a nivel enzimático entre las distintas especies, sino también en aspectos como la expansión celular, PCD, lignificación y fuerzas mecánicas, entre otras (Addicott, 1982; Patterson, 2001; Estornell et al., 2013; Kim et al., 2019).

La investigación del proceso de abscisión, en las últimas décadas, se ha centrado principalmente en Arabidopsis y tomate como plantas modelo, la cual ha aportado una significativa comprensión de la acción coordinada de diferentes componentes de señalización sobre la abscisión de órganos (Meir et al., 2019). En particular, Arabidopsis ha servido como el sistema modelo para estudiar la abscisión floral en dicotiledóneas (Roberts et al., 2000, 2002; Aalen et al., 2013; Binder & Patterson, 2009; Van Nocker, 2009; Liljegren, 2012; Estornell et al., 2013; Niederhuth et al., 2013a; Patterson et al., 2016, Patharkar & Walker, 2019). En base a estos trabajos, la fisiología de la abscisión ha sido dividida en cuatro etapas principales (Patterson, 2001; Roberts et al., 2002; Kim, 2014; Patharkar & Walker, 2018) (Figura 1.3):

- En la primera etapa se diferencia la AZ que es una zona anatómicamente discreta que se diferencia habitualmente entre la planta y la frontera con el órgano que se acabará separando y es a través de este tejido diferenciado donde tendrá lugar la abscisión.
- En la segunda etapa, esta AZ adquiere la competencia para poder responder a estímulos inductores de la abscisión.
- La tercera etapa, consiste en el proceso de activación que es ejecutado principalmente por enzimas remodeladoras de la pared celular y que tiene como consecuencia la separación del órgano.
- En la cuarta y última etapa, tiene lugar la transdiferenciación de la parte proximal de la AZ para formar una capa protectora que está compuesta principalmente de ceras, suberina y lignina. Esta capa cumple la función de proteger de pérdidas de agua, de la entrada de patógenos y, además, ejerce una fuerza mecánica en el plano de fractura que ayuda a la separación celular (Lashbrook & Cai, 2008; Ogawa et al., 2009; Kim et al., 2015; Lee et al., 2018).

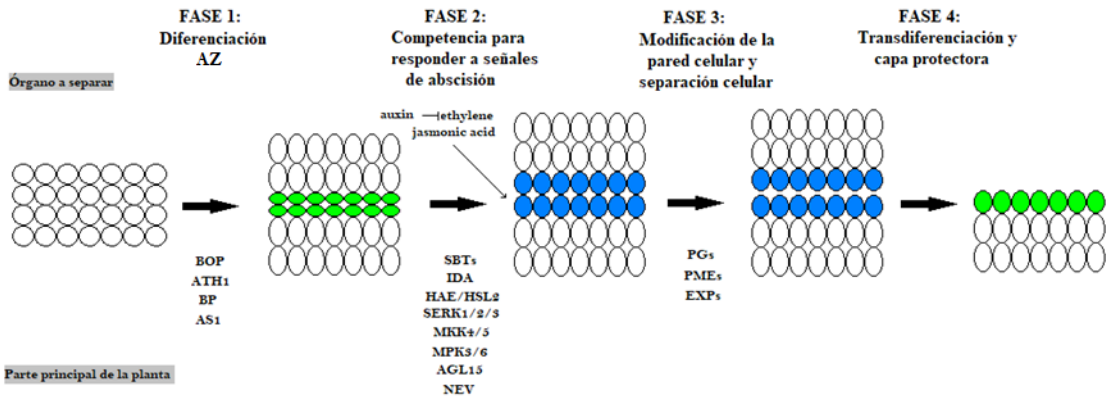

Figura 1.3. Modelo fisiológico de la abscisión. En la fase 1, se desarrollan zonas de abscisión. Se requieren BOP1/2, ATH1, BP y AS1 para el desarrollo de la zona de abscisión. En la fase 2, se activa el circuito de señalización de abscisión y se requieren todas las proteínas indicadas. Las hormonas etileno y ácido jasmónico regulan positivamente la abscisión, mientras que la auxina la regula negativamente al reducir el efecto del etileno. En este paso, las células de la zona de abscisión comienzan a agrandarse y el pH de su citosol se vuelve alcalino. En la fase 3, las poligalacturonasas (PG), las pectinametiltransferasas (PME) y las expansinas (EXP) provocan la separación celular. Estas mismas enzimas, particularmente las expansinas, probablemente estén involucradas en la expansión celular que ocurre antes de la separación celular. Finalmente, en la fase 4, la cicatriz de la zona de abscisión se sella con una capa protectora y el pH de las células de la zona de abscisión vuelve a ser neutro. Las células de la zona de abscisión se representan en color, donde el verde representa el pH citosólico neutro y el azul representa el pH alcalino. Adaptación de figura de Patharkar & Walker (2018).

Varios trabajos utilizando como modelo de estudio el tomate y Arabidopsis, han puesto de manifiesto la existencia de numerosos genes involucrados en la diferenciación y el desarrollo de la AZ (Mao et al., 2000; Pinyopich et al., 2003; Budiman et al., 2004; McKim et al., 2008; Nakano et al., 2012; Wu et al., 2012; Couzigou et al., 2016; Roldan et al., 2017; Meir et al., 2019). Entre ellos se encuentra el factor de transcripción MADS-box, habiéndose demostrado que uno de los miembros de la familia MADS-box, *jointless*, está implicado a nivel funcional en el desarrollo de la AZ, ya que las plantas de tomate con la mutación *jointless* no desarrollan AZ en sus pedicelos y, por tanto, la abscisión de flores o frutos no se produce con normalidad (Mao et al., 2000). Asimismo, también se ha caracterizado otro MADS-box, *MBP21*, que muestra una función similar en la formación de la ZA; en este caso, la pérdida de función de *MBP21* condujo a un *jointless -2* en tomate (Budiman et al., 2004; Roldan et al., 2017). Por último, *Macrocalyx* (*MC*) también es un miembro de la familia MADS-box que se ha confirmado que juega un papel clave en el desarrollo del pedicelo de la AZ en tomate (Nakano et al., 2012).

La formación de la AZ y la propia abscisión de órganos es un proceso oxidativo en la que se ha demostrado la participación de ROS en muchas especies de plantas (Yang et al., 2015; Sakamoto et al., 2008; Liao et al., 2016). En este sentido, el peróxido de hidrógeno (H_2O_2) actúa induciendo la expresión de enzimas que degradan la pared celular durante la fase de ejecución de la abscisión (Sakamoto et al., 2008). A su vez la gran cantidad de ROS producidas en la AZ pueden ser responsables de efectos patológicos en diferentes compartimentos subcelulares, los cuales pueden dañar las bicapas lipídicas debido a su contribución a la degradación de los ácidos grasos liberados de las membranas celulares (Droillard et al., 1989; Mittler et al., 2002).

En Arabidopsis, la abscisión de órganos florales y hojas caulinares está regulada por la interacción entre el péptido IDA, un par de proteínas quinasas de tipo receptor redundantes, HAE y HSL2 y de correceptores de la familia SOMATIC EMBRYOGENESIS RECEPTOR-LIKE KINASE (SERK) (Patharkar & Walker, 2018, 2019; Shi et al., 2019). Los péptidos IDA-like, como elementos de comunicación entre células, parecen estar involucrados además en otros procesos de separación celular como es el caso de la emergencia de raíces laterales a partir de la raíz principal (Kumpf et al., 2013; Liu et al., 2018), el desprendimiento de la caliptra de la raíz (Shi et al., 2018), o incluso en las respuestas a estreses bióticos y abióticos (Vie et al., 2017). Distintos miembros de la familia IDA también se han caracterizado en otras especies de plantas (Tucker & Yang, 2012; Estornell et al., 2015; Ying et al., 2016; Wilmowicz et al., 2018; Tranbarger et al., 2019; Rai et al., 2021; Ventimilla et al., 2021), habiéndose demostrado que algunos de ellos presentan una expresión inducida en las AZs en tomate (*SlIDA1*; Tucker & Yang, 2012), soja (*GmIDA2a*; Tucker & Yang, 2012), cítricos (*CitIDA3*; Estornell et al., 2015), palma aceitera (*EglIDA5*; Stø et al., 2015), litchi (*LcIDL1*; Ying et al., 2016) o lupino amarillo (*LlIDA*; Wilmowicz et al., 2018), lo que sugiere que podrían conservar la función de *IDA* en la regulación de la separación celular durante la abscisión. Asimismo, se ha demostrado que los péptidos sintéticos IDA son también capaces de inducir la abscisión temprana de órganos florales en flores de Arabidopsis (Stenvik et al., 2008), así como la abscisión de flores, frutos maduros y hojas en el lupino amarillo, la palma aceitera y el álamo, respectivamente (Wilmowicz et al., 2018; Tranbarger et al., 2019).

El papel de IDA está regulado por las dos proteínas quinasas similares a receptores redundantes HAE HSL2 y los co-receptores SERK (Patharkar & Walker, 2018; Shi et

al., 2019). Así, una vez que se forma un complejo estable entre el péptido IDA y los heterodímeros tipo HAE/SERK, los dominios quinasa se transfosforilan entre sí y transmiten la señal a una cascada de proteína quinasa activada por MAPK (Meng et al., 2016; Santiago et al., 2016). Se determinó que la cascada MAPK inhibe la actividad del factor de transcripción KNOX, BP/ KNAT1, el cual a su vez desbloquea otros genes KNOX (*KNAT2* y *KNAT6*) para inducir la expresión de un conjunto de enzimas que remodelan la pared celular y modifican las proteínas que permiten la abscisión de los órganos florales (Shi et al.,2011; Butenko et al., 2012). Por otra parte, los genes *IDL6* e *IDL7* son inducidos rápidamente por varios tipos de estrés, sugiriendo que son moduladores negativos de la señalización de ROS inducida por el estrés (Vie et al., 2015; 2017).

Recientemente, mediante la caracterización transcripcional de la AZ del doble mutante hae hsl2 deficiente en abscisión se identificó un nuevo regulador negativo de la señalización de abscisión, MAP KINASE PHOSPHATASE-1/MKP1. La mutación de MKP1 suprime parcialmente el defecto de abscisión del mutante hae hsl2 y se estableció que las bases moleculares de la supresión reactivan de la ruta HAE/HSL2 (Taylor et al., 2022).

ATH1 (*Arabidopsis thaliana* homeobox 1 gene) actúa en conjunto con dos genes KNAT (KNOTTED-like from Arabidopsis thaliana), KNAT6 y KNAT2 para modelar la AZ y facilitar la separación celular. Las actividades de ATH1 e IDA convergen para promover la expresión *KNAT2* **y** *KNAT6* en la AZ (Shi et al., 2011; Khan et al., 2015; Crick et al., 2022). Por el contrario, la expresión *ATH1***,** *BOP1*(blade-on-petiole**) y** *BOP2* en las células de la AZ es independiente de *IDA* (McKim et al., 2008). Sin embargo, se ha mostrado que la sobreexpresión de *BOP1* y *BOP2* durante la separación celular restaura la abscisión en el mutante *IDA* (Crick et al., 2022). Asimismo, a pérdida de función de *BOP1* y *BOP2* provocó la no diferenciación de las AZs florales y foliares, lo que sugiere que las proteínas BOP son esenciales para el establecimiento de las células de la AZ (McKim et al., 2008; Wu et al., 2012; Couzigou et al., 2016) y, por consiguiente, los genes *BOP1* y *BOP2* desempeñan un papel esencial en la formación de la AZ en Arabidopsis.

Por otra parte, también se ha demostrado que *NEVERSHED* (NEV) codifica una proteína activadora de factor de ribosilación de ADP-GTPasa (ARF-GAP) y reguladora

del movimiento de las moléculas que abandonan la red trans-Golgi y/o el ciclo entre la superficie celular y los endosomas (Liljegren et al., 2009; Leslie et al., 2010). Las mutaciones en *NEV* dan como resultado defectos durante el tráfico de membrana e inhibición de la abscisión (Liljegren et al., 2009). Así, mientras que los mutantes *nev* muestran una expansión celular descontrolada al final de la abscisión, la morfología de las células de la AZ al inicio de la abscisión es similar a la de los mutantes *ida* y parece ser normal (Liu et al., 2013). Además de los defectos de abscisión, la organización de la red de Golgi de *nev* se restablece con *EVERSHED (evr)*, *serk1* y *CAST AWAY (cst)*, concluyendo que estos supresores actúan a través de NEV para inhibir espacialmente la separación de órganos (Leslie et al., 2010; Lewis et al., 2010). En particular, las mutaciones en estas 3 quinasas similares a receptores no restauraron el fenotipo en los mutantes *ida* o *hae hsl2* (Leslie et al., 2010; Lewis et al., 2010). Además, mientras que los defectos de abscisión y de la red de Golgi en los mutantes *nev* son restaurados por estos supresores, la expansión celular ectópica de *nev* durante la abscisión tardía no se vio afectada en los mutantes dobles (*nev-3 evr*, nev *-3 serk1*, nev *-3 cst*) ni en los mutantes triples (*nev-3 serk1 ida-2* y *nev-3 ever-2 ida-2*) (Leslie et al., 2010; Lewis et al., 2010). Estos resultados indican que la ruta de señalización de NEV es crucial para la separación celular (etapa 3 del proceso de abscisión) y para la expansión celular (etapa 4 del proceso de abscisión), pudiendo funcionar en paralelo con la ruta de señalización de IDA.

En los últimos años, la combinación de los estudios fisiológicos, genéticos y genómicos han demostrado la implicación de múltiples rutas y procesos coordinados en el proceso de la abscisión (González-Carranza & Roberts, 2012; Estornell et al., 2013; Niederhuth et al., 2013a; Patterson et al., 2016; Patharkar & Walker, 2018, 2019; Kim et al., 2019; Meir et al., 2019, Tranbarger & Tadeo, 2020). En este sentido, se ha demostrado la implicación de la señalización hormonal por parte de etileno, auxina, ABA, y JA (Ogawa et al. 2009), así como la ruta de HAE y HSL2, el tráfico transmembrana y otras respuestas posteriores reguladas por estas señales (Niederhuth et al., 2013a; Patharkar & Walker, 2018, 2019; Kim et al., 2019). Sin embargo, para esclarecer la red que integra estas distintas rutas y procesos se ha requerido de estudios de genómica, como los microarrays y estudios de RNA-seq utilizados principalmente en Arabidopsis (Cai & Lashbrook, 2008; Lashbrook & Cai, 2008; Niederhuth et al., 2013a; Patterson et al., 2016). En otras especies distintas de Arabidopsis, también se han aplicado enfoques

genómicos funcionales para profundizar en el conocimiento de la abscisión. En este sentido, se han utilizado los microarrays o RNA-seq para estudiar los cambios de expresión génica durante la abscisión inducida por etileno en cítricos (Agustí et al., 2009), manzana (Botton et al., 2011; Zhu et al., 2011) y tomate (Meir et al., 2010; Nakano et al., 2013). Estos estudios han revelado cambios entre las distintas especies ensayadas a nivel de las enzimas que modifican la pared celular, así como en la interacción hormonal y frente a factores como el estrés nutricional durante la abscisión. Enfoques basados en la secuenciación del transcriptoma también se han utilizado para analizar la abscisión que puede ser desencadenada por señales del desarrollo como la fertilización o la maduración del fruto (Zhou et al., 2008; Gil-Amado & Gomez-Jimenez, 2013; Corbacho et al., 2013; Goldental-Cohen et al., 2017).

1.2.1. El proceso de abscisión en la agricultura

El conocimiento de los mecanismos implicados en la abscisión del fruto es esencial para desarrollar estrategias de control y mejora de la recolección de la cosecha o la pérdida no deseada de frutos. Hace decenas de miles de años, los primeros agricultores comenzaron a seleccionar cambios en el hábito del crecimiento y del desarrollo de cientos de especies de plantas silvestres para lograr cultivos domesticados con mejores características agronómicas en las que se basa actualmente la agricultura. En comparación con sus progenitores silvestres, los cultivos domesticados producen menos frutos y semillas, pero más grandes, que se convierten en plantas más robustas con una mayor dominancia apical (Doebley et al., 2006). Además, los cultivos domesticados han perdido en gran medida la disposición natural de las especies de plantas silvestres para desprender frutos maduros y dispersar semillas. El hábito de crecimiento vertical y la mayor capacidad de los cultivos domésticos para retener semillas y frutos maduros tiene ventajas agronómicas, como cosechas más fáciles y rápidas y, al mismo tiempo, el rendimiento económico de los cultivos se maximiza porque las pérdidas se reducen. Así, la pérdida de los mecanismos que permiten el desprendimiento de frutos, la dehiscencia de las vainas y la dispersión de semillas puede considerarse imperativa para la domesticación de especies silvestres y necesaria para su cultivo eficiente (Tranbarger & Tadeo, 2020).

El conocimiento sobre la maquinaria molecular que regula la abscisión en especies de plantas de importancia económica es en la actualidad escaso. La abscisión del fruto

carnoso ocurre a través de la activación de las AZs (Figura 1.4), que se encuentran localizadas en diferentes ubicaciones dentro de la estructura de la planta y que son activas en diferentes etapas del desarrollo del fruto, y cuya función depende de contextos fisiológicos y ambientales específicos (Tranbarger & Tadeo, 2020). El tomate ha sido un cultivo modelo para estudiar la abscisión de flores (Abeles et al., 1992; Mao et al., 2000). La fisiología de la abscisión floral del tomate se estudió hace mucho tiempo (Roberts et al., 2000; Sexton & Roberts, 1982), pero los mecanismos moleculares que subyacen al proceso de abscisión en esta planta han sido dilucidados recientemente (Liu et al., 2014; Meir et al., 2010, 2011, 2019; Nakano et al., 2012, 2013, 2014; Wang et al., 2013). Como se mencionó en el apartado anterior, la abscisión de los órganos florales en Arabidopsis está regulada por una hormona peptídica IDA que es liberada de su precursor por una red de subtilasas redundantes. Un reciente trabajo, en tomate, ha descrito cómo la abscisión floral inducida por la sequía está regulada de manera similar, aunque por una ruta distinta, que libera una hormona peptídica, fitosulfocina, PSK (Reichardt et al., 2020), la cual era anteriormente conocida por promover el crecimiento. La formación de PSK en respuesta al estrés por sequía depende de la fitaspasa 2, una proteasa similar a la subtilisina del subtipo de la fitaspasa que genera la hormona peptídica a partir del aspartato, como precursor de PSK en el pedicelo de la flor del tomate. La PSK impulsa la abscisión por inducción de hidrolasas de la pared celular en la AZ floral del tomate. Aunque diferentes estudios han localizado la PSK tanto en monocotiledóneas como en dicotiledóneas, las fitaspasas, y el subtipo de subtilasas que incluye las fitaspasa 2, presentan una distribución menor. En este sentido se ha localizado una fitaspasa en la familia de las solanáceas (incluido el tomate y la patata) y en algunas otras familias de dicotiledoneas (Ranunculaceae, Fabaceae, Lamiaceae y Phrymaceae) pero está ausente de otras familias (por ejemplo, Brassicaceae) (Taylor & Qiu, 2017; Reichardt et al., 2018; Xu et al., 2019). Por tanto, no se conoce todavía si la regulación de la abscisión mediada por PSK solamente se limita a linajes portadores de fitaspasa o si puede estar más ampliamente distribuida en plantas con flores (Schuster & van der Hoorn, 2020; Stintzi & Schaller, 2022).

En monocotiledoneas, a diferencia de las dicotiledóneas, el análisis GWAS (Genome-Wide Association Studies) que compara los transcriptomas de la AZ de inflorescencias de 3 gramíneas como el arroz, el mijo verde (*Setaria viridis*) y *B. distachyon* reveló módulos genéticos específicos de la AZ que en gran medida eran distintos (Yu et al., 2020). De hecho, aunque los genes conocidos de la AZ del arroz estaban en redes de

coexpresión similares para las tres especies, estas redes se implementaron en gran parte fuera de las AZs del mijo verde y *B. distachyon*. Las excepciones se limitaron a tres genes, *YAB2*, *qSH1* y *MYB26*, con alta expresión en la AZ entre las especies, correspondientes a la rama de la flor en el arroz y *B. Distachyon*, y la rama de la espiguilla (pedicelo) en el mijo verde. Por lo tanto, aparentemente y a diferencia de otros rasgos reproductivos importantes que evolucionaron de forma independiente, como los nectarios y la simetría floral bilateral (cigomorfia), las AZ de las gramíneas han surgido a través de la redistribución de mecanismos convergentes en lugar de conservados. Sin embargo, la viabilidad de los estudios comparativos basados en NGS (secuenciación de nueva generación) en una variedad de especies no modelo, combinados con una mayor resolución en todos los enfoques de fenotipado y disección de tejidos, permitirá conocer la mecánica de la evolución de los diferentes rasgos a escala del genoma, incluso para los taxones de plantas más desconocidos.

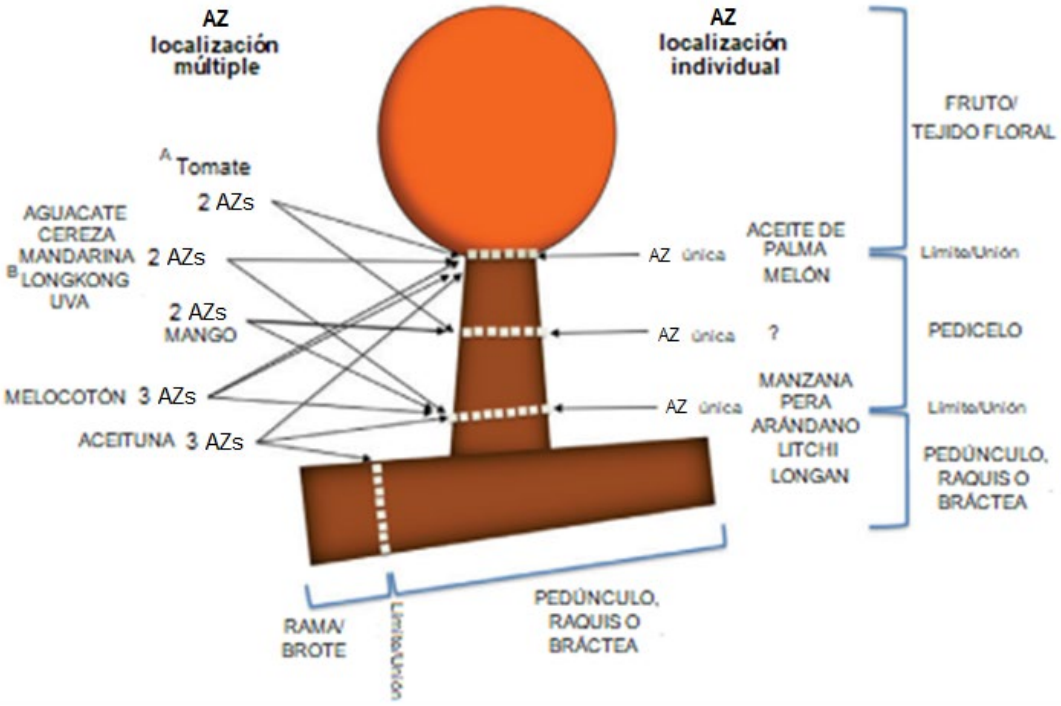

Figura 1.4. Representación esquemática de las diferentes ubicaciones de las AZs de la fruta. La abscisión del fruto se da gracias a la función de la AZ que ocurre en diferentes lugares. **(A)** La AZ del tomate entre la fruta y pedicelo no ha sido confirmada por lo que puede ser una "zona de separación", no una verdadera AZ. **(B)** Longkong no tiene pedicelo, es una fruta sésil, por lo que SZ1 de longkong está en una ubicación similar a AZ-A de cítricos, mientras que SZ2 es similar a AZ-C. Sin embargo, un estudio reciente concluyó que SZ2 no es un verdadero AZ (Taesakul et al., 2018). Figura adaptada de Tranbarger & Tadeo (2020).

Recientemente, con la edición del genoma CRISPR – Cas9, se ha validado al gen *Less Shattering1* (SvLes1) de mijo (*Setaria viridis)*, como un gen cuyo producto controla la rotura de semillas (Mamidi et al., 2020). En *S. italica*, este gen se volvió no funcional por una inserción de retrotransposón en el alelo domesticado de pérdida de rotura SiLes1-TE (elemento transponible) (Mamidi et al., 2020). Es posible que el alelo SiLes1-TE sea un alelo de baja frecuencia que se seleccionó hace aproximadamente 8.000 años durante la domesticación de plantas debido a su fenotipo de baja rotura de semillas y se extendió rápidamente a través del mijo. Más tarde, el fenotipo de baja rotura fue más fortalecido por loci adicionales con efectos positivos durante la reciente mejora de cultivos (Jia et al., 2013; Odonkor et al., 2018). En este sentido, el alelo diseñado SvLes1-CRISPR1 permite recrear un fenotipo de baja rotura de alelos ancestrales de *S. viridis*, imitando la fase inicial de domesticación del mijo (Mamidi et al., 2020).

1.2.2. Control hormonal del proceso de abscisión.

En general, existe evidencia de la interacción entre las hormonas vegetales en la regulación del proceso de abscisión, donde etileno, ABA, JA y citoquininas inducen el proceso, mientras que otras hormonas como auxina, giberelinas, poliaminas y brasinosteroides lo inhiben (Estornell et al., 2013; Tucker & Kim, 2015; Botton & Ruperti, 2019; Meir et al., 2019). El etileno activa la expresión de genes que codifican las enzimas remodeladoras de la pared celular y su secreción a las paredes celulares (Addicott, 1982; Sexton & Roberts, 1982; del Campillo & Bennett, 1996; Lashbrook & Cai, 2008; Sundaresan et al., 2016; Merelo et al., 2017; Botton & Ruperti, 2019; Meir et al., 2019). Todos los datos relevantes recopilados sobre la abscisión de órganos sugieren que el etileno juega un papel importante en el inicio y progresión de la abscisión (Estornell et al., 2013; Botton & Ruperti, 2019: Meir et al., 2019). De hecho, se ha demostrado que tratamientos con etileno exógeno inducen la abscisión floral, de hojas y frutos (Núñez-Elisea & Davenport, 1986; Gomez-Cadenas et al., 1996; Kitsaki et al., 1999; Dal et al., 2005; John-Karuppiah & Burns, 2010; Smith & Whiting, 2010; Gil-Amado & Gomez Jimenez, 2012; Uzquiza et al., 2014; Li et al., 2015b; Wilmowicz et al., 2016; Ma et al., 2021; Hewitt et al., 2021; Singh et al., 2022; Zhang et al., 2022*)*.Sin embargo, los mutantes de Arabidopsis defectuosos en la percepción y sensibilidad a etileno, etr1 (ethylene response 1) e ein2 (ethylene insensitive 2), respectivamente, solo presentan retrasada la abscisión de los órganos florales (Patterson & Bleecker, 2004), sugiriendo que el etileno puede no ser esencial para la activación de este proceso. . Por

otro lado, recientemente también se ha demostrado, en litchi, que LcEIL2/3 (ETHYLENE INSENSITIVE) funcionan como reguladores positivos de la abscisión del fruto, probablemente activando la expresión de genes responsables de la biosíntesis de etileno y la degradación de la pared celular (Ma et al., 2020), mientras que el módulo regulador LcKNAT1-LcEIL2/3 probablemente esté implicado en la abscisión del fruto (Ma et al., 2022) y la represión de la expresión de LcERF2 participe en la reducción de la tasa abscisión de frutos (Yi et al., 2021). Además, se ha propuesto que el factor de transcripción FOREVER YOUNG FLOWER (FYF) funcione a nivel de la señalización del etileno. En este sentido, se ha observado que la sobreexpresión de FYF produce una abscisión retrasada (Chen et al., 2015). Asimismo, en el último año también se ha demostrado que la señal iniciadora de la abscisión en la hoja caulinar de Arabidopsis, es una señal ambiental (estrés hídrico y rehidratación) también está mediada por el etileno (Meir et al., 2022; Figura 1.5).

Contrariamente a lo expuesto para el etileno, la auxina regula negativamente la abscisión al disminuir la sensibilidad de los tejidos al etileno (Sexton & Roberts, 1982; Blanusa et al., 2005; Meir et al., 2006). Es por ello, que, en cítricos y manzano, para prevenir la caída del fruto previa a la cosecha, se aplica un cóctel formado por un bloqueador de etileno (aminoethoxyvinylglycine HCl) y una auxina sintética (ácido 2,4-diclorofenoxiacético) (Yuan & Carbaugh, 2007). Estudios recientes, en uva de mesa, han mostrado que el ácido indol-3-acético (IAA) puede retrasar la abscisión de la baya durante el almacenamiento de la uva (Zhu et al., 2022). La interrelación entre auxina y etileno tiene lugar a través tanto de genes de respuesta a auxinas como a etileno, o a ambas fitohormonas (Muday et al, 2012). No obstante, los factores ambientales también pueden influir en el equilibrio hormonal etileno-auxina de las AZs, provocando tanto activación como inhibición del proceso de abscisión en plantas. En un estudio reciente en se ha puesto de manifiesto que la disminución de luz en la planta reduce la expresión del gen SlWUS (WUSCHEL), lo que resulta en una inducción de la expresión de SlKD1 (KNOX-LIKE HOMEDOMAIN PROTEIN1) y SlFUL2 (FRUITFULL 2) en la AZ, lo que modifica el gradiente de auxina y provoca una mayor producción de etileno, conduciendo así al inicio de la abscisión. Estos resultados indican que los genes SlCLV3 (CLAVATA3)- SlWUS juegan un papel central en la abscisión inducida por la disminución de la luz, afectanado principalmente a la homeostasis de auxina y etileno (Cheng et al., 2022). Por otra parte, trabajos recientes también han mostrado que la interacción de auxina con citoquinina y la de citoquinina con etileno en la AZ también regulan el proceso de abscisión en plantas

(Xu et al., 2019; Jiang et al., 2023). El thidiazuron (citoquinina sintética) que actúa como un defoliante, se usa ampliamente en la agricultura para facilitar la cosecha mecánica de muchos cultivos. Asimismo, otros autores también han demostrado que el etileno y la citoquinina son reguladores de la abscisión foliar en algodón (Xu et al., 2019), ya que el tratamiento con tidiazurón y etefón aumentan la producción endógena de etileno en la AZ a la vez que tiene lugar la degradación de la citoquinina endógena, resultando en la degradación de la pared y la separación celular (Xu et al., 2019).

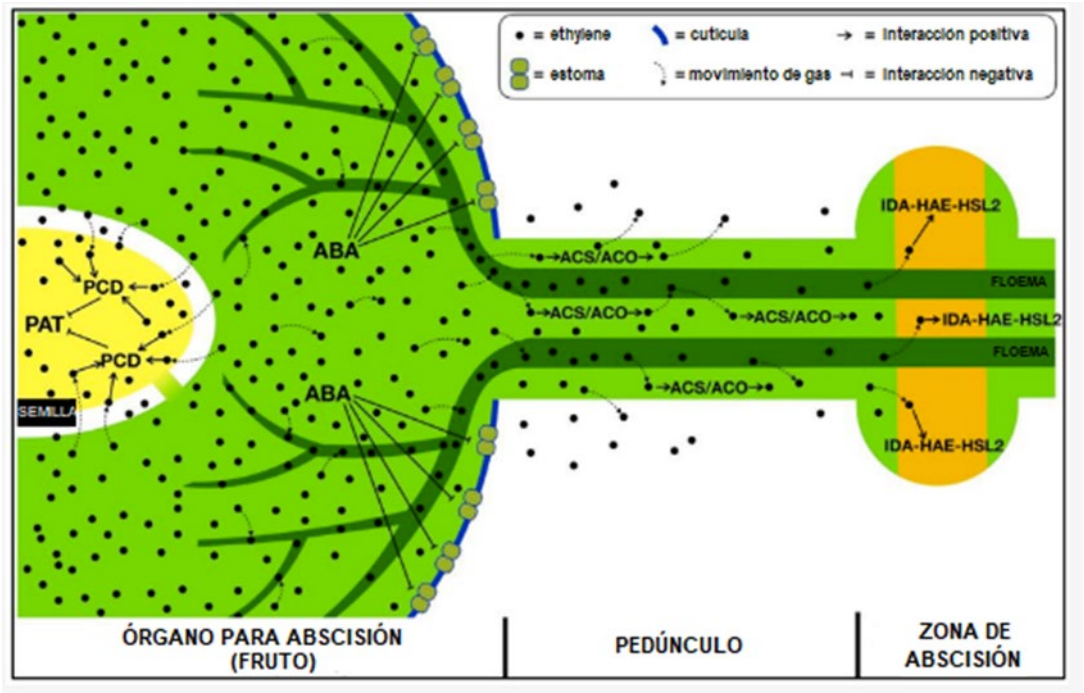

Figura 1.5. Modelo de implicación del etileno en el proceso de abscisión, tomando como referencia el fruto. Tras la inducción de la abscisión, se sintetizan etileno y ácido abscísico (ABA) dentro de la fruta. El etileno ingresa a la semilla y bloquea el transporte polar de auxina (PAT) al inducir la muerte celular programada (PCD) del embrión, de modo que la corriente reducida de auxina permite que la AZ se vuelva sensible al etileno. ABA estimula el cierre de estomas, evitando así que el etileno salga del fruto. La hormona gaseosa está así restringida para difundirse a través de la fase líquida, ya sea de forma apoplástica o simplástica, hacia el sistema vascular (es decir, el floema), a través de la única salida disponible: el pedúnculo. Una vez que el etileno alcanza los tejidos del pedúnculo, puede difundirse o estimular su propia síntesis a través de ACS (aminociclopropano-1-ácido carboxílico sintasa o ACC sintasa;) y ACO (aminociclopropano-1-ácido carboxílico oxidasa o ACC oxidasa), para que se propague progresivamente, llegando finalmente a la AZ en cantidad suficiente para activar las dianas sensibles al etileno, como la vía IDA-HAE-HSL2. Los símbolos se explican en la leyenda. Figura adaptada de Botton & Ruperti (2019).

Igualmente, en estudios llevados a cabo en litchi, se ha visto que la aplicación exógena de brasinosteroides reprime la producción de etileno y, por lo tanto, reduce la abscisión de frutos inducida por etefón., En este caso se ha observado que dos homólogos de BZR (Brassinazole resistant), es decir, LcBZR1/2, reprimen directamente la expresión de *LcACS* (aminocyclopropane-1-carboxylic acid synthase) 1/ 4 y LcACO (aminocyclopropane-1-carboxylic acid oxidase) *2 / 3* regulando así negativamente la abscisión de frutos (Ma et al., 2020).

La literatura científica ha adjudicado un papel importante para el ABA en el proceso de abscisión. Sin embargo, trabajos recientes lo asocian principalmente con su capacidad para desencadenar la senescencia tisular. Así, el efecto de ABA sobre la abscisión no parece ser directo, sino que depende de su interacción con auxina o etileno (Patterson, 2001; Roberts et al., 2002; Wilmowicz et al., 2016). Recientemente, en trabajos llevados a cabo en litchi se han identificado dos nuevos genes, homeodomain-leucine zipper I (HD-Zip I), (LcHB2 (HOMEOBOX2) y LcHB*3* (HOMEOBOX*3*), que están involucrados en la regulación de la abscisión de estos frutos a través de una regulación positiva de los genes biosintéticos de etileno y ABA (*LcACO2/3*, *LcACS1/4/7 y LcNCED3).* Asimismo, también se han identificado otros dos nuevos genes para la poligalacturonasa *(PG) (LcPG1 y LcPG2)* que conducen a un contenido reducido de homogalacturonano (HG) en las AZs del fruto (Ma et al., 2019). Asimismo, el ABA también participa junto con el JA para activar la expresión de algunas enzimas modificadoras de la pared celular durante la abscisión en mutantes de Arabidopsis insensibles a hormonas de (Ogawa et al., 2009).

El JA se asocia tradicionalmente con la regulación de la respuesta de patógenos. Sin embargo, también se ha observado que el JA regula positivamente la abscisión de los órganos florales en Arabidopsis. En este sentido, las mutaciones en el receptor del JA, coronatine insensitive 1 (coi1), provocan una abscisión tardía del órgano floral en Arabidopsis (Kim et al., 2013). Aunque el tratamiento con JA acelera la abscisión (Staswick et al., 1995), esta se comporta como una respuesta de estrés general que finalmente desencadena la producción de etileno (Taylor & Whitelaw, 2001). Por el contrario, algunos estudios sugieren un papel más directo del JA en la activación de la abscisión que no sea el de establecer una respuesta de defensa (Vashisth et al., 2015). Así, en tomate, el factor transcripcional de HD-Zip clase III, SlHB15A, regula la abscisión al reducir los niveles de JA-isoleucina (JA-Ile) induciendo la expresión *SlJAR1*

(JASMONATE-RESISTANT1), un gen implicado en la biosíntesis de JA-Ile, que podría inducir la abscisión de forma dependiente e independiente de la señalización de etileno (Liu et al., 2022).

El SA también puede actuar regulando la abscisión. Los genes que codifican las enzimas necesarias para la síntesis de SA, ISOCHORISMATE SYNTHASE (IS) 1/2, se incrementan transcripcionalmente durante el proceso de abscisión de los órganos florales (Cai & Lashbrook, 2008). El SA presenta además un papel bien establecido en la regulación de la senescencia, y tanto los órganos florales como las hojas son senescentes antes de caer (Patharkar & Walker, 2015, 2016, 2018).

Por último, cabe mencionar que es probable que otras hormonas o moléculas, además de etileno, ABA, auxina, JA o SA, controlen también el proceso de abscisión, como puede ser el caso de péptidos similares a las hormonas peptídicas que actúan en animales (Aalen et al., 2013; Butenko et al., 2003; Estornell et al., 2015; Stø et al., 2015; Kim et al., 2019; Meir et al., 2019; Shi et al., 2019).

1.3. El Olivo

El olivo (*Olea europaea* L. subsp. europaea var. europaea) es el cultivo arbóreo más antiguo de la cuenca mediterránea, cultivado desde hace unos 6000 años (Zohary & Hopf, 1994). Su difusión ha sido fuertemente influenciada por las barreras geográficas, los eventos históricos y las fluctuaciones climáticas que aún continúan. Pertenece a la familia Oleaceae y es la única especie que produce frutos comestibles dentro del género Olea (Green & Wickens, 1989; Green, 2002).

El olivo es una especie caracterizada por su plasticidad fenotípica y por la amplia variabilidad genética lo que le permite sobrevivir bajo diferentes y complejas condiciones agroecológicas (Mousavi et al., 2019; Zelasco et al., 2021). De hecho, la revisión taxonómica más reciente indica que el género Olea incluye 33 especies y 9 subespecies, 6 de ellas (formando la subsección Olea) mostrando una difusión bajo diferentes condiciones climáticas tales como la cuenca mediterránea (subsp. europaea), Macaronesia (subsp. cerasiformis y guanchica), Marruecos (subsp. maroccana), montañas del Sahara (subsp. laperrinei), y de Sudáfrica hasta el sur de Asia (subsp. cuspidata) (Medail et al., 2001; Green 2002; Sebastiani & Busconi, 2017). La subespecie europaea incluye dos variedades botánicas: olivo cultivado (var. europaea) y su pariente

silvestre, generalmente llamado 'oleaster' (var. sylvestris) (Green, 2002). En la actualidad se han descrito más de 2600 variedades (FAO, 2010; Di Rienzo et al., 2018), aunque se espera poder incrementar esta cifra en una revisión más exhaustiva de las mismas.

La mejora genética convencional en olivo presenta un problema asociado con el largo tiempo de generación de la descendencia resultante de los cruces controlados. En olivo, el período juvenil es más largo que en otras especies de árboles frutales, con un promedio de 12 a 13 años después de la germinación (Bellini, 1993; Bellini et al., 2002; Santos-Antunes et al., 2005). Aunque se han ensayado protocolos que permiten proporcionar más del 80 % de las plantas adultas tras 4 años después de la siembra (Moreno-Alías et al., 2012), su utilización no se ha hecho de forma extensiva. En la última década, la rápida evolución y el uso generalizado de las técnicas NGS han contribuido a avanzar en el conocimiento de la genómica del olivo, aunque la complejidad biológica de la especie y de su genoma han ralentizado significativamente el progreso de la investigación en esta especie en comparación con otros cultivos, como arroz, tomate, o vid (Zelasco et al., 2021). En este contexto, nuevos enfoques genómicos serán necesarios en esta especie para contribuir a una fuerte aceleración de la olivicultura en los próximos años. El olivo muestra un genoma nuclear de tamaño mediano (1.4-1.5 Gb), altamente heterocigoto y rico en repeticiones lo que hace que su ensamblaje sea enormemente complejo. Actualmente, se conocen cuatro secuencias genómicas obtenidas a partir de olivo silvestre (Unver et al., 2017) y de diferentes variedades de olivos cultivados, entre los que se encuentran las variedades Farga (Cruz et al., 2016), Picual (Jiménez-Ruiz et al., 2020) y Arbequina (Rao et al., 2021) (Figura 1.6).

1.3.1. Importancia económica.

El olivo es un cultivo de gran interés económico en España, siendo el principal país productor de aceite de oliva y aceituna de mesa a nivel mundial. Según datos del Consejo Oleícola Internacional (COI), el olivar mundial está constituido por unos 850 millones de árboles que ocupan una superficie de más de 10 millones de hectáreas.

Según el Ministerio de Agricultura, Pesca y Alimentación (MAPA, 2023), España cuenta con 2,75 millones de hectáreas, de las cuales 2,55 millones pertenecen a olivar de almazara (93% del total de olivar), lo que representa el 70 % de la producción de aceite de oliva de la Unión europea y el 45 % a nivel mundial (Figura 1.7).

Figura 1.6. Olivos cultivados de la variedad 'Arbequina'.

La Unión Europea es el principal productor, consumidor y exportador de aceite de oliva, produciendo aproximadamente el 67 % del aceite de oliva del mundo. Así, alrededor de 4 millones de hectáreas, localizadas principalmente en los países mediterráneos de la UE, se dedican al cultivo del olivo, combinando olivares tradicionales, intensivos y superintensivos. Italia y España son los mayores consumidores de aceite de oliva en la UE, con un consumo anual de alrededor de 500.000 toneladas cada uno, mientras que Grecia tiene el mayor consumo per cápita de la UE, con alrededor de 12 kg por persona al año. En total, la UE representa alrededor del 53 % del consumo mundial (MAPA, 2023).

En España, el sector del aceite de oliva es un pilar fundamental en el sistema agroalimentario. El sector no solo tiene una indiscutible importancia económica, sino que también tiene una gran repercusión social, ambiental y territorial. Más de 350.000 agricultores se dedican al cultivo del olivar, el sector mantiene unos 15.000 empleos en la industria y genera más de 32 millones de jornales por campaña (MAPA, 2023). En la estimación de la campaña 2022/2023 realizada por SIMO se estima una producción de 780.000 mil toneladas en aceite de oliva, 85,000 de aceite de orujo y 50,000 de aceituna de mesa (Tabla 1.1), situándose España como un líder mundial en producción y exportación de aceite de oliva, las cuales suponen en torno al 65 % de su comercialización

total. El cultivo del olivar posee la mayor superficie de Producción Integrada de España con 477.606 hectáreas (datos 2019) que representa un 57 % del total nacional de este tipo de producción y un 18 % del total de superficie del olivar. Además, 217.864 hectáreas de olivar de almazara se producen en régimen de agricultura ecológica (datos 2020).

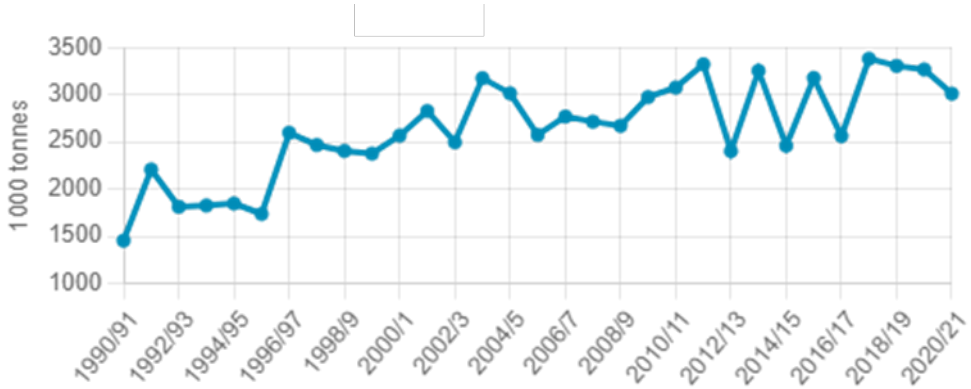

Figura 1.7. Producción de aceite de oliva mundial desde la campaña 1990/91 hasta 2020/2021. Fuente: COI (2022).

En cuanto a producción, el cultivo del olivar se caracteriza por su marcado carácter vecero por lo que la producción de aceite de oliva muestra una gran alternancia productiva entre campañas.

Tabla 1.1. Balance del sector del olivar en España en la campaña 2022/2023. Fuente: SIMO (octubre 2022).

CAMPAÑA 2022/23 (Estimación) ud: miles t	ACEITE DE OLIVA[1]	ACEITE DE ORUJO[1]	ACEITUNA DE MESA[2]
Existencias iniciales	453,768	72,653	439,720
Producción	780,000	85,000	449,423
Importaciones	225,000	85,000	50,000
TOTAL RECURSOS	**1.458,768**	**242,653**	**939,143**
Consumo interior	425,000	65,000	210,000
Exportaciones	800,000	155,000	320,000
Ajustes y Pérdidas[3]	-	-	100,000
Existencias finales	233,768	22,653	309,143
TOTAL REALIZACIÓN	**1.458,768**	**242,653**	**939,143**

1 La campaña comienza el 1 de Octubre y finaliza el 30 de Septiembre del año siguiente
2 La campaña comienza el 1 de Septiembre y finaliza el 31 de Agosto del año siguiente
3 Los ajustes y pérdidas únicamente aplican sobre aceituna de mesa

A nivel regional, la producción de aceite de oliva se localiza fundamentalmente en Andalucía con el 80% del total, donde Jaén es la principal provincia productora con aproximadamente el 37% del total, seguida de Castilla La Mancha con el 8% y de Extremadura con el 4% del total nacional (MAPA, 2023).

1.3.2 La abscisión del fruto en el olivo.

El principal interés del estudio de la abscisión del fruto maduro en olivo es poder facilitar su recolección mecanizada, bien para la producción de aceite o para aceituna de mesa (Barranco et al., 2004; Ferguson et al., 2010; Zipori et al., 2014). En la actualidad, existen variedades de olivo cuyos frutos presentan una alta fuerza de retención en el momento de su recolección y, por consiguiente, la eficacia de la recolección mecanizada es muy baja, lo que provoca una disminución en la producción y, sobre todo, un aumento crítico de los costes de recolección del fruto para el agricultor. En este sentido, el sector demanda el uso de compuestos que promuevan la abscisión selectiva del fruto, sin ocasionar defoliación del olivar, a fin de mejorar la recolección mecanizada de la aceituna de mesa y la destinada a la producción de aceite, y por tanto, reducir los costes de recolección de la cosecha.

Weis et al. (1988) describieron en olivo, múltiples posiciones de la zona de separación dentro de la inflorescencia. Dichas posiciones también representan los diferentes puntos potenciales de separación para la abscisión de frutos. La estructura de la inflorescencia es muy similar entre cultivares y mientras que una inflorescencia puede tener hasta 35 flores, por lo general, sólo uno o dos frutos se establecen por inflorescencia (Figura 1.8) (Lavee, 1986). Diferentes autores han puesto de manifiesto la zona de separación del fruto en el pedicelo (Ben-Tal & Wodner, 1994; Denney & Martin, 1994; Metzidakis, 1999) como una zona situada en las uniones fruto-pedicelo y pedicelo-raquis (Reed & Hartmann, 1976; Bartolini et al., 1992) además de en la unión pedúnculo-brote (Barranco et al., 2002). El estudio de la localización de la zona de abscisión en diferentes variedades de olivo ha revelado que dicha localización varía entre las variedades estudiadas, por lo que es posible que la posición de la zona de separación esté ligada a la variedad. Así, por ejemplo, Reed & Hartmann (1976) localizaron en la variedad 'Manzanilla'la abscisión del fruto a nivel del pedicelo, Barranco et al. (2002) describieron para la variedad 'Arbequina' que la abscisión predominaba en la unión del pedúnculo-brote, mientras que en el fruto de 'Frantoio' y 'Leccino', la separación ocurría tanto en el pedicelo-raquis como en el fruto-pedicelo (Bartolini et al., 1992). Por otra parte, Bartolini et al. (1992) también señalaron que la posición de la abscisión está relacionada con el estado de maduración del fruto. Más recientemente, en un estudio de Castillo-Llanque & Rapoport, (2009) se ha puesto de manifiesto que la abscisión del fruto en las variedades 'Picual' y 'Hojiblanca' puede ocurrir en tres lugares diferentes: pedúnculo-rama (ZA1), pedicelo raquis (ZA2) y

fruto-pedicelo (ZA3). La abscisión del fruto del olivo maduro ocurre principalmente en ZA3, en menor grado en ZA2 y raramente en ZA1 (Figura 1.8).

Figura 1.8. Inflorescencia y fruto de la variedad de olivo 'Picual'. A la izquierda, inflorescencia y a la derecha, localización de las AZs del fruto.

El olivo posee una gran variabilidad genética intraespecífica que puede ser útil para comprender el proceso de abscisión. En los 15 últimos años, nuestro Grupo de Investigación ha estudiado los mecanismos fisiológicos y moleculares implicados en el proceso de abscisión del fruto maduro de olivo.

En estos trabajos, se ha llevado a cabo un estudio fisiológico y molecular del proceso de abscisión del fruto maduro utilizando la variabilidad genética del cultivo con el fin de comprender la regulación hormonal, así como el control transcripcional implicado en dicho proceso. En dicho estudio se han utilizado dos variedades de aceituna, 'Arbequina' y 'Picual', las cuales se caracterizan por presentar en condiciones naturales un diferente patrón de abscisión en el fruto maduro y la misma localización de la zona de abscisión, asociada a la activación de ZA3 (Gomez-Jimenez et al., 2010a).

La aplicación de técnicas de microscopía óptica y de microscopía electrónica, tanto de barrido como de transmisión, han permitido conocer los cambios que ocurren en la AZ del fruto de 'Picual' durante la abscisión natural, y también las diferencias existentes con la AZ del fruto de 'Arbequina' (Gomez-Jimenez et al., 2010a). Además, se han puesto de manifiesto diferentes alteraciones provocadas durante la abscisión en la estructura de las paredes celulares de la AZ del fruto, las cuales implican modificaciones de los polisacáridos de dicha pared relacionadas principalmente con la desesterificación y la solubilización de las pectinas que la componen (Parra et al., 2020). En este sentido, los

estudios de inmunolocalización indican que, en la AZ del fruto, la localización de HGs no esterificados, principalmente en la lámina media, aumenta durante la abscisión y es concomitante con una disminución de HGs esterificados (Parra et al., 2020). Ello sugiere que la desesterificación de HGs que está regulada por las enzimas pectinmetilesterasa (PME) y PG, podría contribuir a la separación celular en la AZ del fruto., Paralelamente también se observó en la AZ del fruto una reducción de pectinas ricas en galactosa y arabinosa, y de proteínas arabinogalactanos (AGP). Por otra parte, los estudios inmunocitoquímicos combinados con el análisis de la expresión génica han permitido establecer una correlación entre la separación celular y la pérdida de extensina, así como niveles inferiores de xiloglucano y nueva deposición de xilano y calosa en la pared celular. Además, existe también una regulación positiva de los genes que codifican para la enzima xiloglucano endotransglicosilasa/hidrolasa (XTH), la cual está involucrada en la desintegración de la unión entre el xiloglucano y las fibras de celulosa en las paredes de las células de la AZ (Parra & Gomez-Jimenez, 2020). Estos resultados, por tanto, indican que la inducción del proceso de abscisión del fruto maduro en olivo se traduce en una secuencia temporal de modificaciones de la pared celular que implican la pérdida, y/o la remodelación de distintos polímeros de la pared celular de las células de la AZ.

Por otra parte, y a pesar del papel regulador atribuido al etileno en el proceso de abscisión como acelerador de este proceso, existe poca información sobre la regulación de la biosíntesis de esta hormona en la propia de la AZ. Para examinar el papel fisiológico del etileno durante la abscisión del fruto de olivo, y su posible interacción con las poliaminas (biosintéticamente relacionadas), se han llevado a cabo trabajos en el grupo de investigación orientados a determinar el contenido del precursor metabólico inmediato del etileno, el ACC, así como de su forma conjugada, el malonil-ACC (MACC) y también el de las poliaminas libres y conjugadas en la AZ Además, se han determinado las actividades de las enzimas asociadas a la síntesis de poliaminas en la AZ del fruto tanto de la variedad 'Picual' como 'Arbequina'. Los resultados indicaron que un proceso de abscisión del fruto maduro en 'Picual' se caracteriza por una disminución de la fuerza de retención del fruto y un incremento en el contenido de ACC en la AZ (Gomez-Jimenez et al., 2010b; Parra-Lobato & Gomez-Jimenez, 2011). El análisis bioquímico indicó también que el metabolismo de poliaminas se encontró alterado en la AZ del fruto de 'Picual' con respecto a la AZ de los frutos de 'Arbequina' que se aracterizan por no caer del árbol. Esto se traduce en la acumulación de putrescina libre y conjugada de la fracción soluble, así como de poliaminas no comunes, tales como la homoespermidina y

cadaverina en la AZ del fruto de 'Picual', en beneficio de la síntesis de etileno (Gomez-Jimenez et al., 2010b). Por tanto, estos resultados sugerían una posible interrelación entre las rutas de etileno y poliaminas en la AZ del fruto en olivo, ya que la inhibición de la actividad S-adenosilmetionina descarboxilasa (SAMDC) (acumulación de putrescina) debe canalizar el SAM principalmente hacia la síntesis de ACC y etileno (Gomez-Jimenez et al., 2010b). Así, la reacción catalizada por la enzima SAMDC es considerada como un punto de regulación clave en la modulación del metabolismo de poliaminas y etileno en la AZ durante la abscisión del fruto maduro en olivo.

A nivel molecular, en este estudio también se abordó el papel del etileno y las poliaminas durante la abscisión del fruto por modulación de los genes implicados en las rutas de biosíntesis y señalización del etileno en la AZ de ambas variedades (Picual y Arbequina). A fin de profundizar en el estudio de la posible interacción del etileno y poliaminas durante la abscisión del fruto, se analizó la expresión de cinco genes relacionados con etileno (*OeACS2*, *OeACO2*, *OeCTR1*, *OeERS1 (ETHYLENE RESPONSE SENSOR)* y *OeEIL2* tanto en la AZ como en otros órganos de la planta. Los genes *OeACS2*, *OeACO2*, y *OeEIL2* fueron encontrados por ser los únicos genes inducidos con la abscisión del fruto (Parra-Lobato & Gomez-Jimenez, 2011). De hecho, se ha demostrado que los tratamientos con etileno e inhibidores de la biosíntesis de poliaminas inducen la abscisión del fruto maduro, sugiriendo papeles antagónicos para ambas fitohormonas (Parra-Lobato & Gomez-Jimenez, 2011). En concreto, usando inhibidores de la biosíntesis de etileno y poliaminas, se puso de manifiesto que la expresión *OeACS2* y O*eEIL2* se produce bajo el control negativo de las poliaminas (espermidina), mientras que el etileno induce su expresión en la AZ del fruto en olivo (Parra-Lobato & Gomez-Jimenez, 2011). Además, también se ha demostrado que la expresión de los genes de la biosíntesis de poliaminas, *OeEIL1* y *OeSPDS1(*spermidine synthase*)*, en la AZ del fruto maduro fue a su vez afectada por tratamientos con etileno exógeno, así como por la aplicación de inhibidores (Gil-Amado & Gomez-Jimenez, 2012), sugiriendo un antagonismo entre ambas rutas a nivel transcripcional. En consecuencia, los resultados previos obtenidos en el grupo de investigación han demostrado la participación de una ruta de biosíntesis y señalización de etileno dependiente de poliaminas, por lo menos parcialmente, en la AZ durante la abscisión del fruto (Parra-Lobato & Gomez-Jimenez, 2011). Además, en estos estudios también se describió por primera vez una implicación del NO en el proceso de abscisión, revelando que el contenido de NO endógeno y el ACC

mantienen una correlación inversa en la AZ del fruto, lo que sugiere una acción opuesta del NO y etileno en el proceso de señalización de la abscisión del fruto maduro del olivo (Parra-Lobato & Gomez-Jimenez, 2011). De la misma manera, también se ha propuesto un posible papel para el H_2O_2 en el proceso de abscisión, cuyo contenido incrementa en la AZ del fruto en respuesta al etileno (Gil-Amado and Gomez-Jimenez, 2012). Aunque no se pudo descifrar cómo se produce el mecanismo de acción con respecto al H_2O_2, el estudio demostró que la síntesis y el catabolismo de la putrescina se vieron inducidos en la variedad 'Arbequina' en respuesta al etileno exógeno, generando a su vez niveles altos de H_2O_2, la cual podría tener un papel en la activación de la expresión de genes relacionados con la abscisión (Gil-Amado & Gomez-Jimenez, 2012). Estos resultados sugieren que la putrescina endógena podría desempeñar un papel complementario al etileno en la abscisión del fruto en olivo y, por consiguiente, demuestran la complejidad metabólica que se produce durante la abscisión, en la que los metabolitos de las poliaminas pueden actuar como antagonistas o complementarios al papel promotor del etileno en dicho proceso.

Posteriormente, los trabajos del grupo de investigación se centraron en identificar genes candidatos y rutas asociadas con la activación del proceso de abscisión, para lo que se llevó a cabo un análisis transcripcional a gran escala del proceso de abscisión del fruto mediante secuenciación de 454 genes en la AZ del fruto de 'Picual' (Gil-Amado & Gomez-Jimenez, 2013). Este estudio constituyóel primer análisis detallado disponible de la actividad transcripcional del proceso de la abscisión del fruto maduro en especies de frutos carnosos. Así, el análisis del transcriptoma en la AZ del fruto maduro del olivo ha demostrado que la abscisión está acoplada a una estimulación del transporte intracelular (de la exocitosis y la endocitosis) gracias a la actividad de miembros específicos de las familias de tipo RAB, ARF, RAN y RHO de las GTPasas (Gil-Amado & Gomez-Jimenez, 2013). El proceso de exocitosis podría estar implicado en la llegada al espacio extracelular de las esterasas e hidrolasas que participan en la desintegración de las paredes de las células de la AZ. En este trabajo, se pudo identificar además la expresión de genes en la AZ relacionados con cambios en los microdominios de membrana que incluyen los esteroles y los esfingolípidos, junto con las proteínas de señalización potencialmente implicadas en la abscisión del fruto en olivo (Gil-Amado & Gomez-Jimenez, 2013). Los cambios en la expresión génica relacionada con el recambio de esfingolípidos sugieren la posible implicación de éstos en el proceso de abscisión, lo que reveló la primera evidencia sobre la posible participación de los esteroles y esfingolípidos

en el proceso de abscisión. Concretamente, estos esfingolípidos forman una familia cuya estructura base es el ácido graso palmitato junto al aminoacido serina. Entre sus integrantes más conocidos están las Cers y LCBs. De hecho, se pudieron visualizar regiones de membrana plasmática y de endomembranas enriquecidas en esfingolípidos en las células de la AZ durante la abscisión del fruto, así como, en el propio fruto al inicio del proceso de maduración del fruto en olivo (Parra-Lobato et al., 2017; Inês et al., 2018). En particular, el análisis del contenido y la composición de LCBs derivados de la hidrólisis de los esfingolípidos demostró un incremento de LCB trihidroxilados en la AZ durante la abscisión del fruto, indicando un enriquecimiento de los esfingolípidos que contienen estas formas LCBs y VLCFAs (Parra-Lobato et al., 2017). Estos resultados sugieren que los esfingolípidos complejos GIPCs son más abundantes que las GlcCers en la AZ durante la abscisión del fruto. Además, los genes de las enzimas biosintéticas clave para la síntesis de esteroles, obtusifoliol 14α-desmetilasa (*CYP51*) y C-24 esterol metiltransferasa2 (*SMT2*), son regulados durante la abscisión del fruto maduro, al mismo tiempo que incrementa el contenido de β-sitosterol, el esterol más predominante (Parra-Lobato et al., 2017). Estos resultados permiten concluir que las diferencias en el contenido y/o composición de esfingolípidos y esteroles en la AZ puede jugar un papel importante durante la abscisión del fruto en olivo.

En un segundo estudio transcriptómico llevado a cabo en el grupo, se realizó una comparación del fruto (pericarpo) y la AZ para identificar la expresión específica de factores de transcripción en cada tejido, que no habían sido previamente relacionados con la abscisión. En dicho estudio, se incluyeron miembros de las familias Aux/IAA, C2H2L y CAMTA que se expresan preferentemente en el fruto, así como otros miembros de las familias HSF (Heat Stress transcription Factor), GRAS, proteína de unión a GAGA, EIN3/EIL, E2F/Dimerization Partner (DP), proteína de unión a CCAAT y WRKY que se expresan preferentemente en la AZ. Los resultados indicaron una, intercomunicación entre los dos tejidos, lo que implica la expresión diferencial de estos factores de transcripción (Parra et al., 2013). Consecuentemente, nuestro Equipo de Investigación ha demostrado, por una parte, que la aplicación en campo de esfingolípidos simples exógenos induce selectivamente la abscisión del fruto y no de la hoja en olivo (Patentes concedidas: ES 2 611 810, ES 2 612 728 y ES 2 616 745), y por otra parte, que la aplicación de secuestradores de NO (cPTIO) o del inhibidor de la enzima NO sintasa (L-NAME) en campo, induce también la abscisión selectiva del fruto,

sin ocasionar defoliación del olivo, a diferencia de lo que ocurre con el etileno (Patentes condedidas: ES 2 611 828 y ES 2 613 583), si bien, el impacto a nivel molecular de estos tratamientos inductores de la abscisión es aún desconocido.

2.OBJETIVOS

2.OBJETIVOS

Desde una perspectiva agrícola, la abscisión puede convertirse en un factor limitante importante para la productividad de los cultivos. En olivo, cultivo de gran interés económico en España, el principal objetivo del estudio de la abscisión del fruto es facilitar su recolección mecánica, ya sea para obtención de aceite o como aceituna de mesa, proceso que incrementa los costes de forma significativa (Barranco et al., 2004; Ferguson et al., 2010; Zipori et al., 2014). Las posibles soluciones son identificar cultivares con un comportamiento de abscisión óptimo o identificar tratamientos que afecten selectivamente a la abscisión de frutos y no de las hojas para facilitar la cosecha mecánica (Banno et al., 1993; Polito & Lavee, 1980; Goldental-Cohen et al., 2017). En los últimos años, nuestro Grupo ha estudiado los mecanismos fisiológicos y moleculares implicados en el proceso de abscisión del fruto maduro en olivo. En estos trabajos, se demostró que el comportamiento de la abscisión del fruto maduro no es homogéneo entre las variedades de olivo cultivadas (Gomez-Jimenez et al., 2010b; Parra-Lobato & Gomez-Jimenez., 2011; Gil-Amado & Gomez -Jiménez, 2012) y se logró la primera evidencia de la posible participación de los esfingolípidos en el proceso de abscisión en plantas (Gil-Amado & Gomez-Jimenez, 2013; Parra-Lobato et al., 2017). La información generada por estos trabajos ha dado lugar a la investigación inicial de nuevos productos químicos (generando patentes) que inducen la abscisión del fruto en olivo. En concreto, se demostró que la aplicación en campo de esfinganina exógena (d18:0) induce selectivamente la abscisión del fruto, pero no de la hoja en olivo (patente: ES 2 612 728), aunque, el impacto de este tratamiento, a nivel molecular, se desconoce.

El **objetivo general** del presente trabajo es profundizar en el conocimiento de los mecanismos fisiológicos y moleculares que regulan la activación del proceso de abscisión del fruto en olivo. En concreto, se pretende conocer el control transcripcional y hormonal implicado en la zona de abscisión del fruto durante la abscisión natural e inducida por esfingolípidos en olivo. La información generada en este trabajo permitiría identificar elementos responsables de esta regulación y así, contribuir a una mejor comprensión de la señalización de este proceso, así como de la función de los esfingolípidos en plantas. En este sentido, la identificación de estos reguladores específicos de la zona de abscisión del fruto permitiría desarrollar estrategias para controlar la recolección de la aceituna, reduciendo, en última

instancia, los costes de recolección y aumentando el beneficio económico para los agricultores.

Para ello, hemos establecido como **objetivos específicos** los siguientes:

1. Analizar el perfil hormonal y transcripcional de la zona de abscisión y del pericarpo del fruto en olivo (cv. 'Picual') durante la abscisión natural del fruto maduro, para establecer distintos patrones de expresión específicos de tejido relacionados con la modificación de la pared celular, el tráfico vesicular, el transporte, y la biosíntesis y señalización de fitohormonas en combinación con el contenido hormonal.

2. Identificar cómo los esfingolípidos afectan la abscisión selectiva del fruto en olivo (cv. 'Manzanilla Sevillana') utilizando un enfoque transcriptómico: analizar el perfil hormonal y transcripcional de la zona de abscisión del fruto y de la hoja durante la abscisión selectiva del fruto inducida por esfinganina (d18:0) para identificar marcadores específicos de la zona de abscisión del fruto que permitan caracterizar la inducción de la abscisión del fruto sobre el árbol.

3.RESULTADOS Y DISCUSIÓN

3.I:

Transcriptome and hormone analyses revealed insights into hormonal and vesicle trafficking regulation among *Olea europaea* fruit tissues in late development

3.I: Transcriptome and hormone analyses revealed insights into hormonal and vesicle trafficking regulation among *Olea europaea* fruit tissues in late development

3.I.1. Abstract

Fruit ripening and abscission are the results of the cell wall modification concerning differentcomponents of the signalling network. However, molecular-genetic information on the cross-talkbetween ripe fruit and their abscission zone (AZ) remains limited. In this study, we investigatedtranscriptional and hormonal changes in olive (*Olea europaea* L. cv Picual) pericarp and AZ tissues offruit at the last stage of ripening, when fruit abscission occurs, to establish distinct tissue-specificexpression patterns related to cell-wall modification, plant-hormone, and vesicle trafficking incombination with data on hormonal content. In this case, transcriptome profiling reveals thatgene encoding members of the α-galactosidase and β-hexosaminidase families associated withup-regulation of RabB, RabD, and RabH classes of Rab-GTPases were exclusively transcribedin ripe fruit enriched in ABA, whereas genes of the arabinogalactan protein, laccase, lyase,endo-β-mannanase, ramnose synthase, and xyloglucan endotransglucosylase/hydrolase familiesassociated with up-regulation of RabC, RabE, and RabG classes of Rab-GTPases were exclusivelytranscribed in AZ-enriched mainly in JA, which provide the first insights into the functionaldivergences among these protein families. The enrichment of these protein families in different tissuesin combination with data on transcript abundance offer a tenable set of key genes of the regulatorynetwork between olive fruit tissues in late development.

Keywords: cell wall; endomembrane trafficking; olive; plant hormone; fruit ripening; transcriptomiccomparative

3.I.2. Introduction

In fleshy fruit, the fruit ripening and abscission are developmentally regulated and genetically programmed processes (Périn et al., 2002) whose induction depends on a complex interplay of plant's hormone content in addition to factors that alter the

sensitivity of the tissues (Pech et al., 2008; Gulfishan et al., 2009; Kumar et al., 2014; Liu et al., 2015; Forlani et al., 2019; Meir et al., 2019). Knowledge of the mechanisms involved in fleshy-fruit ripening and abscission is essential for developing strategies to control yield. Although fully ripe fruit have marked physiological differences with respect to their abscission zone (AZ), both fruit ripening and abscission processes are a result of the cell wall modification, which involves a wide range of structural proteins and hydrolytic enzymes with distinct functions in the tissues (cell separation in the AZ and softening in the fruit), concerning common and different components of the signalling network playing either direct or indirect roles in these processes. However, molecular-genetic information on the cross-talk between ripe fruit and their AZ is still limited.

Olive (*Olea europaea* L.), is one of the most economically important fruit trees worldwide for the oil of its fruit, and has high intra-specific genetic variation with a genome size of about 1,800 Mb (Loureiro et al., 2007; Rugini et al., 2020). Until now, the study of gene function in the olive has been fundamentally advanced by the availability of whole genome sequences (Barghini et al., 2014; Cruz et al., 2016; Unver et al., 2017), while several transcriptomic, proteomic, and metabolic studies have been developed in olive fruit (Alagna et al., 2009; Galla et al., 2009; Alagna et al., 2012; Bianco et al., 2013; Muñoz-Mérida et al., 2013; Carmona et al., 2015; Bruno et al., 2019). However, these studies concern only a few genotypes and little is still known about olive-fruit biology. In particular, information concerning the plant hormone composition of the olive fruit remains to be determined.

Events related fruit ripening in some olive cultivars, such as cv. Picual trigger ripe fruit abscission (Gomez-Jimenez et al., 2010b). In these cases, the patterns of abscission vary according to the cultivar (Gomez-Jimenez et al., 2010b). In olive fruit, several AZs appear in the pedicel (Bartolini et al., 1993), although only one AZ is specifically activated at a time at each stage of development (Gómez-Jimenez et al., 2010b; Parra-Lobato et Gómez-Jimenez, 2011). In a previous study, we reported the comparison of the Picual fruit AZ transcriptomes at two different stages (pre-abscission vs. abscission) using the RNA-Seq technique; 148 Mb of sequences (443,811 good-quality sequence reads) resulted and 4,728 differentially expressed genes were identified from these two samples (Gil-Amado & Gomez-Jimenez, 2013). Additionally, using 454 pyrosequencing technology, we also analyzed the overall transcriptional profile of Picual fruit pericarp

at full ripening to significantly expand the olive transcript catalog (Parra et al., 2013). In this cultivar, abscission of ripe fruit depends on the activation of the AZ located between the pedicel and fruit (Parra-Lobato et Gómez-Jimenez, 2011). The excision of the AZ from olive fruit may lead to a contamination of the tiny AZ tissue with at least as much tissue from the surrounding pericarp/pedicel of the fruit. The comparison between AZ and adjacent tissues enable us to restrict the set of genes putatively related to the abscission process, and in this sense the results may provide worthwhile perspectives for the study of this process. Consequently, we compared the transcriptomes from AZ and pericarp tissues of olive ripe fruit in order to characterize the transcriptional factors enriched in differentially regulated gene clusters, and presumably related to the abscission process, particularly ZF, bHLH, MADS-box, homeobox domain proteins, and bZIP families (Parra et al., 2013). That represented the first effort to elucidate the divergences in transcriptional networks regulating the fruit abscission process in olive. Nevertheless, to date, no transcriptomic analysis has been conducted to determine the genetic changes associated with cell wall modification, plant-hormone, vesicle trafficking, and ion fluxes occurring among olive fruit and their AZ.

The aim of the present work was to analyze whole olive transcriptome changes in order to gain an understanding of the molecular mechanisms and hormonal control in olive fruit with respect to their AZ at last stage of ripening, when fruit abscission occurs. In particular, we focus here on the gene expression pattern involved in cell wall modification, plant hormone, vesicle trafficking and ion fluxes. In addition, the hormonal composition was also examined in the olive fruit and their AZ at last stage of ripening. These findings provide critical information for uncovering the differential hormonal and molecular genetic control between olive fruit tissues in late development.

3.I.3. Results and Discussion

3.I.3.1. Differential abundance of cell-wall-related transcripts between olive fruit tissues in late development

Under natural conditions, olive of cv. Picual displayed around 92% abscission of ripe fruit at 217 days post-anthesis (DPA) (Gómez-Jimenez et al., 2010b). For this study, two adjacent tissues of 'Picual' olive fruit, i.e. the fruit pericarp (epicarp and mesocarp) and the AZ, were selected at the last stage of fruit ripening (217 DPA), when fruit abscission

occurs (Parra-Lobato et Gómez-Jimenez, 2011; Parra et al., 2013). Recently, we have shown that the changes detected in AZ cell wall polysaccharides during 'Picual' fruit abscission are related to pectic polysaccharide de-esterification and solubilization (Parra et al., 2020), which is possibly promoted by cell wall-associated pectin methyl esterases (PMEs) and polygalacturonases (PGs) enzymes. In the present study, to investigate ripening-abscission distinctions in 'Picual' olive, we compared the transcriptomes of olive fruit-pericarp vs. fruit-AZ at 217 DPA to restrict the set of cell wall genes presumably related to the abscission process (Figure 3.I.1).

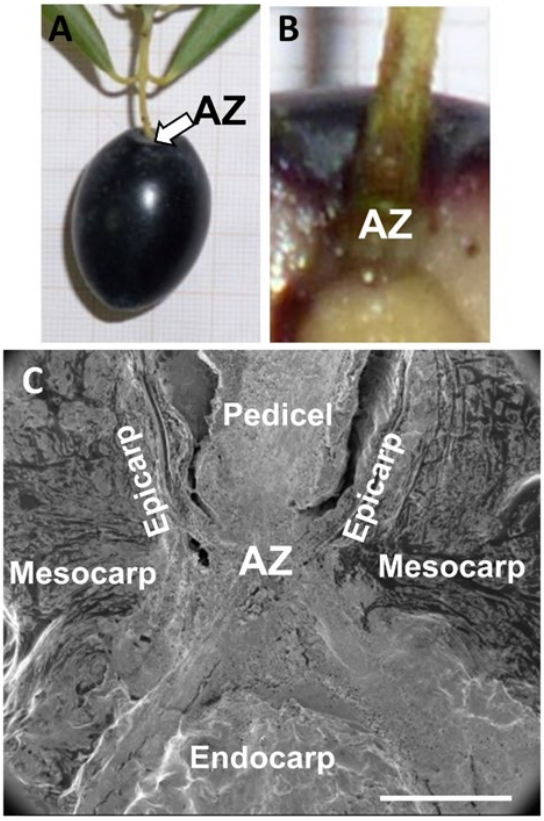

Figure 3.I.1. Tissues of olive (*Olea europaea* L. cv Picual) used for this study: AZ and pericarp (epicarp and mesocarp) of fruit at the last stage of ripening. **(A)** Image of olive ripe-fruit illustrating the location of the AZ between the peduncle (top) and fruit (bottom). **(B)** Longitudinal section of the transition zone between the peduncle (top) and fruit (bottom) showing the AZ of olive ripe-fruit. **(C)** Scanning electron micrograph of a longitudinal section of Picual fruit illustrating the position of the tissue samples used for this study: the fruit (epicarp and mesocarp) and their AZ at 217 DPA. Scale bar 1 mm.

Our pyrosequencing-based approach enabled the identification of 87 differentially expressed genes (P<0.01) in olive AZ compared to fruit at 217 DPA related to cell wall metabolism (Table 3.I.S1, Figure 3.I.2A). Overall, 34 genes had peak read amounts (See Material and Methods) within the set of fruit-induced genes ('fruit-enriched transcripts'), and 53 genes within the set of AZ-induced genes ('AZ-enriched transcripts') (Table 3.I.S1). Among the fruit-enriched genes, the most abundant proved to be a β-glucosidase protein (Table 3.I.S1, Figure 3.I.2B). In olive, several members of the β-glucosidase family have been found in proteomic and transcriptomic studies (Bianco et al., 2013; Corrado et al., 2012). Additionally, it has been proposed that β-glucosidase is a key enzyme in oleuropein catabolism (Gutierrez-Rosales et al., 2010; Koudounas et al., 2015; Cirilli et al., 2017; Velázquez-Palmero et al., 2017). However, in the ripe fruit the well-represented families included expansin (EXP) (7 genes), cellulose synthase (CS) (5 genes), PME (4 genes) and extensin (EXT) (3 genes) proteins (Table 3.I.S1, Figure 3.I.2), suggesting that these cell wall polysaccharide-degrading enzymes regulate olive-fruit softening. In particular, the fact that 7 members of the EXP family showed differential expression in our study, suggests that this family may mediate cell wall loosening in olive ripe fruit.

The 10 most differentially overexpressed genes in the ripe fruit encoding cell wall proteins were one β-glucosidase (*Olea europaea)*, α-EXP 8 (*Ricinus communis)*, one EXP (*Diospyros kaki)*, α-EXP3 (*Triphysaria versicolor)*, one β-1,3-glucanase (*Nicotiana tabacum* NtEIG-E76), α-EXP11 (*Ricinus communis)*, one PME (*Nicotiana benthamiana)*, one EXP (*Vitis vinifera Vexp1)*, one α-EXP (*Nicotiana tabacum*, Nt-EXPA3), and one EXT protein (*Catharanthus roseus* cyc17) (Table 3.I.S1, Figure 3.I.2B).

Our team (Gil-Amado & Gómez-Jimenez, 2013) and others (Roberts et al., 2002; Agustí et al., 2009; Meir et al., 2010; Sun & Van Nocker, 2010; Zhu et al., 2011; Kim et al., 2015; Li et al., 2015b; Glazinska et al., 2017; Xie et al., 2018) have reported AZ-enriched genes related to cell wall rearrangements during fruit abscission. In the present study, the well-represented classes in the AZ included CS (10 genes) and glycosyl hydrolase (GH) proteins (7 genes) (Table 3I.S1, Figure I.2B), indicating a key role for members of these families in abscission-associated cell wall changes. The 10 most differentially overexpressed genes in the AZ encoding cell wall proteins were one β-1,3-glucanase (*Olea europaea*, glu-4), one PG (*Olea europaea)*, 2 laccase proteins *(Rosa hybrid cultivar* and

Populus trichocarpa,), one glycosyl hydrolase GH 18 family protein (*Populus trichocarpa)*, one chitinase protein (*Vitis vinífera)*, 2 lyase proteins (*Ricinus communis)*, one rhamnose synthase protein (RHM1, At1g78570) and one chitinase protein (*Vitis vinífera*) (Table 3.I.S1, Figure 3.I.2B). This finding suggests that these types of enzymes may be required for complete cell separation of ripe fruit, and possibly for cell wall restructuring during AZ-cell separation.

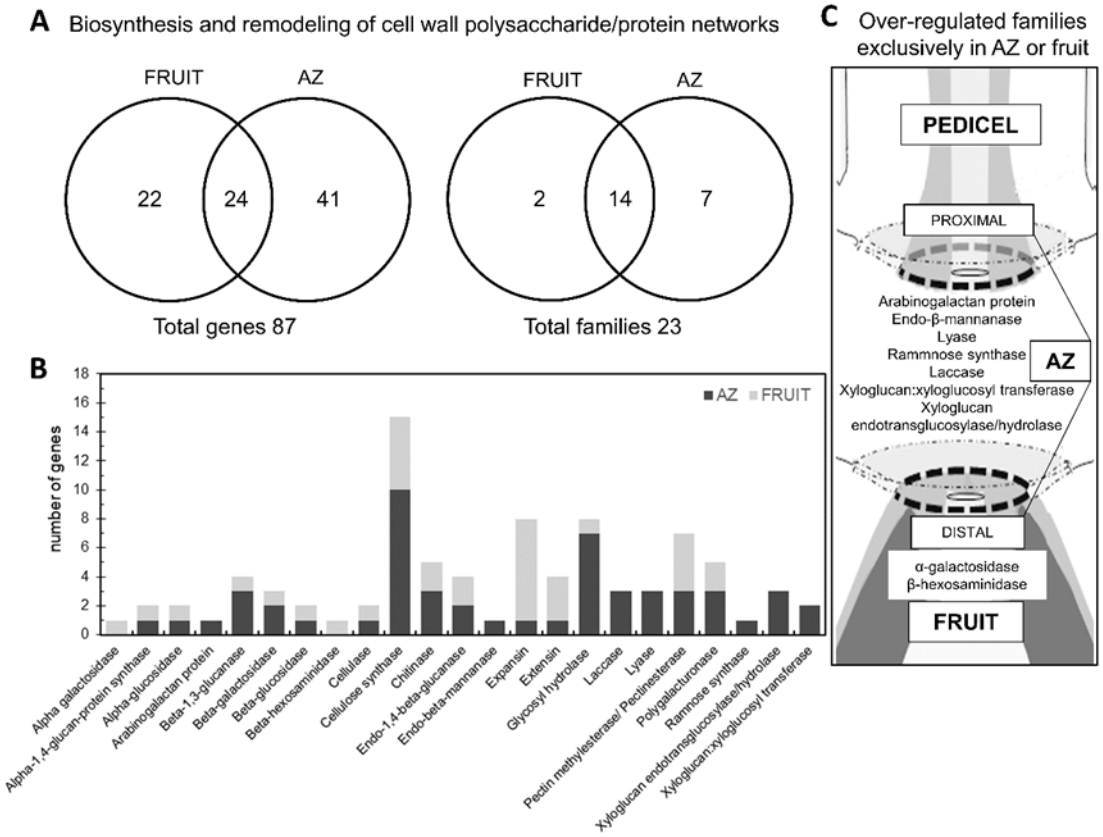

Figure 3.I.2. Differentially expressed cell wall-related genes and classification of cell wall families between olive AZ and fruit (pericarp) at the last stage of ripening (217 DPA). **(A)** Overlap of overexpressed fruit genes, and overexpressed AZ genes. This figure shows the number of transcripts and families that were specific and common for each tissue. **(B)** Comparison of significantly overexpressed transcripts ($P<0.01$) between olive AZ (black) and fruit (gray) at the last stage of ripening. Number of transcripts related to cell wall in each cell wall family. **(C)** Distribution of cell wall-related families that were specific for each olive tissue. Additional information on the cell wall-related genes is presented in Table 3.I.S1.

Among the 34 fruit-enriched transcripts, 22 were exclusively expressed in fruit (Table 3.I.S1). The 22 genes encode 5 EXP proteins, 4 CS proteins, 4 PME proteins, 2 EXT proteins, one cellulase or endo-β-1,4-D-glucanase protein, one α-1,4-glucan-protein

synthase protein, one neutral α-glucosidase protein, one β-1,3-glucanase protein, one β-galactosidase protein, one α-galactosidase protein, one β-hexosaminidase protein, and one glycosyl hydrolase protein, suggesting that cell wall proteins from these families potentially have roles in mediating late events in ripe fruit. Similarly, among the 53 AZ-enriched transcripts (Table 3.I.S1, Figure 3.I.2A), most of them (Taylor et al., 2000) were expressed exclusively in the AZ compared to the ripe fruit. These genes encoding 10 CS proteins, 4 xyloglucan endotransglucosylase/hydrolase (XTH) proteins, 4 glycosyl hydrolase proteins, 3 lyase proteins, 3 PME proteins, 2 PG proteins, 2 laccase proteins, 3 endo-1,4-β-glucanase or cellulase proteins, 2 chitinase proteins, 2 β-galactosidase proteins, 2 β-1,3-glucanase proteins, one α-glucosidase protein, one arabinogalactan protein, one β-glucosidase protein, one EXP protein, and one EXT protein (Table 3.I.S1, Figure 3.I.2B). These data agree with reports published on the expression of genes encoding for cell wall hydrolyzing enzymes associated with olive-fruit abscission (Gil-Amado & Gómez-Jimenez, 2013). Likewise, we recently reported that olive-fruit abscission was correlated with a reduced homogalacturonan methylesterification in the olive AZ (Parra et al., 2020), suggesting that these types of enzymes, 3 PME and 2 PG, may be required in regulating the level of homogalacturonan methylesterification during olive AZ cell separation necessary for abscission.

Here we report that, among all cell wall genes expressed differentially between the two olive tissues, only 22 genes were found to be expressed preferentially in the ripe fruit and 41 genes in the AZ (Table 3.I.S1, Figure 3.I.2A). In this way, although two tissues containing members from several cell wall protein families, in each tissue, a clearly significant difference was found in the proportion of families (Table 3.I.S1, Figure 3.I.2A). We hypothesize that the differences in the bulk of hydrolases and cell-wall-remodeling proteins between olive tissues may reflect differences in cell wall composition in different organs. Moreover, we identified different families of cell wall proteins that are expressed only in AZ (the arabinogalactan protein (AGP), laccase, lyase, endo-β-mannanase, ramnose synthase, XTH families) and families that are regulated only in fruit (the α-galactosidase and β-hexosaminidase families) (Table 3.I.S1, Figure 3.I.2C). Based on expression analyses, we demonstrate that the AGP, laccase, lyase, endo-β-mannanase, ramnose synthase, and XTH families may have a function in cell wall modification related specifically to abscission. The enrichment of

the cell wall protein families in different tissues in combination with data on transcript abundance offer a tenable set of cell wall genes that could be examined in future research.

3.I.3.2. Differential hormonal composition and candidate gene-expression patterns between olive fruit tissues in late development

In olive, although the genomics data have identified hormone-related genes involved in fruit development and abscission processes (Alagna et al., 2009; Alagna et al., 2012; Gil-Amado & Gómez-Jimenez, 2013), the hormonal composition of olive fruit remains to be determined. In previous works, we have reported on the polyamine levels in olive fruit during early development (Cirilli et al., 2017), as well as the 1-aminocyclopropane-1-carboxylic acid (ACC), an ethylene precursor, content (Parra-Lobato & Gómez-Jimenez, 2011) and the polyamine levels in the olive AZ during natural or induced olive-fruit abscission (Gómez-Jimenez et al., 2010b; Gil-Amado & Gómez-Jimenez, 2012).

In the present work, the endogenous levels of indole-3-acetic acid (IAA), gibberellins (GAs), abscisic acid (ABA), jasmonic acid (JA), and salicylic acid (SA) in olive AZ and fruit at last stage of ripening were measured (Figure 3.I.3), while the levels of bioactive free-base cytokinins (CKs) were too low to allow reliable measurement. To our knowledge, this is the first report on the direct measurement of these hormones in olive AZ and fruit. Our results reveal that the total hormonal level was higher in the olive fruit (epicarp and mesocarp) in comparison with the AZ. The highest total hormone level in ripe fruit was due essentially to the highest ABA level. In both olive AZ and ripe fruit tissues, the most abundant hormone was ABA while the least abundant was GA_4, but the ABA and GA_4 levels were higher in the ripe fruit in comparison to the AZ, by 4-fold and 2-fold, respectively (Figure 3.I.3).

A high level of GA_1, the 13-hydroxylated bioactive GA, but not GA_4, the 13-non-hydroxylated bioactive GA, was also detected in the ripe fruit, whereas GA_1 was undetectable in the AZ, indicating the higher activity in the 13-hydroxylated pathway. These results identify GA_1 as the predominant bioactive GA in the olive reproductive organs. Low GA_4 levels were detected in both olive tissues (Figure 3.I.3). By contrast, the profiling of hormone measurement revealed that the IAA and JA levels were higher in the AZ in comparison with the ripe fruit, by 4, and 22-fold, respectively, whereas no significant differences were found in the SA level between olive AZ and ripe fruit (Figure 3.I.3). In olive ripe fruit, it bears noting that the most abundant hormone was ABA,

followed by SA, while, in their AZ, the most abundant hormone was ABA, followed by JA (Figure 3.I.3). Altogether, these results indicate that high ABA and SA contents were found in both olive tissues at late development, and the presence of JA among the major hormones preferentially in the olive AZ.

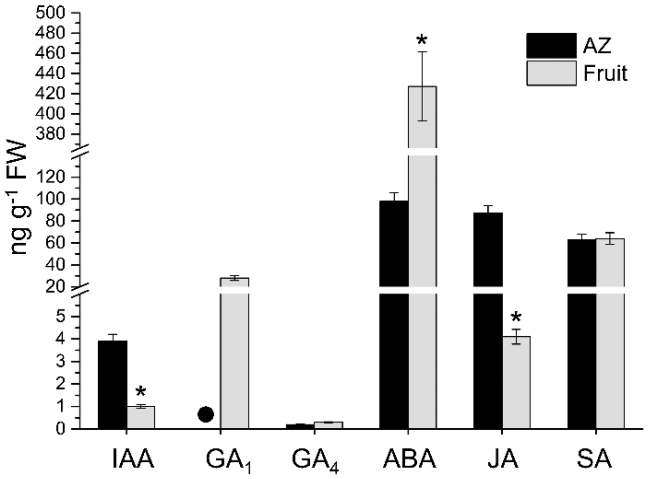

Figure 3.I.3. Profiles of IAA, GA_1, GA_4, ABA, JA and SA levels measured from olive AZ and fruit (pericarp) at the last stage of ripening (217 DPA). Hormone levels not detected are indicated by a black dot (●). Data are the means ±SD of three biological replicates with three technical repeats each. Statistically significant differences based on unpaired Student's *t*-test at $P < 0.05$ are denoted by asterisk.

To determine how gene expression involved in hormone metabolism and signalling correlates with the accumulation of hormone in the olive tissues, we examined the transcriptomic profiling of genes associated with hormone metabolism and signalling in olive fruit and their AZ tissues in late development (217 DPA) through RNA-seq technology. Of 4,391 differentially expressed genes of our pyrosequencing-based approach ($P < 0.01$), 145 genes were related to plant-hormone metabolism and signalling (Figure 3.I.4A, Table 3.I.S2), of which 36 showed a higher expression in the ripe fruit (fruit-enriched transcripts), while 109 were overexpressed in the AZ (AZ-enriched transcripts) (Table 3I.S2). Among the 145 genes, those related to auxin (36 genes), ethylene (35 genes), and ABA (25 genes) were the most represented, followed by those related to JA (15 genes), and GA (14 genes). Few genes related to SA (7 genes),

polyamine (6 genes), brassinosteroid (BR, 5 genes), or CK (2 genes) were found (Figure 3.I.4B, Table 3I.S2).

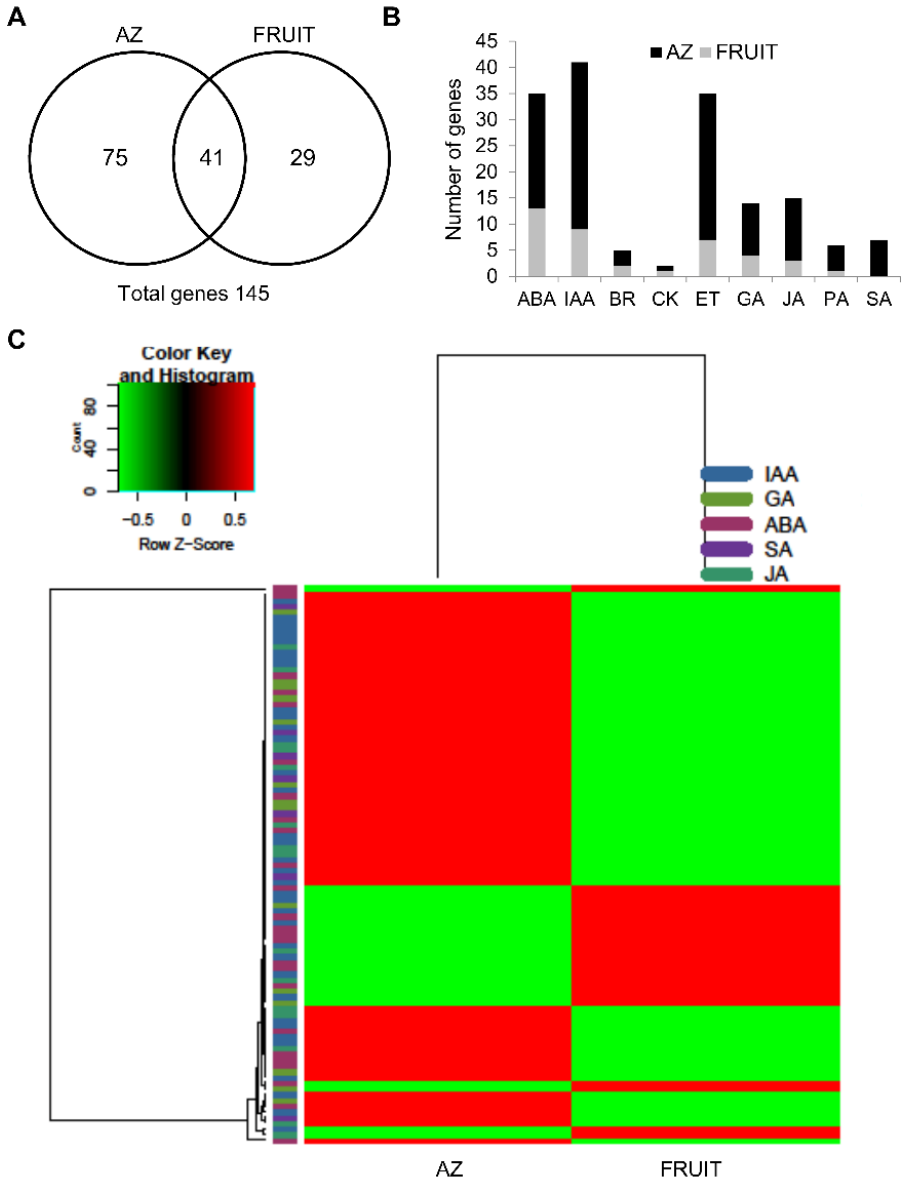

Figure 3.I.4. Differentially expressed hormone-related genes between olive AZ and fruit (pericarp) at the last stage of ripening (217 DPA). **(A)** Overlap of overexpressed fruit genes, and overexpressed AZ genes. This figure shows the number of hormone-related transcripts that were specific and common for each tissue. **(B)** Comparison of significantly overexpressed transcripts (P<0.01) between olive AZ (black) and fruit (gray) at the last stage of ripening. Number of transcripts related to plant hormone in each tissue. **(C)** Heatmap of the expression of differentially expressed genes related to hormone metabolism and signalling in the indicated groups (IAA, GA_1 + GA_4, ABA, SA, JA levels) in olive AZ and fruit at the last stage of ripening. The gene expression of each sample was normalized using the mean expression for each condition. Then, the gene groups were defined in function of hormone relationship. Color codes for expression values are reported on the top. Additional information on the hormones-related genes is presented in Table 3.I.S2.

In particular, a comparison of the 145 hormone-related genes indicated that only 41 genes of these were common in both olive tissues, whereas 29 hormone-related genes were expressed exclusively in ripe fruit (fruit genes), and 75 hormone-related genes were expressed exclusively in their AZ (AZ genes) (Figure 3.I.4A, Table 3I.S2), indicating a tissue-specific regulatory requirement for the expression of these hormone-related genes. Furthermore, we explored the tentatively linking the level of the plant hormones detected to the gene expression involved in their metabolism and signalling in both olive tisssues (Figure 3.I.4C). Taking together the expression analyses and the hormone levels in both olive tissues we built a heat map referring to IAA, GA, ABA, JA and SA (Figure 3.I.4C).

Figure 3.I.5 illustrates the biosynthesis and signalling of plant hormones, and reflects that steps in the pathways of etileno, auxin, ABA, SA, JA, BR, GA, and CK appear to be transcriptionally regulated between olive ripe fruit and their AZ tissues. Notably, among the 145 genes related to plant-hormone, those related to ABA (9 genes) and auxin (9 genes) were the most represented in ripe fruit, whereas those related to ethylene (28 genes) and auxin (27 genes) were the most represented in AZ (Table 3I.S2). *NCED5*, a transcript associated with ABA biosynthesis, was expressed exclusively in ripe fruit (Figure 3.I.5A, Table 3.I.S2). NCED is involved in catalyzing the rate-limiting step in ABA biosynthesis (Taylor et al., 2000). In addition, other transcripts involved in ABA catabolism such as cytochrome P450 *CYP707A*, which encodes ABA 8′-hydroxylase, was expressed exclusively in AZ (Table 3I.S2), consistently with the highest ABA levels detected in olive ripe fruit compared to AZ (Figure 3.I.3). Previously, the downregulation of *NCED5* and upregulation of *CYP707A* genes during abscission in the olive-fruit AZ has been demonstrated (Gil-Amado & Gómez-Jimenez, 2013), suggesting local transcriptional control of the ABA biosynthesis and catabolism rather than transport from other tissues. In the case of auxin, transcripts involved in IAA transport, such as two transcripts encoding auxin influx carrier-like protein 1 (LAX1) and 2 (LAX2), are exclusively overexpressed in olive AZ (Table 3I.S2). This suggests a role in regulating auxin influx and in maintaining auxin sink-strength in this tissue in a manner similar to that of its arabidopsis and tomato orthologs, AtLAX3 and SlLAX3, which have been shown to create cell-specific auxin sinks (Vandenbussche et al., 2010; Pattison & Catalá, 2012). This is consistent with previous studies on abscission, in which genes encoding for protein homologs of this family were found to be up-regulated (Gil-

Amado & Gómez-Jimenez, 2013; Meir et al., 2010; Zhu et al., 2011; Corbacho et al., 2013). In addition, two different transcripts encoding auxin efflux carrier are overexpressed in the AZ or in fruit (Table 3I.S2), indicating altered auxin distribution in these tissues in late development.

In the case of SA, the mRNA for PAL1, which are associated with the SA biosynthesis, was exclusively up-regulated in AZ (Figure 3.I.5B, Table 3I.S2), but SA levels were not significantly different between AZ and ripe fruit, whereas transcripts for some GA biosynthetic enzymes components such as GA 20-oxidase (GA20ox), involved in a late GA biosynthetic step, were enriched exclusively in ripe fruit (Figure 3.I.5A, Table 3I.S2), consistently with the highest GA levels detected in olive ripe fruit compared to AZ. Conversely, *GA2ox5*, a transcript involved in the deactivation of bioactive GAs, was expressed exclusively in AZ (Figure 3.I.5, Table 3I.S2), implying that GA2ox dominantly functions in the AZ, while different transcripts, *GGPS1* and *GGPS2*, for geranylgeranyl pyrophosphate synthase (GGPS), which is involved in an early GA biosynthetic step, were overexpressed in olive fruit (*GGPS1*) or AZ (*GGPS2*) (Figure 3.I.5, Table 3I.S2). The expression of early GA synthesis genes at a low level in the AZ implies that GA may not be actively synthesized in the AZ. These results suggest that GA20ox is the major late-step enzyme responsible for the high level accumulation of GA_1 detected in ripe fruit, whereas the complete absence of GA_1 observed in the AZ may be attributed to the expression of *GA2ox* gene. Moreover, of the 5 differentially expressed genes involved in JA biosynthesis, 4 genes show increased transcript abundance in AZ compared to fruit in good agreement with the highest JA content in the AZ (Figure 3.I.4B, Table 3I.S2). These results indicate that JA may be actively synthesized in the AZ.

On the other hand, several transcripts related to hormonal metabolism were also differentially expressed between olive ripe fruit and AZ tissues, such as genes encoding putative methylesterases, which can hydrolyze MeJA, MeSA, and MeIAA (Table 3.I.S2, Figure 3.I.5). However, transcript levels for some auxin-conjugating enzymes, such as GH3.3, were found to be exclusively expressed in AZ (Table 3.I.S2), which it is consistent with previous studies where *GH3.3* expression is induced during ripe fruit abscission in olive and melon (Gil-Amado & Gómez-Jimenez, 2013; Corbacho et al., 2013). Bioactive forms of CKs are in turn deactivated by CK oxidase/dehydrogenase (CKX), thereby regulating the amount of bioactive CK (Sakakibara et al., 2006). In the

present study, *CKX* gene expression is found exclusively in the ripe fruit, suggesting that the deactivation of CK may actively occur specifically in ripe fruit (Figure 3.I.5A, Table 3.I.S2).

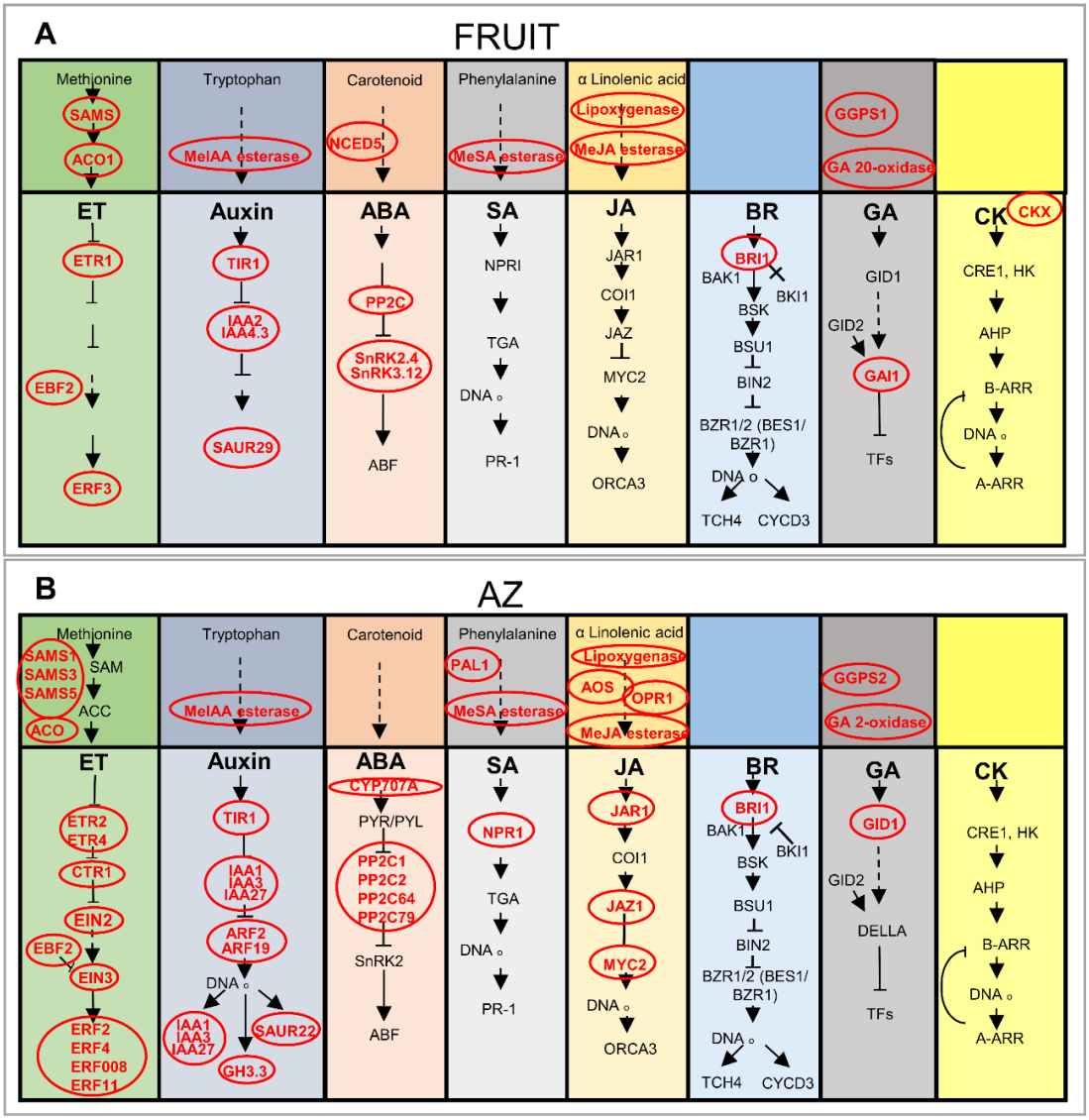

Figure 3.I.5. Simplified schematic representation of the hormone metabolism and signalling pathways in AZ and fruit at the last stage of ripening in olive (217 DPA). **(A)** Fruit-enriched genes encoding various hormone proteins at 217 DPA (P<0.01). **(B)** AZ-enriched genes encoding various hormone proteins at 217 DPA (P<0.01). Genes with elevated mRNA levels are in red typeface (ET = Ethylene). Additional information on the hormone-related genes is presented in Table 3I.S2.

Additionally, our data indicate that numerous genes encode key players related to the ethylene pathway (Table 3.I.S2, Figure 3.I.5). Both ripe fruit and AZ tissues are apparently characterized by an active ethylene biosynthesis at the transcriptional level.

In particular, one S- adenosylmethionine synthase (*SAMS*) gene and one ACC oxidase (*ACO1*) gene were overexpressed in the ripe fruit (Figure 3.I.5A, Table 3.I.S2), while 3 different *SAMS* genes (*SAMS1*, *SAMS3*, *SAMS5*) were up-regulated in the AZ compared to the ripe fruit, and one different *ACO* gene was expressed exclusively in the AZ (Figure 3.I.5B, Table 3.I.S2). Previously, our pyrosequencing data indicated higher olive AZ expression of ethylene-related genes for the SAMS, ACS, and ACO during ripe fruit abscission (Gil-Amado & Gómez-Jimenez, 2013).

The present analysis also detected the differential expression of many genes involved in plant-hormone signalling between ripe fruit and AZ tissues (Figure 3.I.5, Table 3.I.S2). Genes specifying auxin signalling components (IAA2, IAA4.3 and SAUR29) as well as ABA signalling components (PP2C, SnRK2.4, and SnRK3.12) had also raised RNA levels in ripe fruit (Figure 3.I.5B, Table 3.I.S2), while others (IAA1, IAA3, IAA27, ARF2, ARF19, SAUR22, GH3.3, PP2C1, PP2C2, PP2C64 and PP2C79) were overexpressed in AZ. In particular, the specific expression of some *ARF* (*ARF2* and *ARF19*) and *IAA/AUX* (*IAA1*, *IAA3*, *IAA27*) genes in the AZ suggests that ARF2 and ARF19 are involved in the abscission of ripe fruit. Functional studies of ARF2, ARF1, ARF7, and ARF19 suggest that these transcription factors act with partial redundancy to promote senescence and floral abscission (Ellis et al., 2005). Similarly, our previous data indicate that two families of early auxin-responsive genes, IAA27 and GH3.3, which contain a binding motif to the ARF transcription factor, are up-regulated during induction of ripe fruit abscission, whereas one *SAUR1* gene is down-regulated during olive ripe fruit abscission (Gil-Amado & Gómez-Jimenez, 2013). In addition, transcript abundance of putative ABA signalling gene, *ABA-INSENSITIVE 2* (*ABI2*), proved significantly lower in ripe fruit compared to AZ (Table 3I.S2). *ABI2* encodes a member of the 2C class of protein serine/threonine phosphatases (PP2C), which is a negative regulator of ABA responses (Leung et al., 1998). Among fruit-enriched transcripts, *SnRK2.4*, and *SnRK3.12* were exclusively expressed in ripe fruit (Table 3.I.S2). Thus, these differences in auxin- and ABA-related responses suggest that the auxin signalling is more active in the AZ than in ripe fruit, while the ABA signalling is more active in the ripe fruit than in the AZ. In the case of GA, the mRNA for GAI1 (DELLA protein), was also up-regulated in ripe fruit, suggesting that GA signalling is negatively regulated by GAI in ripe fruit. In contrast, some transcripts for SA and JA signalling markers were down-regulated (*NPR1*, *JAR1*, *JAZ1* and *MYC2*) in ripe fruit (Figure

3.I.5A, Table 3.I.S2), whereas they were overexpressed in AZ (Figure 3.I.5B, Table 3.I.S2), suggesting that NPR1, JAR1, JAZ1 and MYC2 may have functions in the AZ cell separation.

The gene profiling data also showed that *ETR1*, and *ERF3* transcripts, which are markers for the ethylene response, were up-regulated in ripe fruit (Figure 3.I.5A, Table 3I.S2), whereas others (*ETR2*, *ETR4*, *CTR1*, *EIN2*, *EIN3*, *ERF2*, *ERF4*, *ERF008* and *ERF11*) were up-regulated in the AZ (Figure 3.I.5B, Table 3I.S3). This is consistent with previous studies where the expression of some *ETR2*, *ETR4*, *CTR1*, *EIL2 (EIN3/EIL)*, and *ERF4* genes are induced during ripe fruit abscission (Parra-Lobato & Gómez-Jimenez, 2011; Gil-Amado & Gómez-Jimenez, 2013). The ERFs are the main mediators of ethylene dependent gene transcription. In apple, ERF3 promotes, whereas ERF2 represses, the expression of *ACS1* (Li et al., 2017). In the tomato genome, 27 ERFs show enhanced expression at the onset of ripening while 28 ERFs display a ripening associated decrease in expression, suggesting that different ERFs may have contrasting roles in fruit ripening (Liu et al., 2016). Here, our results suggest that different ERFs could be involved in triggering the transcriptional cascade in the AZ (ERF2, ERF4, ERF008 and ERF11) or in the ripe fruit (ERF3). Thus, our study demonstrates the induction of the ethylene signalling pathway in both olive tissues via different components.

Up-regulation of BR signalling was unexpected in both olive tissues (Figure 3.I.5, Table 3I.S2). The present work shows that different transcripts encoding BRI1 receptor kinase were up-regulated in AZ and ripe fruit (Figure 3.I.5, Table 3I.S2), suggesting that the up-regulation of receptor BRI1 may be required for complete AZ cell separation in olive.

We used qRT-PCR to verify induction of the ethylene and ABA signalling pathways in both tissues via different components, and up-regulation of the SA and JA signalling pathways in the AZ. In addition, we examined the expression of this set of hormone response genes (*OeERF3*, *OeERF4*, *OeSNRK2.4*, *OeNPR1*, and *OeJAR1*) by qRT-PCR in olive AZ and ripe fruit (Figure 3.I.6). The qRT-PCR analysis confirmed the enrichment of *OeERF3*, and *OeSNRK2.4* genes in ripe fruit and the enrichment of *OeERF4*, *OeNPR1*, and *OeJAR1* genes in the olive AZ.

3.I.3.3. Vesicle trafficking differential gene expression between olive ripe fruit and AZ.

Previously, we have reported that endocytosis, visualized by staining with fluorescent dye FM4-64, was strongly stimulated in AZ during olive ripe fruit abscission (Parra-Lobato et al., 2017), suggesting that endomembrane trafficking probably modulates cell wall modifications during olive fruit abscission. Deposition changes in cell-wall material involve vesicle formation and transport, this being reflected by a high number of up-regulated genes found in ripe fruit and AZ tissues in olive (Figure 3.I.7, Table 3I.S3). In particular, the Rab GTPase is a key component of the membrane trafficking machinery that regulates the targeting and tethering of trafficking vesicles to target compartments by acting as a molecular switch cycling between active and inactive states (Lycett, 2008; Ito et al., 2018; Minamino & Ueda, 2019). However, little is known about Rab-GTPases comparing the transcriptomic responses between fruit and their AZ. Here, among the 24 Rab-GTPases identified in our analysis, 14 Rab-GTPases were up-regulated in ripe fruit and 10 Rab-GTPases in fruit AZ (Figure 3.I.7, Table 3I.S3), indicating that at least some members of Rab-GTPases play major roles in secretion and/or recycling of cell wall components in these olive-fruit tissues in late development.

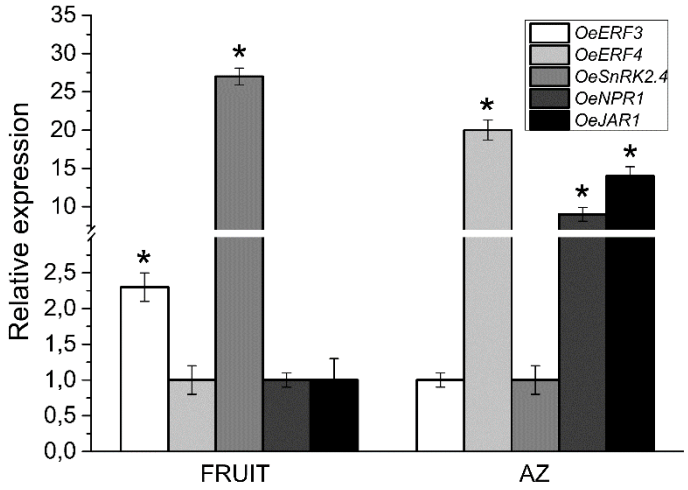

Figure 3.I.6. Expression of *OeERF3*, *OeERF4*, *OeSNRK2.4*, *OeNPR1*, and *OeJAR1* in AZ and fruit at the last stage of ripening (217 DPA) in olive. Data are the means ±SD of three biological replicates with three technical repeats each and were determined by qRT-PCR normalized against *Olea europaea* ubiquitine. Statistically significant differences based on unpaired Student's *t*-test at $P < 0.05$ are denoted by asterisk.

We identified different classes of Rab-GTPases genes that are regulated only in the AZ (the arabidopsis RabC, RabE and RabG clades), in both AZ and fruit (the arabidopsis RabA and RabF clades), or only in the fruit (the arabidopsis RabB, RabD and RabH clades) (Table 3I.S3). 5 Rab11 (corresponding to the arabidopsis RabA clade, gene Identifier AT5G47960.1, AT1G09630.1, AT5G60860.1, AT3G15060.1, and AT5G65270.1 putative orthologs), 3 Rab2 (corresponding to RabB, AT4G35860.1, AT1G02130.1, and AT4G17170.1), 1 Rab1 (corresponding to RabD, AT1G02130.1), 2 Rab5 (corresponding to RabF, AT5G45130.1 and AT4G19640.1) and 2 Rab6 (corresponding to RabH, AT1G18200.1 and AT2G44610.1) genes from olive showed a higher expression in ripe fruit (Figure 3.I.7A, Table 3.I.S3) compared to the AZ, while for 4 Rab11 (corresponding to RabA, putative ortholog AT1G06400.1, AT2G43130.1, AT1G09630.1, and AT1G07410.1), one Rab18 (corresponding to RabC, AT5G03530.1), one Rab8 (corresponding to RabE, AT3G46060.3), one Rab5 (corresponding to RabF, AT3G54840.1) and 2 Rab7 (corresponding to RabG, AT3G18820.1 and AT4G09720.1) genes from olive a higher number of average reads per sample was detected in the AZ (Figure 3.I.7B, Table 3.I.S3).

Of these classes of Rab-GTPases, two (Rab11/RabA and Rab18/RabC) expressed preferentially in apple, peach, and tomato fruits during the final ripening stages (Minamino & Ueda, 2019; Falchi et al., 2010; Lawson et al., 2018). Therefore, these Rab GTPase classes apparently share major trafficking elements related to the cell wall modification in ripe fruit. On the other hand, the Rab5/RabF and Rab7/RabG classes in olive have been determined to be specific to ripe fruit abscission (Gil-Amado & Gómez-Jimenez, 2013). Particularly, the up-regulation of the genes *RabA2A*, *RabA2B*, and *RabA5C* in the AZ of olive during ripe fruit abscission suggests that at least some RAB11 genes play a key part in recycling and/or secretion of cell-wall components in the process of ripe fruit abscission (Gil-Amado & Gómez-Jimenez, 2013). This contention agrees with our prior results demonstrating the up-regulation of genes *RabA2A*, *RabA2B*, and *ARA6* as well as the down-regulation of the *RabH1B* gene in melon AZ during ripe fruit abscission (Parra et al., 2020). Thus, these constitute different classes of Rab-GTPase protein and therefore would presumably regulate either transport to the plasma membrane and the cell wall, exocytosis from the trans-Golgi network, or vacuolar trafficking of these tissues in late development.

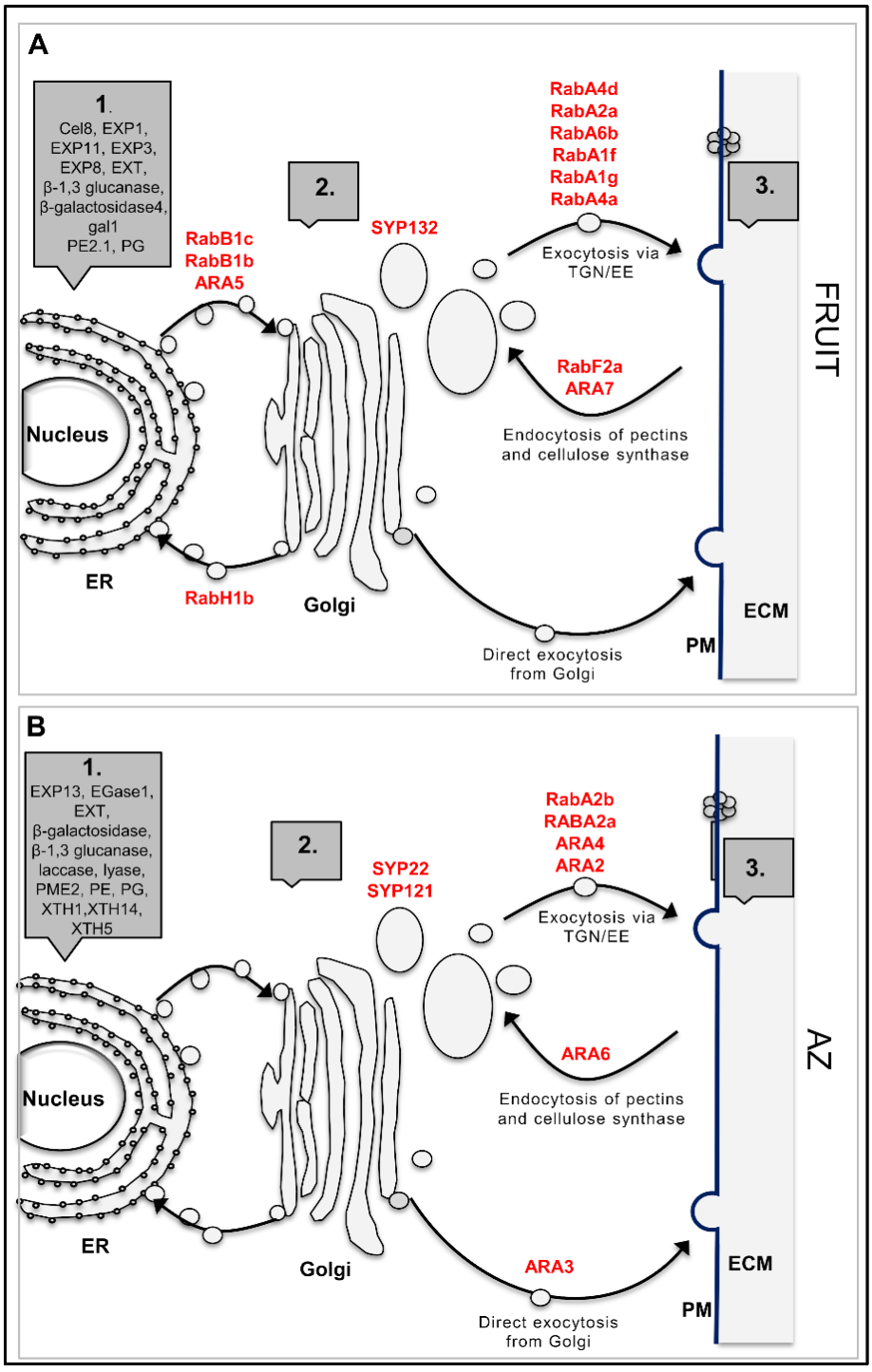

Figure 3.I.7. Simplified schematic representation of the trafficking pathways to and from the cell wall of olive fruit **(A)** and AZ **(B)** at the last stage of ripening. The Rab-GTPases probably involved at each step are indicated in red (up-regulated). 1, Synthesis of proteins in endoplasmic reticulum (ER). 2, Synthesis of matrix polysaccharides and assembly of proteins in Golgi and TGN/EE (the trans-Golgi network and early endosomal compartments). 3, Modification of wall elements by secreted enzymes. Pathways to and from the vacuole have been omitted for simplicity. Additional information on the vesicle-trafficking-related genes is presented in Table 3I.S3. (ECM: equivalent to the "cell wall" or "apoplast"; PM: plasma membrane).

Notably, our data reveal that the ARA6 (RabF1) gene is expressed exclusively in the AZ (Figure 3.I.7B, Table 3.I.S3), this being consistent with previous findings, where the expression of some ARA6 genes was induced in the AZ during fruit abscission (Gil-Amado & Gómez-Jimenez, 2013; Corbacho et al., 2013), whereas ARA7 gene is exclusively expressed in the fruit (Figure 3.I.7A, Table 3I.S3), indicating that transcript levels of ARA6 and ARA7 genes, which regulate endocytic and vacuolar trafficking pathways, are regulated in a tissue-specific manner.

In addition, the synthaxin genes, SYP121 and SYP132 (t-SNARE family), related to ABA-responsive secretion (Leyman et al., 2000; Takemoto et al., 2018), were also up-regulated exclusively in AZ and ripe fruit, respectively. In relation to this, synthaxin SYP121, involved in the regulation of SA and JA (Zhang et al., 2008), is upregulated during ripe fruit abscission in olive and melon (Gil-Amado & Gómez-Jimenez, 2013; Corbacho et al., 2013). Moreover, the synthaxin SYP22, which is required for vacuolar assembly (Carter et al., 2004), is also up-regulated in the AZ (Figure 3.I.7B, Table 3I.S3). Previous work has shown that a strong induction of *ARA6* in the AZ during olive fruit abscission in parallel with the upregulation of *SYP121* and *SYP22* syntaxins, implying the involvement of ARA6 in the trafficking pathway to modulate ripe fruit abscission in olive, and a possible involvement of SYP121 and SYP22 in a common process (Gil-Amado & Gómez-Jimenez, 2013). ARA6 putatively act in a trafficking route that counteracts endocytic trafficking from the endosomes to the vacuoles, where SYP22 fulfills a positive regulatory role. On this basis, it might be asked whether this SYP132 protein plays an essential part together with some of the different up-regulated Rab-GTPases in olive fruit for the transport of proteins and membrane through the endomembrane system to their destination, and whether this transport plays a critical role in mediating plant-hormone signals in ripe fruit.

In this study, some members of Rho GTPase family were also identified (Table 3.I.S3). One gene homologous to MIRO1, which has evolved to regulate mitochondrial trafficking, and one gene homologous to ARAC5 were exclusively transcribed in the AZ, whereas one gene homologous to RAC3 is exclusively transcribed in ripe fruit. Additionally, our data demonstrate that one member of Ran GTPase family homologous to Ran3 (Haizel et al., 1997), involved in the nuclear translocation of proteins in arabidopsis, is up-regulated in the AZ (Table 3I.S3), as previously reported for ripe fruit abscission (Gil-Amado & Gómez-Jimenez, 2013), strengthening the possibility that that

they may help mediate nucleocytoplasmic transport during fruit abscission signalling. Of particular interest is also one member of Sar1 GTPases family, homologous to SAR2 (Takeuchi et al., 2000), which was expressed exclusively in ripe fruit (Table 3I.S3).

Therefore, our results indicate that genes encoding members of small-GTPase Arf and Sar families were exclusively transcribed in ripe fruit. By contrast, small-GTPase genes encoding members of Ran family were exclusively transcribed in the AZ. These results raise the possibility that the Rabs, Rhos, and Ran families of small-GTPases may act in vesicle trafficking in the AZ, while ripe fruit is enriched in the Rabs, Rhos, Arfs, and Sar1 families of small-GTPase, suggesting that Rabs- and Rhos-GTPase families may act in vesicle trafficking in both olive tissues at late development. Moreover, 3 classes of the Rab family, i.e. RabB, RabD and RabH, have been found to be preferentially expressed in the ripe fruit, whereas the classes RabC, RabE, and RabG have been found to be preferentially expressed in olive AZ. Other genes noticeably present in AZ and ripe fruit involved in vesicle trafficking, encode V-type ATPases, called midasins (Table 3I.S3), which were involved in trafficking from the trans-Golgi Network to the central vacuole. Thus, these data provide novel information about small-GTPases in late development, suggesting that vesicular trafficking may regulate fruit and AZ cell wall modifications in late development.

3.I.3.4. Global expression profiling of transport protein genes

Of 4,391 differentially expressed genes, 138 genes related to transport were differentially expressed in olive AZ compared to ripe fruit ($P < 0.01$). Of these genes, 48 genes had peak read amounts in fruit (the set of fruit-induced genes), and 90 genes in AZ (the set of AZ-induced genes) tissues (Figure 3.I.8, Table 3.I.S4). Thus, the majority of these were induced in the AZ (Figure 3.I.8, Table 3.I.S4).

Among the 48 genes enriched in ripe fruit, 31 were exclusively expressed in fruit (Table 3I.S4). The 31 genes encode 3 sugar transporter, 4 N transporter, 3 aquaporin, 4 nutrient transporter, 2 metal ion transporter proteins, and one ATP-binding cassette (ABC) transporter family protein, whereas our analyses have revealed that of 90 transport-related genes induced in the AZ, 75 genes (11 sugar transporter, 20 N transporter, 3 aquaporin, 22 nutrient transposter, 9 metal ion transporter proteins, and 10 ABC transporter family proteins) are exclusively expressed in the AZ (Figure 3.I.8, Table 3.I.S4), indicating that transporters play special roles in the tissue-specific

characteristics of olive ripe fruit. Among these latter proteins, one ERD6 sucrose transporter was upregulated during ripe fruit abscission, whereas one hexose carrier protein HEX6 was downregulated during ripe fruit abscission in olive (Gil-Amado & Gómez-Jimenez, 2013). In addition, of AZ-enriched genes related to nutrient transport in our analysis, 3 are associated with sodium/hydrogen exchangers, 3 cation-transporting ATPases, two nitrate transporters, two potassium transporters, two phosphate transporters, one MATE citrate transporter, one sulfate transporter, one boron transport, and one arsenite transport protein, whereas 3 cation-transporting ATPases, 3 2-oxoglutarate/malate translocator proteins, 2 copper transporters, 2 sulfate transporters and one phosphatidylinositol transporter were induced in ripe fruit, indicating that most of these transporter genes were preferentially expressed in AZ (Figure 3.I.8, Table 3.I.S4). Thus, function enrichment analysis of these genes at the tissue level shows that there are more enriched functions in the AZ than in the pericarp of olive fruit at last stage of ripening, when fruit abscission occurs.

No previous study has been focused on the nutrient transport between olive fruit tissues. In Citrus (*Citrus* spp.), it has been shown that the different flesh-rind transport of nutrients and water due to the anatomic structural differences among citrus varieties might be an important factor that influences fruit senescence behavior (Ding et al., 2015).

Our results appear to reflect differences in nutrient transport between AZ and pericarp tissues of olive fruit at last stage of ripening. For example, the AZ transport results mainly accomplished by the gene activity of nitrate, boron, potassium, and phosphate transporters, and the fruit-pericarp transport by copper transporter, whereas the transport of sulfate and calcium are associated with both olive tissues in late development. Therefore, our results corroborate previous works identifying nitrate and boron transporters as being induced in olive and melon fruit AZ during abscission (Gil-Amado & Gómez-Jimenez, 2013; Corbacho et al., 2013). Based on our data, we suggest that, for the AZ of ripe fruit, these changes could be associate with nutrient re-mobilization prior to abscission. Previous studies have shown that increased ethylene production may be involved in modulating nitrate transporters (Tian et al., 2009) and nitrate metabolism (Leblanc et al., 2008) at high nitrate levels. In the plant, nitrate can serve as a signalling molecule in an array of physiological processes and environmental responses (Fan et al., 2017; Zhang et al., 2018), but the role in abscission played by

nitrate has received little attention. Further studies are needed to explore the exact roles of these transporters in the regulation of olive fruit abscission.

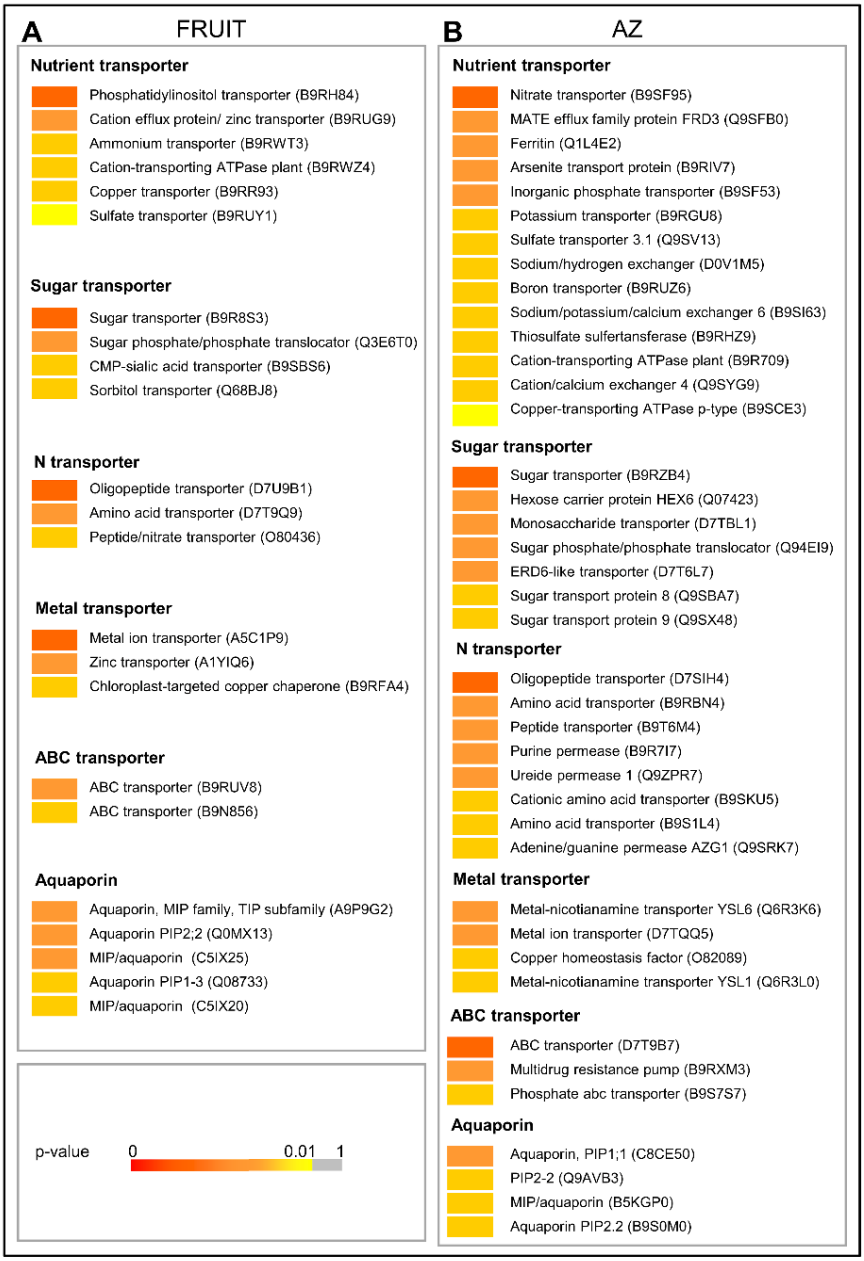

Figure 3.I.8. Expression profiling of **(A)** fruit- or **(B)** AZ- enriched genes related to transport as reconstructed from the pyrosequencing transcriptomes. Sequence transcripts showing significant variations (P<0.01). p-values are visualized in a color-code scale. Additional information on the transport-related genes is presented in Table 3I.S4.

Among differentially expressed genes, we also detected 26 genes related to nitrogen transport and enriched in AZ, different cationic amino acid transporters, amino acid transporters, oligopeptide transporters, purine permeases, one PTR2/POT transporter,

peptide transporters, and one ureide permease (UPS1), among others (Table 3I.S4). Meanwhile, three other amino acid transporters, 7 other oligopeptide transporters and one peptide/nitrate transporter (At2g38100) were overexpressed in ripe fruit (Table 3I.S4). ABC transporter family proteins were also accumulated abundantly in the AZ (Figure 3.I.8, Table 3.I.S4). Among these, 6 encode multidrug resistance-associated protein, known as the ABC transporter of the B class (ABCB) protein, which functions in auxin transport across plant species (Cho & Cho, 2013; Theodoulou & Kerr, 2015; Hwang et al., 2016). At same time, two other ABC transporters are overexpressed in fruit. Thus, the present study provides information for identifying candidate channel and transporter genes possibly involved in a transporter-mediated transportation process from the fruit to the AZ.

3.I.4.Materials and Method

3.I.4.1. Plant material

In an orchard near Badajoz (Spain), 20-year-old olive trees (*Olea europaea* L. cv. Picual) grown under drip irrigation and fertirrigation (irrigation with suitable fertilizers in the solution) were studied. Picual olive flowers were tagged on the day of pollination and the fruit pericarp (fruit mesocarp and epicarp) and fruit-AZ samples were collected from olive fruits subsequently harvested at last stage of ripening (217 DPA), at which time they abscise (Parra-Lobato et Gómez-Jimenez, 2011; Parra et al., 2013). The fruit AZs, located between the pedicel and fruit, were manually dissected from longitudinal sections of the samples with a razor blade into pieces to a maximum width of 1 mm on each side of the abscission fracture plane (Figure 3.I.1). Fresh samples (fruit-pericarp and fruit-AZ at 217 DPA), using 300 fruits, were immediately frozen in liquid nitrogen and stored at -80°C for RNA isolation. For examination of the proximal and distal fracture planes of the fruit AZ by scanning electron microscopy (SEM), following critical-point drying, tissues were mounted onto steel stubs, coated with gold-palladium, and viewed using a LEO 1430 VP scanning electron microscope (Gomez-Jimenez et al., 2010b; Corbacho et al., 2013).

3.I. 4.2. RNA isolation

Total RNA and cDNA synthesis were extracted and purified from fruit-pericarp (mesocarp and epicarp) and-AZ tissues at 217 DPA as detailed in (Parra et al., 2013).

3.I. 4.3. Library preparation for pyro-sequencing

Three micrograms of each cDNA sample were nebulized to produce fragments of a mean size between 400 and 800 bp. Preparation of cDNA fragment libraries and emulsion PCR conditions were performed as described in the Roche GS FLX manual. Pyro-sequencing was performed on a Roche Genome Sequencer FLX instrument (454LifeScience-Roche Diagnostics, http://www.454.com/) at Lifesequencing S.L. (Valencia, Spain). Trimming and assembly of pyro-sequenced reads and annotation were performed as described (Parra et al., 2013).

3.I. 4.4. Quantification of the expression levels

The reference proteins were proteins representative of UniRef90 clusters. This strategy fixed a minimum similarity distance between reference proteins and was the basis of our clustering of isotigs for obtaining unigenes and quantifying their expression levels. The name of each unigene was inferred from the name of the UniRef90 representative proteins that annotated each unigene. We quantified the expression for these unigenes, defined here as clusters of isotigs annotated by the same reference protein. The number of reads assigned to each isotig was calculated taking into account that the reads of each contig were counted only one time. Given that isotigs represent transcribed isoforms, different isotigs sharing some contigs could possibly be clustered within the same unigene. In those cases, the reads of each contig was counted only one time. The normalization of the absolute values of the number of reads was done based on (Mortazavi et al., 2008). We obtained the RPKM (Reads Per Kilobase of exon model per Million mapped reads). In this case, we used the length of the reference protein in nucleotides since we were working without a reference genome and then without exon models. This normalization allows the comparison of the expression values between unigenes from the same or from different simples (Parra et al., 2013).

3.I. 4.5. Differential expression analysis

The method used for the analysis of differential expression in this work was edger (Robinson et al., 2010), a Bioconductor package for differential expression analysis of digital gene-expression data able to account for biological variability. EdgeR models count data using on overdispersed Poisson model and use an empirical Bayes procedure to moderate the degree of over-dispersion across genes. For the analysis of the

differential expression with Edge R the input was a table of counts, with rows corresponding to genes/proteins and columns to samples. EdgeR models the data as negative binomial (NB) distributed, Ygi~NB (Mipgj, Φg) for gene g and sample i. Here Mi is the library size (total number of reads), Φg is the dispersion, and pgj is the relative abundance of gene g in experimental group j to which sample i belongs. The NB distribution reduces to Poisson when Φg = 0. In this work, an isotig was considered differentially expressed when it exhibited highly significant difference in read abundance at $P < 0.01$. The heatmap was drawn using gplots library of R platform and cluster evaluation were defined using Silhouette estimator (Maechler et al., 2019).

3.I. 4.6. Quantification of plant hormones

A pool of 100 mg fresh weight of samples was used for each measurement, and divided into three independent biological replicates. Quantification of plant-hormones was performed as described by (Seo et al., 2011). Aliquots of lyophilized material were extracted with 80% methanol-1% acetic acid. Deuterium-labeled hormones (purchased from Prof. L Mander- Canberra, OlChemim Ltd-Olomouc, or Cambridge Isotope Lab-Andover): [17,17-^{2}H]GAn, [$^2H_5$]IAA and [$^2H_6$]ABA were added as internal standards for quantification SA and ABA. For quantification of JA the compound dhJA was used instead. For collecting the acids fraction containing, SA, ABA, and JA, the extracts passed consecutively through HLB (reverse phase), MCX (cationic exchange) and WAX (ionic exchange) columns (Oasis 30 mg, Waters). The final residue was dissolved in 5% acetonitrile-1% acetic acid, and the hormones were separated by reverse phase UPHL chromatography (2.6 µm Accucore RP-MS column, 100 mm length x 2.1 mm i.d.; ThermoFisher Scientific) with a 5 to 50% acetonitrile gradient. The hormones were analyzed by electrospray ionization and targeted-SIM using a Q-Exactive spectrometer (Orbitrap detector; ThermoFisher Scientific). The concentrations of hormones in the extracts were determined using embedded calibration curves and the Xcalibur 4.1 SP1 build 48 and TraceFinder programs.

3.I.4.7. Quantitative RT-PCR

Total RNA (2 µg) was reverse-transcribed with random hexamers and Superscript III (Invitrogen), according to the manufacturer's instructions. Purified cDNA (2 ng) was used as a template for quantitative RT-PCR (qRT-PCR). qRT-PCR assays were

performed with gene-specific primers (Table 3I.S5). The cDNA was amplified using SYBRGreen-PCR Master kit (Applied Biosystems, Foster City, CA, USA) containing an AmpliTaq Gold polymerase on an iCycler (BioRad Munich, Germany), following the protocol provided by the supplier. Samples were subjected to thermal cycling conditions of DNA polymerase activation at 94°C, 45 s at 55°C, 45 s at 72°C, and 45 s at 80°C; a final elongation step of 7 min at 72°C was performed. The melting curve was designed to increase 0.5°C every 10 s from 62°C. The amplicon was analyzed by electrophoresis and sequenced once for identity confirmation. Also, qRT-PCR efficiency was estimated via a calibration dilution curve and slope calculation. Expression levels were determined as the number of cycles needed for the amplification to reach a threshold fixed in the exponential phase of the PCR (CT). The data were normalized for the quantity of *Olea europaea* ubiquitin (*OeUB*) gene (Gómez-Jimenez et al., 2010). Duplicates from three biological replicates were used in two independent experiments.

3.I.5. Conclusions

In summary, our comprehensive analyses of differential gene expression combined with analysis of differential hormonal composition revealed the unique and common gene signatures between olive fruit tissues in late development. Data here reported represent a significant contribution to the elucidation of transcriptional networks related to cell wall modification, plant hormone, vesicle trafficking and ion fluxes in the AZ and the pericarp of olive fruit at last stage of ripening. Particularly noteworthy are data related to hormones, indicating the complexity of the role played by these compounds in these adjacent tissues. Furthermore, our data reveal that the olive ripe fruit-pericarp was found to be rich in ABA, SA and GA_1, whereas the fruit AZ at the last stage of ripening, when fruit abscission occurs, was enriched mainly in JA. In addition, by qRT-PCR analysis, we confirmed the mRNA-Seq results for five hormone signalling genes, and the induction of the ethylene signalling pathway in both olive tissues via different components. The transcriptomic patterns in AZ and pericarp of olive ripe fruit offer new insights about hormonal and vesicle trafficking regulation potentially involved in cell wall modifications.

3.II.

Impact of sphingolipids on fruit abscission in olive using pharmacological and transcriptomic approaches

3.II. Impact of sphingolipids on fruit abscission in olive using pharmacological and transcriptomic approaches

3.II.1. Abstract

In the olive (*Olea europaea* L.), an economically leading oil crop worldwide, the regulation of fruit abscission constitutes an agricultural problem because of the yield losses in certain cultivars of olive due to the resistance of fruit to release during harvest, a feature that hampers mechanical collection. Recent studies have revealed that olive fruit abscission resulted in quantitative and qualitative changes in sphingolipid long chain bases (LCBs) in the abscission zone (AZ), demonstrating a specific association between the dihydroxylated LCB sphinganine (d18:0) and the olive fruit abscission. In fact, experiments in field showed that sphinganine treatment induced selective olive fruit abscission, without provoking tree defoliation (patent awarded: ES 2 612 728). However, the impact of this treatment at the molecular level remains unknown. The present study investigates the possible role of sphingolipids in olive fruit abscission using pharmacological and transcriptomic approaches. For this, transcriptional and hormonal changes characterizing the fruit AZ and the leaf AZ were analyzed during d18-induced fruit abscission in olive of the cv. 'Manzanilla Sevillana'. Analysis of gene-expression from these AZs revealed that a differential induction of cell-wall-degrading genes is associated with the upregulation of genes involved in ion fluxes, and a shift in plant-hormone metabolism and signalling genes during d18:0-induced fruit abscission. Moreover, *NCER2* and *NCER3* genes that encode enzymes for neutral ceramidase, and *KCS4* and *KCS12* for 3-ketoacyl-CoA synthase were strongly expressed in the fruit AZ and downregulated in the leaf AZ in response to d18:0 treatment, supporting the hypothesis that the homeostasis between LCB and ceramide plays an important role in the execution of fruit abscission in olive. This is accompanied by transcriptional activity of membrane receptor kinases (HSL1, which recognizes a family of IDA/IDL signalling peptides to control cell separation processes, and BAM1), and rapid alkalinization factor (RALF) potentially involved in d18:0-induced fruit abscission signalling. Overall, the data provide a comprehensive

view on selective fruit abscission in response to d18:0 treatment, identifying candidate genes and pathways associated with d18:0-induced fruit abscission in AZ cells. Our comprehensive gene-expression profile, together with hormonal regulators, will help clarify gene regulatory networks during d18:0-induced fruit abscission in olive AZ cells.

Keywords: abscission, fruit detachment force, olive, mechanical harvesting, sphingolipid, transcriptomic comparative

3.II.2. Introduction

Sphingolipids are recognized as critical components of the plant plasma membrane and endomembrane system (Chen et al., 2009; Li et al., 2016; Luttgeharm et al., 2016; Michaelson et al., 2016; Mamode Cassim et al., 2020). These are important structural elements of plant membranes, contributing to its fluidity and biophysical order. Sphingolipids are also involved in multiple cellular and regulatory processes including vesicle trafficking, plant development and defence (Ali et al., 2018; Huby et al., 2020; Liu et al., 2021). The term sphingolipid covers lipids whose defining component is a long-chain or sphingoid base (LCB). The LCB is a carbon aminoalcohol backbone commonly of 18 carbons that is synthesised by the condensation of serine and palmitoyl-CoA catalysed by serine palmitoyl transferase (SPT) in the endoplasmic reticulum (Chen et al., 2006). The product of this reaction, 3-ketosphinganine, is then reduced by the action of the 3-ketosphinganine reductase to sphinganine (d18:0) (Beeler et al., 1998). LCB, considered the simplest functional sphingolipid, can have a range of modifications including phosphorylation, desaturation and hydroxylation and can be in free form or bound in complex sphingolipids. LCB may be linked to a fatty acid (usually 16-26 carbons) via an amide bond to form a ceramide. Ceramides can be phosphorylated in the endoplasmic reticulum by ceramide kinases (CerK) or ACD5 (accelerated cell death 5) or further modified to form the complex sphingolipids glucosylceramides (GlcCers) in the ER and glycosyl inositol phosphorylceramides (GIPCs). These reactions are catalysed by glucosylceramide synthase (GCS) and at least three functional IPC-synthases as well as several glycosyl or glucuronyl transferases (Wang et al., 2008; Mina et al., 2010; Rennie et al., 2014; Msanne et al., 2015).

In plants, treatment with exogenous LCBs stimulates plant cell death and immune responses such as calcium influx, ROS production, expression of defence genes, and callose deposition (Liu et al., 2020b). Among the LCBs, d18:0 and t18:0 are strongly elevated in plants treated with the Cer synthase inhibitor FB1 (Saucedo-Garcia et al., 2011). In contrast to free LCBs, phosphorylated LCBs do not induce PCD and ROS in plant cells (Shi et al., 2007; Saucedo-Garcia et al., 2011).

The olive (*Olea europaea* L. Oleacea) is a crop of prime economic interest in Spain, the world leader in producing olive oil and table olives (Baldoni & Belaj, 2009). In this crop, the regulation of fruit abscission poses an agricultural problem related to recalcitrant fruit release during harvest (Barranco et al., 2004; Ferguson et al., 2010; Zipori et al., 2014). Overall, the harvest operation is costly, exceeding 50% of the total expenses of the crop, and thus in recent decades, the collection has been mechanized. However, for cultivars of table olive ('Manzanilla Sevillana') and early-harvest cultivars, the effectiveness of shaking is poor due to the strong fruit retention, and consequently manual collection is required, increasing the costs of harvesting. In this sense, the production of table olives worldwide is becoming unsustainable due to the stagnation of profitability and the rise in the costs of manual fruit picking. With the need to mechanize the harvest, the sector demands the use of chemical compounds that provoke fruit abscission with minimum effect on the olive (Banno et al., 1993; Polito & Lavee, 1980; Goldental-Cohen et al., 2017).

Previously, we have demonstrated that the behavior of ripe fruit abscission in olive is not homogeneous among the cultivated olive cultivars (Gomez-Jimenez et al., 2010b; Parra- In addition, we have undertaken a pioneer work connecting sphingolipids and the abscission process in plants (Gil-Amado & Gomez-Jimenez, 2013). In particular, this first study found gene expression in the AZ related to changes in membrane microdomains including sphingolipids, sterols, and remorins, along with signalling proteins potentially involved in fruit abscission. In that study, changes in gene activity related to sphingolipid turnover, suggested the potential involvement of LCB metabolism. A more recent study took this subject further to examine the roles of sphingolipids during olive fruit ripening and abscission (Parra-Lobato et al., 2017; Inês et al., 2018). Our study found an increase in both polar lipids and sphingolipids, as well as of endocytosis, which was also stimulated during fruit abscission (Parra-Lobato et al., 2017). In recent years, the information generated by these works has led to initial

research into the new chemical products that induce fruit abscission in olive. In particular, we demonstrated that the application in the field of exogenous sphinganine (d18:0) selectively induces abscission of fruit, but not leaf in olive (patent: ES 2 612 728). However, the impact of this treatment at the molecular level remains unexplored. In this study, transcriptome dynamics associated with d18:0-induced fruit abscission in the fruit AZ and the leaf AZ in combination with data on hormonal content were analysed in olive (cv. 'Manzanilla Sevillana'). Specific potential genes and their associated hormonal pathways were determined to be involved in selective olive fruit abscission.

3.II.3. Results and Discussion

3.II.3.1. The major plant sphingolipid long chain base sphinganine induces fruit abscission in olive

As mentioned above, we have previously demonstrated that exogenous sphinganine induces fruit abscission in olive cultivars (Patente ES 2 612 728). For a fullerunderstanding of the interplay between sphingolipids and abscission, we analysed the effect of d18:0 treatment on the fruit detachment force (FDF) in 'Manzanilla Sevillana' olive fruits. For this, we treated olive tree branches by applying d18:0 at table olive harvest time (September) and conducted daily measurements of the FDF of AZ3 (AZ) for 6 days after treatment (Figure 3.II.1A, B). All measurements were made in the field. After treatment, FDFs were found to decrease continuously in fruit AZs; after 3 days FDFs dropped to 0,40 compared to 0,74 kgf for control. This trend continued until the end of the experiment, 6 days after treatment, by which time FDF of was significantly lower than that of control (Figure 3.II.1B), without provoking tree defoliation (Figure 3.II.1C, D).

In our study of the fruit abscission location in cv. 'Manzanilla Sevillana' in September, the table olive harvest time showed, that the fruits abscised at AZ3 (Figure 3.II.1C), in agreement with previous findings in olive cv. 'Manzanillo', 'Hojiblanca' and 'Picual' (Castillo-Llanque & Rapoport, 2009; Goldental-Cohen et al., 2017). Three days after treatment, only the fruit AZ layer situated above the pedicel was stained darker blue by toluidine blue. Six days after treatment, the toluidine blue staining was at its peak and tissue separation could be clearly seen (Figure 3.II.1E). Similar

labelling was observed in the inactive AZ of leaf at 3 and 6 d after treatment (Figure 3.II.1D).

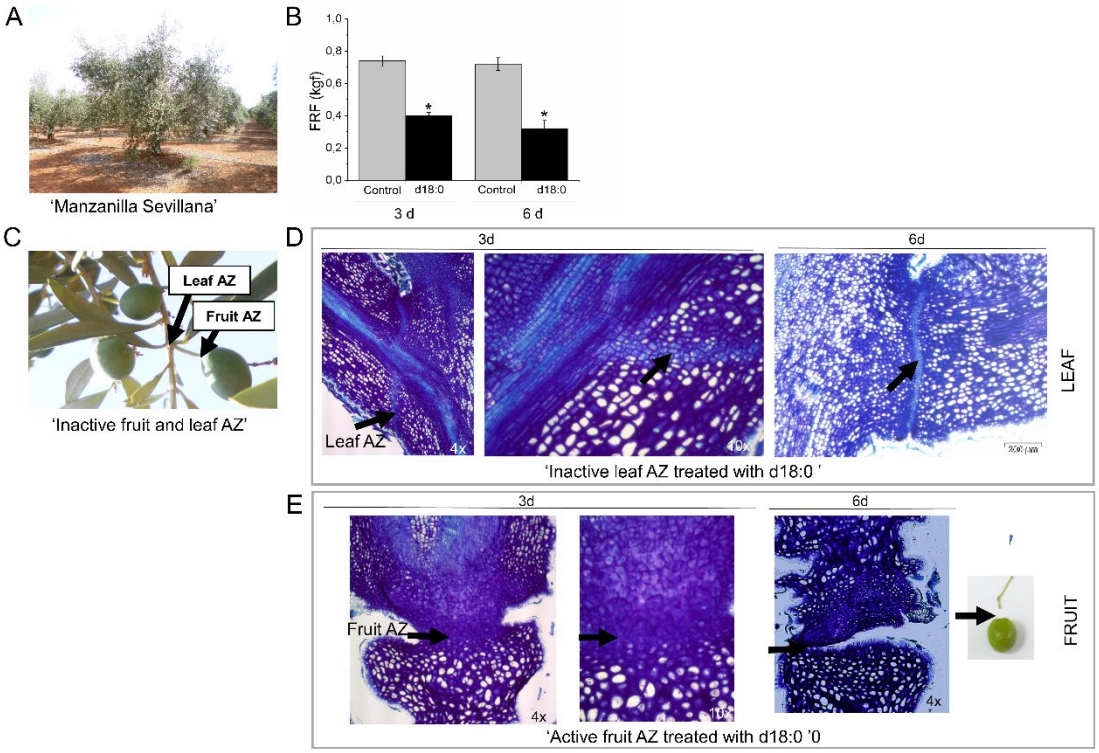

Figure 3.II.1. Plant material used for the experiments included the segments of abscission zone (AZ) excised from olive leaf and fruit of 'Manzanilla Sevillana' cultivar**. (A)** The 'Manzanilla Sevillana' olive trees that were examined in this study were approximately 25 years. **(B)** Effect of sphinganine (d18:0) treatment on changes in the detachment force of the fruit (FDF). Changes in FDF measurements (Kgf) in olive fruit of 'Manzanilla Sevillana' cultivar treated with water (control) and 200 ppm sphinganine (d18:0) at 3 d and 6 d after treatment. Error bars indicate SEs from three replicates. Asterisks above the bars indicate values that were determined by thet-test to be significantly different ($P < 0.05$) from control. **(C)** Positions of the abscission zones (AZs) of olive. Arrows point to the AZ of leaf and fruit of the olive cultivar 'Manzanilla Sevillana'. **(D)** Changes in the anatomy of the leaf AZ at 6 days after d18:0 treatment. **(E)** Changes in the anatomy of fruit AZ at 6 days after d18:0 treatment. Images of longitudinal sections of the leaf AZ (LAZ) stained with toluidine blue (D), and of fruit (AZ) stained with toluidine blue (E) at ×4 and ×10 magnitudes are presented. Active fruit AZ cells situated above the pedicel stained darker blue. Separation of the fruit AZ 6 days after d18:0 treatment is indicated by a black arrow. Photos shown are representative of at least 6 replicate samples. AZs are indicated by black arrows.

3.II.3.2. Effect of the sphinganine (d18:0) treatment on transcriptomic changes in olive AZs

To identify different molecular signals which distinguish the leaf and the fruit abscission process in response to sphinganine (d18:0) treatment, we analysed the transcriptome profiles of the three olive AZs. RNA was extracted from the fruit AZ

(AZ3) before d18:0 treatment (control fruit AZ, C-AZ) and 6 days after (d18:0-AZ), as well as the leaf AZ after the d18:0 treatment (d18:0-LAZ), and then sequenced using Illumina technology.

The RNA-Seq analysis averaged 40 million reads per sample, of which 78% mapped to the 132,819 annotated transcripts from the *Olea europaea* var. *sylvestris* reference genome (Unver et al., 2019). A total of 8,004 differentially expressed genes (DEGs) related to fruit abscission in olive were identified (Figure 3.II.2A; Tables 3.II.S1-3.II.S4).

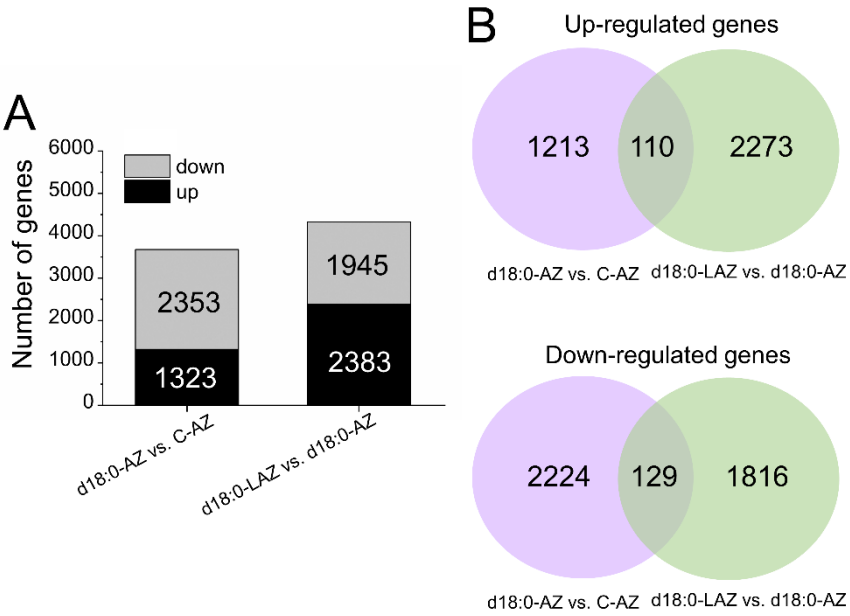

Figure 3.II.2. (A) Distribution of genes differentially expressed during d18:0-induced fruit abscission (d18:0-AZ vs. C-AZ, and 18:0-LAZ vs. d18:0-AZ comparisons). **(B)** Overlap of upregulated and downregulated fruit genes during d18:0-induced fruit abscission. This This Figure shows that 110 were upregulated and 129 were downregulated in both comparisons.

Among the 8,004 DEGs, 3,676 genes were sphinganine (d18:0) responsive in the first comparison (between d18:0-treated fruit AZ and control fruit AZ, d18:0-AZ vs. C-AZ), and 4,328 were abscission responsive in the second comparison (between d18:0-treated leaf AZ, and d18:0-treated fruit AZ, d18:0-LAZ vs. d18:0-AZ) (Figure 3.II.2A; Tables 3.II.S1-3.II.S4). In the first comparison (d18:0-AZ vs. C-AZ), 1,323 genes were upregulated, and 2,353 were downregulated in d18:0-treated fruit AZ (Figure 3.II.2B; Tables 3.II.S1, 3.II.S2). Thus, most of the DEGs were downregulated 6 days after d18:0 treatment in the fruit AZ. In the second comparison (d18:0-LAZ vs. d18:0-AZ),

2,383 genes were upregulated and 1,945 were downregulated in d18:0-treated leaf AZ compared with d18:0-treated fruit AZ (Figure 3.II.2B; Tables 3.II.S3, 3.II.S4). In addition, a comparison of the genes which were d18:0 responsive during olive fruit abscission indicated that 110 were upregulated in both comparisons, and that 129 were downregulated in both comparisons (Figure 3.II.2B; Tables 3.II.S5-S6), while 315 genes were upregulated in the first comparison and downregulated in the second (Table 3.II.S7).

Additionally, 78 transcripts that were identified could be considered as d18:0-treated fruit-AZ specific (specific genes at active fruit AZ) among the transcripts expressed in the d18:0-treated fruit-AZ since they were not detected in other AZs analysed (Table 3.II.1), including homologues of cell wall, transport, transcription factor (TF) and hormone-related genes. However, an appreciable proportion (almost 37%) of them encode proteins with unknown functions or present no homology with any known genes. Among the transcripts specifically expressed in the active fruit AZ, *ERF003*, one of the ethylene-responsive TFs acts as a transcriptional activator through binding to the GCC-box promoter element and regulates expression of the genes involved in the response to stress factors and components of stress signal transduction pathways (Trujillo et al., 2009). According to our study, *ERF003* could be an important regulator of the signalling pathway through modulating ethylene-mediated gene expression during d18:0-induced fruit abscission in olive. Similarly, two ethylene-responsive transcription factors, WIN1 and At1g16060, were found to be detected exclusively in the active fruit AZ (Table 3.II.1). Ethylene was first identified as the primary abscission inductive factor (Abeles, 1992; Botton & Ruperti, 2019). Thus, we identified a large number of specific genes, implying that they may play unique roles in the active fruit AZ. They were considered to be prime candidates for further molecular research on the programme of fruit abscission in olive and their regulation.

Table 3.II.1. Specific genes of the active fruit-AZ in olive.

Gene	log2FoldChange	pvalue	Gene_ID	Description
LOC111365833	3,845262085	5,26E-04	XP_022842116.1	ethylene-responsive transcription factor ERF003-like = *Olea europaea var. Sylvestris*
LOC111365932	2,396588682	2,95E-04	XP_022842267.1	squamosa promoter-binding-like protein 14 = Olea europaea var. Sylvestris
LOC111366215	3,168727093	2,34E-03		uncharacterized LOC111366215 = *Olea europaea var. Sylvestris*
LOC111368316	2,473137831	1,11E-02	XP_022845453.1	ethylene-responsive transcription factor WIN1-like = *Olea europaea var. Sylvestris*
LOC111368591	3,009706953	4,32533E-05	XP_022845697.1	chaperone protein dnaJ 11, chloroplastic-like = *Olea europaea var. Sylvestris*
LOC111370185	3,996317674	2,30E-03	XP_022847648.1	leucine-rich repeat receptor-like tyrosine-protein kinase PXC3 = *Olea europaea var. Sylvestris*
LOC111371536	6,884220433	2,30E-05		uncharacterized
LOC111371554	2,046418298	4,06E-03	XP_022849373.1	deoxynucleotidyltransferase terminal-interacting protein 2-like = *Olea europaea var. Sylvestris*
LOC111372046	2,848793059	0,000703899	XP_022849967.1	AP2-like ethylene-responsive transcription factor At1g16060 = *Olea europaea var. Sylvestris*
LOC111373825	2,506104087	2,11E-04		uncharacterized protein LOC111373825 = *Olea europaea var. Sylvestris*
LOC111375020	2,401802332	1,67E-03	XP_022853581.1	zeatin O-glucosyltransferase-like = *Olea europaea var. Sylvestris*
LOC111375325	2,390144552	9,44E-04	XP_022853899.1	transcription factor MYBC1-like = *Olea europaea var. Sylvestris*
LOC111375664	2,918937442	6,92E-03		uncharacterized
LOC111376313	3,104451658	3,20E-04		uncharacterized
LOC111376579	3,863960241	2,46026E-08	XP_022855314.1	probably inactive leucine-rich repeat receptor-like protein kinase At3g28040 = *Olea europaea var. Sylvestris*
LOC111378221	3,072015778	2,07E-05	XP_022857157.1	uncharacterized LOC111378221 = *Olea europaea var. Sylvestris*
LOC111379026	3,235805092	0,000504311		uncharacterized
LOC111379604	3,061157982	0,011452409	XP_022858782.1	uncharacterized LOC111379604 = *Olea europaea var. Sylvestris*
LOC111380054	2,046359271	1,06E-02	XP_022859288.1	protein kinase G11A-like = *Olea europaea var. Sylvestris*
LOC111380373	2,257446432	3,85E-03	XP_022859680.1	protein XRI1-like = *Olea europaea var. Sylvestris*
LOC111380639	3,200371098	1,48E-04	XP_022860026.1	uncharacterized LOC111380639 = *Olea europaea var. Sylvestris*
LOC111382091	2,055932271	0,003416934	XP_022861731.1	pentatricopeptide repeat-containing protein At1g63330-like = *Olea europaea var. Sylvestris*
LOC111382240	3,180300924	0,008998354	XP_022861926.1	transcription factor MYB61-like = *Olea europaea var. Sylvestris*
LOC111382581	2,489349796	2,76E-04	XP_022862368.1	protein ASPARTIC PROTEASE IN GUARD CELL 2-like = *Olea europaea var. Sylvestris*
LOC111383156	2,153182113	2,66E-03	XP_022863002.1	uncharacterized LOC111383156 = *Olea europaea var. Sylvestris*
LOC111383528	5,717343907	0,0016349	XP_022863412.1	ethylene-responsive transcription factor ERF038-like = *Olea europaea var. Sylvestris*
LOC111385339	2,324111774	0,004656839	XP_022865493.1	protein YLS3-like = *Olea europaea var. Sylvestris*
LOC111385342	2,047686751	0,008068174	XP_022865492.1	expansin-A8-like = *Olea europaea var. Sylvestris*
LOC111385622	2,43015486	1,29E-03	XP_022865804.1	dehydration-responsive element-binding protein 3-like = *Olea europaea var. Sylvestris*
LOC111386067	1,995030483	1,11E-02		uncharacterized
LOC111386400	2,914133022	0,000392185	XP_022866620.1	serine/threonine-protein kinase HT1-like = *Olea europaea var. Sylvestris*
LOC111386803	2,416793673	0,003676585		uncharacterized
LOC111387402	2,021497638	3,30E-03	XP_022867722.1	14 kDa proline-rich protein DC2.15-like = *Olea europaea var. Sylvestris*
LOC111388385	3,548762378	1,77E-03	XP_022868836.1	myb-related protein 306-like = *Olea europaea var. Sylvestris*
LOC111389229	2,850192232	0,003942683	XP_022869886.1	phosphoenolpyruvate carboxylase kinase 1-like = *Olea europaea var. Sylvestris*
LOC111389391	3,708967423	1,62706E-05	XP_022870084.1	gibberellin 2-beta-dioxygenase 8-like = *Olea europaea var. Sylvestris*
LOC111389558	2,338978127	0,00210599		PLAT domain-containing protein 1-like = *Olea europaea var. Sylvestris*
LOC111389582	1,903167787	5,10E-03	XP_022870278.1	uncharacterized LOC111389582 = *Olea europaea var. Sylvestris*
LOC111389820	2,175985687	0,003480067	XP_022870580.1	dormancy-associated protein homolog 3-like = *Olea europaea var. Sylvestris*
LOC111390411	2,199142543	5,39E-03		uncharacterized
LOC111391321	2,50754677	0,000250922	XP_022872291.1	serine/threonine-protein kinase D6PKL2 = *Olea europaea var. Sylvestris*

LOC111391363	2,796177723	0,002256032	XP_022872331.1	probable F-box protein At2g36090 = *Olea europaea var. Sylvestris*
LOC111391767	5,996405168	0,000602719	XP_022872779.1	uncharacterized LOC111391767 = *Olea europaea var. Sylvestris*
LOC111392899	2,147041107	8,63E-03	XP_022874081.1	transcription factor bHLH162-like = *Olea europaea var. Sylvestris*
LOC111392924	3,887137491	4,46E-05	XP_022874105.1	trans-resveratrol di-O-methyltransferase-like = *Olea europaea var. Sylvestris*
LOC111393576	2,731720189	0,002866587	XP_022874944.1	uncharacterized LOC111393576 = *Olea europaea var. Sylvestris*
LOC111393797	2,778416038	0,00093707	XP_022875272.1	uncharacterized LOC111393797 = *Olea europaea var. Sylvestris*
LOC111393814	2,858670791	0,000667957	XP_022875299.1	probable aquaporin TIP1-2 = *Olea europaea var. Sylvestris*
LOC111394796	2,118724683	0,002438332	XP_022876553.1	uncharacterized LOC111394796 = *Olea europaea var. Sylvestris*
LOC111395636	2,002718303	7,23E-03	XP_022877490.1	uncharacterized LOC111395636 = *Olea europaea var. Sylvestris*
LOC111396673	2,261889651	0,002157077	XP_022878895.1	tetrapyrrole-binding protein, chloroplastic = *Olea europaea var. Sylvestris*
LOC111397188	3,639769208	0,000201527	XP_022879735.1	expansin-A8-like = *Olea europaea var. Sylvestris*
LOC111397687	3,370549399	0,000198093	XP_022880454.1	basic leucine zipper 43-like = *Olea europaea var. Sylvestris*
LOC111398343	2,716862849	1,46E-03	XP_022881029.1	uncharacterized LOC111398343 = *Olea europaea var. Sylvestris*
LOC111398513	3,535169654	1,05E-02	XP_022881215.1	uncharacterized LOC111398513 = *Olea europaea var. Sylvestris*
LOC111398571	2,096522709	0,009265824	XP_022881300.1	uncharacterized protein At5g41620-like = *Olea europaea var. Sylvestris*
LOC111398953	2,45293123	0,006575805	XP_022881900.1	cysteine-rich repeat secretory protein 55-like = *Olea europaea var. Sylvestris*
LOC111399295	2,605686795	1,14E-02	XP_022882319.1	uncharacterized LOC111399295 = *Olea europaea var. Sylvestris*
LOC111399535	3,403088723	3,78E-03		uncharacterized LOC111399535 = *Olea europaea var. Sylvestris*
LOC111401081	2,270506831	0,002175843	XP_022884393.1	germin-like protein subfamily 1 member 16 = *Olea europaea var. Sylvestris*
LOC111401258	2,088749607	0,0030106	XP_022884684.1	lysine histidine transporter-like 8 = *Olea europaea var. Sylvestris*
LOC111401913	3,989626162	2,38E-04	XP_022885659.1	putative receptor-like protein kinase At1g80870 = *Olea europaea var. Sylvestris*
LOC111402921	2,462523052	0,001117536		uncharacterized
LOC111403048	2,115265027	0,002343047	XP_022887165.1	protein NRT1/ PTR FAMILY 5.1-like = *Olea europaea var. Sylvestris*
LOC111403273	2,187851812	0,005427169	XP_022887476.1	uncharacterized LOC111403273 = *Olea europaea var. Sylvestris*
LOC111405665	2,914038891	1,01E-03	XP_022890427.1	uncharacterized LOC111405665 = *Olea europaea var. Sylvestris*
LOC111406460	2,570652254	6,37E-03	XP_022891650.1	RING-H2 finger protein ATL73-like = *Olea europaea var. Sylvestris*
LOC111406957	3,529017449	0,01038827		uncharacterized
LOC111406992	2,496871421	0,008708496	XP_022892105.1	glycine-rich protein 5-like = *Olea europaea var. Sylvestris*
LOC111407166	3,618199519	8,59E-03	XP_022892259.1	upstream activation factor subunit UAF30-like = *Olea europaea var. Sylvestris*
LOC111407568	3,702234512	8,05E-04	XP_022892906.1	uncharacterized LOC111407568 = *Olea europaea var. Sylvestris*
LOC111407937	6,401460685	0,000143853	XP_022893431.1	cytochrome P450 734A1-like = *Olea europaea var. Sylvestris*
LOC111407945	2,154915957	0,001212164	XP_022893440.1	uncharacterized protein At1g15400-like = *Olea europaea var. Sylvestris*
LOC111408288	4,290923231	1,7944E-06	XP_022893833.1	probable 1-deoxy-D-xylulose-5-phosphate synthase 2, chloroplastic = *Olea europaea var. Sylvestris*
LOC111409057	2,08801729	1,99E-03	XP_022894720.1	protein CURVATURE THYLAKOID 1D, chloroplastic-like = *Olea europaea var. Sylvestris*
LOC111411688	3,350193603	0,005164869	XP_022898010.1	polyamine oxidase 1-like = *Olea europaea var. Sylvestris*
LOC111411876	2,782514789	1,12E-02		uncharacterized
LOC111411935	2,809043768	0,002244483	XP_022898391.1	beta-Amyrin Synthase 2 = *Olea europaea var. Sylvestris*

3.II.3.3. Gene Ontology functional enrichment analysis of differentially expressed genes

For the analysis of the biological functions and processes regulated in the AZs in response to d18:0 treatment, the DEGs were classified using the Gene Ontology (GO) database. Furthermore, GO accessions were assigned to the DEGs based on similar sequences in known proteins available in the UniProt database in addition to InterPro as well as the Pfam domains that these contain. The GO terms 'Lipid metabolic process', 'Protein binding', and 'Membrane' were most represented among the categories of biological processes (Figure 3.II.3), molecular functions (Figure 3.II.4), and cell components (Figure 3.II.5), respectively. Previously, we have shown that, the GO terms 'Metabolic process', 'Catalytic activity', and 'Membrane' were the most represented ones among the categories during natural fruit abscission in olive (Gil-Amado & Gomez-Jiménez, 2013).

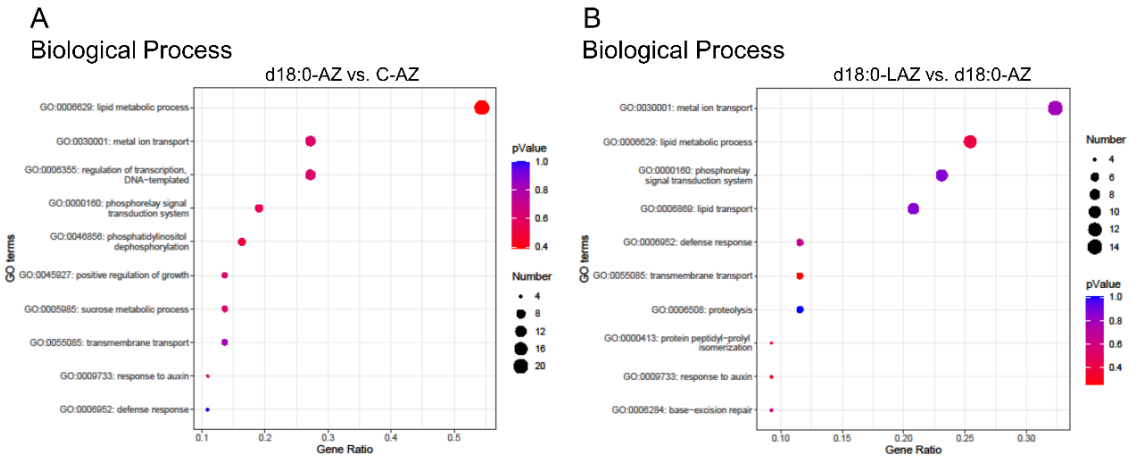

Figure 3.II.3. The top 10 terms from the enrichment analysis of GO 'biological process' based on DEGs in the olive AZs. (**A**) Bubble Plot of GO 'biological process' terms in the GO annotations of the DEG in the d18:0-AZ vs. C-AZ comparison (**B**) Bubble Plot of GO 'biological process' terms in the GO annotations of the genes of the DEG in the d18:0-LAZ vs. d18:0-AZ comparison. The Y-axis and X-axis denote the GO name and gene ratio, respectively. The colour of each bubble represents -$\log_{10}$ (p value), and each bubble size represents the count of DEGs. Additional information is presented in Tables 3.II.S8-3.II.S9.

Within the 'Biological process' category, the list of upregulated transcripts in d18:0-treated fruit AZ (d18:0-AZ) showed enrichment of transcripts involved in "Lipid metabolic process", "Metal ion transport", "Regulation of transcription, DNA-

templated" and "Phosphorelay signal transduction system", which involves autophosphorylation of a histidine kinase and the transfer of the phosphate group to an aspartate that then acts as a phospho-donor to response regulator proteins, such as the ethylene-activated signalling pathway.

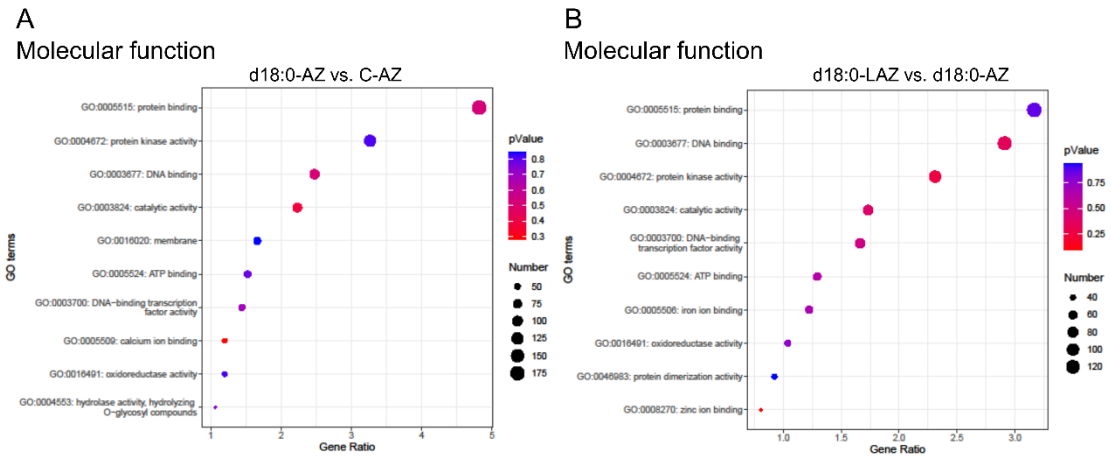

Figure 3.II.4. The top 10 terms from the enrichment analysis of GO 'molecular function' terms based on DEGs in the olive AZs. (**A**) Bubble Plot of GO 'molecular function' terms in the GO annotations of the DEG in the d18:0-AZ vs. C-AZ comparison; and (**B**) Bubble Plot of GO 'molecular function' terms in the GO annotations of the DEG in the d18:0-LAZ vs. d18:0-AZ comparison. The Y-axis and X-axis denote the GO name and gene ratio, respectively. The colourr of each bubble represents -$\log_{10}$ (p value), and each bubble's size of represents the count of DEGs. Additional information is presented in Tables 3.II.S8-3.II.S9.

Marked differences were nevertheless detected between the two comparisons of enriched GO terms. That is, GO terms associated with the "Response to auxin", "Cellulose microfibril organization", "Xyloglucan metabolic process", "Fatty acid biosynthetic process", "Vacuolar transport", "Ubiquitin-dependent protein catabolic process", "Autophagy", "Response to desiccation" and "Response to water" were enriched in the genes that were uniquely upregulated in the fruit AZ (d18:0-AZ vs. C-AZ) compared to the leaf AZ treated with d18:0 (d18:0-LAZ vs. d18:0-AZ). This suggest that such biological processes may be associated with distinctions in the active/inactive AZ in olive.

Within the "molecular function" category, the profile of abundant transcripts in both the active fruit AZ (d18:0-AZ vs. C-AZ) and the inactive leaf AZ (d18:0-LAZ vs. d18:0-

AZ) indicates a predominant expression of proteins related to GO terms "Protein binding", "DNA binding", "ATP binding", "Calcium ion binding", as well as "Protein kinase activity", "Catalytic activity", "Transcription factor activity" and "Oxidoreductase activity", while the "RNA binding", and "Ubiquitin-protein transferase activity" were found to be enriched in genes that were uniquely upregulated in the fruit AZ treated with d18:0 (Figure 3.II.4).

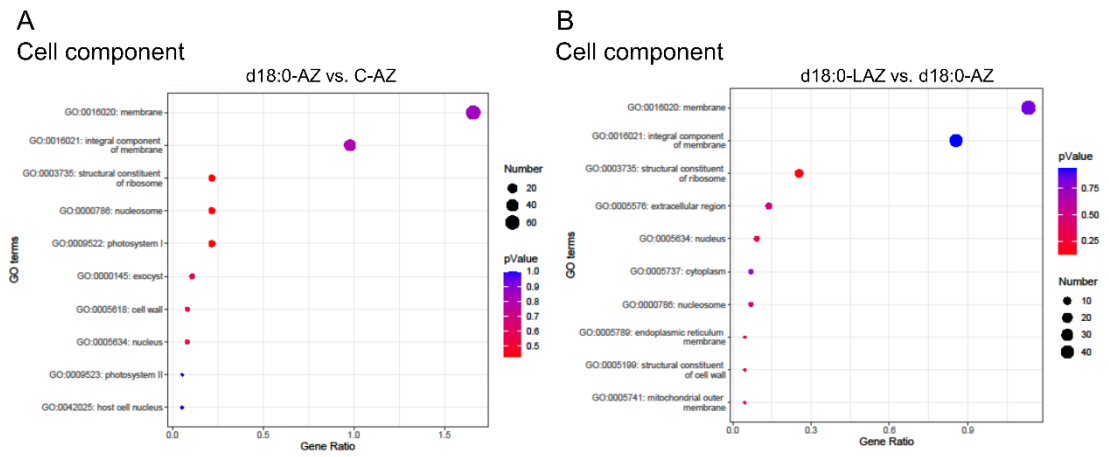

Figure 3.II.5. The top 10 terms from the enrichment analysis of GO 'cellular component' terms based on DEGs in the olive AZs. (**A**) Bubble Plot of GO 'cellular component' terms in the GO annotations of DEG in the d18:0-AZ vs. C-AZ comparison; and (**B**) Bubble Plot of GO 'cellular component' terms in the GO annotations of DEG in the d18:0-LAZ vs. d18:0-AZ comparison. The Y-axis and X-axis denote GO name and gene ratio, respectively. The colourr of each bubble represents -$\log_{10}$ (p value), and each bubble's size of represents the count of DEGs. Additional information is presented in Tables 3.II.S8-3.II.S9.

Finally, within the GO terms "Cellular compartment" category, the "Membrane", and "Integral component of membrane" constituted the most overrepresented category for the genes with increased transcript accumulation in both the fruit and leaf AZs treated with d18:0 (Figure 3.II.5). However, GO terms such as "Nucleosome", "Structural constituent of ribosome", "Cell wall" and "Peroxisome" were found to be enriched among the transcripts that were uniquely upregulated in d18:0-treated fruit AZ.

3.II.3.4. A complex modulation of sphingolipid metabolism during d18:0-induced fruit abscission

As previously observed (Gil-Amado & Gomez-Jimenez, 2013; Parra-Lobato et al., 2017), differences in sphingolipid content/composition and biosynthetic gene expression in the fruit AZ may play a role during natural fruit abscission in olive. Here, we report that several components of the sphingolipid metabolism contribute to abscission signalling during d18:0-induced fruit abscission in olive (Table 3.II.S10, Figure 3.II.6).

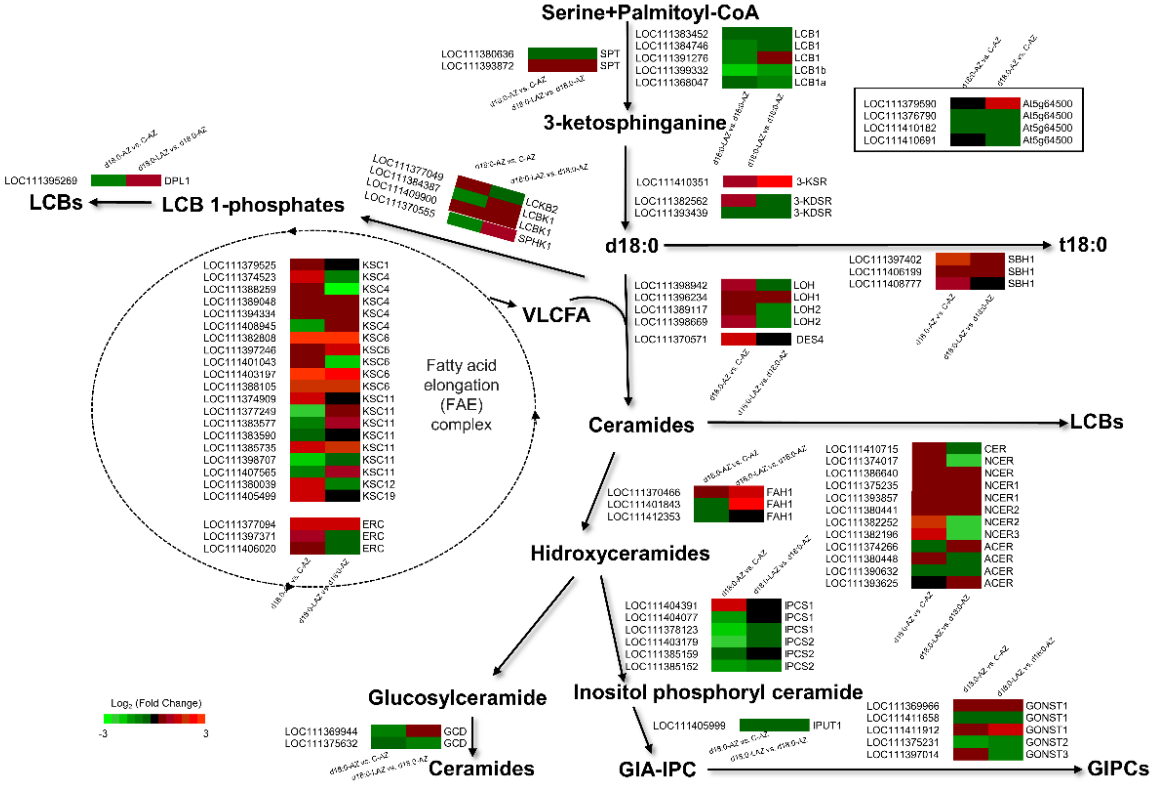

Figure 3.II. 6. Simplified representations of the pathways for the biosynthesis and turnover of sphingolipids, and differential gene expression of sphingolipid metabolism-related genes during d18:0-induced fruit abscission in olive. Expression values are represented in a heatmap as Log_2 Fold Change in both the d18:0-AZ vs. C-AZ, and the d18:0-LAZ vs. d18:0-AZ comparisons; the colour key is indicated at the bottom. Additional information on the sphingolipid metabolism-related genes is presented in Table 3.II.S10.

Several specialised enzymes are involved in the regulation of sphingolipid levels, such as ceramide synthases, ceramidases, ceramide kinase, glucosyl ceramidase and inositol phosphorylceramidase (Warnecke & Heinz, 2003; Luttgeharm et al., 2015; Michaelson

et al., 2016). Our data showed that one *ERH1* gene encoding for ceramide inositolphosphotransferase 1, which catalyses an essential step in sphingolipid biosynthesis, one sphingolipid delta(4)-desaturase gene (*DES1*) required for the biosynthesis of delta-4-unsaturated sphingolipids and derivates, and two 3-ketoacyl-CoA synthase genes (*KCS11* and *KCS19*) involved in the first step of fatty acid elongation, were upregulated exclusively in the fruit AZ treated with d18:0, whereas one dihydroceramide fatty acy 2-hydroxylase gene (FAH1), and one lipid phosphate phosphatase delta gene (LPP) were downregulated only in the fruit AZ treated with d18:0 (Table 3.II.S10, Figure 3.II.16), suggesting an increase of VLCFAs in the fruit AZ during d18:0-induced fruit abscission. This agrees with our previous results demonstrating the upregulation of two 3-keto-acyl-CoA synthases genes, KCS2 and KCS11, during natural fruit abscission in olive (Gil-Amado & Gomez-Jimenez, 2013), implying an increase of VLCFAs in fruit AZ during abscission and thus a correlation between the fruit abscission.

It is noteworthy that genes that encode enzymes for neutral ceramidase (*NCER2* and *NCER3*), and for 3-ketoacyl-CoA synthase (*KCS4* and *KCS12)* were strongly expressed in the fruit AZ treated with d18:0 and downregulated in the leaf AZ treated with d18:0 (Table 3.II.S10, Figure 3.II.6), supporting the hypothesis that the homeostasis between LCB and Cer plays an important role in the execution of fruit abscission in olive, and thus, the d18:0 treatment may play a selective role in modulating fruit abscission by promoting sphingolipid metabolism and regulating ceramide accumulation.

Ceramidases convert Cers into LCBs. We have previously reported that two alkaline ceramidases (ACER) that possibly hydrolyse t18:0-Cers, were upregulated in the fruit AZ during natural olive fruit abscission. Here, two neutral ceramidases (NCER2–3), that may degrade hCers into sphingosine and fatty acids (Li et al., 2015a; Wu et al., 2015a), were exclusively upregulated in the fruit AZ during d18-induced fruit abscission. In particular, NCER2 likely functions as a Cer synthase (Zienkiewicz et al., 2020). It will be useful to establish whether NCER2 and other ceramidases exhibit both ceramidase and reverse ceramidase activity. These ceramidases maintain the balance of Cer and LCB in the ER and Golgi. Previous studies have shown that Arabidopsis ceramidases are key regulators of autophagy, turgor pressure and oxidative stress responses (Chen et al., 2015; Li et al., 2015a; Zheng et al., 2018). In Arabidopsis, disruption of NCER1 and 2 reportedly results in specific sphingolipid imbalances

triggering different phytohormone-dependent plant cell death programmes (Zienkiewicz et al., 2020). Thus, the regulation of Cer and LCB levels by neutral ceramidases (NCER2–3) in the fruit AZ may have some physiological significance during d18:0-induced fruit abscission in olive.

It has been demonstrated that sphingolipids, free LCBs or Cers, play a key part in the regulation of PCD occurring during plant development (Li et al., 2016) or associated with plant defence responses (Ternes et al., 2011; König et al., 2012; Bi et al., 2014; Michaelson et al., 2016), though their precise role in abscission remains unknown. During abscission in tomato, PCD reportedly occurs asymmetrically (Bar-Dror et al., 2011), casting doubts as to whether Cer and LCBs can act as molecules in the olive fruit AZ to promote PCD. Recently, sphingolipid-induced PCD is a salicylic acid and EDS1-dependent phenotype in Arabidopsis fatty acid hydroxylase (FAH1, FAH2) and ceramide synthase (LOH2) triple mutants (König et al., 2022). Conversely, treatment of olive trees with d18:0 resulted in a drop of the transcript levels of FAH1, involved in the alpha-hydroxylation of sphingolipid-associated VLCFA, exclusively in the fruit AZ in association with olive fruit abscission.

3.II.3.5. Transcript changes in cell-wall biosynthesis and remodeling during d18:0-induced fruit abscission

In this study, we identified, among the DEGs, 189 genes that encode proteins with probable functions in cell-wall biosynthesis and remodeling during early olive fruit development (Table 3.II.S11), of which 40 were upregulated and 63 downregulated in the d18:0-AZ versus C-AZ comparison, and 74 were upregulated and 46 downregulated in the d18:0-LAZ versus d18:0-AZ comparison (Figure 3.II.7; Table 3.II.S11). Overall, 8 genes were upregulated in both comparisons, while 5 genes were downregulated in both comparisons (Figure 3.II.7; Table 3.II.S11).

The well-represented families included glucan 1,3-β-glucosidase (BG, 42 genes), xyloglucan endotransglucosylase/hydrolase (XTH, 19 genes), cellulose synthase (CES, 15 genes), expansin (EXP, 15 genes), pectin methylesterase (PME, 12 genes), polygalacturonase (PG, 11 genes), arabinogalactan protein (AGP, 10 genes), endo-1,4-β-glucanase or cellulase (EGase/CEL, 9 genes), extensin (EXT, 9 genes), laccase (LAC, 7 genes) proteins (Table 3.II.S11, Figure 3.II.7). Of these, several genes of each

family were induced in response to sphinganine treatment (Figure 3.II.7; Table 3.II.S11).

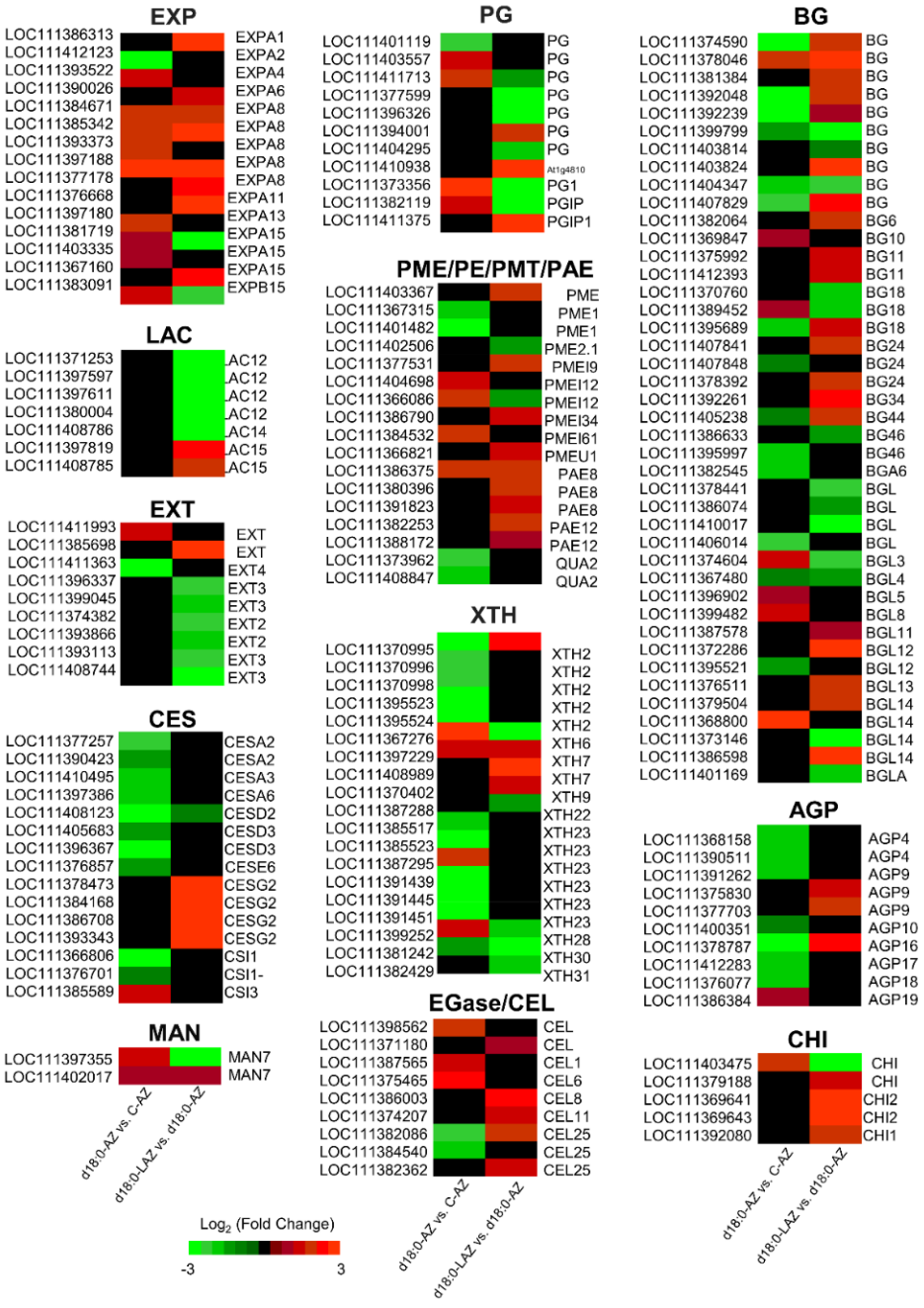

Figure 3.II.7. Expression profile of family genes encoding various cell wall proteins during d18:0-induced fruit abscission in olive. Expression values are represented in a heatmap as Log_2 Fold Change in both the d18:0-AZ vs. C-AZ, and the d18:0-LAZ vs. d18:0-AZ comparisons, and the colour key is indicated at the bottom. Additional information on the cell wall-related genes is presented in Table 3.II.S11.

These results agree with reports on the expression of genes encoding abscission-associated cell wall-hydrolyzing enzymes (Gonzalez-Carranza & Roberts, 2012; Gil-Amado & Gomez-Jimenez, 2013; Corbacho et al., 2013; Kim et al., 2015; Sundaresan et al., 2016). Fruit abscission requires the activity of cell wall degrading enzymes. EGase, PGs and EXP are cell-wall-loosening factors expressed during plant abscission process (Roberts et al., 2002; Agusti et al., 2009; Ogawa et al., 2009; Meir et al., 2010; Botton et al., 2011; Tsuchiya et al., 2015; Roberts & Gonzalez-Carranza, 2018; Botton & Ruperti, 2019; Meir et al., 2019; Kućko et al., 2019). Examining these families, we identified genes that were up-regulated exclusively in the active fruit AZ treated with d18:0, such as genes that encode four EXP (EXPA4, EXPA8, EXPA13, EXPA15), 3 EGase/CELs, one PG, four BG (BG5, BG8, BG10, BG14), one XTH (XTH23), one CS, one EXT, and one AGP protein (Figure 3.II.6; Table 3.II.S10).

According to our RNA-Seq data, in addition, 13 genes were upregulated in d18:0-treated fruit AZ (the first comparison) and were downregulated in d18:0-treated leaf AZ (the second comparison): *CHI (*XP_022887760.1), *XTH6* (XP_022843825.1), *EXPA15* (XP_022861297.1), *PG1* (XP_022851645.1), *PG* (XP_022861759.1), *mannan endo-1,4-beta-mannosidase 7* (XP_022880016.1), *BG3* (XP_022853068.1), *EXPB15* (XP_022862931.1), alpha-galactosidase 3-like (XP_022851936.1), *BG18, XTH28* (XP_022882288.1), *PME12* (XP_022842507.1) proteins, implying that these cell-wall-related enzymes help regulate the activation of olive fruit AZ. Thus, our gene-expression analysis reveals an induction of cell-wall biosynthesis and remodeling genes during d18:0-induced fruit abscission.

3.II.3.6. Characterization of transport related genes associated with d18:0-induced fruit abscission

Furthermore, during d18:0-induced fruit abscission in olive, significant change was identified in the abundance of a subset of 222 genes encoding channel and transporter proteins of 33 diverse families (Table 3.II.S12). Among these, 31 were up- and 85 downregulated in the fruit AZ treated with d18:0 (d18:0-AZ vs. C-AZ), and 81 up- and 25 downregulated in the leaf AZ treated with d18:0 (18:0-LAZ vs. d18:0-AZ). Likewise, of the 33 different families of channel and transporter proteins, one was expressed exclusively in the AZ fruit treated with d18:0 (metal transporter Nramp), 3 families (ammonium transporter, boron transporter, and nitrate transporter) were regulated

only in the leaf AZ treated with d18:0, and 29 families [ATP-binding cassette (ABC) transporter, amino acid transporter, aquaporin, calcium-transporting ATPase, heavy metal-associated isoprenylated plant protein, metal-nicotianamine transporter, potassium transporter, and zinc transporter families, among others] are regulated in both fruit and leaf AZs treated with d18:0 (Table 3.II.S12, Figure 3.II.8).

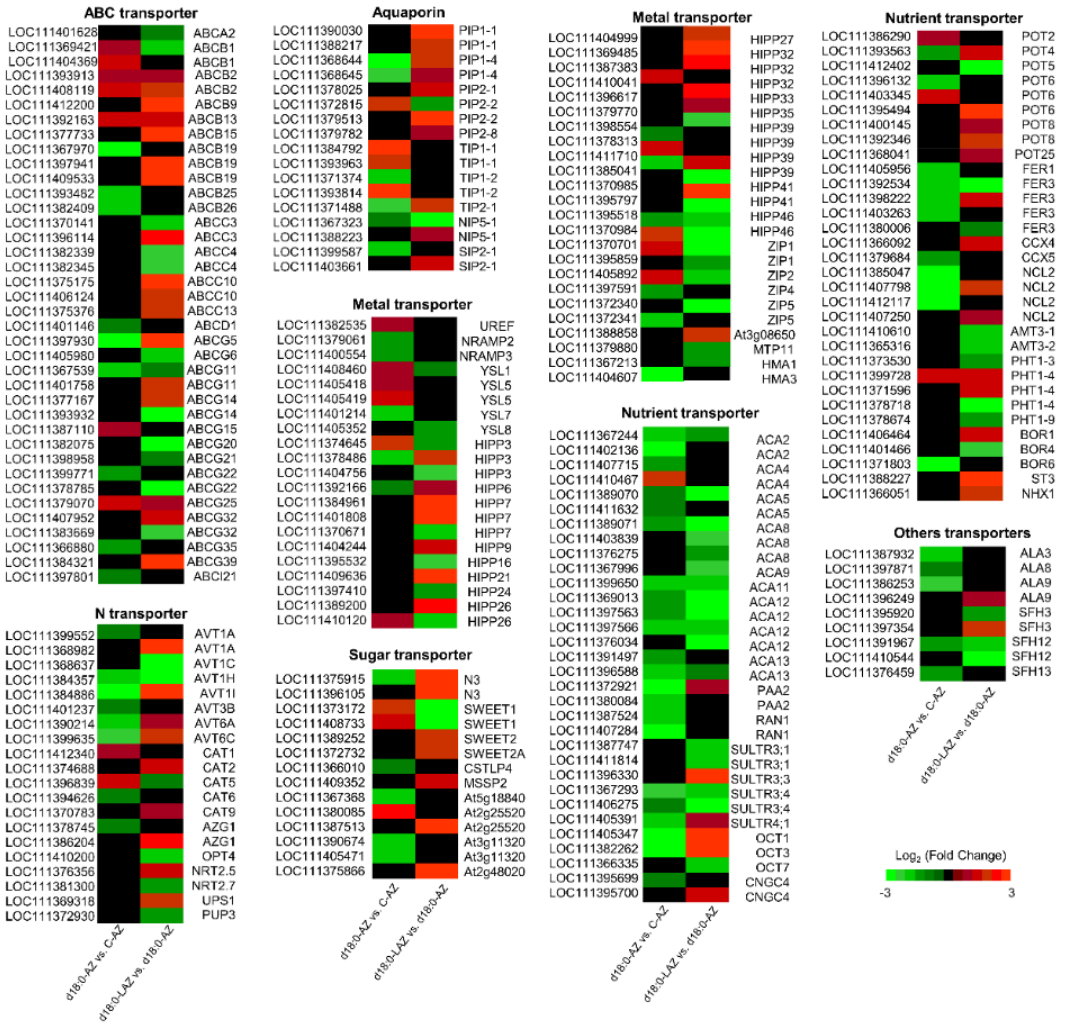

Figure 3.II.8. Expression profile of transport-related genes during d18:0-induced fruit abscission in olive. Expression values are represented in a heatmap as Log_2 Fold Change in both the d18:0-AZ vs. C-AZ, and the d18:0-LAZ vs. d18:0-AZ comparisons, and the color key is indicated at the bottom. Additional information on the transport-related genes is presented in Table 3.II.S12.

Among the specific genes in the fruit AZ treated with d18:0 (d18:0-AZ vs. C-AZ), a homologue of *TIP1-1* encoding a member of the aquaporin family was identified.

Overall, we identified 19 genes that encode aquaporins. Of these, 4 genes (PIP2-2 XP_022850991.1, *TIP1-1* XP_022864884.1, *TIP1-1* XP_022875523.1, *TIP1-2* XP_022875299.1) were upregulated exclusively in the d18:0-AZ vs. C-AZ comparison, while 9 genes were exclusively upregulated in the d18:0-LAZ vs. d18:0-AZ comparison. Furthermore, in the present study, it was notable that the expression levels of some of the calcium-transporting ATPase genes encoding ECA4 proteins were exclusively upregulated in the fruit AZ treated with d18:0 (Figure 3.II.8, Table 3.II.S12), in agreement with our prior study concerning the AZ transcriptome analysis during natural fruit abscission in olive (Gil-Amado & Gomez-Jimenez, 2013), whereas several heavy metal-associated isoprenylated plant protein, metal-nicotianamine transporter, and zinc transporter genes, among other genes, were upregulated in the fruit AZ, and downregulated at the leaf AZ treated with d18:0 (Table 3.II.S11), indicating that these membrane components are essential for diverse cellular functions during d18:0-induced fruit abscission.

On the other hand, among the most abundant upregulated genes in the fruit AZ treated with d18:0, we also found one that encodes zinc transporter 1, ZNT1, which mediates both cellular zinc efflux and zinc sequestration into membrane-bound organelles, suggesting that homeostasis of zinc is tightly modulated by ZNT1 during d18:0-induced fruit abscission in olive (Figure 3.II.8, Table 3.II.S12). Another gene expressed exclusively in the fruit AZ treated with d18:0 was a homologue of *YSL5* encoding a member of the metal-nicotianamine transporter family, suggesting a role for this protein in AZ metal homeostasis. Our data also showed that one ABC transporter G family member 25 gene, *ABCG25*, and two ABC transporter B family member genes, *ABCB2* and *ABCB13*, which function in auxin transport across plant species, were upregulated only in the fruit AZ treated with d18:0 (Figure 3.II.8, Table 3.II.S12). This result may mean that this membrane-localized protein facilitates directed auxin efflux from olive AZ cells for the establishment and maintenance of the gradient of auxin regulating d18:0-induced fruit abscission.

Other genes noticeably present in the fruit AZ treated with d18:0 and involved in vesicle trafficking were found to encode dynamins, kinesins, small GTPases, V-type ATPases, syntaxins and reticulons (Figure 3.II.9, Table 3.II.S13).

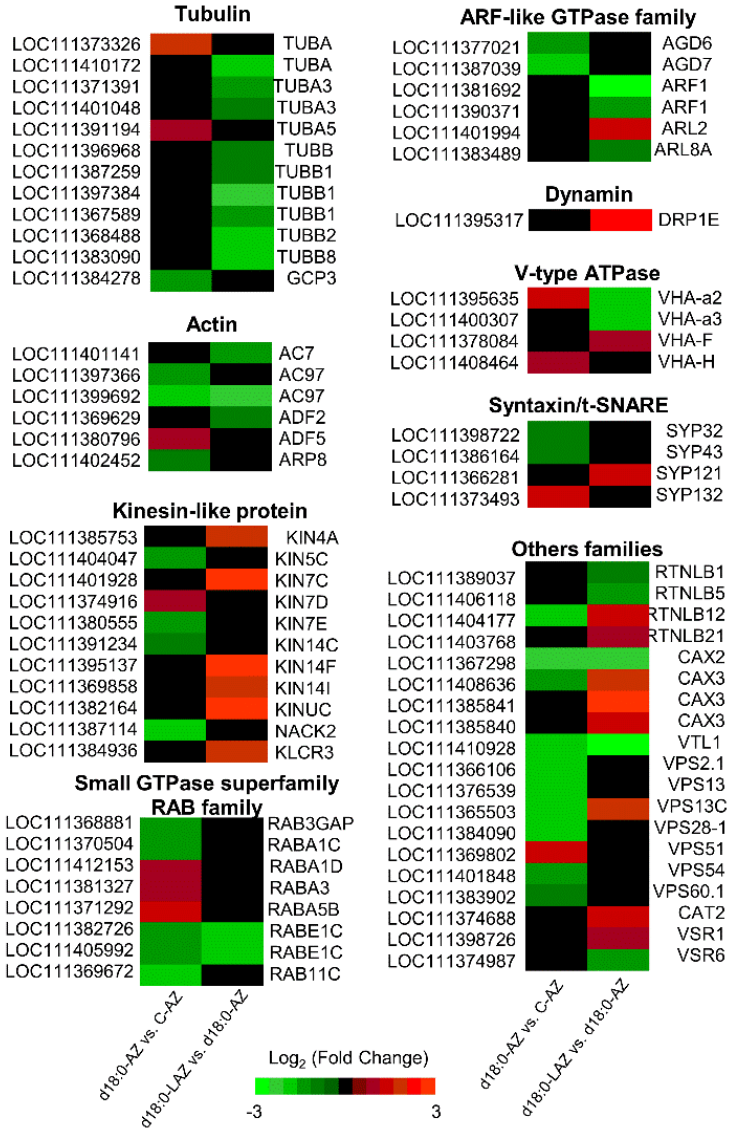

Figure 3.II.9. Expression profile of vesicle trafficking-related genes during d18:0-induced fruit abscission in olive. Expression values are represented in a heatmap as Log_2 Fold Change in both the d18:0-AZ vs. C-AZ, and the d18:0-LAZ vs. d18:0-AZ comparisons; the colour key is indicated at the bottom. Additional information on the vesicle trafficking-related genes is presented in Table 3.II.S13.

Among the RAB-GTPase genes that we identified, only 2 (*RABA1D* and *RABA5B*) were upregulated exclusively in the fruit AZ treated with d18:0, and 3 (*RABA1C*, *Rab11C*, and *RAB3GAP1*) were downregulated only in the fruit AZ treated with d18:0, whereas 2 RAB-GTPases (*RABE1C*) were downregulated in both AZs treated with d18:0 (in both comparisons) (Figure 3.II.9, Table 3.II.S13). By contrast, none of the genes encoding a member of RAB-GTPase gene family was upregulated in both AZs treated with d18:0, indicating that vesicle trafficking is among the most critical cellular

activities for olive fruit abscission. Previously, our pyrosequencing data also indicated higher AZ expression of vesicle trafficking related genes for the small GTPases during natural fruit abscission in olive (Gil-Amado & Gomez-Jimenez, 2013).

In particular, other RAB-GTPase genes, *RABG3A*, *RABG3D*, *ARA4*, *ARA6*, *RABA2B*, *RABA2A/RAB11C* and *RABC2A*, were upregulated during natural fruit abscission (Gil-Amado & Gomez-Jimenez, 2013). Overall, these data are consistent with an increased endomembrane trafficking in olive fruit AZ during abscission, as indicated by FM4-64 staining (Parra-Lobato et al., 2017), suggesting that endomembrane trafficking modulates cell wall modifications during olive fruit abscission.

3.II.3.7. Hormonal composition and gene expression during d18:0-induced fruit abscission

According to the previous data, GO enrichment identified hormone-mediated signalling pathways that may be key during fruit abscission (Figure 3.II.3). Firstly, to determine the changes in hormone levels during d18:0-induced fruit abscission in olive, were examined the hormone profiles of indole-3-acetic acid (IAA), GAs (GA_1 and GA_4), CKs [trans-Zeatin (*t*Z), dihydrozeatin (DHZ), N^6-isopentenyladenine (IP)], abscisic acid (ABA), jasmonic acid (JA), and salicylic acid (SA) in the fruit and leaf AZs 6 days after d18:0 treatment compared to the untreated controls (Figure 3.II.10).

In general, hormonal patterns registered differences between the two AZs (leaf and fruit) during d18:0-induced fruit abscission in olive, but both AZs showed similar variation patterns of the SA levels when exogenous d18:0 was applied (Figure 3.II.10). In fact, the application of exogenous d18:0 significantly elevated the SA level in both leaf and fruit AZs, while IAA and ABA levels rose only in fruit AZ, and GA_1 and *t*Z levels only in the leaf AZ with the d18:0 treatment. By contrast, GA_1, GA_4, DHZ, IP, and *t*Z levels were lowered in the fruit AZ after of d18:0 treatment, whereas ABA and JA levels fell in the leaf AZ by d18:0 in comparison with the control (Figure 3.II.10). Thus, GAs (GA_1) and CKs (tZ) were greater in the leaf AZ than in the fruit AZ suggesting that the GA and CK contents were negatively regulated by d18:0 treatment in the fruit AZ. In addition, JA levels remained unchanged in fruit AZ under treatment, whereas the IAA, GA_4, DHZ and IP contents did not change significantly in the leaf AZ by d18:0 in comparison with the control (Figure 3.II.10). Therefore, our data show that exogenous d18:0 encourages the levels of IAA and ABA, and lowers the GA and

CK levels in the fruit AZ, but not in the leaf AZ, during selective fruit abscission in olive.

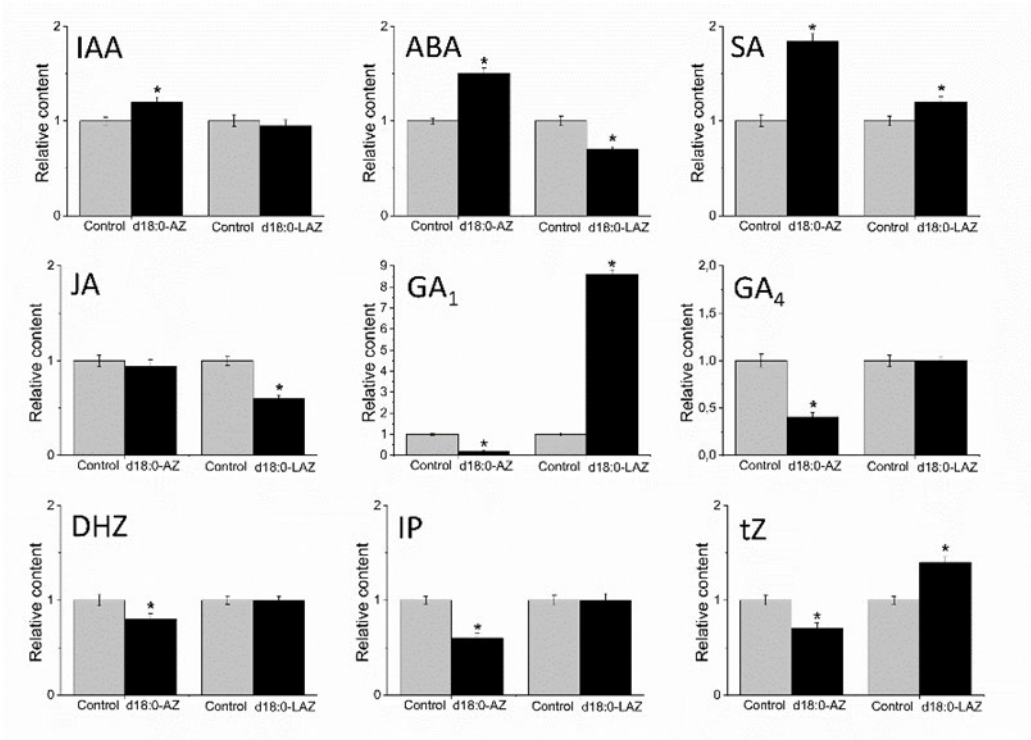

Figure 3.II. 10. Profiles of indole-3-acetic acid (IAA), abscisic acid (ABA), salicylic acid (SA), jasmonic acid (JA), gibberellin 1 (GA_1), gibberellin 4 (GA_4), dihydrozeatin (DHZ), N^6-isopentenyladenine (IP) and trans-Zeatin (*tZ*) levels of AZs from olive fruit and leaf treated with water (control) and 200 ppm sphinganine (d18:0-AZ and d18:0-LAZ) at 6 d after treatment. Values are expressed as a ratio to control values (water treated fruits), which were set to 1. Error bars indicate SEs from three replicates. Asterisks above the bars indicate values that were determined by the t-test to be significantly different ($P < 0.05$) from control. Leaf AZ: LAZ, Fruit AZ: AZ.

Several studies have reported that plant hormones, such as ABA, SA, NO, BR and ethylene, regulate specific aspects of sphingolipid metabolism in plants (Ng et al., 2001; Wang et al., 2008; Guo et al., 2012; Guillas et al., 2013; Sánchez-Rangel et al., 2015; Shi et al., 2015; Wu et al., 2015b; Corbacho et al., 2018). However, our understanding of the molecular mechanisms underlying the crosstalk between plant sphingolipids and hormones is still rudimentary. Sphingolipids activate multiple plant hormone signalling pathways (Asai et al., 2000; Magnin-Robert et al., 2015; Wu et al., 2015b; Zienkiewicz et al., 2020; Huang et al., 2021); therefore, one question is how d18:0

might affect the cross-talk among these signalling pathways in olive fruit AZ during abscission.

The three main plant hormones known to be involved in the abscission process are ethylene, ABA (both accelerating abscission), and auxin (known to delay abscission) (Addicott et al., 1970). Genes involved in auxin biosynthesis and signalling were significantly upregulated in response to d18:0 treatment in fruit AZ. Transcripts involved in IAA synthesis, such as a transcript encoding tryptophan aminotransferase protein 2 (TAR2) was upregulated exclusively in the fruit AZ in response to d18:0 treatment, consistently with the highest IAA levels detected in the fruit AZ. In the leaf AZ, we failed to identify significant regulation of any auxin biosynthesis-related genes (Figure 3.II.11, Table 3.II.S14). However, the IAA-amino acid hydrolase genes (*ILR1-like 1*, *ILR1-like 3*, and *ILR1-like 5*), involved in auxin homeostasis, were found to be downregulated in the fruit AZ and upregulated in the leaf AZ in response to d18:0 treatment (Figure 3.II.11, Table 3.II.S14). Auxin-amino acid hydrolase may provide local concentrations of auxin within the olive leaf AZ during fruit abscission. In addition, expression levels for the auxin-conjugating enzymes *GH3.1*, and *GH3.6* were also found to be boosted in the fruit AZ in response to d18:0 treatment, while *GH3.10* gene shows upregulated expression in the leaf AZ in response to d18:0 treatment (Figure 3.II.11, Table 3.II.S14). Nevertheless, the *GH3.1* and *GH3.6* gene upregulated and downregulated expression in the fruit AZ and the leaf AZ, respectively, in response to d18:0 treatment (Figure 3.II.11, Table 3.II.S14).

Similarly, d18:0 treatment specifically and significantly induced the genes involved in auxin signalling (*TIR1*, *IAA16*, *ARF2B*, *SAUR36*, *SAUR66*, *and SAUR71)* in the fruit AZ, while other genes (*IAA29*, *IAA33)* were upregulated in the fruit AZ and downregulated in the leaf AZ. Conversely, numerous auxin-regulated genes which were specifically downregulated in the fruit AZ during d18:0-induced fruit abscission (*TIR*1, *IAA14*, *IAA29*, *ARF9*, *ARF18*, ARF19 and *SAUR32*, among others) were detected (Figure 3.II.11, Table 3.II.S14). Furthermore, transcript levels for two auxin efflux carriers, *PIN1* and *PIN1b*, rose in the fruit AZ but fell in the leaf AZ, while *PIL2*, and *PIL7* expression increased and *PIN6* and *PIN8* decreased exclusively in the fruit AZ in response to d18:0 treatment. However, transcripts encoding auxin influx carrier-like protein (*LAX5*) diminished while (*LAX2*) augmented exclusively in the

fruit AZ during d18:0-induced fruit abscission, indicating altered auxin distribution in the active fruit AZ. Therefore, the regulation of auxin biosynthesis, conjugation, transport, and signalling may differ in the AZs during d18:0-induced fruit abscission. Rises in endogenous IAA levels in the fruit AZ coincided with higher expression levels for one biosynthesis enzyme, *TAR2*, for the auxin homeostasis enzymes, *ILR1-like 1*, *ILR1-like 3*, and *ILR1-like 5*, and for one auxin influx carrier-like protein, *LAX5*, while the transcripts of IAA16 and ARF2B, involved in auxin signalling, were upregulated exclusively in the fruit AZ, and the transcripts of IAA14, ARF18 and ARF19 were downregulated exclusively in the fruit AZ. This suggests that *IAA16* and *IAA14* may be a key candidate genes of auxin signalling during d18:0-induced fruit abscission in olive.

Xie et al. (2018) have shown that the application of IAA, could block the induction of abscission in AZ of citrus fruitlets also after ovary removal, resulting in the regulation of several ethylene-, ABA- and auxin-related genes, and thus have provided further evidence for the negative role played by auxin on the process of AZ acquisition of sensitivity to abscising signals. Nevertheless, auxin has also been shown to enhance ethylene biosynthesis at the AZ (Abele & Rubinstein, 1964; Morgan & Hall, 1964; Kućko et al., 2019) and auxin signalling is required for abscission to take place, since its abscission-specific inhibition results in a delay of organ shedding (Basu et al., 2013). This evidence raises the issue that auxin may play distinct roles during the early and late phase of the induction of the abscission process, respectively, and indicates the need for further investigation of the complex interplay with the action of ethylene.

In the analysis of genes involved in the ethylene biosynthesis pathway, we focused on the genes encoding the three main enzymes of the pathway, S-adenosyl methionine synthase (SAMS), 1-aminocyclopropane-1-carboxylate synthase (ACS), and 1-aminocyclopropanexoxidase (ACO). Of these, the most abundant genes were found to be SAMS1, OeACO1 and OeACO11 (Figure 3.II.11, Table 3.II.S15). In the fruit AZ, the expression of one SAMS1, two SAMS2, two SAMS3 and one OeAC01 genes was downregulated in response to d18:0 treatment, whereas the expression of one SAMS1 and one ACO11 was enhanced. Unsaturation of VLCFA-containing Cers protects plant from hypoxia-induced damage by modulating ethylene signalling through association with CONSTITUTIVE TRIPLE RESPONSE1, a negative regulator of the ethylene signal transduction pathway (Xie et al., 2015

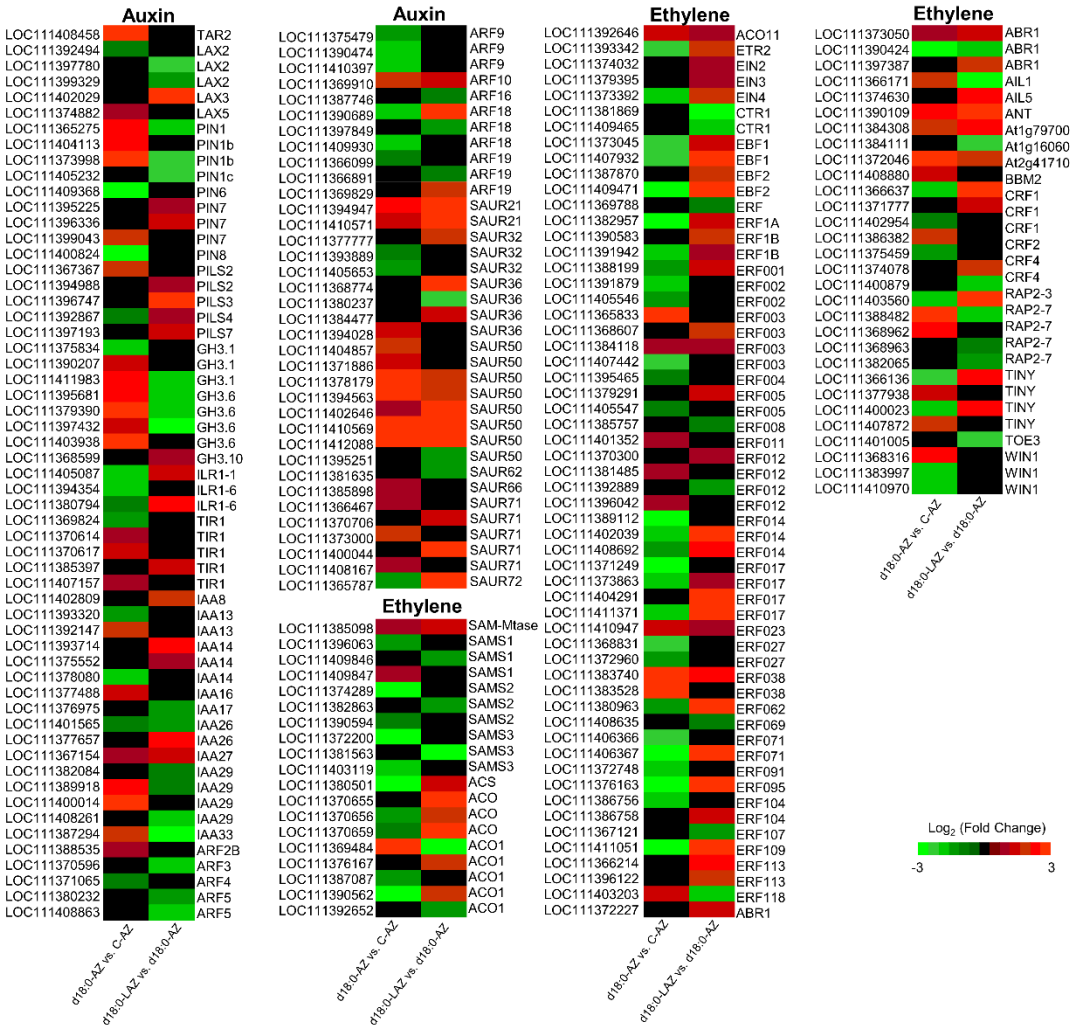

Figure 3.II.11. Expression profile of auxin- and ethylene-related genes during d18:0-induced fruit abscission in olive. Expression values are represented in a heatmap as Log_2 Fold Change in both the d18:0-AZ vs. C-AZ, and the d18:0-LAZ vs. d18:0-AZ comparisons; the colour key is indicated at the bottom. Additional information on the auxin- and ethylene-related genes is presented in Table 3.II.S14-S15.

Conversely, other genes related to ETHYLENE signalling, such as (*ERF2*, *ERF4*, *ERF14*, *ERF17*, *ERF27*, *ERF71*, *ERF91*, and *ERF104*) among others, were downregulated in fruit AZ (Figure 3.II.11, Table 3.II.S15). Likewise, the upregulation of the genes related to ethylene signalling in response to d18:0 treatment was also found (Figure 3.II.11, Table 3.II.S15): *ERF118* was upregulated in the fruit AZ and downregulated in the leaf AZ, whereas *ERF11* and *ERF12* were likely to be associated with d18:0-induced fruit abscission. Thus, d18:0-induced fruit abscission is mediated by upregulated ethylene synthesis (*SAMS1* and *ACO11*) and signalling (*ERF11*, *ERF12* and *ERF118*), whereas a strong induction of *ACO4* and *ERF5* expression in

the fruit AZ during natural fruit abscission (Gil-Amado & Gomez-Jimenez, 2013), suggests that both ACO and ERF may be instrumental in balancing the ethylene biosynthesis needs with the ethylene signalling requirements during olive fruit abscission.

Among the transcripts associated with the ABA biosynthetic process, expression of 3 transcripts representing the gene ZEAXANTHIN EPOXIDASE (OeZEP), were downregulated in the fruit AZ in response to d18:0 treatment, while the upregulated expression of two 9-cis-epoxycarotenoid dioxygenase (NECD), *NECD1*, in the fruit AZ proved to be related to increased ABA content in response to d18:0 treatment (Figure 3.II.12, Table 3.II.S16). Other transcripts involved in ABA catabolism such as ABA 8-OH 4, which encodes ABA 8′-hydroxylase, was upregulated exclusively in the fruit AZ (3 out of the 5 ABA 8-OH 4), in contrast to the ABA levels detected in the fruit AZ during d18:0-induced fruit abscission (Figure 3.II.12, Table 3.II.S16). Notably, the present analysis also found components of ABA signalling upregulated during d18:0-induced fruit abscission, such as *3PYR/PYL (PYL9*, *PYL8* and *PYL4*, ABA receptors) genes, whereas one *ABI5-6* (bZIP TF) gene was exclusively downregulated in the fruit AZ (Figure 3.II.12, Table 3.II.S16), suggesting that this PYL9, PYL8 and PYL4 receptor forms part of an ABA signalling unit that modulates d18:0-induced fruit abscission. Thus, these results suggest that ABA signalling was upregulated during d18:0-induced fruit abscission.

On the other hand, in response to ethephon treatment, several ABA biosynthesis genes, including OeZEP, have been found to be upregulated in the fruit AZ in olive (Goldental-Cohen et al., 2017). Increased ABA biosynthesis in response to exogenous ethylene could be expected since crosstalk between these hormones is well documented (Fedoroff, 2002), and ABA is known to accelerate abscission (Sawicki et al., 2015). In our study, the gene expression pattern and hormonal content indicate the induction of ABA and auxin in a response to d18:0 treatment in the olive fruit AZ.

Many Arabidopsis mutants with abnormal sphingolipid contents show autoimmunity, cell death, and senescence phenotypes, together with constitutively elevated SA levels and the activation of SA-dependent responses (Greenberg et al., 2000; Wang et al., 2008; König et al., 2012; Sánchez-Rangel et al., 2015; Zeng & Yao, 2022). Until recently, it has been difficult to judge which sphingolipid induced SA signalling;

however, recent studies have proposed that LCBs, Cer, hCer, or GIPC may be responsible for activating SA signalling (Zeng & Yao, 2022). However, so far, the regulation of SA biosynthesis by sphingolipids on the molecular level is largely unknown. In the present study, several genes related to SA were upregulated in the fruit AZ and downregulated in the leaf AZ in response to d18:0 treatment, such as *PAL*, and *PR-1* genes, consistently with the highest SA levels being detected in the fruit AZ treated with d18:0 (Figure 3.II.12, Table 3.II.S17). Meanwhile, another, such as one *SAMT* transcript, which encodes SA carboxyl methyltransferase (an enzyme responsible for biosynthesis of methyl salicylate) decreased in the leaf AZ, in good agreement with a rise of SA in content in response to d18:0 treatment in comparison with the control (Figure 3.II.12, Table 3.II.S17). It bears noting that we previously found the activation of the SA pathway during natural fruit abscission, as well as strongly upregulated gene expression related to pathogenesis associated with natural fruit abscission in olive (Gil-Amado & Gomez-Jimenez, 2013). Thus, we report an increase of SA gene expression (via *PAL* and *PR-1*) in the fruit AZ in response to d18:0 treatment. This distinction between both AZs could explain the effect of d18:0 on selective fruit abscission in olive.

On the other hand, *JMT* genes encoding a jasmonate-O-methyltransferase, which catalyses the methylation of JA into methyljasmonate (MeJA), was also downregulated in the fruit AZ during early fruit development, suggesting that the JA could regulate olive fruit abscission. JA conjugation with isoleucine is reportedly catalysed by jasmonoyl-isoleucine (JA-Ile) synthetase (JAR1), this being a member of the GH3 family (Li et al., 2021). The most bioactive of the JAs is JA-Ile. The perception of JA-Ile by its coreceptor, the Skp1-Cullin1-F-box-type (SCF) protein ubiquitin ligase complex SCF^{COI1}-JAZ, counteracts the transcriptional repression of target genes in the nucleus. JA-Ile signalling participates in regulating several developmental processes, such as root growth and architecture, tuber and trichome formation, seed germination, and particularly reproductive-organ development (Huang et al., 2017). Here, it is reported that *JAR1* gene was upregulated and *TPL* (TOPLESS) gene downregulated in the fruit AZ treated with d18:0 (Figure 3.II.11, Table 3.II.S17), suggesting that these components may aid in JA-Ile signalling in the nucleus to regulate olive fruit abscission.

Notably, these results also suggest that *AOC1*, which encodes an allene oxide cyclase (AOC) protein, is the major control point responsible for the drop in JA detected in the leaf AZ treated with d18:0. Remarkably, this analysis showed that *LOX2* (13-LOX member) and *LOX1* (9-LOX member) genes encoding lipoxygenase members were upregulated in the fruit AZ, whereas *LOX3* (13-LOX member) was exclusively downregulated in the fruit AZ during d18-induced fruit abscission (Figure 3.II.11, Table 3.II.S17), indicating that these genes modulate the distribution between 13-LOX- and 9-LOX-derived oxylipins during d18:0-induced fruit abscission in olive.

In the case of GA, the present data suggest that GA synthesis is upregulated by *CPS*, coding ent-copalyl diphosphate synthase (CPS), by *KO* coding ent-kaurene oxidase (KO), by *KAO2* coding ent-kaurenoic acid oxidase 2-like, and by *GA20ox*, coding GA 20-oxidase, these genes being active in the leaf AZ during d18:0-induced fruit abscission (Figure 3.II.11, Table 3.II.S18). Thus, on the basis of these results GA20ox appears to be a major late-step enzyme responsible for the high-level accumulation of GA_1 detected in the leaf AZ, and the drop of GA (GA_1 + GA_4) levels observed in the fruit AZ may be attributed to the downregulation of GA20ox gene expression. It bears mentioning that *GGPS (*geranylgeranyl pyrophosphate synthase*)*, which is a transcript involved in an early GA biosynthetic step, and GA3ox (GA 3-oxidase), which is a transcript involved in a late GA biosynthetic step, were upregulated in the fruit AZ and downregulated in the leaf AZ (Figure 3.II.11, Table 3.II.S18), in contrast to the highest GA_1 levels detected in the leaf AZ in response to d18:0 treatment. Additionally, the data indicate that GA signalling was negatively regulated by *GAI1* and *RGL1* (DELLA proteins) in the fruit AZ, whereas GA signalling (via *GAMYB*) was upregulated in the leaf AZ during d18:0-induced fruit abscission in olive (Figure 3.II.12, Table 3.II.S19).

It is worth noting that we found the upregulation of the expression of three different cytokinin riboside 5'-monophosphate phosphoribohydrolase genes (*LOG1*, *LOG5*, and *LOG10)* in leaf AZ (d18:0-LAZ vs. d18:0-AZ), while LOG8, *LOG5*, and *LOG10* expression were downregulated in fruit AZ (d18:0-AZ vs. C-AZ) during d18:0-induced fruit abscission (Figure 3.II.12, Table 3.II.S20). LOG converts inactive CK nucleotides to the biologically active free-base forms, which is consistent with the highest *tZ* levels detected in olive leaf AZ treated with d18:0 (Figure 3.II.10). In addition, CYP735A (CK hydroxylase), which catalyses the biosynthesis of trans-zeatin (*tZ*) was

downregulated only in the fruit AZ (d18:0-AZ vs. C-AZ), whereas transcripts encoding for zeatin conjugating enzyme *ZOG* (zeatin O-glucosyltransferase) increased in the fruit AZ and decreased in the leaf AZ during d18:0-induced fruit abscission (Figure 3.II.12, Table 3.II.S20), this being consistent with the loss of CKs (DHZ, IP and tZ) detected in the fruit AZ in response to d18:0 treatment (Figure 3.II.10). These results suggest local transcriptional control of the CK biosynthesis and conjugation rather than transport from other tissues. Bioactive forms of CKs were, in turn, deactivated by CK oxidase/dehydrogenase (CKX), thereby regulating the amount of bioactive CK. In the present study, CKX1 gene expression were upregulated in the fruit AZ treated with d18:0 (d18:0-AZ vs. C-AZ), and downregulated in the leaf AZ (d18:0-LAZ vs. d18:0-AZ), while CKX7 gene showed the opposite expression, suggesting that the deactivation of CK may actively occur during d18:0-induced fruit abscission (Figure 3.II.12, Table 3.II.S20). Similarly, CK signalling was stimulated in the leaf AZ and repressed in the fruit AZ in response to d18:0 treatment, since 3 genes coding receptors (CKI1, CKI2, CKI5) and 4 gene-encoding members of the ARR family (ARR10, ARR2, ARR3, ARR7) were exclusively downregulated in the fruit AZ in response to d18:0 treatment, whereas other receptors (CKI2, CKI4) and ARRs (ARR2, ARR5) were exclusively upregulated in the leaf AZ (d18:0-LAZ vs. d18:0-AZ) (Figure 3.II.12, Table 3.II.S20).

Furthermore, the BR signalling was clearly stimulated in fruit AZ during d18:0-induced fruit abscission, since one *BRI1* receptor kinase, 2 *BAK1 (SERK2)* co-receptors, and one *BES1/BZR1* factor transcription were exclusively upregulated in the fruit AZ in response to d18:0 treatment (Figure 3.II.12, Table 3.II.S21), suggesting that the upregulation of receptor *BRI1* may be required for d18:0-induced fruit abscission in olive. Conversely, during early olive fruit development, a BR-induced modulation of long-chain sphingolipids composition and gene expression was found (Corbacho et al., 2018).

In the case of polyamine, the data imply that d18:0-induced fruit abscission is mediated by downregulated polyamine biosynthesis and metabolism, including *ADC* (arginine decarboxylase), *AOase* (acetylornithine deacetylase), *OTCase* (ornithine carbamoyltransferase), *ACAULIS5* (thermospermine synthase), and *PAO* (polyamine oxidase) genes, as well as by upregulated *SAMDC* (S-adenosylmethionine decarboxylase), *SPDS* (spermidine synthase), *PUT* (polyamine uptake transporter),

and *SHT* (spermidine hydroxycinnamoyl transferase) gene expression in the fruit AZ (Figure 3.II.12, Table 3.II.S22). This suggests that polyamine metabolism may have a significant influence on the role of polyamine in the fruit AZ during olive fruit abscission.

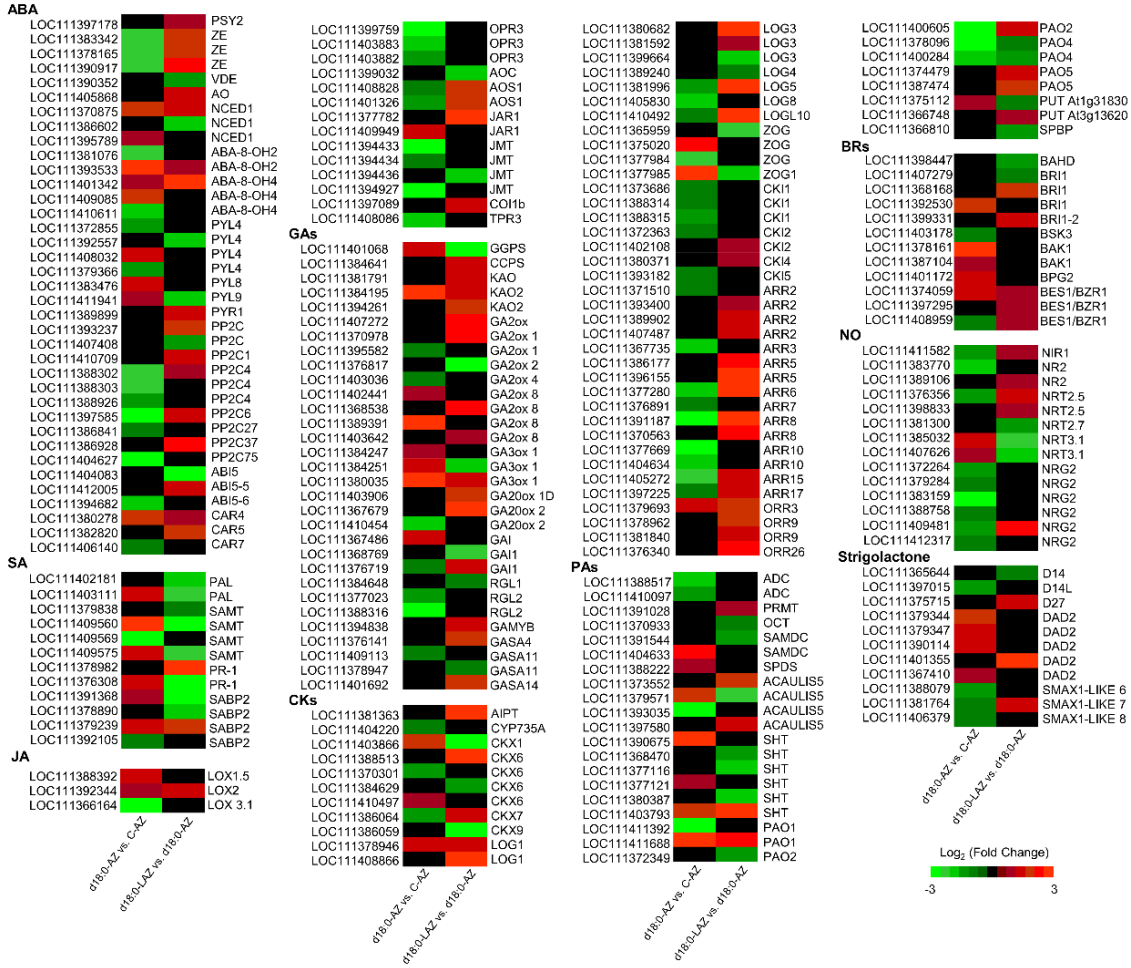

Figure 3.II.12. Expression profile of hormone-related genes during d18:0-induced fruit abscission in olive. Expression values are represented in a heatmap as Log_2 Fold Change in both the d18:0-AZ vs. C-AZ, and the d18:0-LAZ vs. d18:0-AZ comparisons; the colour key is indicated at the bottom.

Finally, the identification of the proteins involved in oxide nitric (NO) formation/transport and strigolactones (SL) signalling in olive AZs constitutes a promising avenue of research for a more complete comprehension of NO and SL physiological functions during fruit abscission. Here, several transcripts related to NO metabolism were also differentially expressed during d18:0-induced fruit abscission, such as *NR1 and NR2* genes, encoding putative nitrate reductase (NR), which were exclusively downregulated in the fruit AZ in response to d18:0 treatment (Figure

3.II.12, Table 3.II.S23). Similarly, *NRT2.5* and *NRT3.1* genes encoding nitrate transporters were downregulated and upregulated in the fruit AZ, respectively. In addition, genes involved in the SL signalling pathway, such as the receptor *DAD2* (SL esterase) was upregulated exclusively in the fruit AZ in response to d18:0 treatment, whereas the transcriptional repressor *SMXL* (SUPPRESSOR OF MAX2 LIKE) genes were downregulated only in the fruit AZ (Figure 3.II.12, Table 3.II.S24), suggesting that these components act to regulate karrikins/strigolactone responses during d18:0-induced fruit abscission in olive. Therefore, the comprehensive study of varying gene expression, together with analyses of different hormonal composition, unveils the complex hormone control underlying d18-induced fruit abscission in the fruit AZ and the leaf AZ, implying different regulatory programmes.

3.II.3.8. Signalling peptides regulating d18:0-induced fruit abscission in olive

Signalling peptides in the role of plant hormones control several features of plant growth and development through cell-cell communication networks, e.g. organ abscission (Ghorbani et al., 2014). Specifically, genetic studies in Arabidopsis have revealed the importance of the small secreted peptide INFLORESCENCE DEFICIENT IN ABSCISSION (IDA), and its two leucine-rich repeat receptor-like kinases (LRR-RLKs) targets, HAESA (HAE) and HAESA-like2 (HSL2), in regulating cell separation during floral organ abscission (Butenko et al., 2003; Santiago et al., 2016; Shi et al., 2018). Based on these studies, it has been proposed that activation of the RLK receptors by the secreted IDA peptide operates through a mitogen-activated protein (MAP) kinase cascade, which in turn activates KNOTTED1- LIKE HOMEOBOX (KNOX) transcription factors, leading to the induction of cell wall remodeling and degrading enzymes genes in the AZ (Cho et al., 2008; Niederhuth et al., 2013b).

The membrane receptor kinases HAESA and HSL2 recognize a family of IDA/IDL signalling peptides to control cell separation processes in different plant organs. The IDA peptide acts as a key component controlling abscission events in Arabidopsis. IDL peptides may assume similar roles in fruit trees. In the present analysis, more than 30 genes encoding putative LRR-RLKs family proteins, involved in plant peptide signalling, were found here to differ in their expression levels during d18:0-induced fruit abscission (Table 3.II.S25, Figure 3.II.13). Among these, one *HSL1* gene

encoding for LRR-RLKs family protein and one *CLE* gene encoding for CLAVATA3/ESR (CLE)-related protein 44-like were exclusively detected in the fruit AZ in response to d18:0 treatment. In Arabidopsis, the homologous HSL1 binds IDA/IDL peptides with high, and CLAVATA3/EMBRYO SURROUNDING REGION-RELATED (CLE) peptides with lower affinity, respectively (Roman et al., 2022). Similarly, one *RALF* gene encoding for rapid alkalinization factor-like and one *BAM1* gene, which encodes a CLAVATA1-related receptor kinase-like protein required for both shoot and flower meristem function (Wang et al., 2018; Roman et al., 2022), were detected exclusively in the fruit AZ in response to d18:0 treatment (Table 3.II.S25, Figure 3.II.13).

Initial studies of AtIDA proposed that this small secreted protein controls floral organ abscission via an ethylene-independent pathway, leading to the activation of cell wall-modifying genes (Butenko et al., 2003; 2006). On the other hand, it was later reported that ethylene could induce *IDA-like* and/or *HSL-like* gene expression in AZ tissues of lychee and lupine flowers, as well as in oil palm and mango fruit AZ, prior to the start of organ abscission (Stø et al., 2015; Ying et al., 2016; Wilmowicz et al., 2018; Rai et al., 2021). Ethylene has also been shown to induce the expression of *IDA-like* genes from tomato and soybean, whereas treatment with the ethylene action inhibitor 2,5-norbornadiene delayed the increase in the expression of these genes (Tucker et al., 2012). These and other findings have led to the establishment of a different concept, suggesting that the IDA/IDL pathway is actually an ethylene-dependent abscission module, which operates downstream of ethylene, serving as a signal for late and/or post-abscission events (Botton & Ruperti, 2019).

It has been reported that there is substantial genetic variation underlying abscission across the plant kingdom based on differences in the morphology and bulk transcriptome of AZs. Nevertheless, a recent report showed that *Nicotiana* lines with silenced HAE and IDA orthologs exhibited reduced perianth abscission (Ventimilla et al., 2021). In addition, expression of both citrus ad litchi orthologs of IDA can complement the abscission-deficient ida mutant phenotype in Arabidopsis (Estornell et al., 2015; Ying et al., 2016). These results suggests that knowledge of the HAE/HSL2 pathway will inform regulation of abscission in other dicots. Additionally, it has been demonstrated abscission of Arabidopsis cauline leaves upon water stress or

pathogen infection is under similar genetic control as floral abscission (Patharkar & Walker, 2016; Patharkar et al., 2017).

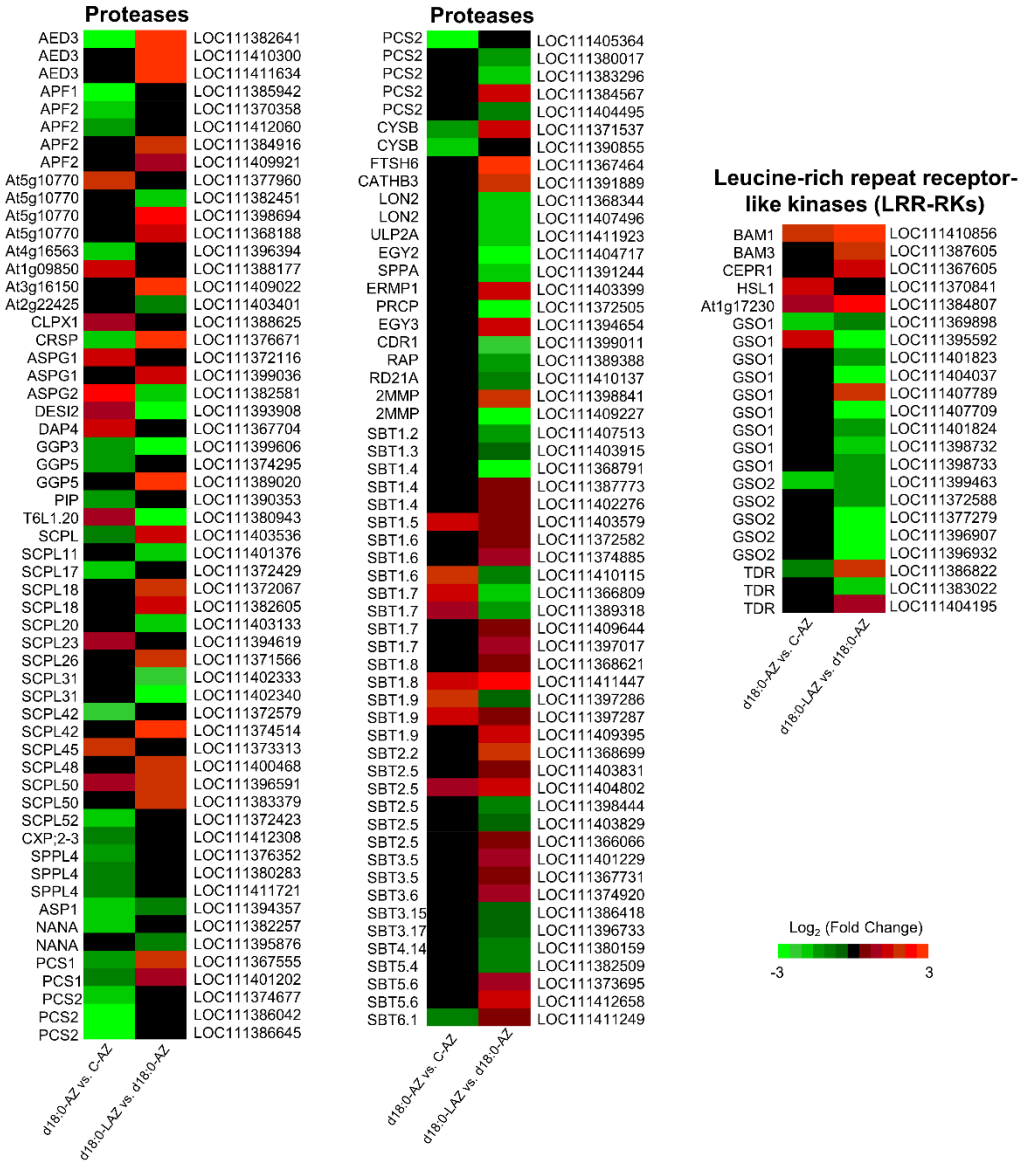

Figure 3.II.13. Differential gene expression of protease and LRR-RKs genes during d18:0-induced fruit abscission in olive. Expression values are represented in a heatmap as Log_2 Fold Change in both the d18:0-AZ vs. C-AZ, and the d18:0-LAZ vs. d18:0-AZ comparisons; the colour key is indicated at the bottom.

In view of the present findings, further research is now required to identify and characterize the different components and targets of the olive IDA-HAE/HSL1-like or HSL2-like module. Whether this olive *HSL1* gene functions as a receptor that interacts with IDA1 or IDA2, remains to be established. Nevertheless, our data provide

different lines of evidences suggesting that the putative olive IDA-HAE/HSL1-like module operates in a d18:0-dependent manner and imposing cytosolic pH changes in olive fruit AZ cells, but not in leaf AZ cells.

Likewise, more than 70 genes have been found to encode putative proteases (also referred to as peptidases or proteinases), including serine proteases, cysteine proteases, aspartic proteases, and Clp proteases, among others (Table 3.II.S26, , Figure 3.II.13). Proteases are enzymes able to participate in almost all stages of plant life (Ghorbani et al., 2014; Stintzi et al., 2022). In particular, *AED3* and *AED2* genes encoding for aspartyl proteases, APOPLASTIC, *EDS1*-DEPENDENT (AED) proteins, were induced exclusively in the fruit AZ treated with d18:0 (Table 3.II.S26, Figure 3.II.13). In addition, the present analysis identified 34 putative SBT genes coding for subtilisin-like protease proteins (also known as subtilases; SBT) in olive fruit AZ that differed in expression levels during d18:0-induced fruit abscission (Table 3.II.S26, Figure 3.II.13). Among 34 SBT genes identified in the analysis, 3 (*SBT1.6*, *SBT1.7* and *SBT1.9*) were upregulated in the fruit AZ treated with d18:0 and downregulated in the leaf AZ treated with d18:0 (Table 3.II.S26, Figure 3.II.13), suggesting that at least some members of SBTs play major roles during d18:0-induced fruit abscission.

3.II.3.9. Identifying transcription factors critical for d18:0-induced fruit abscission in olive

The identification of new transcription factors (TF) genes as well as their function in regulating the expression of candidate genes will aid a fuller understanding of the signalling pathways regulating d18:0-induced fruit abscission. Of the DEGs studied, 394 genes presumably encoding TFs of diverse families were differentially expressed during d18:0-induced fruit abscission in olive, most of them with a downregulation pattern (Table 3.II.S27, Figure 3.II.14). In particular, 178 DEGs were found in the first comparison (the set of d18:0 treatment-related genes), and 278 genes in the second comparison (the set of abscission-related genes). Our RNA-seq analysis revealed that 71 and 107 genes were upregulated and downregulated in the fruit AZ in response to d18:0 treatment (the d18:0-AZ vs. C-AZ comparison), respectively, while 154 and 124 genes were upregulated and downregulated in the leaf AZ (the d18:0-LAZ vs. d18:0-AZ comparison), respectively (Table 3.II.S27). These DEGs proved to be especially related to the TFs AP2/ERF, bHLH, MYB, WRKY, TCP, and bZIP families (Table

3.II.S27, Figure 3.II.14), implying that TFs from these families may take part in triggering the transcriptional cascade during d18:0-induced fruit abscission in olive. Among them, MYB and bZIP TFs are members of TF families abundantly represented during natural fruit abscission in olive (Gil-Amado & Gomez-Jimenez, 2013). This supports the idea that these MYB and bZIP proteins act as critical components of multiple hormone-mediated transcriptional cascades, including auxin, ethylene, ABA, SA and JA, which regulate olive fruit abscission.

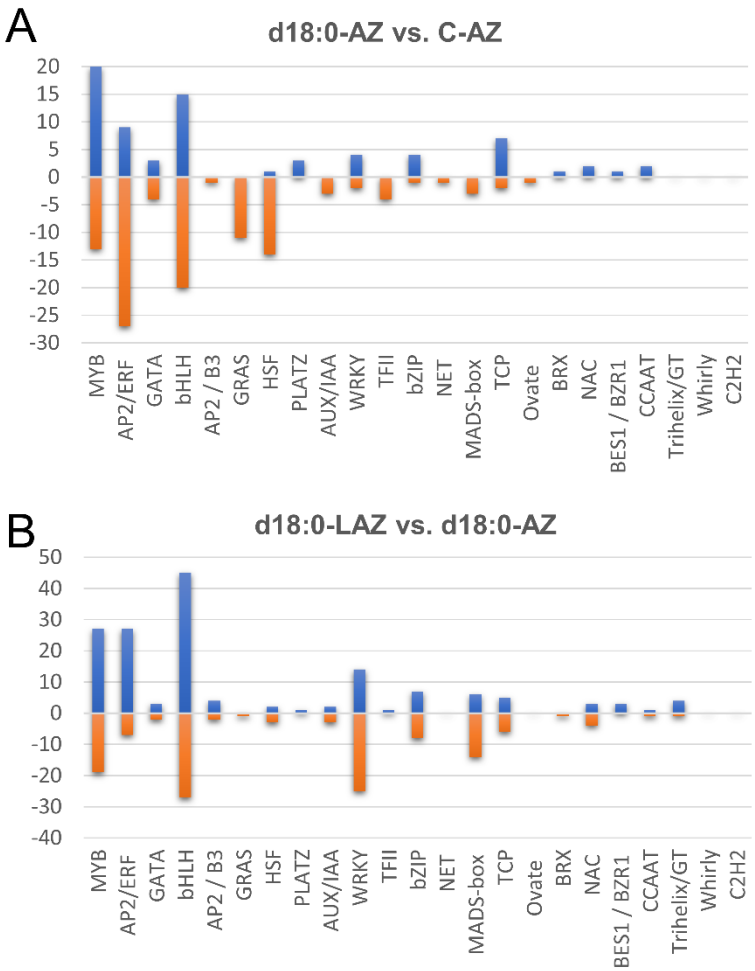

Figure 3.II. 14. Summary of the number of significant changes in olive transcription factor (TF) transcripts between the different families in (A) d18:0-AZ vs. C-AZ comparison and (B) d18:0-LAZ vs. d18:0-AZ comparison. Comparison for significantly upregulated (blue) and downregulated (orange) transcripts revealed differences in the families of TFs during d18:0-induced fruit abscission in olive.

Within the set of DEG in the d18:0-AZ vs. C-AZ comparison, TFs homologous to *ERF038*, *ERF003*, *bHLH30*, *bHLH157*, *bZIP43*, and *MYB61* belonging to AP2/ERF,

bHLH, bZIP, and MYB families, respectively, have been identified as the most abundant TFs. Among these, *ERF038*, *ERF003*, *bZIP43*, and *MYB61* were exclusively overexpressed in the fruit AZ. Indeed, these TF families were among the most widely represented class of proteins in the fruit AZ in response to d18:0 treatment (Table 3.II.S27). Overall, 38 TFs were exclusively upregulated (*PLATZ*, *WIN1*, *MYBC1*, *WRKY11*, *MYB88*, *SRM1*, *CRF1*, among others), and 76 TFs were exclusively downregulated (*LHY*, *DREB1E*, *MYB306*, *WER*, *ABR1*, *HSFA6b*, *SAC51*, among others) in the fruit AZ during d18:0-induced fruit abscission in olive (Table 3.II.S27), implying that these TFs probably mediate abscission-responsive transcription.

Furthermore, the major upregulated differentially expressed TFs in the fruit AZ and downregulated in the leaf AZ were identified during d18:0-induced fruit abscission in olive (Table 3.II.S27), including bZIP43, bHLH30, bHLH157 proteins, while ERF109, ERF095, and ERF071, among others, were downregulated in the fruit AZ and upregulated in the leaf AZ in olive. The abundance of the related transcripts suggests that these TFs play a regulatory role during d18:0-induced fruit abscission in olive. Further study would be needed to reveal the molecular basis of gene expressional regulation.

3.II.4. Materials and Methods

3.II.4.1. Plant material, treatments and fruit-detachment force

Olive trees (*Olea europaea* L.) of the 'Manzanilla Sevillana' cultivar 25 years old in an orchard under drip irrigation (fertigation with suitable liquid fertilizers) near Badajoz (Spain) were studied (Figure 3.II.1A). All experiments and samples collection were performed in September, which is the harvest time of table olives. Fruiting branches on the tree were dipped in a 2-L container filled with a 200 ppm sphinganine (SIGMA, Spain). Control branches were similarly dipped in a 2-L water container. The olive AZ tissues were dissected from the pedicel samples with a razor blade into pieces of ;1 mm3 (Fig. 1C, D). Freshly excised AZ samples were immediately frozen in liquid nitrogen and then stored at −80ºC until analysed.

Fruit breakstrength or FDF, defined as the kg force (kgf) necessary to separate the fruit from the parent plant at the AZ site, was measured in 80 randomly assigned fruits/trees using a dynamometer (Correx, Switzerland) as described by Gomez-

Jimenez et al. (2010). All FDF measurements during the experiment were carried out on fruits while attached to the tree.

3.II.4.2.Anatomical análisis

For the anatomical analysis, the leaf and fruit AZs sampled were excised by hand to a size of approximately 1 mm^3 consisting of the AZ region as well as the adjacent tissues. AZ samples were fixed in formaldehyde: acetic acid: ethanol 70%, 10:5:85, v/v (FAA) solution. Fixation was followed by an ethanol dilution series and a subsequent stepwise exchange of ethanol with histoclear. Samples were embedded in paraffin and cut by microtome (Leica RM2245) into sections, then stained with with 0.04% (w/v) toluidine blue and photographed using a Zeiss Axiophot microscope coupled to a Spot digital camera (Diagnostic Instruments) at 4 and 10 magnifications.

3.II.4.3.AZ transcriptome profiling

The leaf and fruit AZs sampled for transcriptome profiling were excised by hand to approximately 1 mm thick from each side of the AZ region. Tissues were removed from the tree, immediately excised and frozen in liquid nitrogen. AZ enriched tissues were used to prepare six cDNA libraries from total RNA of the three analyzed AZs [Fruit AZ (AZ) and leaf AZ (LAZ)] of 'Manzanilla Sevillana' before and 6 days after LCB sphinganine (d18:0) treatment, using Illumina's TruSeq RNA library preparation kit according to the manufacturer's instructions. Each cDNA library consisted of RNA from about 150 AZs sampled from different fruits or leaves and was sequenced on Illumina HiSeq 2000. Three independent biological replicates (three olive trees) per sample were sequenced, each replicate consisting of an equilibrated pool of three RNAs from three different samples per replicate. The extraction of the total RNA from AZs from fruit and leaf samples was performed as in Gil-Amado & Gomez-Jimenez (2012).

The RNA quality tests were performed with the Agilent 2100 Bioanalyzer (Agilent Technologies, Santa Clara, CA, USA) employing an RNA 6000 Pico assay kit (Agilent Technologies). The poly(A)+ mRNA fraction was isolated from the total RNA and obtained cDNA libraries following the recommendations of Illumina (Truseq stranded Illumina kit). In short, poly(A)+ RNA, after being isolated on poly-T oligo attached magnetic beads, was chemically fragmented before reverse transcription and cDNA generation. Next, in the end-repair process of the cDNA fragments, a single 'A' base

was added to the 3' end, and afterwards the adapters were ligated. Finally, the products were purified and enriched with PCR to compile the final indexed double-stranded cDNA library. The quality of the libraries was checked using a Bioanalyzer 2100, High Sensitivity assay. The quantity within the libraries was assessed by real-time PCR in LightCycler 480 (Roche). Before cluster generation in cbot (Illumina), an equimolar pooling of the DNA libraries was performed and then the pool was sequenced using paired-end sequencing (100 x 2) with an Illumina HiSeq 2000 sequencer. The RNA-seq analysis was ordered from Sistemas Genómicos (Valencia, Spain).

Quality control checks of raw sequencing data were performed with FastQC 0.11.7. The generated reads were cleaned using the Trimgalore 0.6.2 method (http://www.bioinformatics.babraham.ac.uk/projects/trim galore/). Subsequently, all samples were combined, and the complexity of the reads was reduced by removing duplicates and low-quality reads using Picard tools 2.9.2 and Samtools 1.9 algorithms (Li et al., 2009) (>Q20). Reads were mapped to the *Olea europaea* var. sylvestris genome as the reference [*Olea europaea* var. sylvestris Annotation Report (nih.gov)] (Unver et a., 2019). Each sample was then mapped with the latest bowtie2 2.3.3 version (Langmead and Salzberg 2012). The reads of good quality (Phred > 20) were selected to increase the resolution of the count expression. Finally, the expression inference was evaluated by means of the count of properly paired end reads by transcript.

3.II.4.4. Differential expression

For the study of differential gene expression and normalization gene expression using library size, the DESeq 1.36 algorithm was used (Love et al., 2014). This method is based in a negative binomial distribution. The genes with a fold change of less than -2 or greater than 2, and a p adjust by FDR<0.05 were considered differentially expressed (Benjamini and Hochberg, 1995). A functional enrichment study was performed using the information obtained from pFam and uniprot database. This study is based on a hypergeometric distribution using the statistical software R. The principal-component analysis (PCA) was analyzed using the methods described in DESeq using the normalize counts of gene expression obtain from this method. Differential expression was made for each comparison. Then, specific gene expression each comparison was obtained using venn diagram (https://bioinfogp.cnb.csic.es/tools/venny/). The GO enrichment was performance using a hypergeometric test based in R package.

3.II.4.5. Quantification of plant hormones

A pool of 100-mg fresh weight/sample was used for each measurement split into 3 independent biological replicates per sample. The plant hormones were quantified as described by Seo et al. (2011). Aliquots of lyophilized material were extracted with 80% methanol-1% acetic acid. Deuterium-labeled hormones (purchased from Prof. L Mander- Canberra, OlChemim Ltd-Olomouc, or Cambridge Isotope Lab- Andover): [17,17-^{2}H]GAn, [$^2H_5$]IAA, and [$^2H_6$]ABA were added as internal standards for quantification of SA and ABA. For quantification of JA, the compound dhJA was used instead. For collecting the acids fraction containing SA, ABA, and JA, the extracts passed consecutively through HLB (reverse phase), MCX (cationic exchange), and WAX (ionic exchange) columns (Oasis 30 mg, Waters). The final residue was dissolved in 5% acetonitrile-1% acetic acid, and the hormones were separated by reverse phase UPHL chromatography (2.6 μm Accucore RP-MS column, 100 mm length × 2.1 mm i.d., ThermoFisher Scientific) with a 5% to 50% acetonitrile gradient. The hormones were analyzed by electrospray ionization and targeted-SIM using a Q-Exactive spectrometer (Orbitrap detector, ThermoFisher Scientific, Spain). The concentrations of hormones in the extracts were determined using embedded calibration curves and the Xcalibur 4.1 SP1 build 48 and TraceFinder programs.

3.II.5. Conclusions

In conclusion, our study examines various aspects of the distinctive mechanisms characterizing fruit and leaf AZs of 'Manzanilla Sevillana' olive. The results highlight a differential expression of regulatory genes in the fruit AZ (active AZ) and the leaf AZ (inactive AZ) treated with d18:0 compared to the nontreated (inactive AZ). This detailed differential profile of the gene expression in the AZs, together with analyses of different hormonal composition, offers new insights for understanding olive fruit abscission signalling.

4.CONCLUSIONES

CONCLUSIONES

1.Durante la abscisión natural del fruto en el olivo (*Olea europaea* L. 'Picual'), nuestros resultados revelaron complejas rutas reguladoras que controlan los eventos asociados con la abscisión al combinar el análisis de expresión génica diferencial y el perfil hormonal en la zona de abscisión (AZ) y los tejidos del pericarpo del fruto maduro. Estos datos transcriptómicos identificaron transcritos únicos y comunes relacionados con la modificación de la pared celular, el metabolismo y la señalización de hormonas vegetales, el tráfico de vesículas y los flujos de iones entre los tejidos. Esto ofreció una nueva visión de los procesos de regulación metabólica y hormonal que están potencialmente implicados en las modificaciones de la pared celular durante la abscisión natural del fruto.

2. El ácido jasmónico (JA) fue significativamente más abundante en la AZ que en los tejidos del pericarpo del fruto en la etapa de la maduración, que es cuando se produce la abscisión natural del fruto.

3. La caracterización transcripcional de los tejidos de la AZ y del pericarpo del fruto maduro en olivo reveló una inducción de las rutas de señalización de etileno y ácido abscísico (ABA) en ambos tejidos a través de diferentes componentes, y una inducción de la ruta de señalización del ácido salicílico (SA) y del JA en la AZ, validado por análisis qRT-PCR.

4. El presente estudio demostró que la esfinganina (d18:0) puede regular la abscisión selectiva del fruto del olivo principalmente a través de la inducción de los genes *NCER2* y *NCER3* que codifican la ceramidasa neutra, así como de los genes *KCS4* y *KCS12* que codifican la 3-cetoacil-CoA sintasa en la AZ del fruto, apoyando la hipótesis de que la homeostasis entre LCB y ceramida juega un papel importante en la abscisión del fruto en olivo.

5. El análisis transcriptómico de las AZs del fruto y de la hoja de olivo 'Manzanilla Sevillana' mostró que una inducción diferencial de genes que degradan la pared celular está asociada con la inducción de genes implicados en los flujos de iones y un cambio en el metabolismo y señalización de genes de las hormonas vegetales durante la abscisión del fruto inducida por d18:0. Esto se acompañó de la actividad transcripcional

de los receptores de membrana quinasas (HSL1 y BAM1) y del factor de alcalinización rápida (RALF) potencialmente involucrados en la señalización de la abscisión del fruto. En vista de los presentes hallazgos, ahora se requiere más investigación para identificar y caracterizar los diferentes componentes del módulo similar a IDA-HAE/HSL1 o similar a HSL2 del olivo y sugerir que este módulo putativo opera en la AZ del fruto en olivo junto con cambios de pH citosólico.

6. La abscisión del fruto inducida por d18:0 se caracterizó por altos niveles de ABA e IAA, así como bajos niveles de GA y CK en la AZ del fruto en el olivo.

7. Los aumentos en los niveles endógenos de IAA en la AZ del fruto en respuesta al tratamiento d18:0 coincidieron con niveles de expresión más altos de la enzima de biosíntesis, TAR2, de las enzimas de homeostasis de auxina, ILR1-like 1, ILR1-like 3 y ILR1-like 5, así como de un transportador de flujo de entrada de auxina, LAX5. Además, los genes *IAA16* y *ARF2B* de señalización de auxinas fueron inducidos, mientras *IAA14*, *ARF18* y *ARF19* fueron reprimidos exclusivamente en la AZ del fruto, lo que sugiere que *IAA16* e *IAA14* pueden ser genes candidatos clave de la señalización de auxinas durante la indución de la abscisión por d18:0.

8. La abscisión del fruto inducida por d18:0 está mediada por la inducción de la síntesis (SAMS1 y ACO11) y la señalización (ERF11, ERF12 y ERF118) de etileno, lo que sugiere que tanto ACO como ERF pueden ser fundamentales para equilibrar las necesidades de biosíntesis con los requerimientos de señalización de etileno durante la abscisión del fruto del olivo.

9. La esfinganina (d18:0) indujo la biosíntesis (a través de *NECD1*) y la señalización (a través de *PYL9*, *PYL8* y *PYL4)* de ABA exclusivamente en la AZ del fruto durante la abscisión selectiva del fruto en olivo, así como la biosíntesis (a través de PAL) y la señalización (PR-1) de SA, mientras que la señalización de GA está regulada negativamente en la AZ del fruto (a través de GAI1 y RGL1) y aumenta en la AZ de la hoja (a través de GAMYB). De manera similar, la señalización de CK se estimuló en la AZ de la hoja y se reprimió en la AZ del fruto en respuesta al tratamiento con d18:0, lo que reveló un control hormonal complejo que subyace a la abscisión del fruto inducida por d18:0 en la AZ del fruto y de la hoja, lo que implica programas reguladores distintos.

10. Los cambios en las transcripciones de genes estuvieron acompañados por cambios en la expresión de factores de transcripción (TF), especialmente aquellos en las familias AP2/ERF, bHLH, MYB, WRKY, TCP y bZIP durante la abscisión del fruto inducida por d18:0 en olivo. Los genes *ERF038*, *ERF003*, *bZIP43* y *MYB61* se sobreexpresaron exclusivamente en la AZ del fruto, lo que implica que estos TFs desempeñan un papel regulador durante la abscisión del fruto en olivo.

11. Nuestros resultados aportan nuevos conocimientos sobre la biología de la abscisión del fruto del olivo y permitirán desarrollar nuevas estrategias para el control selectivo de la abscisión del fruto del olivo, facilitando la recolección mecánica del cultivo y reduciendo costes sin defoliación del árbol

CONCLUSIONS

1. During natural fruit abscission in olive (*Olea europaea* L. 'Picual'), our results provide evidence of the complex regulatory pathways controlling abscission-associated events by combining differential gene expression analysis and hormonal profiling in the abscission zone (AZ) and pericarp tissues of ripe fruits. These transcriptomic data aided in the characterization of unique and common transcriptional signatures related to cell-wall modification, plant hormone metabolism and signalling, vesicle trafficking, and ion fluxes between the fruit tissues. This offers new insight into the hormonal and metabolic regulation processes that are potentially involved in the cell-wall modifications during natural fruit abscission.

2. Jasmonic acid (JA) was significantly more abundant in the AZ than in fruit pericarp tissues at the ripe stage, which is when natural olive fruit abscission takes place.

3. The transcriptional characterization of the AZ and the pericarp tissues of ripe olive fruits reveal an induction of the ethylene and abscisic acid (ABA) signalling pathways in both tissues via different components, and upregulation of the salicylic acid (SA) and JA signalling pathways in the AZ, validated by qRT-PCR analysis.

4. The present study provides evidence that sphinganine (d18:0) may regulate selective olive fruit abscission mainly through the up-regulation of *NCER2* and *NCER3* genes encoding neutral ceramidase, as well as of *KCS4* and *KCS12* genes that encode 3-ketoacyl-CoA synthase in the fruit AZ, supporting the hypothesis that the homeostasis between LCB and ceramide play an important role in fruit abscission in olive.

5. The transcriptomic analysis of AZs of fruit and leaf in 'Manzanilla Sevillana' olive revealed that a differential induction of cell-wall-degrading genes is associated with the upregulation of genes involved in ion fluxes, and a shift in plant-hormone metabolism and signalling genes during d18:0-induced fruit abscission. This is accompanied by transcriptional activity of membrane receptor kinases (HSL1 and BAM1), and rapid alkalinization factor (RALF) potentially involved in fruit abscission

signalling. In view of the present findings, further research is now required to identify and characterize the different components of the olive IDA-HAE/HSL1-like or HSL2-like module and to suggest that this putative module operates in the olive fruit AZ together with cytosolic pH changes.

6. The d18:0-induced fruit abscission is characterized by high levels of ABA and indole-3-acetic acid (IAA) as well as low gibberellins (GAs) and cytokinins (CKs) levels in the olive fruit AZ.

7. Rises in endogenous IAA levels in the fruit AZ in response to d18:0 treatment coincided with higher expression levels for one biosynthesis enzyme, *TAR2*, for the auxin homeostasis enzymes, *ILR1-like 1*, *ILR1-like 3*, and *ILR1-like 5*, as well as for one auxin influx carrier-like protein, *LAX5*. In addition, *IAA16* and *ARF2B* genes, involved in auxin signalling, were upregulated, and *IAA14*, *ARF18* and *ARF19* were downregulated exclusively in the fruit AZ, suggesting that *IAA16* and *IAA14* may be key candidate genes of auxin signalling during d18:0-induced fruit abscission in olive.

8. The d18:0-induced fruit abscission is mediated by upregulated ethylene synthesis (*SAMS1* and *ACO11*) and signalling (*ERF11*, *ERF12* and *ERF118*), suggests that both ACO and ERF may be instrumental in balancing the ethylene biosynthesis needs with the ethylene signalling requirements during olive fruit abscission.

9. Sphinganine (d18:0) induced ABA biosynthesis (via *NECD1*) and signalling (via *PYL9*, *PYL8* and *PYL4)*, as well as, SA biosynthesis (via PAL) and signalling (PR-1) pathways exclusively in the fruit AZ during selective olive fruit abscission, whereas GA signalling is negatively regulated in the fruit AZ (via *GAI1* and *RGL1*) and is upregulated in the leaf AZ (via *GAMYB*). Similarly, CK signalling was stimulated in the leaf AZ and repressed in the fruit AZ in response to d18:0 treatment, revealing complex hormone control underlying d18-induced fruit abscission in AZs of fruit and leaf, implying distinct regulatory programmes.

10. Changes in gene transcripts were accompanied by changes in expression of TFs, especially those in the TFs AP2/ERF, bHLH, MYB, WRKY, TCP, and bZIP families during d18:0-induced fruit abscission in olive. *ERF038*, *ERF003*, *bZIP43*, and *MYB61* genes were exclusively overexpressed in the fruit AZ, implying that these TFs play a regulatory role during olive fruit abscission.

11. Our results provide new insight into the biology of olive fruit abscission and this will enable the development of new strategies for the selective control of the fruit abscission in olive, facilitating mechanical harvest of the crop and reducing costs without tree defoliation.

5.REFERENCIAS

Aalen, R. B., Wildhagen, M., Stø, I. M., & Butenko, M. A. (2013). IDA: a peptide ligand regulating cell separation processes in Arabidopsis. *Journal of Experimental Botany*, *64*(17), 5253-5261. doi: https://doi.org/10.1093/jxb/ert338

Abbas, H. K., Tanaka, T., Duke, S. O., Porter, J. K., Wray, E. M., Hodges, L., Sessions, A.E., Wang, E., Merril Jr, A.E., & Riley, R. T. (1994). Fumonisin- and AAL-toxin-induced disruption of sphingolipid metabolism with accumulation of free sphingoid bases. *Plant Physiology*, *106*(3), 1085-1093. doi: https://doi.org/10.1104/pp.106.3.1085

Abeles, F. B., Morgan, P. W., & Saltveit Jr, M. E. (2012). *Ethylene in plant biology*. Academic press.

Abeles, F. B., & Rubinstein, B. (1964). Regulation of ethylene evolution and leaf abscission by auxin. *Plant Physiology*, *39*(6), 963. Doi: 10.1104/pp.39.6.963

Addicott, F. T. (1970). Plant hormones in the control of abscission. *Biological Reviews*, *45*(4), 485-524.

Addicott, F. T. (1982). *Abscission*. Univ of California Press.

Agustí, J., Merelo, P., Cercós, M., Tadeo, F. R., & Talón, M. (2009). Comparative transcriptional survey between laser-microdissected cells from laminar abscission zone and petiolar cortical tissue during ethylene-promoted abscission in citrus leaves. *BMC Plant Biology*, *9*, 1-20. doi: https://doi.org/10.1186/1471-2229-9-127

Alagna, F., D'Agostino, N., Torchia, L., Servili, M., Rao, R., Pietrella, M., Giuliano, G., Chiusano, M.L., Baldoni, L., & Perrotta, G. (2009). Comparative 454 pyrosequencing of transcripts from two olive genotypes during fruit development. *BMC genomics*, *10*(1), 1-15. doi: https://doi.org/10.1186/1471-2164-10-399

Alagna, F., Mariotti, R., Panara, F., Caporali, S., Urbani, S., Veneziani, G., Esposto, S., Taticchi, A., Rosati, A., Rao, R., Perrotta, G., Servili, M., & Baldoni, L. (2012). Olive phenolic compounds: metabolic and transcriptional profiling during fruit development. *BMC plant biology*, *12*, 1-19. doi: https://doi.org/10.1186/1471-2229-12-162

Alden, K. P., Dhondt-Cordelier, S., McDonald, K. L., Reape, T. J., Ng, C. K. Y., McCabe, P. F., & Leaver, C. J. (2011). Sphingolipid long chain base phosphates can regulate apoptotic-like programmed cell death in plants. *Biochemical and Biophysical Research Communications*, *410*(3), 574-580. Doi: https://doi.org/10.1016/j.bbrc.2011.06.028

Ali, U., Li, H., Wang, X., & Guo, L. (2018). Emerging roles of sphingolipid signalling in plant response to biotic and abiotic stresses. *Molecular plant*, *11*(11), 1328-1343. Doi: https://doi.org/10.1016/j.molp.2018.10.001

Asai, T., Stone, J. M., Heard, J. E., Kovtun, Y., Yorgey, P., Sheen, J., & Ausubel, F. M. (2000). Fumonisin B1–induced cell death in Arabidopsis protoplasts requires jasmonate-, ethylene-, and salicylate-dependent signalling pathways. *The Plant Cell*, *12*(10), 1823-1835. doi: https://doi.org/10.1105/tpc.12.10.1823

Baldoni, L., & Belaj, A. (2009). Olive. *Oil crops*, 397-421. doi: https://doi.org/10.1007/978-0-387-77594-4_13

Banno, K., Martin, G. C., & Carlson, R. M. (1993). The role of phosphorus as an abscission-inducing agent for olive leaves and fruit. *Journal of the American*

Society for Horticultural Science, *118*(5), 599-604. doi: https://doi.org/10.21273/JASHS.118.5.599

Bar-Dror, T., Dermastia, M., Kladnik, A., Žnidarič, M. T., Novak, M. P., Meir, S., Burd, S., Philoshop-Hadas, S., Ori, N., Sonego, L., Dickman, M. B., & Lers, A. (2011). Programmed cell death occurs asymmetrically during abscission in tomato. *The Plant Cell*, *23*(11), 4146-4163. doi: 10.1105/tpc.111.092494

Barghini, E., Natali, L., Cossu, R. M., Giordani, T., Pindo, M., Cattonaro, F., Scalabrin, S., Velasco, R., Morgante, Michele., & Cavallini, A. (2014). The peculiar landscape of repetitive sequences in the olive (Olea europaea L.) genome. *Genome biology and evolution*, *6*(4), 776-791. doi: 10.1093/gbe/evu058

Barranco, D., Arquero, O., Navarro García, C., & Rapoport, H. F. (2004). Monopotassium phosphate for olive fruit abscission. American Society for Horticultural Science. Doi: https://doi.org/10.21273/HORTSCI.39.6.1313

Barranco, D., De Toro, C. C., Oria, M., & Rapoport, H. F. (2002). Monpotasium phosphate (PO4H2K) for olive fruit abscission. In *IV International Symposium on Olive Growing 586* (pp. 263-266). doi: 10.17660/ActaHortic.2002.586.50

Bartolini, S., Cantini, C., & Vitagliano, C. (1992). Olive fruit abscission: anatomical observations following application of ethylene-releasing compound. In *VII International Symposium on Plant Growth Regulators in Fruit Production 329* (pp. 249-251). doi: 10.17660/ActaHortic.1993.329.55

Basu, M. M., González-Carranza, Z. H., Azam-Ali, S., Tang, S., Shahid, A. A., & Roberts, J. A. (2013). The manipulation of auxin in the abscission zone cells of Arabidopsis flowers reveals that indoleacetic acid signalling is a prerequisite for organ shedding. *Plant physiology*, *162*(1), 96-106. doi: 10.1104/pp.113.216234

Beeler, T., Bacikova, D., Gable, K., Hopkins, L., Johnson, C., Slife, H., & Dunn, T. (1998). The Saccharomyces cerevisiae TSC10/YBR265w gene encoding 3-ketosphinganine reductase is identified in a screen for temperature-sensitive suppressors of the Ca2+-sensitive csg2Δ mutant. *Journal of Biological Chemistry*, *273*(46), 30688-30694. doi:10.1074/jbc.273.46.30688

Bellini, E. (1993). Behaviour of some genetic characters in olive seedlings obtained by cross-breeding. *Fruit Breeding and Genetics 317*, 197-208. doi: 10.17660/ActaHortic.1992.317.24

Bellini, E., Giordani, E., Parlati, M. V., & Pandolfi, S. (2000). Olive genetic improvement: thirty years of research. In *IV International Symposium on Olive Growing 586* (pp. 105-108). doi: 10.17660/ActaHortic.2002.586.13

Ben-Tal, Y., & Wodner, M. (1993). Chemical loosening of olive pedicel's for mechanical harvesting. In *II International Symposium on Olive Growing 356* (pp. 297-301). doi: 10.17660/ActaHortic.1994.356.62

Berkey, R., Bendigeri, D., & Xiao, S. (2012). Sphingolipids and plant defense/disease: the "death" connection and beyond. *Frontiers in plant science*, *3*, 68.

Bi, F. C., Liu, Z., Wu, J. X., Liang, H., Xi, X. L., Fang, C., Sun, T.J., Yin, J., Dai, G.J., Rong, C., Greenberg, J.T., Su, W.W., & Yao, N. (2014). Loss of ceramide kinase in Arabidopsis impairs defenses and promotes ceramide accumulation and mitochondrial H2O2 bursts. *The Plant Cell*, *26*(8), 3449-3467. doi: 10.1105/tpc.114.127050

Bianco, L., Alagna, F., Baldoni, L., Finnie, C., Svensson, B., & Perrotta, G. (2013). Proteome regulation during Olea europaea fruit development. *PLoS one*, *8*(1), e53563. Doi: https://doi.org/10.1371/journal.pone.0053563

Binder, B. M., & Patterson, S. E. (2009). Ethylene-dependent and-independent regulation of abscission. *Stewart Postharvest Review*, *5*(1), 1-10. doi: 10.2212/spr.2009.1.1

Blanusa, T., Else, M. A., Atkinson, C. J., & Davies, W. J. (2005). The regulation of sweet cherry fruit abscission by polar auxin transport. *Plant growth regulation*, *45*, 189-198. doi: 10.1007/s10725-005-3568-9

Bohn, M., Heinz, E., & Lüthje, S. (2001). Lipid composition and fluidity of plasma membranes isolated from corn (Zea mays L.) roots. *Archives of Biochemistry and Biophysics*, *387*(1), 35-40. doi: https://doi.org/10.1006/abbi.2000.2224

Botton, A., Eccher, G., Forcato, C., Ferrarini, A., Begheldo, M., Zermiani, M., Moscatello, S., Batistelli, A., Velasco, R., Ruperti, B., & Ramina, A. (2011). Signalling pathways mediating the induction of apple fruitlet abscission. *Plant physiology*, *155*(1), 185-208. doi: https://doi.org/10.1104/pp.110.165779

Botton, A., & Ruperti, B. (2019). The yes and no of the ethylene involvement in abscission. *Plants*, *8*(6), 187. doi: https://doi.org/10.3390/plants8060187

Brodersen, P., Petersen, M., Pike, H. M., Olszak, B., Skov, S., Ødum, N., Jorgensen, L. B., Brown, R.E., & Mundy, J. (2002). Knockout of Arabidopsis accelerated-cell-death11 encoding a sphingosine transfer protein causes activation of programmed cell death and defense. *Genes & development*, *16*(4), 490-502. doi: 10.1101/gad.218202

Bromley, P. E., Li, Y. O., Murphy, S. M., Sumner, C. M., & Lynch, D. V. (2003). Complex sphingolipid synthesis in plants: characterization of inositolphosphorylceramide synthase activity in bean microsomes. *Archives of Biochemistry and Biophysics*, *417*(2), 219-226. doi: 10.1016/S0003-9861(03)00339-4

Bruno, L., Picardi, E., Pacenza, M., Chiappetta, A., Muto, A., Gagliardi, O., Muzzalupo, I., Pesole, G., & Bitonti, M. B. (2019). Changes in gene expression and metabolic profile of drupes of Olea europaea L. cv Carolea in relation to maturation stage and cultivation area. *BMC Plant Biology*, *19*(1), 1-17. doi: 10.1186/s12870-019-1969-6

Budiman, M. A., Chang, S. B., Lee, S., Yang, T. J., Zhang, H. B., De Jong, H., & Wing, R. A. (2004). Localization of jointless-2 gene in the centromeric region of tomato chromosome 12 based on high resolution genetic and physical mapping. *Theoretical and applied genetics*, *108*, 190-196. doi: 10.1007/s00122-003-1429-3

Buré, C., Cacas, J. L., Badoc, A., Mongrand, S., & Schmitter, J. M. (2016). Branched glycosylated inositolphosphosphingolipid structures in plants revealed by MS3 analysis. *Journal of Mass Spectrometry*, *51*(4), 305-308. doi: 10.1002/jms.3758

Buré, C., Cacas, J. L., Mongrand, S., & Schmitter, J. M. (2014). Characterization of glycosyl inositol phosphoryl ceramides from plants and fungi by mass spectrometry. *Analytical and bioanalytical chemistry*, *406*, 995-1010. doi: 10.1007/s00216-013-7130-8

Buré, C., Cacas, J. L., Wang, F., Gaudin, K., Domergue, F., Mongrand, S., & Schmitter, J. M. (2011). Fast screening of highly glycosylated plant sphingolipids by tandem mass spectrometry. *Rapid Communications in Mass Spectrometry*, *25*(20), 3131-3145. doi: 10.1002/rcm.5206

Butenko, M. A., Patterson, S. E., Grini, P. E., Stenvik, G. E., Amundsen, S. S., Mandal, A., & Aalen, R. B. (2003). Inflorescence deficient in abscission controls floral organ abscission in Arabidopsis and identifies a novel family of putative ligands in plants. *The Plant Cell*, *15*(10), 2296-2307. doi: 10.1105/tpc.014365

Butenko, M. A., Shi, C. L., & Aalen, R. B. (2012). KNAT1, KNAT2 and KNAT6 act downstream in the IDA-HAE/HSL2 signalling pathway to regulate floral organ abscission. *Plant signalling & behavior*, *7*(1), 135-138. doi: 10.4161/psb.7.1.18379

Butenko, M. A., Stenvik, G. E., Alm, V., Sæther, B., Patterson, S. E., & Aalen, R. B. (2006). Ethylene-dependent and-independent pathways controlling floral abscission are revealed to converge using promoter: reporter gene constructs in the ida abscission mutant. *Journal of Experimental Botany*, *57*(14), 3627-3637. doi: 10.1093/jxb/erl130

Cacas, J. L., Bure, C., Furt, F., Maalouf, J. P., Badoc, A., Cluzet, S., Schmitter, J. M., Antajan, E., & Mongrand, S. (2013). Biochemical survey of the polar head of plant glycosylinositolphosphoceramides unravels broad diversity. *Phytochemistry*, *96*, 191-200. doi: j.phytochem.2013.08.002

Cacas, J. L., Buré, C., Grosjean, K., Gerbeau-Pissot, P., Lherminier, J., Rombouts, Y., Maes, E., Bossard, E., Granier, J., Furt, F., Fouillen, L., Germain, V., Bayer, E., Cluzet, S., Robert, F., Schmitter, J.M., Deleu, M., Lins, L., Simons-Plas, F., & Mongrand, S. (2016). Revisiting plant plasma membrane lipids in tobacco: a focus on sphingolipids. *Plant physiology*, *170*(1), 367-384. doi: 10.1104/pp.15.00564

Cacas, J. L., Furt, F., Le Guédard, M., Schmitter, J. M., Buré, C., Gerbeau-Pissot, P., Moreau, P., Bessoule, J. J., Simon-Plas, F., & Mongrand, S. (2012). Lipids of plant membrane rafts. *Progress in lipid research*, *51*(3), 272-299. doi: 10.1016/j.plipres.2012.04.001

Cai, S., & Lashbrook, C. C. (2008). Stamen abscission zone transcriptome profiling reveals new candidates for abscission control: enhanced retention of floral organs in transgenic plants overexpressing Arabidopsis ZINC FINGER PROTEIN2. *Plant physiology*, *146*(3), 1305-1321. doi: 10.1104/pp.107.110908

Cantrel, C., Vazquez, T., Puyaubert, J., Rezé, N., Lesch, M., Kaiser, W. M., Dutilleul, C., Guillas, I., Zachowski, A., & Baudouin, E. (2011). Nitric oxide participates in cold-responsive phosphosphingolipid formation and gene expression in Arabidopsis thaliana. *New Phytologist*, *189*(2), 415-427. doi: 10.1111/j.1469-8137.2010.03500.x

Carmona-Salazar, L., Cahoon, R. E., Gasca-Pineda, J., González-Solís, A., Vera-Estrella, R., Treviño, V., Cahoon, E.B., & Gavilanes-Ruiz, M. (2021). Plasma and vacuolar membrane sphingolipidomes: composition and insights on the role of main molecular species. *Plant physiology*, *186*(1), 624-639. doi: 10.1093/plphys/kiab064

Carmona, R., Zafra, A., Seoane, P., Castro, A. J., Guerrero-Fernández, D., Castillo-Castillo, T., Medina-García, A., Cánovas, F.M., & Claros, M. G. (2015). ReprOlive: a database with linked data for the olive tree (Olea europaea L.) reproductive transcriptome. *Frontiers in Plant Science*, *6*, 625. doi: 10.3389/fpls.2015.00625

Carter, C., Pan, S., Zouhar, J., Avila, E. L., Girke, T., & Raikhel, N. V. (2004). The vegetative vacuole proteome of Arabidopsis thaliana reveals predicted and

unexpected proteins. *The Plant Cell*, *16*(12), 3285-3303. doi: 10.1105/tpc.104.027078

Cassim, A. M., Gouguet, P., Gronnier, J., Laurent, N., Germain, V., Grison, M., Boutté, Y., Gerbeau-Pissot, P., Simon-Plas, F., & Mongrand, S. (2019). Plant lipids: Key players of plasma membrane organization and function. *Progress in Lipid Research*, *73*, 1-27. doi: 10.1016/j.plipres.2018.11.002

Castillo-Llanque, F., & Rapoport, H. F. (2009). Identifying the location of olive fruit abscission. *Scientia horticulturae*, *120*(2), 292-295. doi: 10.1016/j.scienta.2008.11.006

Chao, D. Y., Gable, K., Chen, M., Baxter, I., Dietrich, C. R., Cahoon, E. B., Guerinot, M. L., Lahaner, B., Lü, S., Markham, J. E., Morrisey, J., Han, G., Gupta, S. D., Harmon, J. M., Jaworski, J. G., Dunn, T. M., & Salt, D. E. (2011). Sphingolipids in the root play an important role in regulating the leaf ionome in Arabidopsis thaliana. *The Plant Cell*, *23*(3), 1061-1081. doi: 10.1105/tpc.110.079095

Chen, J., Li, Z., Cheng, Y., Gao, C., Guo, L., Wang, T., & Xu, J. (2020). Sphinganine-analog mycotoxins (SAMs): chemical structures, bioactivities, and genetic controls. *Journal of Fungi*, *6*(4), 312. doi: 10.3390/jof6040312

Chen, Q., Xu, F., Wang, L., Suo, X., Wang, Q., Meng, Q., Huang, L., Ma, C., Li, G., & Luo, M. (2021). Sphingolipid profile during cotton fiber growth revealed that a phytoceramide containing hydroxylated and saturated VLCFA is important for fiber cell elongation. *Biomolecules*, *11*(9), 1352. doi: 10.3390/biom11091352

Chen, M., Cahoon, E. B., Saucedo-García, M., Plasencia, J., & Gavilanes-Ruíz, M. (2009). Plant sphingolipids: structure, synthesis and function. *Lipids in photosynthesis: essential and regulatory functions*, 77-115. doi: 10.1007/978-90-481-2863-1_5

Chen, M., Han, G., Dietrich, C. R., Dunn, T. M., & Cahoon, E. B. (2006). The essential nature of sphingolipids in plants as revealed by the functional identification and characterization of the Arabidopsis LCB1 subunit of serine palmitoyltransferase. *The Plant Cell*, *18*(12), 3576-3593. doi: https://doi.org/10.1105/tpc.105.040774

Chen, M., Markham, J. E., & Cahoon, E. B. (2012). Sphingolipid Δ8 unsaturation is important for glucosylceramide biosynthesis and low-temperature performance in Arabidopsis. *The Plant Journal*, *69*(5), 769-781. doi: 10.1111/j.1365-313X.2011.04829.x

Chen, M., Markham, J. E., Dietrich, C. R., Jaworski, J. G., & Cahoon, E. B. (2008). Sphingolipid long-chain base hydroxylation is important for growth and regulation of sphingolipid content and composition in Arabidopsis. *The Plant Cell*, *20*(7), 1862-1878. doi: 10.1105/tpc.107.057851

Chen, W. H., Li, P. F., Chen, M. K., Lee, Y. I., & Yang, C. H. (2015). FOREVER YOUNG FLOWER negatively regulates ethylene response DNA-binding factors by activating an ethylene-responsive factor to control Arabidopsis floral organ senescence and abscission. *Plant Physiology*, *168*(4), 1666-1683. doi: 10.1104/pp.15.00433

Cheng, L., Li, R., Wang, X., Ge, S., Wang, S., Liu, X., He, J., Jiang, C. Z., Qi, M., Xu, T., & Li, T. (2022). A SlCLV3-SlWUS module regulates auxin and ethylene homeostasis in low light-induced tomato flower abscission. *The Plant Cell*, *34*(11), 4388-4408. doi: 10.1093/plcell/koac254

Cho, M., & Cho, H. (2013). The function of ABCB transporters in auxin transport. *Plant signalling & behavior*, *8*(2), 642-54. doi: 10.4161/psb.22990

Cho, S. K., Larue, C. T., Chevalier, D., Wang, H., Jinn, T. L., Zhang, S., & Walker, J. C. (2008). Regulation of floral organ abscission in Arabidopsis thaliana. *Proceedings of the National Academy of Sciences*, *105*(40), 15629-15634. doi: 10.1073/pnas.0805539105

Chueasiri, C., Chunthong, K., Pitnjam, K., Chakhonkaen, S., Sangarwut, N., Sangsawang, K., Suksangpanomrung, M., Michaelson, L.V., Napier, J.A., & Muangprom, A. (2014). Rice ORMDL controls sphingolipid homeostasis affecting fertility resulting from abnormal pollen development. *PLoS One*, *9*(9), e106386. doi: 10.1371/journal.pone.0106386

Cirilli, M., Caruso, G., Gennai, C., Urbani, S., Frioni, E., Ruzzi, M., Servili, M., Gucci, R., Poerio, E., & Muleo, R. (2017). The role of polyphenoloxidase, peroxidase, and β-glucosidase in phenolics accumulation in Olea europaea L. fruits under different water regimes. *Frontiers in plant science*, *8*, 717. doi: 10.3389/fpls.2017.00717

Coll, N. S., Epple, P., & Dangl, J. L. (2011). Programmed cell death in the plant immune system. *Cell Death & Differentiation*, *18*(8), 1247-1256. doi: 10.1038/cdd.2011.37

Corbacho, J., Inês, C., Paredes, M. A., Labrador, J., Cordeiro, A. M., Gallardo, M., & Gomez-Jimenez, M. C. (2018). Modulation of sphingolipid long-chain base composition and gene expression during early olive-fruit development, and putative role of brassinosteroid. *Journal of plant physiology*, *231*, 383-392. doi:10.1016/j.jplph.2018.10.018

Corbacho, J., Romojaro, F., Pech, J. C., Latché, A., & Gomez-Jimenez, M. C. (2013). Transcriptomic events involved in melon mature-fruit abscission comprise the sequential induction of cell-wall degrading genes coupled to a stimulation of endo and exocytosis. *PloS one*, *8*(3), e58363. doi: 10.1371/journal.pone.0058363

Corrado, G., Alagna, F., Rocco, M., Renzone, G., Varricchio, P., Coppola, V., Garonna, A., Baldoni, L., Scaloni, A., & Rao, R. (2012). Molecular interactions between the olive and the fruit fly Bactrocera oleae. *BMC Plant Biology*, *12*. doi: 10.1186/1471-2229-12-86

Coursol, S., Fan, L. M., Stunff, H. L., Spiegel, S., Gilroy, S., & Assmann, S. M. (2003). Sphingolipid signalling in Arabidopsis guard cells involves heterotrimeric G proteins. *Nature*, *423*(6940), 651-654. doi: 10.1038/nature01643

Coursol, S., Le Stunff, H., Lynch, D. V., Gilroy, S., Assmann, S. M., & Spiegel, S. (2005). Arabidopsis sphingosine kinase and the effects of phytosphingosine-1-phosphate on stomatal aperture. *Plant Physiology*, *137*(2), 724-737. doi: 10.1104/pp.104.055806

Couzigou, J. M., Magne, K., Mondy, S., Cosson, V., Clements, J., & Ratet, P. (2016). The legume NOOT-BOP-COCH-LIKE genes are conserved regulators of abscission, a major agronomical trait in cultivated crops. *New Phytologist*, *209*(1), 228-240. doi: 10.1111/nph.13634

Crick, J., Corrigan, L., Belcram, K., Khan, M., Dawson, J. W., Adroher, B., Hepwoeth, S. R., & Pautot, V. (2022). Floral organ abscission in Arabidopsis requires the combined activities of three TALE homeodomain transcription factors. *Journal of Experimental Botany*, *73*(18), 6150-6169. doi: 10.1093/jxb/erac255

Cruz, F., Julca, I., Gómez-Garrido, J., Loska, D., Marcet-Houben, M., Cano, E., Galán, B., Frias, L., Ribeca, P, Derdak, S., Gut, M., Sánchez-Fernández, M., García, J. L., Gut, I. G., Vargas, P., Alioto, T. S., & Gabaldón, T. (2016). Genome sequence of the olive tree, Olea europaea. *Gigascience*, *5*(1), s13742-016. doi: 10.1186/s13742-016-0134-5

Da Silva, D., Lachaud, C., Cotelle, V., Brière, C., Grat, S., Mazars, C., & Thuleau, P. (2011). Nitric oxide production is not required for dihydrosphingosine-induced cell death in tobacco BY-2 cells. *Plant signalling & behavior*, *6*(5), 736-739. doi: 10.4161/psb.6.5.15126

Dai, G. Y., Yin, J., Li, K. E., Chen, D. K., Liu, Z., Bi, F. C., Rong, C., & Yao, N. (2020). The Arabidopsis AtGCD3 protein is a glucosylceramidase that preferentially hydrolyzes long-acyl-chain glucosylceramides. *Journal of Biological Chemistry*, *295*(3), 717-728. doi: 10.1016/S0021-9258(17)49930-3

Dal Cin, V., Danesin, M., Boschetti, A., Dorigoni, A., & Ramina, A. (2005). Ethylene biosynthesis and perception in apple fruitlet abscission (Malus domestica L. Borck). *Journal of Experimental Botany*, *56*(421), 2995-3005. doi: 10.1093/jxb/eri296

Davis, J. A., Pares, R. B., Palmgren, M., López-Marqués, R. L., & Harper, J. F. (2020). A potential pathway for flippase-facilitated glucosylceramide catabolism in plants. *Plant Signalling & Behavior*, *15*(10), 1783486. doi: 10.1080/15592324.2020.1783486

De Bigault Du Granrut, A., & Cacas, J. L. (2016). How very-long-chain fatty acids could signal stressful conditions in plants?. *Frontiers in plant science*, *7*, 1490. doi: 10.3389/fpls.2016.01490

Degenkolbe, T., Giavalisco, P., Zuther, E., Seiwert, B., Hincha, D. K., & Willmitzer, L. (2012). Differential remodeling of the lipidome during cold acclimation in natural accessions of Arabidopsis thaliana. *The Plant Journal*, *72*(6), 972-982. doi: 10.1111/tpj.12007

Del Campillo, E., & Bennett, A. B. (1996). Pedicel breakstrength and cellulase gene expression during tomato flower abscission. *Plant Physiology*, *111*(3), 813-820. doi: 10.1104/pp.111.3.813

Denney, J. O., & Martin, G. C. (1994). Ethephon tissue penetration and harvest effectiveness in olive as a function of solution pH, application time, and BA or NAA addition. *Journal of the American Society for Horticultural Science*, *119*(6), 1185-1192. doi: 10.21273/JASHS.119.6.1185

Di Rienzo, V., Sion, S., Taranto, F., D'Agostino, N., Montemurro, C., Fanelli, V., Sabetta, W., Boucheffa, S., Tamendjari, A., Pasqualone, A., Zammit-Mangion, M., & Miazzi, M. M. (2018). Genetic flow among olive populations within the Mediterranean basin. *Peer J*, *6*, e5260. doi: 10.7717/peerj.5260

Dietrich, C. R., Han, G., Chen, M., Berg, R. H., Dunn, T. M., & Cahoon, E. B. (2008). Loss-of-function mutations and inducible RNAi suppression of Arabidopsis LCB2 genes reveal the critical role of sphingolipids in gametophytic and sporophytic cell viability. *The Plant Journal*, *54*(2), 284-298. doi: j.1365-313X.2008.03420.x

Ding, Y., Chang, J., Ma, Q., Chen, L., Liu, S., Jin, S., Han, J., Xu, R., Zhu, A., Guo, J., Luo, Y., Xu, J., Xu, Q., Zeng, Y., Deng, X., & Cheng, Y. (2015). Network analysis of postharvest senescence process in citrus fruits revealed by transcriptomic and metabolomic profiling. *Plant physiology*, *168*(1), 357-376. doi: 10.1104/pp.114.255711

Doebley, J. F., Gaut, B. S., & Smith, B. D. (2006). The molecular genetics of crop domestication. *Cell*, *127*(7), 1309-1321. doi: 10.1016/j.cell.2006.12.006

Droillard, M. J., Bureau, D., & Paulin, A. (1989). Changes in activities of superoxide dismutases during aging of petals of cut carnations (Dianthus caryophyllus). *Physiologia Plantarum*, *76*(2), 149-154. doi: h10.1111/j.1399-3054.1989.tb05624.x

Dunn, T. M., Lynch, D. V., Michaelson, L. V., & Napier, J. A. (2004). A post-genomic approach to understanding sphingolipid metabolism in Arabidopsis thaliana. *Annals of Botany*, *93*(5), 483-497. doi: 10.1093/aob/mch071

Dutilleul, C., Benhassaine-Kesri, G., Demandre, C., Rézé, N., Launay, A., Pelletier, S., Renou, J. P., Zachowski, A., Baudouin, E., & Guillas, I. (2012). Phytosphingosine-phosphate is a signal for AtMPK6 activation and Arabidopsis response to chilling. *New Phytologist*, *194*(1), 181-191. doi: 10.1111/j.1469-8137.2011.04017.x

Dutilleul, C., Chavarria, H., Rézé, N., Sotta, B., Baudouin, E., & Guillas, I. (2015). Evidence for ACD 5 ceramide kinase activity involvement in A rabidopsis response to cold stress. *Plant, Cell & Environment*, *38*(12), 2688-2697. Doi: https://doi.org/10.1111/pce.12578

Ebert, B., Rautengarten, C., McFarlane, H. E., Rupasinghe, T., Zeng, W., Ford, K., Scheller H. V., Bacic., Roessner, U., Persson, S., & Heazlewood, J. L. (2018). A Golgi UDP-GlcNAc transporter delivers substrates for N-linked glycans and sphingolipids. *Nature Plants*, *4*(10), 792-801. doi: 10.1038/s41477-018-0235-5

Ellis, C. M., Nagpal, P., Young, J. C., Hagen, G., Guilfoyle, T. J., & Reed, J. W. (2005). AUXIN RESPONSE FACTOR1 and AUXIN RESPONSE FACTOR2 regulate senescence and floral organ abscission in Arabidopsis thaliana. doi: https: 10.1242/dev.02012

Estornell, L. H., Agustí, J., Merelo, P., Talón, M., & Tadeo, F. R. (2013). Elucidating mechanisms underlying organ abscission. *Plant Science*, *199*, 48-60. doi: 10.1016/j.plantsci.2012.10.008

Estornell, L. H., Wildhagen, M., Pérez-Amador, M. A., Talón, M., Tadeo, F. R., & Butenko, M. A. (2015). The IDA peptide controls abscission in Arabidopsis and Citrus. *Frontiers in plant science*, *6*, 1003. doi: https://doi.org/10.3389/fpls.2015.01003

Falchi, R., Cipriani, G., Marrazzo, T., Nonis, A., Vizzotto, G., & Ruperti, B. (2010). Identification and differential expression dynamics of peach small GTPases encoding genes during fruit development and ripening. *Journal of Experimental Botany*, *61*(10), 2829-2842. doi: 10.1093/jxb/erq116

Fan, X., Naz, M., Fan, X., Xuan, W., Miller, A. J., & Xu, G. (2017). Plant nitrate transporters: from gene function to application. *Journal of Experimental Botany*, *68*(10), 2463-2475. doi: 10.1093/jxb/erx011

Fanani, M. L., & Maggio, B. (2017). The many faces (and phases) of ceramide and sphingomyelin I–single lipids. *Biophysical reviews*, *9*, 589-600. doi: 10.1007/s12551-017-0297-z

Fang, L., Ishikawa, T., Rennie, E. A., Murawska, G. M., Lao, J., Yan, J., Tsai, A. I-L., Baidoo, E. E. K., Xu, J., Keasling, J. D., Demura, T., Kawai-Yamada, M., Scheller, H. V., & Mortimer, J. C. (2016). Loss of inositol phosphorylceramide sphingolipid mannosylation induces plant immune responses and reduces

cellulose content in Arabidopsis. *The Plant Cell*, *28*(12), 2991-3004. doi: 10.1105/tpc.16.00186

Fedoroff, N. V. (2002). Cross-talk in abscisic acid signalling. *Science's STKE*, *2002*(140), re10-re10. doi: 10.1126/stke.2002.140.re10

Fehling, E., & Mukherjee, K. D. (1991). Acyl-CoA elongase from a higher plant (Lunaria annua): metabolic intermediates of very-long-chain acyl-CoA products and substrate specificity. *Biochimica et Biophysica Acta (BBA)-Lipids and Lipid Metabolism*, *1082*(3), 239-246. doi: 10.1016/0005-2760(91)90198-Q

Ferguson, L., Rosa, U. A., Castro-Garcia, S., Krueger, G., & JX, B. (2010). Mechanical harvesting of California table and oil olives. *Mechanical Harvesting of California Table and Oil Olives*, 1000-1011.

Forlani, S., Masiero, S., & Mizzotti, C. (2019). Fruit ripening: the role of hormones, cell wall modifications, and their relationship with pathogens. *Journal of experimental botany*, *70*(11), 2993-3006. doi: 10.1093/jxb/erz112

Fouillen, L., Maneta-Peyret, L., & Moreau, P. (2018). ER membrane lipid composition and metabolism: lipidomic analysis. *The Plant Endoplasmic Reticulum: Methods and Protocols*, 125-137.

Fujimoto, T., & Parmryd, I. (2017). Interleaflet coupling, pinning, and leaflet asymmetry—major players in plasma membrane nanodomain formation. *Frontiers in cell and developmental biology*, *4*, 155. doi: https://doi.org/10.3389/fcell.2016.00155

Galla, G., Barcaccia, G., Ramina, A., Collani, S., Alagna, F., Baldoni, L., Cultrera. N. GM., Martinelli, F., Sebastiani, L., & Tonutti, P. (2009). Computational annotation of genes differentially expressed along olive fruit development. *BMC Plant Biology*, *9*, 1-17. doi: d10.1186/1471-2229-9-128

Ghorbani, S., Fernandez Salina, A., Hilson, P., & Beeckman, T. (2014). Signalling peptides in plants. *Cell & Developmental Biology*, *3*(2). doi: 10.4172/2168-9296.1000141

Gil-Amado, J. A., & Gomez-Jimenez, M. C. (2012). Regulation of polyamine metabolism and biosynthetic gene expression during olive mature-fruit abscission. *Planta*, *235*, 1221-1237. doi: 10.1007/s00425-011-1570-1

Gil-Amado, J. A., & Gomez-Jimenez, M. C. (2013). Transcriptome analysis of mature fruit abscission control in olive. *Plant and Cell Physiology*, *54*(2), 244-269. doi: 10.1093/pcp/pcs179

Giussani, P., Brioschi, L., Bassi, R., Riboni, L., & Viani, P. (2009). Phosphatidylinositol 3-kinase/AKT pathway regulates the endoplasmic reticulum to golgi traffic of ceramide in glioma cells: a link between lipid signalling pathways involved in the control of cell survival. *Journal of Biological Chemistry*, *284*(8), 5088-5096. doi: 10.1074/jbc.M808934200

Glazebrook, J. (2005). Contrasting mechanisms of defense against biotrophic and necrotrophic pathogens. *Annu. Rev. Phytopathol.*, *43*, 205-227. doi: 10.1146/annurev.phyto.43.040204.135923

Glazinska, P., Wojciechowski, W., Kulasek, M., Glinkowski, W., Marciniak, K., Klajn, N., Kesy, J., & Kopcewicz, J. (2017). De novo transcriptome profiling of flowers, flower pedicels and pods of Lupinus luteus (yellow lupine) reveals complex expression changes during organ abscission. *Frontiers in Plant Science*, *8*, 641. doi:10.3389/fpls.2017.00641

Goldental-Cohen, S., Burstein, C., Biton, I., Ben Sasson, S., Sadeh, A., Many, Y., Doron-Faigenboim, A., Zemach, H., Mugira, Y., Schneider, D., Birger, R., Meir, S., Philosoph-Hadas, S., Irihomovitch, V., Lavee, S., Avidan, B., & Ben-

Ari, G. (2017). Ethephon induced oxidative stress in the olive leaf abscission zone enables development of a selective abscission compound. *BMC Plant Biology*, *17*, 1-17. doi: 10.1186/s12870-017-1035-1.

Gömann, J., Herrfurth, C., Zienkiewicz, K., Haslam, T. M., & Feussner, I. (2021). Sphingolipid Δ4-desaturation is an important metabolic step for glycosylceramide formation in Physcomitrium patens. *Journal of Experimental Botany*, *72*(15), 5569-5583. doi: 10.1093/jxb/erab238

Gómez-Cadenas, A., Tadeo, F. R., Talon, M., & Primo-Millo, E. (1996). Leaf abscission induced by ethylene in water-stressed intact seedlings of Cleopatra mandarin requires previous abscisic acid accumulation in roots. *Plant Physiology*, *112*(1), 401-408. doi: 10.1104/pp.112.1.401.

Gomez-Jimenez, M. C., Paredes, M. A., Gallardo, M., Fernandez-Garcia, N., Olmos, E., & Sanchez-Calle, I. M. (2010a). Tissue-specific expression of olive S-adenosyl methionine decarboxylase and spermidine synthase genes and polyamine metabolism during flower opening and early fruit development. *Planta*, *232*, 629-647. doi:10.1007/s00425-010-1198-6

Gomez-Jimenez, M. C., Paredes, M. A., Gallardo, M., & Sanchez-Calle, I. M. (2010b). Mature fruit abscission is associated with up-regulation of polyamine metabolism in the olive abscission zone. *Journal of plant physiology*, *167*(17), 1432-1441. doi: 10.1016/j.jplph.2010.05.020

Gonzalez-Carranza, Z. H., & Roberts, J. A. (2012). Ethylene and cell separation processes. *Annual Plant Reviews Volume 44: The Plant Hormone Ethylene*, *44*, 243-273. doi: 10.1002/9781118223086.ch10

Gonzalez-Solis, A., Han, G., Gan, L., Li, Y., Markham, J. E., Cahoon, R. E., Dunn, T. M., & Cahoon, E. B. (2020). Unregulated sphingolipid biosynthesis in gene-edited Arabidopsis ORM mutants results in nonviable seeds with strongly reduced oil content. *Plant Cell*, *32*(8), 2474-2490. doi: 10.1105/tpc.20.00015

Green, P. S. (2002). A revision of Olea L. (Oleaceae). *Kew Bulletin*, 91-140.

Green, P. S., Wickens, G. E., Tan, K., Mill, R. R., & Elias, T. S. (1989). The Olea europaea complex. The Davis and Hedge Festschrift.

Greenberg, J. T., Silverman, F. P., & Liang, H. (2000). Uncoupling salicylic acid-dependent cell death and defense-related responses from disease resistance in the Arabidopsis mutant acd5. *Genetics*, *156*(1), 341-350. doi: 10.1093/genetics/156.1.341

Grison, M. S., Brocard, L., Fouillen, L., Nicolas, W., Wewer, V., Dörmann, P., Nacir, H., Benitez-Alfonso, Y., Claverol, S., Germain, V., Boutté, Y., Mongrand, S., & Bayer, E. M. (2015). Specific membrane lipid composition is important for plasmodesmata function in Arabidopsis. *The Plant Cell*, *27*(4), 1228-1250. doi: 10.1105/tpc.114.135731

Gronnier, J., Crowet, J. M., Habenstein, B., Nasir, M. N., Bayle, V., Hosy, E., Platre, P., Gouguet, P., Raffaele, S., Martinez, D., Grelard, A., Loquet, A., Simon-Plas, F., Gerbeau-Pissot, P., Der, C., Bayer, E. M., Jaillais, Y., Deleu, M., Germain, V., Lins, L., & Mongrand, S. (2017). Structural basis for plant plasma membrane protein dynamics and organization into functional nanodomains. *Elife*, *6*, e26404. Elife, 6, e26404. doi: 10.7554/eLife.26404

Gronnier, J., Legrand, A., Loquet, A., Habenstein, B., Germain, V., & Mongrand, S. (2019). Mechanisms governing subcompartmentalization of biological membranes. *Current opinion in plant biology*, *52*, 114-123. doi: 10.1016/j.pbi.2019.08.003

Grosjean, K., Der, C., Robert, F., Thomas, D., Mongrand, S., Simon-Plas, F., & Gerbeau-Pissot, P. (2018). Interactions between lipids and proteins are critical for organization of plasma membrane-ordered domains in tobacco BY-2 cells. *Journal of experimental botany*, *69*(15), 3545-3557. doi: 10.1093/jxb/ery152

Groux, R., Fouillen, L., Mongrand, S., & Reymond, P. (2022). Sphingolipids are involved in insect egg-induced cell death in Arabidopsis. *Plant Physiology*, *189*(4), 2535-2553. doi: 10.1093/plphys/kiac242

Guillas, I., Guellim, A., Rezé, N., & Baudouin, E. (2013). Long chain base changes triggered by a short exposure of Arabidopsis to low temperature are altered by AHb1 non-symbiotic haemoglobin overexpression. *Plant physiology and biochemistry*, *63*, 191-195. doi: 10.1016/j.plaphy.2012.11.020

Gulfishan, M., Jahan, A., Bhat, T. A., & Shahab, D. (2009). Senescence Signalling and Control in Plants.

Gutierrez-Rosales, F., Romero, M. P., Casanovas, M., Motilva, M. J., & Mínguez-Mosquera, M. I. (2010). Metabolites involved in oleuropein accumulation and degradation in fruits of Olea europaea L.: Hojiblanca and Arbequina varieties. *Journal of Agricultural and Food Chemistry*, *58*(24), 12924-12933. doi: 10.1021/jf103083u

Guo, L., Mishra, G., Taylor, K., & Wang, X. (2011). Phosphatidic acid binds and stimulates Arabidopsis sphingosine kinases. *Journal of Biological Chemistry*, *286*(15), 13336-13345. doi: 10.1074/jbc.M110.190892

Guo, L., & Wang, X. (2012). Crosstalk between phospholipase D and sphingosine kinase in plant stress signalling. *Frontiers in plant science*, *3*, 51.

Guo, W. L., Chen, R. G., Gong, Z. H., Yin, Y. X., Ahmed, S. S., & He, Y. M. (2012). Exogenous abscisic acid increases antioxidant enzymes and related gene expression in pepper (Capsicum annuum) leaves subjected to chilling stress. *Genet. Mol. Res*, *11*(4), 4063-80. doi: 10.4238/2012.September.10.5

Haizel, T., Merkle, T., Pay, A., Fejes, E., & Nagy, F. (1997). Characterization of proteins that interact with the GTP-bound form of the regulatory GTPase Ran in Arabidopsis. *The Plant Journal*, *11*(1), 93-103. doi: 10.1046/j.1365-313X.1997.11010093.x

Hannun, Y. A., & Obeid, L. M. (2018). Sphingolipids and their metabolism in physiology and disease. *Nature reviews Molecular cell biology*, *19*(3), 175-191. doi: 10.1038/nrm.2017.107

Hasi, R. Y., Miyagi, M., Morito, K., Ishikawa, T., Kawai-Yamada, M., Imai, H., Fukuta, T., Kogure, K., Kanemaru, K., Hayaski, J., Kawakami, R., & Tanaka, T. (2019). Glycosylinositol phosphoceramide-specific phospholipase D activity catalyzes transphosphatidylation. *The Journal of Biochemistry*, *166*(5), 441-448. doi: 10.1093/jb/mvz056

Haslam, T. M., & Feussner, I. (2022). Diversity in sphingolipid metabolism across land plants. *Journal of Experimental Botany*, *73*(9), 2785-2798. doi: 10.1093/jxb/erab558

Haslam, T. M., & Kunst, L. (2013). Extending the story of very-long-chain fatty acid elongation. *Plant Science*, *210*, 93-107. doi: 10.1016/j.plantsci.2013.05.008

Hegebarth, D., Buschhaus, C., Wu, M., Bird, D., & Jetter, R. (2016). The composition of surface wax on trichomes of Arabidopsis thaliana differs from wax on other epidermal cells. *The Plant Journal*, *88*(5), 762-774. doi: 10.1111/tpj.13294

Hewitt, S., Kilian, B., Koepke, T., Abarca, J., Whiting, M., & Dhingra, A. (2021). Transcriptome Analysis Reveals Potential Mechanisms for Ethylene-Inducible Pedicel–Fruit Abscission Zone Activation in Non-Climacteric Sweet Cherry (Prunus avium L.). *Horticulturae*, *7*(9), 270. doi: 10.3390/horticulturae7090270

Holthuis, J., & Levine, T. P. (2005). Lipid traffic: floppy drives and a superhighway. *Nature reviews molecular cell biology*, *6*(3), 209-220. doi: 10.1038/nrm1591

Huang, L. Q., Chen, D. K., Li, P. P., Bao, H. N., Liu, H. Z., Yin, J., Zeng, H. Y., Yang, Y. B., Li, Y. K., Xiao, S., & Yao, N. (2021). Jasmonates modulate sphingolipid metabolism and accelerate cell death in the ceramide kinase mutant acd5. *Plant Physiology*, *187*(3), 1713-1727. doi: 10.1093/plphys/kiab362

Huang, X., Zhang, Y., Zhang, X., & Shi, Y. (2017). Long-chain base kinase1 affects freezing tolerance in Arabidopsis thaliana. *Plant Science*, *259*, 94-103. doi: 10.1016/j.plantsci.2017.03.009

Huby, E., Napier, J. A., Baillieul, F., Michaelson, L. V., & Dhondt-Cordelier, S. (2020). Sphingolipids: towards an integrated view of metabolism during the plant stress response. *New Phytologist*, *225*(2), 659-670. doi: 10.1111/nph.15997

Hunter, J. E., Brandsma, J., Dymond, M. K., Koster, G., Moore, C. M., Postle, A. D., Mills, R. A., & Attard, G. S. (2018). Lipidomics of Thalassiosira pseudonana under phosphorus stress reveal underlying phospholipid substitution dynamics and novel diglycosylceramide substitutes. *Applied and Environmental Microbiology*, *84*(6), e02034-17. doi: 10.1128/AEM.02034-17

Hurlock, A. K., Roston, R. L., Wang, K., & Benning, C. (2014). Lipid trafficking in plant cells. *Traffic*, *15*(9), 915-932. doi: 10.1111/tra.12187

Huysmans, M., Coll, N. S., & Nowack, M. K. (2017). Dying two deaths—programmed cell death regulation in development and disease. *Current Opinion in Plant Biology*, *35*, 37-44. doi: 10.1016/j.pbi.2016.11.005

Hwang, J. U., Song, W. Y., Hong, D., Ko, D., Yamaoka, Y., Jang, S., Yim, S., Lee, E., Khare, D., Kim, K., Palmgren, M., Yoon, H. S., Martinoia, E., & Lee, Y. (2016). Plant ABC transporters enable many unique aspects of a terrestrial plant's lifestyle. *Molecular Plant*, *9*(3), 338-355. doi: 10.1016/j.molp.2016.02.003

Imai, H., & Nishiura, H. (2005). Phosphorylation of sphingoid long-chain bases in Arabidopsis: functional characterization and expression of the first sphingoid long-chain base kinase gene in plants. *Plant and cell physiology*, *46*(2), 375-380. doi: 10.1093/pcp/pci023

Inês, C., Parra-Lobato, M. C., Paredes, M. A., Labrador, J., Gallardo, M., Saucedo-García, M., Gavilanes-Ruiz, M., & Gomez-Jimenez, M. C. (2018). Sphingolipid distribution, content and gene expression during olive-fruit development and ripening. *Frontiers in Plant Science*, *9*, 28. doi: 10.3389/fpls.2018.00028

Ishikawa, T., Fang, L., Rennie, E. A., Sechet, J., Yan, J., Jing, B., Moore, W., Cahoon, E. B., Scheller, H. V., Kawai-Yamada, M., & Mortimer, J. C. (2018). GLUCOSAMINE INOSITOLPHOSPHORYLCERAMIDE TRANSFERASE1 (GINT1) is a GlcNAc-containing glycosylinositol phosphorylceramide glycosyltransferase. *Plant physiology*, *177*(3), 938-952. doi: 10.1104/pp.18.00396

Ishikawa, T., Ito, Y., & Kawai-Yamada, M. (2016). Molecular characterization and targeted quantitative profiling of the sphingolipidome in rice. *The Plant Journal*, *88*(4), 681-693. doi: 10.1111/tpj.13281

Islam, M. N., Jacquemot, M. P., Coursol, S., & Ng, C. K. Y. (2012). Sphingosine in plants–more riddles from the Sphinx?. *New Phytologist*, *193*(1), 51-57. doi: 10.1111/j.1469-8137.2011.03963.x

Ito, E., Ebine, K., Choi, S. W., Ichinose, S., Uemura, T., Nakano, A., & Ueda, T. (2018). Integration of two RAB5 groups during endosomal transport in plants. *Elife*, *7*, e34064. doi: 10.7554/eLife.34064

Ito, S., Ohnishi, M., & Fujino, Y. (1985). Investigation of sphingolipids in pea seeds. *Agricultural and biological chemistry*, *49*(2), 539-540. doi: 10.1080/00021369.1985.10866760

Jia, G., Huang, X., Zhi, H., Zhao, Y., Zhao, Q., Li, W., Chai, Y., Yang, L., Liu, K., Lu, H., Zhu, C., Lu, Y., Zhou, C., Fan, D., Weng, Q., Guo, Y., Huang, T., Zhang, L., Lu, T., Feng, Q., Hao, H., Liu, H., Lu, P., Zhang, N., Li, Y., Guo, E., Wang, S., Wang, S., Liu, J., Zhang, W., Chen, G., Zhang, B., Wei, L., Wang, Y., Li, H., Zhao, B., Li, J., Diao, X., & Han, B. (2013). A haplotype map of genomic variations and genome-wide association studies of agronomic traits in foxtail millet (*Setaria italica*). *Nature genetics*, *45*(8), 957-961. doi: 10.1038/ng.2673

Jiang, C., Liang, Y., Deng, S., Liu, Y., Zhao, H., Li, S., Jiang, C. Z., Gao, J., & Ma, C. (2023). The Rh LOL1–Rh ILR3 module mediates cytokinin-induced petal abscission in rose. *New Phytologist*, *237*(2), 483-496. doi: 10.1111/nph.18556

Jiang, Z., Zhou, X., Tao, M., Yuan, F., Liu, L., Wu, F., Wu, X., Xiang, Y., Niu, Y., Liu, F., Li, C., Ye, R., Byeon, B., Xue, Y., Zhao, H., Wang, H. N., Crawford, B. M., Jonhson, D. M., Hu, C., Pei, C., Zhou, W., Swift, G. B., Zhang, H., Vo-Dinh, T., Hu, Z., Siedow, J. N., & Pei, Z. M. (2019). Plant cell-surface GIPC sphingolipids sense salt to trigger Ca2+ influx. *Nature*, *572*(7769), 341-346. doi: 10.1038/s41586-019-1449-z

Jiménez-Ruiz, J., Ramírez-Tejero, J. A., Fernández-Pozo, N., Leyva-Pérez, M. D. L. O., Yan, H., Rosa, R. D. L., Belaj, A., Montes, E., Rodriguez-Ariza, M. O., Navarro, F., Barroso, J. B., Beuzón, C. R., Valpuesta, V., Bombarely, A., & Luque, F. (2020). Transposon activation is a major driver in the genome evolution of cultivated olive trees (Olea europaea L.). *The Plant Genome*, *13*(1), e20010. doi: 10.1002/tpg2.20010

Jing, B., Ishikawa, T., Soltis, N., Inada, N., Liang, Y., Murawska, G., Fang, L., Andeberhan, F., Pidatala, R., Yu, X., Baidoo, E., Kawai-Yamada, M., Loque, D., Kliebenstein, D. J., Dupree, P., & Mortimer, J. C. (2021). The Arabidopsis thaliana nucleotide sugar transporter GONST2 is a functional homolog of GONST1. *Plant Direct*, *5*(3), e00309. doi: 10.1002/pld3.309

John-Karuppiah, K. J., & Burns, J. K. (2010). Expression of ethylene biosynthesis and signalling genes during differential abscission responses of sweet orange leaves and mature fruit. *Journal of the American Society for Horticultural Science*, *135*(5), 456-464. doi: 10.21273/JASHS.135.5.456

Kajiwara, K., Watanabe, R., Pichler, H., Ihara, K., Murakami, S., Riezman, H., & Funato, K. (2008). Yeast ARV1 is required for efficient delivery of an early GPI intermediate to the first mannosyltransferase during GPI assembly and controls lipid flow from the endoplasmic reticulum. *Molecular biology of the cell*, *19*(5), 2069-2082. doi: 10.1091/mbc.e07-08-0740

Kawaguchi, M., Imai, H., Naoe, M., Yasui, Y., & Ohnishi, M. (2000). Cerebrosides in grapevine leaves: distinct composition of sphingoid bases among the grapevine species having different tolerances to freezing temperature. *Bioscience, Biotechnology, and Biochemistry*, *64*(6), 1271-1273.

Khan, M., Ragni, L., Tabb, P., Salasini, B. C., Chatfield, S., Datla, R., Lock, J., Kuai, X., Després, C., Proveniers, M., Yongguo, C., Xiang, D., Morin, H., Rullière, J. P., Citerne, S., Hepworth, S. R., & Pautot, V. (2015). Repression of lateral organ boundary genes by PENNYWISE and POUND-FOOLISH is essential for meristem maintenance and flowering in Arabidopsis. *Plant Physiology*, *169*(3), 2166-2186. doi: 10.1104/pp.15.00915

Kihara, A., Mitsutake, S., Mizutani, Y., & Igarashi, Y. (2007). Metabolism and biological functions of two phosphorylated sphingolipids, sphingosine 1-phosphate and ceramide 1-phosphate. *Progress in lipid research*, *46*(2), 126-144. doi: https://doi.org/10.1016/j.plipres.2007.03.001

Kim, J. (2014). Four shades of detachment: regulation of floral organ abscission. *Plant signalling & behavior*, *9*(11), e976154. doi: 10.4161/15592324.2014.976154

Kim, J., Chun, J. P., & Tucker, M. L. (2019). Transcriptional regulation of abscission zones. *Plants*, *8*(6), 154. doi: 10.3390/plants8060154

Kim, J., Dotson, B., Rey, C., Lindsey, J., Bleecker, A. B., Binder, B. M., & Patterson, S. E. (2013). New clothes for the jasmonic acid receptor COI1: delayed abscission, meristem arrest and apical dominance. *PloS one*, *8*(4), e60505. doi: 10.1371/journal.pone.0060505.

Kim, J., Sundaresan, S., Philosoph-Hadas, S., Yang, R., Meir, S., & Tucker, M. L. (2015). Examination of the abscission-associated transcriptomes for soybean, tomato, and Arabidopsis highlights the conserved biosynthesis of an extensible extracellular matrix and boundary layer. *Frontiers in Plant Science*, *6*, 1109. doi: 10.1186/1471-2229-10-152

Kimberlin, A. N., Majumder, S., Han, G., Chen, M., Cahoon, R. E., Stone, J. M., Dunn, T. M., Cahoon, E. B. (2013). Arabidopsis 56–amino acid serine palmitoyltransferase-interacting proteins stimulate sphingolipid synthesis, are essential, and affect mycotoxin sensitivity. *The Plant Cell*, *25*(11), 4627-4639. doi: 10.1105/tpc.113.116145

Kitsaki, C. K., Drossopoulos, J. B., Aivalakis, G., Anastasiadou, F., & Delis, C. (1999). In vitro studies of ABA and ethephon induced abscission in olive organs. *The Journal of Horticultural Science and Biotechnology*, *74*(1), 19-25. doi: 10.1080/14620316.1999.11511065

König, S., Feussner, K., Schwarz, M., Kaever, A., Iven, T., Landesfeind, M., Ternes, P., Karlovsky, P., Lipka, V., & Feussner, I. (2012). A rabidopsis mutants of sphingolipid fatty acid α-hydroxylases accumulate ceramides and salicylates. *New Phytologist*, *196*(4), 1086-1097. doi: 10.1111/j.1469-8137.2012.04351.x

Koudounas, K., Banilas, G., Michaelidis, C., Demoliou, C., Rigas, S., & Hatzopoulos, P. (2015). A defence-related Olea europaea β-glucosidase hydrolyses and activates oleuropein into a potent protein cross-linking agent. *Journal of Experimental Botany*, *66*(7), 2093-2106. doi: 10.1093/jxb/erv002

Kućko, A., Wilmowicz, E., & Ostrowski, M. (2019). Spatio-temporal IAA gradient is determined by interactions with ET and governs flower abscission. *Journal of Plant Physiology*, *236*, 51-60. doi: 10.1016/j.jplph.2019.02.014

Kumar, R., Khurana, A., & Sharma, A. K. (2014). Role of plant hormones and their interplay in development and ripening of fleshy fruits. *Journal of experimental botany*, *65*(16), 4561-4575. doi: 10.1093/jxb/eru277

Kumpf, R. P., Shi, C. L., Larrieu, A., Stø, I. M., Butenko, M. A., Péret, B., Riiser, E. S., Bennet, M. J., Aalen, R. B. (2013). Floral organ abscission peptide IDA and its HAE/HSL2 receptors control cell separation during lateral root emergence. *Proceedings of the National Academy of Sciences*, *110* (13), 5235-5240. doi: 10.1073/pnas.1210835110

Lachaud, C., Prigent, E., Thuleau, P., Grat, S., Da Silva, D., Brière, C., Mazars, C., & Cotelle, V. (2013). 14-3-3-regulated Ca2+-dependent protein kinase CPK3 is required for sphingolipid-induced cell death in Arabidopsis. *Cell Death & Differentiation*, *20*(2), 209-217. doi: 10.1038/cdd.2012.114

Laloi, M., Perret, A. M., Chatre, L., Melser, S., Cantrel, C., Vaultier, M. N., Zachowski, A., Bathany, K., Schmitter, J. M., Vallet, M., Lessire, R., Hartmann, M. A., & Moreau, P. (2007). Insights into the role of specific lipids in the formation and delivery of lipid microdomains to the plasma membrane of plant cells. *Plant physiology*, *143*(1), 461-472. doi: 10.1104/pp.106.091496

Lashbrook, C. C., & Cai, S. (2008). Cell wall remodeling in Arabidopsis stamen abscission zones: temporal aspects of control inferred from transcriptional profiling. *Plant signalling & behavior*, *3*(9), 733-736. doi: 10.4161/psb.3.9.6489

Lavee, S., Haskal, A., & Wodner, M. (1986). Barnea: anew olive cultivar from first breeding generation. *Olea 17*, 95-99.

Lawson, T., Mayes, S., Lycett, G. W., & Chin, C. F. (2018). Plant Rabs and the role in fruit ripening. *Biotechnology and Genetic Engineering Reviews*, *34*(2), 181-197. doi: 10.1080/02648725.2018.1482092

Leblanc, A., Renault, H., Lecourt, J., Etienne, P., Deleu, C., & Le Deunff, E. (2008). Elongation changes of exploratory and root hair systems induced by aminocyclopropane carboxylic acid and aminoethoxyvinylglycine affect nitrate uptake and BnNrt2. 1 and BnNrt1. 1 transporter gene expression in oilseed rape. *Plant Physiology*, *146*(4), 1928-1940. doi: 10.1104/pp.107.109363

Lee, Y., Yoon, T. H., Lee, J., Jeon, S. Y., Lee, J. H., Lee, M. K., Chen, H., Yun, J., Oh, S. Y., Wen, X., Cho, H. K., Mang, H., & Kwak, J. M. (2018). A lignin molecular brace controls precision processing of cell walls critical for surface integrity in Arabidopsis. *Cell*, *173*(6), 1468-1480. doi: 10.1016/j.cell.2018.03.060

Leipelt, M., Warnecke, D., Zähringer, U., Ott, C., Muller, F., Hube, B., & Heinz, E. (2001). Glucosylceramide synthases, a gene family responsible for the biosynthesis of glucosphingolipids in animals, plants, and fungi. *Journal of Biological Chemistry*, *276*(36), 33621-33629. doi: 10.1074/jbc.M104952200

Lenarčič, T., Albert, I., Böhm, H., Hodnik, V., Pirc, K., Zavec, A. B., Podobnik, M., Pahovnik, D., Žagar, E., Pruitt, R., Greimel, P., Yamaji-Hasegawa, A., Kobayashi, T., Zienkiewicz, A., Gömann, J., Mortimer, J. C., Fang, L., Mamode-Cassim, A., Deleu, M., Lins, L., Oecking, C., Feussner, I., Mongrand, S., Anderluh, G., & Nürnberger, T. (2017). Eudicot plant-specific sphingolipids determine host selectivity of microbial NLP cytolysins. *Science*, *358*(6369), 1431-1434. doi: 10.1126/science.aan6874

Leslie, M. E., Lewis, M. W., Liljegren, S. J., & Roberts, J. A. (2007). Organ abscission. *Annual Plant Reviews*, *25*, 106-136. doi: 10.1002/9780470988824.ch6

Leslie, M. E., Lewis, M. W., Youn, J. Y., Daniels, M. J., & Liljegren, S. J. (2010). The EVERSHED receptor-like kinase modulates floral organ shedding in Arabidopsis. *Development*, *137*(3), 467-476. doi: 10.1242/dev.041335

Leung, J., & Giraudat, J. (1998). Abscisic acid signal transduction. *Annual review of plant biology*, *49*(1), 199-222. doi: 10.1146/annurev.arplant.49.1.199

Lewis, M. W., Leslie, M. E., Fulcher, E. H., Darnielle, L., Healy, P. N., Youn, J. Y., & Liljegren, S. J. (2010). The SERK1 receptor-like kinase regulates organ separation in Arabidopsis flowers. *The Plant Journal*, *62*(5), 817-828. doi: 10.1111/j.1365-313X.2010.04194.x

Leyman, B., Geelen, D., & Blatt, M. R. (2000). Localization and control of expression of Nt-Syr1, a tobacco SNARE protein. *The Plant Journal*, *24*(3), 369-382. doi: 10.1046/j.1365-313x.2000.00886.x

Li, C., Wang, Y., Ying, P., Ma, W., & Li, J. (2015b). Genome-wide digital transcript analysis of putative fruitlet abscission related genes regulated by ethephon in litchi. *Frontiers in Plant Science*, *6*, 502. doi: 10.3389/fpls.2015.00502

Li, G., Wang, Q., Meng, Q., Wang, G., Xu, F., Chen, Q., Liu, F., Hu, Y., & Luo, M. (2022). Overexpression of a ceramide synthase gene, GhCS1, inhibits fiber cell initiation and elongation by promoting the synthesis of ceramides containing dihydroxy LCB and VLCFA. *Frontiers in Plant Science*, 13:1000348

Li, J., Bi, F. C., Yin, J., Wu, J. X., Rong, C., Wu, J. L., & Yao, N. (2015a). An Arabidopsis neutral ceramidase mutant ncer1 accumulates hydroxyceramides and is sensitive to oxidative stress. *Frontiers in Plant Science*, *6*, 460.

Li, J., Yin, J., Rong, C., Li, K. E., Wu, J. X., Huang, L. Q., Zeng, H. Y., Sahu, S. K., & Yao, N. (2016). Orosomucoid proteins interact with the small subunit of serine palmitoyltransferase and contribute to sphingolipid homeostasis and stress responses in Arabidopsis. *The Plant Cell*, *28*(12), 3038-3051. doi: 10.1105/tpc.16.00574

Li, T., Xu, Y., Zhang, L., Ji, Y., Tan, D., Yuan, H., & Wang, A. (2017). The jasmonate-activated transcription factor MdMYC2 regulates ETHYLENE RESPONSE FACTOR and ethylene biosynthetic genes to promote ethylene biosynthesis during apple fruit ripening. *The Plant Cell*, *29*(6), 1316-1334. doi: 10.1105/tpc.17.00349

Li, Y., Li, S., Du, R., Wang, J., Li, H., Xie, D., & Yan, J. (2021). Isoleucine enhances plant resistance against Botrytis cinerea via jasmonate signalling pathway. *Frontiers in Plant Science*, 1738. doi: 10.3389/fpls.2021.628328

Liang, H., Yao, N., Song, J. T., Luo, S., Lu, H., & Greenberg, J. T. (2003). Ceramides modulate programmed cell death in plants. *Genes & Development*, *17*(21), 2636-2641. doi: 10.1101/gad.1140503

Liao, W., Wang, G., Li, Y., Wang, B., Zhang, P., & Peng, M. (2016). Reactive oxygen species regulate leaf pulvinus abscission zone cell separation in response to water-deficit stress in cassava. *Scientific Reports*, *6*(1), 1-17. doi: 10.1038/srep21542

Liljegren, S. J. (2012). Organ abscission: exit strategies require signals and moving traffic. *Current Opinion in Plant Biology*, *15*(6), 670-676. doi: 10.1016/j.pbi.2012.09.012

Liljegren, S. J., Leslie, M. E., Darnielle, L., Lewis, M. W., Taylor, S. M., Luo, R., Geldner, N., Chory, J., Randazzo, P. A., Yanofsky, M. F., & Ecker, J. R. (2009). Regulation of membrane trafficking and organ separation by the NEVERSHED ARF-GAP protein. doi: 10.1242/dev.033605

Liu, B., Butenko, M. A., Shi, C. L., Bolivar, J. L., Winge, P., Stenvik, G. E., Vie, A. K., Leslie, M. E., Brembu, T., Kristiansen, W., Bones, A. M., Patterson, S. E., Liljegren, S. J., & Aalen, R. B. (2013). NEVERSHED and INFLORESCENCE DEFICIENT IN ABSCISSION are differentially required for cell expansion and cell separation during floral organ abscission in Arabidopsis thaliana. *Journal of Experimental Botany*, *64*(17), 5345-5357. doi: 10.1093/jxb/ert232

Liu, C., Zhang, C., Fan, M., Ma, W., Chen, M., Cai, F., Liu, K., & Lin, F. (2018). GmIDL2a and GmIDL4a, encoding the inflorescence deficient in abscission-like protein, are involved in soybean cell wall degradation during lateral root emergence. *International Journal of Molecular Sciences*, *19*(8), 2262. doi: 10.3390/ijms19082262

Liu, D., Wang, D., Qin, Z., Zhang, D., Yin, L., Wu, L., Colasanti, J., Li, A., & Mao, L. (2014). The SEPALLATA MADS-box protein SLMBP 21 forms protein complexes with JOINTLESS and MACROCALYX as a transcription activator for development of the tomato flower abscission zone. *The Plant Journal*, *77*(2), 284-296. doi: 10.1111/tpj.12387

Liu, M., Gomes, B. L., Mila, I., Purgatto, E., Peres, L. E., Frasse, P., Maza, E., Zouine, M., Roustan, J. P., Bouzayen, M., & Pirrello, J. (2016). Comprehensive profiling of ethylene response factor expression identifies ripening-associated ERF genes and their link to key regulators of fruit ripening in tomato. *Plant Physiology*, *170*(3), 1732-1744. doi: 10.1104/pp.15.01859

Liu, M., Pirrello, J., Chervin, C., Roustan, J. P., & Bouzayen, M. (2015). Ethylene control of fruit ripening: revisiting the complex network of transcriptional regulation. *Plant physiology*, *169*(4), 2380-2390. doi: 10.1104/pp.15.01361

Liu, N. J., Hou, L. P., Bao, J. J., Wang, L. J., & Chen, X. Y. (2021). Sphingolipid metabolism, transport, and functions in plants: Recent progress and future perspectives. *Plant Communications*, *2*(5), 100214. doi: 10.1016/j.xplc.2021.100214

Liu, N. J., Wang, N., Bao, J. J., Zhu, H. X., Wang, L. J., & Chen, X. Y. (2020a). Lipidomic analysis reveals the importance of GIPCs in Arabidopsis leaf extracellular vesicles. *Molecular Plant*, *13*(10), 1523-1532. doi: 10.1016/j.molp.2020.07.016

Liu, N. J., Zhang, T., Liu, Z. H., Chen, X., Guo, H. S., Ju, B. H., Zhang, Y. Y., Li, G. Z., Zhou, Q. H., Qin, Y. M., & Zhu, Y. X. (2020b). Phytosphinganine affects plasmodesmata permeability via facilitating PDLP5-stimulated callose accumulation in Arabidopsis. *Molecular Plant*, *13*(1), 128-143. doi: 10.1016/j.molp.2019.10.013

Liu, X., Cheng, L., Li, R., Cai, Y., Wang, X., Fu, X., Dong, X., Qi, M., Jiang, Tao., Xu, C-Z., & Li, T. (2022). The HD-Zip transcription factor SlHB15A regulates abscission by modulating jasmonoyl-isoleucine biosynthesis. *Plant Physiology*, *189*(4), 2396-2412. doi: 10.1093/plphys/kiac212

Loureiro, J., Rodriguez, E., Costa, A., & Santos, C. (2007). Nuclear DNA content estimations in wild olive (*Olea europaea* L. ssp. europaea var. sylvestris Brot.)

and portuguese cultivars of O. europaea using flow cytometry. *Genetic Resources and Crop Evolution*, *54*, 21-25. doi: 10.1007/s10722-006-9115-3

Love, M. I., Huber, W., & Anders, S. (2014). Moderated estimation of fold change and dispersion for RNA-seq data with DESeq2. *Genome biology*, *15*(12), 1-21. doi: 10.1186/s13059-014-0550-8

Luttgeharm, K. D., Chen, M., Mehra, A., Cahoon, R. E., Markham, J. E., & Cahoon, E. B. (2015). Overexpression of Arabidopsis ceramide synthases differentially affects growth, sphingolipid metabolism, programmed cell death, and mycotoxin resistance. *Plant physiology*, *169*(2), 1108-1117. doi: 10.1104/pp.15.00987

Luttgeharm, K. D., Kimberlin, A. N., & Cahoon, E. B. (2016). Plant sphingolipid metabolism and function. *Lipids in plant and algae development*, 249-286.

Lycett, G. (2008). The role of Rab GTPases in cell wall metabolism. *Journal of Experimental Botany*, *59*(15), 4061-4074. doi: 10.1093/jxb/ern255

Lynch, S. M., & Frei, B. (1993). Mechanisms of copper-and iron-dependent oxidative modification of human low-density lipoprotein. *Journal of Lipid Research*, *34*(10), 1745-1753. doi: 10.1016/S0022-2275(20)35737-0

Ma, C., Jiang, C. Z., & Gao, J. (2021). Regulatory mechanisms underlying activation of organ abscission. *Annual Plant Reviews online*, 27-56. doi:10.1002/9781119312994.apr0741

Ma, X., Li, C., Huang, X., Wang, H., Wu, H., Zhao, M., & Li, J. (2019). Involvement of HD-ZIP I transcription factors LcHB2 and LcHB3 in fruitlet abscission by promoting transcription of genes related to the biosynthesis of ethylene and ABA in litchi. *Tree Physiology*, *39*(9), 1600-1613. doi: 10.1093/treephys/tpz071

Ma, X., Ying, P., He, Z., Wu, H., Li, J., & Zhao, M. (2022). The LcKNAT1-LcEIL2/3 regulatory module is involved in fruitlet abscission in litchi. *Frontiers in Plant Science*, *12*, 3258. doi: 10.3389/fpls.2021.802016

Ma, X., Yuan, Y., Wu, Q., Wang, J., Li, J., & Zhao, M. (2020). LcEIL2/3 are involved in fruitlet abscission via activating genes related to ethylene biosynthesis and cell wall remodeling in litchi. *The Plant Journal*, *103*(4), 1338-1350. doi: https://doi.org/10.1111/tpj.14804

Maechler, M., Rousseeuw, P., Struyf, A., Hubert, M., & Hornik, K. (2019). cluster: Cluster Analysis Basics and Extensions. R package version 2.1.0.

Magnin-Robert, M., Le Bourse, D., Markham, J., Dorey, S., Clément, C., Baillieul, F., & Dhondt-Cordelier, S. (2015). Modifications of sphingolipid content affect tolerance to hemibiotrophic and necrotrophic pathogens by modulating plant defense responses in Arabidopsis. *Plant physiology*, *169*(3), 2255-2274. doi: 10.1104/pp.15.01126

Mamidi, S., Healey, A., Huang, P., Grimwood, J., Jenkins, J., Barry, K., Sreedasyam, A., Shu, S., Lovell, J. T., Feldman, M., Wu, J., Yu, Y., Chen, C., Johnson, J., Sakakibara, H., Kiba, T., Sakurai, T., Tavares, R., Nusinow, D. A., Baxter, I., Schmutz, J., Brutnell, T. P., & Kellogg, E. A. (2020). A genome resource for green millet Setaria viridis enables discovery of agronomically valuable loci. *Nature Biotechnology*, *38*(10), 1203-1210. doi: 10.1038/s41587-020-0681-2

Mamode Cassim, A., Grison, M., Ito, Y., Simon-Plas, F., Mongrand, S., & Boutté, Y. (2020). Sphingolipids in plants: a guidebook on their function in membrane architecture, cellular processes, and environmental or

developmental responses. *FEBS letters*, *594*(22), 3719-3738. doi: 10.1002/1873-3468.13987

Mamode Cassim, A., Gouguet, P., Gronnier, J., Laurent, N., Germain, V., Grison, M., Boutté, Y., Gerbeau-Pissot, P., Simon-Plas, F., & Mongrand, S. (2019). Plant lipids: Key players of plasma membrane organization and function. *Progress in Lipid Research*, *73*, 1-27. doi: 10.1016/j.plipres.2018.11.002

Mandon, E. C., Ehses, I., Rother, J., van Echten, G., & Sandhoff, K. (1992). Subcellular localization and membrane topology of serine palmitoyltransferase, 3-dehydrosphinganine reductase, and sphinganine N-acyltransferase in mouse liver. *Journal of Biological Chemistry*, *267*(16), 11144-11148. doi: 10.1016/S0021-9258(19)49887-6

Mao, C., & Obeid, L. M. (2008). Ceramidases: regulators of cellular responses mediated by ceramide, sphingosine, and sphingosine-1-phosphate. *Biochimica et Biophysica Acta (BBA)-Molecular and Cell Biology of Lipids*, *1781*(9), 424-434. doi: 10.1016/j.bbalip.2008.06.002

Mao, L., Begum, D., Chuang, H. W., Budiman, M. A., Szymkowiak, E. J., Irish, E. E., & Wing, R. A. (2000). JOINTLESS is a MADS-box gene controlling tomato flower abscissionzone development. *Nature*, *406*(6798), 910-913. doi: 10.1038/35022611

Markham, J. E., Li, J., Cahoon, E. B., & Jaworski, J. G. (2006). Separation and identification of major plant sphingolipid classes from leaves. *Journal of Biological Chemistry*, *281*(32), 22684-22694. doi: 10.1074/jbc.M604050200

Markham, J. E., Lynch, D. V., Napier, J. A., Dunn, T. M., & Cahoon, E. B. (2013). Plant sphingolipids: function follows form. *Current opinion in plant biology*, *16*(3), 350-357. doi: 10.1016/j.pbi.2013.02.009

Markham, J. E., Molino, D., Gissot, L., Bellec, Y., Hématy, K., Marion, J., Belcram, K., Palauqui, J. C., Satiat-JeuneMaître, B., & Faure, J. D. (2011). Sphingolipids containing very-long-chain fatty acids define a secretory pathway for specific polar plasma membrane protein targeting in Arabidopsis. *The Plant Cell*, *23*(6), 2362-2378. doi: 10.1105/tpc.110.080473

Markham, J. E., & Jaworski, J. G. (2007). Rapid measurement of sphingolipids from Arabidopsis thaliana by reversed-phase high-performance liquid chromatography coupled to electrospray ionization tandem mass spectrometry. *Rapid Communications in Mass Spectrometry: An International Journal Devoted to the Rapid Dissemination of Up-to-the-Minute Research in Mass Spectrometry*, *21*(7), 1304-1314. doi: 10.1002/rcm.2962

Marquês, J. T., Cordeiro, A. M., Viana, A. S., Herrmann, A., Marinho, H. S., & de Almeida, R. F. (2015). Formation and properties of membrane-ordered domains by phytoceramide: role of sphingoid base hydroxylation. *Langmuir*, *31*(34), 9410-9421. doi: 10.1021/acs.langmuir.5b02550

Maula, T., Al Sazzad, M. A., & Slotte, J. P. (2015). Influence of hydroxylation, chain length, and chain unsaturation on bilayer properties of ceramides. *Biophysical Journal*, *109*(8), 1639-1651. doi: 10.1016/j.bpj.2015.08.040

McKim, S. M., Stenvik, G. E., Butenko, M. A., Kristiansen, W., Cho, S. K., Hepworth, S. R., Aalen, R. B., & Haughn, G. W. (2008). The BLADE-ON-PETIOLE genes are essential for abscission zone formation in Arabidopsis. doi: 10.1242/dev.012807

Medail, F., Quezel, P., Besnard, G., & Khadari, B. (2001). Systematics, ecology and phylogeographic significance of Olea europaea L. ssp. maroccana (Greuter & Burdet) P. Vargas et al., a relictual olive tree in south-west Morocco. *Botanical Journal of the Linnean Society*, *137*(3), 249-266. doi: 10.1111/j.1095-8339.2001.tb01121.x

Meir, S., Hunter, D. A., Chen, J. C., Halaly, V., & Reid, M. S. (2006). Molecular changes occurring during acquisition of abscission competence following auxin depletion in Mirabilis jalapa. *Plant Physiology*, *141*(4), 1604-1616. doi: 10.1104/pp.106.079277

Meir, S., Philosoph-Hadas, S., Riov, J., Tucker, M. L., Patterson, S. E., & Roberts, J. A. (2019). Re-evaluation of the ethylene-dependent and-independent pathways in the regulation of floral and organ abscission. *Journal of experimental botany*, *70*(5), 1461-1467. doi: 10.1093/jxb/erz038

Meir, S., Philosoph-Hadas, S., Salim, S., Segev, A., & Riov, J. (2022). Reevaluation of ethylene role in Arabidopsis cauline leaf abscission induced by water stress and rewatering. *Plant Direct*, *6*(9), e444. doi: 10.1002/pld3.444

Meir, S., Philosoph-Hadas, S., Sundaresan, S., Selvaraj, K. V., Burd, S., Ophir, R., Kochanek, B., Reid, M. S., Jiang, C. Z., & Lers, A. (2010). Microarray analysis of the abscission-related transcriptome in the tomato flower abscission zone in response to auxin depletion. *Plant Physiology*, *154*(4), 1929-1956. doi: 10.1104/pp.110.160697

Meir, S., Philosoph-Hadas, S., Sundaresan, S., Selvaraj, K. V., Burd, S., Ophir, R., Kochanek, K. S. B., Reid, M. S., Jianj, C. Z., & Lers, A. (2011). Identification of defense-related genes newly-associated with tomato flower abscission. *Plant signalling & behavior*, *6*(4), 590-593. doi: 10.4161/psb.6.4.15043

Melser, S., Batailler, B., Peypelut, M., Poujol, C., Bellec, Y., Wattelet-Boyer, V., Maneta-Peyret, L., Faure, J. D., & Moreau, P. (2010). Glucosylceramide biosynthesis is involved in Golgi morphology and protein secretion in plant cells. *Traffic*, *11*(4), 479-490. doi: 10.1111/j.1600-0854.2009.01030.x

Meng, X., Zhou, J., Tang, J., Li, B., de Oliveira, M. V., Chai, J., He, P., & Shan, L. (2016). Ligand-induced receptor-like kinase complex regulates floral organ abscission in Arabidopsis. *Cell Reports*, *14*(6), 1330-1338. doi: 10.1016/j.celrep.2016.01.023

Merelo, P., Agustí, J., Arbona, V., Costa, M. L., Estornell, L. H., Gómez-Cadenas, A., Coimbra, S., Gómez, M. D., Pérez-Amador, M. A., Domingo, C., Talón, M., & Tadeo, F. R. (2017). Cell wall remodeling in abscission zone cells during ethylene-promoted fruit abscission in citrus. *Frontiers in plant science*, *8*, 126. doi: 10.3389/fpls.2017.00126

Merrill, A. H., Stokes, T. H., Momin, A., Park, H., Portz, B. J., Kelly, S., Elaine, W., Cameron, S. M., & Wang, M. D. (2009). Sphingolipidomics: a valuable tool for understanding the roles of sphingolipids in biology and disease. *Journal of Lipid Research*, *50*, S97-S102. doi: 10.1194/jlr.R800073-JLR200

Merrill Jr, A. H., Van Echten, G., Wang, E., & Sandhoff, K. (1993). Fumonisin B1 inhibits sphingosine (sphinganine) N-acyltransferase and de novo sphingolipid biosynthesis in cultured neurons in situ. *Journal of Biological Chemistry*, *268*(36), 27299-27306. doi: 10.1016/S0021-9258(19)74249-5

Metzidakis, I., Gerasopoulos, D., & Naoufel, E. (1997). Olive oil quality characteristics of 'mastoides' olives remaining on the tree after ethephon

spray. In *III International Symposium on Olive Growing 474* (pp. 677-682). doi: 10.17660/ActaHortic.1999.474.140

Michaelson, L. V., Napier, J. A., Molino, D., & Faure, J. D. (2016). Plant sphingolipids: Their importance in cellular organization and adaption. *Biochimica et Biophysica Acta (BBA)-Molecular and Cell Biology of Lipids*, *1861*(9), 1329-1335. doi: 10.1016/j.bbalip.2016.04.003

Michaelson, L. V., Zauner, S., Markham, J. E., Haslam, R. P., Desikan, R., Mugford, S., Albrecht, S., Warnecke, D., Sperling, P., Heinz, E., & Napier, J. A. (2009). Functional characterization of a higher plant sphingolipid Δ4-desaturase: defining the role of sphingosine and sphingosine-1-phosphate in Arabidopsis. *Plant physiology*, *149*(1), 487-498. doi: 10.1104/pp.108.129411

Miller, R., Wu, G., Deshpande, R. R., Vieler, A., Gärtner, K., Li, X., Moellering, E. R., Zäuner, S., Cornish, A. J., Liu, B., Bullard, B., Sears, B. B., Kuo, M. H., Hegg, E. L., Shachar-Hill, Y., Shiu, S. H., & Benning, C. (2010). Changes in transcript abundance in Chlamydomonas reinhardtii following nitrogen deprivation predict diversion of metabolism. *Plant physiology*, *154*(4), 1737-1752. doi: 10.1104/pp.110.165159

Mina, J. G., Okada, Y., Wansadhipathi-Kannangara, N. K., Pratt, S., Shams-Eldin, H., Schwarz, R. T., Steel, P. G., Fawcett, T., & Denny, P. W. (2010). Functional analyses of differentially expressed isoforms of the Arabidopsis inositol phosphorylceramide synthase. *Plant Molecular Biology*, *73*, 399-407.

Minami, A., Fujiwara, M., Furuto, A., Fukao, Y., Yamashita, T., Kamo, M., Kawamura, Y., & Uemura, M. (2009). Alterations in detergent-resistant plasma membrane microdomains in Arabidopsis thaliana during cold acclimation. *Plant and Cell Physiology*, *50*(2), 341-359. doi: 10.1093/pcp/pcn202

Minamino, N., & Ueda, T. (2019). RAB GTPases and their effectors in plant endosomal transport. *Current opinion in plant biology*, *52*, 61-68. doi: 10.1016/j.pbi.2019.07.007

Mittler, R. (2002). Oxidative stress, antioxidants and stress tolerance. *Trends in plant science*, *7*(9), 405-410. Doi: 10.1016/S1360-1385(02)02312-9

Miyake, Y., Kozutsumi, Y., Nakamura, S., Fujita, T., & Kawasaki, T. (1995). Serine palmitoyltransferase is the primary target of a sphingosine-like immunosuppressant, ISP-1/myriocin. *Biochemical and biophysical research communications*, *211*(2), 396-403. doi: 10.1006/bbrc.1995.1827

Moreno-Alias, I., Rapoport, HF., & Martins, PC. (2012) Morphological limitations in floral development among olive tree cultivars. *In XXVIII International Horticultural Congress on Science and Horticulture for People (Ihc2010): International Symposium on Plant 932* (pp. 23-27). doi: 10.17660/ActaHortic.2012.932.2

Morgan, P. W., & Hall, W. C. (1964). Accelerated release of ethylene by cotton following application of indolyl-3-acetic acid. *Nature*, *201*(4914), 99-99. Doi: https://doi.org/10.1038/201099a0

Mortazavi, A., Williams, B. A., McCue, K., Schaeffer, L., & Wold, B. (2008). Mapping and quantifying mammalian transcriptomes by RNA-Seq. *Nature methods*, *5*(7), 621-628. doi: 10.1038/nmeth.1226

Mortimer, J. C., Yu, X., Albrecht, S., Sicilia, F., Huichalaf, M., Ampuero, D., Michaelson, L. V., Murphy, A. M., Matsunaga, T., Kurz, S., Stephens, E., Baldwin, T. C., Ishii, T., Napier, J. A., Weber, A. P. M., Handford, M. G., & Dupree, P. (2013). Abnormal glycosphingolipid mannosylation triggers

salicylic acid–mediated responses in Arabidopsis. *The Plant Cell*, *25*(5), 1881-1894. doi: 10.1105/tpc.113.111500

Mousavi, S., Regni, L., Bocchini, M., Mariotti, R., Cultrera, N. G., Mancuso, S., Googlani, J., Chakerolhosseini, M. R., Guerrero, C., Albertini, E., Baldoni, L., & Proietti, P. (2019). Physiological, epigenetic and genetic regulation in some olive cultivars under salt stress. *Scientific reports*, *9*(1), 1-17. doi: 10.1038/s41598-018-37496-5

Msanne, J., Chen, M., Luttgeharm, K. D., Bradley, A. M., Mays, E. S., Paper, J. M., Boyle, D, L., Cahoon, R. E., Schrick, K., & Cahoon, E. B. (2015). Glucosylceramides are critical for cell-type differentiation and organogenesis, but not for cell viability in Arabidopsis. *The Plant Journal*, *84*(1), 188-201. doi: 10.1111/tpj.13000

Muday, G. K., Rahman, A., & Binder, B. M. (2012). Auxin and ethylene: collaborators or competitors?. *Trends in plant science*, *17*(4), 181-195. doi: 10.1016/j.tplants.2012.02.001

Munro, S. (2003). Lipid rafts: elusive or illusive?. *Cell*, *115*(4), 377-388. doi: 10.1016/S0092-8674(03)00882-1

Muñoz-Mérida, A., González-Plaza, J. J., Canada, A. N., Blanco, A. M., García-López, M. D. C., Rodríguez, J. M., Pedrola, L., Sicardo, M. D., Hernández, M. L., De la Rosa, R., Belaj, A., Gil-Borja, M., Luque, F., Martínez-Rivas, J. M., Pisano, D. G., Trelles, O., Valpuesta, V., & Beuzón, C. R. (2013). De novo assembly and functional annotation of the olive (*Olea europaea*) transcriptome. *DNA research*, *20*(1), 93-108. doi: 10.1093/dnares/dss036

Nagano, M., Ishikawa, T., Fujiwara, M., Fukao, Y., Kawano, Y., Kawai-Yamada, M., & Shimamoto, K. (2016). Plasma membrane microdomains are essential for Rac1-RbohB/H-mediated immunity in rice. *The Plant Cell*, *28*(8), 1966-1983. doi: 10.1105/tpc.16.00201

Nagano, M., Ishikawa, T., Ogawa, Y., Iwabuchi, M., Nakasone, A., Shimamoto, K., Uchimiya, H., & Kawai-Yamada, M. (2014). Arabidopsis Bax inhibitor-1 promotes sphingolipid synthesis during cold stress by interacting with ceramide-modifying enzymes. *Planta*, *240*, 77-89.

Nagano, M., Takahara, K., Fujimoto, M., Tsutsumi, N., Uchimiya, H., & Kawai-Yamada, M. (2012). Arabidopsis sphingolipid fatty acid 2-hydroxylases (AtFAH1 and AtFAH2) are functionally differentiated in fatty acid 2-hydroxylation and stress responses. *Plant physiology*, *159*(3), 1138-1148. doi: 10.1104/pp.112.199547

Nakano, T., Fujisawa, M., Shima, Y., & Ito, Y. (2013). Expression profiling of tomato pre-abscission pedicels provides insights into abscission zone properties including competence to respond to abscission signals. *BMC Plant Biology*, *13*, 1-19. doi: 10.1186/1471-2229-13-40

Nakano, T., Fujisawa, M., Shima, Y., & Ito, Y. (2014). The AP2/ERF transcription factor SlERF52 functions in flower pedicel abscission in tomato. *Journal of Experimental Botany*, *65*(12), 3111-3119. doi: 10.1093/jxb/eru154

Nakano, T., Kimbara, J., Fujisawa, M., Kitagawa, M., Ihashi, N., Maeda, H., Kasumi, T., & Ito, Y. (2012). MACROCALYX and JOINTLESS interact in the transcriptional regulation of tomato fruit abscission zone development. *Plant Physiology*, *158*(1), 439-450. doi: 10.1104/pp.111.183731

Nakagawa, N., Kato, M., Takahashi, Y., Shimazaki, K. I., Tamura, K., Tokuji, Y., Kihara, A., & Imai, H. (2012). Degradation of long-chain base 1-phosphate

(LCBP) in Arabidopsis: functional characterization of LCBP phosphatase involved in the dehydration stress response. *Journal of Plant Research*, *125*, 439-449.

Niederhuth, C. E., Cho, S. K., Seitz, K., & Walker, J. C. (2013b). Letting Go is Never Easy: Abscission and Receptor-L ike Protein Kinases. *Journal of Integrative Plant Biology*, *55*(12), 1251-1263. doi: 10.1111/jipb.12116

Niederhuth, C. E., Patharkar, O. R., & Walker, J. C. (2013a). Transcriptional profiling of the Arabidopsis abscission mutant hae hsl2 by RNA-Seq. *BMC genomics*, *14*, 1-12. doi: 10.1186/1471-2164-14-37

Niemelä, P. S., Hyvönen, M. T., & Vattulainen, I. (2009). Atom-scale molecular interactions in lipid raft mixtures. *Biochimica et Biophysica Acta (BBA)-Biomembranes*, *1788*(1), 122-135. doi: 10.1016/j.bbamem.2008.08.018

Nishikawa, M., Hosokawa, K., Ishiguro, M., Minamioka, H., Tamura, K., Hara-Nishimura, I.,Takahashi, Y., Shimazaki, K. I., & Imai, H. (2008). Degradation of sphingoid long-chain base 1-phosphates (LCB-1Ps): functional characterization and expression of AtDPL1 encoding LCB-1P lyase involved in the dehydration stress response in Arabidopsis. *Plant and Cell Physiology*, *49*(11), 1758-1763. doi: 10.1093/pcp/pcn149

Nishiura, H., Tamura, K., Morimoto, Y., & Imai, H. (2000). Characterization of sphingolipid long-chain base kinase in Arabidopsis thaliana. doi: 10.1042/bst0280747

Ng, C. K. Y., Carr, K., McAinsh, M. R., Powell, B., & Hetherington, A. M. (2001). Drought-induced guard cell signal transduction involves sphingosine-1-phosphate. *Nature*, *410*(6828), 596-599. doi: 10.1038/35069092

Ng, C. K. Y., & Coursol, S. (2012). New insights into phospholipase D and sphingosine kinase activation in Arabidopsis. *Frontiers in Physiology*, *3*, 67. doi: 10.3389/fphys.2012.00067

Ngo, T. N., Nguyen, N. D. P., Nguyen, N. T. L., Pham, N. K. T., Phan, N. M., Bui, T. D., Dang, V. S., Tran, C. L., Mai, D. T., & Nguyen, T. P. (2020). Markhasphingolipid A, new phytosphingolipid from the leaves of Markhamia stipulata var. canaense VS Dang. *Natural product research*, *34*(13), 1820-1826.doi: 10.1080/14786419.2018.1561686

Núñez-Elisea, R., & Davenport, T. L. (1986). Abscission of mango fruitlets as influenced by enhanced ethylene biosynthesis. *Plant physiology*, *82*(4), 991-994. doi: 10.1104/pp.82.4.991

Odonkor, S., Choi, S., Chakraborty, D., Martinez-Bello, L., Wang, X., Bahri, B. A., Tenaillon, M. I., Panaud, O., & Devos, K. M. (2018). QTL mapping combined with comparative analyses identified candidate genes for reduce. doi: 10.3389/fpls.2018.00918

Ogawa, M., Kay, P., Wilson, S., & Swain, S. M. (2009). ARABIDOPSIS DEHISCENCE ZONE POLYGALACTURONASE1 (ADPG1), ADPG2, and QUARTET2 are polygalacturonases required for cell separation during reproductive development in Arabidopsis. *The Plant Cell*, *21*(1), 216-233. doi: 10.1105/tpc.108.06376

Ohnishi, M., Ito, S., & Fujino, Y. (1983). Characterization of sphingolipids in spinach leaves. *Biochimica et Biophysica Acta (BBA)-Lipids and Lipid Metabolism*, *752*(3), 416-422. doi: 10.1016/0005-2760(83)90271-0

Panzenboeck, L., Troppmair, N., Schlachter, S., Koellensperger, G., Hartler, J., & Rampler, E. (2020). Chasing the major sphingolipids on earth: automated

annotation of plant Glycosyl inositol Phospho ceramides by Glycolipidomics. *Metabolites*, *10*(9), 375. doi: 10.3390/metabo10090375

Parra, R., Paredes, M. A., Labrador, J., Nunes, C., Coimbra, M. A., Fernandez-Garcia, N., Olmos, E., Gallardo, M., & Gomez-Jimenez, M. C. (2020). Cell wall composition and ultrastructural immunolocalization of pectin and arabinogalactan protein during *Olea europaea* L. fruit abscission. *Plant and Cell Physiology*, *61*(4), 814-825. doi: 10.1093/pcp/pcaa009

Parra, R., Paredes, M. A., Sanchez-Calle, I. M., & Gomez-Jimenez, M. C. (2013). Comparative transcriptional profiling analysis of olive ripe-fruit pericarp and abscission zone tissues shows expression differences and distinct patterns of transcriptional regulation. *BMC Genomics*, *14*, 1-20. doi: 10.1186/1471-2164-14-866

Parra, R., & Gomez-Jimenez, M. C. (2020). Spatio–temporal immunolocalization of extensin protein and hemicellulose polysaccharides during olive fruit abscission. *Planta*, *252*, 1-15. doi: 10.1007/s00425-020-03439-6

Parra-Lobato, M. C., Paredes, M. A., Labrador, J., Saucedo-García, M., Gavilanes-Ruiz, M., & Gomez-Jimenez, M. C. (2017). Localization of sphingolipid enriched plasma membrane regions and long-chain base composition during mature-fruit abscission in olive. *Frontiers in Plant Science*, *8*, 1138. doi: 10.3389/fpls.2017.01138

Parra-Lobato, M. C., & Gomez-Jimenez, M. C. (2011). Polyamine-induced modulation of genes involved in ethylene biosynthesis and signalling pathways and nitric oxide production during olive mature fruit abscission. *Journal of Experimental Botany*, *62*(13), 4447-4465. doi: 10.1093/jxb/err124.

Pata, M. O., Hannun, Y. A., & Ng, C. K. Y. (2010). Plant sphingolipids: decoding the enigma of the Sphinx. *New Phytologist*, *185*(3), 611-630. doi: 10.1111/j.1469-8137.2009.03123.x

Pata, M. O., Wu, B. X., Bielawski, J., Xiong, T. C., Hannun, Y. A., & Ng, C. K. Y. (2008). Molecular cloning and characterization of OsCDase, a ceramidase enzyme from rice. *The Plant Journal*, *55*(6), 1000-1009. doi: https://doi.org/10.1111/j.1365-313X.2008.03569.x

Patharkar, O. R., Gassmann, W., & Walker, J. C. (2017). Leaf shedding as a bacterial defense in Arabidopsis cauline leaves. *bioRxiv*, 189720.

Patharkar, O. R., & Walker, J. C. (2018). Advances in abscission signalling. *Journal of Experimental Botany*, *69*(4), 733-740. doi: 10.1093/jxb/erx256

Patharkar, O. R., & Walker, J. C. (2019). Connections between abscission, dehiscence, pathogen defense, drought tolerance, and senescence. *Plant Science*, *284*, 25-29. doi: 10.1016/j.plantsci.2019.03.016

Patharkar, O. R., & Walker, J. C. (2016). Core mechanisms regulating developmentally timed and environmentally triggered abscission. *Plant Physiology*, *172*(1), 510-520. doi: 10.1104/pp.16.01004

Patharkar, O. R., & Walker, J. C. (2015). Floral organ abscission is regulated by a positive feedback loop. *Proceedings of the National Academy of Sciences*, *112*(9), 2906-2911. doi: 10.1073/pnas.1423595112

Patterson, S. E. (2001). Cutting loose. Abscission and dehiscence in Arabidopsis. *Plant physiology*, *126*(2), 494-500. doi: 10.1104/pp.126.2.494

Patterson, S. E., Bolivar-Medina, J. L., Falbel, T. G., Hedtcke, J. L., Nevarez-McBride, D., Maule, A. F., & Zalapa, J. E. (2016). Are we on the right track: can our understanding of abscission in model systems promote or derail

making improvements in less studied crops?. *Frontiers in Plant Science*, *6*, 1268. doi: 10.3389/fpls.2015.01268

Patterson, S. E., & Bleecker, A. B. (2004). Ethylene-dependent and-independent processes associated with floral organ abscission in Arabidopsis. *Plant Physiology*, *134*(1), 194-203. doi: stable/4281547

Pattison, R. J., & Catalá, C. (2012). Evaluating auxin distribution in tomato (Solanum lycopersicum) through an analysis of the PIN and AUX/LAX gene families. *The Plant Journal*, *70*(4), 585-598. doi: j.1365-313X.2011.04895.x

Paul, S., Gable, K., Beaudoin, F., Cahoon, E., Jaworski, J., Napier, J. A., & Dunn, T. M. (2006). Members of the Arabidopsis FAE1-like 3-ketoacyl-CoA synthase gene family substitute for the Elop proteins of Saccharomyces cerevisiae. *Journal of Biological Chemistry*, *281*(14), 9018-9029. doi: 10.1074/jbc.M507723200

Pech, J. C., Bouzayen, M., & Latché, A. J. P. S. (2008). Climacteric fruit ripening: ethylene-dependent and independent regulation of ripening pathways in melon fruit. *Plant science*, *175*(1-2), 114-120. doi: 10.1016/j.plantsci.2008.01.003

Périn, C., Gomez-Jimenez, M., Hagen, L., Dogimont, C., Pech, J. C., Latché, A., Pitrat, M., & Lelièvre, J. M. (2002). Molecular and genetic characterization of a non-climacteric phenotype in melon reveals two loci conferring altered ethylene response in fruit. *Plant Physiology*, *129*(1), 300-309. doi: 10.1104/pp.010613

Pike, L. J. (2006). Rafts defined: a report on the Keystone Symposium on Lipid Rafts and Cell Function. *Journal of lipid research*, *47*(7), 1597-1598. doi: 10.1194/jlr.E600002-JLR200

Pinyopich, A., Ditta, G. S., Savidge, B., Liljegren, S. J., Baumann, E., Wisman, E., & Yanofsky, M. F. (2003). Assessing the redundancy of MADS-box genes during carpel and ovule development. *Nature*, *424*(6944), 85-88. doi: 10.1038/nature01741

Polito, V. S., & Lavee, S. (1980). Anatomical and histochemical aspects of ethephon-induced leaf abscission in Olive (Olea europaea L.). *Botanical Gazette*, *141*(4), 413-417. doi: 10.1086/337175

Qin, X., Zhang, R. X., Ge, S., Zhou, T., & Liang, Y. K. (2017). Sphingosine kinase AtSPHK1 functions in fumonisin B1-triggered cell death in Arabidopsis. *Plant Physiology and Biochemistry*, *119*, 70-80. doi: 10.1016/j.plaphy.2017.08.008

Rai, A. C., Halon, E., Zemach, H., Zviran, T., Sisai, I., Philosoph-Hadas, S., Meir, S., Cohen, Y., & Irihimovitch, V. (2021). Characterization of two ethephon-induced IDA-like genes from mango, and elucidation of their involvement in regulating organ abscission. *Genes*, *12*(3), 439. doi: 10.3390/genes12030439

Rao, G., Zhang, J., Liu, X., Lin, C., Xin, H., Xue, L., & Wang, C. (2021). De novo assembly of a new Olea europaea genome accession using nanopore sequencing. *Horticulture research*, *8*. doi: 10.1038/s41438-021-00498-y

Reed, N. M. R., & Hartmann, H. T. (1976). Histochemical and ultrastructural studies of fruit abscission in the olive after treatment with 2-chloroethyl-tris-(2-methoxyethoxy)-silane. *Journal American Society for Horticultural Science*.

Reichardt, S., Piepho, H. P., Stintzi, A., & Schaller, A. (2020). Peptide signalling for drought-induced tomato flower drop. *Science*, *367*(6485), 1482-1485. doi: 10.1126/science.aaz5641

Reichardt, S., Repper, D., Tuzhikov, A. I., Galiullina, R. A., Planas-Marquès, M., Chichkova, N. V., Vartapetian, A. B., Stintzi, A., & Schaller, A. (2018). The tomato subtilase family includes several cell death-related proteinases with caspase specificity. *Scientific reports*, *8*(1), 10531. doi: 10.1038/s41598-018-28769-0

Rennie, E. A., Ebert, B., Miles, G. P., Cahoon, R. E., Christiansen, K. M., Stonebloom, S., Khatab, H., Twell, D., Petzold, C. J., Adams, P. D., Dupree, P., Heazlewood, J. L., Cahoon, E. B., & Scheller, H. V. (2014). Identification of a sphingolipid α-glucuronosyltransferase that is essential for pollen function in Arabidopsis. *The Plant Cell*, *26*(8), 3314-3325. doi: 10.1105/tpc.114.129171

Riboni, L., Giussani, P., & Viani, P. (2010). Sphingolipid transport. *Sphingolipids as signalling and regulatory molecules*, 24-45.

Rivas-San Vicente, M., Larios-Zarate, G., & Plasencia, J. (2013). Disruption of sphingolipid biosynthesis in Nicotiana benthamiana activates salicylic acid-dependent responses and compromises resistance to Alternaria alternata f. sp. lycopersici. *Planta*, *237*, 121-136. doi: 10.1007/s00425-012-1758-z

Roberts, J. A., Elliott, K. A., & Gonzalez-Carranza, Z. H. (2002). Abscission, dehiscence, and other cell separation processes. *Annual review of plant biology*, *53*(1), 131-158. doi: 10.1146/annurev.arplant.53.092701.180236.

Roberts, J. A., Whitelaw, C. A., Gonzalez-Carranza, Z. H., & McManus, M. T. (2000). Cell separation processes in plants—models, mechanisms and manipulation. *Annals of Botany*, *86*(2), 223-235. doi: 10.1006/anbo.2000.1203

Roberts, J. A., & Gonzalez-Carranza, Z. (Eds.). (2007). *Plant cell separation and adhesion*. Oxford, UK: Blackwell.

Roberts, J. A., & Gonzalez-Carranza, Z. (2018). Cell Separation and Adhesion Processes in Plants. In *Annual Plant Reviews online*, J.A. Roberts (Ed.). doi: 10.1002/9781119312994.apr0253

Robinson, M. D., McCarthy, D. J., & Smyth, G. K. (2010). edgeR: a Bioconductor package for differential expression analysis of digital gene expression data. *bioinformatics*, *26*(1), 139-140. doi: 10.1093/bioinformatics/btp616

Roldan, M. V. G., Périlleux, C., Morin, H., Huerga-Fernandez, S., Latrasse, D., Benhamed, M., & Bendahmane, A. (2017). Natural and induced loss of function mutations in SlMBP21 MADS-box gene led to jointless-2 phenotype in tomato. *Scientific reports*, *7*(1), 1-10. doi: 10.1038/s41598-017-04556-1

Roman, A. O., Jimenez-Sandoval, P., Augustin, S., Broyart, C., Hothorn, L. A., & Santiago, J. (2022). HSL1 and BAM1/2 impact epidermal cell development by sensing distinct signalling peptides. *Nature communications*, *13*(1), 876. doi: 10.1038/s41467-022-28558-4

Roongsattham, P., Morcillo, F., Fooyontphanich, K., Jantasuriyarat, C., Tragoonrung, S., Amblard, P., Collin, M., Mouille, G., Verdeil, J. L., & Tranbarger, T. J. (2016). Cellular and pectin dynamics during abscission zone development and ripe fruit abscission of the monocot oil palm. *Frontiers in Plant Science*, *7*, 540. doi: 10.3389/fpls.2016.00540

Rugini, E., Baldoni, L., Silvestri, C., Mariotti, R., Narváez, I., Cultrera, N., Cristofori, V., Bashir, M. A., Mousavi, S., Palomo-Rios, E., Mercado, J. A., & Pliego-Alfaro, F. (2020). Olea europaea olive. In *Biotechnology of fruit and nut crops* (pp. 343-376). Wallingford UK: CAB International. doi: 10.1079/9781780648279.0343

Sakakibara, H., Takei, K., & Hirose, N. (2006). Interactions between nitrogen and cytokinin in the regulation of metabolism and development. *Trends in plant science*, *11*(9), 440-448. doi: 10.1016/j.tplants.2006.07.004

Sakamoto, M., Munemura, I., Tomita, R., & Kobayashi, K. (2008). Involvement of hydrogen peroxide in leaf abscission signalling, revealed by analysis with an in vitro abscission system in Capsicum plants. *The Plant Journal*, *56*(1), 13-27. doi: 10.1111/j.1365-313X.2008.03577.x

Sánchez-Rangel, D., Rivas-San Vicente, M., De la Torre-Hernandez, M. E., Nájera-Martínez, M., & Plasencia, J. (2015). Deciphering the link between salicylic acid signalling and sphingolipid metabolism. *Frontiers in plant science*, *6*, 125. doi: 10.3389/fpls.2015.00125

Santiago, J., Brandt, B., Wildhagen, M., Hohmann, U., Hothorn, L. A., Butenko, M. A., & Hothorn, M. (2016). Mechanistic insight into a peptide hormone signalling complex mediating floral organ abscission. *Elife*, *5*, e15075. Elife *5*: e15075. doi: 10.7554/eLife.15075

Santos-Antunes, F., León, L., de la Rosa, R., Alvarado, J., Mohedo, A., Trujillo, I., & Rallo, L. (2005). The length of the juvenile period in olive as influenced by vigor of the seedlings and the precocity of the parents. *HortScience*, *40*(5), 1213-1215. doi: 10.21273/HORTSCI.40.5.1213

Saucedo-García, M., Guevara-García, A., González-Solís, A., Cruz-García, F., Vázquez-Santana, S., Markham, J. E., Lozano-Rosas, M. G., Dietrich, C. R., Ramos-Vega, M., Cahoon, E. B., & Gavilanes-Ruíz, M. (2011). MPK6, sphinganine and the LCB2a gene from serine palmitoyltransferase are required in the signalling pathway that mediates cell death induced by long chain bases in Arabidopsis. *New Phytologist*, *191*(4), 943-957. doi: 10.1111/j.1469-8137.2011.03727.x

Sawicki, M., Aït Barka, E., Clément, C., Vaillant-Gaveau, N., & Jacquard, C. (2015). Cross-talk between environmental stresses and plant metabolism during reproductive organ abscission. *Journal of Experimental Botany*, *66*(7), 1707-1719. doi: 10.1093/jxb/eru533

Schuster, M., & van der Hoorn, R. A. (2020). Plant biology: distinct new players in processing peptide hormones during abscission. *Current Biology*, *30*(12), R715-R717. doi: 10.1016/j.cub.2020.04.072

Sebastiani, L., & Busconi, M. (2017). Recent developments in olive (Olea europaea L.) genetics and genomics: applications in taxonomy, varietal identification, traceability and breeding. *Plant cell reports*, *36*, 1345-1360. doi: 10.1007/s00299-017-2145-9

Seo, M., Jikumaru, Y., & Kamiya, Y. (2011). Profiling of hormones and related metabolites in seed dormancy and germination studies. *Seed dormancy: methods and protocols*, 99-111. doi: 10.1007/978-1-61779-231-1_7

Sexton, R., & Roberts, J. A. (1982). Cell biology of abscission. *Annual Review of Plant Physiology*, *33*(1), 133-162. doi: 10.1016/j.plaphy.2018.03.035

Shi, C., Yin, J., Liu, Z., Wu, J. X., Zhao, Q., Ren, J., & Yao, N. (2015). A systematic simulation of the effect of salicylic acid on sphingolipid metabolism. *Frontiers in Plant Science*, *6*, 186. doi: 10.3389/fpls.2015.00186

Shi, C. L., Alling, R. M., Hammerstad, M., & Aalen, R. B. (2019). Control of organ abscission and other cell separation processes by evolutionary conserved peptide signalling. *Plants*, *8*(7), 225. doi: 10.3390/plants8070225

Shi, C. L., Stenvik, G. E., Vie, A. K., Bones, A. M., Pautot, V., Proveniers, M., Aalen, R. B., & Butenko, M. A. (2011). Arabidopsis class I KNOTTED-like homeobox proteins act downstream in the IDA-HAE/HSL2 floral abscission signalling pathway. *The Plant Cell*, *23*(7), 2553-2567. doi: 10.1105/tpc.111.084608

Shi, C. L., Von Wangenheim, D., Herrmann, U., Wildhagen, M., Kulik, I., Kopf, A., Ishida, T., Olsson, V., Anker, M. K., Albert, M., Butenko, M. A., Felix, G., Sawa, S., Claassen, M., Friml, J., & Aalen, R. B. (2018). The dynamics of root cap sloughing in Arabidopsis is regulated by peptide signalling. *Nature plants*, *4*(8), 596-604. doi: 10.1038/s41477-018-0212-z

Shi, L., Bielawski, J., Mu, J., Dong, H., Teng, C., Zhang, J., Yang, X., Tomishige, N., Hanada, K., Hannun, Y, A., & Zuo, J. (2007). Involvement of sphingoid bases in mediating reactive oxygen intermediate production and programmed cell death in Arabidopsis. *Cell research*, *17*(12), 1030-1040. doi: 10.1038/cr.2007.100

Simons, K., & Sampaio, J. L. (2011). Membrane organization and lipid rafts. *Cold Spring Harbor perspectives in biology*, *3*(10), a004697. doi: 10.1101/cshperspect.a004697

Simon-Plas, F., Perraki, A., Bayer, E., Gerbeau-Pissot, P., & Mongrand, S. (2011). An update on plant membrane rafts. *Current opinion in plant biology*, *14*(6), 642-649. doi: 10.1016/j.pbi.2011.08.003

Singh, P., Maurya, S. K., Pradhan, L., & Sane, A. P. (2022). The JA pathway is rapidly down-regulated in petal abscission zones prior to flower opening and affects petal abscission in fragrant roses during natural and ethylene-induced petal abscission. *Scientia Horticulturae*, *300*, 111072. doi: 10.1016/j.scienta.2022.111072

Smith, E., & Whiting, M. (2010). Effect of ethephon on sweet cherry pedicel-fruit retention force and quality is cultivar dependent. *Plant Growth Regulation*, *60*, 213-223.

Sperling, P., Franke, S., Lüthje, S., & Heinz, E. (2005). Are glucocerebrosides the predominant sphingolipids in plant plasma membranes?. *Plant Physiology and Biochemistry*, *43*(12), 1031-1038. doi: 10.1016/j.plaphy.2005.10.004

Sperling, P., & Heinz, E. (2003). Plant sphingolipids: structural diversity, biosynthesis, first genes and functions. *Biochimica et Biophysica Acta (BBA)-Molecular and Cell Biology of Lipids*, *1632*(1-3), 1-15. doi: 10.1016/S1388-1981(03)00033-7

Staswick, P. E., Raskin, I., & Arteca, R. N. (1995). Jasmonates, salicylic acid and brassinosteroids. *Plant Hormones: Physiology, Biochemistry and Molecular Biology*, 179-213. doi: 10.1007/978-94-011-0473-9_9

Stenvik, G. E., Tandstad, N. M., Guo, Y., Shi, C. L., Kristiansen, W., Holmgren, A., Clark, S. E., Aalen, R. B., & Butenko, M. A. (2008). The EPIP peptide of INFLORESCENCE DEFICIENT IN ABSCISSION is sufficient to induce abscission in Arabidopsis through the receptor-like kinases HAESA and HAESA-LIKE2. *The Plant Cell*, *20*(7), 1805-1817. doi: 10.1105/tpc.108.059139

Stintzi, A., & Schaller, A. (2022). Biogenesis of post-translationally modified peptide signals for plant reproductive development. *Current Opinion in Plant Biology*, *69*, 102274. doi: 10.1016/j.pbi.2022.102274.

Stø, I. M., Orr, R. J., Fooyontphanich, K., Jin, X., Knutsen, J. M., Fischer, U., Tranbarger, T. J., Nordal, I., & Aalen, R. B. (2015). Conservation of the abscission signalling peptide IDA during Angiosperm evolution: withstanding genome duplications and gain and loss of the receptors HAE/HSL2. *Frontiers in Plant Science*, *6*, 931. doi: 10.3389/fpls.2015.00931

Sun, L., & van Nocker, S. (2010). Analysis of promoter activity of members of the PECTATE LYASE-LIKE (PLL) gene family in cell separation in Arabidopsis. *BMC Plant Biology*, *10*, 1-13. doi: 10.1186/1471-2229-10-152

Sundaresan, S., Philosoph-Hadas, S., Riov, J., Mugasimangalam, R., Kuravadi, N. A., Kochanek, B., Salim, S., Tucker, M. L., & Meir, S. (2016). De novo transcriptome sequencing and development of abscission zone-specific microarray as a new molecular tool for analysis of tomato organ abscission. *Frontiers in Plant Science*, *6*, 1258. doi: 10.3389/fpls.2015.01258

Takahashi, D., Imai, H., Kawamura, Y., & Uemura, M. (2016). Lipid profiles of detergent resistant fractions of the plasma membrane in oat and rye in association with cold acclimation and freezing tolerance. *Cryobiology*, *72*(2), 123-134. doi: 10.1016/j.cryobiol.2016.02.003

Takemoto, K., Ebine, K., Askani, J. C., Krüger, F., Gonzalez, Z. A., Ito, E., Goh, T., Schumacher, K., Nakano, A., & Ueda, T. (2018). Distinct sets of tethering complexes, SNARE complexes, and Rab GTPases mediate membrane fusion at the vacuole in Arabidopsis. *Proceedings of the National Academy of Sciences*, *115*(10), E2457-E2466. doi: 10.1073/pnas.1717839115

Takeuchi, M., Ueda, T., Sato, K., Abe, H., Nagata, T., & Nakano, A. (2000). A dominant negative mutant of sar1 GTPase inhibits protein transport from the endoplasmic reticulum to the Golgi apparatus in tobacco and Arabidopsis cultured cells. *The Plant Journal*, *23*(4), 517-525. doi: 10.1046/j.1365-313x.2000.00823.x

Tanaka, T., Abbas, H. K., & Duke, S. O. (1993). Structure-dependent phytotoxicity of fumonisins and related compounds in a duckweed bioassay. *Phytochemistry*, *33*(4), 779-785. doi: 10.1016/0031-9422(93)85274-U

Tanner, W., Malinsky, J., & Opekarová, M. (2011). In plant and animal cells, detergent-resistant membranes do not define functional membrane rafts. *The Plant Cell*, *23*(4), 1191-1193. doi: 10.1105/tpc.111.086249

Tapken, W., & Murphy, A. S. (2015). Membrane nanodomains in plants: capturing form, function, and movement. *Journal of experimental botany*, *66*(6), 1573-1586. doi: 10.1093/jxb/erv054

Tarazona, P., Feussner, K., & Feussner, I. (2015). An enhanced plant lipidomics method based on multiplexed liquid chromatography–mass spectrometry reveals additional insights into cold-and drought-induced membrane remodeling. *The Plant Journal*, *84*(3), 621-633. doi: 10.1111/tpj.13013

Tartaglio, V., Rennie, E. A., Cahoon, R., Wang, G., Baidoo, E., Mortimer, J. C., Cahoon, E. B., & Scheller, H. V. (2017). Glycosylation of inositol phosphorylceramide sphingolipids is required for normal growth and reproduction in Arabidopsis. *The Plant Journal*, *89*(2), 278-290. doi: 10.1111/tpj.13382

Taylor, A., & Qiu, Y. L. (2017). Evolutionary history of subtilases in land plants and their involvement in symbiotic interactions. *Molecular Plant-Microbe Interactions*, *30*(6), 489-501. doi: 10.1094/MPMI-10-16-0218-R

Taylor, I. B., Burbidge, A., & Thompson, A. J. (2000). Control of abscisic acid synthesis. *Journal of experimental Botany*, *51*(350), 1563-1574. doi: 10.1093/jexbot/51.350.1563

Taylor, J. E., & Whitelaw, C. A. (2001). Signals in abscission. *New Phytologist*, *151*(2), 323-340. doi: 10.1046/j.0028-646x.2001.00194.x

Taylor, I.W., Patharkar, O.R., Hsu, C.W., Baer, J., Niederhuth, C.E., Ohler, U., Benfey, P.N., & Walker, J.C. (2022). Single-cell transcriptomics of the Arabidopsis floral abscission zone. *bioRxiv*, 2022-07.

Teng, C., Dong, H., Shi, L., Deng, Y., Mu, J., Zhang, J., Yang, X., & Zuo, J. (2008). Serine palmitoyltransferase, a key enzyme for de novo synthesis of sphingolipids, is essential for male gametophyte development in Arabidopsis. *Plant Physiology*, *146*(3), 1322-1332. doi: 10.1104/pp.107.113506

Ternes, P., Feussner, K., Werner, S., Lerche, J., Iven, T., Heilmann, I., Reizman, H., & Feussner, I. (2011). Disruption of the ceramide synthase LOH1 causes spontaneous cell death in Arabidopsis thaliana. *New Phytologist*, *192*(4), 841-854. doi: 10.1111/j.1469-8137.2011.03852.x

Theodoulou, F. L., & Kerr, I. D. (2015). ABC transporter research: going strong 40 years on. *Biochemical Society Transactions*, *43*(5), 1033-1040. doi: 10.1042/BST20150139

Thomma, B. P., Penninckx, I. A., Cammue, B. P., & Broekaert, W. F. (2001). The complexity of disease signalling in Arabidopsis. *Current opinion in immunology*, *13*(1), 63-68. doi: 10.1016/S0952-7915(00)00183-7

Thudichum, J. L. W. (1874). Reports of the Medical Officer of Privy Council and Local Government Board. *N. Ser.*, *3*, 113-113.

Tian, Q. Y., Sun, P., & Zhang, W. H. (2009). Ethylene is involved in nitrate-dependent root growth and branching in Arabidopsis thaliana. *New Phytologist*, *184*(4), 918-931. doi: 10.1111/j.1469-8137.2009.03004.x

Tjellström, H.; Hellgren, L. I.; Wieslander, Å.; Sandelius, A. S. (2010). Tjellström, H., Hellgren, L. I., Wieslander, Å., & Sandelius, A. S. (2010). Lipid asymmetry in plant plasma membranes: phosphate deficiency-induced phospholipid replacement is restricted to the cytosolic leaflet. *The FASEB Journal*, *24*(4), 1128-1138. doi: 10.1096/fj.09-139410

Tortosa, M., Cartea, M. E., Rodríguez, V. M., & Velasco, P. (2018). Unraveling the metabolic response of Brassica oleracea exposed to Xanthomonas campestris pv. campestris. *Journal of the Science of Food and Agriculture*, *98*(10), 3675-3683. doi: 10.1002/jsfa.8876

Tranbarger, T. J., Domonhédo, H., Cazemajor, M., Dubreuil, C., Fischer, U., & Morcillo, F. (2019). The PIP peptide of INFLORESCENCE DEFICIENT IN ABSCISSION enhances Populus leaf and Elaeis guineensis fruit abscission. *Plants*, *8*(6), 143. doi: 10.3390/plants8060143

Tranbarger, T. J., & Tadeo, F. R. (2020). Diversity and functional dynamics of fleshy fruit abscission zones. *Annual Plant Reviews online*, 1-64. doi: 10.1002/9781119312994.apr0652

Trujillo, L. E., Menéndez, C., Ochogavía, M. E., Hernández, I., Borrás, O., Rodríguez, R., ... & Hernández, L. (2009). Engineering drought and salt

tolerance in plants using SodERF3, a novel sugarcane ethylene responsive factor. *Biotecnología Aplicada*, *26*(2), 168-171.

Tsegaye, Y., Richardson, C. G., Bravo, J. E., Mulcahy, B. J., Lynch, D. V., Markham, J. E., Jaworski, J. G., Chen, M., Cahoon, E. B., & Dunn, T. M. (2007). Arabidopsis mutants lacking long chain base phosphate lyase are fumonisin-sensitive and accumulate trihydroxy-18: 1 long chain base phosphate. *Journal of Biological Chemistry*, *282*(38), 28195-28206. doi: 10.1074/jbc.M705074200

Tucker, M. L., & Kim, J. (2015). Abscission research: what we know and what we still need to study. doi: 10.2212/spr.2015.2.1

Tucker, M. L., & Yang, R. (2012). IDA-like gene expression in soybean and tomato leaf abscission and requirement for a diffusible stelar abscission signal. *AoB plants*, *2012*. doi: 10.1093/aobpla/pls035

Unver, T., Wu, Z., Sterck, L., Turktas, M., Lohaus, R., Li, Z., Yang, M., He, L., Deng, T., Escalante, F. J., Llorens, C., Roig, F. J., Parmaksiz, I., Dundar, E., Xie, F., Zhang, B., Ipek, A., Uranbey, S., Erayman, M., Ilhan, E., Badad, O., Ghazal, H., Lightfoot, D. A., Kasarla, P., Colantonio, V., Tombuloglu, H., Hernandez, P., Mete, N., Cetin, O., Van Montagu, M., Yang, H., Gao, Q., Dorado, G., & Van de Peer, Y. (2017). Genome of wild olive and the evolution of oil biosynthesis. *Proceedings of the National Academy of Sciences*, *114*(44), E9413-E9422. doi: 10.1073/pnas.1708621114

Uzquiza, L., Martin, P., Sievert, J. R., Arpaia, M. L., & Fidelibus, M. W. (2014). Methyl jasmonate and 1-aminocyclopropane-1-carboxylic acid interact to promote grape berry abscission. *American Journal of Enology and Viticulture*, *65*(4), 504-509. doi: 10.5344/ajev.2014.14038

Van Nocker, S. (2009). Development of the abscission zone. *Stewart Postharvest Review*, *5*(1), 5. doi: 10.2212/spr.2009.1.5

Vashisth, T., NeSmith, D. S., & Malladi, A. (2015). Anatomical and gene expression analyses of two blueberry genotypes displaying differential fruit detachment. *Journal of the American Society for Horticultural Science*, *140*(6), 620-626. doi: 10.21273/JASHS.140.6.620

Vandenbussche, F., Petrášek, J., Žádníková, P., Hoyerová, K., Pešek, B., Raz, V., Swarup, R., Bennett, M., Zažímalová, E., Benková, E., & Van Der Straeten, D. (2010). The auxin influx carriers AUX1 and LAX3 are involved in auxin-ethylene interactions during apical hook development in Arabidopsis thaliana seedlings. *Development*, *137*(4), 597-606. doi: 10.1242/dev.040790

Velázquez-Palmero, D., Romero-Segura, C., García-Rodríguez, R., Hernández, M. L., Vaistij, F. E., Graham, I. A., Pérez, A. G., & Martínez-Rivas, J. M. (2017). An oleuropein β-glucosidase from olive fruit is involved in determining the phenolic composition of virgin olive oil. *Frontiers in plant science*, *8*, 1902. doi: 10.3389/fpls.2017.01902

Ventimilla, D., Velázquez, K., Ruiz-Ruiz, S., Terol, J., Pérez-Amador, M. A., Vives, M. C., Guerri, J., Talon, M., & Tadeo, F. R. (2021). IDA (INFLORESCENCE DEFICIENT IN ABSCISSION)-like peptides and HAE (HAESA)-like receptors regulate corolla abscission in Nicotiana benthamiana flowers. *BMC Plant Biology*, *21*(1), 226. doi. 10.1186/s12870-021-02994-8

Verhoek, B., Haas, R., Wrage, K., Linscheid, M., & Heinz, E. (1983). Lipids and enzymatic activities in vacuolar membranes isolated via protoplasts from

oat primary leaves. *Zeitschrift für Naturforschung C*, *38*(9-10), 770-777. doi: 10.1515/znc-1983-9-1018

Vie, A. K., Najafi, J., Liu, B., Winge, P., Butenko, M. A., Hornslien, K. S., Kumpf, R., Aalen, R. B., Bones, A, M., & Brembu, T. (2015). The IDA/IDA-LIKE and PIP/PIP-LIKE gene families in Arabidopsis: phylogenetic relationship, expression patterns, and transcriptional effect of the PIPL3 peptide. *Journal of Experimental Botany*, *66*(17), 5351-5365. doi: 10.1093/jxb/erv285

Vie, A. K., Najafi, J., Winge, P., Cattan, E., Wrzaczek, M., Kangasjärvi, J., Miller, G., Brembu, T., & Bones, A. M. (2017). The IDA-LIKE peptides IDL6 and IDL7 are negative modulators of stress responses in Arabidopsis thaliana. *Journal of Experimental Botany*, *68*(13), 3557-3571. doi: 10.1093/jxb/erx168

Vu, H. S., Shiva, S., Roth, M. R., Tamura, P., Zheng, L., Li, M., Sarowar, S., Honey, S., McEllhiney, D., Hinkes, P., Seib, L., Williams, T. D., Gadbury, G., Wang, X., Shah, J., & Welti, R. (2014). Lipid changes after leaf wounding in Arabidopsis thaliana: Expanded lipidomic data form the basis for lipid co-occurrence analysis. *The Plant Journal*, *80*(4), 728-743. doi: 10.1111/tpj.12659

Wang, J., Lin, G., Ma, R., Han, Z., & Chai, J. (2018). Structural Insight into Recognition of Plant Peptide Hormones by Plant Receptor Kinases. *Plant Structural Biology: Hormonal Regulations*, 31-46. doi: 10.1007/978-3-319-91352-0_3

Wang, J., Ye, B., Yin, J., Yuan, C., Zhou, X., Li, W., He, M., Wang, J., Chen, W., Qin, P., Ma, B., Wang, Y., Li, S., & Chen, X. (2015). Characterization and fine mapping of a light-dependent leaf lesion mimic mutant 1 in rice. *Plant Physiology and Biochemistry*, *97*, 44-51. doi: 10.1016/j.plaphy.2015.09.001

Wang, L., Liu, C., Liu, Y., & Luo, M. (2020b). Fumonisin B1-induced changes in cotton fiber elongation revealed by sphingolipidomics and proteomics. *Biomolecules*, *10*(9), 1258. doi: 10.3390/biom10091258

Wang, L., Suo, X., Liu, Y., Liu, C., & Luo, M. (2021). Sphingosine promotes embryo biomass in upland cotton: A biochemical and Transcriptomic analysis. *Biomolecules*, *11*(4), 525. doi: 10.3390/biom11040525

Wang, R., Shi, C., Wang, X., Li, R., Meng, Y., Cheng, L., Qi, M., Xu, T., & Li, T. (2020a). Tomato SlIDA has a critical role in tomato fertilization by modifying reactive oxygen species homeostasis. *The Plant Journal*, *103*(6), 2100-2118. Doi: 10.1111/tpj.14886

Wang, X., Liu, D., Li, A., Sun, X., Zhang, R., Wu, L., Liang, Y., & Mao, L. (2013). Transcriptome analysis of tomato flower pedicel tissues reveals abscission zone-specific modulation of key meristem activity genes. *PLoS One*, *8*(2), e55238. doi: 10.1371/journal.pone.0055238

Wang, W., Yang, X., Tangchaiburana, S., Ndeh, R., Markham, J. E., Tsegaye, Y., Dunn, T. M., Wang, G. L., Bellizi, M., Parsons, J. F., Morrissey, D., Bravo, J. E., Lynch, D. V., & Xiao, S. (2008). An inositolphosphorylceramide synthase is involved in regulation of plant programmed cell death associated with defense in Arabidopsis. *The Plant Cell*, *20*(11), 3163-3179. doi: 10.1105/tpc.108.060053

Warnecke, D., & Heinz, E. (2003). Recently discovered functions of glucosylceramides in plants and fungi. *Cellular and Molecular Life Sciences CMLS*, *60*, 919-941.

Weis, K. G., Goren, R., Martin, G. C., & Webster, B. D. (1988). Leaf and inflorescence abscission in olive. I. Regulation by ethylene and ethephon. *Botanical Gazette*, *149*(4), 391-397. doi: 10.1086/337731

West, G., Viitanen, L., Alm, C., Mattjus, P., Salminen, T. A., & Edqvist, J. (2008). Identification of a glycosphingolipid transfer protein GLTP1 in Arabidopsis thaliana. *The FEBS journal*, *275*(13), 3421-3437. doi: 10.1111/j.1742-4658.2008.06498.x

Wilmowicz, E., Frankowski, K., Kućko, A., Świdziński, M., de Dios Alché, J., Nowakowska, A., & Kopcewicz, J. (2016). The influence of abscisic acid on the ethylene biosynthesis pathway in the functioning of the flower abscission zone in Lupinus luteus. *Journal of plant physiology*, *206*, 49-58. Doi: https://doi.org/10.1016/j.jplph.2016.08.018

Wilmowicz, E., Kućko, A., Ostrowski, M., & Panek, K. (2018). INFLORESCENCE DEFICIENT IN ABSCISSION-like is an abscission-associated and phytohormone-regulated gene in flower separation of Lupinus luteus. *Plant Growth Regulation*, *85*, 91-100. doi: 10.1007/s10725-018-0375-7

Worrall, D., Liang, Y. K., Alvarez, S., Holroyd, G. H., Spiegel, S., Panagopulos, M., Gray, J. E., & Hetherington, A. M. (2008). Involvement of sphingosine kinase in plant cell signalling. *The Plant Journal*, *56*(1), 64-72. doi: 10.1111/j.1365-313X.2008.03579.x

Wu, J., Qin, X., Tao, S., Jiang, X., Liang, Y. K., & Zhang, S. (2014). Long-chain base phosphates modulate pollen tube growth via channel-mediated influx of calcium. *The Plant Journal*, *79*(3), 507-516. doi: 10.1111/tpj.12576

Wu, J. X., Li, J., Liu, Z., Yin, J., Chang, Z. Y., Rong, C., Wu, J. L., Bi, F. C., & Yao, N. (2015a). The Arabidopsis ceramidase At ACER functions in disease resistance and salt tolerance. *The Plant Journal*, *81*(5), 767-780. doi: 10.1111/tpj.12769

Wu, J. X., Wu, J. L., Yin, J., Zheng, P., & Yao, N. (2015b). Ethylene modulates sphingolipid synthesis in Arabidopsis. *Frontiers in Plant Science*, *6*, 1122. doi: 10.3389/fpls.2015.01122

Wu, X. M., Yu, Y., Han, L. B., Li, C. L., Wang, H. Y., Zhong, N. Q., Yao, Y., & Xia, G. X. (2012). The tobacco BLADE-ON-PETIOLE2 gene mediates differentiation of the corolla abscission zone by controlling longitudinal cell expansion. *Plant physiology*, *159*(2), 835-850. doi: 10.1104/pp.112.193482

Xie, L. J., Chen, Q. F., Chen, M. X., Yu, L. J., Huang, L., Chen, L., Wang, F. Z., Xia, F. N., Zhu, T. R., Wu, J. X., Yin, J., Liao, B., Shi, J., Zhang, J. H., Aharoni, A., Yao, N., Shu, W., & Xiao, S. (2015). Unsaturation of very-long-chain ceramides protects plant from hypoxia-induced damages by modulating ethylene signalling in Arabidopsis. *PLoS genetics*, *11*(3), e1005143. doi: 10.1371/journal.pgen.1005143

Xie, R., Ge, T., Zhang, J., Pan, X., Ma, Y., Yi, S., & Zheng, Y. (2018). The molecular events of IAA inhibiting citrus fruitlet abscission revealed by digital gene expression profiling. *Plant Physiology and Biochemistry*, *130*, 192-204. doi: 10.1016/j.plaphy.2018.07.006

Xu, J., Chen, L., Sun, H., Wusiman, N., Sun, W., Li, B., Gao, Y., Kong, J., Zhang, D., Zhang, X., Xu, H., & Yang, X. (2019). Crosstalk between cytokinin and ethylene signalling pathways regulates leaf abscission in cotton in response to chemical defoliants. *Journal of experimental botany*, *70*(5), 1525-1538. doi: 10.1093/jxb/erz036

Yan, D., Yadav, S. R., Paterlini, A., Nicolas, W. J., Petit, J. D., Brocard, L., Belevich, I., Grison, M. S., Vaten, A., Karami, L., el-Showk, S., Lee, J. Y., Murawska, G. M., Mortimer, J., Knoblauch, M., Jokitalo, E., Markham, J. E., Bayer, E. M., & Helariutta, Y. (2019). Sphingolipid biosynthesis modulates plasmodesmal ultrastructure and phloem unloading. *Nature plants*, *5*(6), 604-615. doi: 10.1038/s41477-019-0429-5

Yang, B., Li, M., Phillips, A., Li, L., Ali, U., Li, Q., Lu, S., Hong, Y., Wang, X., & Guo, L. (2021). Nonspecific phospholipase C4 hydrolyzes phosphosphingolipids and sustains plant root growth during phosphate deficiency. *The Plant Cell*, *33*(3), 766-780. doi: 10.1093/plcell/koaa054

Yang, C., Lu, X., Ma, B., Chen, S. Y., & Zhang, J. S. (2015). Ethylene signalling in rice and Arabidopsis: conserved and diverged aspects. *Molecular plant*, *8*(4), 495-505. doi: 10.1016/j.molp.2015.01.003

Yi, J. W., Wang, Y., Ma, X. S., Zhang, J. Q., Zhao, M. L., Huang, X. M., Li, J. G., HU, G. B., & Wang, H. C. (2021). LcERF2 modulates cell wall metabolism by directly targeting a UDP-glucose-4-epimerase gene to regulate pedicel development and fruit abscission of litchi. *The Plant Journal*, *106*(3), 801-816. doi: 10.1111/tpj.15201

Ying, P., Li, C., Liu, X., Xia, R., Zhao, M., & Li, J. (2016). Identification and molecular characterization of an IDA-like gene from litchi, LcIDL1, whose ectopic expression promotes floral organ abscission in Arabidopsis. *Scientific Reports*, *6*(1), 37135. doi: 10.1038/srep37135

Yu, L., Nie, J., Cao, C., Jin, Y., Yan, M., Wang, F., Liu, J., Xiao, Y., Liang, Y., & Zhang, W. (2010). Phosphatidic acid mediates salt stress response by regulation of MPK6 in Arabidopsis thaliana. *New Phytologist*, *188*(3), 762-773. doi: 10.1111/j.1469-8137.2010.03422.x

Yu, Y., Leyva, P., Tavares, R. L., & Kellogg, E. A. (2020). The anatomy of abscission zones is diverse among grass species. *American Journal of Botany*, *107*(4), 549-561. doi: 10.1002/ajb2.1454

Yuan, R., & Carbaugh, D. H. (2007). Effects of NAA, AVG, and 1-MCP on ethylene biosynthesis, preharvest fruit drop, fruit maturity, and quality of 'Golden Supreme'and 'Golden Delicious' apples. *HortScience*, *42*(1), 101-105. doi: 10.21273/HORTSCI.42.1.101

Zelasco, S., Carbone, F., Lombardo, L., & Salimonti, A. (2021). Olive tree genetics, genomics, and transcriptomics for the olive oil quality improvement. In *Olives and Olive Oil in Health and Disease Prevention* (pp. 27-49). Academic Press. doi: 10.1016/B978-0-12- 819528-4.00017-1.

Zeng, H. Y., & Yao, N. (2022). Sphingolipids in plant immunity. *Phytopathology Research*, *4*(1), 1-19. doi: 10.1186/s42483-022-00125-1

Zhang, G. B., Meng, S., & Gong, J. M. (2018). The expected and unexpected roles of nitrate transporters in plant abiotic stress resistance and their regulation. *International journal of molecular sciences*, *19*(11), 3535. doi: 10.3390/ijms19113535

Zhang, H., Huang, L., Li, X., Ouyang, Z., Yu, Y., Li, D., & Song, F. (2013). Overexpression of a rice long-chain base kinase gene OsLCBK1 in tobacco improves oxidative stress tolerance. *Plant Biotechnology*, *30*(1), 9-16. doi: 10.5511/plantbiotechnology.12.1101b

Zhang, X., Li, B., Zhang, X., Wang, C., Zhang, Z., & Sun, P. (2022). Exogenous application of ethephon regulates flower abscission, shoot growth, and secondary metabolites in Camellia sinensis. *Scientia Horticulturae*, *304*, 111333. doi: 10.1016/j.scienta.2022.111333

Zhang, Y., Zhu, H., Zhang, Q., Li, M., Yan, M., Wang, R., Wang, L., Welti, R., Zhang, W., & Wang, X. (2009). Phospholipase Dα1 and phosphatidic acid regulate NADPH oxidase activity and production of reactive oxygen species in ABA-mediated stomatal closure in Arabidopsis. *The Plant Cell*, *21*(8), 2357-2377. doi: 10.1105/tpc.108.062992

Zhang, Z., Lenk, A., Andersson, M. X., Gjetting, T., Pedersen, C., Nielsen, M. E., Newman, M, Hou, B. H., Somerville, S. C., & Thordal-Christensen, H. (2008). A lesion-mimic syntaxin double mutant in Arabidopsis reveals novel complexity of pathogen defense signalling. *Molecular plant*, *1*(3), 510-527. doi: 10.1093/mp/ssn011

Zheng, G., Bao, Z., Pérez-Juste, J., Du, R., Liu, W., Dai, J., Zhang, W., Lee, L. Y. S., & Wong, K. Y. (2018). Tuning the morphology and chiroptical properties of discrete gold nanorods with amino acids. *Angewandte Chemie International Edition*, *57*(50), 16452-16457. doi: 10.1002/anie.201810693

Zhou, C., Lakso, A. N., Robinson, T. L., & Gan, S. (2008). Isolation and characterization of genes associated with shade-induced apple abscission. *Molecular Genetics and Genomics*, *280*, 83-92. doi: 10.1007/s00438-008-0348-z

Zhou, Y., Zeng, L., Fu, X., Mei, X., Cheng, S., Liao, Y., Deng, R., Xu, X., Jiang, Y., Duan, X., Baldermann, S & Yang, Z. (2016). The sphingolipid biosynthetic enzyme Sphingolipid delta8 desaturase is important for chilling resistance of tomato. *Scientific reports*, *6*(1), 1-10. doi: 10.1038/srep38742

Zhu, H., Dardick, C. D., Beers, E. P., Callanhan, A. M., Xia, R., & Yuan, R. (2011). Transcriptomics of shading-induced and NAA-induced abscission in apple (Malus domestica) reveals a shared pathway involving reduced photosynthesis, alterations in carbohydrate transport and signalling and hormone crosstalk. *BMC Plant Biology*, *11*, 1-20. doi: 10.1186/1471-2229-11-138

Zhu, M., Zheng, L., Zeng, Y., & Yu, J. (2022). Susceptibility of two grape varieties to berry abscission. *Scientia Horticulturae*, *304*, 111280. doi: 10.1016/j.scienta.2022.111280

Zienkiewicz, A., Gömann, J., König, S., Herrfurth, C., Liu, Y. T., Meldau, D., & Feussner, I. (2020). Disruption of Arabidopsis neutral ceramidases 1 and 2 results in specific sphingolipid imbalances triggering different phytohormone-dependent plant cell death programmes. *New Phytologist*, *226*(1), 170-188. doi: 10.1111/nph.16336

Zipori, I., Dag, A., Tugendhaft, Y., & Birger, R. (2014). Mechanical harvesting of table olives: Harvest efficiency and fruit quality. *HortScience*, *49*(1), 55-58. doi: 10.21273/HORTSCI.49.1.55

Zohary, D., Hopf, M. (1994). Domestication of plants in the Old World, 2nd edn. Clarendon.

6.ANEXOS

Table 3.I.S1. Fruit- or AZ-enriched genes encoding various cell-wall proteins at the last stage of olive fruit ripening. Sequences were selected after establishing a P<0.01. The table shows the total read count in RPKMx1000 for each gene after normalization across the two samples: fruit-pericarp and their AZ at 217 DPA.

Uniprot ID	AZ	Fruit	P value	Description
α-galactosidase				
Enriched in fruit				
Q5DUH8	2.00	26.19	2,27E-07	Alpha galactosidase, gal1 = *Coffea arabica*
α-1,4-glucan-protein synthase				
Enriched in fruit				
Q2HV87	0.00	150.81	2,70E-44	Alpha-1,4-glucan-protein synthase (UDP-forming) = *Medicago truncatula*
Enriched in AZ				
B9RAC8	83.00	54.32	2,41E-03	Alpha-1,4-glucan-protein synthase [UDP-forming] = *Ricinus communis*
α-glucosidase				
Enriched in fruit				
B9STU2	0.00	3.97	9,77E-04	Neutral alpha-glucosidase ab = *Ricinus communis*
Enriched in AZ				
Q9LEC9	12.00	0.00	2,91E-11	Alpha-glucosidase, mal2 = *Solanum tuberosum*
arabinogalactan protein				
Enriched in AZ				
Q8LCE4	22.56	0.00	1,95E-03	Classical arabinogalactan protein 5, AGP5, At1g35230
β-1,3-glucanase				
Enriched in fruit				
Q9FXL4	0.00	642.39	8,53E-252	Elicitor inducible beta-1,3-glucanase NtEIG-E76 = *Nicotiana tabacum*
Enriched in AZ				
Q68V46	1350.00	0.00	0,00E+00	Beta-1,3-glucanase, glu-4 = *Olea europaea*
B9RSS2	42.00	0.00	9,31E-10	Endo-1,3-1,4-beta-d-glucanase = *Ricinus communis*
B9SCU1	94.00	11.13	5,10E-22	Glucan endo-1,3-beta-glucosidase = *Ricinus communis*
β-galactosidase				
Enriched in fruit				
O81100	0.00	27.16	6,94E-18	Beta-galactosidase, TBG4 = *Solanum lycopersicum*
Enriched in AZ				
O65736	25.00	0.00	1,39E-17	Beta-galactosidase = *Cicer arietinum*
B9N0S6	3.00	0.00	7,81E-03	Beta-galactosidase = *Populus trichocarpa*
β-glucosidase				
Enriched in fruit				
Q8GVD0	215.00	5033.87	0,00E+00	Beta-glucosidase, bglc = *Olea europaea*
Enriched in AZ				
O82151	59.00	0.00	4,81E-35	Beta-D-glucan exohydrolase = *Nicotiana tabacum*
β-hexosaminidase				
Enriched in fruit				
D3TI69	0.00	27.24	2,84E-14	Beta-hexosaminidase 1 = *Solanum lycopersicum*
Cellulase				
Enriched in fruit				
Q9XF22	0.00	6.23	3,91E-03	Cellulase = *Nicotiana alata*

Enriched in AZ				
Q43149	20.00	0.00	9,31E-10	Cellulase = *Sambucus nigra*
cellulose synthase				
Enriched in fruit				
B9IKV7	0.00	46.74	8,35E-43	Cellulose synthase = *Populus trichocarpa*
B9S9V9	4.00	24.16	1,05E-10	Cellulose synthase = *Ricinus communis*
D7U7F7	0.00	6.06	4,88E-04	Cellulose synthase = *Vitis vinifera*
B9GFE1	0.00	12.33	3,64E-12	Cellulose synthase = *Populus trichocarpa*
D7T308	0.00	11.84	2,33E-10	Cellulose synthase = *Vitis vinifera*
Enriched in AZ				
Q6XP47	13.00	0.00	9,09E-13	Cellulose synthase, StCesA1 = *Solanum tuberosum*
C6KF43	11.00	0.00	2,38E-07	Cellulose synthase catalytic subunit, cesA7 = *Gossypium hirsutum*
Q4PKB6	5.00	0.00	6,10E-05	Cellulose synthase CesA1 = *Boehmeria nivea*
Q45KQ0	26.00	0.00	1,73E-18	Cellulose synthase-like protein CslE = *Nicotiana tabacum*
Q3Y6V1	14.00	0.00	4,66E-10	Cellulose synthase-like protein CslG = *Nicotiana tabacum*
B9I7Q4	12.00	0.00	9,09E-13	Cellulose synthase = *Populus trichocarpa*
B9RYN4	3.00	0.00	7,81E-03	Cellulose synthase = *Ricinus communis*
D7T7B9	6.00	0.00	7,81E-03	Cellulose synthase = *Vitis vinifera*
D7THX8	11.00	0.00	1,14E-13	Cellulose synthase = *Vitis vinifera*
D7SUS1	5.00	0.00	1,22E-04	Cellulose synthase = *Vitis vinifera*
chitinase				
Enriched in fruit				
A5B1C7	25.00	71.65	3,67E-05	Chitinase = *Vitis vinifera*
D7T2C4	19.00	113.28	1,81E-14	Chitinase = *Vitis vinifera*
Enriched in AZ				
Q9FS45	134.00	10.25	5,46E-30	Chitinase = *Vitis vinifera*
A1IJ67	10.00	0.00	3,91E-03	Class IV chitinase = *Nicotiana tabacum*
D7SSZ8	350.00	0.00	1,92E-93	Chitinase = *Vitis vinifera*
endo-1,4-β-glucanase				
Enriched in fruit				
Q9ZSP9	0.00	20.80	7,28E-12	Endo-beta-1,4-D-glucanase, Cel8 = *Solanum lycopersicum*
B9S075	103.00	146.00	4,49E-03	Endo-1,4-beta-glucanase = *Ricinus communis*
Enriched in AZ				
B9RLZ9	4.00	0.00	7,81E-03	Endo-1,4-beta-glucanase = *Ricinus communis*
Q0KIX2	68.00	0.00	3,67E-40	Endoglucanase, CmEGase1 = *Cucumis melo*
endo-β-mannanase				
Enriched in AZ				
C7A7X6	44.00	18.47	8,72E-05	Endo-beta-mannanase, MAN1 = *Actinidia arguta*
expansin				
Enriched in fruit				
Q9ZP37	0.00	232.00	7,35E-51	Alpha-expansin, Nt-EXPA3 = *Nicotiana tabacum*
B9R8E5	0.00	457.03	1,31E-98	Alpha-expansin 11 = *Ricinus communis*
Q9M5I7	132.00	658.56	4,56E-56	Alpha-expansin 3 = *Triphysaria versicolor*
B9S4E4	0.00	2111.11	0,00E+00	Alpha-expansin 8 = *Ricinus communis*
Q84UT0	0.00	247.96	4,70E-52	Expansin, Vexp-1 = *Vitis vinifera*
B7U8J4	52.00	1418.63	1,22E-244	Expansin, CDK3 = *Diospyros kaki*

A5BA94	0.00	120.83	5,17E-26	Expansin = *Vitis vinifera*
Enriched in AZ				
B9IGR9	10.00	0.00	3,91E-03	PtEXPA13 = *Populus trichocarpa*
extensin				
Enriched in fruit				
Q39600	0.00	216.58	7,98E-40	Extensin, cyc17 = *Catharanthus roseus*
P13983	0.00	213.97	2,39E-119	Extensin, HRGPNT3 = *Nicotiana tabacum*
B9RPC0	9.29	41.51	3,64E-08	leucine-rich repeat family protein / extensin family protein LRX1 = *Ricinus communis*
Enriched in AZ				
C3VPW8	9.00	0.00	7,81E-03	Extensin = *Lithospermum erythrorhizon*
glycosyl hydrolase				
Enriched in fruit				
D7U290	0.00	2.71	7,81E-03	Glycosyl hydrolase 1 family protein = *Vitis vinifera*
Enriched in AZ				
B9HAA3	32.00	0.00	1,16E-10	Glycosyl hydrolase 17 family = *Populus trichocarpa*
D7TQ09	19.00	4.08	1,17E-04	Glycosyl hydrolase 17 family = *Populus trichocarpa*
B9GQH4	10.00	0.00	1,95E-03	Glycosyl hydrolase 18 family protein = *Populus trichocarpa*
B9HYK4	404.00	39.21	8,46E-70	Glycosyl hydrolase 18 family protein = *Populus trichocarpa*
A5BD25	4.00	0.00	7,81E-03	Glycosyl hydrolase 18 family protein = *Vitis vinifera*
D7U285	120.00	58.68	2,47E-11	Glycosyl hydrolase 1 family protein = *Vitis vinifera*
D7U288	8.00	0.00	9,54E-07	Glycosyl hydrolase 1 family protein = *Vitis vinifera*
laccase				
Enriched in AZ				
B2M153	518.00	0.00	4,51E-277	Laccase = *Rosa hybrid cultivar*
B9H7Z9	170.00	35.39	9,82E-42	Laccase = *Populus trichocarpa*
B9IEA5	14.00	0.00	2,98E-08	Laccase = *Populus trichocarpa*
l				
Enriched in AZ				
B9SMY4	31.00	0.00	8,67E-19	Lyase = *Ricinus communis*
B9SMM6	156.00	0.00	4,91E-91	Lyase = *Ricinus communis*
B9SML0	215.00	0.00	6,88E-136	Lyase = *Ricinus communis*
pectin methylesterase/ Pectinesterase				
Enriched in fruit				
Q84V57	0.00	368.45	1,16E-180	Pectinesterase = *Nicotiana benthamiana*
B9H3W4	0.00	9.49	3,91E-03	Pectinesterase = *Populus trichocarpa*
D7SXF6	0.00	8.43	7,81E-03	Pectinesterase = *Vitis vinifera*
P09607	0.00	24.84	1,82E-12	Pectinesterase 2.1 (PE 2.1) (Pectin methylesterase 2.1), PME2.1 = *Solanum lycopersicum*
Enriched in AZ				
A0ZNK0	10.00	0.00	7,63E-06	Pectin methylesterase 2, PcPME2 = *Pyrus communis*
B9SP63	4.00	0.00	7,81E-03	Pectinesterase = *Ricinus communis*
B9RD90	8.00	0.00	2,44E-04	Pectinesterase = *Ricinus communis*
polygalacturonase				
Enriched in fruit				
D7U2D3	2.00	67.78	2,38E-23	Polygalacturonase = *Vitis vinifera*
D7U2D3	2.00	67.78	2,38E-23	Polygalacturonase = *Vitis vinifera*

Enriched in AZ				
B9RCG6	24.00	0.00	2,91E-11	Polygalacturonase = *Ricinus communis*
B1PK08	616.00	114.23	3,23E-100	Polygalacturonase = *Olea europaea*
A7PZL3	10.00	0.00	3,05E-05	Polygalacturonase = *Vitis vinifera*
ramnose synthase				
Enriched in AZ				
Q9SYM5	206.78	84.21	6,03E-30	Probable rhamnose biosynthetic enzyme, RHM1, At1g78570
xyloglucan endotransglucosylase/hydrolase				
Enriched in AZ				
Q6EJD2	72.00	0.00	2,17E-19	Xyloglucan endotransglucosylase, XTH-1 = *Beta vulgaris*
C0IRH3	105.00	38.01	5,79E-10	Xyloglucan endotransglucosylase/hydrolase 14 = *Actinidia deliciosa*
C0IRG4	80.00	0.00	2,12E-22	Xyloglucan endotransglucosylase/hydrolase 5 = *Actinidia deliciosa*
xyloglucan:xyloglucosyl transferase				
Enriched in AZ				
B9HAM2	25.00	0.00	9,54E-07	Xyloglucan:xyloglucosyl transferase = *Populus trichocarpa*
A5BND5	94.00	0.00	2,58E-26	Xyloglucan: xyloglucosyl transferase = *Vitis vinifera*

Table 3.I.S2. Fruit- or AZ-enriched genes encoding various plant-hormone metabolism and signalling proteins at the last stage of olive fruit ripening. Sequences were selected after establishing a P<0.01. The table shows the total read count in RPKMx1000 for each gene after normalization across the two samples: fruit-pericarp and their AZ at 217 DPA.

	Uniprot ID	AZ	Fruit	P value	Description
Ethylene					
	Enriched in fruit				
	C6KMJ4	1423.76	4795.00	0.00E+00	ACC oxidase, ACO1 = *Boea hygrometrica*
	A1E4D3	13.51	611.00	0.00E+00	Ethylene receptor, ETR1 = *Coffea canephora*
	Q2PQJ0	0.00	68.00	2.46E-38	EIN3-binding F-box protein 1 (EIN3-binding F-box protein 2), EBF2 EBF1 = *Solanum lycopersicum*
	Q39026	0.00	45.00	4.44E-16	Mitogen-activated protein kinase 6 (AtMPK6), MPK6 At2g43790 F18O19.10
	O48631	0.00	29.00	1.86E-09	Ethylene-forming-enzyme-like dioxygenase = *Prunus armeniaca*
	Q8GTL5	0.00	10.00	2.44E-04	S-adenosylmethionine synthase (AdoMet synthase) (Methionine adenosyltransferase) (MAT), SAMS = *Carica papaya*
	Q9SXS8	100.74	169.00	4.60E-03	Ethylene-responsive transcription factor 3 (Ethylene-responsive element-binding factor 3 homolog) (Ethylene-responsive element-binding factor 5) (EREBP-5) (NtERF5), ERF3 ERF-5 ERF5 = *Nicotiana tabacum*
	Enriched in AZ				
	Q5IWL7	319.17	0.00	1.73E-77	Ethylene-responsive element binding protein 5 = *Nicotiana tabacum*
	Q84QD4	166.12	18.00	3.87E-62	EIL1 = *Nicotiana tabacum*
	A7Q0V4	326.51	70.00	3.00E-53	S-adenosylmethionine synthase 5 (AdoMet synthase 5) (Methionine adenosyltransferase 5) (MAT 5), METK5= *Vitis vinifera*
	Q9SFB0	91.25	0.00	2.80E-45	MATE efflux family protein FRD3 (MATE citrate transporter) (Protein DTX43) (Protein FERRIC REDUCTASE DEFECTIVE 3) (AtFRD3) (Protein MANGANESE ACCUMULATOR 1), FRD3 DTX43 MAN1 At3g08040 F17A17.38 T8G24.8
	Q2PQJ1	79.01	2.00	6.88E-44	EIN3-binding F-box protein 1 (EIN3-binding F-box protein 2), EBF1 EBF2 = *Solanum lycopersicum*
	Q9FHW7	608.18	207.00	5.50E-29	SKP1-like protein 1B (SKP1-like 2) (UFO-binding protein 2), SKP1B ASK2 UIP2 At5g42190 MJC20.30
	Q38950	256.67	111.00	2.31E-29	Serine/threonine-protein phosphatase 2A 65 kDa regulatory subunit A beta isoform (AtA beta) (PP2A. subunit A. beta isoform), PP2AA2 DF1 At3g25800 K13N2.14
	Q6R567	133.59	11.00	1.49E-23	E3 ubiquitin-protein ligase RMA1H1 (EC 6.3.2.-) (Protein RING membrane-anchor 1 homolog 1), RMA1H1 = *Capsicum annuum*
	P31237	66.87	0.00	1.36E-20	1-aminocyclopropane-1-carboxylate oxidase (ACC oxidase), ACO = *Actinidia deliciosa*
	A9P822	242.34	105.00	3.08E-19	S-adenosylmethionine synthase 1 (AdoMet synthase 1) (Methionine adenosyltransferase 1) (MAT 1), METK1 = *Populus trichocarpa*
	Q9LW49	83.70	0.00	3.47E-18	Ethylene-responsive transcription factor 4 (Ethylene-responsive element-binding factor 3) (EREBP-3) (Ethylene-responsive element-binding factor 4 homolog) (NsERF3), ERF4 ERF-3 ERF3 = *Nicotiana sylvestris*
	Q32W74	56.76	0.00	3.55E-15	Ethylene responsive element binding protein C2 = *Capsicum annuum*
	Q9SJL8	343.58	215.00	1.59E-12	S-adenosylmethionine synthase 3 (AdoMet synthase 3) (Methionine adenosyltransferase 3) (MAT 3), METK3 At2g36880 T1J8.6
	B9HK87	15.47	0.00	3.73E-09	Ethylene-insensitive 3d, EIN3D = *Populus trichocarpa*
	D8VD38	35.15	0.00	1.86E-09	Ethylene response factor 11, ERF11 = *Actinidia deliciosa*

	B9S1K1	35.26	7.00	3.54E-09	S-adenosylmethionine-dependent methyltransferase = *Ricinus communis*
	Q9XET8	9.63	0.00	2.38E-07	Ethylene receptor (Ethylene receptor homolog) ETR4 = *Solanum lycopersicum*
	Q39227	21.23	0.00	1.19E-07	24-methylenesterol C-methyltransferase 2 (24-sterol C-methyltransferase 2) (Sterol-C-methyltransferase 2) (EC 2.1.1.143) (Protein COTYLEDON VASCULAR PATTERN 1), SMT2 CVP1 At1g20330 F14O10.7
	B3FIB0	13.30	0.00	1.91E-06	Ethylene receptor ETR2 = *Actinidia deliciosa*
	Q6V397	4.58	0.00	3.81E-06	EIN2 = *Petunia hybrida*
	O22587	6.99	0.00	1.53E-05	Ethylene receptor homolog, NTHK1 = *Nicotiana tabacum*
	A6ZI64	110.63	52.00	1.96E-05	Putative ethylene-responsive element binding protein = *Salvia miltiorrhiza*
	P28186	310.18	231.00	4.28E-04	Ras-related protein ARA-3, ARA-3 At3g46060 F12M12_30
	Q6RJ36	14.10	0.00	4.88E-04	Ethylene responsive factor 2 (Ethylene-binding protein), ERF2 = *Solanum lycopersicum*
	Q9SHE7	115.38	53.00	4.52E-04	Ubiquitin-NEDD8-like protein RUB1 [Cleaved into: Ubiquitin; NEDD8-like protein RUB1 (Ubiquitin-related protein 1) (AtRUB1)], RUB1 NEDD8 UBQ15 At1g31340 T19E23.13
	Q8W231	7.05	0.00	4.88E-04	Putative serine/threonine-specific protein kinase, CTR1 = *Pyrus communis*
	Q6V398	5.16	0.00	9.77E-04	EIL1 = *Petunia hybrida*
	O22174	17.04	0.00	1.95E-03	Ethylene-responsive transcription factor ERF008, ERF008 At2g23340 T20D16.3
Auxin					
	Enriched in fruit				
	Q940X7	172.31	1565.00	3.56E-91	RING-box protein 1a (At-Rbx1;1) (Protein RING of cullins 1) (RBX1-2) (RBX1a-At), RBX1A ROC1 At5g20570 F7C8.160
	P31414	0.00	16.00	2.91E-11	Pyrophosphate-energized vacuolar membrane proton pump 1 (Pyrophosphate-energized inorganic pyrophosphatase 1) (H(+)-PPase 1) (Vacuolar proton pyrophosphatase 1) (Vacuolar proton pyrophosphatase 3) = AVP1 AVP AVP-3 AVP3 At1g15690 F7H2.3
	B9RUW0	0.00	51.00	2.33E-10	Auxin-responsive protein IAA1 = *Ricinus communis*
	Q5ZF70	0.00	35.00	1.19E-07	Auxin resistance protein, axr2 = *Plantago major*
	D1MWZ6	69.44	228.00	4.33E-07	Auxin-repressed protein, CitAuR = *Citrullus lanatus*
	B9H0Z6	0.00	64.00	1.91E-06	SAUR family protein, SAUR29 = *Populus trichocarpa*
	D7M6D2	0.00	12.00	6.10E-05	Auxin efflux carrier family protein, ARALYDRAFT_486870
	Q9LTX2	0.00	6.00	9.77E-04	Transport inhibitor response 1-like protein (TIR1-like protein), At5g49980 K9P8.12
	Q9XEY3	18.15	54.00	3.66E-03	Nt-iaa4.3 deduced protein = *Nicotiana tabacum*
	Enriched in AZ				
	O04951	277.95	0.00	3.37E-80	Serine/threonine-protein phosphatase PP2A-5 catalytic subunit (Protein phosphatase 2A isoform 5), PP2A5 At1g69960 F20P5.30 T17F3.1
	B9HCL2	85.41	0.00	1.18E-38	Auxin influx carrier component, PtrAUX1 = *Populus trichocarpa*
	D9ZIM5	148.34	15.00	5.73E-35	ARF domain class transcription factor, IAA1 = Malus domestica
	B9H216	58.72	0.00	2.47E-32	F-box family protein, FBL5 = *Populus trichocarpa*
	Q9FHW7	608.18	207.00	5.50E-29	SKP1-like protein 1B (SKP1-like 2) (UFO-binding protein 2), SKP1B ASK2 UIP2 At5g42190 MJC20.30
	P46423	196.54	20.00	6.29E-26	Glutathione S-transferase (EC 2.5.1.18) (25 kDa auxin-binding protein) (GST class-phi) = *Hyoscyamus muticus*
	A5C819	39.24	0.00	2.65E-23	Putative uncharacterized protein = *Vitis vinifera*
	B9IGX9	82.93	19.00	4.48E-15	Auxin efflux carrier component. auxin transport protein = *Populus trichocarpa*

	Q1W389	52.41	0.00	9.09E-13	Auxin-regulated protein = *Striga asiatica*
	C0SU68	25.91	0.00	3.64E-12	Auxin influx carrier protein, ZeLAX1 = *Zinnia elegans*
	B9I233	118.51	7.00	5.52E-12	SAUR family protein, SAUR22 = *Populus trichocarpa*
	C0SU69	23.35	0.00	5.82E-11	Auxin influx carrier protein, ZeLAX2 = *Zinnia elegans*
	B9SHS8	27.30	0.00	2.91E-11	Auxin-induced protein 5NG4 = *Ricinus communis*
	Q949J8	21.61	0.00	4.66E-10	Putative auxin growth promotor protein = *Solanum lycopersicum*
	B9R824	27.77	0.00	1.16E-10	Auxin-induced protein 5NG4 = *Ricinus communis*
	C8CBW3	30.78	0.00	1.19E-07	Auxin/indole-3-acetic acid 3, IAA3 = *Solanum tuberosum*
	B9RQI4	16.08	0.00	3.81E-06	Auxin-responsive protein IAA27 = *Nicotiana tabacum*
	Q2LAJ3	10.63	1.00	4.65E-06	Auxin response factor 2, ARF2 = *Solanum lycopersicum*
	B9SN97	10.60	0.00	1.91E-06	Indole-3-acetic acid-amido synthetase GH3.3 = *Ricinus communis*
	P40691	15.20	0.00	6.10E-05	Auxin-induced protein PCNT115 = *Nicotiana tabacum*
	B9RJT7	5.24	0.00	9.77E-04	TRANSPORT INHIBITOR RESPONSE 1 protein = *Ricinus communis*
	Q9SHE7	115.38	53.00	4.52E-04	Ubiquitin-NEDD8-like protein RUB1 [Cleaved into: Ubiquitin; NEDD8-like protein RUB1 (Ubiquitin-related protein 1) (AtRUB1)], RUB1 NEDD8 UBQ15 At1g31340 T19E23.13
	D7SH69	9.66	3.00	1.32E-03	Whole genome shotgun sequence of line PN40024. Scaffold 0.assembly12x (Fragment) = *Vitis vinifera*
	B9S0L2	3.79	0.00	3.91E-03	Auxin response factor = *Ricinus communis*
	B9S1E4	2.70	0.00	1.95E-03	Auxin response factor = *Ricinus communis*
	D9IA29	2.69	0.00	1.95E-03	Auxin response factor 19, ARF19 = *Solanum lycopersicum*
	C7E4R3	4.01	0.00	7.81E-03	Transport inhibitor response 1, TIR1 = *Nicotiana tabacum*
Abscisic acid					
	Enriched in fruit				
	Q39026	0.00	45.00	4.44E-16	Mitogen-activated protein kinase 6 (AtMPK6) (MAP kinase 6), MPK6 At2g43790 F18O19.10
	Q944A7	0.00	29.00	2.27E-13	Probable serine/threonine-protein kinase At4g35230
	P43291	0.00	39.00	9.09E-13	Serine/threonine-protein kinase SRK2A (EC 2.7.11.1) (Arabidopsis protein SK1) (OST1-kinase-like 7) (SNF1-related kinase 2.4) (SnRK2.4), SRK2A ASK1 OSKL7 SNRK2.4 At1g10940 T19D16.14
	Q8RXD3	0.00	13.00	4.88E-04	E3 ubiquitin-protein ligase AIP2 (EC 6.3.2.-) (ABI3-interacting protein 2), AIP2 At5g20910 F22D1.80
	Q8LGH4	0.00	4.00	1.95E-03	Cullin-4 (AtCUL4), CUL4 At5g46210 MDE13.3
	B9SE77	59.10	447.00	4.33E-29	Abscisic stress ripening protein = *Ricinus communis*
	A0SE34	0.00	9.00	3.05E-05	9-cis-epoxycarotenoid dioxygenase 5, NCED5 = *Citrus clementina*
	B9S5U9	0.00	5.00	7.81E-03	Protein phosphatase 2c = *Ricinus communis*
	Q9MAM1	0.00	6.00	7.81E-03	CBL-interacting serine/threonine-protein kinase 9 (EC 2.7.11.1) (SNF1-related kinase 3.12) (SOS2-like protein kinase PKS6), CIPK9 PKS6 SnRK3.12 At1g01140 F6F3.28 T25K16.13
	Enriched in AZ				
	B9RNU7	1060.01	145.00	1.01E-205	Protein phosphatase 2c = *Ricinus communis*
	Q2TUW1	1196.07	20.74	0.00E+00	Abscisic stress ripening-like protein = *Glycine max*
	Q9ZUU4	235.29	5.00	1.24E-58	Ribonucleoprotein At2g37220. Chloroplastic, At2g37220 F3G5.1
	O80653	11.96	0.00	2.38E-07	At1g77180/T14N5_5 (Putative nuclear protein) (Putative uncharacterized protein At1g77180), At1g77180 T14N5.5

	P22240	74.35	0.00	1.86E-09	Abscisic acid and environmental stress-inducible protein TAS14 (Dehydrin TAS14) = *Solanum lycopersicum*
	A9QNE7	9.10	0.00	1.22E-04	ABA 8'-hydroxylase, CYP707A1 = *Solanum lycopersicum*
	B9SVA1	93.10	13.00	6.79E-25	Dihydrolipoamide succinyltransferase component of 2-oxoglutarate dehydrogenase = *Ricinus communis*
	Q9M3V1	6.45	0.00	3.91E-03	Protein phpsphatase 2C (PP2C), pp2C1 = Fagus sylvatica
	B9RK51	7.44	0.00	2.44E-04	Protein phosphatase 2c = *Ricinus communis*
	B9RVV7	18.84	0.00	1.53E-05	Protein phosphatase 2c = *Ricinus communis*
	B9R8Q9	22.39	0.00	1.49E-08	Protein phosphatase 2c = *Ricinus communis*
	C8KHU4	36.94	0.00	1.42E-14	Protein phosphatase 2C AHG3 homolog, SlPP2C-2 = *Solanum lycopersicum*
	B9RJK5	94.22	0.00	2.07E-25	Protein phosphatase 2c putative = *Ricinus communis*
	Q5PNS9	120.83	0.00	1.40E-45	Probable protein phosphatase 2C 64 (AtPP2C64) (EC 3.1.3.16)
	Q9FKX4	129.00	0.00	8.76E-47	Probable protein phosphatase 2C 79 (AtPP2C79), At5g66080 K2A18.16
	C8KHU3	93.75	0.00	5.47E-48	Protein phosphatase 2C ABI2 homolog, SlPP2C-1 = *Solanum lycopersicum*
Jasmonate					
	Enriched in fruit				
	B9SG47	0.00	43.00	5,82E-11	Sigma factor sigb regulation protein rsbq (methyl esterase activity, MES: methyl jasmonate (MeJA) esterase activity , methyl salicylate (MeSA) esterase activity and methyl indole-3-acetate (MeIAA) esterase activity)
	O24370	0	161.29	4,16E-123	Lipoxygenase = *Solanum tuberosum*
	Q39026	0.00	45.00	4.44E-16	Mitogen-activated protein kinase 6 (AtMPK6) (MAP kinase 6), MPK6 At2g43790 F18O19.10
	Enriched in AZ				
	B9SEM5	12.91	0.00	9,77E-04	Acyl-protein thioesterase (methyl indole-3-acetate esterase activity; methyl jasmonate esterase activity; methyl salicylate esterase activity) = *Ricinus communis*
	Q8S8S9	16.47	0.00	1,22E-04	At2g23620 (Putative acetone-cyanohydrin lyase), methyl indole-3-acetate esterase activity; methyl jasmonate esterase activity; methyl salicylate esterase activity; systemic acquired resistance
	Q8LAH7	341.39	0.00	4.96E-119	12-oxophytodienoate reductase 1 (12-oxophytodienoate-10.11-reductase 1) (AtOPR1) (OPDA-reductase 1) (FS-AT-I), OPR1 At1g76680 F28O16.5
	B9RRB8	83.54	5.00	1,38E-24	12-oxophytodienoate reductase opr = *Ricinus communis*
	B6D1W5	44.75	16.00	5,70E-11	Lipoxygenase = *Olea europaea*
	O24371	18.23	0.00	4,44E-16	Lipoxygenase =*Solanum tuberosum*
	Q9M464	13.10	0.00	4,77E-07	Allene oxide synthase AOS = *Solanum lycopersicum*
	Q9SQK8	22.49	0.00	2.38E-07	Jasmonic acid 3, LEJA3 = *Solanum lycopersicum*
	D8V3L7	112.67	7.00	5.01E-24	Plastid jasmonates ZIM-domain protein = *Hevea brasiliensis*
	A7XXZ0	26.45	0.00	9.54E-07	Jasmonate ZIM-domain protein = *Solanum lycopersicum*
	B0VXR3	21.26	0.00	3.64E-12	JAR1-like protein, JAR6 = *Nicotiana attenuata*
	A6NAB4	4.93	0.00	1.95E-03	Myc2 bHLH protein = *Vitis vinifera*
Cytokinins					
	Enriched in fruit				

	D7TDN8	0.00	5.00	1.95E-03	cytokinin dehydrogenase = *Vitis vinifera*
	Enriched in AZ				
	Q3ECF7	8.05	0.00	4.88E-04	Uncharacterized protein, At1g69040
Polyamine					
	Enriched in fruit				
	Q8GTQ5	0.00	12.00	4.88E-04	Spermidine synthase, MdSPDS2a = *Malus domestica*
	Enriched in AZ				
	B9SIY7	142.06	0.00	5.47E-48	S-adenosylmethionine decarboxylase proenzyme = *Ricinus communis*
	A5AFT0	133.33	0.00	2.80E-45	S-adenosylmethionine decarboxylase proenzyme = *Vitis vinifera*
	B9RT51	20.33	4.00	1.38E-06	Protein arginine n-methyltransferase = *Ricinus communis*
	B3Y023	337.01	6.00	1.24E-210	Arginine decarboxylase, PpADC = *Prunus persica*
	D2K8S6	52.42	0.00	5.55E-17	Spermidine synthase = *Olea europaea*
Brassinosteroid					
	Enriched in fruit				
	B9RI66	0.00	51.00	3.61E-34	BRASSINOSTEROID INSENSITIVE 1-associated receptor kinase 1 = *Ricinus communis*
	Q944A7	0.00	29.00	2.27E-13	Probable serine/threonine-protein kinase At4g35230
	Enriched in AZ				
	Q39011	252.63	75.00	7.52E-31	Shaggy-related protein kinase eta (ASK-eta) (Protein BRASSINOSTEROID INSENSITIVE 2) (Protein ULTRACURVATA 1), ASK7 BIN2 DWF12 UCU1 At4g18710 F28A21.120
	B9S318	11.61	0.00	9.77E-04	Brassinosteroid-regulated protein BRU1 = *Ricinus communis*
	B9RAQ8	5.79	0.00	4.88E-04	BRASSINOSTEROID INSENSITIVE 1-associated receptor kinase 1 = *Ricinus communis*
Salicylic acid					
	Enriched in AZ				
	Q8H6W0	35.33	3.00	2.44E-17	Phenylalanine ammonia-lyase, PAL1 = *Coffea canephora*
	O23924	7.01	0.00	3.05E-05	Phenylalanine ammonia-lyase = *Digitalis lanata*
	Q6RYA0	584.61	51.00	1.32E-98	Salicylic acid-binding protein 2 = *Nicotiana tabacum*
	Q9FGY9	3.69	0.00	3.91E-03	Peptide-N(4)-(N-acetyl-beta-glucosaminyl)asparagine amidase (Peptide:N-glycanase) (AtPNG1), PNG1 At5g49570 K6M13.12
	Q8S8S9	16.47	0.00	1.22E-04	At2g23620 (Putative acetone-cyanohydrin lyase) = At2g23620
	B9H966	12.47	0.00	3.81E-06	BOP/NPR1/NIM1-like regulatory protein = *Populus trichocarpa*
	B9S3I0	12.42	0.00	2.38E-07	Regulatory protein NPR1 = *Ricinus communis*
Gibberellin					
	Enriched in fruit				
	Q9SLQ9	0.00	139.00	1.06E-43	Gibberellin 3beta-hydroxylase, Nty = *Nicotiana tabacum*
	B9SME4	0.00	77.00	1.29E-26	Gibberellin 20-oxidase = *Ricinus communis*
	Q42698	0.00	58.00	8.67E-19	Geranylgeranyl pyrophosphate synthase. chloroplastic (GGPP synthase) (GGPS) ((2E.6E)-farnesyl diphosphate synthase) (Dimethylallyltranstransferase) (Farnesyl diphosphate synthase) (Farnesyltranstransferase) (Geranyltranstransferase), GGPS1 GGC1 = *Catharanthus roseus*
	Q1ZYL0	0.00	19.00	2.98E-08	Geranylgeranyl reductase = *Olea europaea*

Enriched in AZ				
Q8S4W7	35.59	19.00	4.90E-04	DELLA protein GAI1 (Gibberellic acid-insensitive mutant protein 1) (VvGAI1), GAI1 = *Vitis vinifera*
B9SST2	9.29	0.00	3.05E-05	Chitin-inducible gibberellin-responsive protein = *Ricinus communis*
C6GMF4	18.07	0.00	3.81E-06	Gibberellin 2-oxidase, gao = *Nicotiana plumbaginifolia*
A4URE9	27.21	0.00	3.73E-09	Gibberellin 2-oxidase 5, GA2ox5 = *Nicotiana tabacum*
B9S2K0	92.06	0.00	1.86E-09	Gibberellin-regulated protein 3 = *Ricinus communis*
B9S2N0	17.29	0.00	1.86E-09	Chitin-inducible gibberellin-responsive protein = *Ricinus communis*
B9SFJ8	238.64	0.00	3.45E-77	Gibberellin receptor GID1 = *Ricinus communis*
Q1A7S9	12.85	3.00	7.54E-03	Geranylgeranyl pyrophosphate synthase 2, GGPS2 = *Solanum lycopersicum*
B9SVW8	12.78	0.00	1.53E-05	Geranylgeranyl pyrophosphate synthase = *Ricinus communis*
Q9SFB0	91.25	0.00	2.80E-45	MATE efflux family protein FRD3 (MATE citrate transporter) (Protein DTX43) (Protein FERRIC REDUCTASE DEFECTIVE 3) (AtFRD3) (Protein MANGANESE ACCUMULATOR 1), FRD3 DTX43 MAN1 At3g08040 F17A17.38 T8G24.8

Table 3.I.S3. Fruit- or AZ-enriched genes encoding various vesicle trafficking proteins at the last stage of olive fruit ripening. Sequences were selected after establishing a P<0.01. The table shows the total read count in RPKMx1000 for each gene after normalization across the two samples: fruit-pericarp and their AZ at 217 DPA.

	Uniprot ID	ZA	Fruit	P value	Putative ortholog	Description
Tubulin family						
	Enriched in fruit					
	D7TVZ8	0.00	203.53	6.32E^{-59}	AT5G12250.1, TUB6	Tubulin = *Vitis vinifera*
	Q3EA24	0.00	41.37	4.44E^{-16}	AT4G14960.1, TUA6	AT4G14960 protein
	B9S382	22.01	949.23	0.00E^{+00}	AT5G23860.2, TUB8	Tubulin beta chain = *Ricinus communis*
	P29512	180.74	1812.59	0.00E^{+00}	AT5G62700.1, TUB3	Tubulin beta-2/beta-3 chain. TUBB2 TUB2 At5g62690 MRG21.11; TUBB3 TUB3 At5g62700 MRG21.12
	Enriched in AZ					
	E0CNV2	6.75	0.00	3.91E^{-03}	AT1G50010.1, TUA2	Tubulin = *Vitis vinifera*
	B9SB77	41.06	0.00	2.22E^{-16}	AT5G12250.1, TUB6	Tubulin beta chain = *Ricinus communis*
Actin family						
	Enriched in fruit					
	B9SXZ4	0.00	47.22	1.16E^{-10}	AT3G53750.1, ACT3	Actin = Ricinus communis
	P53496	0.00	7.95	3.91E^{-03}	AT3G12110.1, ACT11	Actin-11. ACT11 At3g12110 T21B14.7 T23B7.5 T21B14_108
	D7U423	285.13	834.96	1.85E^{-64}	AT5G09810.1, ACT7	Actin = *Vitis vinifera*
	Enriched in AZ					
	D7SMF4	27.92	0.00	1.16E^{-10}	AT1G13180.1, DIS1, ARP3, ATARP3	Actin = *Vitis vinifera*
	B9RR79	84.21	0.00	3.16E^{-30}	AT5G09810.1, ACT7	Actin = *Ricinus communis*
Kinesin-like protein family						
	Enriched in fruit					
	B9RB32	0.00	21.29	7.11E^{-15}	AT1G27500.1, KLCR3	Kinesin light chain = *Ricinus communis*
Small GTPase superfamily. RAB family						
	Enriched in fruit					

D7T2X5	0.00	1244.83	2.22E-235	AT5G47960.1 ATRABA4D, RABA4D, RAB GTPase homolog A4D	RAB GTPase = *Vitis vinifera*
A9PCE2	0.00	62.01	3.64E-12	AT1G09630.1, ATRAB11C, ATRABA2A, ATRAB-A2A, RAB-A2A, RAB11c, RAB	RAB GTPase = *Populus trichocarpa*
D7U0K6	0.00	35.17	9.54E-07	AT5G45130.1, ATRAB5A, ATRABF2A, RABF2A, RAB5A, RHA1, ATRAB-F2A	RAB GTPase = *Vitis vinifera*
B9RRP3	0.00	20.74	1.22E-04	AT4G19640.1, ARA7, ARA-7, ATRABF2B, ATRAB5B, RABF2B, ATRAB-F2B,RAB-F2B, Ras-related small GTP-binding family protein	RAB GTPase = *Ricinus communis*
D7SJ99	0.00	21.40	1.22E-04	AT1G18200.1, AtRABA6b, RABA6b (RabH)	RAB GTPase = *Vitis vinifera*
B9N9L9	0.00	16.89	9.77E-04	AT5G60860.1, AtRABA1f, RABA1f, RAB GTPase homolog A1F	RAB GTPase = *Populus trichocarpa*
B9IQR9	13.88	254.62	4.73E-35	AT3G15060.1, AtRABA1g, RABA1g,RAB GTPase homolog A1G	RAB GTPase = *Populus trichocarpa*
A5BGY6	4.42	63.42	4.62E-10	AT5G65270.1,AtRABA4a, RABA4a,RAB GTPase homolog A4A	RAB GTPase = *Vitis vinifera*
C0LSK7	73.57	724.47	4.71E-164	AT3G59920.1, ATGDI2, GDI2, RAB GDP dissociation inhibitor 2	Rab GDP dissociation inhibitor. GDI = *Nicotiana benthamiana*
Q38922	14.21	110.58	9.71E-12	AT4G35860.1, ATRABB1B, ATGB2, ATRAB2C, GB2,GTP-binding 2	ATGB2 (GTP-binding protein GB2) (Putative GTP-binding protein GB2). AT4g35860
P28188	37.76	259.44	1.25E-23	AT1G02130.1, ATRAB1B, ARA5, ARA-5, ATRABD2A, RABD2A	Ras-related protein RABD2A (Ras-related protein ARA-5) (Ras-related protein RAB1B) (AtRab1b). RABD2A ARA-5 RAB1B At1g02130 T7I23.6
P92963	30.01	165.87	5.82E-14	AT4G17170.1, AT-RAB2, ATRABB1C, ATRAB2A, RAB2A, RABB1C, ATRAB-B1B,	At4g17170 (GTP-binding RAB2A like protein) (Rab2-like protein). rab2 A T4g17170 dl4620c At4g17170

O80501	30.44	128.20	2.87E-09	AT2G44610.1, RAB6, ATRABH1B, ATRAB6A, RAB6A	Ras-related protein RABH1B. RABH1B RAB6A At2g44610 F16B22.10
B9MUT7	198.68	384.23	1.53E-07	AT1G02130.1, ATRAB1B, ARA5, ARA-5, ATRABD2A, RABD2A,	RAB GTPase = *Populus trichocarpa*
Enriched in AZ					
P28186	310.18	231.48	4.28E-04	AT3G46060.3, ARA3, RAB GTPase homolog 8A (RAB E)	Ras-related protein ARA-3. ARA-3 At3g46060 F12M12_30
D7TQ04	106.71	55.33	9.65E-05	AT3G18820.1, ATRABG3F, ATRAB7B, RAB71, RABG3F, RAB7B	RAB GTPase = *Vitis vinifera*
B9HUI6	175.78	71.31	6.47E-09	AT3G54840.1, ARA6, ATRABF1, ARA-6, ATRAB5C	RAB GTPase = *Populus trichocarpa*
Q01111	90.21	21.40	8.40E-09	AT1G06400.1, ARA9	Ras-related protein YPT3 = *Nicotiana plumbaginifolia*
A5C9K9	15.50	0.00	9.77E-04	AT2G43130.1, ARA4	RAB GTPase = *Vitis vinifera*
Q43463	40.45	0.00	2.98E-08	AT4G09720.1, ATRABG3A	Ras-related protein Rab7 = Glycine max
O04486	46.08	0.00	9.31E-10	AT1G09630.1, ATRAB11C, ATRABA2a	Ras-related protein RABA2a (Ras-related protein Rab11C). RABA2A RAB11C At1g09630
D7TIU1	50.55	0.00	1.16E-10	AT5G03530.1, ATRAB ALPHA, ATRAB, ATRAB18B, ATRABC2A, RABC2A, RAB GTPase homolog C2A	RAB GTPase = *Vitis vinifera*
A5AR55	62.98	0.00	2.27E-13	AT1G07410.1, ATRABA2B, RAB-A2B, ATRAB-A2B, RABA2b	RAB GTPase = *Vitis vinifera*
A9PC79	117.11	0.00	6.84E-49	AT2G44100.1, ATGDI1, AT-GDI1, GDI1, guanosine nucleotide diphosphate dissociation inhibitor 1	RAB GTPase = *Populus trichocarpa*
Small GTPase superfamily. ARF-like GTPase family					
Enriched in fruit					
P51824	0.00	79.52	2.84217 1E-14	AT5G14670.1, ATARFA1B, ARFA1B, ADP-ribosylation factor A1B	ADP-ribosylation factor 1 = *Solanum tuberosum*

Small GTPase superfamily. RAN family

Enriched in AZ					
P54765	14.35	0.00	1.95E-03	AT5G55190.1, RAN3, ATRAN3, RAN GTPase 3	GTP-binding nuclear protein Ran1 = *Lotus japonicus*

Small GTPase superfamily. Rho GTPase family

Enriched in fruit					
Q38912	0.00	106.06	4.336809E-19	AT4G35020.3, RAC3	Rac-like GTP-binding protein ARAC3 (GTPase protein ROP6). ARAC3 RAC1 ROP6 At4g35020 M4E13.80
Enriched in AZ					
D7U1Z9	102.82	2.92	1.515424E-59	AT5G27540.2, MIRO1	Mitochondrial Rho GTPase = *Vitis vinifera*
Q6EP31	213.19	0.00	7.34684E-40	AT1G75840.1, ARAC5, ATGP3,	Rac-like GTP-binding protein 5 (GTPase protein RacD) (OsRac5) = *Oryza sativa*

Small GTPase superfamily. SAR1 family

Enriched in fruit					
O04834	407.59	1017.27	2.92844E-29	AT4G02080.1, ASAR1, ATSARA1C, ATSAR2, SAR2	GTP-binding protein SAR1A. SAR1A At4g02080 T10M13.9 AGAA.4

Dynamin family

Enriched in fruit					
B9MVC5	0.00	17.51	2.33E-10	AT3G60190.1, ADL4, ADLP2, EDR3, DRP1E, ADL1E, DL1E	Dynamin = *Populus trichocarpa*
Enriched in AZ					
B9SRI2	11.32	0.00	1.49E-08	AT3G19720.1, ARC5, DRP5B	Dynamin = *Ricinus communis*
D7TGM4	10.14	0.00	3.73E-09	AT1G59610.1, ADL3, CF1, DRP2B, DL3	Dynamin = *Vitis vinifera*
D7SN01	12.88	0.00	7.28E-12	AT1G10290.1, ADL6, DRP2A	Dynamin = *Vitis vinifera*
D7U670	17.69	0.00	8.88E-16	AT4G33650.1, ADL2, DRP3A	Dynamin = *Vitis vinifera*

	A5CA51	32.22	0.00	2.17E-19	AT3G60190.1, ADL4, ADLP2, EDR3, DRP1E, ADL1E, DL1E	Dynamin = *Vitis vinifera*
V-type ATPase family						
	Enriched in fruit					
	D7SX66	0.00	25.13	2.38E-07	AT3G28715.1, ATPase, V0/A0 complex, subunit C/D	V-type ATPase = *Vitis vinifera*
	Q9FLN5	28.57	147.61	4.13E-05	AT5G55290.2, ATPase, V0 complex, subunit E	AT5G55290 protein (AT5g55290/MCO15_24) (Genomic DNA. chromosome 5. P1 clone :MCO15) AT5G55290 At5g55290 AT5G55290 At5g55290
	P59227	516.26	1674.79	3.12E-60	AT4G34720.1, VHA-C1 AVA-P1 AVAP1 At4g34720	V-type proton ATPase 16 kDa proteolipid subunit c1/c3/c5 (V-ATPase 16 kDa proteolipid subunit c1/c3/c5) (Vacuolar H(+)-ATPase subunit c isoform 1/3/5) (Vacuolar proton pump 16 kDa proteolipid subunit c1/c3/c5)
	Q9SZY7	57.40	120.37	2.88E-03	T4L20.300; VHA-C3 AVA-P1, VHA-C1, ATVHA-C1	H+-transporting ATPase-like protein (Vacuolar membrane ATPase subunit c")
	D7T7L1	40.02	69.70	4.16E-03	AT3G42050.1, Vacuolar-ATP-synthase subunit H family protein	V-type ATPase = *Vitis vinifera*
	Enriched in AZ					
	D7SS06	252.00	190.47	1.48E-07	AT1G78900.2, VHA-A, vacuolar-	V-type ATPase = *Vitis vinifera*
	Q6KAA4	117.94	35.89	7.67E-06	AT4G02620.1, vacuolar ATPase subunit F family protein	V-type proton ATPase subunit F = *Oryza sativa*

	Q9LJI5	494.77	50.33	6.20E-107	AT3G28710.1, ATPase, V0/A0 complex, subunit C/D	V-type proton ATPase subunit d1 (V-ATPase subunit d1) (Vacuolar H(+)-ATPase subunit d. VHA-D1 At3g28710 MZN14.21
	Q9LX65	7.55	0.00	9.77E-04	AT3G42050.1, Vacuolar-ATP-synthase subunit H family protein	V-type proton ATPase subunit H (V-ATPase subunit H) (Vacuolar H(+)-ATPase subunit H) (Vacuolar proton pump subunit H). VHA-H At3g42050 F4M19_10
	B9S253	48.57	0.00	6.78E-21	AT3G42050.1, vacuolar ATP synthase subunit H family protein	Vacuolar ATP synthase subunit h = *Ricinus communis*
	Q8RU33	242.16	0.00	6.75E-80	AT3G28715.1, ATPase, V0/A0 complex, subunit C/D	Probable V-type proton ATPase subunit d (V-ATPase subunit d) (Vacuolar proton pump subunit d) = *Oryza sativa*
Syntaxin/ t-SNARE family						
	Enriched in fruit					
	D7U8L0	0.00	13.02	4.88E-04	AT5G08080.1, SYP132,ATSYP132 syntaxin of plants 132	Syntaxin = *Vitis vinifera*
	B9SUS4	0.00	8.65	7.81E-03	AT5G08080.1, SYP132,ATSYP132 syntaxin of plants 132	Syntaxin = *Ricinus communis*
	Enriched in AZ					
	B9T2S1	243.53	108.06	7.08E-11	AT5G06320.1, NHL3, NDR1/HIN1-	Syntaxin = *Ricinus communis*
	B9MU58	26.76	0.00	2.38E-07	AT5G46860.1, VAM3, ATVAM3, SYP22, ATSYP22, SGR3,	Syntaxin = *Populus trichocarpa*

					AT3G11820.1, SYP121,	
	B9SDJ9	136.07	0.00	9.18E-41	AT-SYR1,ATSYP121, SYR1, ATSYR1, PEN1, syntaxin	Syntaxin = *Ricinus communis*
Others families						
	B9S5U3	0.50	0.00	3.91E-03		Midasin = *Ricinus communis*
	Q9SUT9	44.28	0.00	7.28E-12	At4g11220 F8L21.10	Reticulon-like protein B2 (AtRTNLB2) (VirB2-interacting protein 2). RTNLB2 BTI2 At4g11220 F8L21.10

Table 3.I.S4. Fruit- or AZ-enriched genes encoding various transport proteins at the last stage of olive fruit ripening. Sequences were selected after establishing a P<0.01. The table shows the total read count in RPKMx1000 for each gene after normalization across the two samples: fruit-pericarp and their AZ at 217 DPA.

	Uniprot ID	ZA	Fruit	P value	Description
Sugar transporter					
	D7SH34	0.00	696.00	1,50E-158	Sugar transporter= *Vitis vinifera*
	D7UDD8	0.00	185.00	1,10E-103	Major facilitator superfamily, Sugar transporter family = *Vitis vinifera*
	Q3E6T0	0.00	156.00	4,38E-46	Probable sugar phosphate/phosphate translocator At5g25400
	B9SJK9	0.00	102.00	1,06E-22	Sugar transporter = *Ricinus communis*
	D7U4Q9	0.00	56.00	6,94E-18	Sugar transporter = *Vitis vinifera*
	B9SBS6	0.00	43.00	5,68E-14	CMP-sialic acid transporter = *Ricinus communis*
	B9RM94	3.68	71.00	9,08E-13	Sugar transporter = *Ricinus communis*
	B9R8S3	51.87	470.00	4,59E-170	Sugar transporter = *Ricinus communis*
	Q68BJ8	285.36	386.00	5,01E-04	Sorbitol transporter = *Malus domestica*
	D7TBL1	17.08	2.00	1,52E-05	Monosaccharide transporter = *Vitis vinifera*
	B9RP33	6.55	0.00	7,81E-03	UDP-sugar transporter = *Ricinus communis*
	B9RTN4	4.52	0.00	7,81E-03	Sugar transporter = *Ricinus communis*
	Q9SX48	4.51	0.00	7,81E-03	Sugar transport protein 9 (Hexose transporter 9) STP9 At1g50310 F14I3.9
	D7TJV0	11.49	0.00	3,91E-03	Sugar transporter = *Vitis vinifera*
	Q9SBA7	6.57	0.00	9,77E-04	Sugar transport protein 8 (Hexose transporter 8) STP8 At5g26250 F9D12.9 T19G15.100
	D7T6L7	8.37	0.00	4,88E-04	ERD6-like transporter = *Vitis vinifera*
	Q94EI9	11.76	0.00	2,44E-04	Sugar phosphate/phosphate translocator At3g14410
	Q07423	9.8	0.00	3,05E-05	Hexose carrier protein HEX6 = *Ricinus communis*
	B9RTZ7	45.28	0.00	5,29E-23	Sugar transporter = *Ricinus communis*
	B9SZL0	85.85	0.00	1,84E-40	Sugar transporter = *Ricinus communis*
	B9RZB4	192.95	0.00	2,34E-97	Sugar transporter= *Ricinus communis*
N transporter					
	D7U9B7	0.00	115.00	2,69E-101	Oligopeptide transporter = *Vitis vinifera*
	D7TNF6	0.00	70.00	1,50E-36	Oligopeptide transporter = *Vitis vinifera*
	A5C8T7	0.00	44.00	5,29E-23	Oligopeptide transporter = *Vitis vinifera*
	D7U9C1	0.00	19.00	7,28E-12	Oligopeptide transporter = *Vitis vinifera*
	D7T4G2	0.00	12.00	9,54E-07	Oligopeptide transporter = *Vitis vinifera*
	D7SLW7	0.00	7.00	2,44E-04	Oligopeptide transporter = *Vitis vinifera*
	O80436	0.00	7.00	9,77E-04	Peptide/nitrate transporter At2g38100
	D7U9B1	1.39	69.00	3,33E-112	Oligopeptide transporter = *Vitis vinifera*
	B9SM54	6.45	23.00	1,45E-03	Amino acid transporter = *Ricinus communis*

	D7T9Q9	14.25	45.00	9,74E-08	Amino acid transporter = *Vitis vinifera*
	B9S4A3	23.65	61.00	3,30E-05	Amino acid transporter = *Ricinus communis*
	D7TL72	17.23	9.00	9,40E-03	Amino acid transporter = *Vitis vinifera*
	Q9ZTX4	42.53	4.00	8,45E-17	Oligopeptide transporter, LeOPT1 = *Solanum lycopersicum*
	B9RBN4	103.03	8.00	9,43E-31	Amino acid transporter = *Ricinus communis*
	D7TJT3	1.86	0.00	7,81E-03	Oligopeptide transporter = *Vitis vinifera*
	B9RD13	4.69	0.00	3,91E-03	Cationic amino acid transporter = *Ricinus communis*
	B9S4A2	6.06	0.00	3,91E-03	Amino acid transporter = *Ricinus communis*
	B9T755	2.35	0.00	3,91E-03	Peptide transporter = *Ricinus communis*
	Q9SRK7	5.76	0.00	9,77E-04	Adenine/guanine permease AZG1 (AzgA-homolog protein) (Protein AZAGUANINE RESISTANT 1) (AtAzg1), AZG1
	B9S1L4	7.54	0.00	4,88E-04	Amino acid transporter = *Ricinus communis*
	D7T9A4	4.14	0.00	4,88E-04	Oligopeptide transporter = *Vitis vinifera*
	Q9LFX9	6.94	0.00	2,44E-04	Nitrate transporter 1.6
	B9RYS3	6.14	0.00	6,10E-05	Oligopeptide transporter = *Ricinus communis*
	B9SI71	8.81	0.00	7,63E-06	Cationic amino acid transporter = *Ricinus communis*
	B9SKU5	10.22	0.00	3,81E-06	Cationic amino acid transporter = Ricinus communis
	Q9ZPR7	18.80	0.00	2,38E-07	Ureide permease 1 (AtUPS1), UPS1 At2g03590 F19B11.4
	B9RPK4	11.43	0.00	1,19E-07	Oligopeptide transporter = *Ricinus communis*
	A5BUN8	13.76	0.00	1,49E-08	Oligopeptide transporter = *Vitis vinifera*
	B9RAN2	18.32	0.00	9,31E-10	Purine permease = *Ricinus communis*
	B9SJX4	18.94	0.00	9,31E-10	GABA-specific permease = *Ricinus communis*
	Q7XAK5	19.57	0.00	1,46E-11	Nitrate transporter = *Prunus persica*
	B9R7I7	23.11	0.00	1,82E-12	Purine permease = *Ricinus communis*
	B9T6M4	13.08	0.00	2,84E-14	Peptide transporter= *Ricinus communis*
	B9S275	41.31	0.00	3,23E-27	Oligopeptide transporter = *Ricinus communis*
	D7SZL3	54.05	0.00	1,58E-30	Oligopeptide transporter = *Vitis vinifera*
	B9R934	162.79	0.00	6,14E-92	Nitrate transporter = *Ricinus communis*
	D7SIH4	110.16	0.00	8,52E-109	Oligopeptide transporter = *Vitis vinifera*
Aquaporin					
	Q08733	0.00	61.00	8,88E-16	Aquaporin PIP1-3 (AtPIP1;3) (Plasma membrane intrinsic protein 1c) (PIP1c) (TMP-B), PIP1-3 PIP1C TMPB At1g01620
	B9RS20	0.00	38.00	7,45E-09	Tonoplast intrinsic protein, MIP/aquaporin family = *Ricinus communis*
	C5IX25	16.61	225.00	2,30E-37	Plasma intrinsic protein 2;5, MIP/aquaporin family = Juglans regia
	Q0MX13	26.28	319.00	3,33E-50	Aquaporin PIP2;2 = *Vitis vinifera*
	A9P9G2	148.45	729.00	4,38E-61	Aquaporin, MIP family, TIP subfamily = *Populus trichocarpa*

	C5IX20	27.87	84.00	1,18E-05	Plasma intrinsic protein 1;1, MIP/aquaporin family = *Juglans regia*
	B5KGP0	361.00	181.00	1,07E-13	Small basic intrinsic protein 1-2, MIP/aquaporin family = *Olea europaea*
	B9S0M0	84.49	36.00	5,05E-06	Aquaporin PIP2.2 = *Ricinus communis*
	A9PFE8	8.13	0.00	7,81E-03	Aquaporin, MIP family, PIP subfamily = *Populus trichocarpa*
	Q9AVB3	60.39	0.00	1,11E-16	Plasma membrane intrinsic protein 2-2, Py-PIP2-2 = *Pyrus communis*
	C8CE50	117.24	0.00	2,47E-32	Aquaporin, PIP1;1 = *Fragaria ananassa*
ABC transporter					
	B9RUV8	0.00	35.00	1,06E-22	ATP-dependent transporter, ABC transporter = *Ricinus communis*
	B9N856	125.69	203.00	3,07E-06	ABC transporter family protein = *Populus trichocarpa*
	B9R7N6	6.9	0.00	9,77E-04	Multidrug resistance pump = *Ricinus communis*
	B9RIN7	4.28	0.00	1,91E-06	Multidrug resistance-associated protein 1, 3 (Mrp1, 3), abc-transoprter = Ricinus communis
	B9R6R0	15.78	0.00	2,98E-08	Multidrug resistance pump = *Ricinus communis*
	B9S7S7	35.02	0.00	1,86E-09	Phosphate abc transporter = *Ricinus communis*
	B9T0A5	19.66	0.00	1,14E-13	ATP-binding cassette transporter = *Ricinus communis*
	D7UBX7	10.57	0.00	2,84E-14	ABC transporter = *Vitis vinifera*
	B9RXM4	67.97	0.00	6,16E-33	Multidrug resistance pump = *Ricinus communis*
	B9T6V3	71.92	0.00	6,16E-33	Multidrug resistance pump = *Ricinus communis*
	B9RXM3	71.09	0.00	1,54E-33	Multidrug resistance pump = *Ricinus communis*
	D7T9B7	122.29	0.00	1,73E-77	ABC transporter = *Vitis vinifera*
Metal transporter					
	A5C1P9	0.00	354.00	1,22E-92	Metal ion transporter= *Vitis vinifera*
	B9T4M0	0.00	111.00	9,18E-35	Urease accessory protein ureH = *Ricinus communis*
	B9RAC5	0.00	46.00	1,42E-14	Metal ion binding protein = *Ricinus communis*
	E0CUG6	0.00	136.00	1,14E-13	Metal ion transporter = *Vitis vinifera*
	D7TBR6	0.00	82.00	2,33E-10	Metal ion transporter = *Vitis vinifera*
	B9RFA4	0.00	10.00	9,77E-04	Chloroplast-targeted copper chaperone, Metal ion transporter = *Ricinus communis*
	D7SND2	0.00	9.00	7,81E-03	Metal ion transporter = *Vitis vinifera*
	A1YIQ6	16.19	150.00	5,93E-27	Zinc transporter = *Solanum lycopersicum*
	Q9FJH5	95.41	240.00	3,50E-11	At5g60800 (Gb|AAC98457.1) Metal ion transporter
	O82089	190.08	69.00	4,76E-07	AT3g56240/F18O21_200 (Copper homeostasis factor)
	D7TQQ5	184.54	57.00	3,91E-20	Metal ion transporter = *Vitis vinifera*
	A5C6S4	79.57	9.00	5,65E-08	Metal ion transporter = *Vitis vinifera*
	Q6R3K6	65.09	2.00	6,56E-37	Metal-nicotianamine transporter YSL6 (Protein YELLOW STRIPE LIKE 6) (AtYSL6), YSL6 At3g27020 MOJ10.9
	D7TV62	17.41	0.00	7,81E-03	Metal ion transporter = *Vitis vinifera*

	A5APE7	21.13	0.00	1,95E-03	Metal ion transporter = *Vitis vinifera*
	Q8RY06	6.91	0.00	1,95E-03	Metal ion transmembrane transporter At2g04305/T23O15.7
	D7T3V8	9.42	0.00	9,77E-04	Metal ion transporter = *Vitis vinifera*
	Q6R3L0	4.95	0.00	9,77E-04	Metal-nicotianamine transporter YSL1 (Protein YELLOW STRIPE LIKE 1) (AtYSL1), YSL1 At4g24120 T19F6.8
	A5BBJ4	13.00	0.00	4,88E-04	Metal ion transporter = *Vitis vinifera*
	D7T8F6	7.59	0.00	4,88E-04	Metal ion transporter = *Vitis vinifera*
	D7UCD8	22.36	0.00	4,88E-04	Metal ion transporter = *Vitis vinifera*
	B9TAG3	189.39	0.00	6,62E-24	Metal ion binding protein = *Ricinus communis*
Nutrient transporter					
	B9SIK0	0.00	350.00	1,67E-99	2-oxoglutarate/malate translocator, chloroplast = *Ricinus communis*
	Q9FMF7	0.00	198.00	3,92E-94	2-oxoglutarate/malate translocator (At5g64290) (Putative 2-oxoglutarate/malate translocator) (Putative 2-
	B9RID8	0.00	89.00	3,30E-42	2-oxoglutarate/malate translocator, chloroplast = *Ricinus communis*
	B9RUG9	0.00	37.00	8,88E-16	Cation efflux protein/ zinc transporter = *Ricinus communis*
	B9SH00	0.00	8.00	9,54E-07	Cation-transporting atpase plant = *Ricinus communis*
	Q8GWP3	0.00	44.00	3,81E-06	Copper transporter 6 (AtCOPT6), COPT6 At2g26975
	B9SJ59	0.00	7.00	2,44E-04	Sulfate transporter = *Ricinus communis*
	B9RR93	0.00	28.00	4,88E-04	Copper transporter = *Ricinus communis*
	B9RH84	138.90	358.00	9,13E-151	Phosphatidylinositol transporter = *Ricinus communis*
	B9T1L0	3.45	30.00	4,52E-15	Cation-transporting atpase plant = *Ricinus communis*
	B9RWZ4	1.86	10.00	4,13E-05	Cation-transporting atpase plant = *Ricinus communis*
	B9RUY1	12.93	30.00	6,22E-03	Sulfate transporter = *Ricinus communis*
	B9RWT3	17.93	3.00	6,62E-05	Ammonium transporter = *Ricinus communis*
	B9RHZ9	56.74	7.00	2,12E-13	Thiosulfate sulfertansferase = *Ricinus communis*
	B9STR6	17.23	2.00	3,11E-08	Cyclic nucleotide-gated ion channel = *Ricinus communis*
	B9R709	18.20	2.00	5,91E-12	Cation-transporting atpase plant = *Ricinus communis*
	B9S7C7	3.18	0.00	7,81E-03	Potassium transporter = *Ricinus communis*
	B9SCE3	2.33	0.00	7,81E-03	Copper-transporting atpase p-type = *Ricinus communis*
	Q9SYG9	5.18	0.00	9,77E-04	Cation/calcium exchanger 4 (AtCCX4) (Protein CATION CALCIUM EXCHANGER 4), CCX4 At1g54115 F15I1.21
	B9RKV6	3.61	0.00	4,88E-04	Cation-transporting atpase plant = *Ricinus communis*
	A8D009	17.81	0.00	6,10E-05	Ferritin = *Ricinus communis*
	B9SZW3	14.30	0.00	1,19E-07	Inorganic phosphate transporter = *Ricinus communis*
	Q93YH1	13.18	0.00	4,77E-07	Sodium/hydrogen exchanger, NHX2 = *Solanum lycopersicum*
	B9SI63	26.89	0.00	1,78E-15	Sodium/potassium/calcium exchanger 6 = *Ricinus communis*

B9RUZ6	24.88	0.00	4,44E-16	Boron transporter = *Ricinus communis*
Q1JRA3	31.66	0.00	2,22E-16	Sodium/hydrogen exchanger, NHX3 = *Solanum lycopersicum*
D0V1M5	34.08	0.00	1,39E-17	Sodium/hydrogen exchanger = *Vitis vinifera*
Q9SV13	30.9	0.00	2,17E-19	Sulfate transporter 3.1 (AST12) (AtST1), SULTR3;1 ST1 At3g51895 F4F15.10 ATEM1.15
B9RGU8	35.33	0.00	2,58E-26	Potassium transporter = *Ricinus communis*
B9SF53	62.81	0.00	4,93E-32	Inorganic phosphate transporter = *Ricinus communis*
B9SPI0	71.43	0.00	3,85E-34	Nitrate transporter = *Ricinus communis*
B9RIV7	70.92	0.00	9,40E-38	Arsenite transport protein = *Ricinus communis*
Q1L4E2	158.84	0.00	1,15E-41	Ferritin = *Malus domestica*
Q9SFB0	91.25	0.00	2,80E-45	MATE efflux family protein FRD3 (MATE citrate transporter) (Protein DTX43) (Protein FERRIC REDUCTASE DEFECTIVE 3) (AtFRD3) (Protein MANGANESE
B9SF95	614.34	0.00	7,75E-267	Nitrate transporter = *Ricinus communis*

Table 3.I.S5. PCR-primers used in this study.

Primer	Sequence	Gene (Uniprot ID)
ERF5-F	5'-TTCATCCAGCATCGGAGTAAC-3'	ERF5 (Q9SXS8)
ERF5-R	5'-GAGGGCTGTGCATGCAAGCTC-3'	
ERF4-F	5'-GTTAATGGAGTTAAGGATAAG -3'	ERF4 (Q9LW49)
ERF4-R	5'-TCAAGCTCAACCGGCGGTTG-3'	
SnRK2.4-F	5'-TACCGGAGAGAAAACCCAACC-3'	SnRK2.4 (P43291)
SnRK2.4-R	5'-TATGCCTCCCCAACCAAAGCC-3'	
NPR1-F	5'-CTGAATAATGTGTCATATCCG-3'	NPR1 (B9H966)
NPR1-R	5'-ATGCTCATTCTTTGTTAGTTG-3'	
JAR1-F	5'-AACATCGACAAGAATACGGAG-3'	JAR1 (B0VXR3)
JAR1-R	5'-GTCTAAACGGTTGCAGCATTC-3'	

Table 3.II.S1. Genes up-regulated in the fruit AZ treated with d18:0 compared with the control fruit AZ (first comparison, d18:0-AZ vs. C-AZ).

Formato (*.xlsx).

Table 3.II.S2. Genes down-regulated in the fruit AZ treated with d18:0 compared with the control fruit AZ (first comparison, 18:0-AZ vs. C-AZ).

Formato (*.xlsx).

Table 3II.S3. Genes up-regulated in the leaf AZ treated with d18:0 compared with the fruit AZ treated with d18:0 (2º comparison, d18:0-LAZ vs. d18:0-AZ).

Formato (*.xlsx).

Table 3II.S4. Genes down-regulated in the leaf AZ treated with d18:0 compared with the fruit AZ treated with d18:0 (2º comparison, d18:0-LAZ vs. d18:0-AZ).

Formato (*.xlsx).

Table 3.II.S5. Genes down-regulated in both the first and second comparisons.

Gene	log2FoldChange	pvalue	Gene_ID	Description
LOC111365331	2,52466779	4,06E-05	XP_022841563.1	putative late blight resistance protein homolog R1B-14 = *Olea europaea var. Sylvestris*
LOC111365332	1,136878629	2,07E-05	XP_022841564.1	putative late blight resistance protein homolog R1A-10 = *Olea europaea var. Sylvestris*
LOC111365353	1,670502278	1,56E-10	XP_022841608.1	pentatricopeptide repeat-containing protein At2g20540-like = *Olea europaea var. Sylvestris*
LOC111365358	3,8000555	8,58E-14	XP_022841616.1	uncharacterized LOC111365358 = *Olea europaea var. Sylvestris*
LOC111366215	3,168727093	0,002340176	-	uncharacterized LOC111366215 = *Olea europaea var. Sylvestris*
LOC111366237	1,060227012	1,17E-09	XP_022842719.1	uncharacterized LOC111366237 = *Olea europaea var. Sylvestris*
LOC111366302	1,531378335	6,66E-06	XP_022842802.1	protein WVD2-like 4 = *Olea europaea var. Sylvestris*
LOC111366500	2,81021448	2,51E-11	-	uncharacterized LOC111366500 = *Olea europaea var. Sylvestris*
LOC111366991	1,651249614	0,008722872	XP_022843436.1	dof zinc finger protein DOF5.6-like = *Olea europaea var. Sylvestris*
LOC111367154	1,106567393	2,03E-09	XP_022843651.1	auxin-responsive protein IAA27-like = *Olea europaea var. Sylvestris*
LOC111367558	1,499055774	4,66E-06	XP_022844263.1	15.7 kDa heat shock protein, peroxisomal = *Olea europaea var. Sylvestris*
LOC111367630	1,013266959	6,95E-05	XP_022844386.1	receptor-like serine/threonine-protein kinase ALE2 = *Olea europaea var. Sylvestris*
LOC111367858	1,865199768	2,77E-11	XP_022844704.1	uncharacterized LOC111367858 = *Olea europaea var. Sylvestris*
LOC111368046	1,435608951	3,82E-08	XP_022844984.1	transcription factor bHLH137-like = *Olea europaea var. Sylvestris*
LOC111368450	1,533835518	0,000675926	XP_022845437.1	E3 ubiquitin-protein ligase RHA1B-like = *Olea europaea var. Sylvestris*
LOC111369356	1,658879202	2,31E-15	XP_022846608.1	defensin-like protein P322 = *Olea europaea var. Sylvestris*
LOC111369486	1,317074372	0,004241118	XP_022846779.1	uncharacterized LOC111369486 = *Olea europaea var. Sylvestris*
LOC111369543	1,932117489	0,000282266	-	uncharacterized LOC111369543 = *Olea europaea var. Sylvestris*
LOC111370381	2,035333147	1,10E-20	XP_022847830.1	36.4 kDa proline-rich protein-like = *Olea europaea var. Sylvestris*
LOC111370418	2,156391159	6,28E-05	XP_022847876.1	BOI-related E3 ubiquitin-protein ligase 1-like = *Olea europaea var. Sylvestris*
LOC111370634	1,319751875	9,13E-06	XP_022848214.1	uncharacterized LOC111370634 = *Olea europaea var. Sylvestris*
LOC111370635	1,487981795	0,002478804	XP_022848216.1	uncharacterized LOC111370635 = *Olea europaea var. Sylvestris*
LOC111370745	1,718229009	0,003584937	XP_022848371.1	E3 ubiquitin-protein ligase At1g63170-like = *Olea europaea var. Sylvestris*
LOC111371515	2,947890651	4,53E-12	XP_022849319.1	uncharacterized LOC111371515 = *Olea europaea var. Sylvestris*
LOC111371536	6,884220433	2,30E-05	uncharacterized	uncharacterized
LOC111371759	1,424274426	0,000369714	XP_022849667.1	alcohol dehydrogenase-like 3 = *Olea europaea var. Sylvestris*
LOC111372046	2,848793059	0,000703899	XP_022849967.1	AP2-like ethylene-responsive transcription factor At1g16060 = *Olea europaea var. Sylvestris*
LOC111373919	1,115596838	0,006308008	XP_022852283.1	uncharacterized LOC111373919 = *Olea europaea var. Sylvestris*
LOC111374056	1,682219541	1,02E-07	XP_022852444.1	protein indeterminate-domain 1-like = *Olea europaea var. Sylvestris*
LOC111374059	1,455966823	1,35E-05	XP_022852449.1	protein BRASSINAZOLE-RESISTANT 1-like = *Olea europaea var. Sylvestris*
LOC111375465	1,204478371	0,000287711	XP_022854059.1	endoglucanase 6-like = *Olea europaea var. Sylvestris*
LOC111375943	1,463453823	0,000653666	XP_022854633.1	putative E3 ubiquitin-protein ligase XBAT31 = *Olea europaea var. Sylvestris*
LOC111376429	2,689696132	6,34E-07	XP_022855161.1	transcription factor MYB61-like = *Olea europaea var. Sylvestris*
LOC111376925	1,315355774	1,02E-05	XP_022855709.1	phosphoenolpyruvate carboxylase kinase 2-like = *Olea europaea var. Sylvestris*
LOC111377094	1,024821369	0,001660121	XP_022855909.1	very-long-chain enoyl-CoA reductase-like = *Olea europaea var. Sylvestris*
LOC111378041	1,458409369	0,000721231	XP_022856968.1	uncharacterized LOC111378041 = *Olea europaea var. Sylvestris*
LOC111378046	1,785327826	0,000939071	XP_022856975.1	beta-glucosidase-like = *Olea europaea var. Sylvestris*
LOC111378102	2,543174821	2,55E-05	-	PH, RCC1 and FYVE domains-containing protein 1-like = *Olea europaea var. Sylvestris*
LOC111378946	1,514995283	0,000169112	XP_022858013.1	cytokinin riboside 5-monophosphate phosphoribohydrolase LOG1-like = *Olea europaea var. Sylvestris*
LOC111378975	1,891882349	2,63E-07	XP_022858048.1	protein DETOXIFICATION 16-like = *Olea europaea var. Sylvestris*
LOC111379070	1,505745075	0,003245374	XP_022858163.1	ABC transporter G family member 25-like = *Olea europaea var. Sylvestris*
LOC111380186	1,10129491	0,003658854	XP_022859446.1	plastid division protein PDV1 = *Olea europaea var. Sylvestris*

LOC111380331	1,87921014	0,001205441	XP_022859627.1	uncharacterized LOC111380331 =*Olea europaea var. Sylvestris*
LOC111380489	1,940111245	1,05E-10	XP_022859839.1	thaumatin-like protein = *Olea europaea var. Sylvestris*
LOC111380683	1,51605244	1,98E-10	XP_022860081.1	beta-galactosidase 8 = *Olea europaea var. Sylvestris*
LOC111381574	1,456572839	0,001176442	XP_022861134.1	transcriptional activator DEMETER-like = *Olea europaea var. Sylvestris*
LOC111382617	1,289865588	0,003361191	XP_022862413.1	sulfite exporter TauE/SafE family protein 4-like = *Olea europaea var. Sylvestris*
LOC111383156	2,153182113	0,002660317	XP_022863002.1	uncharacterized LOC111383156 =*Olea europaea var. Sylvestris*
LOC111384577	1,016952233	0,005829921	-	uncharacterized protein LOC111384577 =*Olea europaea var. Sylvestris*
LOC111384671	1,938784795	1,91E-07	XP_022864754.1	expansin-A8-like = *Olea europaea var. Sylvestris*
LOC111385342	2,047686751	0,008068174	XP_022865492.1	expansin-A8-like = *Olea europaea var. Sylvestris*
LOC111385622	2,43015486	0,001287204	XP_022865804.1	dehydration-responsive element-binding protein 3-like = *Olea europaea var. Sylvestris*
LOC111386375	1,603780356	0,007952981	-	pectin acetylesterase 8-like = *Olea europaea var. Sylvestris*
LOC111386400	2,914133022	3,92E-04	XP_022866620.1	serine/threonine-protein kinase HT1-like = *Olea europaea var. Sylvestris*
LOC111386881	1,285769232	2,20E-09	XP_022867140.1	cytochrome P450 81D11-like =*Olea europaea var. Sylvestris*
LOC111387506	1,173903124	0,004583307	XP_022867836.1	SPX domain-containing protein 1-like = *Olea europaea var. Sylvestris*
LOC111387950	1,465294867	0,000931895	XP_022868351.1	TORTIFOLIA1-like protein 4 = *Olea europaea var. Sylvestris*
LOC111387965	1,118446835	2,63E-09	XP_022868377.1	protein NRT1/ PTR FAMILY 2.13 = *Olea europaea var. Sylvestris*
LOC111388105	1,78406392	1,97E-08	XP_022868534.1	3-ketoacyl-CoA synthase 10 = *Olea europaea var. Sylvestris*
LOC111388385	3,548762378	0,001771447	XP_022868836.1	myb-related protein 306-like = *Olea europaea var. Sylvestris*
LOC111388504	2,227164751	0,000231824	XP_022869005.1	purple acid phosphatase 2-like = *Olea europaea var. Sylvestris*
LOC111389898	1,164284555	2,79E-08	XP_022870649.1	uncharacterized LOC111389898 =*Olea europaea var. Sylvestris*
LOC111390411	2,199142543	0,005392266	uncharacterized	uncharacterized
LOC111390931	1,289828997	0,000955621	XP_022871823.1	peptide-N4-(N-acetyl-beta-glucosaminyl)asparagine amidase A-like = *Olea europaea var. Sylvestris*
LOC111391402	1,721991129	0,006985924	XP_022872384.1	protein NRT1/ PTR FAMILY 5.1-like = *Olea europaea var. Sylvestris*
LOC111392256	1,763986251	1,53E-14	XP_022873319.1	protein NLP1-like = *Olea europaea var. Sylvestris*
LOC111392344	1,182390112	9,34E-09	XP_022873439.1	linoleate 13S-lipoxygenase 2-1, chloroplastic-like = *Olea europaea var. Sylvestris*
LOC111392646	1,373518724	0,001346872	XP_022873791.1	1-aminocyclopropane-1-carboxylate oxidase homolog 11-like = *Olea europaea var. Sylvestris*
LOC111392899	2,147041107	0,008634933	XP_022874081.1	transcription factor bHLH162-like = *Olea europaea var. Sylvestris*
LOC111392924	3,887137491	4,46E-05	XP_022874105.1	trans-resveratrol di-O-methyltransferase-like = *Olea europaea var. Sylvestris*
LOC111393536	1,555689929	2,95E-11	XP_022874877.1	chlorophyll a-b binding protein 7, chloroplastic = *Olea europaea var. Sylvestris*
LOC111393576	2,731720189	0,002866587	XP_022874944.1	uncharacterized LOC111393576 =*Olea europaea var. Sylvestris*
LOC111393913	1,076754393	0,0083965	XP_022875454.1	ABC transporter B family member 2-like = *Olea europaea var. Sylvestris*
LOC111394603	1,092073561	0,010470528	XP_022876271.1	protein MIZU-KUSSEI 1-like =*Olea europaea var. Sylvestris*
LOC111396591	1,063208189	3,88E-06	XP_022878768.1	serine carboxypeptidase-like 50 = *Olea europaea var. Sylvestris*
LOC111397188	3,639769208	0,000201527	XP_022879735.1	expansin-A8-like = *Olea europaea var. Sylvestris*
LOC111397229	1,236281552	6,27E-05	XP_022879818.1	probable xyloglucan endotransglucosylase/hydrolase protein 7 = *Olea europaea var. Sylvestris*
LOC111398633	1,068315219	0,004130963	XP_022881394.1	uncharacterized LOC111398633 =*Olea europaea var. Sylvestris*
LOC111398953	2,45293123	0,006575805	XP_022881900.1	cysteine-rich repeat secretory protein 55-like = *Olea europaea var. Sylvestris*
LOC111399002	1,586031131	1,78E-04	uncharacterized	uncharacterized
LOC111399354	1,265831033	5,36E-05	XP_022882385.1	axial regulator YABBY 5 = *Olea europaea var. Sylvestris*
LOC111399450	1,136936376	0,006955997	-	uncharacterized LOC111399450 =*Olea europaea var. Sylvestris*
LOC111399610	1,622743325	9,66E-05	uncharacterized	uncharacterized
LOC111399728	1,258757377	4,91E-07	XP_022882966.1	inorganic phosphate transporter 1-4-like = *Olea europaea var. Sylvestris*
LOC111400171	3,928815987	5,50E-19	XP_022883368.1	protein LONGIFOLIA 1-like = *Olea europaea var. Sylvestris*
LOC111401697	1,208520193	1,02E-07	XP_022885324.1	TORTIFOLIA1-like protein 4 = *Olea europaea var. Sylvestris*
LOC111401891	1,537141914	2,62E-12	XP_022885633.1	cytochrome P450 71A1-like = *Olea europaea var. Sylvestris*
LOC111402017	1,169341072	1,23E-07	XP_022885802.1	mannan endo-1,4-beta-mannosidase 7 = *Olea europaea var. Sylvestris*
LOC111402921	2,462523052	0,001117536	uncharacterized	uncharacterized
LOC111403048	2,115265027	0,002343047	XP_022887165.1	protein NRT1/ PTR FAMILY 5.1-like = *Olea europaea var. Sylvestris*

LOC111403273	2,187851812	0,005427169	XP_022887476.1	uncharacterized LOC111403273 = *Olea europaea var. Sylvestris*
LOC111403314	1,492845327	0,000277681	XP_022887534.1	ninja-family protein AFP2-like = *Olea europaea var. Sylvestris*
LOC111403359	1,150675018	0,000181554	uncharacterized	uncharacterized
LOC111403994	1,849120836	5,57E-10	XP_022888459.1	receptor protein kinase TMK1-like = *Olea europaea var. Sylvestris*
LOC111404371	1,499772107	1,13E-06	uncharacterized	uncharacterized
LOC111404802	1,242141908	0,001296496	-	subtilisin-like protease SBT2.5 = *Olea europaea var. Sylvestris*
LOC111405743	1,104727677	0,000510821	XP_022890535.1	receptor-like cytosolic serine/threonine-protein kinase RBK2 = *Olea europaea var. Sylvestris*
LOC111405925	1,000123512	0,011281978	XP_022890810.1	dCTP pyrophosphatase 1-like = *Olea europaea var. Sylvestris*
LOC111406396	1,666321169	1,84E-07	XP_022891592.1	uncharacterized LOC111406396 = *Olea europaea var. Sylvestris*
LOC111407242	1,399618018	1,02E-14	XP_022892374.1	chlorophyll a-b binding protein of LHCII type 1 = *Olea europaea var. Sylvestris*
LOC111407568	3,702234512	0,000804671	XP_022892906.1	uncharacterized LOC111407568 = *Olea europaea var. Sylvestris*
LOC111407816	1,591577963	2,81E-08	XP_022893267.1	zinc finger CCCH domain-containing protein 20-like = *Olea europaea var. Sylvestris*
LOC111408119	1,429300267	3,09E-08	XP_022893683.1	ABC transporter B family member 2-like = *Olea europaea var. Sylvestris*
LOC111408423	1,061065924	0,009362579	XP_022893952.1	serine/threonine-protein kinase CTR1-like = *Olea europaea var. Sylvestris*
LOC111409237	1,5403713	4,56E-14	XP_022895015.1	glycerophosphodiester phosphodiesterase GDPD1, chloroplastic-like = *Olea europaea var. Sylvestris*
LOC111409311	1,34496629	5,34E-06	XP_022895113.1	LOB domain-containing protein 25-like = *Olea europaea var. Sylvestris*
LOC111409999	1,176541016	2,38E-12	XP_022895919.1	transcription factor MYB1R1-like = *Olea europaea var. Sylvestris*
LOC111410250	1,220770793	1,43E-08	XP_022896283.1	protein ZINC INDUCED FACILITATOR-LIKE 1-like = *Olea europaea var. Sylvestris*
LOC111410856	1,679612628	0,002200741	XP_022897200.1	leucine-rich repeat receptor-like serine/threonine-protein kinase BAM1 = *Olea europaea var. Sylvestris*
LOC111411447	1,311732513	1,29E-05	XP_022897749.1	subtilisin-like protease SBT1.8 = *Olea europaea var. Sylvestris*

Table 3.II.S6. Genes down-regulated in both the first and second comparisons

LOC111400284	-2,518485882	2,03E-06	XP_022883468.1	probable polyamine oxidase 4 = *Olea europaea var. Sylvestris*
LOC111400933	-2,202858656	0,000334012	XP_022884173.1	solute carrier family 25 member 44-like = *Olea europaea var. Sylvestris*
LOC111400934	-311,0947163	9,43E-08	XP_022884174.1	developmental protein SEPALLATA 1 = *Olea europaea var. Sylvestris*
LOC111400940	-2,131757905	0,023881323	XP_022884185.1	glutathione transferase GST 23-like = *Olea europaea var. Sylvestris*
LOC111401060	-226,8530264	4,55E-06	uncharacterized	uncharacterized
LOC111401565	-2,549223896	0,000652085	XP_022885126.1	auxin-responsive protein IAA26-like = *Olea europaea var. Sylvestris*
LOC111401691	-3,424991257	1,22E-07	XP_022885320.1	calmodulin-binding protein 60 A-like = *Olea europaea var. Sylvestris*
LOC111403387	-2,52492614	0,001326626	XP_022887648.1	cysteine-rich receptor-like protein kinase 2 = *Olea europaea var. Sylvestris*
LOC111403728	-7,725947301	2,93E-10	XP_022888104.1	tetraspanin-8-like = *Olea europaea var. Sylvestris*
LOC111403868	-2,256533758	8,84E-08	XP_022888272.1	probable calcium-binding protein CML49 = *Olea europaea var. Sylvestris*
LOC111404273	-2,837480037	2,12E-07	XP_022888866.1	uncharacterized LOC111404273 = *Olea europaea var. Sylvestris*
LOC111404347	-5,611178423	4,70E-06	XP_022888932.1	beta-glucosidase-like = *Olea europaea var. Sylvestris*
LOC111404719	-2,519555896	8,11E-09	XP_022889253.1	IQ domain-containing protein IQM3-like = *Olea europaea var. Sylvestris*
LOC111405234	-2,001030231	1,11E-05	XP_022889805.1	calcium-binding allergen Ole e 8-like = *Olea europaea var. Sylvestris*
LOC111405992	-3,453194516	1,17E-18	XP_022890914.1	ras-related protein RABE1c-like = *Olea europaea var. Sylvestris*
LOC111406337	-4,312475116	1,82E-06	XP_022891495.1	2-methylene-furan-3-one reductase-like = *Olea europaea var. Sylvestris*
LOC111407177	-79,53249436	0,000184434	XP_022892277.1	homeobox protein SBH1-like = *Olea europaea var. Sylvestris*
LOC111407490	-3,352954621	0,001484911	XP_022892766.1	type I inositol polyphosphate 5-phosphatase 2-like = *Olea europaea var. Sylvestris*
LOC111408024	-3,614610379	0,030433117	XP_022893537.1	putative wall-associated receptor kinase-like 16 = *Olea europaea var. Sylvestris*
LOC111408823	-6,739267306	0,019305329	uncharacterized	uncharacterized
LOC111408953	-2,082929436	2,40E-06	XP_022894574.1	isoflavone reductase-like protein = *Olea europaea var. Sylvestris*
LOC111408990	-11,8469955	0,007240138	XP_022894639.1	transcription factor MYB87-like = *Olea europaea var. Sylvestris*
LOC111409135	-2,138955754	5,49E-10	XP_022894863.1	G-type lectin S-receptor-like serine/threonine-protein kinase At1g11330 = *Olea europaea var. Sylvestris*
LOC111409172	-2,131426176	1,13E-06	XP_022894919.1	AAA-ATPase ASD, mitochondrial-like = *Olea europaea var. Sylvestris*
LOC111409261	-6,547374816	0,003641253	uncharacterized	uncharacterized
LOC111409741	-2,274095039	3,95E-09	XP_022895517.1	desiccation protectant protein Lea14 homolog = *Olea europaea var. Sylvestris*
LOC111409839	-26,92386796	3,71E-07	XP_022895689.1	uncharacterized LOC111409839 = *Olea europaea var. Sylvestris*
LOC111409970	-4,016010953	0,003500494	XP_022895879.1	uncharacterized protein ZK1098.3-like = *Olea europaea var. Sylvestris*
LOC111410082	-4,652096921	4,86E-22	XP_022896028.1	purple acid phosphatase 2-like = *Olea europaea var. Sylvestris*
LOC111410171	-2,092760693	6,19E-05	XP_022896169.1	cysteine-rich and transmembrane domain-containing protein WIH2-like = *Olea europaea var. Sylvestris*
LOC111410340	-2,38741566	4,74E-05	XP_022896386.1	ascorbate transporter, chloroplastic = *Olea europaea var. Sylvestris*
LOC111410928	-18,87316721	7,96E-09	XP_022897290.1	vacuolar iron transporter homolog 1-like = *Olea europaea var. Sylvestris*
LOC111411182	-2,118858143	0,002364841	XP_022897507.1	mannosylglycoprotein endo-beta-mannosidase-like = *Olea europaea var. Sylvestris*
LOC111411240	-9,331901958	0,022359227	XP_022897562.1	ATP-dependent 6-phosphofructokinase 6-like = *Olea europaea var. Sylvestris*
LOC111411636	-2,012645871	0,045030963	XP_022897966.1	uncharacterized LOC111411636 = *Olea europaea var. Sylvestris*
LOC111411655	-3,504271319	1,66E-08	XP_022897964.1	rust resistance kinase Lr10-like = *Olea europaea var. Sylvestris*
LOC111412112	-2,055098515	0,00037048	XP_022898655.1	chaperone protein dnaJ 10-like = *Olea europaea var. Sylvestris*
LOC111412591	-2,417914001	3,22E-09	-	UDP-D-apiose/UDP-D-xylose synthase 1-like = *Olea europaea var. Sylvestris*

Table 3.II.S7. Genes up-regulated in the first comparison and down-regulated in the second comparison.

Formato (*.xlsx).

Table 3.II. S8. The enrichment analysis of GO terms based on DEGs in the first comparison.
Formato (*.xlsx).

Table 3.II.S9. The enrichment analysis of GO terms based on DEGs in the second comparison.
Formato (*.xlsx).

Table 3.II.S10. Sphingolipids genes repressed or induced in the first comparison (d18:0-AZ vs. C-AZ) and the second comparison (d18:0-LAZ vs. d18:0-AZ).

d18:0-AZ vs. C-AZ					
Gene	**log2FoldChange**	**FoldChange**	**p value**	**Gene_ID**	**Description**
UP					
LOC111382808	3,22142757	9,327093436	0,32033777	XP_022862615.1	3-ketoacyl-CoA synthase 6-like = *Olea europaea var. Sylvestris*
LOC111403197	2,605848132	6,087492679	0,04607355	XP_022887373.1	3-ketoacyl-CoA synthase 6-like = *Olea europaea var. Sylvestris*
LOC111397402	1,968044105	3,912373498	0,05724023	XP_022880076.1	sphinganine C4-monooxygenase 1-like = *Olea europaea var. Sylvestris*
LOC111388105	1,78406392	3,443949338	1,966E-08	XP_022868534.1	3-ketoacyl-CoA synthase 10 = *Olea europaea var. Sylvestris*
LOC111382252	1,555941303	2,940255045	2,6089E-11		neutral ceramidase 2-like = *Olea europaea var. Sylvestris*
LOC111405499	1,447755453	2,727833243	1,667E-06	XP_022890179.1	3-ketoacyl-CoA synthase 19 = *Olea europaea var. Sylvestris*
LOC111382196	1,380965675	2,604426412	6,2703E-05	XP_022861871.1	neutral ceramidase 3-like = *Olea europaea var. Sylvestris*
LOC111374523	1,307679478	2,475430557	0,02926899	XP_022852962.1	3-ketoacyl-CoA synthase 4-like = *Olea europaea var. Sylvestris*
LOC111370571	1,29356892	2,451337147	0,53459419	XP_022848108.1	sphingolipid delta(4)-desaturase DES1-like = *Olea europaea var. Sylvestris*
LOC111404391	1,247107701	2,373650789	0,80200342	XP_022888971.1	phosphatidylinositol: ceramide inositolphosphotransferase 1-like = *Olea europaea var. Sylvestris*
LOC111385735	1,20205924	2,300678256	0,1004797	XP_022865919.1	3-ketoacyl-CoA synthase 11-like = *Olea europaea var. Sylvestris*
LOC111380039	1,126602109	2,183438822	0,13067706	XP_022859273.1	3-ketoacyl-CoA synthase 12-like = *Olea europaea var. Sylvestris*
LOC111374909	1,061005899	2,086385719	3,6161E-05	XP_022853429.1	3-ketoacyl-CoA synthase 11-like = *Olea europaea var. Sylvestris*
LOC111377094	1,024821369	2,034707436	0,00166012	XP_022855909.1	very-long-chain enoyl-CoA reductase-like = *Olea europaea var. Sylvestris*
LOC111397246	0,904670291	1,872116599	0,01431618	XP_022879839.1	3-ketoacyl-CoA synthase 6 = *Olea europaea var. Sylvestris*
LOC111410351	0,881020615	1,841677711	0,26747078	XP_022896406.1	3-ketodihydrosphingosine reductase-like = *Olea europaea var. Sylvestris*
LOC111397371	0,788634548	1,727438739	0,00198536	XP_022880040.1	very-long-chain enoyl-CoA reductase-like = *Olea europaea var. Sylvestris*
LOC111398942	0,736227888	1,665814652	0,00592851	XP_022881881.1	ASC1-like protein = *Olea europaea var. Sylvestris*
LOC111401043	0,733397628	1,662549883	0,65044186	XP_022884342.1	3-ketoacyl-CoA synthase 6-like = *Olea europaea var. Sylvestris*
LOC111382562	0,684199872	1,606810586	0,03253358	XP_022862350.1	3-dehydrosphinganine reductase TSC10A-like = *Olea europaea var. Sylvestris*
LOC111369966	0,6650573	1,585631249	0,34152152	XP_022847471.1	GDP-mannose transporter GONST1-like = *Olea europaea var. Sylvestris*
LOC111408777	0,564054099	1,478417869	0,81258603	XP_022894316.1	sphinganine C4-monooxygenase 1-like = *Olea europaea var. Sylvestris*
LOC111398669	0,502408554	1,416576539	0,28058744	XP_022881460.1	LAG1 longevity assurance homolog 2-like = *Olea europaea var. Sylvestris*
LOC111394334	0,501075829	1,415268546	0,05950011	XP_022875864.1	3-ketoacyl-CoA synthase 4-like = *Olea europaea var. Sylvestris*
LOC111389048	0,492955096	1,407324571	0,13225617	XP_022869672.1	3-ketoacyl-CoA synthase 4-like = *Olea europaea var. Sylvestris*
LOC111374017	0,483131914	1,397774773	0,12046493	XP_022852392.1	neutral ceramidase-like = *Olea europaea var. Sylvestris*
LOC111380441	0,432055225	1,349154178	0,07820079		neutral ceramidase 2-like = *Olea europaea var. Sylvestris*
LOC111388259	0,429098213	1,346391723	0,55499054	XP_022868715.1	3-ketoacyl-CoA synthase 4-like = *Olea europaea var. Sylvestris*
LOC111370466	0,414905727	1,333211556	0,41279288	XP_022847947.1	dihydroceramide fatty acyl 2-hydroxylase FAH1-like = *Olea europaea var. Sylvestris*
LOC111389117	0,369642214	1,292032369	0,38321173	XP_022869743.1	LAG1 longevity assurance homolog 2-like = *Olea europaea var. Sylvestris*
LOC111406020	0,364903737	1,287795699	0,10148843	XP_022890953.1	very-long-chain enoyl-CoA reductase-like = *Olea europaea var. Sylvestris*
LOC111393857	0,331322751	1,25816641	0,06686375	XP_022875371.1	neutral ceramidase 1-like = Olea europaea var. Sylvestris
LOC111393872	0,280699547	1,214783777	0,22317719	XP_022875405.1	Small subunit of serine palmitoyltransferase-like = *Olea europaea var. Sylvestris*
LOC111386640	0,269078582	1,20503795	0,22081511	XP_022866875.1	neutral ceramidase-like = *Olea europaea var. Sylvestris*
LOC111397014	0,222688045	1,166905754	0,59320773	XP_022879444.1	GDP-mannose transporter GONST3 = *Olea europaea var. Sylvestris*
LOC111411912	0,218446578	1,163480134	0,51327509	XP_022898347.1	GDP-mannose transporter GONST1-like = *Olea europaea var. Sylvestris*

LOC111409900	0,202733127	1,15087658	0,53974799	XP_022895776.1	sphingoid long-chain bases kinase 1-like = *Olea europaea var. Sylvestris*
LOC111379590	0,195984159	1,14550532	0,49532833	XP_022858766.1	probable sphingolipid transporter spinster homolog 2 = *Olea europaea var. Sylvestris*
LOC111377049	0,143429777	1,104527835	0,64858622		sphingoid long-chain bases kinase 2, mitochondrial = *Olea europaea var. Sylvestris*
LOC111410715	0,119319069	1,08622206	0,54182746	XP_022896961.1	Ceramidase = *Olea europaea var. Sylvestris*
LOC111406199	0,113411266	1,081783101	0,64619317	XP_022891239.1	sphinganine C4-monooxygenase 1-like = *Olea europaea var. Sylvestris*
LOC111379525	0,091756875	1,065667134	0,7700022	XP_022858684.1	3-ketoacyl-CoA synthase 1 = *Olea europaea var. Sylvestris*
LOC111396234	0,029311206	1,020524775	0,90277469	XP_022878370.1	ASC1-like protein = *Olea europaea var. Sylvestris*
LOC111375235	0,002548778	1,00176824	0,99084029	XP_022853805.1	neutral ceramidase 1-like = *Olea europaea var. Sylvestris*
LOC111380448	0,001105657	1,000766677	0,99650756	XP_022859788.1	alkaline ceramidase-like = *Olea europaea var. Sylvestris*
DOWN					
LOC111403179	-2,473833144	-5,555178019	8,4644E-25	XP_022887351.1	phosphatidylinositol: ceramide inositolphosphotransferase 2-like = *Olea europaea var. Sylvestris*
LOC111377249	-2,210646998	-4,628828138	4,7702E-12	XP_022856081.1	3-ketoacyl-CoA synthase 11 = *Olea europaea var. Sylvestris*
LOC111398707	-1,919609835	-3,783207312	9,8003E-17	XP_022881518.1	3-ketoacyl-CoA synthas 11-like = *Olea europaea var. Sylvestris*
LOC111399332	-1,826610267	-3,547026888	4,5018E-10	XP_022882355.1	long chain base biosynthesis protein 1b-like = *Olea europaea var. Sylvestris*
LOC111378123	-1,664860327	-3,17082955	2,9046E-28	XP_022857063.1	phosphatidylinositol: ceramide inositolphosphotransferase 1-like = *Olea europaea var. Sylvestris*
LOC111385152	-1,235713529	-2,354977913	7,5854E-05	XP_022865296.1	phosphatidylinositol: ceramide inositolphosphotransferase 2-like = *Olea europaea var. Sylvestris*
LOC111391093	-1,234173683	-2,352465692	1,0951E-08	XP_022872004.1	lipid phosphate phosphatase delta-like = *Olea europaea var. Sylvestris*
LOC111408945	-1,189767262	-2,281159402	4,9397E-10	XP_022894566.1	3-ketoacyl-CoA synthase 4-like = *Olea europaea var. Sylvestris*
LOC111375231	-1,130443105	-2,189259703	1,1E-05	XP_022853801.1	GDP-mannose transporter GONST2-like = *Olea europaea var. Sylvestris*
LOC111404077	-1,029136486	-2,04080238	2,5971E-09	XP_022888576.1	phosphatidylinositol: ceramide inositolphosphotransferase 1-like = *Olea europaea var. Sylvestris*
LOC111383577	-0,934767231	-1,91158219	9,4927E-07	XP_022863459.1	3-ketoacyl-CoA synthase 11-like = *Olea europaea var. Sylvestris*
LOC111395269	-0,863584839	-1,819553964	0,00162755	XP_022877023.1	sphingosine-1-phosphate lyase = *Olea europaea var. Sylvestris*
LOC111391276	-0,839291061	-1,789170729	0,00214443	XP_022872217.1	long chain base biosynthesis protein 1-like = *Olea europaea var. Sylvestris*
LOC111384746	-0,723842806	-1,651575367	0,00538581		long chain base biosynthesis protein 1-like= *Olea europaea var. Sylvestris*
LOC111407565	-0,661199344	-1,581396727	0,00117242	XP_022892904.1	3-ketoacyl-CoA synthase 11-like = *Olea europaea var. Sylvestris*
LOC111369944	-0,615699621	-1,532300891	0,00255488	XP_022847443.1	non-lysosomal glucosylceramidase = *Olea europaea var. Sylvestris*
LOC111384387	-0,585027282	-1,500067356	0,00283486	XP_022864440.1	sphingoid long-chain bases kinase 1 = *Olea europaea var. Sylvestris*
LOC111410182	-0,455313943	-1,371081132	0,24428513	XP_022896184.1	probable sphingolipid transporter spinster homolog 2 = *Olea europaea var. Sylvestris*
LOC111405999	-0,435180679	-1,352080153	0,10811594	XP_022890928.1	inositol phosphorylceramide glucuronosyltransferase 1-like = *Olea europaea var. Sylvestris*
LOC111374266	-0,429428483	-1,346699982	0,10478962	XP_022852690.1	alkaline ceramidase-like = *Olea europaea var. Sylvestris*
LOC111383590	-0,405139812	-1,324217234	0,92053227	XP_022863475.1	3-ketoacyl-CoA synthase 11-like = *Olea europaea var. Sylvestris*
LOC111390632	-0,40404459	-1,323212336	0,06588822	XP_022871465.1	alkaline ceramidase-like = *Olea europaea var. Sylvestris*
LOC111393439	-0,360950571	-1,284271807	0,06615722	XP_022874741.1	3-dehydrosphinganine reductase TSC10B-like = *Olea europaea var. Sylvestris*
LOC111380636	-0,287064333	-1,220154919	0,18558293	XP_022860024.1	Small subunit of serine palmitoyltransferase-like = *Olea europaea var. Sylvestris*
LOC111401843	-0,240173014	-1,181134299	0,70646438	XP_022885549.1	dihydroceramide fatty acyl 2-hydroxylase FAH1-like = *Olea europaea var. Sylvestris*
LOC111385159	-0,223744621	-1,167760665	0,95401125	XP_022865303.1	phosphatidylinositol: ceramide inositolphosphotransferase 2-like = *Olea europaea var. Sylvestris*
LOC111383452	-0,184551836	-1,136463883	0,33859207		long chain base biosynthesis protein 1-like = *Olea europaea var. Sylvestris*
LOC111411658	-0,183858369	-1,135917745	0,51939736	XP_022897973.1	GDP-mannose transporter GONST1-like = *Olea europaea var. Sylvestris*
LOC111368047	-0,156716597	-1,114747217	0,32269382	XP_022844985.1	long chain base biosynthesis protein 2a-like = *Olea europaea var. Sylvestris*

LOC111375632	-0,138322855	-1,100624886	0,69001833	XP_022854255.1	non-lysosomal glucosylceramidase-like = *Olea europaea var. Sylvestris*
LOC111370555	-0,108481391	-1,078092817	0,55801735	XP_022848084.1	sphingosine kinase 1-like = *Olea europaea var. Sylvestris*
LOC111412353	-0,106098882	-1,076313892	0,90891866	XP_022899017.1	dihydroceramide fatty acy 2-hydroxylas FAH1-like = *Olea europaea var. Sylvestris*
LOC111376790	-0,015344986	-1,010693101	0,94276468	XP_022855564.1	probable sphingolipid transporter spinster homolog 2 = *Olea europaea var. Sylvestris*
d18:0 LAZ vs. d18:0-AZ					
Gene	**log2FoldChange**	**FoldChange**	**p value**	**Gene_ID**	**Description**
UP					
LOC111382808	3,35589257	10,2382169	0,00070684	XP_022862615.1	3-ketoacyl-CoA synthase 6-like = *Olea europaea var. Sylvestris*
LOC111403197	2,498431264	5,650706526	1,73E-06	XP_022887373.1	3-ketoacyl-CoA synthase 6-like = *Olea europaea var. Sylvestris*
LOC111401843	2,311322569	4,963378817	3,6463E-08	XP_022885549.1	dihydroceramide fatty acyl 2-hydroxylase FAH1-like = *Olea europaea var. Sylvestris*
LOC111410351	2,286117864	4,87741883	2,1982E-07	XP_022896406.1	3-ketodihydrosphingosine reductase-like = *Olea europaea var. Sylvestris*
LOC111385735	1,822880202	3,537867954	3,3029E-05	XP_022865919.1	3-ketoacyl-CoA synthase 11-like = *Olea europaea var. Sylvestris*
LOC111388105	1,565623862	2,960054753	2,3768E-12	XP_022868534.1	3-ketoacyl-CoA synthase 10 = *Olea europaea var. Sylvestris*
LOC111397246	1,296603456	2,456498666	5,7425E-07	XP_022879839.1	3-ketoacyl-CoA synthase 6 = *Olea europaea var. Sylvestris*
LOC111370466	1,286338995	2,439083241	0,00051901	XP_022847947.1	dihydroceramide fatty acyl 2-hydroxylase FAH1-like = *Olea europaea var. Sylvestris*
LOC111377094	1,09412879	2,134841246	3,435E-06	XP_022855909.1	very-long-chain enoyl-CoA reductase-like = *Olea europaea var. Sylvestris*
LOC111379590	1,071597765	2,101759748	5,3978E-06	XP_022858766.1	probable sphingolipid transporter spinster homolog 2 = *Olea europaea var. Sylvestris*
LOC111411912	1,063327462	2,089745801	8,5556E-05	XP_022898347.1	GDP-mannose transporter GONST1-like = *Olea europaea var. Sylvestris*
LOC111383577	0,91928509	1,891177911	1,5173E-06	XP_022863459.1	3-ketoacyl-CoA synthase 11-like = *Olea europaea var. Sylvestris*
LOC111407565	0,850126668	1,802659191	1,8683E-05	XP_022892904.1	3-ketoacyl-CoA synthase 11-like = *Olea europaea var. Sylvestris*
LOC111369966	0,771214379	1,706705788	0,12743341	XP_022847471.1	GDP-mannose transporter GONST1-like = *Olea europaea var. Sylvestris*
LOC111395269	0,683039323	1,605518538	0,01209599	XP_022877023.1	sphingosine-1-phosphate lyase = *Olea europaea var. Sylvestris*
LOC111408945	0,499459841	1,413684166	0,01420491	XP_022894566.1	3-ketoacyl-CoA synthase 4-like = *Olea europaea var. Sylvestris*
LOC111393857	0,479821312	1,394570929	0,00444371	XP_022875371.1	neutral ceramidase 1-like = *Olea europaea var. Sylvestris*
LOC111386640	0,404602008	1,323723688	0,05358785	XP_022866875.1	neutral ceramidase-like = *Olea europaea var. Sylvestris*
LOC111384387	0,37737701	1,298978011	0,04928305	XP_022864440.1	sphingoid long-chain bases kinase 1 = *Olea europaea var. Sylvestris*
LOC111375235	0,363041322	1,286134321	0,09182414	XP_022853805.1	neutral ceramidase 1-like = *Olea europaea var. Sylvestris*
LOC111393625	0,337888639	1,263905534	0,71072595	XP_022875020.1	alkaline ceramidase-like = *Olea europaea var. Sylvestris*
LOC111374266	0,302636084	1,23339601	0,2469271	XP_022852690.1	alkaline ceramidase-like = *Olea europaea var. Sylvestris*
LOC111389048	0,294854664	1,226761388	0,30707715	XP_022869672.1	3-ketoacyl-CoA synthase 4-like = *Olea europaea var. Sylvestris*
LOC111409900	0,228464167	1,171587063	0,45142732	XP_022895776.1	sphingoid long-chain bases kinase 1-like = *Olea europaea var. Sylvestris*
LOC111391276	0,228323643	1,171472951	0,4324772	XP_022872217.1	long chain base biosynthesis protein 1-like = *Olea europaea var. Sylvestris*
LOC111369944	0,128181387	1,092915141	0,54335284	XP_022847443.1	non-lysosomal glucosylceramidase = *Olea europaea var. Sylvestris*
LOC111394334	0,116948703	1,08443885	0,62930949	XP_022875864.1	3-ketoacyl-CoA synthase 4-like = *Olea europaea var. Sylvestris*
LOC111396234	0,099955747	1,071740587	0,66826209	XP_022878370.1	ASC1-like protein = *Olea europaea var. Sylvestris*
LOC111380441	0,098290931	1,070504552	0,66875308		neutral ceramidase 2-like = *Olea europaea var. Sylvestris*
LOC111406199	0,092898147	1,066510483	0,69693807	XP_022891239.1	sphinganine C4-monooxygenase 1-like = *Olea europaea var. Sylvestris*
LOC111397402	0,067020467	1,047550988	0,92519352	XP_022880076.1	sphinganine C4-monooxygenase 1-like = *Olea europaea var. Sylvestris*
LOC111377249	0,051200429	1,036126699	0,90819925	XP_022856081.1	3-ketoacyl-CoA synthase 11 = *Olea europaea var. Sylvestris*
LOC111393872	0,007178661	1,004988269	0,97405421	XP_022875405.1	Small subunit of serine palmitoyltransferase-like = *Olea europaea var. Sylvestris*
DOWN					
LOC111388259	-6,402876886	-84,61707351	0,00011408	XP_022868715.1	3-ketoacyl-CoA synthase 4-like = *Olea europaea var. Sylvestris*

LOC111382252	-2,166832211	-4,490363418	2,9698E-18		neutral ceramidase 2-like = *Olea europaea var. Sylvestris*
LOC111382196	-2,116944804	-4,337743673	1,3072E-08	XP_022861871.1	neutral ceramidase 3-like = *Olea europaea var. Sylvestris*
LOC111374017	-2,000207485	-4,000575312	2,1746E-08	XP_022852392.1	neutral ceramidase-like = *Olea europaea var. Sylvestris*
LOC111401043	-1,622938668	-3,080017755	0,37408252	XP_022884342.1	3-ketoacyl-CoA synthase 6-like = *Olea europaea var. Sylvestris*
LOC111399332	-1,313746339	-2,485862225	0,00357857	XP_022882355.1	long chain base biosynthesis protein 1b-like = *Olea europaea var. Sylvestris*
LOC111398669	-0,978840109	-1,970880233	0,04176292	XP_022881460.1	LAG1 longevity assurance homolog 2-like = *Olea europaea var. Sylvestris*
LOC111385152	-0,976096598	-1,967135857	0,01875751	XP_022865296.1	phosphatidylinositol: ceramide inositolphosphotransferase 2-like = *Olea europaea var. Sylvestris*
LOC111375231	-0,930029534	-1,905315	0,0050464	XP_022853801.1	GDP-mannose transporter GONST2-like = *Olea europaea var. Sylvestris*
LOC111378123	-0,793551327	-1,733335982	2,9099E-06	XP_022857063.1	phosphatidylinositol: ceramide inositolphosphotransferas 1-like = *Olea europaea var. Sylvestris*
LOC111375632	-0,646593562	-1,565467505	0,08885566	XP_022854255.1	non-lysosomal glucosylceramidase-like = *Olea europaea var. Sylvestris*
LOC111389117	-0,642503777	-1,561035966	0,1135309	XP_022869743.1	LAG1 longevity assurance homolog 2-like = *Olea europaea var. Sylvestris*
LOC111374523	-0,629873649	-1,547429464	0,23155343	XP_022852962.1	3-ketoacyl-CoA synthase 4-like = *Olea europaea var. Sylvestris*
LOC111380039	-0,592827153	-1,508199371	0,37209256	XP_022859273.1	3-ketoacyl-CoA synthase 12-like = *Olea europaea var. Sylvestris*
LOC111368047	-0,555724351	-1,469906461	0,0005592	XP_022844985.1	long chain base biosynthesis protein 2a-like = *Olea europaea var. Sylvestris*
LOC111397371	-0,496139732	-1,410434561	0,04038544	XP_022880040.1	very-long-chain enoyl-CoA reductase-like = *Olea europaea var. Sylvestris*
LOC111393439	-0,412973238	-1,331426915	0,05039789	XP_022874741.1	3-dehydrosphinganine reductase TSC10B-like = *Olea europaea var. Sylvestris*
LOC111406020	-0,408022113	-1,326865478	0,06657018	XP_022890953.1	very-long-chain enoyl-CoA reductase-like = *Olea europaea var. Sylvestris*
LOC111380448	-0,379814086	-1,301174168	0,12154897	XP_022859788.1	alkaline ceramidase-like = *Olea europaea var. Sylvestris*
LOC111410715	-0,373633004	-1,295611343	0,06497415	XP_022896961.1	Ceramidase = *Olea europaea var. Sylvestris*
LOC111370555	-0,332292371	-1,259012295	0,08158345	XP_022848084.1	sphingosine kinase 1-like = *Olea europaea var. Sylvestris*
LOC111398942	-0,289640039	-1,22233526	0,25325492	XP_022881881.1	ASC1-like protein = *Olea europaea var. Sylvestris*
LOC111405999	-0,266173861	-1,202614169	0,34654318	XP_022890928.1	inositol phosphorylceramide glucuronosyltransferase 1-like = *Olea europaea var. Sylvestris*
LOC111405999	-0,266173861	-1,202614169	0,34654318	XP_022890928.1	inositol phosphorylceramide glucuronosyltransferase 1-like = *Olea europaea var. Sylvestris*
LOC111376790	-0,263072384	-1,20003159	0,22775546	XP_022855564.1	probable sphingolipid transporter spinster homolog 2 = *Olea europaea var. Sylvestris*
LOC111380636	-0,249177196	-1,188529074	0,27552212	XP_022860024.1	Small subunit of serine palmitoyltransferase-like = *Olea europaea var. Sylvestris*
LOC111383452	-0,246338931	-1,186193138	0,21887175		long chain base biosynthesis protein 1-like = *Olea europaea var. Sylvestris*
LOC111390632	-0,230231927	-1,173023509	0,32022341	XP_022871465.1	alkaline ceramidase-like = *Olea europaea var. Sylvestris*
LOC111410182	-0,19057806	-1,14122089	0,65591846	XP_022896184.1	probable sphingolipid transporter spinster homolog 2 = *Olea europaea var. Sylvestris*
LOC111397014	-0,158461619	-1,116096383	0,69579782	XP_022879444.1	GDP-mannose transporter GONST3 = *Olea europaea var. Sylvestris*
LOC111377049	-0,141257624	-1,102866086	0,64913324		sphingoid long-chain bases kinase 2, mitochondrial = *Olea europaea var. Sylvestris*
LOC111384746	-0,132387657	-1,096106254	0,64244175		long chain base biosynthesis protein 1-like = *Olea europaea var. Sylvestris*
LOC111398707	-0,079855966	-1,056912517	0,78952723	XP_022881518.1	3-ketoacyl-CoA synthase 11-like = *Olea europaea var. Sylvestris*
LOC111403179	-0,077264073	-1,055015411	0,81929012	XP_022887351.1	phosphatidylinositol: ceramide inositolphosphotransferase 2-like = *Olea europaea var. Sylvestris*
LOC111410691	-0,053139414	-1,037520192	0,7954185		probable sphingolipid transporter spinster homolog 2 = *Olea europaea var. Sylvestris*
LOC111382562	-0,038440803	-1,027003289	0,89160361	XP_022862350.1	3-dehydrosphinganine reductase TSC10A-like = *Olea europaea var. Sylvestris*
LOC111411658	-0,008891009	-1,006181807	0,97487841	XP_022897973.1	GDP-mannose transporter GONST1-like = *Olea europaea var. Sylvestris*

Table 3.II. S11. Cell-wall-related genes induced or repressed in the first comparison (d18:0-AZ vs. C-AZ) and the second comparison (d18:0-LAZ vs. d18:0-AZ).

	d18:0-AZ vs. C-AZ		d18:0-LAZ vs. d18:0-AZ			
Gene	log2FoldChange	pvalue	log2FoldChange	pvalue	Gene_ID	Description
LOC111376911			-1,010185633	2,62E-01	-	alpha-1,4-glucan-protein synthase [UDP-forming] 2-like = *Olea europaea var. Sylvestris*
LOC111399050			1,30100591	2,96E-05	XP_022882036.1	alpha-galactosidase 1-like = *Olea europaea var. Sylvestris*
LOC111373614	1,366727969	3,13E-17	-1,368275667	1,46E-16	XP_022851936.1	alpha-galactosidase 3-like = *Olea europaea var. Sylvestris*
LOC111397171			1,321705668	6,63E-09	XP_022879712.1	alpha-galactosidase 3-like = *Olea europaea var. Sylvestris*
LOC111401756			-1,446529629	1,20E-05	XP_022885408.1	alpha-galactosidase-like = *Olea europaea var. Sylvestris*
LOC111400865			1,451443074	2,37E-04	XP_022884074.1	ALTERED XYLOGLUCAN 4-like = *Olea europaea var. Sylvestris*
LOC111368078	-2,175769716	1,14E-04			XP_022845035.1	ALTERED XYLOGLUCAN 4-like = *Olea europaea var. Sylvestris*
LOC111379188			1,426042601	4,09E-17	XP_022858302.1	basic endochitinase-like = *Olea europaea var. Sylvestris*
LOC111367036			-1,57431532	5,35E-08	XP_022843486.1	beta-galactosidase 10 = *Olea europaea var. Sylvestris*
LOC111374877	-3,377308584	2,83E-01			XP_022853404.1	beta-galactosidase 13-like = *Olea europaea var. Sylvestris*
LOC111409129	-1,257081223	6,81E-01			XP_022894854.1	beta-galactosidase 16 = *Olea europaea var. Sylvestris*
LOC111380683	1,51605244	1,98E-10	1,370089838	8,37E-14	XP_022860081.1	beta-galactosidase 8 = *Olea europaea var. Sylvestris*
LOC111367696	-1,139689305	5,97E-06			XP_022844468.1	beta-galactosidase-like = *Olea europaea var. Sylvestris*
LOC111401551			1,969304912	9,44E-03	XP_022885106.1	beta-galactosidase-like = *Olea europaea var. Sylvestris*
LOC111369847	1,296676489	8,66E-12			XP_022847306.1	beta-glucosidase 10-like = *Olea europaea var. Sylvestris*
LOC111375992			1,480655117	3,10E-19	XP_022854687.1	beta-glucosidase 11-like =*Olea europaea var. Sylvestris*
LOC111412393			1,360805101	3,99E-14	XP_022899078.1	beta-glucosidase 11-like =*Olea europaea var. Sylvestris*
LOC111370760			-1,612963979	3,15E-05	XP_022848392.1	beta-glucosidase 18-like = *Olea europaea var. Sylvestris*
LOC111389452	1,023171426	1,02E-03	-1,863052147	3,45E-08	-	beta-glucosidase 18-like = *Olea europaea var. Sylvestris*
LOC111395689	-2,199736337	1,37E-16	1,375042323	2,05E-06	XP_022877573.1	beta-glucosidase 18-like = *Olea europaea var. Sylvestris*
LOC111407841			2,005180994	3,63E-03	XP_022893296.1	beta-glucosidase 24-like = *Olea europaea var. Sylvestris*
LOC111407848	-1,237410815	1,16E-02			XP_022893301.1	beta-glucosidase 24-like = *Olea europaea var. Sylvestris*
LOC111392261			2,325727202	5,46E-06	-	beta-glucosidase 34-like = *Olea europaea var. Sylvestris*
LOC111405238	-1,12383383	6,73E-03	2,1556798	1,23E-10	XP_022889809.1	beta-glucosidase 44-like = *Olea europaea var. Sylvestris*
LOC111386633			-1,554067596	5,13E-07	XP_022866868.1	beta-glucosidase 46-like = *Olea europaea var. Sylvestris*
LOC111395997	-1,745221158	3,06E-26			XP_022878014.1	beta-glucosidase 46-like = *Olea europaea var. Sylvestris*
LOC111382064			1,798634988	3,05E-04	XP_022861696.1	beta-glucosidase 6-like = *Olea europaea var. Sylvestris*
LOC111374590	-4,87249204	4,88E-44	1,600921726	3,92E-03	XP_022853054.1	beta-glucosidase-like = *Olea europaea var. Sylvestris*
LOC111378046	1,785327826	9,39E-04	4,039098999	2,10E-60	XP_022856975.1	beta-glucosidase-like = *Olea europaea var. Sylvestris*
LOC111381384			2,072782228	5,74E-08	XP_022860931.1	beta-glucosidase-like = *Olea europaea var. Sylvestris*
LOC111392048	-6,64762646	3,66E-49	2,164217172	3,06E-03	XP_022873099.1	beta-glucosidase-like = *Olea europaea var. Sylvestris*
LOC111392239	-4,723093672	4,59E-10	1,197023167	1,43E-04	XP_022873293.1	beta-glucosidase-like = *Olea europaea var. Sylvestris*
LOC111399799	-1,494972584	2,99E-10	-9,277840838	3,59E-10	XP_022883058.1	beta-glucosidase-like = *Olea europaea var. Sylvestris*
LOC111403814			-1,170626093	8,34E-09	XP_022888202.1	beta-glucosidase-like = *Olea europaea var. Sylvestris*
LOC111403824			5,457685188	3,49E-21	XP_022888218.1	beta-glucosidase-like = *Olea europaea var. Sylvestris*

LOC111404347	-2,083732992	4,43E-17	-2,488303788	3,35E-07	XP_022888932.1	beta-glucosidase-like = *Olea europaea var. Sylvestris*
LOC111407829	-2,298839497	4,17E-05	2,429110982	7,02E-06	XP_022893286.1	beta-glucosidase-like = *Olea europaea var. Sylvestris*
LOC111390423	-1,332011528	1,17E-02			XP_022871230.1	cellulose synthase A catalytic subunit 2 [UDP-forming]-like
LOC111377257	-2,203171831	3,44E-31			XP_022856087.1	cellulose synthase A catalytic subunit 2 [UDP-forming]-like = *Olea europaea var. Sylvestris*
LOC111410495	-2,026616436	4,82E-26			XP_022896619.1	cellulose synthase A catalytic subunit 3 [UDP-forming]-like = *Olea europaea var. Sylvestris*
LOC111397386	-2,105110061	3,26E-07			XP_022880055.1	cellulose synthase A catalytic subunit 6 [UDP-forming]-like = *Olea europaea var. Sylvestris*
LOC111366806	-2,647690436	9,81E-04			XP_022843270.1	CELLULOSE SYNTHASE INTERACTIVE 1-like = *Olea europaea var. Sylvestris*
LOC111376701	-1,00518735	2,85E-06			XP_022855441.1	CELLULOSE SYNTHASE INTERACTIVE 1-like = *Olea europaea var. Sylvestris*
LOC111385589	1,432515509	7,52E-07			XP_022865765.1	CELLULOSE SYNTHASE INTERACTIVE 3-like = *Olea europaea var. Sylvestris*
LOC111408123	-2,632850786	4,33E-36	-1,149927623	5,56E-04	XP_022893693.1	cellulose synthase-like protein D2 = *Olea europaea var. Sylvestris*
LOC111396367	-2,664160509	1,57E-65			XP_022878564.1	cellulose synthase-like protein D3 = *Olea europaea var. Sylvestris*
LOC111405683	-1,264145534	8,08E-03			XP_022890451.1	cellulose synthase-like protein D3 = *Olea europaea var. Sylvestris*
LOC111376857	-1,347087233	7,61E-06			XP_022855631.1	cellulose synthase-like protein E6 = *Olea europaea var. Sylvestris*
LOC111378473			3,740753903	2,84E-15	XP_022857450.1	cellulose synthase-like protein G2 = *Olea europaea var. Sylvestris*
LOC111384168			4,08711623	1,01E-12	XP_022864188.1	cellulose synthase-like protein G2 = *Olea europaea var. Sylvestris*
LOC111386708			2,735939465	1,02E-04	XP_022866941.1	cellulose synthase-like protein G2 = *Olea europaea var. Sylvestris*
LOC111393343			4,515978739	2,07E-24	XP_022874611.1	cellulose synthase-like protein G2 = *Olea europaea var. Sylvestris*
LOC111369641			3,511436636	6,29E-04	XP_022847003.1	chitinase 2-like = *Olea europaea var. Sylvestris*
LOC111369643			3,848178437	5,25E-03	XP_022847006.1	chitinase 2-like = *Olea europaea var. Sylvestris*
LOC111392080			2,008764552	1,12E-06	XP_022873127.1	chitinase-like protein 1 = *Olea europaea var. Sylvestris*
LOC111403475	1,776604802	2,13E-12	-5,239400995	6,19E-32	XP_022887760.1	endochitinase, basic endochitinase-like = *Olea europaea var. Sylvestris*
LOC111386313			2,806758104	5,74E-08	-	expansin-A1 =*Olea europaea var. Sylvestris*
LOC111376668			3,958674645	6,04E-11	XP_022855408.1	expansin-A11-like =*Olea europaea var. Sylvestris*
LOC111397180	1,71581243	2,61E-09			XP_022879718.1	expansin-A13 =*Olea europaea var. Sylvestris*
LOC111367160			2,25413	3,28E-05	XP_022843661.1	expansin-A15-like =*Olea europaea var. Sylvestris*
LOC111381719	1,125875399	8,29E-03	-4,157842665	1,44E-09	XP_022861297.1	expansin-A15-like =*Olea europaea var. Sylvestris*
LOC111403335	1,14880954	4,95E-05			XP_022887560.1	expansin-A15-like =*Olea europaea var. Sylvestris*
LOC111393522	1,432394225	6,72E-04			XP_022874855.1	expansin-A4-like = *Olea europaea var. Sylvestris*
LOC111390026			1,561734876	5,17E-03	XP_022870782.1	expansin-A6-like = *Olea europaea var. Sylvestris*
LOC111377178			2,424531987	5,91E-03	XP_022856000.1	expansin-A8-like = *Olea europaea var. Sylvestris*
LOC111384671	1,938784795	1,91E-07	2,73883079	2,74E-35	XP_022864754.1	expansin-A8-like = *Olea europaea var. Sylvestris*
LOC111385342	2,047686751	8,07E-03	2,76556506	9,98E-16	XP_022865492.1	expansin-A8-like = *Olea europaea var. Sylvestris*
LOC111393373	1,67132695	3,37E-03			XP_022874649.1	expansin-A8-like = *Olea europaea var. Sylvestris*
LOC111397188	3,639769208	2,02E-04	5,462708694	4,22E-102	XP_022879735.1	expansin-A8-like = *Olea europaea var. Sylvestris*
LOC111383091	1,353178472	8,20E-05	-2,235680168	8,16E-10	XP_022862931.1	expansin-B15-like =*Olea europaea var. Sylvestris*
LOC111412123	-2,908314351	1,30E-77			XP_022898668.1	expansin-like A2 = *Olea europaea var. Sylvestris*
LOC111396337			-2,239123496	3,10E-09	XP_022878514.1	Extensin, leucine-rich repeat extensin-like protein 3 = *Olea europaea var. Sylvestris*

LOC111399045			-1,904151506	4,28E-06	XP_022882025.1	extensin, leucine-rich repeat extensin-like protein 3 = *Olea europaea var. Sylvestris*
LOC111411363	-2,723674854	2,10E-22			XP_022897674.1	extensin, leucine-rich repeat extensin-like protein 4 = *Olea europaea var. Sylvestris*
LOC111374382			-2,276771871	6,25E-06	XP_022852815.1	extensin-2-like = *Olea europaea var. Sylvestris*
LOC111393866			-1,889250965	9,08E-13	XP_022875386.1	extensin-2-like = *Olea europaea var. Sylvestris*
LOC111393113			-2,286373756	1,36E-26	XP_022874278.1	extensin-3-like = *Olea europaea var. Sylvestris*
LOC111408744			-7,046002594	1,09E-06	XP_022894274.1	extensin-3-like = *Olea europaea var. Sylvestris*
LOC111385698			3,20305005	2,59E-16	XP_022865890.1	extensin-like = *Olea europaea var. Sylvestris*
LOC111411993	1,237034428	8,96E-05			XP_022898478.1	extensin-like = *Olea europaea var. Sylvestris*
LOC111401169			-2,013543807	1,17E-06	XP_022884550.1	glucan 1,3-beta-glucosidase A = *Olea europaea var. Sylvestris*
LOC111387578			1,251264979	1,11E-02	XP_022867920.1	glucan endo-1,3-beta-glucosidase 11-like = *Olea europaea var. Sylvestris*
LOC111372286			3,424142441	3,44E-11	XP_022850312.1	glucan endo-1,3-beta-glucosidase 12-like = *Olea europaea var. Sylvestris*
LOC111395521	-1,419402944	1,04E-03			XP_022877311.1	glucan endo-1,3-beta-glucosidase 12-like = *Olea europaea var. Sylvestris*
LOC111376511			2,021299027	5,23E-04	XP_022855243.1	glucan endo-1,3-beta-glucosidase 13-like = *Olea europaea var. Sylvestris*
LOC111379504			1,773448364	8,48E-13	XP_022858657.1	glucan endo-1,3-beta-glucosidase 14 = *Olea europaea var. Sylvestris*
LOC111368800	3,785813479	8,20E-17			XP_022846026.1	glucan endo-1,3-beta-glucosidase 14-like = *Olea europaea var. Sylvestris*
LOC111373146			-4,245099643	5,37E-11	XP_022851396.1	glucan endo-1,3-beta-glucosidase 14-like = *Olea europaea var. Sylvestris*
LOC111386598			2,851484084	5,09E-08	XP_022866836.1	glucan endo-1,3-beta-glucosidase 14-like = *Olea europaea var. Sylvestris*
LOC111374604	1,399543151	2,42E-03	-2,619936815	3,64E-07	XP_022853068.1	glucan endo-1,3-beta-glucosidase 3-like = *Olea europaea var. Sylvestris*
LOC111367480	-1,062454401	8,59E-05	-1,290499501	2,72E-04	XP_022844153.1	glucan endo-1,3-beta-glucosidase 4-like = *Olea europaea var. Sylvestris*
LOC111396902	1,246503992	3,82E-03			XP_022879272.1	glucan endo-1,3-beta-glucosidase 5 = *Olea europaea var. Sylvestris*
LOC111399482	1,397106308	2,45E-03			XP_022882595.1	glucan endo-1,3-beta-glucosidase 8-like = *Olea europaea var. Sylvestris*
LOC111382545	-1,840110028	3,82E-07			XP_022862332.1	glucan endo-1,3-beta-glucosidase A6 = *Olea europaea var. Sylvestris*
LOC111378392			1,732502548	6,02E-26	XP_022857353.1	glucan endo-1,3-beta-glucosidase, acidic-like (BG2)
LOC111378441			-2,433846244	1,12E-35	XP_022857406.1	glucan endo-1,3-beta-glucosidase, acidic-like = *Olea europaea var. Sylvestris*
LOC111386074			-1,524482027	5,09E-19	XP_022866268.1	glucan endo-1,3-beta-glucosidase, acidic-like = *Olea europaea var. Sylvestris*
LOC111410017			-3,118405755	3,68E-16	XP_022895940.1	glucan endo-1,3-beta-glucosidase, acidic-like = *Olea europaea var. Sylvestris*
LOC111406014	-2,535225411	3,29E-62			XP_022890945.1	glucan endo-1,3-beta-glucosidase-like = *Olea europaea var. Sylvestris*
LOC111373520			4,359005346	3,62E-05	XP_022851829.1	glucomannan 4-beta-mannosyltransferase 1-like = *Olea europaea var. Sylvestris*
LOC111379915			1,723052065	4,72E-09	XP_022859127.1	glucomannan 4-beta-mannosyltransferase 2-like = *Olea europaea var. Sylvestris*
LOC111412010			2,364270364	7,98E-05	XP_022898505.1	glucomannan 4-beta-mannosyltransferase 2-like = *Olea europaea var. Sylvestris*
LOC111371253			-4,649219641	1,43E-04	XP_022848908.1	laccase-12-like = *Olea europaea var. Sylvestris*
LOC111380004			-5,795868688	1,29E-04	XP_022859235.1	laccase-12-like = *Olea europaea var. Sylvestris*
LOC111397597			-5,091886121	7,92E-03	XP_022880370.1	laccase-12-like = *Olea europaea var. Sylvestris*
LOC111397611			-5,574781306	1,92E-03	XP_022880385.1	laccase-12-like = *Olea europaea var. Sylvestris*
LOC111408786			-5,123865371	7,61E-03	XP_022894322.1	laccase-14-like = *Olea europaea var. Sylvestris*
LOC111397819			2,41171314	1,54E-41	XP_022880563.1	laccase-15-like = *Olea europaea var. Sylvestris*
LOC111408785			1,64383932	3,02E-27	XP_022894321.1	laccase-15-like = *Olea europaea var. Sylvestris*
LOC111402017	1,169341072	1,23E-07	1,111454207	7,86E-10	XP_022885802.1	mannan endo-1,4-beta-mannosidase 7 = *Olea europaea var. Sylvestris*

LOC111397355	1,495516992	1,65E-04	-2,683620462	6,41E-09	XP_022880016.1	mannan endo-1,4-beta-mannosidase 7-like = *Olea europaea var. Sylvestris*
LOC111382253			1,773944895	3,36E-11	XP_022861935.1	pectin acetylesterase 12-like = *Olea europaea var. Sylvestris*
LOC111388172			1,192917603	7,35E-05	XP_022868623.1	pectin acetylesterase 12-like = *Olea europaea var. Sylvestris*
LOC111380396			1,906288817	3,42E-08	-	pectin acetylesterase 8-like = *Olea europaea var. Sylvestris*
LOC111386375	1,603780356	7,95E-03	2,001207169	1,23E-09	-	pectin acetylesterase 8-like = *Olea europaea var. Sylvestris*
LOC111391823			1,412871149	9,51E-16	-	pectin acetylesterase 8-like = *Olea europaea var. Sylvestris*
LOC111373962	-2,292460081	2,91E-16			XP_022852332.1	pectin methyltransferase QUA2 = *Olea europaea var. Sylvestris*
LOC111408847	-1,721622136	1,36E-25			XP_022894425.1	pectin methyltransferase QUA2 = Olea europaea var. Sylvestris
LOC111367315	-1,770120433	1,60E-26			XP_022843895.1	pectinesterase 1-like = *Olea europaea var. Sylvestris*
LOC111401482	-4,586199872	2,61E-08			XP_022884988.1	pectinesterase 1-like = *Olea europaea var. Sylvestris*
LOC111402506			-1,408845214	4,81E-05	XP_022886639.1	pectinesterase 2.1-like = *Olea europaea var. Sylvestris*
LOC111377531			2,158730367	4,42E-11	XP_022856426.1	pectinesterase inhibitor 9-like = *Olea europaea var. Sylvestris*
LOC111366086	2,12620927	6,93E-04	-1,569479287	3,35E-03	XP_022842507.1	pectinesterase/pectinesterase inhibitor 12 =*Olea europaea var. Sylvestris*
LOC111404698	1,599024932	1,27E-03			XP_022889233.1	pectinesterase/pectinesterase inhibitor 12 =*Olea europaea var. Sylvestris*
LOC111386790			1,542447116	4,02E-04	XP_022867034.1	pectinesterase/pectinesterase inhibitor 34 = *Olea europaea var. Sylvestris*
LOC111384532	1,689605776	1,04E-07			XP_022864586.1	pectinesterase/pectinesterase inhibitor 61 =*Olea europaea var. Sylvestris*
LOC111366821			1,521384268	1,15E-11	XP_022843285.1	pectinesterase/pectinesterase inhibitor U1-like =*Olea europaea var. Sylvestris*
LOC111403367			2,194573812	2,01E-29	XP_022887658.1	pectinesterase-like = *Olea europaea var. Sylvestris*
LOC111394001			1,62928319	4,81E-20	XP_022875561.1	polygalacturonase = *Olea europaea var. Sylvestris*
LOC111401119	-2,229758467	1,84E-14			XP_022884463.1	polygalacturonase = *Olea europaea var. Sylvestris*
LOC111403557	1,210243841	2,13E-06			XP_022887880.1	polygalacturonase = *Olea europaea var. Sylvestris*
LOC111404295			-2,15111266	5,25E-03	XP_022888892.1	polygalacturonase = *Olea europaea var. Sylvestris*
LOC111411713	1,969133956	5,77E-28	-1,540829316	2,89E-19	XP_022898049.1	polygalacturonase = *Olea europaea var. Sylvestris*
LOC111410938			5,507787869	3,92E-03	XP_022897298.1	polygalacturonase At1g48100-like = *Olea europaea var. Sylvestris*
LOC111411375			3,913909324	5,62E-05	XP_022897680.1	polygalacturonase inhibitor 1-like = *Olea europaea var. Sylvestris*
LOC111382119	1,335398902	3,34E-04	-3,974125923	6,35E-14	XP_022861759.1	polygalacturonase inhibitor-like = *Olea europaea var. Sylvestris*
LOC111373356	4,828099873	4,14E-03	-3,242594614	4,51E-03	XP_022851645.1	polygalacturonase-1 non-catalytic subunit beta-like = *Olea europaea var. Sylvestris*
LOC111377599			-5,3656396	4,73E-03	XP_022856498.1	polygalacturonase-like = *Olea europaea var. Sylvestris*
LOC111396326			-5,449553969	3,44E-03	XP_022878501.1	polygalacturonase-like = *Olea europaea var. Sylvestris*
LOC111396344	-2,881253202	1,12E-12			XP_022878525.1	trifunctional UDP-glucose 4,6-dehydratase/UDP-4-keto-6-deoxy-D-glucose 3,5-epimerase/UDP-4-keto-L-rhamnose-reductase RHM2-like = *Olea europaea var. Sylvestris*
LOC111371080	-1,432292966	1,46E-13			XP_022848762.1	xyloglucan 6-xylosyltransferase 2-like = *Olea europaea var. Sylvestris*
LOC111384804	-1,450692495	2,87E-11			-	xyloglucan 6-xylosyltransferase 2-like = *Olea europaea var. Sylvestris*
LOC111367983	-1,474189205	4,57E-15			XP_022844909.1	xyloglucan 6-xylosyltransferase 5 = *Olea europaea var. Sylvestris*
LOC111370995	-2,600326941	4,35E-29	2,541697063	5,22E-28	XP_022848695.1	xyloglucan endotransglucosylase/hydrolase 2-like = *Olea europaea var. Sylvestris*
LOC111370996	-2,54878484	4,30E-08			XP_022848696.1	xyloglucan endotransglucosylase/hydrolase 2-like = *Olea europaea var. Sylvestris*
LOC111370998	-2,521254663	1,53E-19			XP_022848697.1	xyloglucan endotransglucosylase/hydrolase 2-like = *Olea europaea var. Sylvestris*

LOC111395523	-3,435965084	2,45E-12			XP_022877313.1	xyloglucan endotransglucosylase/hydrolase 2-like = *Olea europaea var. Sylvestris*
LOC111395524	-3,756568568	3,47E-21			XP_022877314.1	xyloglucan endotransglucosylase/hydrolase 2-like = *Olea europaea var. Sylvestris*
LOC111387288			-1,300951008	1,44E-03	XP_022867600.1	xyloglucan endotransglucosylase/hydrolase protein 22-like = *Olea europaea var. Sylvestris*
LOC111391439	-3,178681972	8,83E-64			XP_022872431.1	xyloglucan endotransglucosylase/hydrolase protein 23 = *Olea europaea var. Sylvestris*
LOC111391445	-2,745013371	1,47E-50			XP_022872439.1	xyloglucan endotransglucosylase/hydrolase protein 23 = *Olea europaea var. Sylvestris*
LOC111391451	-2,811285994	1,58E-16			XP_022872444.1	xyloglucan endotransglucosylase/hydrolase protein 23 = *Olea europaea var. Sylvestris*
LOC111385517	-1,649309329	8,39E-15			XP_022865681.1	xyloglucan endotransglucosylase/hydrolase protein 23 = *Olea europaea var. Sylvestris*
LOC111385523	-3,257817606	5,00E-74			-	xyloglucan endotransglucosylase/hydrolase protein 23 = *Olea europaea var. Sylvestris*
LOC111387295	2,039651592	7,15E-33			XP_022867613.1	xyloglucan endotransglucosylase/hydrolase protein 23 = *Olea europaea var. Sylvestris*
LOC111399252	1,48673082	4,98E-15	-1,610827166	2,58E-16	XP_022882288.1	xyloglucan endotransglucosylase/hydrolase protein 28 = *Olea europaea var. Sylvestris*
LOC111381242	-1,411073267	3,91E-09	-9,182447489	5,79E-10	XP_022860765.1	xyloglucan endotransglucosylase/hydrolase protein 30 = *Olea europaea var. Sylvestris*
LOC111382429			-1,839312808	5,81E-13	XP_022862171.1	xyloglucan endotransglucosylase/hydrolase protein 31-like =*Olea europaea var. Sylvestris*
LOC111367276	2,603340538	2,68E-14	-4,537635745	4,24E-22	XP_022843825.1	xyloglucan endotransglucosylase/hydrolase protein 6 = *Olea europaea var. Sylvestris*
LOC111408989			4,427767363	4,72E-14	XP_022894638.1	xyloglucan endotransglucosylase/hydrolase protein 7 = *Olea europaea var. Sylvestris*
LOC111397229	1,236281552	6,27E-05	1,288615774	9,33E-09	XP_022879818.1	xyloglucan endotransglucosylase/hydrolase protein 7 = *Olea europaea var. Sylvestris*
LOC111370402			1,456068256	3,18E-04	XP_022847859.1	xyloglucan endotransglucosylase/hydrolase protein 9-like = *Olea europaea var. Sylvestris*
LOC111405825	1,049588562	4,98E-03			XP_022890649.1	xyloglucan galactosyltransferase MUR3-like = *Olea europaea var. Sylvestris*
LOC111376073	2,027172612	1,38E-07			XP_022854768.1	xyloglucan galactosyltransferase XLT2-like = *Olea europaea var. Sylvestris*
LOC111371769	-1,950065021	2,21E-22			XP_022849689.1	xyloglucan glycosyltransferase 12 = *Olea europaea var. Sylvestris*
LOC111384947	-1,577379685	4,99E-05			XP_022865062.1	xyloglucan glycosyltransferase 12 = *Olea europaea var. Sylvestris*
LOC111368079			3,887197675	2,21E-11	XP_022845037.1	xyloglucan glycosyltransferase 4-like = *Olea europaea var. Sylvestris*
LOC111400143	-2,424168496	7,50E-13			XP_022883348.1	xyloglucan glycosyltransferase 4-like = *Olea europaea var. Sylvestris*
LOC111375465	2,304539301	0,0002877			XP_022854059.1	endoglucanase 6-like = *Olea europaea var. Sylvestris*

LOC111382086	-2,542247715	-1,24E+01			XP_022861725.1	endoglucanase 25-like = *Olea europaea var. Sylvestris*
LOC111384540	-1,848592798	-1,00E+01			XP_022864594.1	endoglucanase 25-like = *Olea europaea var. Sylvestris*
LOC111387565	1,405435535	8,70E-07			XP_022867905.1	endoglucanase 1-like = *Olea europaea var. Sylvestris*
LOC111398562	1,742044804	0,0071994			XP_022881291.1	endoglucanase-like = *Olea europaea var. Sylvestris*
LOC111382362			1,221663327	1,09E-14	XP_022862078.1	endoglucanase 25-like = *Olea europaea var. Sylvestris*
LOC111371180			1,047379308	5,81E-07	XP_022848852.1	endoglucanase-like = *Olea europaea var. Sylvestris*
LOC111374207			1,289408849	0,0049883	XP_022852619.1	endoglucanase 11-like =*Olea europaea var. Sylvestris*
LOC111382086			1,895804214	1,17E-21	XP_022861725.1	endoglucanase 25-like = *Olea europaea var. Sylvestris*
LOC111386003			2,374159209	0,0031007	XP_022866199.1	endoglucanase 8-like = *Olea europaea var. Sylvestris*
LOC111367161	-1,749694498	1,29E-05	1,330887105	0,0013184	XP_022843666.1	fasciclin-like arabinogalactan protein 16 = *Olea europaea var. Sylvestris*
LOC111368158	-1,831884514	9,30E-13			XP_022845161.1	classical arabinogalactan protein 4-like = *Olea europaea var. Sylvestris*
LOC111376077	-1,731641536	1,88E-12			XP_022854773.1	lysine-rich arabinogalactan protein 18-like = *Olea europaea var. Sylvestris*
LOC111378787	-3,027223361	1,28E-05	2,258442168	0,0035787	XP_022857804.1	fasciclin-like arabinogalactan protein 16 =*Olea europaea var. Sylvestris*
LOC111386384	1,156289033	6,48E-05			XP_022866610.1	lysine-rich arabinogalactan protein 19 = *Olea europaea var. Sylvestris*
LOC111390511	-1,73438668	1,76E-13			XP_022871328.1	classical arabinogalactan protein 4-like = *Olea europaea var. Sylvestris*
LOC111391262	-2,04760408	3,77E-22			XP_022872206.1	classical arabinogalactan protein 9-like = *Olea europaea var. Sylvestris*
LOC111400351	-1,214022203	0,0021563			XP_022883534.1	classical arabinogalactan protein 10-like = *Olea europaea var. Sylvestris*
LOC111412283	-1,800518888	2,76E-26			XP_022898911.1	fasciclin-like arabinogalactan protein 17 =*Olea europaea var. Sylvestris*
LOC111375830			1,625986544	0,0089459	XP_022854510.1	classical arabinogalactan protein 9-like = *Olea europaea var. Sylvestris*
LOC111377703			1,98918682	0,0011387	XP_022856601.1	classical arabinogalactan protein 9-like = *Olea europaea var. Sylvestris*

Table 3II. S12. Transport-related genes induced or repressed in the first comparison (d18:0-AZ vs. C-AZ) and the second comparison (d18:0-LAZ vs. d18:0-AZ).

Fruit AZ d18:0 vs Fruit Az Control					
Gene	**log2FoldChange**	**FoldChange**	**pvalue**	**Gene_ID**	**Description**
Sugar transporter					
LOC111367368	-1,971739902	-3,922408795	8,19E-12	XP_022843973.1	sugar transporter ERD6-like 16 = *Olea europaea var. Sylvestris*
LOC111375915	-1,821298347	-3,533990953	9,39E-10	XP_022854600.1	bidirectional sugar transporter N3-like = *Olea europaea var. Sylvestris*
LOC111373172	1,972950124	3,925700535	7,05E-04	XP_022851443.1	bidirectional sugar transporter SWEET1-like = *Olea europaea var. Sylvestris*
LOC111408733	1,269309843	2,410462261	3,14E-04	XP_022894260.1	bidirectional sugar transporter SWEET1-like = *Olea europaea var. Sylvestris*
LOC111366010	-1,176580354	-2,260403541	2,27E-05	XP_022842389.1	CMP-sialic acid transporter 4-like = *Olea europaea var. Sylvestris*
LOC111380085	2,377338118	5,195771978	1,05E-05	XP_022859317.1	probable sugar phosphate/phosphate translocator At2g25520 = *Olea europaea var. Sylvestris*
LOC111390674	-1,7283834	-3,313563115	1,62E-07	XP_022871508.1	probable sugar phosphate/phosphate translocator At3g11320 =*Olea europaea var. Sylvestris*
LOC111405471	-1,805887065	-3,496440767	1,48E-15	XP_022890136.1	probable sugar phosphate/phosphate translocator At3g11320 =*Olea europaea var. Sylvestris*
N transporter					
LOC111399552	-1,191069499	-2,283219402	3,82E-06	XP_022882712.1	amino acid transporter AVT1A-like = *Olea europaea var. Sylvestris*
LOC111384357	-2,024369355	-4,068140074	3,73E-06	XP_022864395.1	amino acid transporter AVT1H = *Olea europaea var. Sylvestris*
LOC111384886	-3,842544964	-14,34568511	3,94E-63	XP_022864995.1	amino acid transporter AVT1I-like = *Olea europaea var. Sylvestris*
LOC111401237	-1,057369846	-2,081133979	1,18E-06	XP_022884652.1	amino acid transporter AVT3B-like = *Olea europaea var. Sylvestris*
LOC111390214	-1,551404161	-2,931022739	5,88E-20	XP_022870989.1	amino acid transporter AVT6A-like = *Olea europaea var. Sylvestris*
LOC111399635	-2,2393992	-4,722003792	6,94E-25	XP_022882870.1	amino acid transporter AVT6C-like = *Olea europaea var. Sylvestris*
LOC111412340	1,065593546	2,093030806	4,23E-03	XP_022898994.1	cationic amino acid transporter 1-like = *Olea europaea var. Sylvestris*
LOC111396839	1,408062943	2,653806061	5,42E-13	XP_022879145.1	cationic amino acid transporter 5 = *Olea europaea var. Sylvestris*
LOC111394626	-1,089570049	-2,128106053	6,11E-03	XP_022876303.1	cationic amino acid transporter 6, chloroplastic-like = *Olea europaea var. Sylvestris*
LOC111378745	-1,06308562	-2,089395522	3,15E-04	XP_022857751.1	adenine/guanine permease AZG1-like = *Olea europaea var. Sylvestris*
Aquaporin					
LOC111368644	-2,722307731	-6,599275882	1,35E-10	XP_022845778.1	probable aquaporin PIP1-4 = *Olea europaea var. Sylvestris*
LOC111368645	-2,581588569	-5,985984609	8,48E-39	XP_022845779.1	probable aquaporin PIP1-4 = *Olea europaea var. Sylvestris*
LOC111372815	1,613586696	3,06011675	5,09E-17	XP_022850991.1	aquaporin PIP2-2-like = *Olea europaea var. Sylvestris*
LOC111384792	2,98394542	7,911468021	2,09E-54	XP_022864884.1	aquaporin TIP1-1-like =*Olea europaea var. Sylvestris*
LOC111393963	2,069481283	4,197357314	4,51E-24	XP_022875523.1	aquaporin TIP1-1-like =*Olea europaea var. Sylvestris*

LOC111371488	-2,396846633	-5,266507798	1,68E-35	XP_022849284.1	aquaporin TIP2-1-like = *Olea europaea var. Sylvestris*
LOC111371374	-1,649074651	-3,136324098	2,70E-03	XP_022849083.1	probable aquaporin TIP1-2 = *Olea europaea var. Sylvestris*
LOC111393814	2,858670791	7,25346727	6,68E-04	XP_022875299.1	probable aquaporin TIP1-2 = *Olea europaea var. Sylvestris*
LOC111367323	-1,160334341	-2,235092193	1,58E-06	XP_022843902.1	probable aquaporin NIP5-1 = *Olea europaea var. Sylvestris*
LOC111399587	-1,819186981	-3,528822784	3,26E-23	XP_022882754.1	probable aquaporin SIP2-1 = *Olea europaea var. Sylvestris*
ABC transporter					
LOC111369421	1,177840606	2,262378957	1,76E-06	XP_022846703.1	ABC transporter B family member 1 = *Olea europaea var. Sylvestris*
LOC111392163	1,426366046	2,687688695	4,58E-03	XP_022873197.1	ABC transporter B family member 13-like = *Olea europaea var. Sylvestris*
LOC111367970	-3,544259424	-11,66617264	1,62E-12	XP_022844890.1	ABC transporter B family member 19 = *Olea europaea var. Sylvestris*
LOC111404369	1,357587611	2,562563244	3,77E-06	XP_022888953.1	ABC transporter B family member 1-like = *Olea europaea var. Sylvestris*
LOC111393482	-2,006822431	-4,018960593	1,40E-17	XP_022874797.1	ABC transporter B family member 25, mitochondrial-like = *Olea europaea var. Sylvestris*
LOC111382409	-1,846115253	-3,595307714	2,27E-13	XP_022862148.1	ABC transporter B family member 26, chloroplastic = *Olea europaea var. Sylvestris*
LOC111393913	1,076754393	2,109285515	8,40E-03	XP_022875454.1	ABC transporter B family member 2-like = *Olea europaea var. Sylvestris*
LOC111408119	1,429300267	2,693160606	3,09E-08	XP_022893683.1	ABC transporter B family member 2-like = *Olea europaea var. Sylvestris*
LOC111401143	-1,072265624	-2,10273293	4,70E-05	XP_022884513.1	ABC transporter D family member 1 = *Olea europaea var. Sylvestris*
LOC111367539	-1,712862336	-3,278105614	4,54E-22	XP_022844245.1	ABC transporter G family member 11-like = *Olea europaea var. Sylvestris*
LOC111387110	1,172096799	2,253389646	2,30E-03	XP_022867397.1	ABC transporter G family member 15-like = *Olea europaea var. Sylvestris*
LOC111399771	-1,222746552	-2,333906155	1,10E-03	XP_022883015.1	ABC transporter G family member 22-like = *Olea europaea var. Sylvestris*
LOC111379070	1,505745075	2,839712895	3,25E-03	XP_022858163.1	ABC transporter G family member 25-like = *Olea europaea var. Sylvestris*
LOC111366880	-1,290801642	-2,446639667	5,74E-13	XP_022843334.1	ABC transporter G family member 35-like = *Olea europaea var. Sylvestris*
LOC111397930	-3,003285252	-8,018238065	3,71E-03	XP_022880662.1	ABC transporter G family member 5-like = *Olea europaea var. Sylvestris*
LOC111397801	-1,001738457	-2,002411466	6,47E-05	XP_022880548.1	ABC transporter I family member 21-like = *Olea europaea var. Sylvestris*
Metal transporter					
LOC111382535	1,122540907	2,177301062	3,01E-04	XP_022862317.1	urease accessory protein F = *Olea europaea var. Sylvestris*
LOC111379061	-1,543545573	-2,9151004	3,24E-03	XP_022858158.1	metal transporter Nramp2-like = *Olea europaea var. Sylvestris*
LOC111400554	-1,448112162	-2,72850779	2,56E-08	XP_022883728.1	metal transporter Nramp3-like = *Olea europaea var. Sylvestris*
LOC111408460	1,128109524	2,185721403	1,67E-11	XP_022893983.1	metal-nicotianamine transporter YSL1-like = *Olea europaea var. Sylvestris*
LOC111405418	1,177509349	2,261859551	1,90E-12	XP_022890050.1	probable metal-nicotianamine transporter YSL5 = *Olea europaea var. Sylvestris*

LOC111405419	1,573928326	2,9771426	5,35E-12	XP_022890051.1	probable metal-nicotianamine transporter YSL5 = *Olea europaea var. Sylvestris*
LOC111401214	-1,650184812	-3,138738444	1,61E-19	XP_022884614.1	probable metal-nicotianamine transporter YSL7 = *Olea europaea var. Sylvestris*
LOC111374645	1,976272733	3,934752069	1,19E-40	XP_022853126.1	heavy metal-associated isoprenylated plant protein 3-like = *Olea europaea var. Sylvestris*
LOC111378486	-1,877781883	-3,675095865	4,60E-08	XP_022857466.1	heavy metal-associated isoprenylated plant protein 3-like = *Olea europaea var. Sylvestris*
LOC111392166	-1,034757288	-2,048768942	1,10E-03	XP_022873201.1	heavy metal-associated isoprenylated plant protein 6-like = *Olea europaea var. Sylvestris*
LOC111410120	1,05008465	2,07065134	2,03E-09	XP_022896093.1	heavy metal-associated isoprenylated plant protein 26-like = *Olea europaea var. Sylvestris*
LOC111410041	1,322313102	2,500667255	3,58E-03	XP_022895965.1	heavy metal-associated isoprenylated plant protein 32-like = *Olea europaea var. Sylvestris*
LOC111378313	-1,019637362	-2,027409282	1,07E-06	XP_022857252.1	heavy metal-associated isoprenylated plant protein 39-like = *Olea europaea var. Sylvestris*
LOC111411710	1,445406004	2,723394545	4,59E-13	XP_022898042.1	heavy metal-associated isoprenylated plant protein 39-like = *Olea europaea var. Sylvestris*
LOC111385041	-1,991026128	-3,975196366	8,06E-27	XP_022865173.1	heavy metal-associated isoprenylated plant protein 39-like = *Olea europaea var. Sylvestris*
LOC111370984	-1,322238778	-2,500538431	2,02E-16	XP_022848679.1	heavy metal-associated isoprenylated plant protein 46-like = *Olea europaea var. Sylvestris*
LOC111370701	1,68039666	3,205160629	1,06E-23	XP_022848307.1	zinc transporter 1-like = *Olea europaea var. Sylvestris*
LOC111395859	1,413013811	2,662928719	1,07E-19	XP_022877827.1	zinc transporter 1-like = *Olea europaea var. Sylvestris*
LOC111397591	1,261125011	2,396825721	1,07E-11	XP_022880355.1	zinc transporter 4, chloroplastic = *Olea europaea var. Sylvestris*
LOC111372340	-1,403703139	-2,645798402	1,09E-10	XP_022850398.1	zinc transporter 5-like = *Olea europaea var. Sylvestris*
LOC111388858	-2,014430301	-4,040210052	1,34E-26	XP_022869437.1	putative zinc transporter At3g08650 = *Olea europaea var. Sylvestris*
LOC111404607	-3,60341909	-12,15450378	6,29E-06	XP_022889160.1	cadmium/zinc-transporting ATPase HMA3-like = *Olea europaea var. Sylvestris*
Nutrient transporter					
LOC111367244	-1,938027568	-3,831814092	1,87E-30	XP_022843776.1	calcium-transporting ATPase 2, plasma membrane-type-like = *Olea europaea var. Sylvestris*
LOC111402136	-3,386956024	-10,46105191	3,79E-20	XP_022885993.1	calcium-transporting ATPase 2, plasma membrane-type-like = *Olea europaea var. Sylvestris*
LOC111407715	-1,284459585	-2,435907896	1,49E-15	XP_022893126.1	calcium-transporting ATPase 4, endoplasmic reticulum-type-like = *Olea europaea var. Sylvestris*
LOC111410467	2,050985795	4,143890253	1,13E-06	XP_022896585.1	calcium-transporting ATPase 4, plasma membrane-type-like = *Olea europaea var. Sylvestris*
LOC111389070	-1,196650887	-2,292069654	4,56E-04	XP_022869691.1	calcium-transporting ATPase 5, plasma membrane-type-like = *Olea europaea var. Sylvestris*
LOC111411632	-1,136811043	-2,198944273	1,55E-04	XP_022897918.1	calcium-transporting ATPase 5, plasma membrane-type-like = *Olea europaea var. Sylvestris*
LOC111389071	-1,24508389	-2,370323368	6,09E-03	XP_022869692.1	calcium-transporting ATPase 8, plasma membrane-type-like = *Olea europaea var. Sylvestris*
LOC111399650	-1,906100526	-3,747946934	1,46E-33	XP_022882853.1	putative calcium-transporting ATPase 11, plasma membrane-type = *Olea europaea var. Sylvestris*
LOC111369013	-1,465130672	-2,760884763	1,53E-03	XP_022846270.1	calcium-transporting ATPase 12, plasma membrane-type-like = *Olea europaea var. Sylvestris*
LOC111397563	-1,486710133	-2,802491763	2,87E-09	XP_022880322.1	calcium-transporting ATPase 12, plasma membrane-type-like = *Olea europaea var. Sylvestris*

LOC111397566	-2,021916545	-4,061229468	7,18E-14	XP_022880325.1	calcium-transporting ATPase 12, plasma membrane-type-like = *Olea europaea var. Sylvestris*
LOC111391497	-1,321868069	-2,499895985	5,56E-03	XP_022872498.1	putative calcium-transporting ATPase 13, plasma membrane-type = *Olea europaea var. Sylvestris*
LOC111396588	-2,078831624	-4,224649418	1,23E-18	XP_022878764.1	putative calcium-transporting ATPase 13, plasma membrane-type = *Olea europaea var. Sylvestris*
LOC111372921	-2,664287466	-6,339141476	3,74E-17	XP_022851117.1	copper-transporting ATPase PAA2, chloroplastic-like = *Olea europaea var. Sylvestris*
LOC111380084	-2,123499529	-4,357496572	8,85E-27	XP_022859316.1	copper-transporting ATPase PAA2, chloroplastic-like = *Olea europaea var. Sylvestris*
LOC111387524	-2,107645358	-4,309873	1,71E-18	XP_022867861.1	copper-transporting ATPase RAN1-like = *Olea europaea var. Sylvestris*
LOC111407284	-3,002518769	-8,013979219	5,33E-18	XP_022892439.1	copper-transporting ATPase RAN1-like = *Olea europaea var. Sylvestris*
LOC111367293	-2,303011017	-4,934866363	2,45E-22	XP_022843864.1	probable sulfate transporter 3.4 = *Olea europaea var. Sylvestris*
LOC111406275	-1,06564501	-2,09310547	4,82E-07	XP_022891378.1	probable sulfate transporter 3.4 = *Olea europaea var. Sylvestris*
LOC111405391	-1,809734883	-3,505778586	2,09E-13	XP_022890015.1	sulfate transporter 4.1, chloroplastic-like = *Olea europaea var. Sylvestris*
LOC111405347	-3,047319653	-8,266746532	2,45E-10	XP_022889943.1	organic cation/carnitine transporter 1 = *Olea europaea var. Sylvestris*
LOC111382262	-3,818816237	-14,11166426	1,31E-04	XP_022861947.1	organic cation/carnitine transporter 3-like = *Olea europaea var. Sylvestris*
LOC111395699	-1,199798428	-2,297075742	3,92E-03	XP_022877587.1	cyclic nucleotide-gated ion channel 4-like = *Olea europaea var. Sylvestris*
LOC111386290	1,107890515	2,155302719	1,19E-07	XP_022866774.1	potassium transporter 2-like = *Olea europaea var. Sylvestris*
LOC111393563	-1,254186518	-2,385326111	3,36E-13	XP_022874923.1	potassium transporter 4-like = *Olea europaea var. Sylvestris*
LOC111396132	-2,038755967	-4,108910672	2,58E-20	XP_022878211.1	potassium transporter 6-like = *Olea europaea var. Sylvestris*
LOC111403345	1,316048273	2,48983178	9,98E-07	XP_022887579.1	potassium transporter 6-like = *Olea europaea var. Sylvestris*
LOC111405956	-1,723311808	-3,301935201	1,14E-25	XP_022890860.1	ferritin-1, chloroplastic-like = *Olea europaea var. Sylvestris*
LOC111392534	-1,881510533	-3,684606446	1,72E-34	XP_022873666.1	ferritin-3, chloroplastic-like = *Olea europaea var. Sylvestris*
LOC111398222	-1,902442908	-3,73845692	7,08E-12	XP_022880923.1	ferritin-3, chloroplastic-like = *Olea europaea var. Sylvestris*
LOC111403263	-1,684426568	-3,214126181	2,30E-20	XP_022887462.1	ferritin-3, chloroplastic-like = *Olea europaea var. Sylvestris*
LOC111379684	-1,226236402	-2,339558659	3,73E-04	XP_022858880.1	cation/calcium exchanger 5-like = *Olea europaea var. Sylvestris*
LOC111385047	-3,049425092	-8,278819657	1,30E-82	-	sodium/calcium exchanger NCL2-like = *Olea europaea var. Sylvestris*
LOC111407798	-3,788713536	-13,82026655	6,23E-51	XP_022893246.1	sodium/calcium exchanger NCL2-like = *Olea europaea var. Sylvestris*
LOC111412117	-3,132221566	-8,767840573	1,34E-39	XP_022898660.1	sodium/calcium exchanger NCL2-like = *Olea europaea var. Sylvestris*
LOC111399728	1,258757377	2,39289547	4,91E-07	XP_022882966.1	inorganic phosphate transporter 1-4-like = *Olea europaea var. Sylvestris*
LOC111371803	-2,853938788	-7,22971506	1,57E-67	XP_022849740.1	probable boron transporter 6 = *Olea europaea var. Sylvestris*

Others transporters					
LOC111387932	-1,926607861	-3,80160295	1,92E-25	XP_022868332.1	phospholipid-transporting ATPase 3-like = *Olea europaea var. Sylvestris*
LOC111397871	-1,123541995	-2,178812418	6,38E-11	XP_022880608.1	probable phospholipid-transporting ATPase 8 = *Olea europaea var. Sylvestris*
LOC111386253	-2,288049978	-4,88395524	3,01E-05	XP_022866478.1	putative phospholipid-transporting ATPase 9 = *Olea europaea var. Sylvestris*
LOC111391967	-1,456941017	-2,745256624	7,08E-10	XP_022873017.1	phosphatidylinositol/phosphatidylcholine transfer protein SFH12-like = *Olea europaea var. Sylvestris*
LOC111376459	-1,214437323	-2,320502615	8,42E-12	XP_022855186.1	phosphatidylinositol/phosphatidylcholine transfer protein SFH13-like = *Olea europaea var. Sylvestris*
Leaf AZ + d18:0 vs Fruit AZ d18:0					
Gene	**log2FoldChange**	**FoldChange**	**pvalue**	**Gene_ID**	**Description**
Sugar transporter					
LOC111375866	3,414829607	10,66512971	5,86E-03	XP_022854547.1	sugar transporter ERD6-like 7 = *Olea europaea var. Sylvestris*
LOC111396105	4,881054676	29,46753906	2,39E-83	XP_022878165.1	bidirectional sugar transporter N3-like = *Olea europaea var. Sylvestris*
LOC111375915	4,844097151	28,72225572	4,00E-95	XP_022854600.1	bidirectional sugar transporter N3-like = *Olea europaea var. Sylvestris*
LOC111373172	-7,750735784	-215,3792991	4,26E-07	XP_022851443.1	bidirectional sugar transporter SWEET1-like = *Olea europaea var. Sylvestris*
LOC111408733	-3,398810466	-10,54736316	5,43E-12	XP_022894260.1	bidirectional sugar transporter SWEET1-like = *Olea europaea var. Sylvestris*
LOC111389252	1,74226979	3,345611185	3,16E-14	XP_022869919.1	bidirectional sugar transporter SWEET2-like = *Olea europaea var. Sylvestris*
LOC111372732	1,694530589	3,236715562	2,47E-08	XP_022850891.1	bidirectional sugar transporter SWEET2a-like = *Olea europaea var. Sylvestris*
LOC111409352	1,473295932	2,776554919	2,39E-10	XP_022895178.1	monosaccharide-sensing protein 2-like = *Olea europaea var. Sylvestris*
LOC111387513	5,35679678	40,97854287	8,10E-04	XP_022867843.1	probable sugar phosphate/phosphate translocator At2g25520 = *Olea europaea var. Sylvestris*
N transporter					
LOC111410200	-1,733308144	-3,324893531	1,51E-23	XP_022896208.1	oligopeptide transporter 4 = *Olea europaea var. Sylvestris*
LOC111368982	2,914968353	7,542110841	6,03E-15	XP_022846250.1	amino acid transporter AVT1A-like = *Olea europaea var. Sylvestris*
LOC111368637	-3,300219001	-9,850650524	1,18E-49	XP_022845764.1	amino acid transporter AVT1C-like = *Olea europaea var. Sylvestris*
LOC111384357	-3,109388486	-8,630167055	2,21E-03	XP_022864395.1	amino acid transporter AVT1H = *Olea europaea var. Sylvestris*
LOC111384886	3,438181937	10,83916665	2,10E-44	XP_022864995.1	amino acid transporter AVT1I-like = *Olea europaea var. Sylvestris*
LOC111390214	1,01470577	2,020490782	1,20E-08	XP_022870989.1	amino acid transporter AVT6A-like = *Olea europaea var. Sylvestris*
LOC111399635	1,899098339	3,729800173	1,32E-16	XP_022882870.1	amino acid transporter AVT6C-like = *Olea europaea var. Sylvestris*
LOC111374688	1,222822462	2,334028961	1,08E-12	XP_022853168.1	cationic amino acid transporter 2, vacuolar-like = *Olea europaea var. Sylvestris*
LOC111396839	-1,009961499	-2,013857356	1,32E-07	XP_022879145.1	cationic amino acid transporter 5 = *Olea europaea var. Sylvestris*
LOC111370783	1,127092754	2,184181513	2,10E-04	XP_022848415.1	cationic amino acid transporter 9, chloroplastic = *Olea europaea var. Sylvestris*
LOC111386204	2,544803155	5,835285143	1,87E-05	XP_022866456.1	adenine/guanine permease AZG1-like = *Olea europaea var. Sylvestris*

LOC111376356	1,482438749	2,794206703	9,12E-03	XP_022855081.1	high affinity nitrate transporter 2.5-like = *Olea europaea var. Sylvestris*
LOC111381300	-1,472294981	-2,774629196	8,37E-20	XP_022860840.1	high affinity nitrate transporter 2.7 = *Olea europaea var. Sylvestris*
LOC111369318	1,707726107	3,266455774	3,86E-08	XP_022846559.1	ureide permease 1-like =*Olea europaea var. Sylvestris*
LOC111372930	-1,316460133	-2,490542677	4,67E-09	XP_022851125.1	purine permease 3-like = *Olea europaea var. Sylvestris*
Aquaporin					
LOC111390030	2,750609715	6,730014973	5,28E-22	XP_022870789.1	aquaporin PIP1-1 =*Olea europaea var. Sylvestris*
LOC111388217	2,181277327	4,535549429	9,88E-08	XP_022868671.1	aquaporin PIP1-1-like =*Olea europaea var. Sylvestris*
LOC111368644	2,185254906	4,548071408	2,83E-06	XP_022845778.1	probable aquaporin PIP1-4 = *Olea europaea var. Sylvestris*
LOC111368645	1,187242274	2,277170434	1,43E-07	XP_022845779.1	probable aquaporin PIP1-4 = *Olea europaea var. Sylvestris*
LOC111378025	1,419747662	2,675387123	3,36E-13	XP_022856958.1	aquaporin PIP2-1-like = *Olea europaea var. Sylvestris*
LOC111372815	-1,331649754	-2,516903239	7,47E-12	XP_022850991.1	aquaporin PIP2-2-like = *Olea europaea var. Sylvestris*
LOC111379513	5,226090266	37,42914704	1,24E-03	XP_022858669.1	aquaporin PIP2-2-like = Olea europaea var. Sylvestris
LOC111379782	1,130139854	2,188799573	3,88E-10	XP_022858990.1	probable aquaporin PIP2-8 = *Olea europaea var. Sylvestris*
LOC111371488	1,800501326	3,483412503	9,63E-21	XP_022849284.1	aquaporin TIP2-1-like = *Olea europaea var. Sylvestris*
LOC111367323	-3,000347597	-8,001927721	1,14E-12	XP_022843902.1	probable aquaporin NIP5-1 = *Olea europaea var. Sylvestris*
LOC111388223	1,162395022	2,23828698	8,72E-04	XP_022868680.1	probable aquaporin NIP5-1 = *Olea europaea var. Sylvestris*
LOC111403661	1,466148432	2,762833137	2,38E-03	XP_022888013.1	probable aquaporin SIP2-1 = *Olea europaea var. Sylvestris*
ABC transporter					
LOC111401628	-1,031392305	-2,043995904	1,55E-03	XP_022885220.1	ABC transporter A family member 2 = *Olea europaea var. Sylvestris*
LOC111369421	-2,005869658	-4,0163073	4,22E-14	XP_022846703.1	ABC transporter B family member 1 = *Olea europaea var. Sylvestris*
LOC111392163	1,48035782	2,790179273	2,48E-06	XP_022873197.1	ABC transporter B family member 13-like = *Olea europaea var. Sylvestris*
LOC111377733	5,222494266	37,3359689	6,70E-12	XP_022856629.1	ABC transporter B family member 15-like = *Olea europaea var. Sylvestris*
LOC111397941	3,557356132	11,77255968	2,32E-88	XP_022880672.1	ABC transporter B family member 19-like = *Olea europaea var. Sylvestris*
LOC111409533	5,202720528	36,82772894	9,22E-16	XP_022895341.1	ABC transporter B family member 19-like = Olea europaea var. Sylvestris
LOC111393913	1,114974989	2,165912542	1,06E-04	XP_022875454.1	ABC transporter B family member 2-like = *Olea europaea var. Sylvestris*
LOC111408119	1,645402831	3,128351952	3,62E-18	XP_022893683.1	ABC transporter B family member 2-like = *Olea europaea var. Sylvestris*
LOC111412200	5,655327929	50,3991651	3,17E-04	XP_022898780.1	ABC transporter B family member 9-like = *Olea europaea var. Sylvestris*
LOC111375175	7,756608484	216,2578188	7,32E-08	XP_022853743.1	ABC transporter C family member 10-like = *Olea europaea var. Sylvestris*
LOC111406124	2,058065427	4,164275238	2,43E-31	XP_022891109.1	ABC transporter C family member 10-like = *Olea europaea var. Sylvestris*

LOC111375376	1,706137523	3,262860987	1,67E-14	XP_022853958.1	ABC transporter C family member 13 = *Olea europaea var. Sylvestris*
LOC111370141	-2,173907168	-4,512438182	2,43E-03	XP_022847607.1	ABC transporter C family member 3-like = *Olea europaea var. Sylvestris*
LOC111396114	2,221422782	4,66353124	4,45E-11	XP_022878182.1	ABC transporter C family member 3-like = *Olea europaea var. Sylvestris*
LOC111382339	-2,205355234	-4,61188083	2,21E-31	XP_022862046.1	ABC transporter C family member 4-like = *Olea europaea var. Sylvestris*
LOC111382345	-2,236051351	-4,71105884	1,43E-16	-	ABC transporter C family member 4-like = *Olea europaea var. Sylvestris*
LOC111401758	1,642096564	3,121190824	9,83E-04	XP_022885409.1	ABC transporter G family member 11 = *Olea europaea var. Sylvestris*
LOC111367539	-1,008851856	-2,012309001	8,67E-06	XP_022844245.1	ABC transporter G family member 11-like = *Olea europaea var. Sylvestris*
LOC111377167	1,789042462	3,455854462	2,30E-12	XP_022855990.1	ABC transporter G family member 14-like = *Olea europaea var. Sylvestris*
LOC111393932	-2,987210483	-7,929393288	7,31E-17	XP_022875488.1	ABC transporter G family member 14-like = *Olea europaea var. Sylvestris*
LOC111382075	-5,235463257	-37,6731107	5,52E-03	XP_022861708.1	ABC transporter G family member 20-like = *Olea europaea var. Sylvestris*
LOC111398958	-1,14177427	-2,206522211	4,87E-07	XP_022881906.1	ABC transporter G family member 21-like = *Olea europaea var. Sylvestris*
LOC111378785	-4,932331618	-30,5337233	1,28E-02	XP_022857796.1	ABC transporter G family member 22-like = *Olea europaea var. Sylvestris*
LOC111379070	1,163490447	2,239987137	3,78E-04	XP_022858163.1	ABC transporter G family member 25-like = *Olea europaea var. Sylvestris*
LOC111407952	1,312537836	2,483780762	1,86E-13	XP_022893446.1	ABC transporter G family member 32-like = *Olea europaea var. Sylvestris*
LOC111383669	-2,549937392	-5,856088645	2,72E-03	XP_022863569.1	ABC transporter G family member 32-like = *Olea europaea var. Sylvestris*
LOC111384321	7,17115235	144,1225577	9,01E-07	XP_022864354.1	ABC transporter G family member 39-like = *Olea europaea var. Sylvestris*
LOC111397930	4,722503795	26,40069117	2,09E-09	XP_022880662.1	ABC transporter G family member 5-like = *Olea europaea var. Sylvestris*
LOC111405980	-1,745177132	-3,352360112	2,30E-03	XP_022890898.1	ABC transporter G family member 6-like = *Olea europaea var. Sylvestris*
Metal transporter					
LOC111374645	-1,345286297	-2,540806128	1,35E-18	XP_022853126.1	heavy metal-associated isoprenylated plant protein 3-like = *Olea europaea var. Sylvestris*
LOC111378486	1,879663352	3,679891811	1,78E-08	XP_022857466.1	heavy metal-associated isoprenylated plant protein 3-like = *Olea europaea var. Sylvestris*
LOC111404756	-2,528720108	-5,770595105	2,09E-45	-	heavy metal-associated isoprenylated plant protein 3-like = *Olea europaea var. Sylvestris*
LOC111392166	1,187502698	2,277581529	6,68E-05	XP_022873201.1	heavy metal-associated isoprenylated plant protein 6-like = *Olea europaea var. Sylvestris*
LOC111384961	4,763511757	27,1618861	4,66E-56	XP_022865078.1	heavy metal-associated isoprenylated plant protein 7-like = *Olea europaea var. Sylvestris*
LOC111401808	6,26457022	76,88180059	2,02E-08	XP_022885488.1	heavy metal-associated isoprenylated plant protein 7-like = *Olea europaea var. Sylvestris*
LOC111370671	-2,062486888	-4,177057166	1,74E-18	XP_022848265.1	heavy metal-associated isoprenylated plant protein 7-like = *Olea europaea var. Sylvestris*
LOC111404244	1,446229771	2,724950024	3,91E-10	XP_022888808.1	heavy metal-associated isoprenylated plant protein 9-like = *Olea europaea var. Sylvestris*
LOC111395532	-2,230952675	-4,694438717	3,58E-12	XP_022877322.1	heavy metal-associated isoprenylated plant protein 16-like = *Olea europaea var. Sylvestris*

LOC111409636	4,341993446	20,28010823	7,23E-04	XP_022895430.1	heavy metal-associated isoprenylated plant protein 21-like = *Olea europaea var. Sylvestris*
LOC111397410	-1,209677076	-2,312858613	8,51E-03	XP_022880090.1	heavy metal-associated isoprenylated plant protein 24-like = *Olea europaea var. Sylvestris*
LOC111389200	2,466751842	5,527977878	5,08E-04	XP_022869859.1	heavy metal-associated isoprenylated plant protein 26-like = *Olea europaea var. Sylvestris*
LOC111410120	-1,714370834	-3,281535029	3,45E-21	XP_022896093.1	heavy metal-associated isoprenylated plant protein 26-like = *Olea europaea var. Sylvestris*
LOC111404999	1,743710834	3,348954635	9,50E-03	XP_022889486.1	heavy metal-associated isoprenylated plant protein 27 = *Olea europaea var. Sylvestris*
LOC111369485	4,452167166	21,88950106	7,06E-57	XP_022846778.1	heavy metal-associated isoprenylated plant protein 32-like = *Olea europaea var. Sylvestris*
LOC111387383	2,251330623	4,761217792	4,80E-05	XP_022867707.1	heavy metal-associated isoprenylated plant protein 32-like = *Olea europaea var. Sylvestris*
LOC111396617	2,426466718	5,375752501	1,02E-02	XP_022878801.1	heavy metal-associated isoprenylated plant protein 33-like = *Olea europaea var. Sylvestris*
LOC111379770	1,051285845	2,072376092	2,00E-03	XP_022858980.1	heavy metal-associated isoprenylated plant protein 35-like = *Olea europaea var. Sylvestris*
LOC111385041	1,518186707	2,864308143	4,80E-15	XP_022865173.1	heavy metal-associated isoprenylated plant protein 39-like = *Olea europaea var. Sylvestris*
LOC111398554	-2,381990413	-5,21255396	1,37E-36	XP_022881282.1	heavy metal-associated isoprenylated plant protein 39-like = *Olea europaea var. Sylvestris*
LOC111370985	-2,884880198	-7,386445085	3,79E-35	XP_022848680.1	heavy metal-associated isoprenylated plant protein 41-like = *Olea europaea var. Sylvestris*
LOC111395797	5,406945872	42,42803245	6,92E-04	XP_022877714.1	heavy metal-associated isoprenylated plant protein 41-like = *Olea europaea var. Sylvestris*
LOC111370984	-2,062625436	-4,177458326	5,21E-30	XP_022848679.1	heavy metal-associated isoprenylated plant protein 46-like = *Olea europaea var. Sylvestris*
LOC111395518	-3,801553733	-13,94381794	1,48E-26	XP_022877307.1	heavy metal-associated isoprenylated plant protein 46-like = *Olea europaea var. Sylvestris*
LOC111408460	-1,170733076	-2,251260612	8,33E-11	XP_022893983.1	metal-nicotianamine transporter YSL1-like = *Olea europaea var. Sylvestris*
LOC111405352	-1,298904179	-2,460419267	4,00E-08	XP_022889948.1	probable metal-nicotianamine transporter YSL8 = *Olea europaea var. Sylvestris*
LOC111379880	1,633172002	3,101942625	3,74E-16	XP_022859089.1	metal tolerance protein 11 = *Olea europaea var. Sylvestris*
LOC111370701	-4,566313656	-23,69176303	1,28E-93	XP_022848307.1	zinc transporter 1-like = *Olea europaea var. Sylvestris*
LOC111395859	-4,102272658	-17,17541029	2,38E-10	XP_022877827.1	zinc transporter 1-like = *Olea europaea var. Sylvestris*
LOC111405892	-1,588816611	-3,008025112	1,15E-05	XP_022890754.1	zinc transporter 2 = *Olea europaea var. Sylvestris*
LOC111397591	-1,850561378	-3,606404894	2,58E-21	XP_022880355.1	zinc transporter 4, chloroplastic = *Olea europaea var. Sylvestris*
LOC111372341	-2,959844458	-7,780400702	1,79E-44	XP_022850400.1	zinc transporter 5-like = *Olea europaea var. Sylvestris*
LOC111367213	-1,390932923	-2,622482095	1,20E-09	XP_022843736.1	probable cadmium/zinc-transporting ATPase HMA1, chloroplastic = *Olea europaea var. Sylvestris*
Nutrient transporter					
LOC111367244	-1,206951134	-2,308492642	7,84E-11	XP_022843776.1	calcium-transporting ATPase 2, plasma membrane-type-like = *Olea europaea var. Sylvestris*
LOC111389070	-4,970889662	-31,36078271	2,07E-10	XP_022869691.1	calcium-transporting ATPase 5, plasma membrane-type-like = *Olea europaea var. Sylvestris*
LOC111389071	-4,587545842	-24,04301376	1,07E-05	XP_022869692.1	calcium-transporting ATPase 8, plasma membrane-type-like = *Olea europaea var. Sylvestris*

LOC111403839	-2,284753664	-4,872808964	2,71E-16	XP_022888234.1	calcium-transporting ATPase 8, plasma membrane-type-like = *Olea europaea var. Sylvestris*
LOC111376275	-1,205679272	-2,306458401	4,43E-10	XP_022854992.1	calcium-transporting ATPase 8, plasma membrane-type-like = *Olea europaea var. Sylvestris*
LOC111367996	-2,513502327	-5,710045836	8,58E-08	XP_022844924.1	calcium-transporting ATPase 9, plasma membrane-type-like = *Olea europaea var. Sylvestris*
LOC111399650	-2,076047676	-4,216505033	1,68E-36	XP_022882853.1	putative calcium-transporting ATPase 11, plasma membrane-type = *Olea europaea var. Sylvestris*
LOC111369013	-5,288782325	-39,09148065	7,08E-04	XP_022846270.1	calcium-transporting ATPase 12, plasma membrane-type-like = *Olea europaea var. Sylvestris*
LOC111376034	-6,713777821	-104,9659663	3,26E-05	XP_022854728.1	calcium-transporting ATPase 12, plasma membrane-type-like = *Olea europaea var. Sylvestris*
LOC111397563	-3,098893454	-8,567613828	5,82E-13	XP_022880322.1	calcium-transporting ATPase 12, plasma membrane-type-like = *Olea europaea var. Sylvestris*
LOC111397566	-1,735457171	-3,329849956	4,75E-05	XP_022880325.1	calcium-transporting ATPase 12, plasma membrane-type-like = *Olea europaea var. Sylvestris*
LOC111396588	-1,009132524	-2,012700522	4,22E-03	XP_022878764.1	putative calcium-transporting ATPase 13, plasma membrane-type = *Olea europaea var. Sylvestris*
LOC111372921	1,159767876	2,234214772	2,33E-03	XP_022851117.1	copper-transporting ATPase PAA2, chloroplastic-like = *Olea europaea var. Sylvestris*
LOC111396249	1,069843759	2,099206015	6,98E-07	XP_022878389.1	putative phospholipid-transporting ATPase 9 = *Olea europaea var. Sylvestris*
LOC111388227	2,909969601	7,516023622	2,84E-09	XP_022868686.1	low affinity sulfate transporter 3-like = *Olea europaea var. Sylvestris*
LOC111387747	-1,92123539	-3,787472437	3,28E-04	XP_022868100.1	sulfate transporter 3.1-like = *Olea europaea var. Sylvestris*
LOC111411814	-2,104478377	-4,300422413	1,74E-03	XP_022898198.1	sulfate transporter 3.1-like = *Olea europaea var. Sylvestris*
LOC111396330	2,601287318	6,068278579	1,54E-17	XP_022878506.1	probable sulfate transporter 3.3 = *Olea europaea var. Sylvestris*
LOC111367293	-1,978175629	-3,939945377	1,18E-06	XP_022843864.1	probable sulfate transporter 3.4 = *Olea europaea var. Sylvestris*
LOC111406275	-3,874367304	-14,66563165	2,37E-24	XP_022891378.1	probable sulfate transporter 3.4 = *Olea europaea var. Sylvestris*
LOC111405391	1,16844717	2,247696382	2,66E-05	XP_022890015.1	sulfate transporter 4.1, chloroplastic-like = *Olea europaea var. Sylvestris*
LOC111405347	4,720124861	26,35719358	8,24E-36	XP_022889943.1	organic cation/carnitine transporter 1 = *Olea europaea var. Sylvestris*
LOC111382262	4,052146072	16,58889715	1,68E-05	XP_022861947.1	organic cation/carnitine transporter 3-like = *Olea europaea var. Sylvestris*
LOC111366335	-2,153046903	-4,447661225	1,18E-12	XP_022842851.1	organic cation/carnitine transporter 7-like = *Olea europaea var. Sylvestris*
LOC111410610	-2,179679129	-4,530527791	4,41E-03	XP_022896814.1	ammonium transporter 3 member 1-like = *Olea europaea var. Sylvestris*
LOC111365316	-1,658533173	-3,156953854	4,60E-07	XP_022841531.1	ammonium transporter 3 member 2-like = *Olea europaea var. Sylvestris*
LOC111395700	1,581708467	2,993241053	3,23E-05	XP_022877588.1	cyclic nucleotide-gated ion channel 4-like = *Olea europaea var. Sylvestris*
LOC111393563	1,218205632	2,326571672	4,43E-12	XP_022874923.1	potassium transporter 4-like = *Olea europaea var. Sylvestris*
LOC111412402	-2,823411804	-7,078343641	1,20E-03	XP_022899092.1	potassium transporter 5-like = *Olea europaea var. Sylvestris*
LOC111395494	2,641495547	6,239781656	2,35E-05	XP_022877284.1	potassium transporter 6-like = *Olea europaea var. Sylvestris*
LOC111400145	1,11016542	2,158703977	7,11E-06	XP_022883350.1	potassium transporter 8-like = *Olea europaea var. Sylvestris*

LOC111392346	1,946397627	3,854109677	4,82E-28	XP_022873447.1	potassium transporter 8-like = *Olea europaea var. Sylvestris*
LOC111368041	1,000813738	2,001128399	1,56E-03	XP_022844973.1	potassium transporter 25-like = *Olea europaea var. Sylvestris*
LOC111380006	-1,004097627	-2,005688592	1,37E-05	XP_022859236.1	ferritin-3, chloroplastic-like = *Olea europaea var. Sylvestris*
LOC111392534	-2,708407525	-6,535997925	6,54E-41	XP_022873666.1	ferritin-3, chloroplastic-like = *Olea europaea var. Sylvestris*
LOC111398222	1,401664554	2,642062425	1,62E-06	XP_022880923.1	ferritin-3, chloroplastic-like = *Olea europaea var. Sylvestris*
LOC111366092	1,542260246	2,912504433	2,70E-11	XP_022842514.1	cation/calcium exchanger 4-like = *Olea europaea var. Sylvestris*
LOC111407798	1,822208984	3,536222333	6,88E-08	XP_022893246.1	sodium/calcium exchanger NCL2-like = *Olea europaea var. Sylvestris*
LOC111407250	1,11292233	2,162833084	1,01E-04	XP_022892398.1	sodium/calcium exchanger NCL2-like = *Olea europaea var. Sylvestris*
LOC111366051	1,917994379	3,77897344	6,22E-22	XP_022842465.1	sodium/hydrogen exchanger 1-like = *Olea europaea var. Sylvestris*
LOC111373530	-1,410582247	-2,658444314	1,65E-15	XP_022851837.1	probable inorganic phosphate transporter 1-3 = *Olea europaea var. Sylvestris*
LOC111371596	1,440954761	2,715004824	1,42E-07	XP_022849431.1	inorganic phosphate transporter 1-4-like = *Olea europaea var. Sylvestris*
LOC111378718	-3,008405627	-8,04674674	1,28E-87	XP_022857721.1	inorganic phosphate transporter 1-4-like = *Olea europaea var. Sylvestris*
LOC111399728	1,396797052	2,633163404	7,70E-12	XP_022882966.1	inorganic phosphate transporter 1-4-like = *Olea europaea var. Sylvestris*
LOC111378674	-1,251197596	-2,380389397	2,91E-03	XP_022857670.1	probable inorganic phosphate transporter 1-9 = *Olea europaea var. Sylvestris*
LOC111406464	1,20280766	2,301872077	5,83E-03	XP_022891654.1	boron transporter 1-like = *Olea europaea var. Sylvestris*
LOC111401466	-2,305037931	-4,941804477	8,23E-07	XP_022884973.1	boron transporter 4-like = *Olea europaea var. Sylvestris*
Other transporters					
LOC111395920	-1,230843224	-2,347041292	1,94E-11	XP_022877916.1	phosphatidylinositol/phosphatidylcholine transfer protein SFH3 = *Olea europaea var. Sylvestris*
LOC111397354	2,099266444	4,28491458	1,86E-15	XP_022880015.1	phosphatidylinositol/phosphatidylcholine transfer protein SFH3-like = *Olea europaea var. Sylvestris*
LOC111391967	-2,171773931	-4,505770808	8,90E-09	XP_022873017.1	phosphatidylinositol/phosphatidylcholine transfer protein SFH12-like = *Olea europaea var. Sylvestris*
LOC111410544	-4,317187373	-19,9343875	1,10E-02	XP_022896718.1	phosphatidylinositol/phosphatidylcholine transfer protein SFH12-like =*Olea europaea var. Sylvestris*

Table 3.II. S13. Vesicle-trafficking-related genes induced or repressed in the first comparison (d18:0-AZ vs. C-AZ) and the second comparison (d18:0-LAZ vs. d18:0-AZ).

Fruit AZ d18:0 vs Fruit Az Control					
Gene	**log2FoldChange**	**FoldChange**	**pvalue**	**Gene_ID**	**Description**
Tubulin family					
LOC111373326	1,845319455	3,593325072	0,00400647	-	tubulin alpha chain-like = *Olea europaea var. Sylvestris*
LOC111391194	1,089868051	2,128545679	1,54E-08	XP_022872123.1	tubulin beta-5 chain = *Olea europaea var. Sylvestris*
LOC111384278	-1,498320316	-2,825135994	0,00674603	-	gamma-tubulin complex component 3 = *Olea europaea var. Sylvestris*
Actin family					
LOC111397366	-1,320048956	-2,49674582	4,57E-15	XP_022880028.1	actin-97 = *Olea europaea var. Sylvestris*
LOC111399692	-1,791932904	-3,462785212	2,54E-06	XP_022882916.1	actin-97-like = *Olea europaea var. Sylvestris*
LOC111380796	1,080983458	2,115477671	1,01E-05	XP_022860214.1	actin-depolymerizing factor 5-like = *Olea europaea var. Sylvestris*
LOC111402452	-1,022498352	-2,031433801	1,04E-05	XP_022886530.1	actin-related protein 8 = *Olea europaea var. Sylvestris*
Kinesin-like protein family					
LOC111404047	-1,432315996	-2,698796125	0,01049261	XP_022888530.1	kinesin-like protein KIN-5C = *Olea europaea var. Sylvestris*
LOC111374916	1,000095036	2,000131752	0,00433597	XP_022853442.1	kinesin-like protein KIN-7D, mitochondrial = *Olea europaea var. Sylvestris*
LOC111380555	-1,218304782	-2,326731573	4,33E-12	XP_022859928.1	kinesin-like protein KIN-7E = *Olea europaea var. Sylvestris*
LOC111391234	-1,088830263	-2,127015082	0,00892753	XP_022872170.1	kinesin-like protein KIN-14C = *Olea europaea var. Sylvestris*
LOC111387114	-2,006048086	-4,016804052	0,00164034	-	kinesin-like protein NACK2 = *Olea europaea var. Sylvestris*
Small GTPase superfamily. RAB family					
LOC111368881	-1,560334363	-2,949221875	3,41E-16	XP_022846137.1	rab3 GTPase-activating protein non-catalytic subunit = *Olea europaea var. Sylvestris*
LOC111370504	-1,281169932	-2,430359834	0,00191932	XP_022847990.1	ras-related protein RABA1c = *Olea europaea var. Sylvestris*
LOC111412153	1,120382743	2,174046417	0,00108389	XP_022898711.1	ras-related protein RABA1d-like = *Olea europaea var. Sylvestris*
LOC111381327	1,137567645	2,200097782	0,00366017	XP_022860877.1	ras-related protein RABA3 = *Olea europaea var. Sylvestris*
LOC111371292	1,208718482	2,311322353	5,70E-05	XP_022848959.1	ras-related protein RABA5b-like = *Olea europaea var. Sylvestris*
LOC111382726	-1,267559642	-2,40753979	8,08E-13	XP_022862535.1	ras-related protein RABE1c-like = *Olea europaea var. Sylvestris*
LOC111405992	-1,462711047	-2,756258208	6,22E-20	XP_022890914.1	ras-related protein RABE1c-like = *Olea europaea var. Sylvestris*
LOC111369672	-1,80455482	-3,493213498	1,04E-09	XP_022847043.1	ras-related protein Rab11C-like =*Olea europaea var. Sylvestris*
Small GTPase superfamily. ARF-like GTPase family					
LOC111377021	-1,478946275	-2,787450673	1,07E-09	XP_022855805.1	probable ADP-ribosylation factor GTPase-activating protein AGD6 = *Olea europaea var. Sylvestris*
LOC111387039	-1,60516932	-3,042314542	1,96E-09	-	ADP-ribosylation factor GTPase-activating protein AGD7-like = *Olea europaea var. Sylvestris*
V-type ATPase family					
LOC111395635	1,391079748	2,622749003	3,59E-09	XP_022877489.1	V-type proton ATPase subunit a2-like = *Olea europaea var. Sylvestris*
LOC111408464	1,091171309	2,130469368	0,00015994	XP_022893986.1	V-type proton ATPase subunit H-like = *Olea europaea var. Sylvestris*
Syntaxin/t-SNARE family					
LOC111398722	-1,090348149	-2,129254131	0,00021382	XP_022881547.1	syntaxin-32-like = *Olea europaea var. Sylvestris*
LOC111386164	-1,01975707	-2,027577515	0,00194262	XP_022866386.1	syntaxin-43-like = *Olea europaea var. Sylvestris*
LOC111373493	1,341303307	2,533801149	7,58E-06	XP_022851792.1	syntaxin-132-like =*Olea europaea var. Sylvestris*
Others families					
LOC111404177	-2,112636997	-4,324810733	9,00E-12	XP_022888712.1	reticulon-like protein B12 = *Olea europaea var. Sylvestris*
LOC111367298	-2,431689646	-5,395249381	1,71E-09	XP_022843876.1	vacuolar cation/proton exchanger 2-like = *Olea europaea var. Sylvestris*

LOC111408636	-1,213272335	-2,318629547	7,56E-09	-	vacuolar cation/proton exchanger 3-like = *Olea europaea var. Sylvestris*
LOC111410928	-1,6169186	-3,067192256	5,41E-09	XP_022897290.1	vacuolar iron transporter homolog 1-like = *Olea europaea var. Sylvestris*
LOC111366106	-1,702640618	-3,254961813	1,03E-28	XP_022842530.1	vacuolar protein sorting-associated protein 2 homolog 1 = *Olea europaea var. Sylvestris*
LOC111376539	-1,612001731	-3,056756709	0,00015786	XP_022855275.1	vacuolar protein sorting-associated protein 13-like = *Olea europaea var. Sylvestris*
LOC111365503	-1,693465595	-3,234327109	0,00042608	XP_022841826.1	vacuolar protein sorting-associated protein 13C-like = *Olea europaea var. Sylvestris*
LOC111384090	-1,753133595	-3,370899453	1,85E-24	XP_022864085.1	vacuolar protein sorting-associated protein 28 homolog 1-like = *Olea europaea var. Sylvestris*
LOC111369802	1,552167592	2,93257416	0,00736474	XP_022847234.1	vacuolar protein sorting-associated protein 51 homolog = *Olea europaea var. Sylvestris*
LOC111401848	-1,40651039	-2,650951711	3,37E-10	XP_022885558.1	vacuolar protein sorting-associated protein 54, chloroplastic = *Olea europaea var. Sylvestris*
LOC111383902	-1,166282903	-2,244327015	4,68E-10	XP_022863858.1	vacuolar protein sorting-associated protein 60.1-like = *Olea europaea var. Sylvestris*

Leaf AZ + d18:0 vs Fruit AZ d18:0					
Gene	**log2FoldChange**	**FoldChange**	**pvalue**	**Gene_ID**	**Description**
Tubulin family					
LOC111410172	-1,746016422	-3,354310919	4,77E-07	XP_022896170.1	tubulin alpha chain-like = *Olea europaea var. Sylvestris*
LOC111371391	-1,308417353	-2,476696955	2,61E-15	XP_022849110.1	tubulin alpha-3 chain = *Olea europaea var. Sylvestris*
LOC111401048	-1,054555133	-2,077077624	1,28E-07	XP_022884352.1	tubulin alpha-3 chain-like = *Olea europaea var. Sylvestris*
LOC111396968	-1,188963194	-2,27988838	1,75E-09	XP_022879377.1	tubulin beta chain-like = *Olea europaea var. Sylvestris*
LOC111387259	-1,139529374	-2,203091438	7,89E-04	XP_022867570.1	tubulin beta-1 chain = *Olea europaea var. Sylvestris*
LOC111397384	-2,318008804	-4,986435205	2,91E-16	XP_022880052.1	tubulin beta-1 chain = *Olea europaea var. Sylvestris*
LOC111367589	-1,309394448	-2,478374916	4,39E-11	XP_022844311.1	tubulin beta-1 chain-like = *Olea europaea var. Sylvestris*
LOC111368488	-2,037641684	-4,10573833	1,09E-27	XP_022845513.1	tubulin beta-2 chain-like = *Olea europaea var. Sylvestris*
LOC111383090	-1,682159941	-3,209080413	3,75E-16	XP_022862927.1	tubulin beta-8 chain-like = *Olea europaea var. Sylvestris*
Actin family					
LOC111401141	-1,222149315	-2,33294018	6,67E-14	XP_022884507.1	actin-7-like = *Olea europaea var. Sylvestris*
LOC111399692	-2,290911996	-4,893653645	1,55E-03	XP_022882916.1	actin-97-like = *Olea europaea var. Sylvestris*
LOC111369629	-1,053836657	-2,076043477	2,32E-06	XP_022846987.1	actin-depolymerizing factor 2-like = *Olea europaea var. Sylvestris*
Kinesin-like protein family					
LOC111385753	1,718360096	3,29062151	1,51E-17	XP_022865937.1	kinesin-like protein KIN-4A = *Olea europaea var. Sylvestris*
LOC111401928	2,989174001	7,940192592	1,08E-05	XP_022885678.1	kinesin-like protein KIN-7C = *Olea europaea var. Sylvestris*
LOC111395137	2,969772907	7,834129123	8,21E-06	XP_022876916.1	kinesin-like protein KIN-14F = *Olea europaea var. Sylvestris*
LOC111369858	1,934588356	3,822690387	3,17E-05	XP_022847322.1	kinesin-like protein KIN-14I = *Olea europaea var. Sylvestris*
LOC111382164	3,556625489	11,76659907	7,04E-15	XP_022862054.1	kinesin-like protein KIN-UC = *Olea europaea var. Sylvestris*
LOC111384936	1,704967108	3,260215	1,20E-02	-	protein KINESIN LIGHT CHAIN-RELATED 3-like = *Olea europaea var. Sylvestris*
Small GTPase superfamily. RAB family					
LOC111382726	-1,656590638	-3,152705994	2,05E-13	XP_022862535.1	ras-related protein RABE1c-like = *Olea europaea var. Sylvestris*
LOC111405992	-1,787931602	-3,453194516	1,97E-20	XP_022890914.1	ras-related protein RABE1c-like = *Olea europaea var. Sylvestris*
Small GTPase superfamily. ARF-like GTPase family					
LOC111381692	-3,534958018	-11,59119993	2,87E-07	XP_022861272.1	ADP-ribosylation factor 1-like = *Olea europaea var. Sylvestris*
LOC111390371	-1,311388159	-2,481802237	2,12E-12	XP_022871179.1	ADP-ribosylation factor 1-like = *Olea europaea var. Sylvestris*
LOC111401994	1,373976641	2,591839966	6,90E-07	XP_022885768.1	ADP-ribosylation factor 2-like = *Olea europaea var. Sylvestris*
LOC111383489	-1,164916102	-2,24220176	7,93E-03	XP_022863373.1	ADP-ribosylation factor-like protein 8a = *Olea europaea var. Sylvestris*
Dynamin family					
LOC111395317	2,516279323	5,721047501	3,70E-10	XP_022877067.1	dynamin-related protein 1E-like = *Olea europaea var. Sylvestris*

V-type ATPase family					
LOC111395635	-1,757670991	-3,381517901	4,75E-14	XP_022877489.1	V-type proton ATPase subunit a2-like = *Olea europaea var. Sylvestris*
LOC111400307	-1,744057697	-3,349759913	5,31E-13	XP_022883492.1	V-type proton ATPase subunit a3-like = *Olea europaea var. Sylvestris*
LOC111378084	1,14340951	2,209024639	4,05E-03	XP_022857017.1	V-type proton ATPase subunit F-like = *Olea europaea var. Sylvestris*
Syntaxin/t-SNARE family					
LOC111366281	1,4328822	2,69985551	9,33E-13	XP_022842778.1	syntaxin-121-like =*Olea europaea var. Sylvestris*
Others families					
LOC111389037	-1,068637062	-2,097450934	1,41E-05	-	reticulon-like protein B1 = *Olea europaea var. Sylvestris*
LOC111406118	-1,318919847	-2,494792534	1,04E-07	XP_022891102.1	reticulon-like protein B5 = *Olea europaea var. Sylvestris*
LOC111404177	1,518807576	2,865541076	4,37E-06	XP_022888712.1	reticulon-like protein B12 = *Olea europaea var. Sylvestris*
LOC111403768	1,049298657	2,069523538	4,41E-03	XP_022888156.1	reticulon-like protein B21 = *Olea europaea var. Sylvestris*
LOC111374688	1,222822462	2,334028961	1,08E-12	XP_022853168.1	cationic amino acid transporter 2, vacuolar-like = *Olea europaea var. Sylvestris*
LOC111367298	-2,34463345	-5,079313249	7,17E-03	XP_022843876.1	vacuolar cation/proton exchanger 2-like = *Olea europaea var. Sylvestris*
LOC111385841	3,172597851	9,01668956	2,97E-09	XP_022866040.1	vacuolar cation/proton exchanger 3-like = *Olea europaea var. Sylvestris*
LOC111408636	2,038330132	4,107698039	6,04E-23	-	vacuolar cation/proton exchanger 3-like = *Olea europaea var. Sylvestris*
LOC111385840	1,435828534	2,705374905	8,04E-04	XP_022866039.1	vacuolar cation/proton exchanger 3-like = *Olea europaea var. Sylvestris*
LOC111410928	-4,238264645	-18,87316721	3,71E-10	XP_022897290.1	vacuolar iron transporter homolog 1-like = *Olea europaea var. Sylvestris*
LOC111365503	1,707718602	3,266438782	1,03E-04	XP_022841826.1	vacuolar protein sorting-associated protein 13C-like = *Olea europaea var. Sylvestris*
LOC111398726	1,058718363	2,083080168	2,38E-08	XP_022881557.1	vacuolar-sorting receptor 1-like = *Olea europaea var. Sylvestris*
LOC111374987	-1,350716395	-2,550387379	6,19E-11	XP_022853529.1	vacuolar-sorting receptor 6-like = *Olea europaea var. Sylvestris*

Table 3.II.S14. Auxin related genes induced or repressed in the first comparison (d18:0-AZ vs. C-AZ) and the second comparison (d18:0-LAZ vs. d18:0-AZ).

	d18:0-AZ vs. C-AZ		d18:0-LAZ vs. d18:0-AZ			
Gene	log2FoldChange	pvalue	log2FoldChange	pvalue	Gene_ID	Description
LOC111408458	3,386480119	0,2315787			XP_022893981.1	TAR2 tryptophan aminotransferase-related protein 2-like = *Olea europaea var. Sylvestris*
LOC111392494	-1,239117609	0,7038278			XP_022873616.1	LAX2 auxin transporter-like protein 2 = Olea europaea var. Sylvestris
LOC111397780			-2,495935596	5,68E-02	XP_022880537.1	LAX2 auxin transporter-like protein 2 = *Olea europaea var. Sylvestris*
LOC111399329			-1,647847893	2,44E-04	XP_022882353.1	LAX2 auxin transporter-like protein 2 = *Olea europaea var. Sylvestris*
LOC111402029			2,817286515	2,11E-19	XP_022885827.1	LAX3 auxin transporter-like protein 3 = *Olea europaea var. Sylvestris*
LOC111374882	1,031005812	0,8362085			XP_022853409.1	LAX5 auxin transporter-like protein 5= *Olea europaea var. Sylvestris*
LOC111365275	2,563601029	3,767E-19	-2,170683607	1,26E-15	XP_022841487.1	PIN1 auxin efflux carrier component 1-like= *Olea europaea var. Sylvestris*
LOC111404113	2,610701657	0,2460836			XP_022888622.1	PIN1b probable auxin efflux carrier component 1b = *Olea europaea var. Sylvestris*
LOC111373998	3,961185858	0,0313809	-2,424314382	6,39E-02	XP_022852367.1	PIN1b probable auxin efflux carrier component 1b= *Olea europaea var. Sylvestris*
LOC111405232			-2,401241902	1,93E-04	XP_022889803.1	PIN1c probable auxin efflux carrier component 1c = *Olea europaea var. Sylvestris*
LOC111409368	-4,112063623	0,1198514			XP_022895191.1	PIN6 auxin efflux carrier component 6 = *Olea europaea var. Sylvestris*
LOC111395225			1,106697206	2,47E-06	XP_022876988.1	PIN7 auxin efflux carrier component 7-like = *Olea europaea var. Sylvestris*
LOC111396336			1,395984814	3,08E-07	XP_022878513.1	PIN7 auxin efflux carrier component 7-like = *Olea europaea var. Sylvestris*
LOC111399043	1,758177827	8,918E-16			XP_022882020.1	PIN7 auxin efflux carrier component 7-like= *Olea europaea var. Sylvestris*
LOC111400824	-3,908535975	0,0409745			XP_022884006.1	PIN8 auxin efflux carrier component 8 = *Olea europaea var. Sylvestris*
LOC111367367	1,835412452	7,715E-18			XP_022843960.1	PIN-LIKES 2 = *Olea europaea var. Sylvestris*
LOC111394988			1,294614285	3,88E-02	XP_022876783.1	PIN-LIKES 2 protein = *Olea europaea var. Sylvestris*
LOC111396747			3,731205643	3,47E-05	XP_022879017.1	PIN-LIKES 3 protein = *Olea europaea var. Sylvestris*
LOC111392867	-1,045931049	0,0209792	1,29044036	1,96E-03	XP_022874037.1	PIN-LIKES 4 protein = *Olea europaea var. Sylvestris*
LOC111397193			1,370397139	4,58E-15	XP_022879740.1	PIN-LIKES 7 protein = *Olea europaea var. Sylvestris*
LOC111375834	-1,766475522	7,808E-09			XP_022854515.1	GH3.1 probable indole-3-acetic acid-amido synthetase = *Olea europaea var. Sylvestris*
LOC111390207	1,425449931	0,2599443			XP_022870980.1	GH3.1 probable indole-3-acetic acid-amido synthetase = *Olea europaea var. Sylvestris*
LOC111411983	2,386489899	2,109E-10	-1,972136816	1,44E-08	XP_022898464.1	GH3.1 probable indole-3-acetic acid-amido synthetase = *Olea europaea var. Sylvestris*
LOC111368599			1,125361586	2,99E-02	XP_022845709.1	GH3.10 indole-3-acetic acid-amido synthetase = *Olea europaea var. Sylvestris*
LOC111395681	2,545065098	1,472E-10	-1,984094045	5,09E-08	XP_022877558.1	GH3.6 indole-3-acetic acid-amido synthetase = *Olea europaea var. Sylvestris*
LOC111379390	3,185257042	0,0313106	-1,737055479	1,36E-01	XP_022858515.1	GH3.6 indole-3-acetic acid-amido synthetase = *Olea europaea var. Sylvestris*

LOC111397432	1,48024924	0,0005729	-5,075190137	1,01E-09	XP_022880124.1	GH3.6 indole-3-acetic acid-amido synthetase = *Olea europaea var. Sylvestris*
LOC111403938	3,019849129	1,109E-08			XP_022888388.1	GH3.6 indole-3-acetic acid-amido synthetase = *Olea europaea var. Sylvestris*
LOC111380794	-1,044443514	4,953E-06	2,207883984	7,06E-29	XP_022860209.1	ILR1- 6 IAA-amino acid hydrolase = Olea europaea var. Sylvestris
LOC111405087	-2,186230694	6,197E-16	1,301430805	1,86E-05	XP_022889573.1	ILR1-1 IAA-amino acid hydrolase = *Olea europaea var. Sylvestris*
LOC111394354	-2,0759856	1,011E-35			XP_022875891.1	ILR1-6 IAA-amino acid hydrolase = *Olea europaea var. Sylvestris*
LOC111369824	-1,433828875	1,017E-12			XP_022847260.1	TIR1 protein TRANSPORT INHIBITOR RESPONSE 1-like = *Olea europaea var. Sylvestris*
LOC111370614	1,247107701	0,8020034			XP_022848180.1	TIR1 protein TRANSPORT INHIBITOR RESPONSE 1-like = *Olea europaea var. Sylvestris*
LOC111370617	1,300063732	0,6493017			XP_022848187.1	TIR1 protein TRANSPORT INHIBITOR RESPONSE 1-like = *Olea europaea var. Sylvestris*
LOC111385397			1,392585208	2,74E-02	XP_022865551.1	TIR1 protein TRANSPORT INHIBITOR RESPONSE 1-like = *Olea europaea var. Sylvestris*
LOC111407157	1,077447414	1,772E-11			XP_022892250.1	TIR1 protein TRANSPORT INHIBITOR RESPONSE 1-like= *Olea europaea var. Sylvestris*
LOC111393320	-1,364621851	1,157E-16			XP_022874572.1	IAA13 auxin-responsive protein = *Olea europaea var. Sylvestris*
LOC111393714			2,532373477	2,79E-30	XP_022875154.1	IAA14 auxin-responsive protein = *Olea europaea var. Sylvestris*
LOC111377657			2,21983285	6,77E-39	XP_022856551.1	IAA26 auxin-responsive protein = *Olea europaea var. Sylvestris*
LOC111367154	1,106567393	2,025E-09	1,492032288	7,84E-21	XP_022843651.1	IAA27 auxin-responsive protein= *Olea europaea var. Sylvestris*
LOC111392147	1,684463735	0,2730146			XP_022873182.1	IAA13 auxin-responsive protein IAA13-like= *Olea europaea var. Sylvestris*
LOC111375552			1,147678359	6,21E-15	XP_022854159.1	IAA14 auxin-responsive protein = *Olea europaea var. Sylvestris*
LOC111378080	-1,694038738	0,0004245			XP_022857015.1	IAA14 auxin-responsive protein = Olea europaea var. Sylvestris
LOC111377488	1,360289309	9,088E-15			XP_022856362.1	IAA16 auxin-responsive protein = *Olea europaea var. Sylvestris*
LOC111376975			-1,434871092	1,31E-05	XP_022855756.1	IAA17 auxin-responsive protein = *Olea europaea var. Sylvestris*
LOC111401565	-1,039870527	4,657E-05	-1,35005809	7,90E-05	XP_022885126.1	IAA26 auxin-responsive protein = *Olea europaea var. Sylvestris*
LOC111382084			-1,019729179	1,80E-07	XP_022861723.1	IAA29 auxin-responsive protein = *Olea europaea var. Sylvestris*
LOC111389918	2,500791522	1,113E-17	-1,133789422	4,94E-06	XP_022870673.1	IAA29 auxin-responsive protein = *Olea europaea var. Sylvestris*
LOC111400014	2,915555563	0,0532652			XP_022883260.1	IAA29 auxin-responsive protein = *Olea europaea var. Sylvestris*

LOC111408261			-2,102300793	6,03E-03	XP_022893814.1	IAA29 auxin-responsive protein = *Olea europaea var. Sylvestris*
LOC111387294	1,762776142	0,0015177	-4,219062912	4,65E-07	XP_022867612.1	IAA33 auxin-responsive protein = *Olea europaea var. Sylvestris*
LOC111402809			1,885556713	2,45E-26	XP_022886908.1	IAA8 auxin-responsive protein = *Olea europaea var. Sylvestris*
LOC111369910	1,613794605	0,3902104	1,547237655	1,35E-01	XP_022847394.1	ARF10 auxin response factor 10-like= *Olea europaea var. Sylvestris*
LOC111387746			-1,091652529	4,59E-02	-	ARF16 auxin response factor 16-like = *Olea europaea var. Sylvestris*
LOC111390689	-1,778776608	0,0664554	4,260754889	9,06E-12	XP_022871540.1	ARF18 auxin response factor 18 = *Olea europaea var. Sylvestris*
LOC111397849			-1,516253549	1,57E-05	XP_022880587.1	ARF18 auxin response factor 18-like = *Olea europaea var. Sylvestris*
LOC111409930	-1,874930721	2,059E-23			XP_022895821.1	ARF18 auxin response factor 18-like = Olea europaea var. Sylvestris
LOC111366099	-1,062942407	2,594E-10			XP_022842521.1	ARF19 auxin response factor 19-like = *Olea europaea var. Sylvestris*
LOC111366891			-1,040152963	3,59E-10	XP_022843346.1	ARF19 auxin response factor 19-like = *Olea europaea var. Sylvestris*
LOC111369829			1,729655827	7,14E-16	XP_022847289.1	ARF19 auxin response factor 19-like = *Olea europaea var. Sylvestris*
LOC111388535	1,031005812	0,8362085			XP_022869037.1	ARF2B auxin response factor 2B-like= *Olea europaea var. Sylvestris*
LOC111370596			-1,648776036	2,90E-02	XP_022848157.1	ARF3 auxin response factor 3-like = *Olea europaea var. Sylvestris*
LOC111371065	-1,150008131	0,2266741			XP_022848749.1	ARF4 auxin response factor 4-like = *Olea europaea var. Sylvestris*
LOC111380232			-1,450337012	3,27E-04	XP_022859505.1	ARF5 auxin response factor 5-like = *Olea europaea var. Sylvestris*
LOC111408863			-1,630810453	3,75E-03	XP_022894443.1	ARF5 auxin response factor 5-like = *Olea europaea var. Sylvestris*
LOC111375479	-1,45042148	0,0124937			XP_022854076.1	ARF9 auxin response factor 9-like = Olea europaea var. Sylvestris
LOC111390474	-1,950010328	4,127E-18			XP_022871290.1	ARF9 auxin response factor 9-like = *Olea europaea var. Sylvestris*
LOC111410397	-1,79219187	0,7198538			XP_022896478.1	ARF9 auxin response factor 9-like = Olea europaea var. Sylvestris
LOC111394947	2,279140502	0,5829192	4,03977591	2,18E-03	XP_022876755.1	SAUR21 auxin-responsive protein = *Olea europaea var. Sylvestris*
LOC111410571	1,247107701	0,8020034	5,011673146	2,20E-03	XP_022896751.1	SAUR21 auxin-responsive protein = *Olea europaea var. Sylvestris*
LOC111377777			1,728792192	3,66E-02	XP_022856671.1	SAUR32 auxin-responsive protein = *Olea europaea var. Sylvestris*
LOC111393889	-1,007928203	6,716E-06			XP_022875429.1	SAUR32 auxin-responsive protein = Olea europaea var. Sylvestris
LOC111405653	-1,346144589	1,704E-11			XP_022890399.1	SAUR32 auxin-responsive protein = *Olea europaea var. Sylvestris*

LOC111368774			2,973741831	2,11E-25	XP_022845979.1	SAUR36 auxin-responsive protein = *Olea europaea var. Sylvestris*
LOC111380237			-2,215775458	6,57E-02	XP_022859512.1	SAUR36 auxin-responsive protein = *Olea europaea var. Sylvestris*
LOC111384477			1,37414517	3,25E-02	XP_022864521.1	SAUR36 auxin-responsive protein = *Olea europaea var. Sylvestris*
LOC111394028	1,36965948	7,993E-06			XP_022875586.1	SAUR36 auxin-responsive protein = *Olea europaea var. Sylvestris*
LOC111404857	1,958056243	0,3094238			XP_022889361.1	SAUR50 auxin-responsive protein = *Olea europaea var. Sylvestris*
LOC111371886	1,564753479	0,5665039			XP_022849809.1	SAUR50 auxin-responsive protein = *Olea europaea var. Sylvestris*
LOC111378179	5,34003874	0,0049742	1,887980146	2,95E-03	XP_022857113.1	SAUR50 auxin-responsive protein = *Olea europaea var. Sylvestris*
LOC111394563	3,438340588	0,0814065	1,777182537	1,80E-02	XP_022876198.1	SAUR50 auxin-responsive protein = *Olea europaea var. Sylvestris*
LOC111402646	1,031005812	0,8362085	3,854388135	4,22E-02	XP_022886787.1	SAUR50 auxin-responsive protein = *Olea europaea var. Sylvestris*
LOC111410569	3,882654309	0,1217359	4,095719848	1,16E-08	XP_022896750.1	SAUR50 auxin-responsive protein = *Olea europaea var. Sylvestris*
LOC111412088	2,877819974	0,0573843	2,772281346	8,85E-07	XP_022898615.1	SAUR50 auxin-responsive protein = *Olea europaea var. Sylvestris*
LOC111395251			-1,315930107	6,53E-09	XP_022877005.1	SAUR50 auxin-responsive protein= *Olea europaea var. Sylvestris*
LOC111381635			-1,267382768	1,53E-01	XP_022861202.1	SAUR62 auxin-responsive protein = *Olea europaea var. Sylvestris*
LOC111385898	1,059616738	0,0556983			XP_022866088.1	SAUR66 auxin-responsive protein = *Olea europaea var. Sylvestris*
LOC111366467	1,031005812	0,8362085			XP_022842991.1	SAUR71 auxin-responsive protein = *Olea europaea var. Sylvestris*
LOC111370706			1,307274585	8,12E-07	XP_022848311.1	SAUR71 auxin-responsive protein = *Olea europaea var. Sylvestris*
LOC111373000	1,825083011	0,5130226			XP_022851215.1	SAUR71 auxin-responsive protein = *Olea europaea var. Sylvestris*
LOC111400044			3,803400992	3,82E-07	XP_022883272.1	SAUR71 auxin-responsive protein = *Olea europaea var. Sylvestris*
LOC111408167	1,031005812	0,8362085			XP_022893737.1	SAUR71 auxin-responsive protein = *Olea europaea var. Sylvestris*
LOC111365787	-1,458597481	0,0008132	3,927476516	2,53E-40	XP_022842078.1	SAUR72 auxin-responsive protein = *Olea europaea var. Sylvestris*

Table 3.II.S15. Ethylene-related genes induced or repressed in the first comparison (d18:0-AZ vs. C-AZ) and the second comparison (d18:0-LAZ vs. d18:0-AZ).

	d18:0-AZ vs. C-AZ		d18:0-LAZ vs. d18:0-AZ			
Gene	log2FoldChange	pvalue	log2FoldChange	pvalue	Gene_ID	Description
LOC111385098	1,161581988	4,235E-08	1,235596104	1,90E-12	XP_022865232.1	SAM-Mtase At5g37990 probable S-adenosylmethionine-dependent methyltransferase = *Olea europaea var. Sylvestris*
LOC111396063	-1,281607803	3,401E-11			XP_022878101.1	SAMS1 S-adenosylmethionine synthase 1=*Olea europaea var. Sylvestris*
LOC111409846			-1,356020944	3,923E-12	XP_022895694.1	SAMS1 S-adenosylmethionine synthase 1-like=*Olea europaea var. Sylvestris*
LOC111409847	1,059370223	3,52E-07			XP_022895695.1	SAMS1 S-adenosylmethionine synthase 1-like=*Olea europaea var. Sylvestris*
LOC111374289	-2,904053196	4,598E-05			XP_022852716.1	SAMS2 S-adenosylmethionine synthase 2-like= *Olea europaea var. Sylvestris*
LOC111382863			-1,378911631	4,404E-11	XP_022862667.1	SAMS2 S-adenosylmethionine synthase 2-like= *Olea europaea var. Sylvestris*
LOC111390594	-1,163203951	3,675E-13			XP_022871420.1	SAMS2 S-adenosylmethionine synthase 2-like= *Olea europaea var. Sylvestris*
LOC111372200	-2,742003931	4,7E-51			XP_022850196.1	SAMS3 S-adenosylmethionine synthase 3= *Olea europaea var. Sylvestris*
LOC111381563			-3,145518571	0,0002604	XP_022861124.1	SAMS3 S-adenosylmethionine synthase 3-like= *Olea europaea var. Sylvestris*
LOC111403119	-1,834406666	1,021E-28			XP_022887275.1	SAMS3 S-adenosylmethionine synthase 3-like= *Olea europaea var. Sylvestris*
LOC111380501	-3,305007259	9,095E-39	1,497246987	4,36E-06	XP_022859853.1	ACS 1-aminocyclopropane-1-carboxylate synthase-like = *Olea europaea var. Sylvestris*
LOC111370655			3,831037118	9,24E-31	XP_022848244.1	ACO 1-aminocyclopropane-1-carboxylate oxidase-like= *Olea europaea var. Sylvestris*
LOC111370656	-1,208636204	1,264E-12	2,161004602	9,73E-39	XP_022848245.1	ACO 1-aminocyclopropane-1-carboxylate oxidase-like= *Olea europaea var. Sylvestris*
LOC111370659	-1,041264759	0,5789102	10,89089989	1,47E-37	XP_022848247.1	ACO 1-aminocyclopropane-1-carboxylate oxidase-like= *Olea europaea var. Sylvestris*
LOC111369484	4,460194175	0,0448121	-4,474132139	0,0362981	XP_022846777.1	ACO1 1-aminocyclopropane-1-carboxylate oxidase homolog 1-like = *Olea europaea var. Sylvestris*
LOC111376167			1,813509507	1,20E-13	XP_022854875.1	ACO1 1-aminocyclopropane-1-carboxylate oxidase homolog 1-like= *Olea europaea var. Sylvestris*
LOC111387087	-1,344419716	4,598E-09			XP_022867370.1	ACO1 1-aminocyclopropane-1-carboxylate oxidase homolog 1-like= *Olea europaea var. Sylvestris*
LOC111390562	-2,748890366	4,317E-09	1,654051874	3,01E-03	XP_022871389.1	ACO1 1-aminocyclopropane-1-carboxylate oxidase homolog 1-like= *Olea europaea var. Sylvestris*

LOC111392652			-1,584780371	6,288E-05	XP_022873797.1	ACO1_1-aminocyclopropane-1-carboxylate oxidase homolog 1-like= *Olea europaea var. Sylvestris*
LOC111392646	1,373518724	0,0013469	1,01726009	3,64E-04	XP_022873791.1	ACO11_1-aminocyclopropane-1-carboxylate oxidase homolog 11-like= *Olea europaea var. Sylvestris*
LOC111393342	-2,263268308	4,461E-23	1,778168545	1,04E-13	XP_022874608.1	ETR2 ethylene receptor 2-like= *Olea europaea var. Sylvestris*
LOC111373392	-1,659489945	5,057E-22	1,816480732	3,20E-25	XP_022851687.1	EIN4 = *Olea europaea var. Sylvestris*
LOC111381869			-3,160269127	0,1043172	XP_022861485.1	CTR1 serine/threonine-protein kinase = *Olea europaea var. Sylvestris*
LOC111409465			-1,782188913	0,1569613	XP_022895279.1	CTR1 serine/threonine-protein kinase = *Olea europaea var. Sylvestris*
LOC111374032			1,152631809	1,37E-10	XP_022852416.1	EIN2 ethylene-insensitive protein 2-like= *Olea europaea var. Sylvestris*
LOC111379395			1,082620687	2,62E-13	XP_022858519.1	EIN3 protein ETHYLENE INSENSITIVE 3-like= *Olea europaea var. Sylvestris*
LOC111387870			1,617787998	2,40E-28	XP_022868235.1	EIN3-binding F-box protein 2-like= *Olea europaea var. Sylvestris*
LOC111373045	-2,348386685	9,757E-44	1,453067391	1,44E-15		EBF1_EIN3-binding F-box protein 1-like= Olea europaea var. Sylvestris
LOC111407932	-2,232164905	9,843E-07	5,340495508	1,88E-68	XP_022893426.1	EBF1_EIN3-binding F-box protein 1-like= *Olea europaea var. Sylvestris*
LOC111409471	-2,942501487	9,829E-20	3,53359776	7,86E-34		EBF2_EIN3-binding F-box protein 2-like= *Olea europaea var. Sylvestris*
LOC111369788			-1,015713731	6,78E-05	XP_022847201.1	ERF At4g13040 ethylene-responsive transcription factor-like protein = *Olea europaea var. Sylvestris*
LOC111365833	3,845262085	0,0005263			XP_022842116.1	ERF003 ethylene-responsive transcription factor = *Olea europaea var. Sylvestris*
LOC111368607			1,806743542	1,19E-02	XP_022845722.1	ERF003 ethylene-responsive transcription factor = *Olea europaea var. Sylvestris*
LOC111384118	1,072332118	0,4753515	1,106656532	2,57E-01	XP_022864125.1	ERF003 ethylene-responsive transcription factor = *Olea europaea var. Sylvestris*
LOC111407442	-2,407709758	4,344E-26			XP_022892676.1	ERF003 ethylene-responsive transcription factor = *Olea europaea var. Sylvestris*
LOC111385757			-1,04131887	5,812E-05	XP_022865941.1	ERF008 ethylene-responsive transcription factor = *Olea europaea var. Sylvestris*
LOC111401352	1,150695316	3,871E-08			XP_022884823.1	ERF011 ethylene-responsive transcription factor = *Olea europaea var. Sylvestris*
LOC111389112	-2,840833667	0,0197677			XP_022869737.1	ERF014 ethylene-responsive transcription factor = *Olea europaea var. Sylvestris*
LOC111402039	-2,114962834	8,795E-07	2,75890815	1,22E-13	XP_022885843.1	ERF014 ethylene-responsive transcription factor = *Olea europaea var. Sylvestris*

LOC111408692	-1,373170631	0,0055847	2,430250435	8,76E-10	XP_022894210.1	ERF014 ethylene-responsive transcription factor = *Olea europaea var. Sylvestris*
LOC111371249	-3,031417447	1,943E-10			XP_022848905.1	ERF017 ethylene-responsive transcription factor = *Olea europaea var. Sylvestris*
LOC111373863	-2,044926531	0,0001501	1,002429797	1,11E-01	XP_022852217.1	ERF017 ethylene-responsive transcription factor = *Olea europaea var. Sylvestris*
LOC111404291			3,074218473	8,03E-52	XP_022888889.1	ERF017 ethylene-responsive transcription factor = *Olea europaea var. Sylvestris*
LOC111411371	-1,852630572	1,241E-08	4,134643884	2,14E-65	XP_022897679.1	ERF017 ethylene-responsive transcription factor = *Olea europaea var. Sylvestris*
LOC111410947	1,533671155	0,077495	1,092726514	4,91E-02	XP_022897305.1	ERF023-like ethylene-responsive transcription factor = *Olea europaea var. Sylvestris*
LOC111368831	-2,299911414	8,903E-27			XP_022846068.1	ERF027 ethylene-responsive transcription factor = *Olea europaea var. Sylvestris*
LOC111372960	-1,378682301	2,373E-12			XP_022851160.1	ERF027 ethylene-responsive transcription factor = *Olea europaea var. Sylvestris*
LOC111383740	3,686772068	0,1604268	2,487864915	1,17E-02	XP_022863649.1	ERF038 ethylene-responsive transcription factor = *Olea europaea var. Sylvestris*
LOC111383528	5,717343907	0,0016349			XP_022863412.1	ERF038 ethylene-responsive transcription factor= *Olea europaea var. Sylvestris*
LOC111380963	-1,345300529	0,5386562	3,420963806	1,99E-02	XP_022860415.1	ERF062 ethylene-responsive transcription factor = *Olea europaea var. Sylvestris*
LOC111408635			-1,051911057	0,1233852	XP_022894144.1	ERF069 ethylene-responsive transcription factor = *Olea europaea var. Sylvestris*
LOC111406366	-2,260353684	4,189E-09			XP_022891565.1	ERF071 ethylene-responsive transcription factor = *Olea europaea var. Sylvestris*
LOC111406367	-3,858247732	1,701E-58	3,388270479	5,40E-42	XP_022891566.1	ERF071 ethylene-responsive transcription factor = *Olea europaea var. Sylvestris*
LOC111372748	-1,807450988	0,4105609			XP_022850908.1	ERF091 ethylene-responsive transcription factor = *Olea europaea var. Sylvestris*
LOC111376163	-4,622537896	0,0086075	5,595559156	3,67E-04	XP_022854872.1	ERF095 ethylene-responsive transcription factor = *Olea europaea var. Sylvestris*
LOC111388199	-1,392621106	1,551E-14	1,273489808	3,57E-11	XP_022868653.1	ERF1 ethylene-responsive transcription factor 1-like= *Olea europaea var. Sylvestris*
LOC111386756	-1,642498638	8,39E-07			XP_022866990.1	ERF104 ethylene-responsive transcription factor = *Olea europaea var. Sylvestris*
LOC111386758			1,37652933	2,16E-05	XP_022866991.1	ERF104 ethylene-responsive transcription factor = *Olea europaea var. Sylvestris*
LOC111367121			-1,310550973	0,0005126	XP_022843617.1	ERF107 ethylene-responsive transcription factor = *Olea europaea var. Sylvestris*
LOC111411051	-5,198277039	1,33E-20	2,723872478	5,00E-04	XP_022897392.1	ERF109 ethylene-responsive transcription factor = *Olea europaea var. Sylvestris*

LOC111366214			2,275944636	1,54E-06	XP_022842691.1	ERF113 ethylene-responsive transcription factor = *Olea europaea var. Sylvestris*
LOC111396122			2,010675871	2,44E-15	XP_022878201.1	ERF113 ethylene-responsive transcription factor = *Olea europaea var. Sylvestris*
LOC111403203	1,396797453	2,152E-05	-2,005652908	6,456E-09	XP_022887380.1	ERF118 ethylene-responsive transcription factor = *Olea europaea var. Sylvestris*
LOC111370300			1,139997956	6,14E-02	XP_022847741.1	ERF12 ethylene-responsive transcription factor 12-like= *Olea europaea var. Sylvestris*
LOC111381485	1,111094366	0,0442995			XP_022861036.1	ERF12 ethylene-responsive transcription factor 12-like= *Olea europaea var. Sylvestris*
LOC111392889			-1,421470686	0,034543	XP_022874066.1	ERF12 ethylene-responsive transcription factor 12-like= *Olea europaea var. Sylvestris*
LOC111396042	1,128234006	0,000273			XP_022878070.1	ERF12 ethylene-responsive transcription factor 12-like= *Olea europaea var. Sylvestris*
LOC111382957	-3,47519957	9,438E-08	1,39865028	1,22E-01	XP_022862772.1	ERF1A ethylene-responsive transcription factor 1A-like= *Olea europaea var. Sylvestris*
LOC111390583			2,18082865	1,20E-06	XP_022871411.1	ERF1B ethylene-responsive transcription factor 1B-like= *Olea europaea var. Sylvestris*
LOC111391942	-1,858400417	0,0007694	1,150157113	5,58E-02		ERF1B ethylene-responsive transcription factor 1B-like= *Olea europaea var. Sylvestris*
LOC111391879	-1,625415391	2,468E-05			XP_022872924.1	ERF2 ethylene-responsive transcription factor 2-like= *Olea europaea var. Sylvestris*
LOC111405546	-1,38175771	1,528E-16			XP_022890259.1	ERF2 ethylene-responsive transcription factor 2-like= *Olea europaea var. Sylvestris*
LOC111395465	-1,018805801	4,886E-09			XP_022877236.1	ERF4 ethylene-responsive transcription factor 4-like= *Olea europaea var. Sylvestris*
LOC111379291			1,598890517	9,72E-18		ERF5 ethylene-responsive transcription factor 5-like= *Olea europaea var. Sylvestris*
LOC111405547	-1,075099018	2,861E-07			XP_022890260.1	ERF5 ethylene-responsive transcription factor 5-like= *Olea europaea var. Sylvestris*
LOC111372227			1,544499305	1,38E-07	XP_022850227.1	ABR1 ethylene-responsive transcription factor = *Olea europaea var. Sylvestris*
LOC111373050	1,143538876	0,3846278	1,633244607	3,39E-02	XP_022851284.1	ABR1 ethylene-responsive transcription factor = *Olea europaea var. Sylvestris*
LOC111390424	-3,958647482	1,025E-18	-2,049386287	0,0914605	XP_022871231.1	ABR1 ethylene-responsive transcription factor = *Olea europaea var. Sylvestris*
LOC111397387			1,873740892	2,19E-20	XP_022880057.1	ABR1 ethylene-responsive transcription factor = *Olea europaea var. Sylvestris*
LOC11136617	2,010123412	0,1128439	-3,100224346	0,0363848	XP_022842633.1	AIL1 AP2-like ethylene-responsive transcription factor = *Olea europaea var. Sylvestris*
LOC111374630			2,517536023	8,84E-07	XP_022853103.1	AIL5 AP2-like ethylene-responsive transcription factor = *Olea europaea var. Sylvestris*

LOC111390109	2,272388417	0,0998642	3,603836029	1,15E-13	XP_022870872.1	ANT AP2-like ethylene-responsive transcription factor = *Olea europaea var. Sylvestris*
LOC111384308	2,044367201	0,0495286	2,241005174	2,61E-06	XP_022864341.1	ANT AP2-like ethylene-responsive transcription factor= *Olea europaea var. Sylvestris*
LOC111384111			-2,546803678	0,0438424	XP_022864119.1	At1g79700 AP2-like ethylene-responsive transcription factor = *Olea europaea var. Sylvestris*
LOC111372046	2,848793059	0,0007039	1,775312381	3,96E-06	XP_022849967.1	At1g16060 AP2-like ethylene-responsive transcription factor = Olea europaea var. Sylvestris
LOC111408880	1,308401903	0,1184874			XP_022894466.1	At2g41710 AP2-like ethylene-responsive transcription factor = *Olea europaea var. Sylvestris*
LOC111366637	-1,614346604	0,1908219	3,928606007	8,40E-07	XP_022843119.1	BBM2 AP2-like ethylene-responsive transcription factor = *Olea europaea var. Sylvestris*
LOC111371777			1,582239598	4,76E-04	XP_022849697.1	CRF1 ethylene-responsive transcription factor = *Olea europaea var. Sylvestris*
LOC111402954	-1,119666089	0,000968			XP_022887053.1	CRF1 ethylene-responsive transcription factor = *Olea europaea var. Sylvestris*
LOC111386382	2,017469395	9,708E-07			XP_022866607.1	CRF1 ethylene-responsive transcription factor= *Olea europaea var. Sylvestris*
LOC111375459	-1,485938291	0,5191252			XP_022854050.1	CRF2 ethylene-responsive transcription factor = *Olea europaea var. Sylvestris*
LOC111374078			1,787255404	5,22E-10	XP_022852475.1	CRF4 ethylene-responsive transcription factor = *Olea europaea var. Sylvestris*
LOC111400879			-1,7925384	0,2234593	XP_022884093.1	CRF4 ethylene-responsive transcription factor = *Olea europaea var. Sylvestris*
LOC111403560	-2,150034981	2,127E-12	2,843285973	4,43E-25	XP_022887882.1	RAP2-3 ethylene-responsive transcription factor = *Olea europaea var. Sylvestris*
LOC111388482	5,230281122	0,0068464	-2,187320546	0,1023113	XP_022868974.1	RAP2-7 ethylene-responsive transcription factor = *Olea europaea var. Sylvestris*
LOC111368962	2,329350016	0,3343874			XP_022846223.1	RAP2-7 ethylene-responsive transcription factor = *Olea europaea var. Sylvestris*
LOC111368963			-1,148877322	0,1769305		RAP2-7 ethylene-responsive transcription factor = *Olea europaea var. Sylvestris*
LOC111382065			-1,328335933	0,0006876	XP_022861697.1	RAP2-7 ethylene-responsive transcription factor = *Olea europaea var. Sylvestris*
LOC111366136	-2,435213025	4,453E-23	2,491227248	4,80E-24	XP_022842585.1	TINY ethylene-responsive transcription factor = *Olea europaea var. Sylvestris*
LOC111377938	1,431448415	1,572E-07			XP_022856866.1	TINY ethylene-responsive transcription factor = *Olea europaea var. Sylvestris*
LOC111400023	-1,966585604	0,2240479	2,241936872	1,25E-01	XP_022883264.1	TINY ethylene-responsive transcription factor = *Olea europaea var. Sylvestris*
LOC111407872	1,875403816	0,1476052			XP_022893335.1	TINY ethylene-responsive transcription factor = *Olea europaea var. Sylvestris*

LOC111401005			-2,286014035	9,494E-19	XP_022884297.1	TOE3 AP2-like ethylene-responsive transcription factor = *Olea europaea var. Sylvestris*
LOC111368316	2,473137831	0,0110788			XP_022845453.1	WIN1 ethylene-responsive transcription factor = *Olea europaea var. Sylvestris*
LOC111383997	-1,801997461	0,7183482			XP_022863964.1	WIN1 ethylene-responsive transcription factor = *Olea europaea var. Sylvestris*
LOC111410970	-1,79219187	0,7198538			XP_022897334.1	WIN1 ethylene-responsive transcription factor = *Olea europaea var. Sylvestris*

Table 3.II.S16. ABA-related genes induced or repressed in the first comparison (d18:0-AZ vs. C-AZ) and the second comparison (d18:0-LAZ vs. d18:0-AZ).

	d18:0-AZ vs. C-AZ		d18:0-LAZ vs. d18:0-AZ			
Gene	log2FoldChange	pvalue	log2FoldChange	pvalue	Gene_ID	Description
LOC111397178			1,100455357	4,014E-07	XP_022879717.1	PSY2 phytoene synthase 2, chloroplastic = *Olea europaea var. Sylvestris*
LOC111383342	-2,500119779	3,06E-46	1,239954379	2,197E-10	XP_022863205.1	ZEP zeaxanthin epoxidase, chloroplastic = *Olea europaea var. Sylvestris*
LOC111378165	-2,341851199	3,88E-11	2,105200539	2,356E-09	XP_022857097.1	ZEP zeaxanthin epoxidase, chloroplastic-like = *Olea europaea var. Sylvestris*
LOC111390917	-2,446270225	4,3E-24	2,459072491	1,088E-24	XP_022871809.1	ZEP zeaxanthin epoxidase, chloroplastic-like = *Olea europaea var. Sylvestris*
LOC111390352			-1,427884404	0,0041043	XP_022871146.1	VDE violaxanthin de-epoxidase, chloroplastic = *Olea europaea var. Sylvestris*
LOC111405868			1,392283539	2,486E-13	XP_022890717.1	AAO3 abscisic-aldehyde oxidase-like = *Olea europaea var. Sylvestris*
LOC111370875	1,683088116	0,026309	1,2871023	0,0038927	XP_022848544.1	NCED1 9-cis-epoxycarotenoid dioxygenase , chloroplastic-like = *Olea europaea var. Sylvestris*
LOC111386602			-2,176903218	0,0024923	XP_022866840.1	NCED1 9-cis-epoxycarotenoid dioxygenase , chloroplastic-like = *Olea europaea var. Sylvestris*
LOC111395789	1,11813998	0,000327			XP_022877706.1	NCED1 9-cis-epoxycarotenoid dioxygenase , chloroplastic-like = *Olea europaea var.*
LOC111381076	-2,459429505	0,191968			XP_022860562.1	ABA-8-OH2 abscisic acid 8-hydroxylase 2-like = *Olea europaea var. Sylvestris*
LOC111393533	4,510174283	0,040076	1,160647166	0,2253059	XP_022874870.1	ABA-8-OH2 abscisic acid 8-hydroxylase 2-like= *Olea europaea var. Sylvestris*
LOC111401342	1,092082568	0,085529	3,295652273	9,334E-28	XP_022884809.1	ABA-8-OH4 abscisic acid 8-hydroxylase 4-like = *Olea europaea var. Sylvestris*
LOC111409085	1,900838068	0,684337			XP_022894768.1	ABA-8-OH4 abscisic acid 8-hydroxylase 4-like = *Olea europaea var. Sylvestris*
LOC111410611	-1,801997461	0,718348			XP_022896810.1	ABA-8-OH4 abscisic acid 8-hydroxylase 4-like = *Olea europaea var. Sylvestris*
LOC111372855	-1,518282855	0,158759			XP_022851036.1	PYL4 abscisic acid receptor = *Olea europaea var. Sylvestris*
LOC111392557			-1,791075739	3,378E-06	XP_022873689.1	PYL4 abscisic acid receptor = *Olea europaea var. Sylvestris*
LOC111408032	1,564753479	0,566504			XP_022893547.1	PYL4 abscisic acid receptor = *Olea europaea var. Sylvestris*
LOC111379366	-1,529333014	9,2E-17			XP_022858493.1	PYL4 abscisic acid receptor PYL4-like = *Olea europaea var. Sylvestris*
LOC111383476	1,231755951	0,000251			XP_022863355.1	PYL8 abscisic acid receptor = *Olea europaea var. Sylvestris*
LOC111411941	1,066453289	7,53E-07	-2,047234606	7,344E-19	XP_022898402.1	PYL9 abscisic acid receptor = *Olea europaea var. Sylvestris*
LOC111389899			1,398930182	1,277E-05	XP_022870650.1	PYR1 abscisic acid receptor = *Olea europaea var. Sylvestris*
LOC111384648			-1,007432766	0,4314874	XP_022864727.1	RGL1-DELLA protein RGL1-like = *Olea europaea var. Sylvestris*
LOC111377023	-1,494649685	0,044103			XP_022855807.1	RGL2-DELLA protein = *Olea europaea var. Sylvestris*
LOC111388316	-3,06503032	5,86E-17			XP_022868763.1	RGL2-DELLA protein = *Olea europaea var. Sylvestris*
LOC111367486	1,366207587	2,62E-07			XP_022844159.1	GAI-DELLA protein = *Olea europaea var. Sylvestris*
LOC111386841	-1,177525785	1,07E-08			XP_022867092.1	PP2C 27 probable protein phosphatase 2C 27 = *Olea europaea var. Sylvestris*
LOC111386928			2,278644148	0,0171379	-	PP2C 37 protein phosphatase 2C 37-like = *Olea europaea var. Sylvestris*
LOC111388926	-1,383889857	2,85E-06			XP_022869523.1	PP2C 4 probable protein phosphatase 2C 4 = *Olea europaea var. Sylvestris*
LOC111404627	-5,117003134	0,014946			XP_022889380.1	PP2C 75 probable protein phosphatase 2C 75 = *Olea europaea var. Sylvestris*
LOC111393237			1,734257755	1,799E-06	XP_022874444.1	PP2C 4 probable protein phosphatase 2C 4 = *Olea europaea var. Sylvestris*
LOC111407408			-1,507063134	1,063E-15	XP_022892626.1	PP2C 37 protein phosphatase 2C 37-like = *Olea europaea var. Sylvestris*
LOC111410709			1,502343627	1,191E-12	XP_022896953.1	BIPP2C1 probable protein phosphatase 2C = *Olea europaea var. Sylvestris*
LOC111388302	-2,638363101	2,21E-28	1,01788582	0,0004153	-	PP2C4 probable protein phosphatase 2C 4 = *Olea europaea var. Sylvestris*
LOC111388303	-2,30174373	1,43E-22			XP_022868748.1	PP2C4 probable protein phosphatase 2C 4 = *Olea europaea var. Sylvestris*
LOC111397585	-3,016599805	1,08E-09	1,479499139	0,0206256	XP_022880349.1	PP2C6 probable protein phosphatase 2C 6 = *Olea europaea var. Sylvestris*

LOC111412005			1,411266948	6,939E-14	XP_022898495.1	ABI5 5 ABSCISIC ACID-INSENSITIVE 5-like protein 5 = *Olea europaea var. Sylvestris*
LOC111394682	-1,887354987	3,72E-33			XP_022876389.1	ABI5 6 ABSCISIC ACID-INSENSITIVE 5-like protein 6 = *Olea europaea var. Sylvestris*
LOC111404083			-3,797681999	0,0357273	XP_022888584.1	ABI5 protein ABSCISIC ACID-INSENSITIVE 5-like = *Olea europaea var. Sylvestris*
LOC111380278	1,831103767	0,070367	1,132500369	0,0604932	XP_022859558.1	CAR4 protein C2-DOMAIN ABA-RELATED 4-like = *Olea europaea var. Sylvestris*
LOC111382820			2,00901372	0,1430984	XP_022862629.1	CAR5 protein C2-DOMAIN ABA-RELATED 5-like = *Olea europaea var. Sylvestris*
LOC111406140	-1,168199169	4,26E-10			XP_022891134.1	CAR7 protein C2-DOMAIN ABA-RELATED 7-like = *Olea europaea var. Sylvestris*

Table 3.II.S17. SA-related genes induced or repressed in the first comparison (d18:0-AZ vs. C-AZ) and the second comparison (d18:0-LAZ vs. d18:0-AZ).

	d18:0-AZ vs. C-AZ		d18:0-LAZ vs. d18:0-AZ			
Gene	**log2FoldChange**	**pvalue**	**log2FoldChange**	**pvalue**	**Gene_ID**	**Description**
LOC111402181			-1,785166413	2,06E-26	XP_022886100.1	PAL phenylalanine ammonia-lyase-like = *Olea europaea var. sylvestris*
LOC111403111	1,501745842	4,118E-20	-2,686322698	1,13E-52	XP_022887263.1	PAL phenylalanine ammonia-lyase-like = *Olea europaea var. sylvestris*
LOC111379838			-1,096168847	2,78E-01	XP_022859041.1	SAMT salicylate carboxymethyltransferase-like = *Olea europaea var. sylvestris*
LOC111409560	3,462223968	3,2E-09	-4,071120469	2,69E-10	XP_022895367.1	SAMT salicylate carboxymethyltransferase-like = *Olea europaea var. sylvestris*
LOC111409569	-3,795067035	0,1773434			XP_022895373.1	SAMT salicylate carboxymethyltransferase-like = *Olea europaea var. sylvestris*
LOC111409575	1,278619985	1,564E-05	-2,606475501	6,61E-15	XP_022895378.1	SAMT salicylate carboxymethyltransferase-like = *Olea europaea var. sylvestris*
LOC111378982			3,981958128	3,00E-03	XP_022858058.1	PR-1 pathogenesis-related protein PR-1-like = *Olea europaea var. sylvestris*
LOC111376308	1,570368155	0,2150305	-5,340528938	4,30E-03	XP_022855025.1	PR-1 pathogenesis-related protein = *Olea europaea var. sylvestris*
LOC111391368	1,143538876	0,3846278	-3,450637385	6,41E-02	XP_022872333.1	SABP2 salicylic acid-binding protein 2-like = *Olea europaea var. sylvestris*
LOC111378890			-1,899946362	4,04E-04	XP_022857938.1	SABP2 salicylic acid-binding protein 2-like = *Olea europaea var. sylvestris*
LOC111379239	1,765177851	2,262E-08	2,176181778	1,40E-27	XP_022858350.1	SABP2 salicylic acid-binding protein 2-like = *Olea europaea var. sylvestris*
LOC111392105	-1,010706889	3,89E-10			XP_022873147.1	SABP2 salicylic acid-binding protein 2-like = *Olea europaea var. sylvestris*

Table 3.II.S18. JA-related genes induced or repressed in the first comparison (d18:0-AZ vs. C-AZ) and the second comparison (d18:0-LAZ vs. d18:0-AZ).

	d18:0-AZ vs. C-AZ		d18:0-LAZ vs. d18:0-AZ			
Gene	log2FoldChange	pvalue	log2FoldChange	pvalue	Gene_ID	Description
LOC111366164	-2,692768148	1,152E-53			XP_022842625.1	LOX 3-1linoleate 13S-lipoxygenase 3-1, chloroplastic-like= *Olea europaea var. Sylvestris*
LOC111388392	1,46318433	3,822E-17			XP_022868846.1	LOX1.5 probable linoleate 9S-lipoxygenase 5 = *Olea europaea var. Sylvestris*
LOC111392344	1,182390112	9,337E-09	1,325747043	1,499E-13	XP_022873439.1	LOX2 linoleate 13S-lipoxygenase 2-1, chloroplastic-like= *Olea europaea var. Sylvestris*
LOC111399759	-2,846965263	1,196E-74			XP_022882998.1	OPR3 12-oxophytodienoate reductase 3 = *Olea europaea var. Sylvestris*
LOC111403883	-1,841722808	9,471E-14			XP_022888288.1	OPR3 12-oxophytodienoate reductase 3-like = *Olea europaea var. Sylvestris*
LOC111403882	-1,6115776	9,056E-22			XP_022888287.1	OPR3 12-oxophytodienoate reductase 3-like= *Olea europaea var. Sylvestris*
LOC111399032			-1,973479004	0,0003501	XP_022881999.1	AOC allene oxide cyclase, chloroplastic-like = *Olea europaea var. Sylvestris*
LOC111408828	-1,178297026	3,74E-10	2,009324622	1,203E-29	XP_022894376.1	AOS1 allene oxide synthase 1, chloroplastic-like = Olea europaea var. Sylvestris
LOC111401326	-1,373395592	0,1007263	2,172605005	0,0014029	XP_022884787.1	AOS1 allene oxide synthase 1, chloroplastic-like= *Olea europaea var. Sylvestris*
LOC111377782			3,698544953	5,669E-97	XP_022856678.1	JAR1 jasmonic acid-amido synthetase = *Olea europaea var. Sylvestris*
LOC111409949	1,406414511	2,691E-11			XP_022895848.1	JAR1 jasmonic acid-amido synthetase = *Olea europaea var. Sylvestris*
LOC111394433	-3,703753353	0,065013			XP_022876027.1	JMT jasmonate O-methyltransferase-like = *Olea europaea var. Sylvestris*
LOC111394434	-1,221161311	0,1496693			XP_022876028.1	JMT jasmonate O-methyltransferase-like = *Olea europaea var. Sylvestris*
LOC111394436			-1,838251269	0,1374706	XP_022876029.1	JMT jasmonate O-methyltransferase-like = *Olea europaea var. Sylvestris*
LOC111394927	-2,786656368	0,4864548			XP_022876741.1	JMT jasmonate O-methyltransferase-like = *Olea europaea var. Sylvestris*
LOC111397089			1,391978391	4,945E-12	XP_022879601.1	COI1b coronatine-insensitive protein homolog 1b-like = *Olea europaea var. Sylvestris*
LOC111408086	-1,860494451	4,671E-31			XP_022893634.1	TPR3 topless-related protein 3-like = *Olea europaea var. Sylvestris*

Table 3.II.S19. GA-related genes induced or repressed in the first comparison (d18:0-AZ vs. C-AZ) and the second comparison (d18:0-LAZ vs. d18:0-AZ).

	d18:0-AZ vs. C-AZ		d18:0-LAZ vs. d18:0-AZ			
Gene	log2FoldChange	pvalue	log2FoldChange	pvalue	Gene_ID	Description
LOC111401068	1,365260207	0,24483689	-3,946711369	0,02540888	XP_022884378.1	GGPS geranylgeranyl pyrophosphate synthase, chloroplastic-like = *Olea europaea var. Sylvestris*
LOC111384641			1,301648121	0,1850691	XP_022864719.1	CCPS ent-copalyl diphosphate synthase, chloroplastic-like = *Olea europaea var. Sylvestris*
LOC111381791			1,411885726	0,0002905	XP_022861387.1	KAO ent-kaurene oxidase, chloroplastic-like = *Olea europaea var. Sylvestris*
LOC111384195	4,147226384	0,08068977	1,553598509	0,12838779	XP_022864227.1	KAO2 ent-kaurenoic acid oxidase 2-like = *Olea europaea var. Sylvestris*
LOC111394261			1,637770861	0,04577549	XP_022875786.1	KAO2 ent-kaurenoic acid oxidase 2-like = *Olea europaea var. Sylvestris*
LOC111403906			2,198781119	0,21502877	XP_022888330.1	GA20ox 1D gibberellin 20 oxidase 1-D-like = *Olea europaea var. Sylvestris*
LOC111367679			2,790606321	0,00707035	XP_022844439.1	GA20ox 2 gibberellin 20 oxidase 2-like = *Olea europaea var. Sylvestris*
LOC111410454	-1,801997461	0,71834824			XP_022896564.1	GA20ox 2 gibberellin 20 oxidase 2-like = *Olea europaea var. Sylvestris*
LOC111384247	1,18645434	0,68415148			XP_022864276.1	GA3ox 1 gibberellin 3-beta-dioxygenase 1-like = *Olea europaea var. Sylvestris*
LOC111384251	1,497170469	0,00474685	-1,8201347	0,00061654	XP_022864280.1	GA3ox 1 gibberellin 3-beta-dioxygenase 1-like = *Olea europaea var. Sylvestris*
LOC111380035	3,151891261	0,12972041	1,431972786	0,12246585	XP_022859269.1	GA3ox gibberellin 3-beta-dioxygenase 1-like = *Olea europaea var. Sylvestris*
LOC111370978			2,472592423	1,726E-07	XP_022848673.1	GA2ox 1 gibberellin 2-beta-dioxygenase 1-like = *Olea europaea var. Sylvestris*
LOC111395582	-1,086744245	1,1796E-13			XP_022877393.1	GA2ox 1 gibberellin 2-beta-dioxygenase 1-like = *Olea europaea var. Sylvestris*
LOC111376817			-4,320287859	0,05244654	XP_022855586.1	GA2ox 2 gibberellin 2-beta-dioxygenase 2-like = *Olea europaea var. Sylvestris*
LOC111403036	-1,005638639	0,05928618			XP_022887149.1	GA2ox 4 gibberellin 2-beta-dioxygenase 4 = *Olea europaea var. Sylvestris*
LOC111402441	1,034804149	0,0117665			XP_022886508.1	GA2ox 8 gibberellin 2-beta-dioxygenase 8 = *Olea europaea var. Sylvestris*
LOC111368538			2,298802245	3,5137E-08	XP_022845590.1	GA2ox 8 gibberellin 2-beta-dioxygenase 8-like = *Olea europaea var. Sylvestris*
LOC111389391	3,708967423	1,6271E-05			XP_022870084.1	GA2ox 8 gibberellin 2-beta-dioxygenase 8-like = *Olea europaea var. Sylvestris*
LOC111403642			1,053888537	0,02984675	XP_022887988.1	GA2ox 8 gibberellin 2-beta-dioxygenase 8 = *Olea europaea var. Sylvestris*
LOC111407272			2,312153214	9,5467E-15	XP_022892423.1	GA2ox gibberellin 2-beta-dioxygenase-like = *Olea europaea var. Sylvestris*
LOC111368769			-2,349282914	3,7055E-06	XP_022845970.1	GAI1-DELLA protein = *Olea europaea var. Sylvestris*
LOC111376719	-1,00759109	0,00164992	1,210983873	6,2796E-05	XP_022855465.1	GAI1-DELLA protein = *Olea europaea var. Sylvestris*
LOC111367486	1,366207587	2,6196E-07			XP_022844159.1	GAI-DELLA protein -like = *Olea europaea var. Sylvestris*
LOC111384648			-1,007432766	0,43148745	XP_022864727.1	RGL1-DELLA protein = *Olea europaea var. Sylvestris*
LOC111377023	-1,494649685	0,04410273			XP_022855807.1	RGL2-DELLA protein = *Olea europaea var. Sylvestris*
LOC111388316	-3,06503032	5,8551E-17			XP_022868763.1	RGL2-DELLA protein = *Olea europaea var. Sylvestris*
LOC111394838			1,373227402	0,0007432	XP_022876628.1	GAMYB transcription factor GAMYB = *Olea europaea var. Sylvestris*
LOC111409113	-1,16810187	0,01380462			XP_022894821.1	GASA 11 gibberellin-regulated protein 11-like = *Olea europaea var. Sylvestris*
LOC111378947			-1,212690278	0,0794941	-	GASA11 gibberellin-regulated protein 11-like = *Olea europaea var. Sylvestris*
LOC111401692			2,138658819	0,03009777	XP_022885321.1	GASA14 gibberellin-regulated protein 14-like = *Olea europaea var. Sylvestris*
LOC111376141			1,689815168	0,01265472	XP_022854851.1	GASA4 gibberellin-regulated protein 4-like = *Olea europaea var. Sylvestris*

Table 3II.S20. CK-related genes induced or repressed in the first comparison (d18:0-AZ vs. C-AZ) and the second comparison (d18:0-LAZ vs. d18:0-AZ).

	d18:0-AZ vs. C-AZ		d18:0-LAZ vs. d18:0-AZ			
Gene	log2FoldChange	pvalue	log2FoldChange	pvalue	Gene_ID	Description
LOC111381363			6,127498363	1,92E-11	XP_022860907.1	AIPT adenylate isopentenyltransferase 5, chloroplastic-like= *Olea europaea var. Sylvestris*
LOC111404220	-1,082694989	6,67E-01			XP_022888772.1	CYP735A cytokinin hydroxylase-like = *Olea europaea var. Sylvestris*
LOC111403866	1,875551176	2,24E-01	-4,922688444	1,25E-02	XP_022888270.1	CKX1 cytokinin dehydrogenase 1-like = *Olea europaea var. Sylvestris*
LOC111388513			3,03085313	4,27E-04	XP_022869012.1	CKX6 cytokinin dehydrogenase 5-like = *Olea europaea var. Sylvestris*
LOC111370301	-1,500768767	1,04E-02			XP_022847745.1	CKX6 cytokinin dehydrogenase 6-like = *Olea europaea var. Sylvestris*
LOC111384629			-1,446772381	2,59E-02	XP_022864705.1	CKX6 cytokinin dehydrogenase 6-like = *Olea europaea var. Sylvestris*
LOC111410497	1,241745791	5,35E-01			XP_022896625.1	CKX6 cytokinin dehydrogenase 6-like = *Olea europaea var. Sylvestris*
LOC111386064	-1,30100988	2,05E-01	1,400743587	1,44E-01	-	CKX7 cytokinin dehydrogenase 7-like = *Olea europaea var. Sylvestris*
LOC111386059			-3,500135053	3,28E-18	XP_022866256.1	CKX9 cytokinin dehydrogenase 9-like = *Olea europaea var. Sylvestris*
LOC111378946	1,514995283	1,69E-04	1,457203941	1,47E-08	XP_022858013.1	LOG1 cytokinin riboside 5-monophosphate phosphoribohydrolase = *Olea europaea var. Sylvestris*
LOC111408866			3,377112253	6,52E-17	XP_022894450.1	LOG1 cytokinin riboside 5-monophosphate phosphoribohydrolase = *Olea europaea var. Sylvestris*
LOC111380682			3,953731911	3,99E-02	XP_022860079.1	LOG3 cytokinin riboside 5-monophosphate phosphoribohydrolase = *Olea europaea var. Sylvestris*
LOC111381592			1,040599369	7,27E-03	XP_022861155.1	LOG3 cytokinin riboside 5-monophosphate phosphoribohydrolase = *Olea europaea var. Sylvestris*
LOC111399664			-2,037112138	2,07E-04	XP_022882873.1	LOG3 cytokinin riboside 5-monophosphate phosphoribohydrolase = *Olea europaea var. Sylvestris*
LOC111389240			-1,249276535	4,12E-01	XP_022869899.1	LOG4 cytokinin riboside 5-monophosphate phosphoribohydrolase = *Olea europaea var. Sylvestris*
LOC111381996	-1,411315115	6,73E-01	5,705330837	2,58E-04	XP_022861619.1	LOG5 cytokinin riboside 5-monophosphate phosphoribohydrolase = *Olea europaea var. Sylvestris*
LOC111405830	-1,958144628	2,35E-16			XP_022890657.1	LOG8 cytokinin riboside 5-monophosphate phosphoribohydrolase = *Olea europaea var. Sylvestris*
LOC111410492	-1,198750467	2,70E-01	3,061220223	2,37E-05	XP_022896611.1	LOGL10 probable cytokinin riboside 5-monophosphate phosphoribohydrolase = *Olea europaea var. Sylvestris*
LOC111365959			-2,335190078	2,53E-06	XP_022842309.1	ZOG zeatin O-glucosyltransferase-like = *Olea europaea var. Sylvestris*
LOC111375020	2,401802332	1,67E-03			XP_022853581.1	ZOG zeatin O-glucosyltransferase-like = *Olea europaea var. Sylvestris*
LOC111377984	-2,354900219	1,90E-01			XP_022856912.1	ZOG zeatin O-glucosyltransferase-like = *Olea europaea var. Sylvestris*
LOC111377985	4,015839307	2,82E-12	-1,630143478	2,27E-05	XP_022856913.1	ZOG1 zeatin O-glucosyltransferase-like = *Olea europaea var. Sylvestris*
LOC111373686	-1,116468145	1,21E-01			-	CKI1 histidine kinase =*Olea europaea var. Sylvestris*
LOC111388314	-1,149062445	1,60E-05			XP_022868760.1	CKI1 histidine kinase =*Olea europaea var. Sylvestris*
LOC111388315	-1,493305632	2,60E-02			XP_022868762.1	CKI1 histidine kinase= *Olea europaea var. Sylvestris*
LOC111372363	-1,272744518	3,92E-07			XP_022850441.1	CKI2 histidine kinase 2-like = *Olea europaea var. Sylvestris*
LOC111402108			1,243071568	9,80E-09	XP_022885947.1	CKI2 histidine kinase 2-like = *Olea europaea var. Sylvestris*

LOC111380371			1,225599116	2,82E-09	XP_022859678.1	CKI4 histidine kinase 4 = *Olea europaea var. Sylvestris*
LOC111393182	-1,082694989	6,67E-01			XP_022874362.1	CKI5 histidine kinase 5-like = *Olea europaea var. Sylvestris*
LOC111377669	-4,460990113	1,56E-02			XP_022856560.1	ARR10 two-component response regulator = *Olea europaea var. Sylvestris*
LOC111404634	-1,801997461	7,18E-01			XP_022889184.1	ARR10 two-component response regulator = *Olea europaea var. Sylvestris*
LOC111405272	-2,431194442	3,03E-20	1,587057904	4,29E-08	XP_022889846.1	ARR15 two-component response regulator = *Olea europaea var. Sylvestris*
LOC111397225	-1,006733515	4,06E-06	1,358271561	8,13E-11	XP_022879794.1	ARR17 two-component response regulator = *Olea europaea var. Sylvestris*
LOC111371510	-1,156952417	2,18E-08			XP_022849311.1	ARR2 two-component response regulator = *Olea europaea var. Sylvestris*
LOC111393400			1,298150882	9,30E-12	XP_022874680.1	ARR2 two-component response regulator = *Olea europaea var. Sylvestris*
LOC111389902			1,494481423	9,54E-23	XP_022870654.1	ARR2 two-component response regulator-like = *Olea europaea var. Sylvestris*
LOC111407487			1,420260656	8,45E-17	XP_022892759.1	ARR2 two-component response regulator-like = *Olea europaea var. Sylvestris*
LOC111367735	-1,747006857	3,12E-28			XP_022844535.1	ARR3 two-component response regulator = *Olea europaea var. Sylvestris*
LOC111386177			2,346314795	3,01E-09	XP_022866401.1	ARR5 two-component response regulator = *Olea europaea var. Sylvestris*
LOC111396155			3,756320209	2,29E-13	XP_022878244.1	ARR5 two-component response regulator = *Olea europaea var. Sylvestris*
LOC111377280	-1,79219187	7,20E-01	7,064229754	1,27E-05	XP_022856121.1	ARR6 two-component response regulator = *Olea europaea var. Sylvestris*
LOC111376891	-1,232712252	6,99E-07			XP_022855666.1	ARR7 two-component response regulator = *Olea europaea var. Sylvestris*
LOC111391187	-3,194073489	1,45E-01	3,788273365	4,81E-02	XP_022872116.1	ARR8 two-component response regulator = *Olea europaea var. Sylvestris*
LOC111370563			2,622345375	2,31E-03	XP_022848106.1	ARR8 two-component response regulator A = *Olea europaea var. Sylvestris*
LOC111381840			1,321930008	3,87E-03	XP_022861454.1	ORR9 two-component response regulator = *Olea europaea var. Sylvestris*
LOC111376340			2,264661805	1,04E-06	XP_022855060.1	ORR26 two-component response regulator = *Olea europaea var. Sylvestris*
LOC111379693	1,572736051	4,29E-01	1,707863381	1,05E-01	XP_022858889.1	ORR3 (tipe A) two-component response regulator -like = *Olea europaea var. Sylvestris*
LOC111378962			2,132232354	2,16E-02	XP_022858035.1	ORR9 two-component response regulator = *Olea europaea var. Sylvestris*

Table 3.II.S21. BR-related genes induced or repressed in the first comparison (d18:0-AZ vs. C-AZ) and the second comparison (d18:0-LAZ vs. d18:0-AZ).

	d18:0-AZ vs. C-AZ		d18:0-LAZ vs. d18:0-AZ			
Gene	**log2FoldChange**	**pvalue**	**log2FoldChange**	**pvalue**	**Gene_ID**	**Description**
LOC111398447			-1,227299158	5,49E-02	XP_022881116.1	BAHD acyltransferase BIA1-like = *Olea europaea var. sylvestris*
LOC111407279			-1,142906228	3,77E-09	XP_022892434.1	BRI1 brassinosteroid LRR receptor kinase-like = *Olea europaea var. sylvestris*
LOC111368168			1,818393093	2,25E-10	XP_022845178.1	BRI1 kinase inhibitor 1-like =*Olea europaea var. sylvestris*
LOC111392530	1,846500793	0,3060868			XP_022873661.1	BRI1 serine/threonine-protein kinase BRI1-like 2 =*Olea europaea var. sylvestris*
LOC111399331			1,562379596	1,26E-03	XP_022882357.1	BRI1-2 serine/threonine-protein kinase = *Olea europaea var. sylvestris*
LOC111403178	-1,110803809	0,0007521			XP_022887350.1	BSK3 probable serine/threonine-protein kinase = *Olea europaea var. sylvestris*
LOC111378161	4,251163124	0,0659732			XP_022857094.1	BAK1 BRASSINOSTEROID INSENSITIVE 1-associated receptor kinase 1-like =*Olea europaea var. sylvestris*
LOC111387104	1,294027307	0,6504209			XP_022867392.1	BAK1 BRASSINOSTEROID INSENSITIVE 1-associated receptor kinase 1-like =*Olea europaea var. sylvestris*
LOC111401172	1,475545217	3,634E-05			XP_022884565.1	BPG2 GTP-binding protein BRASSINAZOLE INSENSITIVE PALE GREEN 2, chloroplastic = *Olea europaea var. sylvestris*
LOC111374059	1,455966823	1,35E-05	1,173355912	6,44E-07	XP_022852449.1	BES1/BZR1 protein BRASSINAZOLE-RESISTANT 1-like = *Olea europaea var. sylvestris*
LOC111397295			1,047437366	2,69E-06	XP_022879910.1	BES1/BZR1 protein BRASSINAZOLE-RESISTANT 1-like = *Olea europaea var. sylvestris*
LOC111408959	-1,231647669	6,823E-12	1,07525885	1,05E-08	XP_022894588.1	BES1/BZR1 protein BRASSINAZOLE-RESISTANT 1-like = *Olea europaea var. sylvestris*

Table 3.II.S22. PA-related genes induced or repressed in the first comparison (d18:0-AZ vs. C-AZ) and the second comparison (d18:0-LAZ vs. d18:0-AZ).

	d18:0-AZ vs. C-AZ		d18:0-LAZ vs. d18:0-AZ			
Gene	log2FoldChange	pvalue	log2FoldChange	pvalue	Gene_ID	Description
LOC111388517	-1,674597614	1,36E-28			XP_022869017.1	ADC arginine decarboxylase-like = *Olea europaea var. sylvestris*
LOC111410097	-1,59094796	6,67E-24			XP_022896062.1	ADC arginine decarboxylase-like = *Olea europaea var. sylvestris*
LOC111391028			1,007854495	1,56E-01	XP_022871928.1	PRMT protein arginine N-methyltransferase 1.5-like = *Olea europaea var. sylvestris*
LOC111370933			-1,217574416	4,35E-04	XP_022848608.1	OCT ornithine carbamoyltransferase, chloroplastic-like = *Olea europaea var. sylvestris*
LOC111391544			-1,42585346	1,19E-17	XP_022872548.1	SAMDC S-adenosylmethionine decarboxylase proenzyme-like = *Olea europaea var. sylvestris*
LOC111404633	2,279140502	5,83E-01			-	SAMDC S-adenosylmethionine decarboxylase proenzyme-like = *Olea europaea var. sylvestris*
LOC111388222	1,177856955	1,69E-01			XP_022868679.1	SPDS probable polyamine aminopropyl transferase = *Olea europaea var. sylvestris*
LOC111373552			1,69773865	2,49E-11	XP_022851867.1	ACAULIS5 thermospermine synthase = *Olea europaea var. Sylvestris*
LOC111379571	2,142829082	1,31E-14	-2,585927904	5,03E-19	XP_022858735.1	ACAULIS5 thermospermine synthase = *Olea europaea var. sylvestris*
LOC111393035	-3,207733016	1,78E-01			XP_022874205.1	ACAULIS5 thermospermine synthase = *Olea europaea var. sylvestris*
LOC111397580			1,394718578	2,07E-02	XP_022880342.1	ACAULIS5 thermospermine synthase = *Olea europaea var. sylvestris*
LOC111390675	3,48409986	2,51E-01			XP_022871509.1	SHT spermidine hydroxycinnamoyl transferase = *Olea europaea var. sylvestris*
LOC111368470			-1,382617292	8,20E-07	XP_022845483.1	SHT spermidine hydroxycinnamoyl transferase-like = *Olea europaea var. sylvestris*
LOC111377116			-1,610502713	1,68E-01	XP_022855938.1	SHT spermidine hydroxycinnamoyl transferase-like = *Olea europaea var. sylvestris*
LOC111377121	1,129033424	4,47E-01			XP_022855948.1	SHT spermidine hydroxycinnamoyl transferase-like = *Olea europaea var. sylvestris*
LOC111380387			-1,948364947	7,30E-03	XP_022859703.1	SHT spermidine hydroxycinnamoyl transferase-like = *Olea europaea var. sylvestris*
LOC111403793	1,900838068	6,84E-01	3,023615081	6,06E-02	XP_022888181.1	SHT spermidine hydroxycinnamoyl transferase-like = *Olea europaea var. sylvestris*
LOC111411392	-3,972401968	3,11E-17			XP_022897695.1	PAO1 polyamine oxidase 1-like =*Olea europaea var. sylvestris*
LOC111411688	3,350193603	5,16E-03	2,481454849	3,43E-09	XP_022898010.1	PAO1 polyamine oxidase 1-like =*Olea europaea var. sylvestris*
LOC111372349			-1,42177066	2,35E-01	XP_022850415.1	PAO2 probable polyamine oxidase 2 = *Olea europaea var. sylvestris*
LOC111400605	-3,592310052	1,73E-08	1,25187832	1,86E-01	XP_022883777.1	PAO2 probable polyamine oxidase 2 = *Olea europaea var. sylvestris*
LOC111378096	-2,681207744	8,53E-12	-1,050515253	1,41E-01	XP_022857034.1	PAO4 probable polyamine oxidase 4 = *Olea europaea var. sylvestris*
LOC111400284	-1,88115648	5,55E-25	-1,332556643	1,36E-07	XP_022883468.1	PAO4 probable polyamine oxidase 4 = *Olea europaea var. sylvestris*
LOC111374479			1,354274983	3,25E-02	XP_022852917.1	PAO5 probable polyamine oxidase 5 = *Olea europaea var. sylvestris*
LOC111387474			1,75522606	5,91E-03	XP_022867797.1	PAO5 probable polyamine oxidase 5 = *Olea europaea var. sylvestris*
LOC111375112	1,00903383	1,98E-01	-1,205811597	1,00E-01	XP_022853669.1	PUT At1g31830 probable polyamine transporter = *Olea europaea var. sylvestris*
LOC111366748			1,274519127	7,49E-03	-	PUT At3g13620 probable polyamine transporter = *Olea europaea var. sylvestris*
LOC111366810			-1,369956732	6,08E-03	XP_022843273.1	SPBP spermine-binding protein-like = *Olea europaea var. sylvestris*

Table 3.II.S23. NO-related genes induced or repressed in the first comparison (d18:0-AZ vs. C-AZ) and the second comparison (d18:0-LAZ vs. d18:0-AZ).

	d18:0-AZ vs. C-AZ		d18:0-LAZ vs. d18:0-AZ			
Gene	**log2FoldChange**	**pvalue**	**log2FoldChange**	**pvalue**	**Gene_ID**	**Description**
LOC111411582	-1,524011709	5,334E-07	1,166418366	0,000189	XP_022897851.1	NIR1 ferredoxin--nitrite reductase, chloroplastic = *Olea europaea var. sylvestris*
LOC111383770	-1,699800847	0,02909			XP_022863688.1	NR2 nitrate reductase [NADH] 2-like = *Olea europaea var. sylvestris*
LOC111389106			1,267449269	0,0004608	XP_022869728.1	NR2 nitrate reductase [NADH] 2-like = *Olea europaea var. sylvestris*
LOC111376356	-1,233878578	0,0575697	1,482438749	0,0091239	XP_022855081.1	NRT2.5 high affinity nitrate transporter 2.5-like = *Olea europaea var. sylvestris*
LOC111398833			1,111745201	0,0180097	XP_022881712.1	NRT2.5 high affinity nitrate transporter 2.5-like = *Olea europaea var. Sylvestris*
LOC111381300			-1,472294981	8,367E-20	XP_022860840.1	NRT2.7 high affinity nitrate transporter 2.7 = *Olea europaea var. sylvestris*
LOC111385032	1,472253504	0,2428838	-2,26104547	0,0979196	XP_022865164.1	NRT3.1 high-affinity nitrate transporter 3.1-like =*Olea europaea var. sylvestris*
LOC111407626	1,046003594	0,1653643	-1,697628899	0,0321793	XP_022893008.1	NRT3.1 high-affinity nitrate transporter 3.1-like =*Olea europaea var. sylvestris*
LOC111372264	-1,584586875	0,2372466			XP_022850275.1	NRG2 nitrate regulatory gene2 protein-like = *Olea europaea var. sylvestris*
LOC111379284	-1,026857732	3,082E-06			XP_022858410.1	NRG2 nitrate regulatory gene2 protein-like = *Olea europaea var. sylvestris*
LOC111383159	-3,799149514	0,1805516			XP_022863005.1	NRG2 nitrate regulatory gene2 protein-like = *Olea europaea var. sylvestris*
LOC111388758	-1,003195334	7,468E-08			XP_022869322.1	NRG2 nitrate regulatory gene2 protein-like = *Olea europaea var. sylvestris*
LOC111409481	-1,352679748	0,5359149	2,461455146	0,1465204	XP_022895296.1	NRG2 nitrate regulatory gene2 protein-like = *Olea europaea var. sylvestris*
LOC111412317	-1,031390731	2,662E-07			XP_022898967.1	NRG2 nitrate regulatory gene2 protein-like = *Olea europaea var. sylvestris*

Table 3.II.S24. Strigolactone-related genes induced or repressed in the first comparison (d18:0-AZ vs. C-AZ) and the second comparison (d18:0-LAZ vs. d18:0-AZ).

	d18:0-AZ vs. C-AZ		d18:0-LAZ vs. d18:0-AZ			
Gene	**log2FoldChange**	**pvalue**	**log2FoldChange**	**pvalue**	**Gene_ID**	**Description**
LOC111365644			-1,093660307	0,3144092	XP_022841952.1	D14 strigolactone esterase = *Olea europaea var. Sylvestris*
LOC111397015	-1,358612514	2,98E-07			XP_022879442.1	D14L probable esterase = *Olea europaea var. Sylvestris*
LOC111375715			1,592638557	1,186E-09	XP_022854350.1	D27 beta-carotene isomerase chloroplastic = *Olea europaea var. Sylvestris*
LOC111379344	2,137173245	4,38E-13			-	DAD2 probable strigolactone esterase = *Olea europaea var. Sylvestris*
LOC111379347	1,587210189	2,99E-03			XP_022858475.1	DAD2 probable strigolactone esterase = *Olea europaea var. Sylvestris*
LOC111390114	1,581140362	1,49E-18			XP_022870880.1	DAD2 probable strigolactone esterase = *Olea europaea var. Sylvestris*
LOC111401355			3,408048211	0,0011334	XP_022884825.1	DAD2 probable strigolactone esterase = *Olea europaea var. Sylvestris*
LOC111367410	1,225091318	7,70E-03			XP_022844031.1	DAD2 probable strigolactone esterase = *Olea europaea var. Sylvestris*
LOC111388079	-1,48213474	5,81E-08			XP_022868511.1	SMAX1-LIKE 6 protein = *Olea europaea var. Sylvestris*
LOC111381764	-1,082371751	3,06E-02	1,45503331	0,0010538	-	SMAX1-LIKE 7-like protein = *Olea europaea var. Sylvestris*
LOC111406379	-1,138086437	4,14E-02			XP_022891577.1	SMAX1-LIKE 8 protein = *Olea europaea var. Sylvestris*

Table 3.II.S25. Peptide-signalling-related genes induced or repressed in the first comparison (d18:0-AZ vs. C-AZ) and the second comparison (d18:0-LAZ vs. d18:0-AZ).

d18:0-AZ vs. C-AZ					
Gene	**log2FoldChange**	**FoldChange**	**pvalue**	**Gene_ID**	**Description**
UP					
LOC111410856	1,679612628	3,203419259	2,20E-03	XP_022897200.1	leucine-rich repeat receptor-like serine/threonine-protein kinase BAM1 = *Olea europaea var. Sylvestris*
LOC11137264	1,419385087	2,674714836	7,64E-03	XP_022850793.1	receptor-like protein kinase FERONIA = *Olea europaea var. Sylvestris*
LOC11139559	1,40420386	2,646716848	1,84E-06	XP_022877413.1	LRR receptor-like serine/threonine-protein kinase GSO1 = *Olea europaea var. Sylvestris*
LOC111370841	1,269863854	2,411388083	2,00E-13	XP_022848503.1	receptor-like protein kinase HSL1 = *Olea europaea var. Sylvestris*
LOC11139755	1,251659519	2,381151673	2,22E-04	XP_022880316.1	rop guanine nucleotide exchange factor 1-like = *Olea europaea var. Sylvestris*
LOC11138480	1,172778005	2,254453894	7,88E-03	XP_022864902.1	leucine-rich repeat receptor-like serine/threonine-protein kinase At1g17230 =*Olea europaea var. Sylvestris*
LOC11140807	1,123822338	2,179235844	8,60E-03	XP_022893613.1	rapid alkalinization factor-like = *Olea europaea var. Sylvestris*
DOWN					
LOC11138682	-1,081020305	-2,115531702	8,87E-03	XP_022867066.1	leucine-rich repeat receptor-like protein kinase TDR = *Olea europaea var. Sylvestris*
LOC11138592	-3,626372847	-12,34943255	5,34E-33	XP_022866112.1	receptor-like protein kinase FERONIA = *Olea europaea var. Sylvestris*
LOC11138706	-2,345913237	-5,083821008	1,96E-24	-	GPI-anchored protein LLG1-like = *Olea europaea var. Sylvestris*
LOC11137477	-2,13636526	-4,39652984	2,52E-42	XP_022853283.1	receptor-like protein kinase FERONIA = *Olea europaea var. Sylvestris*
LOC11139946	-1,957117697	-3,882854634	9,94E-21	XP_022882542.1	LRR receptor-like serine/threonine-protein kinase GSO2 = *Olea europaea var. Sylvestris*
LOC11136989	-1,716123508	-3,285524061	1,35E-14	XP_022847381.1	LRR receptor-like serine/threonine-protein kinase GSO1 = *Olea europaea var. Sylvestris*
LOC11140245	-1,657860185	-3,155481542	4,36E-17	XP_022886532.1	GPI-anchored protein LLG1-like = *Olea europaea var. Sylvestris*
LOC11138257	-1,522611947	-2,873107446	1,53E-05	XP_022862364.1	rapid alkalinization factor-like = *Olea europaea var. Sylvestris*
LOC11138958	-1,409431948	-2,656325512	2,12E-12	XP_022870287.1	rapid alkalinization factor = *Olea europaea var. Sylvestris*
d18:0-LAZ vs. d18:0-AZ					
Gene	**log2FoldChange**	**FoldChange**	**pvalue**	**Gene_ID**	**Description**
UP					
LOC111410856	2,764239197	6,793896299	1,89E-25	XP_022897200.1	leucine-rich repeat receptor-like serine/threonine-protein kinase BAM1 = *Olea europaea var. Sylvestris*
LOC11138480	2,218472036	4,654002663	5,69E-18	XP_022864902.1	leucine-rich repeat receptor-like serine/threonine-protein kinase At1g17230 =*Olea europaea var. Sylvestris*
LOC11138760	2,183921916	4,543871123	6,98E-05	XP_022867945.1	leucine-rich repeat receptor-like serine/threonine-protein kinase BAM3 = *Olea europaea var. Sylvestris*
LOC11138257	2,048903181	4,137912623	3,27E-10	XP_022862364.1	rapid alkalinization factor-like = *Olea europaea var. Sylvestris*
LOC11138682	1,959385917	3,888964101	1,02E-08	XP_022867066.1	leucine-rich repeat receptor-like protein kinase TDR = *Olea europaea var. Sylvestris*
LOC11138958	1,924116503	3,795043712	1,11E-23	XP_022870287.1	rapid alkalinization factor = *Olea europaea var. Sylvestris*
LOC11140778	1,726978222	3,310337294	1,42E-03	XP_022893236.1	LRR receptor-like serine/threonine-protein kinase GSO1 = *Olea europaea var. Sylvestris*
LOC11136760	1,557104413	2,942626452	3,15E-09	XP_022844336.1	receptor protein-tyrosine kinase CEPR1-like = *Olea europaea var. Sylvestris*

LOC11138592	1,267573162	2,407562352	2,23E-03	XP_022866112.1	receptor-like protein kinase FERONIA = *Olea europaea var. Sylvestris*
LOC111404195	1,134613038	2,195596642	4,56E-03	XP_022888732.1	leucine-rich repeat receptor-like protein kinase TDR = *Olea europaea var. Sylvestris*
DOWN					
LOC11140403	-5,143192279	-35,33907271	4,04E-10	XP_022888522.1	LRR receptor-like serine/threonine-protein kinase GSO1 = *Olea europaea var. Sylvestris*
LOC11139826	-4,99479593	-31,88477798	1,73E-03	XP_022880957.1	receptor-like protein kinase FERONIA = *Olea europaea var. Sylvestris*
LOC11137727	-3,885478347	-14,77901637	2,61E-06	XP_022856120.1	LRR receptor-like serine/threonine-protein kinase GSO2 = *Olea europaea var. Sylvestris*
LOC11139690	-3,808257293	-14,00875941	4,40E-06	XP_022879278.1	LRR receptor-like serine/threonine-protein kinase GSO2 = *Olea europaea var. Sylvestris*
LOC11139559	-3,487177244	-11,21359717	2,23E-20	XP_022877413.1	LRR receptor-like serine/threonine-protein kinase GSO1 = *Olea europaea var. Sylvestris*
LOC11139693	-2,942969805	-7,689926477	4,56E-11	XP_022879317.1	LRR receptor-like serine/threonine-protein kinase GSO2 = *Olea europaea var. Sylvestris*
LOC11137264	-2,892289169	-7,424475801	7,11E-06	XP_022850793.1	receptor-like protein kinase FERONIA = *Olea europaea var. Sylvestris*
LOC11140770	-2,668863914	-6,359282123	2,08E-06	XP_022893121.1	LRR receptor-like serine/threonine-protein kinase GSO1 = *Olea europaea var. Sylvestris*
LOC11136936	-2,497752507	-5,648048618	7,84E-06	XP_022846622.1	rop guanine nucleotide exchange factor 7-like = *Olea europaea var. Sylvestris*
LOC11137264	-2,246042936	-4,743799175	1,84E-19	XP_022850792.1	receptor-like protein kinase FERONIA = *Olea europaea var. Sylvestris*
LOC11139873	-2,03615133	-4,101499152	3,18E-23	XP_022881560.1	LRR receptor-like serine/threonine-protein kinase GSO1 = *Olea europaea var. Sylvestris*
LOC11138302	-1,892908458	-3,713831751	2,87E-05	XP_022862844.1	leucine-rich repeat receptor-like protein kinase TDR = *Olea europaea var. Sylvestris*
LOC11139873	-1,585474036	-3,001063896	3,32E-10	XP_022881567.1	LRR receptor-like serine/threonine-protein kinase GSO1 = *Olea europaea var. Sylvestris*
LOC11137258	-1,468635493	-2,767600091	2,25E-12	-	LRR receptor-like serine/threonine-protein kinase GSO2 = Olea europaea var. Sylvestris
LOC11140427	-1,390194015	-2,621139278	2,09E-06	XP_022888869.1	rop guanine nucleotide exchange factor 14-like = *Olea europaea var. Sylvestris*
LOC11139946	-1,290214427	-2,445644024	3,64E-05	XP_022882542.1	LRR receptor-like serine/threonine-protein kinase GSO2 = *Olea europaea var. Sylvestris*
LOC111401824	-1,254393718	-2,385668716	8,82E-08	XP_022885515.1	LRR receptor-like serine/threonine-protein kinase GSO1 = *Olea europaea var. Sylvestris*
LOC111401823	-1,236200234	-2,355772518	1,27E-08	XP_022885512.1	LRR receptor-like serine/threonine-protein kinase GSO1 = *Olea europaea var. Sylvestris*
LOC11136989	-1,124846827	-2,180783916	4,48E-04	XP_022847381.1	LRR receptor-like serine/threonine-protein kinase GSO1 = *Olea europaea var. Sylvestris*

Table 3.II. S26. Proteases genes induced or repressed in the first comparison (d18:0-AZ vs. C-AZ) and the second comparison (d18:0-LAZ vs. d18:0-AZ).

d18:0-AZ vs. C-AZ					
Gene	**log2FoldChange**	**FoldChange**	**pvalue**	**Gene_ID**	**Description**
UP					
LOC111382581	2,489349796	5,615248215	0,00027622	XP_022862368.1	protein ASPARTIC PROTEASE IN GUARD CELL 2-like = *Olea europaea var. Sylvestris*
LOC111397286	1,929610177	3,809522501	3,9268E-06	XP_022879899.1	subtilisin-like protease SBT1.9 = *Olea europaea var. Sylvestris*
LOC111373313	1,880115576	3,681045483	8,0309E-06	XP_022851592.1	serine carboxypeptidase-like 45 = *Olea europaea var. Sylvestris*
LOC111410115	1,752069021	3,368412961	1,7396E-18	XP_022896089.1	subtilisin-like protease SBT1.6 = *Olea europaea var. Sylvestris*
LOC111377960	1,636098609	3,108241519	8,1736E-06	XP_022856889.1	aspartyl protease family protein At5g10770-like = *Olea europaea var. Sylvestris*
LOC111403579	1,573325978	2,975899856	4,4719E-05	XP_022887944.1	subtilisin-like protease SBT1.5 = *Olea europaea var. Sylvestris*
LOC111372116	1,555931439	2,94023494	7,183E-18	XP_022850062.1	protein ASPARTIC PROTEASE IN GUARD CELL 1-like = *Olea europaea var. Sylvestris*
LOC111397287	1,539129322	2,906190595	1,7461E-05	XP_022879901.1	subtilisin-like protease SBT1.9 = *Olea europaea var. Sylvestris*
LOC111366809	1,492499216	2,813759877	0,00167848	XP_022843272.1	subtilisin-like protease SBT1.7 = *Olea europaea var. Sylvestris*
LOC111388177	1,383429031	2,608877187	2,264E-15	XP_022868628.1	low-temperature-induced cysteine proteinase-like = *Olea europaea var. Sylvestris*
LOC111367704	1,365671079	2,57696167	4,7186E-09	XP_022844479.1	dipeptidyl aminopeptidase 4-like = *Olea europaea var. Sylvestris*
LOC111411447	1,311732513	2,482394684	1,287E-05	XP_022897749.1	subtilisin-like protease SBT1.8 = *Olea europaea var. Sylvestris*
LOC111404802	1,242141908	2,365494666	0,0012965	-	subtilisin-like protease SBT2.5 = *Olea europaea var. Sylvestris*
LOC111389318	1,120464911	2,174170242	4,8906E-06	XP_022870004.1	subtilisin-like protease SBT1.7 = *Olea europaea var. Sylvestris*
LOC111380943	1,110391382	2,15904211	9,01E-14	XP_022860388.1	prolyl endopeptidase-like = *Olea europaea var. Sylvestris*
LOC111388625	1,078176171	2,111365244	0,00487519	XP_022869149.1	CLP protease regulatory subunit CLPX1, mitochondrial-like = *Olea europaea var. Sylvestris*
LOC111396591	1,063208189	2,089573041	3,8752E-06	XP_022878768.1	serine carboxypeptidase-like 50 = *Olea europaea var. Sylvestris*
LOC111394619	1,036591254	2,05137501	0,00068943	XP_022876297.1	putative serine carboxypeptidase-like 23 = *Olea europaea var. Sylvestris*
LOC111393908	1,006528765	2,0090713	2,0746E-08	XP_022875448.1	desumoylating isopeptidase 2-like = *Olea europaea var. Sylvestris*
DOWN					
LOC111382641	-4,627253532	-24,71394699	0,00900033	-	aspartyl protease AED3-like = *Olea europaea var. Sylvestris*
LOC111386042	-3,09913656	-8,569057664	1,5547E-46	XP_022866241.1	aspartic proteinase-like protein 2 = *Olea europaea var. Sylvestris*
LOC111386645	-2,692403355	-6,463893172	4,8629E-14	XP_022866880.1	aspartic proteinase-like protein 2 = *Olea europaea var. Sylvestris*
LOC111385942	-2,678921968	-6,403772111	4,1763E-65	XP_022866134.1	aspartyl protease family protein 1-like = *Olea europaea var. Sylvestris*
LOC111405364	-2,638023958	-6,224784785	9,3749E-56	XP_022889964.1	aspartic proteinase-like protein 2 = *Olea europaea var. Sylvestris*
LOC111372579	-2,302183151	-4,932035385	9,7606E-14	XP_022850721.1	serine carboxypeptidase-like 42 = *Olea europaea var. Sylvestris*
LOC111390855	-1,993821807	-3,982907036	9,2475E-08	XP_022871750.1	cysteine proteinase inhibitor B-like = *Olea europaea var. Sylvestris*
LOC111370358	-1,950804693	-3,865901	9,6274E-10	XP_022847796.1	aspartyl protease family protein 2-like = O*lea europaea var. Sylvestris*
LOC111372429	-1,909375409	-3,756464347	7,3022E-12	XP_022850554.1	serine carboxypeptidase-like 17 = *Olea europaea var. Sylvestris*
LOC111376671	-1,856349742	-3,620903535	5,2961E-11	XP_022855410.1	CO(2)-response secreted protease-like = *Olea europaea var. Sylvestris*

LOC111394357	-1,82012899	-3,531127685	1,2404E-28	XP_022875893.1	aspartic proteinase Asp1-like = *Olea europaea var. Sylvestris*
LOC111374677	-1,809395756	-3,504954598	2,2391E-06	XP_022853186.1	aspartic proteinase-like protein 2 = *Olea europaea var. Sylvestris*
LOC111382257	-1,634708075	-3,105247098	0,01065075	XP_022861939.1	aspartic proteinase NANA, chloroplast-like = *Olea europaea var. Sylvestris*
LOC111396394	-1,62826548	-3,091411017	1,1534E-17	XP_022878600.1	probable aspartyl protease At4g16563 = *Olea europaea var. Sylvestris*
LOC111372423	-1,6068778	-3,04591947	8,7033E-21	XP_022850537.1	putative serine carboxypeptidase-like 52 = *Olea europaea var. Sylvestris*
LOC111371537	-1,594112268	-3,019086868	2,1713E-06	XP_022849348.1	cysteine proteinase inhibitor B-like = *Olea europaea var. Sylvestris*
LOC111376352	-1,58780185	-3,005910075	1,7893E-17	-	signal peptide peptidase-like 4 = *Olea europaea var. Sylvestris*
LOC111412060	-1,478788005	-2,787144894	8,8073E-09	XP_022898573.1	aspartyl protease family protein 2-like = *Olea europaea var. Sylvestris*
LOC111374295	-1,414608647	-2,665874098	0,00011853	XP_022852720.1	gamma-glutamyl peptidase 5-like = *Olea europaea var. Sylvestris*
LOC111399606	-1,36180806	-2,570070723	1,6704E-12	XP_022882780.1	gamma-glutamyl peptidase 3-like = *Olea europaea var. Sylvestris*
LOC111367555	-1,238811758	-2,36004073	7,2238E-17	XP_022844259.1	aspartic proteinase PCS1-like = *Olea europaea var. Sylvestris*
LOC111390353	-1,201925634	-2,300465202	2,0455E-11	XP_022871149.1	proline iminopeptidase = *Olea europaea var. Sylvestris*
LOC111411249	-1,190774977	-2,282753337	5,4055E-08	XP_022897569.1	subtilisin-like protease SBT6.1 = *Olea europaea var. Sylvestris*
LOC111412308	-1,17613646	-2,259708158	0,00221058	XP_022898952.1	serine carboxypeptidase II-3-like = *Olea europaea var. Sylvestris*
LOC111403536	-1,167453023	-2,246148051	1,2759E-05	XP_022887850.1	serine carboxypeptidase-like = *Olea europaea var. Sylvestris*
LOC111380283	-1,070397575	-2,100012005	1,7782E-10	XP_022859563.1	signal peptide peptidase-like 4 = *Olea europaea var. Sylvestris*
LOC111411721	-1,032208765	-2,045152983	1,1839E-10	XP_022898061.1	signal peptide peptidase-like 4 = *Olea europaea var. Sylvestris*
LOC111401202	-1,019759308	-2,02758066	1,0584E-07	XP_022884599.1	aspartic proteinase PCS1-like = *Olea europaea var. Sylvestris*

d18:0-LAZ vs. d18:0-AZ					
Gene	**log2FoldChange**	**FoldChange**	**pvalue**	**Gene_ID**	**Description**
UP					
LOC111411634	6,611172483	97,76000698	8,4048E-06	XP_022897920.1	aspartyl protease AED3-like = *Olea europaea var. Sylvestris*
LOC111382641	5,643706497	49,99481232	0,00039112	-	aspartyl protease AED3-like = *Olea europaea var. Sylvestris*
LOC111409022	3,848035996	14,40039017	1,1458E-10	XP_022894684.1	probable isoaspartyl peptidase/L-asparaginase 2 = *Olea europaea var. Sylvestris*
LOC111374514	3,606893463	12,18381016	0,00191996	XP_022852953.1	serine carboxypeptidase-like 42 = *Olea europaea var. Sylvestris*
LOC111367464	3,350229474	10,19810699	1,6115E-08	XP_022844121.1	ATP-dependent zinc metalloprotease FTSH 6, chloroplastic = *Olea europaea var. Sylvestris*
LOC111376671	3,214986437	9,285544019	7,9435E-43	XP_022855410.1	CO(2)-response secreted protease-like = *Olea europaea var. Sylvestris*
LOC111389020	2,880731817	7,365236324	0,01187137	XP_022869638.1	gamma-glutamyl peptidase 5-like = *Olea europaea var. Sylvestris*
LOC111410300	2,618257416	6,140079845	0,00028124	XP_022896336.1	aspartyl protease AED3-like = *Olea europaea var. Sylvestris*
LOC111411447	2,326538481	5,016003939	4,7618E-33	XP_022897749.1	subtilisin-like protease SBT1.8 = *Olea europaea var. Sylvestris*
LOC111398694	2,219886342	4,658567321	9,2687E-47	XP_022881501.1	aspartyl protease family protein At5g10770-like = *Olea europaea var. Sylvestris*
LOC111398841	2,194881629	4,578520965	1,2499E-17	XP_022881729.1	metalloendoproteinase 2-MMP-like = *Olea europaea var. Sylvestris*
LOC111368699	2,180619506	4,53348184	0,00104039	XP_022845874.1	subtilisin-like protease SBT2.2 = *Olea europaea var. Sylvestris*
LOC111391889	2,05498344	4,155388717	0,00488642	XP_022872937.1	cathepsin B-like protease 3 = *Olea europaea var. Sylvestris*
LOC111371566	1,995103436	3,986446854	8,1905E-19	XP_022849392.1	serine carboxypeptidase-like 26 = *Olea europaea var. Sylvestris*

LOC111400468	1,922245923	3,790126294	0,00399029	XP_022883652.1	serine carboxypeptidase-like 48 = *Olea europaea var. Sylvestris*
LOC111384916	1,914180973	3,768997852	5,0615E-05	XP_022865030.1	aspartyl protease family protein 2-like = *Olea europaea var. Sylvestris*
LOC111372067	1,832191276	3,560774998	9,8711E-30	XP_022849992.1	serine carboxypeptidase-like 18 = *Olea europaea var. Sylvestris*
LOC111367555	1,709271579	3,269956807	1,0238E-28	XP_022844259.1	aspartic proteinase PCS1-like = *Olea europaea var. Sylvestris*
LOC111396591	1,626687585	3,088031747	7,254E-18	XP_022878768.1	serine carboxypeptidase-like 50 = *Olea europaea var. Sylvestris*
LOC111383379	1,601138952	3,033827277	0,00334977	XP_022863255.1	serine carboxypeptidase-like 50 = *Olea europaea var. Sylvestris*
LOC111382605	1,591172721	3,012941623	1,9092E-16	XP_022862402.1	serine carboxypeptidase-like 18 = *Olea europaea var. Sylvestris*
LOC111394654	1,498849444	2,82617234	1,7349E-06	XP_022876340.1	probable zinc metallopeptidase EGY3, chloroplastic = *Olea europaea var. Sylvestris*
LOC111404802	1,497346699	2,823230066	4,5835E-09	-	subtilisin-like protease SBT2.5 = *Olea europaea var. Sylvestris*
LOC111403399	1,451102735	2,734169598	3,5308E-09	XP_022887666.1	endoplasmic reticulum metallopeptidase 1 = *Olea europaea var. Sylvestris*
LOC111384567	1,38996407	2,620721538	0,00392225	XP_022864630.1	aspartic proteinase-like protein 2 = *Olea europaea var. Sylvestris*
LOC111371537	1,380084681	2,602836483	5,0833E-05	XP_022849348.1	cysteine proteinase inhibitor B-like = *Olea europaea var. Sylvestris*
LOC111409395	1,325080443	2,505468575	0,01208018	XP_022895215.1	subtilisin-like protease SBT1.9 = *Olea europaea var. Sylvestris*
LOC111403536	1,277775894	2,424648967	1,1452E-06	XP_022887850.1	serine carboxypeptidase-like = *Olea europaea var. Sylvestris*
LOC111399036	1,263414297	2,400632053	0,00015192	XP_022882007.1	protein ASPARTIC PROTEASE IN GUARD CELL 1 = *Olea europaea var. Sylvestris*
LOC111368188	1,236561444	2,35636241	1,8082E-07	XP_022845204.1	aspartyl protease family protein At5g10770-like = *Olea europaea var. Sylvestris*
LOC111401202	1,151174115	2,220945691	1,1754E-09	XP_022884599.1	aspartic proteinase PCS1-like = *Olea europaea var. Sylvestris*
LOC111409921	1,047874717	2,067481926	0,00182037	XP_022895802.1	aspartyl protease family protein 2-like = *Olea europaea var. Sylvestris*
			DOWN		
LOC111372505	-6,6980288	-103,8263485	5,4627E-10	XP_022850621.1	lysosomal Pro-X carboxypeptidase = *Olea europaea var. Sylvestris*
LOC111368791	-5,257075303	-38,24171458	0,00540766	XP_022846003.1	subtilisin-like protease SBT1.4 = *Olea europaea var. Sylvestris*
LOC111409227	-4,41086071	-21,27165989	2,9352E-08	XP_022895004.1	metalloendoproteinase 2-MMP-like = *Olea europaea var. Sylvestris*
LOC111402340	-4,266722653	-19,24914756	2,7516E-09	XP_022886337.1	serine carboxypeptidase-like 31 = *Olea europaea var. Sylvestris*
LOC111393908	-3,474976543	-11,11916497	8,6056E-61	XP_022875448.1	desumoylating isopeptidase 2-like = *Olea europaea var. Sylvestris*
LOC111404717	-2,902860929	-7,479080587	0,0021754	XP_022889252.1	probable zinc metalloprotease EGY2, chloroplastic = *Olea europaea var. Sylvestris*
LOC111399606	-2,722195383	-6,598761992	5,7765E-20	XP_022882780.1	gamma-glutamyl peptidase 3-like = *Olea europaea var. Sylvestris*
LOC111380943	-2,654649847	-6,296935315	6,9124E-59	XP_022860388.1	prolyl endopeptidase-like = *Olea europaea var. Sylvestris*
LOC111402333	-2,404379955	-5,294079848	9,1516E-19	XP_022886330.1	serine carboxypeptidase-like 31 = *Olea europaea var. Sylvestris*
LOC111399011	-2,226626156	-4,680381587	1,0983E-15	XP_022881974.1	aspartic proteinase CDR1-like = *Olea europaea var. Sylvestris*
LOC111366809	-2,157745374	-4,462169678	1,9935E-05	XP_022843272.1	subtilisin-like protease SBT1.7 = *Olea europaea var. Sylvestris*
LOC111383296	-2,01660095	-4,046293443	1,3469E-16	XP_022863146.1	aspartic proteinase-like protein 2 = *Olea europaea var. Sylvestris*
LOC111407496	-1,891800885	-3,710981695	3,2442E-23	XP_022892775.1	lon protease homolog 2, peroxisomal-like = *Olea europaea var. Sylvestris*
LOC111382581	-1,857649749	-3,624167788	0,00187573	XP_022862368.1	protein ASPARTIC PROTEASE IN GUARD CELL 2-like = *Olea europaea var. Sylvestris*
LOC111391244	-1,828465801	-3,551591862	1,7435E-06	XP_022872180.1	serine protease SPPA, chloroplastic-like = *Olea europaea var. Sylvestris*
LOC111382451	-1,799253514	-3,480400942	4,7406E-11	XP_022862197.1	aspartyl protease family protein At5g10770-like = *Olea europaea var. Sylvestris*

LOC111401376	-1,731173343	-3,319977222	0,00266373	XP_022884850.1	serine carboxypeptidase-like 11 =*Olea europaea var. Sylvestris*
LOC111403133	-1,705060725	-3,260426562	3,3742E-11	XP_022887298.1	serine carboxypeptidase-like 20 = *Olea europaea var. Sylvestris*
LOC111411923	-1,674130131	-3,191268799	1,6176E-08	XP_022898368.1	probable ubiquitin-like-specific protease 2A = *Olea europaea var. Sylvestris*
LOC111368344	-1,646495043	-3,130721211	0,0001653	XP_022845343.1	lon protease homolog 2, peroxisomal-like = *Olea europaea var. Sylvestris*
LOC111389318	-1,464798224	-2,76024863	1,0945E-08	XP_022870004.1	subtilisin-like protease SBT1.7 = *Olea europaea var. Sylvestris*
LOC111407513	-1,410173652	-2,657691506	1,5579E-13	XP_022892810.1	subtilisin-like protease SBT1.2 = *Olea europaea var. Sylvestris*
LOC111389388	-1,383918082	-2,609761706	1,253E-17	XP_022870077.1	aspartic proteinase-like = *Olea europaea var. Sylvestris*
LOC111380017	-1,322897545	-2,501680494	0,00529213	XP_022859245.1	aspartic proteinase-like protein 2 = *Olea europaea var. Sylvestris*
LOC111394357	-1,136274653	-2,198126864	2,3713E-08	XP_022875893.1	aspartic proteinase Asp1-like = *Olea europaea var. Sylvestris*
LOC111403401	-1,125409261	-2,181634259	1,181E-06	XP_022887668.1	probable signal peptidase complex subunit 1 = *Olea europaea var. Sylvestris*
LOC111404495	-1,114259416	-2,164838521	0,00038499	XP_022889059.1	aspartic proteinase-like protein 2 = *Olea europaea var. Sylvestris*
LOC111410115	-1,077551994	-2,110451966	7,2576E-09	XP_022896089.1	subtilisin-like protease SBT1.6 = *Olea europaea var. Sylvestris*
LOC111410137	-1,059128738	-2,083672785	0,0016081	XP_022896123.1	cysteine proteinase RD21A-like = *Olea europaea var. Sylvestris*
LOC111395876	-1,020390115	-2,028467397	0,00029888	XP_022877845.1	aspartic proteinase NANA, chloroplast-like = *Olea europaea var. Sylvestris*

Table 3.II.S27. Transcription factors (TF) genes repressed or induced in the first comparison (d18:0-AZ vs. C-AZ) and the second comparison (d18:0-LAZ vs. d18:0-AZ).

d18:0-AZ vs. C-AZ					
Gene	**log2FoldChange**	**FoldChange**	**p value**	**Gene_ID**	**Description**
UP					
LOC111383528	5,717343907	52,6128722	1,63E-03	XP_022863412.1	Ethylene-responsive transcription factor ERF038-like = *Olea europaea var. Sylvestris*
LOC111367898	4,987557681	31,7252072	2,34E-05	XP_022844772.1	Basic leucine zipper 43-like = *Olea europaea var. Sylvestris*
LOC111365833	3,845262085	14,3727287	5,26E-04	XP_022842116.1	Ethylene-responsive transcription factor ERF003-like = *Olea europaea var. Sylvestris*
LOC111397687	3,370549399	10,3427606	1,98E-04	XP_022880454.1	Basic leucine zipper 43-like = *Olea europaea var. Sylvestris*
LOC111401184	3,216946536	9,29816828	4,63E-05	XP_022884570.1	Transcription factor bHLH30-like = *Olea europaea var. Sylvestris*
LOC111382240	3,180300924	9,0649617	9,00E-03	XP_022861926.1	Transcription factor MYB61-like = *Olea europaea var. Sylvestris*
LOC111371745	2,900721516	7,46799787	2,78E-06	XP_022849653.1	Transcription factor bHLH157-like = *Olea europaea var. Sylvestris*
LOC111372046	2,848793059	7,20397442	7,04E-04	XP_022849967.1	AP2-like ethylene-responsive transcription factor At1g16060 = *Olea europaea var. Sylvestris*
LOC111366352	2,708620677	6,53696366	5,42E-14	XP_022842873.1	Protein Brevis radix-like 4 = *Olea europaea var. Sylvestris*
LOC111376429	2,689696132	6,45177502	6,34E-07	XP_022855161.1	Transcription factor MYB61-like= *Olea europaea var. Sylvestris*
LOC111399295	2,605686795	6,08681195	1,14E-02	XP_022882319.1	PLATZ transcription factor = *Olea europaea var. Sylvestris*
LOC111368316	2,473137831	5,55250132	1,11E-02	XP_022845453.1	Ethylene-responsive transcription factor WIN1-like =*Olea europaea var. Sylvestris*
LOC111375325	2,390144552	5,24209883	9,44E-04	XP_022853899.1	Transcription factor MYBC1-like = *Olea europaea var. Sylvestris*
LOC111395589	2,369023667	5,16591415	8,47E-14	XP_022877412.1	Transcription factor TCP15-like = *Olea europaea var. Sylvestris*
LOC111365917	2,286678864	4,87931581	1,53E-05	XP_022842243.1	Transcription factor bHLH48-like = *Olea europaea var. Sylvestris*
LOC111392899	2,147041107	4,42918454	8,63E-03	XP_022874081.1	Transcription factor bHLH162-like = *Olea europaea var. Sylvestris*
LOC111378634	2,067968804	4,19295924	7,45E-08	XP_022857636.1	Probable WRKY transcription factor 11 = *Olea europaea var. Sylvestris*
LOC111372511	2,061960254	4,17553267	2,10E-08	XP_022850626.1	Transcription factor MYB88-like = *Olea europaea var. Sylvestris*
LOC111399169	2,031768092	4,08905677	2,80E-03	XP_022882203.1	Transcription factor SRM1-like = *Olea europaea var. Sylvestris*
LOC111386382	2,017469395	4,04872988	9,71E-07	XP_022866607.1	Ethylene-responsive transcription factor CRF1-like = *Olea europaea var. Sylvestris*
LOC111374728	1,992988908	3,98060828	1,07E-15	XP_022853226.1	Transcription factor CRF1-like = *Olea europaea var. Sylvestris*
LOC111371806	1,929326322	3,80877304	1,73E-07	XP_022849745.1	Probable WRKY transcription factor 60 = *Olea europaea var. Sylvestris*
LOC111384800	1,78623368	3,44913281	1,92E-03	XP_022864892.1	GATA transcription factor 16-like = *Olea europaea var. Sylvestris*
LOC111399867	1,784315362	3,44454962	8,98E-05	XP_022883124.1	Transcription factor MYBS3-like = *Olea europaea var. Sylvestris*
LOC111402385	1,764391625	3,39730707	4,34E-03	XP_022886397.1	Transcription factor JUNGBRUNNEN 1- like = *Olea europaea var. Sylvestris*
LOC111382117	1,764234682	3,39693752	1,30E-16	XP_022861755.1	Transcription factor LHW-like= *Olea europaea var. Sylvestris*
LOC111405261	1,741275036	3,34330515	4,75E-03	XP_022889834.1	Transcription factor TCP14-like = *Olea europaea var. Sylvestris*
LOC111385494	1,713616126	3,27981883	3,74E-04	XP_022865658.1	Trihelix transcription factor GTL1-like = *Olea europaea var. Sylvestris*
LOC111401704	1,650401211	3,13920928	1,13E-12	XP_022885330.1	Transcription factor MYB61-like= *Olea europaea var. Sylvestris*
LOC111411485	1,641111031	3,11905941	1,72E-04	XP_022897801.1	Transcription factor UNE12-like= *Olea europaea var. Sylvestris*
LOC111389185	1,617733908	3,0689261	3,04E-17	XP_022869846.1	Transcription factor bHLH69-like= *Olea europaea var. Sylvestris*

LOC111407653	1,60452796	3,04096236	9,91E-07	XP_022893036.1	Transcription factor MYB8-like = *Olea europaea var. Sylvestris*
LOC111380516	1,600318879	3,03210325	7,06E-03	XP_022859868.1	Transcription factor TCP11-like= *Olea europaea var. Sylvestris*
LOC111380252	1,575356074	2,98009036	3,11E-04	XP_022859533.1	Transcription factor KUA1-like = *Olea europaea var. Sylvestris*
LOC111365662	1,540839498	2,90963765	1,26E-06	XP_022841973.1	Transcription factor DIVARICATA-like = *Olea europaea var. Sylvestris*
LOC111369120	1,508958528	2,84604511	9,98E-04	XP_022846382.1	Transcription factor MYBC1-like = *Olea europaea var. Sylvestris*
LOC111411535	1,499554132	2,82755313	3,65E-04	XP_022897847.1	Transcription factor UNE12-like= *Olea europaea var. Sylvestris*
LOC111411782	1,492176405	2,81313035	2,20E-05	XP_022898148.1	Transcription factor TCP8-like= *Olea europaea var. Sylvestris*
LOC111387172	1,487065737	2,80318262	6,40E-06	XP_022867480.1	Heat stress transcription factor C-1-like = *Olea europaea var. Sylvestris*
LOC111372036	1,475537116	2,78087157	3,63E-09	XP_022849953.1	Probable WRKY transcription factor 28 = *Olea europaea var. Sylvestris*
LOC111374059	1,455966823	2,74340349	1,35E-05	XP_022852449.1	Protein BRASSINAZOLE-RESISTANT 1- like= *Olea europaea var. Sylvestris*
LOC111381309	1,448260665	2,72878866	1,22E-03	XP_022860857.1	Nuclear transcription factor Y subunit A-8-like= *Olea europaea var. Sylvestris*
LOC111368046	1,435608951	2,70496317	3,82E-08	XP_022844984.1	Transcription factor bHLH137-like = *Olea europaea var. Sylvestris*
LOC111411684	1,431514582	2,69729737	1,36E-19	XP_022898002.1	Nuclear transcription factor Y subunit A-4-like = *Olea europaea var. Sylvestris*
LOC111377938	1,431448415	2,69717366	1,57E-07	XP_022856866.1	Ethylene-responsive transcription factor TINY-like = *Olea europaea var. Sylvestris*
LOC111402519	1,429237851	2,69304409	6,59E-16	XP_022886657.1	NAC transcription factor 56-like = *Olea europaea var. Sylvestris*
LOC111410442	1,405159722	2,64847102	9,60E-12	XP_022896540.1	Transcription factor PHL5-like = *Olea europaea var. Sylvestris*
LOC111403203	1,396797453	2,63316414	2,15E-05	XP_022887380.1	Ethylene-responsive transcription factor ERF118-like =*Olea europaea var. Sylvestri* s
LOC111370737	1,384447938	2,61072036	2,86E-10	XP_022848358.1	Trihelix transcription factor PTL-like = *Olea europaea var. Sylvestri* s
LOC111389866	1,349975339	2,54907768	2,29E-03	XP_022870611.1	Transcription factor AS1-like = *Olea europaea var. Sylvestris*
LOC111365350	1,337184237	2,52657716	4,56E-05	XP_022841600.1	Transcription factor TCP7-like = *Olea europaea var. Sylvestris*
LOC111393537	1,327427815	2,50954848	8,91E-06	XP_022874881.1	Transcription factor PCL1-like = *Olea europaea var. Sylvestris*
LOC111376054	1,318282057	2,49368987	2,86E-07	XP_022854747.1	Trihelix transcription factor ASIL2 = *Olea europaea var. Sylvestris*
LOC111372110	1,29270611	2,44987155	7,58E-09	XP_022850050.1	Transcription factor CYCLOIDEA-like = *Olea europaea var. Sylvestris*
LOC111383943	1,290252864	2,44570918	1,33E-05	XP_022863905.1	Basic leucine zipper 4-like = *Olea europaea var. Sylvestris*
LOC111373408	1,219120066	2,32804681	1,05E-08	XP_022851719.1	Transcription factor UNE12-like = *Olea europaea var. Sylvestris*
LOC111374684	1,19701574	2,29264938	5,06E-07	XP_022853163.1	PLATZ transcription factor = *Olea europaea var. Sylvestris*
LOC111409999	1,176541016	2,26034191	2,38E-12	XP_022895919.1	Transcription factor MYB1R1-like = *Olea europaea var. Sylvestris*
LOC111412780	1,16829129	2,24745354	4,12E-03	XP_022899457.1	Trihelix transcription factor PTL-like = *Olea europaea var. Sylvestris*
LOC111376049	1,156810368	2,22963935	3,28E-04	XP_022854744.1	Transcription factor UNE12-like = *Olea europaea var. Sylvestris*
LOC111401352	1,150695316	2,22020873	3,87E-08	XP_022884823.1	Ethylene-responsive transcription factor ERF011-like =*Olea europaea var. Sylvestris*
LOC111405697	1,150290315	2,21958555	9,75E-09	XP_022890463.1	PLATZ transcription factor = *Olea europaea var. Sylvestris*
LOC111405523	1,150113499	2,21931353	2,80E-03	XP_022890220.1	Probable WRKY transcription factor 70 = *Olea europaea var. Sylvestris*
LOC111369046	1,144754578	2,21108514	8,93E-07	XP_022846318.1	Transcription factor TGA2.2-like = *Olea europaea var. Sylvestris*
LOC111396042	1,128234006	2,18591	2,73E-04	XP_022878070.1	Ethylene-responsive transcription factor 12-like =*Olea europaea var. Sylvestris*
LOC111368040	1,107442352	2,15463329	1,59E-03	XP_022844972.1	Transcription factor TCP14-like = *Olea europaea var. Sylvestris*
LOC111368603	1,091830615	2,13144321	9,58E-04	XP_022845716.1	Transcription factor bHLH30-like = *Olea europaea var. Sylvestris*
LOC111378403	1,080313159	2,11449501	4,12E-04	XP_022857365.1	GATA transcription factor 26-like = *Olea europaea var. Sylvestris*

LOC111373997	1,05767148	2,08156914	2,28E-06	XP_022852366.1	Transcription factor bHLH106-like = *Olea europaea var. Sylvestris*
LOC111405134	1,047134682	2,06642168	9,61E-03	XP_022889656.1	Transcription factor bHLH68-like = *Olea europaea var. Sylvestris*
LOC111398971	1,040800952	2,05736954	6,24E-03	XP_022881923.1	Transcription factor bHLH30-like = *Olea europaea var. Sylvestris*
LOC111401959	1,002951356	2,00409564	1,33E-03	XP_022885719.1	GATA transcription factor 5-like = *Olea europaea var. Sylvestris*
DOWN					
LOC111411051	-5,198277039	-36,714474	1,33E-20	XP_022897392.1	Ethylene-responsive transcription factor ERF109-like = *Olea europaea var. Sylvestris*
LOC111392782	-4,784461875	-27,559196	1,19E-132	XP_022873948.1	Protein LHY-like = *Olea europaea var. Sylvestris*
LOC111376163	-4,622537896	-24,633298	8,61E-03	XP_022854872.1	Ethylene-responsive transcription factor ERF095-like = *Olea europaea var. Sylvestris*
LOC111407525	-4,263801352	-19,21021	7,49E-63	XP_022892829.1	Dehydration-responsive element-binding protein 1E-like = *Olea europaea var. Sylvestris*
LOC111400894	-4,263084603	-19,200668	1,20E-03	XP_022884114.1	Myb-related protein 306-like = *Olea europaea var. Sylvestris*
LOC111389739	-4,078283976	-16,892184	6,99E-38	XP_022870458.1	Transcription factor WER-like = *Olea europaea var. Sylvestris*
LOC111390424	-3,958647482	-15,547896	1,03E-18	XP_022871231.1	Ethylene-responsive transcription factor ABR1-like = *Olea europaea var. Sylvestris*
LOC111406367	-3,858247732	-14,502681	1,70E-58	XP_022891566.1	Ethylene-responsive transcription factor ERF071-like = *Olea europaea var. Sylvestris*
LOC111368833	-3,765486097	-13,599541	2,13E-102	XP_022846069.1	Dehydration-responsive element-binding protein 1E-like = *Olea europaea var. Sylvestris*
LOC111402033	-3,548892873	-11,703701	1,96E-06	XP_022885842.1	Heat stress transcription factor A-6b-like = *Olea europaea var. Sylvestris*
LOC111382957	-3,47519957	-11,120884	9,44E-08	XP_022862772.1	Ethylene-responsive transcription factor 1A-like = *Olea europaea var. Sylvestris*
LOC111388895	-3,277152561	-9,6944064	3,27E-87	XP_022869488.1	Transcription factor SAC51-like= Olea europaea var. Sylvestris
LOC111377398	-3,238508767	-9,4381805	2,10E-46	XP_022856260.1	Transcription factor bHLH47-like = *Olea europaea var. Sylvestris*
LOC111410604	-3,190061033	-9,1264958	8,73E-37	XP_022896802.1	At5g42700-like = *Olea europaea var. Sylvestris*
LOC111378532	-3,096761156	-8,5549603	1,55E-20	XP_022857521.1	Transcription factor bHLH35-like = *Olea europaea var. Sylvestris*
LOC111382532	-3,073043657	-8,4154689	6,55E-05	XP_022862308.1	MADS-box protein AGL42-like = *Olea europaea var. Sylvestris*
LOC111388316	-3,06503032	-8,3688554	5,86E-17	XP_022868763.1	DELLA protein RGL2-like = *Olea europaea var. Sylvestris*
LOC111371249	-3,031417447	-8,1761261	1,94E-10	XP_022848905.1	Ethylene-responsive transcription factor ERF017-like = *Olea europaea var. Sylvestris*
LOC111409243	-2,67175679	-6,3720465	5,03E-22	XP_022895022.1	Transcription factor bHLH93-like = *Olea europaea var. Sylvestris*
LOC111411950	-2,663833355	-6,3371464	1,32E-07	XP_022898412.1	Transcription factor bHLH13-like = *Olea europaea var. Sylvestris*
LOC111403895	-2,636421948	-6,2178764	4,81E-56	XP_022888317.1	Dehydration-responsive element-binding protein 1B-like = *Olea europaea var. Sylvestris*
LOC111370521	-2,631768445	-6,1978526	1,72E-04	XP_022848010.1	Transcription factor TCP3-like = *Olea europaea var. Sylvestris*
LOC111391691	-2,593193496	-6,0343296	6,50E-04	XP_022872708.1	bHLH23/11/2021 transcription factor bHLH18-like = *Olea europaea var. Sylvestris*
LOC111386018	-2,473857719	-5,5552726	4,36E-40	XP_022866230.1	Transcription factor ABA-INDUCIBLE bHLH-TYPE-like = *Olea europaea var. Sylvestris*
LOC111371771	-2,442194207	-5,4346767	6,85E-38	XP_022849690.1	Transcription factor bHLH74-like = *Olea europaea var. Sylvestris*
LOC111366136	-2,435213025	-5,4084419	4,45E-23	XP_022842585.1	Ethylene-responsive transcription factor TINY-like = *Olea europaea var. Sylvestris*
LOC111407442	-2,407709758	-5,3063129	4,34E-26	XP_022892676.1	Ethylene-responsive transcription factor ERF003-like = *Olea europaea var. Sylvestris*
LOC111379833	-2,341287291	-5,067546	6,73E-44	XP_022859036.1	Disease resistance RPP13-like protein 4 = *Olea europaea var. Sylvestris*
LOC111384917	-2,320836889	-4,9962196	8,05E-06	XP_022865031.1	Transcription factor ABA-INDUCIBLE bHLH-TYPE-like= *Olea europaea var. Sylvestris*
LOC111405443	-2,317752321	-4,9855488	4,44E-49	XP_022890098.1	GATA transcription factor 8-like = *Olea europaea var. Sylvestris*
LOC111368831	-2,299911414	-4,9242753	8,90E-27	XP_022846068.1	Ethylene-responsive transcription factor ERF027-like= *Olea europaea var. Sylvestris*
LOC111373846	-2,279934039	-4,8565575	1,57E-29	XP_022852196.1	Putative late blight resistance protein homolog R1B-17 = *Olea europaea var. Sylvestris*

LOC111406366	-2,260353684	-4,7910892	4,19E-09	XP_022891565.1	Ethylene-responsive transcription factor ERF071-like= *Olea europaea var. Sylvestris*
LOC111411949	-2,195198075	-4,5795253	5,08E-07	XP_022898411.1	Transcription factor bHLH13-like = *Olea europaea var. Sylvestris*
LOC111380711	-2,180754364	-4,5339056	7,71E-14	XP_022860118.1	GATA transcription factor 7-like = *Olea europaea var. Sylvestris*
LOC111403560	-2,150034981	-4,4383855	2,13E-12	XP_022887882.1	Ethylene-responsive transcription factor RAP2-3-like = *Olea europaea var. Sylvestris*
LOC111399633	-2,145579184	-4,4246986	2,38E-30	XP_022882834.1	Transcription activator GLK2-like = *Olea europaea var. Sylvestris*
LOC111402039	-2,114962834	-4,3317886	8,79E-07	XP_022885843.1	Ethylene-responsive transcription factor ERF014-like =*Olea europaea var. Sylvestris*
LOC111387898	-2,061261116	-4,1735097	2,97E-21	XP_022868274.1	Scarecrow-like protein 13 = *Olea europaea var. Sylvestris*
LOC111373863	-2,044926531	-4,1265226	1,50E-04	XP_022852217.1	Ethylene-responsive transcription factor ERF017-like =*Olea europaea var. Sylvestris*
LOC111393263	-1,979930649	-3,9447412	5,44E-34	XP_022874491.1	Scarecrow-like protein 8 = *Olea europaea var. Sylvestris*
LOC111390474	-1,950010328	-3,863773	4,13E-18	XP_022871290.1	Auxin response factor 9-like = *Olea europaea var. Sylvestris*
LOC111403672	-1,911892717	-3,7630246	1,89E-10	XP_022888025.1	Protein FAR1-RELATED SEQUENCE 5- like = *Olea europaea var. Sylvestris*
LOC111391416	-1,890367014	-3,7072952	9,24E-28	XP_022872401.1	Transcription factor bHLH3-like = *Olea europaea var. Sylvestris*
LOC111365496	-1,879948386	-3,6806189	2,30E-12	XP_022841819.1	Protein REVEILLE 8 = *Olea europaea var. Sylvestris*
LOC111409930	-1,874930721	-3,66784	2,06E-23	XP_022895821.1	Auxin response factor 18-like = *Olea europaea var. Sylvestris*
LOC111401887	-1,85554195	-3,6188767	9,86E-28	XP_022885625.1	Transcription factor BIM1-like = *Olea europaea var. Sylvestris*
LOC111411371	-1,852630572	-3,6115811	1,24E-08	XP_022897679.1	Ethylene-responsive transcription factor ERF017-like =*Olea europaea var. Sylvestris*
LOC111392167	-1,780129934	-3,4345711	3,75E-20	XP_022873203.1	Transcription factor IIS, N-terminal = *Olea europaea var. Sylvestris*
LOC111408990	-1,777762801	-3,4289403	1,07E-04	XP_022894639.1	Transcription factor MYB87-like = *Olea europaea var. Sylvestris*
LOC111399557	-1,755208193	-3,3757503	4,76E-13	XP_022882723.1	Transcription factor TGA2.2-like = *Olea europaea var. Sylvestris*
LOC111409927	-1,738490018	-3,3368574	2,53E-27	XP_022895816.1	Transcription factor bHLH13-like= *Olea europaea var. Sylvestris*
LOC111395898	-1,703596548	-3,2571193	1,92E-30	XP_022877882.1	Scarecrow-like protein 13 = *Olea europaea var. Sylvestris*
LOC111386251	-1,690784618	-3,2283223	2,18E-07	XP_022866476.1	RNA polymerase sigma factor sigE, chloroplastic/mitochondrial-like = *Olea europaea var.*
LOC111403941	-1,676777783	-3,1971308	1,00E-09	XP_022888392.1	Scarecrow-like protein 21= *Olea europaea var. Sylvestris*
LOC111386756	-1,642498638	-3,1220608	8,39E-07	XP_022866990.1	Ethylene-responsive transcription factor ERF104-like =*Olea europaea var. Sylvestris*
LOC111409864	-1,627527728	-3,0898306	5,52E-03	XP_022895713.1	Transcription factor bHLH149-like = *Olea europaea var. Sylvestris*
LOC111391879	-1,625415391	-3,0853099	2,47E-05	XP_022872924.1	Ethylene-responsive transcription factor 2-like = *Olea europaea var. Sylvestris*
LOC111384435	-1,622045118	-3,0781107	1,30E-12	XP_022864479.1	Trihelix transcription factor GT-3b-like = *Olea europaea var. Sylvestris*
LOC111391209	-1,611965389	-3,0566797	7,57E-23	XP_022872140.1	Transcription factor GTE8-like = *Olea europaea var. Sylvestris*
LOC111375523	-1,579292908	-2,9882335	1,22E-14	XP_022854130.1	GATA transcription factor 8-like = Olea europaea var. Sylvestris
LOC111374139	-1,573347074	-2,9759434	6,52E-09	XP_022852538.1	Transcription factor MYB1R1-like = *Olea europaea var. Sylvestris*
LOC111400934	-1,57122037	-2,9715597	4,21E-14	XP_022884174.1	Developmental protein SEPALLATA 1 = *Olea europaea var. Sylvestris*
LOC111392361	-1,565557104	-2,9599178	5,31E-07	XP_022873463.1	Transcription initiation factor IIB-2-like = *Olea europaea var. Sylvestris*
LOC111399031	-1,563888704	-2,9564968	8,71E-25	XP_022881998.1	AP2/ERF and B3 domain-containing transcription factor RAV1 = *Olea europaea var.*
LOC111393769	-1,549612674	-2,9273854	8,50E-14	XP_022875233.1	Transcription factor bHLH78-like = *Olea europaea var. Sylvestris*
LOC111380382	-1,514958266	-2,8579056	1,98E-08	XP_022859694.1	Transcription factor TCP23-like = *Olea europaea var. Sylvestris*
LOC111407350	-1,48951464	-2,8079449	2,39E-17	XP_022892541.1	General transcription factor IIE subunit 1 =*Olea europaea var. Sylvestris*
LOC111392598	-1,481717508	-2,7928102	4,80E-06	XP_022873722.1	Transcription factor bHLH128-like = *Olea europaea var. Sylvestris*

LOC111379136	-1,480369307	-2,7902015	1,58E-06	XP_022858238.1	Transcription factor bHLH34-like = *Olea europaea var. Sylvestris*
LOC111372629	-1,452965036	-2,7377013	1,54E-05	XP_022850778.1	Protein EJ2-like;SRF-type transcription factor = *Olea europaea var. Sylvestris*
LOC111398443	-1,42453365	-2,6842772	1,41E-14	XP_022881109.1	Transcription factor MYC2-like = *Olea europaea var. Sylvestris*
LOC111373832	-1,41008144	-2,6575216	5,25E-15	XP_022852180.1	Putative late blight resistance protein homolog R1B-14 = *Olea europaea var. Sylvestris*
LOC111388199	-1,392621106	-2,6255526	1,55E-14	XP_022868653.1	Ethylene-responsive transcription factor 1-like =*Olea europaea var. Sylvestris*
LOC111405546	-1,38175771	-2,6058566	1,53E-16	XP_022890259.1	Ethylene-responsive transcription factor 2-like = Olea europaea var. Sylvestris
LOC111372960	-1,378682301	-2,6003076	2,37E-12	XP_022851160.1	Ethylene-responsive transcription factor ERF027-like = *Olea europaea var. Sylvestris*
LOC111408692	-1,373170631	-2,5903924	5,58E-03	XP_022894210.1	Ethylene-responsive transcription factor ERF014-like = Olea europaea var. Sylvestris
LOC111396299	-1,347620391	-2,5449202	8,08E-14	XP_022878458.1	Transcription factor MYB62-like = *Olea europaea var. Sylvestris*
LOC111399124	-1,34663672	-2,5431855	9,83E-09	XP_022882132.1	Heat stress transcription factor A-8 = *Olea europaea var. Sylvestris*
LOC111385802	-1,322901412	-2,5016872	1,26E-11	XP_022865984.1	Putative late blight resistance protein homolog R1B-17 = *Olea europaea var. Sylvestris*
LOC111370253	-1,302969664	-2,4673625	2,50E-15	XP_022847705.1	Transcription initiation factor IIB-2-like = *Olea europaea var. Sylvestris*
LOC111374856	-1,300978543	-2,4639595	4,03E-03	XP_022853374.1	Transcription factor MYB3R-1-like = *Olea europaea var. Sylvestris*
LOC111395674	-1,299888071	-2,4620978	1,42E-17	XP_022877549.1	Scarecrow-like protein 21 = *Olea europaea var. Sylvestris*
LOC111367031	-1,262998203	-2,3999398	7,02E-04	XP_022843477.1	Myb-like DNA-binding domain = *Olea europaea var. Sylvestris*
LOC111407422	-1,246897803	-2,3733055	2,71E-03	XP_022892651.1	Putative late blight resistance protein homolog R1B-23 = *Olea europaea var. Sylvestris*
LOC111373845	-1,223921868	-2,3358083	1,70E-10	XP_022852194.1	Putative late blight resistance protein homolog R1B-14 = *Olea europaea var. Sylvestris*
LOC111365376	-1,196485561	-2,291807	3,21E-03	XP_022841638.1	Putative late blight resistance protein homolog R1B-17 = *Olea europaea var. Sylvestris*
LOC111369670	-1,139027806	-2,2023256	1,50E-08	XP_022847042.1	Scarecrow-like protein 30 = *Olea europaea var. Sylvestris*
LOC111388121	-1,128216593	-2,1858836	1,93E-05	XP_022868562.1	Transcription factor MYB124-like = *Olea europaea var. Sylvestris*
LOC111402954	-1,119666089	-2,1729667	9,68E-04	XP_022887053.1	Ethylene-responsive transcription factor CRF1-like = *Olea europaea var. Sylvestris*
LOC111369660	-1,109861342	-2,158249	1,66E-10	XP_022847027.1	Scarecrow-like protein 33 = *Olea europaea var. Sylvestris*
LOC111408732	-1,10952961	-2,1577528	3,75E-14	XP_022894259.1	Scarecrow-like protein 1 = *Olea europaea var. Sylvestris*
LOC111374921	-1,107818455	-2,1551951	2,88E-09	XP_022853453.1	NHR/GATA-type, GATA transcription factor 5-like = *Olea europaea var. Sylvestris*
LOC111371296	-1,094856589	-2,1359185	7,09E-03	XP_022848964.1	Transcription factor bHLH62-like = *Olea europaea var. Sylvestris*
LOC111405547	-1,075099018	-2,1068667	2,86E-07	XP_022890260.1	Ethylene-responsive transcription factor 5-like = *Olea europaea var. Sylvestris*
LOC111392955	-1,067229797	-2,095406	4,20E-03	XP_022874133.1	Transcription repressor OFP1-like = *Olea europaea var. Sylvestris*
LOC111366099	-1,062942407	-2,0891881	2,59E-10	XP_022842521.1	Auxin response factor 19-like = *Olea europaea var. Sylvestris*
LOC111367212	-1,05967668	-2,0844643	7,76E-04	XP_022843735.1	Transcription factor MYB44-like = *Olea europaea var. Sylvestris*
LOC111403278	-1,037258417	-2,0523239	1,02E-07	XP_022887481.1	Putative disease resistance RPP13-like protein 3 = *Olea europaea var. Sylvestris*
LOC111383844	-1,032578849	-2,0456777	1,60E-04	XP_022863784.1	Heat stress transcription factor A-3-like = *Olea europaea var. Sylvestris*
LOC111403762	-1,023393256	-2,0326943	1,70E-09	XP_022888150.1	Transcription factor bHLH66-like = *Olea europaea var. Sylvestris*
LOC111395465	-1,018805801	-2,026241	4,89E-09	XP_022877236.1	Ethylene-responsive transcription factor 4-like = *Olea europaea var. Sylvestris*
LOC111405590	-1,017878774	-2,0249395	1,93E-10	XP_022890308.1	Heat stress transcription factor B-2a-like = *Olea europaea var. Sylvestris*
LOC111403423	-1,015481803	-2,0215779	2,55E-03	XP_022887693.1	Transcription initiation factor IIB-2-like = *Olea europaea var. Sylvestris*
LOC111394710	-1,010860189	-2,0151122	8,48E-10	XP_022876423.1	Probable WRKY transcription factor 23= *Olea europaea var. Sylvestris*
LOC111395773	-1,007592818	-2,0105536	5,54E-10	XP_022877687.1	Scarecrow-like protein 21 = *Olea europaea var. Sylvestris*
LOC111376719	-1,00759109	-2,0105512	1,65E-03	XP_022855465.1	DELLA protein GAI1-like = *Olea europaea var. Sylvestris*

LOC111402954	-1,119666089	-2,1729667	9,68E-04	XP_022887053.1	Ethylene-responsive transcription factor CRF1-like = *Olea europaea var. Sylvestris*
LOC111369660	-1,109861342	-2,158249	1,66E-10	XP_022847027.1	Scarecrow-like protein 33 = *Olea europaea var. Sylvestris*
LOC111408732	-1,10952961	-2,1577528	3,75E-14	XP_022894259.1	Scarecrow-like protein 1 = *Olea europaea var. Sylvestris*
LOC111374921	-1,107818455	-2,1551951	2,88E-09	XP_022853453.1	NHR/GATA-type, GATA transcription factor 5-like = *Olea europaea var. Sylvestris*
LOC111371296	-1,094856589	-2,1359185	7,09E-03	XP_022848964.1	Transcription factor bHLH62-like = *Olea europaea var. Sylvestris*
LOC111405547	-1,075099018	-2,1068667	2,86E-07	XP_022890260.1	Ethylene-responsive transcription factor 5-like = *Olea europaea var. Sylvestris*
LOC111392955	-1,067229797	-2,095406	4,20E-03	XP_022874133.1	Transcription repressor OFP1-like = *Olea europaea var. Sylvestris*
LOC111366099	-1,062942407	-2,0891881	2,59E-10	XP_022842521.1	Auxin response factor 19-like = *Olea europaea var. Sylvestris*
LOC111367212	-1,05967668	-2,0844643	7,76E-04	XP_022843735.1	Transcription factor MYB44-like = *Olea europaea var. Sylvestris*
LOC111403278	-1,037258417	-2,0523239	1,02E-07	XP_022887481.1	Putative disease resistance RPP13-like protein 3 = *Olea europaea var. Sylvestris*
LOC111383844	-1,032578849	-2,0456777	1,60E-04	XP_022863784.1	Heat stress transcription factor A-3-like = *Olea europaea var. Sylvestris*
LOC111403762	-1,023393256	-2,0326943	1,70E-09	XP_022888150.1	Transcription factor bHLH66-like = *Olea europaea var. Sylvestris*
LOC111395465	-1,018805801	-2,026241	4,89E-09	XP_022877236.1	Ethylene-responsive transcription factor 4-like = *Olea europaea var. Sylvestris*
LOC111405590	-1,017878774	-2,0249395	1,93E-10	XP_022890308.1	Heat stress transcription factor B-2a-like = *Olea europaea var. Sylvestris*
LOC111403423	-1,015481803	-2,0215779	2,55E-03	XP_022887693.1	Transcription initiation factor IIB-2-like = *Olea europaea var. Sylvestris*
LOC111394710	-1,010860189	-2,0151122	8,48E-10	XP_022876423.1	Probable WRKY transcription factor 23= *Olea europaea var. Sylvestris*
LOC111395773	-1,007592818	-2,0105536	5,54E-10	XP_022877687.1	Scarecrow-like protein 21 = *Olea europaea var. Sylvestris*
LOC111376719	-1,00759109	-2,0105512	1,65E-03	XP_022855465.1	DELLA protein GAI1-like = *Olea europaea var. Sylvestris*

Leaf AZ + d18:0 vs Fruit AZ d18:0					
Gene	**log2FoldChange**	**FoldChange**	**p value**	**Gene_ID**	**Description**
UP					
LOC111400898	7,999049987	255,83148	2,41E-07	XP_022884120.1	Transcription factor PRE1 = *Olea europaea var. Sylvestris*
LOC111386286	7,303574429	157,977406	4,61E-06	XP_022866517.1	Transcription factor bHLH36-like = *Olea europaea var. Sylvestris*
LOC111383445	6,705160313	104,340852	5,91E-06	XP_022863326.1	Transcription factor MYB1-like = *Olea europaea var. Sylvestris*
LOC111410395	6,346843387	81,3935962	2,21E-04	XP_022896477.1	Transcription factor bHLH13-like = Olea europaea var. Sylvestris
LOC111391969	6,24437431	75,8130504	2,02E-18	XP_022873018.1	Transcription factor HBI1-like = *Olea europaea var. Sylvestris*
LOC111398941	6,169436321	71,9756157	3,50E-08	XP_022881879.1	Basic leucine zipper 43-like = *Olea europaea var. Sylvestris*
LOC111376163	5,595559156	48,35386	3,67E-04	XP_022854872.1	Ethylene-responsive transcription factor ERF095-like = *Olea europaea var. Sylvestris*
LOC111386271	5,403437618	42,324984	7,57E-04	XP_022866502.1	Transcription factor MYB52-like = *Olea europaea var. Sylvestris*
LOC111391692	5,163527164	35,8407063	1,49E-03	XP_022872709.1	Transcription factor bHLH93-like = *Olea europaea var. Sylvestris*
LOC111383678	5,008282267	32,1842349	9,38E-26	XP_022863579.1	Trihelix transcription factor GTL2 = *Olea europaea var. Sylvestris*
LOC111375491	4,838075233	28,6026167	3,97E-03	XP_022854097.1	Transcription factor MYB8-like = *Olea europaea var. Sylvestris*
LOC111373107	4,787097425	27,6095874	7,17E-90	XP_022851356.1	Transcription factor MYB108-like = *Olea europaea var. Sylvestris*
LOC111397282	4,737844034	26,6829086	5,15E-03	XP_022879895.1	Heat stress transcription factor B-4-like = *Olea europaea var. Sylvestris*
LOC111372416	4,703341617	26,0523501	1,76E-04	XP_022850528.1	Transcription factor TCP5-like = *Olea europaea var. Sylvestris*
LOC111388132	4,619153107	24,5755723	6,64E-06	XP_022868576.1	Transcription factor PRE6-like = *Olea europaea var. Sylvestris*
LOC111398467	4,583652752	23,9782215	1,50E-28	XP_022881148.1	MADS-box protein SOC1-like = *Olea europaea var. Sylvestris*

LOC111404291	3,074218473	8,42232457	8,03E-52	XP_022888889.1	Ethylene-responsive transcription factor ERF017-like = *Olea europaea var. Sylvestris*
LOC111392899	3,028415839	8,15913289	4,93E-20	XP_022874081.1	Transcription factor bHLH162-like = *Olea europaea var. Sylvestris*
LOC111410316	2,955708367	7,75812686	2,08E-23	XP_022896352.1	Transcription factor HBI1-like = *Olea europaea var. Sylvestris*
LOC111392113	2,924904612	7,59423483	3,85E-21	XP_022873149.1	Transcription factor bHLH148-like = *Olea europaea var. Sylvestris*
LOC111403560	2,843285973	7,17652768	4,43E-25	XP_022887882.1	Ethylene-responsive transcription factor RAP2-3-like = O *lea europaea var. Sylvestris*
LOC111410287	2,817798923	7,05085848	1,24E-13	XP_022896322.1	MADS-box protein SVP-like = *Olea europaea var. Sylvestris*
LOC111384917	2,800755368	6,96805189	9,68E-10	XP_022865031.1	Transcription factor ABA-INDUCIBLE bHLH-TYPE-like = *Olea europaea var. Sylvestris*
LOC111402039	2,75890815	6,76883782	1,22E-13	XP_022885843.1	Ethylene-responsive transcription factor ERF014-like = *Olea europaea var. Sylvestris*
LOC111411051	2,723872478	6,60643734	5,00E-04	XP_022897392.1	Ethylene-responsive transcription factor ERF109-like = *Olea europaea var. Sylvestris*
LOC111397706	2,702763396	6,51047767	1,25E-02	XP_022880472.1	GATA transcription factor 18-like = *Olea europaea var. Sylvestris*
LOC111385758	2,700160403	6,49874168	7,71E-33	XP_022865945.1	Transcription factor MYC4-like = *Olea europaea var. Sylvestris*
LOC111409864	2,632291557	6,20010031	2,88E-08	XP_022895713.1	Transcription factor bHLH149-like = *Olea europaea var. Sylvestris*
LOC111383288	2,577418411	5,9687069	9,07E-19	XP_022863135.1	Transcription factor IBH1-like 1 = *Olea europaea var. Sylvestris*
LOC111367387	2,56028036	5,89822296	9,74E-03	XP_022844001.1	GATA transcription factor 5-like = *Olea europaea var. Sylvestris*
LOC111412977	2,551009681	5,86044282	3,43E-03	XP_022899601.1	Transcription factor MYB56-like = *Olea europaea var. Sylvestris*
LOC111408796	2,540992215	5,81989133	6,13E-03	XP_022894336.1	Heat stress transcription factor B-4-like = *Olea europaea var. Sylvestris*
LOC111410289	2,538234251	5,80877621	8,82E-12	XP_022896327.1	MADS-box protein SVP-like = *Olea europaea var. Sylvestris*
LOC111374630	2,517536023	5,72603315	8,84E-07	XP_022853103.1	AP2-like ethylene-responsive transcription factor AIL5 = *Olea europaea var.*
LOC111366136	2,491227248	5,62256038	4,80E-24	XP_022842585.1	Ethylene-responsive transcription factor TINY-like = *Olea europaea var. Sylvestris*
LOC111375927	2,488633638	5,61246148	8,68E-07	XP_022854620.1	Probable WRKY transcription factor 75 = *Olea europaea var. Sylvestris*
LOC111383740	2,487864915	5,60947174	1,17E-02	XP_022863649.1	Ethylene-responsive transcription factor ERF038-like = *Olea europaea var. Sylvestris*
LOC111410012	2,474545094	5,5579201	7,25E-16	XP_022895932.1	Myb family transcription factor EFM-like = *Olea europaea var. Sylvestris*
LOC111376814	2,45653595	5,48897188	7,00E-29	XP_022855584.1	Transcription factor MYB108-like = *Olea europaea var. Sylvestris*
LOC111397280	2,442709591	5,43661849	1,53E-48	XP_022879888.1	bZIP transcription factor 46-like = *Olea europaea var. Sylvestris*
LOC111408692	2,430250435	5,38986984	8,76E-10	XP_022894210.1	Ethylene-responsive transcription factor ERF014-like = *Olea europaea var. Sylvestris*
LOC111399557	2,423764832	5,36569419	7,90E-28	XP_022882723.1	Transcription factor TGA2.2-like = *Olea europaea var. Sylvestris*
LOC111402874	2,396216597	5,26420838	1,39E-26	XP_022886946.1	Probable WRKY transcription factor 53 = *Olea europaea var. Sylvestris*
LOC111411896	2,386957424	5,23053103	2,54E-20	XP_022898320.1	Transcription factor BEE 1-like = *Olea europaea var. Sylvestris*
LOC111409243	2,356807149	5,12235467	1,24E-16	XP_022895022.1	Transcription factor bHLH93-like = *Olea europaea var. Sylvestris*
LOC111370802	2,329041034	5,02471244	1,55E-43	XP_022848444.1	Protein RICE SALT SENSITIVE 3-like = *Olea europaea var. Sylvestris*
LOC111394783	2,290303177	4,89158895	2,65E-09	XP_022876534.1	Transcription factor TCP8-like = *Olea europaea var. Sylvestris*
LOC111389809	2,283127519	4,86731964	1,13E-02	XP_022870557.1	Transcription factor MYB52-like = Olea europaea var. Sylvestris
LOC111366214	2,275944636	4,84314648	1,54E-06	XP_022842691.1	Ethylene-responsive transcription factor ERF113-like =*Olea europaea var. Sylvestris*
LOC111393013	2,271709999	4,82895158	2,72E-12	XP_022874213.1	MADS-box protein AGL42-like = *Olea europaea var. Sylvestris*
LOC111391984	2,270963136	4,82645235	6,17E-07	XP_022873043.1	Transcription factor BEE 1-like = Olea europaea var. Sylvestris
LOC111384308	2,241005174	4,72726314	2,61E-06	XP_022864341.1	AP2-like ethylene-responsive transcription factor ANT = *Olea europaea var.*
LOC111410636	2,234118956	4,70475291	3,11E-22	XP_022896843.1	Transcription factor MYB44-like = *Olea europaea var. Sylvestris*

LOC111387224	2,218381156	4,6537095	3,22E-04	XP_022867535.1	Transcription factor UNE10-like = Olea europaea var. Sylvestris
LOC111411950	2,206783629	4,61644926	3,44E-05	XP_022898412.1	Transcription factor bHLH13-like = *Olea europaea var. Sylvestris*
LOC111390583	2,18082865	4,5341391	1,20E-06	XP_022871411.1	Ethylene-responsive transcription factor 1B-like = *Olea europaea var. Sylvestris*
LOC111410366	2,152833467	4,44700328	4,19E-08	XP_022896430.1	B3 domain-containing protein At3g18960-like = *Olea europaea var. Sylvestris*
LOC111403738	2,123543348	4,35762892	7,13E-03	XP_022888115.1	Transcription factor IBH1-like 1 = *Olea europaea var. Sylvestris*
LOC111410459	2,072547873	4,2062887	1,35E-03	XP_022896567.1	Transcription factor bHLH130-like = *Olea europaea var. Sylvestris*
LOC111376429	2,052696039	4,14880554	8,47E-16	XP_022855161.1	Transcription factor MYB61-like = *Olea europaea var. Sylvestris*
LOC111388449	2,020956744	4,0585285	1,25E-12	XP_022868921.1	Probable WRKY transcription factor 23 = *Olea europaea var. Sylvestris*
LOC111396122	2,010675871	4,02970959	2,44E-15	XP_022878201.1	Ethylene-responsive transcription factor ERF113-like =*Olea europaea var. Sylvestris*
LOC111399538	1,926074878	3,80019876	2,40E-13	XP_022882676.1	Nuclear transcription factor Y subunit A-10-like =*Olea europaea var. Sylvestris*
LOC111382652	1,907520772	3,75163838	9,04E-03	XP_022862451.1	bZIP transcription factor 11-like = *Olea europaea var. Sylvestris*
LOC111386053	1,876044011	3,67067151	1,42E-16	XP_022866251.1	Probable WRKY transcription factor 41 = *Olea europaea var. Sylvestris*
LOC111397387	1,873740892	3,66481632	2,19E-20	XP_022880057.1	Ethylene-responsive transcription factor ABR1-like = *Olea europaea var. Sylvestris*
LOC111378658	1,846437186	3,59611009	6,02E-11	XP_022857656.1	Transcription factor bHLH147-like = *Olea europaea var. Sylvestris*
LOC111390345	1,807983141	3,5015244	2,12E-11	XP_022871142.1	WRKY transcription factor 22-like = *Olea europaea var. Sylvestris*
LOC111368607	1,806743542	3,4985171	1,19E-02	XP_022845722.1	Ethylene-responsive transcription factor ERF003-like = *Olea europaea var. Sylvestris*
LOC111396884	1,788914418	3,45554776	5,04E-04	XP_022879249.1	Transcription factor ICE1 = *Olea europaea var. Sylvestris*
LOC111368046	1,788129205	3,45366752	8,60E-22	XP_022844984.1	Transcription factor bHLH137-like = *Olea europaea var. Sylvestris*
LOC111374078	1,787255404	3,45157636	5,22E-10	XP_022852475.1	Ethylene-responsive transcription factor CRF4-like = *Olea europaea var. Sylvestris*
LOC111372046	1,775312381	3,42312122	3,96E-06	XP_022849967.1	AP2-like ethylene-responsive transcription factor At1g16060 = *Olea europaea var.*
LOC111410858	1,774539536	3,42128796	1,44E-21	XP_022897201.1	Transcription factor UNE10-like = *Olea europaea var. Sylvestris*
LOC111409737	1,736166043	3,33148649	2,35E-11	XP_022895514.1	WRKY transcription factor 22-like = *Olea europaea var. Sylvestris*
LOC111369829	1,729655827	3,3164869	7,14E-16	XP_022847289.1	Auxin response factor 19-like, = *Olea europaea var. Sylvestris*
LOC111396393	1,726619859	3,30951511	2,26E-25	XP_022878599.1	Transcription factor MYC4-like = *Olea europaea var. Sylvestris*
LOC111399313	1,70543476	3,26127198	1,42E-21	XP_022882328.1	Probable WRKY transcription factor 33 = *Olea europaea var. Sylvestris*
LOC111401887	1,631921382	3,09925483	5,38E-21	XP_022885625.1	Transcription factor BIM1-like = *Olea europaea var. Sylvestris*
LOC111388766	1,627605756	3,08999768	1,26E-17	XP_022869333.1	Transcription factor LHW-like = *Olea europaea var. Sylvestris*
LOC111405948	1,609046625	3,05050189	1,48E-13	XP_022890848.1	Probable WRKY transcription factor 33 = *Olea europaea var. Sylvestris*
LOC111379291	1,598890517	3,02910275	9,72E-18		Ethylene-responsive transcription factor 5-like = *Olea europaea var. Sylvestris*
LOC111371777	1,582239598	2,99434322	4,76E-04	XP_022849697.1	Ethylene-responsive transcription factor CRF1-like = *Olea europaea var. Sylvestris*
LOC111396299	1,578899879	2,98741958	2,77E-19	XP_022878458.1	Transcription factor MYB62-like = *Olea europaea var. Sylvestris*
LOC111372227	1,544499305	2,91702814	1,38E-07	XP_022850227.1	Ethylene-responsive transcription factor ABR1-like= *Olea europaea var. Sylvestris*
LOC111411949	1,492017694	2,8128209	1,85E-03	XP_022898411.1	Transcription factor bHLH13-like = *Olea europaea var. Sylvestris*
LOC111406027	1,453781886	2,73925179	6,08E-10	XP_022890966.1	Transcription factor IIS, transcription elongation factor TFIIS-like = *Olea europaea var.*
LOC111371771	1,41825014	2,6726115	2,43E-11	XP_022849690.1	Transcription factor bHLH74-like = *Olea europaea var. Sylvestris*
LOC111412005	1,411266948	2,65970631	6,94E-14	XP_022898495.1	ABSCISIC ACID-INSENSITIVE 5-like protein 5 = *Olea europaea var. Sylvestris*
LOC111410604	1,406840566	2,65155848	8,01E-06	XP_022896802.1	B3 domain-containing protein At5g42700-like = *Olea europaea var. Sylvestris*

LOC111411538	1,402958462	2,64443307	2,26E-05		Trihelix transcription factor GTL2-like = *Olea europaea var. Sylvestris*
LOC111386758	1,37652933	2,59643	2,16E-05	XP_022866991.1	Ethylene-responsive transcription factor ERF104-like =*Olea europaea var. Sylvestris*
LOC111394838	1,373227402	2,59049429	7,43E-04	XP_022876628.1	Transcription factor GAMYB = *Olea europaea var. Sylvestris*
LOC111374802	1,368942071	2,58281099	3,20E-09	XP_022853307.1	Transcription factor bHLH78-like = *Olea europaea var. Sylvestris*
LOC111409999	1,36433287	2,57457245	1,36E-17	XP_022895919.1	Transcription factor MYB1R1-like = *Olea europaea var. Sylvestris*
LOC111381748	1,347063352	2,54393772	8,53E-13	XP_022861425.1	GATA transcription factor 8-like = *Olea europaea var. Sylvestris*
LOC111384934	1,34259919	2,53607813	1,07E-08	XP_022865052.1	Transcription factor bHLH149-like = *Olea europaea var. Sylvestris*
LOC111409989	1,340355071	2,53213631	5,48E-05	XP_022895900.1	Transcription factor bHLH149-like = *Olea europaea var. Sylvestris*
LOC111387638	1,33945477	2,53055665	9,89E-13	XP_022867982.1	Transcription factor CPC-like = *Olea europaea var. Sylvestris*
LOC111371312	1,326117948	2,50727101	2,22E-04	XP_022848988.1	Transcription factor TCP14-like = *Olea europaea var. Sylvestris*
LOC111399031	1,300766742	2,4635978	6,20E-16	XP_022881998.1	AP2/ERF and B3 domain-containing transcription factor RAV1 = *Olea europaea var.*
LOC111398904	1,292204357	2,44901966	6,75E-14	XP_022881834.1	NAC transcription factor 29-like = *Olea europaea var. Sylvestris*
LOC111373658	1,277141956	2,42358378	1,25E-03	XP_022851995.1	Transcription factor TCP19-like = *Olea europaea var. Sylvestris*
LOC111388199	1,273489808	2,4174563	3,57E-11	XP_022868653.1	Ethylene-responsive transcription factor 1-like =*Olea europaea var. Sylvestris*
LOC111380810	1,259080117	2,39343084	2,30E-05	XP_022860233.1	B3 domain-containing protein REM16- like = *Olea europaea var. Sylvestris*
LOC111388121	1,238926618	2,36022863	1,08E-06	XP_022868562.1	Transcription factor MYB124-like= *Olea europaea var. Sylvestris*
LOC111373841	1,210154962	2,31362486	5,52E-03	XP_022852190.1	Transcription factor HHO3-like = *Olea europaea var. Sylvestris*
LOC111401434	1,208550096	2,3110526	2,61E-04	XP_022884934.1	Transcription factor CYCLOIDEA-like = *Olea europaea var. Sylvestris*
LOC111406159	1,200957525	2,29892201	1,96E-06	XP_022891165.1	NAC transcription factor 29-like = *Olea europaea var. Sylvestris*
LOC111390480	1,190184428	2,28181911	1,90E-03	XP_022871296.1	Transcription factor MYB8-like = *Olea europaea var. Sylvestris*
LOC111391938	1,18215321	2,26915193	8,60E-05	XP_022872992.1	Transcription factor MYB14-like = *Olea europaea var. Sylvestris*
LOC111374059	1,173355912	2,25535715	6,44E-07	XP_022852449.1	Protein BRASSINAZOLE-RESISTANT 1- like = *Olea europaea var. Sylvestris*
LOC111391416	1,16053808	2,23540786	3,53E-10	XP_022872401.1	Transcription factor bHLH3-like = *Olea europaea var. Sylvestris*
LOC111408750	1,143263346	2,20880085	6,62E-07	XP_022894282.1	Trihelix transcription factor GT-2-like = *Olea europaea var. Sylvestris*
LOC111398443	1,139009026	2,20229698	7,47E-11	XP_022881109.1	Transcription factor MYC2-like = *Olea europaea var. Sylvestris*
LOC111402064	1,130425722	2,18923332	4,83E-11	XP_022885876.1	Trihelix transcription factor GT-2-like = *Olea europaea var. Sylvestris*
LOC111371528	1,125121796	2,1811996	2,08E-03	XP_022849337.1	Transcription factor bHLH148 = *Olea europaea var. Sylvestris*
LOC111378532	1,125105448	2,18117488	1,24E-02	XP_022857521.1	Transcription factor bHLH35-like = *Olea europaea var. Sylvestris*
LOC111401347	1,123524446	2,17878592	8,47E-10	XP_022884813.1	bZIP transcription factor 46-like = *Olea europaea var. Sylvestris*
LOC111399146	1,12290425	2,17784948	1,07E-04	XP_022882158.1	PLATZ transcription factor = *Olea europaea var. Sylvestris*
LOC111374139	1,11743907	2,16961502	7,91E-05	XP_022852538.1	Transcription factor MYB1R1-like = *Olea europaea var. Sylvestris*
LOC111389584	1,117242342	2,16931919	1,41E-08	XP_022870279.1	Probable WRKY transcription factor 31 = *Olea europaea var. Sylvestris*
LOC111367560	1,09135778	2,13074475	4,29E-03	XP_022844265.1	Transcription factor MYB20-like = *Olea europaea var. Sylvestris*
LOC111367212	1,083991448	2,119893	3,74E-04	XP_022843735.1	transcription factor MYB44-like = *Olea europaea var. Sylvestris*
LOC111410288	1,082915331	2,11831235	4,02E-04	XP_022896325.1	MADS-box protein SVP-like = *Olea europaea var. Sylvestris*
LOC111408959	1,07525885	2,1071001	1,05E-08	XP_022894588.1	protein BRASSINAZOLE-RESISTANT 1- like = *Olea europaea var. Sylvestris*
LOC111408558	1,070172227	2,09968401	4,89E-07		transcription factor bHLH68-like = *Olea europaea var. Sylvestris*

LOC111407693	1,067160742	2,0953057	6,80E-06	XP_022893099.1	probable WRKY transcription factor 23 = *Olea europaea var. Sylvestris*
LOC111372244	1,061288246	2,08679408	1,37E-05	XP_022850256.1	transcription factor bHLH80-like = *Olea europaea var. Sylvestris*
LOC111376796	1,058016438	2,08206692	1,14E-08	XP_022855569.1	Transcription factor bHLH143-like = *Olea europaea var. Sylvestris*
LOC111371256	1,05613273	2,07935016	7,44E-11	XP_022848910.1	Probable WRKY transcription factor 26 = *Olea europaea var. Sylvestris*
LOC111397295	1,047437366	2,06685527	2,69E-06	XP_022879910.1	Protein BRASSINAZOLE-RESISTANT 1- like = Olea europaea var. Sylvestris
LOC111411839	1,047218427	2,06654163	8,18E-06	XP_022898240.1	Transcription factor UNE12-like = *Olea europaea var. Sylvestris*
LOC111385983	1,038361043	2,05389303	1,70E-03	XP_022866171.1	Basic leucine zipper 9-like = *Olea europaea var. Sylvestris*
LOC111398889	1,035365516	2,04963287	3,76E-08	XP_022881807.1	Transcription factor MYB1R1-like = *Olea europaea var. Sylvestris*
LOC111391020	1,00607517	2,00843973	2,34E-04	XP_022871920.1	Trihelix transcription factor GT-3b-like = *Olea europaea var. Sylvestris*
DOWN					
LOC111406228	-12,23159626	-4809,2502	4,10E-17	XP_022891279.1	Agamous-like MADS-box protein AGL9 homolog = *Olea europaea var. Sylvestris*
LOC111391554	-12,21867048	-4766,3543	4,59E-17	XP_022872561.1	MADS-box transcription factor = *Olea europaea var. Sylvestris*
LOC111393458	-10,21717125	-1190,3509	3,25E-12	XP_022874757.1	NAC transcription factor 56-like = Olea europaea var. Sylvestris
LOC111410442	-9,000945669	-512,33572	5,57E-18	XP_022896540.1	Transcription factor PHL5-like = *Olea europaea var. Sylvestris*
LOC111378040	-8,635140034	-397,59065	7,70E-09	XP_022856967.1	Floral homeotic protein DEFICIENS = *Olea europaea var. Sylvestris*
LOC111400934	-8,281210082	-311,09472	5,08E-09	XP_022884174.1	Developmental protein SEPALLATA 1 = *Olea europaea var. Sylvestris*
LOC111367898	-7,443776617	-174,10051	1,62E-06	XP_022844772.1	Basic leucine zipper 43-like = *Olea europaea var. Sylvestris*
LOC111398121	-7,210392336	-148,09636	4,31E-06	XP_022880858.1	Developmental protein SEPALLATA 3 = *Olea europaea var. Sylvestris*
LOC111412195	-7,095796802	-136,7879	7,16E-06	XP_022898776.1	Floral homeotic protein AGAMOUS-like = Olea europaea var. Sylvestris
LOC111400987	-6,6448585	-100,0695	4,36E-05	XP_022884261.1	Transcription factor CYCLOIDEA-like = *Olea europaea var. Sylvestris*
LOC111403403	-6,235318803	-75,338678	4,72E-57	XP_022887671.1	Agamous-like MADS-box protein AGL9 homolog = *Olea europaea var. Sylvestris*
LOC111375095	-6,165598493	-71,784402	1,88E-21	XP_022853651.1	Transcription factor HHO5-like = *Olea europaea var. Sylvestris*
LOC111396223	-5,483121118	-44,728458	1,09E-50	XP_022878350.1	Truncated transcription factor CAULIFLOWER A-like = *Olea europaea var. Sylvestris*
LOC111401437	-5,354917825	-40,925207	7,57E-04	XP_022884937.1	Transcription factor RADIALIS-like = *Olea europaea var. Sylvestris*
LOC111387344	-5,270411684	-38,596863	7,44E-04	XP_022867670.1	Probable WRKY transcription factor 12 = *Olea europaea var. Sylvestris*
LOC111410797	-4,992852254	-31,84185	1,19E-02	XP_022897098.1	B3 domain-containing protein At3g18960-like= *Olea europaea var. Sylvestris*
LOC111406553	-4,720526971	-26,364541	3,82E-03	XP_022891726.1	Probable WRKY transcription factor 53 = *Olea europaea var. Sylvestris*
LOC111402519	-4,583973241	-23,983549	5,97E-76	XP_022886657.1	NAC transcription factor 56-like = *Olea europaea var. Sylvestris*
LOC111403309	-4,54143733	-23,286749	6,39E-20	XP_022887526.1	Truncated transcription factor CAULIFLOWER A-like = Olea europaea var. Sylvestris
LOC111393537	-4,538110184	-23,233107	4,20E-20	XP_022874881.1	Transcription factor PCL1-like = *Olea europaea var. Sylvestris*
LOC111407640	-4,246799279	-18,985147	2,74E-05	XP_022893024.1	Transcription factor MYB61-like = *Olea europaea var. Sylvestris*
LOC111372629	-4,145595766	-17,698998	2,23E-07	XP_022850778.1	MADS-box protein EJ2-like = *Olea europaea var. Sylvestris*
LOC111375227	-4,048163859	-16,543171	9,58E-18	XP_022853794.1	Transcription factor DIVARICATA-like = *Olea europaea var. Sylvestris*
LOC111399240	-3,99296994	-15,922224	1,83E-06	XP_022882273.1	Probable WRKY transcription factor 50 = *Olea europaea var. Sylvestris*
LOC111371806	-3,975432385	-15,729843	4,91E-15	XP_022849745.1	Probable WRKY transcription factor 60 = *Olea europaea var. Sylvestris*
LOC111373696	-3,958216813	-15,543256	3,88E-13	XP_022852042.1	Floral homeotic protein AGAMOUS-like = *Olea europaea var. Sylvestris*
LOC111403006	-3,702373638	-13,017438	6,18E-03	XP_022887113.1	WRKY transcription factor 55-like = *Olea europaea var. Sylvestris*

LOC111373118	-3,660151865	-12,641992	5,13E-10	XP_022851371.1	Agamous-like MADS-box protein AGL12 = *Olea europaea var. Sylvestris*
LOC111408990	-3,566449321	-11,846996	1,25E-03	XP_022894639.1	Transcription factor MYB87-like = *Olea europaea var. Sylvestris*
LOC111374728	-3,513886983	-11,423137	4,62E-32	XP_022853226.1	Transcription factor PCL1-like = *Olea europaea var. Sylvestris*
LOC111401009	-3,245304404	-9,4827428	1,38E-03	XP_022884305.1	Transcription factor SPATULA-like = *Olea europaea var. Sylvestris*
LOC111367828	-3,23720699	-9,4296681	1,40E-03	XP_022844658.1	Transcription factor MYBS3-like = *Olea europaea var. Sylvestris*
LOC111372078	-3,178685393	-9,0548164	3,64E-05	XP_022850017.1	Probable WRKY transcription factor 282 = *Olea europaea var. Sylvestris*
LOC111391977	-3,107433479	-8,6184802	5,38E-24	XP_022873027.1	bZIP transcription factor 44-like = *Olea europaea var. Sylvestris*
LOC111405523	-3,094598417	-8,5421452	5,07E-10	XP_022890220.1	Probable WRKY transcription factor 70 = *Olea europaea var. Sylvestris*
LOC111380693	-3,059070477	-8,3343546	5,42E-27	XP_022860094.1	Transcription factor TCP13-like = *Olea europaea var. Sylvestri* s
LOC111373566	-2,973208512	-7,8528074	5,00E-03	XP_022851886.1	Probable WRKY transcription factor 50 = Olea europaea var. Sylvestris
LOC111411962	-2,96271312	-7,7958867	1,06E-05	XP_022898434.1	Transcription factor MYC2-like = Olea europaea var. Sylvestris
LOC111381309	-2,870613945	-7,3137633	4,08E-08	XP_022860857.1	Nuclear transcription factor Y subunit A-8-like = *Olea europaea var. Sylvestris*
LOC111380252	-2,768380733	-6,8134275	1,51E-07	XP_022859533.1	Transcription factor KUA1-like = *Olea europaea var. Sylvestris*
LOC111393855	-2,754678806	-6,7490236	1,46E-23	XP_022875364.1	Transcription factor DIVARICATA-like = *Olea europaea var. Sylvestris*
LOC111402385	-2,577526459	-5,9691539	1,39E-04	XP_022886397.1	Transcription factor JUNGBRUNNEN 1- like = *Olea europaea var. Sylvestris*
LOC111403024	-2,561517237	-5,9032819	1,65E-53	XP_022887137.1	Probable WRKY transcription factor 53 = *Olea europaea var. Sylvestris*
LOC111378859	-2,542804769	-5,8272078	9,54E-04	XP_022857912.1	Protein FD-like = *Olea europaea var. Sylvestris*
LOC111365917	-2,479199183	-5,5758787	3,13E-06	XP_022842243.1	Transcription factor bHLH48-like = *Olea europaea var. Sylvestris*
LOC111382510	-2,366106165	-5,1554779	3,52E-05		GATA transcription factor 26-like = *Olea europaea var. Sylvestris*
LOC111401704	-2,356441096	-5,1210552	1,46E-21	XP_022885330.1	Transcription factor MYB61-like = *Olea europaea var. Sylvestris*
LOC111401184	-2,345757514	-5,0832723	3,02E-04	XP_022884570.1	Transcription factor bHLH30-like = *Olea europaea var. Sylvestris*
LOC111401005	-2,286014035	-4,8770678	9,49E-19	XP_022884297.1	AP2-like ethylene- responsive transcription factor TOE3 = *Olea europaea var.*
LOC111398171	-2,180758435	-4,5339184	5,31E-11	XP_022880873.1	Transcription factor IBH1-like = *Olea europaea var. Sylvestris*
LOC111399867	-2,149621843	-4,4371147	1,60E-06	XP_022883124.1	Transcription factor MYBS3-like = *Olea europaea var. Sylvestris*
LOC111404141	-2,136161064	-4,3959076	6,31E-05	XP_022888664.1	Transcription factor RAX2 = *Olea europaea var. Sylvestris*
LOC111382706	-2,124410321	-4,3602484	2,92E-09	XP_022862513.1	Transcription factor bHLH162-like = *Olea europaea var. Sylvestris*
LOC111412214	-2,110681402	-4,3189524	1,84E-03	XP_022898810.1	Probable WRKY transcription factor 28 = *Olea europaea var. Sylvestris*
LOC111392938	-2,076053189	-4,2165211	2,40E-37	XP_022874117.1	Probable WRKY transcription factor 70 = *Olea europaea var. Sylvestris*
LOC111371188	-2,053609428	-4,151433	1,17E-06	XP_022848858.1	Probable WRKY transcription factor 40 = *Olea europaea var. Sylvestris*
LOC111368020	-2,008481943	-4,0235862	1,52E-05	XP_022844951.1	Agamous-like MADS-box protein AGL65 = *Olea europaea var. Sylvestris*
LOC111403203	-2,005652908	-4,0157039	6,46E-09	XP_022887380.1	Ethylene-responsive transcription factor ERF118-like =*Olea europaea var. Sylvestris*
LOC111399525	-1,971774786	-3,9225036	1,48E-09	XP_022882657.1	Transcription factor bHLH130 = *Olea europaea var. Sylvestris*
LOC111380516	-1,967949151	-3,912116	9,31E-04	XP_022859868.1	Transcription factor TCP11-like = *Olea europaea var. Sylvestris*
LOC111384244	-1,921252216	-3,7875166	2,76E-03	XP_022864272.1	Probable WRKY transcription factor 50 = *Olea europaea var. Sylvestris*
LOC111400926	-1,909776026	-3,7575076	1,35E-04	XP_022884165.1	Transcription factor TCP13-like = *Olea europaea var. Sylvestris*
LOC111407653	-1,8716475	-3,6595024	1,07E-07	XP_022893036.1	Transcription factor MYB8-like = *Olea europaea var. Sylvestris*
LOC111372198	-1,865420518	-3,6437413	4,34E-05	XP_022850193.1	Transcription factor RAX2-like = *Olea europaea var. Sylvestris*

LOC111411849	-1,848289212	-3,6007295	9,11E-20	XP_022898251.1	Probable WRKY transcription factor 21 = *Olea europaea var. Sylvestris*
LOC111368603	-1,803861524	-3,4915352	2,12E-07	XP_022845716.1	Transcription factor bHLH30-like = *Olea europaea var. Sylvestris*
LOC111374780	-1,803180105	-3,4898865	1,55E-21	XP_022853284.1	Probable WRKY transcription factor 70 = *Olea europaea var. Sylvestris*
LOC111387943	-1,763909532	-3,396172	2,20E-04	XP_022868345.1	Transcription factor BPE = *Olea europaea var. Sylvestris*
LOC111394582	-1,752080745	-3,3684403	2,75E-23	XP_022876240.1	bZIP transcription factor 44-like = *Olea europaea var. Sylvestris*
LOC111412780	-1,719208388	-3,2925569	6,16E-05	XP_022899457.1	Trihelix transcription factor PTL-like = *Olea europaea var. Sylvestris*
LOC111385988	-1,717993531	-3,2897855	2,03E-14	XP_022866179.1	Transcription factor BHLH089-like = *Olea europaea var. Sylvestris*
LOC111366744	-1,709429293	-3,2703143	3,00E-15	XP_022843213.1	Ethylene-responsive transcription factor RAP2-12-like = *Olea europaea var. Sylvestris*
LOC111371413	-1,700782924	-3,2507732	8,92E-09	XP_022849162.1	Transcription factor bHLH154-like = *Olea europaea var. Sylvestris*
LOC111409915	-1,700101974	-3,2492392	3,67E-03	XP_022895793.1	Probable WRKY transcription factor 30 = *Olea europaea var. Sylvestris*
LOC111409880	-1,663526898	-3,1679002	5,73E-08	XP_022895741.1	Transcription factor UNE10-like = *Olea europaea var. Sylvestris*
LOC111384800	-1,651932769	-3,1425436	2,87E-03	XP_022864892.1	GATA transcription factor 16-like= *Olea europaea var. Sylvestris*
LOC111408863	-1,630810453	-3,0968692	3,75E-03	XP_022894443.1	Auxin response factor 5-like = *Olea europaea var. Sylvestris*
LOC111406121	-1,526979039	-2,8818176	1,89E-09	XP_022891105.1	Probable WRKY transcription factor 19 = *Olea europaea var. Sylvestris*
LOC111377804	-1,524065038	-2,8760027	6,56E-16	XP_022856700.1	Transcription factor bHLH162-like = *Olea europaea var. Sylvestris*
LOC111377241	-1,517552205	-2,8630487	1,49E-03	XP_022856069.1	WRKY transcription factor 18-like = *Olea europaea var. Sylvestris*
LOC111371745	-1,515915361	-2,8598022	1,57E-03	XP_022849653.1	Transcription factor bHLH157-like = *Olea europaea var. Sylvestris*
LOC111377264	-1,500069098	-2,8285626	3,70E-04	XP_022856105.1	Probable WRKY transcription factor 43 = *Olea europaea var. Sylvestris*
LOC111402312	-1,49059155	-2,8100417	1,71E-04	XP_022886300.1	Transcription factor bHLH112-like = *Olea europaea var. Sylvestris*
LOC111370636	-1,455356161	-2,7422425	1,43E-09	XP_022848222.1	B3 domain-containing transcription repressor VAL2-like = *Olea europaea var. Sylvestris*
LOC111380232	-1,450337012	-2,7327188	3,27E-04	XP_022859505.1	Auxin response factor 5-like = *Olea europaea var. Sylvestris*
LOC111397902	-1,449525165	-2,7311814	2,28E-09	XP_022880637.1	Transcription factor DIVARICATA-like = *Olea europaea var. Sylvestris*
LOC111403319	-1,448866364	-2,7299346	1,06E-04	XP_022887540.1	Probable WRKY transcription factor 3 = *Olea europaea var. Sylvestris*
LOC111382117	-1,442858997	-2,7185908	4,26E-12	XP_022861755.1	Transcription factor LHW-like = *Olea europaea var. Sylvestris*
LOC111388546	-1,424397134	-2,6840232	2,17E-03	XP_022869058.1	Basic helix-loop-helix protein A = *Olea europaea var. Sylvestris*
LOC111383207	-1,401428802	-2,6416307	3,54E-04	XP_022863054.1	Protein Brevis radix-like 4 = *Olea europaea var. Sylvestris*
LOC111383485	-1,371959621	-2,5882189	6,29E-07	XP_022863365.1	bZIP transcription factor 2-like= *Olea europaea var. Sylvestris*
LOC111401666	-1,35871755	-2,5645711	2,93E-03	XP_022885281.1	Transcription factor bHLH79-like = *Olea europaea var. Sylvestris*
LOC111412269	-1,32965011	-2,5134171	1,60E-04	XP_022898892.1	Transcription factor E2FB-like = *Olea europaea var. Sylvestris*
LOC111382065	-1,328335933	-2,5111286	6,88E-04	XP_022861697.1	Ethylene-responsive transcription factor RAP2-7-like = *Olea europaea var. Sylvestris*
LOC111368499	-1,313463707	-2,4853753	1,28E-12	XP_022845535.1	Transcription factor ILR3-like = *Olea europaea var. Sylvestris*
LOC111367121	-1,310550973	-2,4803625	5,13E-04	XP_022843617.1	Ethylene-responsive transcription factor ERF107-like =*Olea europaea var. Sylvestris*
LOC111405984	-1,29069536	-2,4464594	7,43E-05	XP_022890903.1	Transcription factor DIVARICATA-like = *Olea europaea var. Sylvestris*
LOC111367203	-1,284781909	-2,4364522	3,27E-09	XP_022843726.1	Probable WRKY transcription factor 7 = *Olea europaea var. Sylvestris*
LOC111389185	-1,279087462	-2,4268542	9,88E-12	XP_022869846.1	Transcription factor bHLH69-like = *Olea europaea var. Sylvestris*
LOC111389402	-1,277021322	-2,4233811	2,78E-04	XP_022870093.1	Transcription factor DIVARICATA-like = *Olea europaea var. Sylvestris*
LOC111384067	-1,250165019	-2,3786863	3,39E-06	XP_022864056.1	Protein FD-like = *Olea europaea var. Sylvestris*

LOC111407238	-1,234531054	-2,3530485	1,62E-06	XP_022892370.1	Probable WRKY transcription factor 71 = *Olea europaea var. Sylvestris*
LOC111383943	-1,225031619	-2,3376057	3,00E-05	XP_022863905.1	Basic leucine zipper 4-like = *Olea europaea var. Sylvestris*
LOC111378339	-1,199531586	-2,2966509	4,50E-10	XP_022857290.1	MADS-box protein 04g005320-like = *Olea europaea var. Sylvestris*
LOC111389453	-1,198059781	-2,2943091	3,32E-12	XP_022870138.1	NAC transcription factor 56-like = *Olea europaea var. Sylvestris*
LOC111396272	-1,193737904	-2,2874463	4,05E-07	XP_022878424.1	Transcription factor bHLH30-like = *Olea europaea var. Sylvestris*
LOC111407314	-1,17447845	-2,2571127	8,96E-06	XP_022892495.1	Probable WRKY transcription factor 35 = *Olea europaea var. Sylvestris*
LOC111403872	-1,170627455	-2,2510958	3,93E-04	XP_022888274.1	Heat stress transcription factor B-3-like = *Olea europaea var. Sylvestris*
LOC111412051	-1,166067072	-2,2439913	1,38E-08	XP_022898562.1	Scarecrow-like transcription factor PAT1 = *Olea europaea var. Sylvestris*
LOC111403584	-1,160876629	-2,2359325	5,94E-03	XP_022887920.1	Probable WRKY transcription factor 21 = Olea europaea var. Sylvestris
LOC111389357	-1,159896078	-2,2344133	4,16E-05	XP_022870049.1	Transcription factor bHLH115-like = *Olea europaea var. Sylvestris*
LOC111398971	-1,158429166	-2,2321426	1,03E-03	XP_022881923.1	Transcription factor bHLH30-like = *Olea europaea var. Sylvestris*
LOC111365512	-1,143617233	-2,2093427	7,99E-03	XP_022841835.1	Transcription factor E2FA-like = *Olea europaea var. Sylvestris*
LOC111393752	-1,141357224	-2,2058845	5,22E-06	XP_022875210.1	Transcription factor IBH1-like = *Olea europaea var. Sylvestris*
LOC111403479	-1,137621704	-2,2001802	1,59E-10	XP_022887773.1	Transcription factor bHLH153-like = *Olea europaea var. Sylvestris*
LOC111395589	-1,096058908	-2,1376993	7,15E-05	XP_022877412.1	Transcription factor TCP15-like = *Olea europaea var. Sylvestris*
LOC111387409	-1,095931904	-2,1375111	6,60E-10	XP_022867730.1	bZIP transcription factor 60-like = *Olea europaea var. Sylvestris*
LOC111379078	-1,063551744	-2,0900707	9,10E-05	XP_022858170.1	Transcription factor TCP23-like = *Olea europaea var. Sylvestris*
LOC111397429	-1,048889665	-2,0689369	1,12E-02	XP_022880119.1	Transcription factor bHLH123-like = *Olea europaea var. Sylvestris*
LOC111372036	-1,041556151	-2,0584468	1,37E-05	XP_022849953.1	Probable WRKY transcription factor 28 = *Olea europaea var. Sylvestris*
LOC111385757	-1,04131887	-2,0581083	5,81E-05	XP_022865941.1	Ethylene-responsive transcription factor ERF008-like = *Olea europaea var. Sylvestris*
LOC111366891	-1,040152963	-2,0564457	3,59E-10	XP_022843346.1	Auxin response factor 19-like = *Olea europaea var. Sylvestris*
LOC111373997	-1,032124117	-2,045033	3,09E-06	XP_022852366.1	Transcription factor bHLH106-like = *Olea europaea var. Sylvestris*
LOC111369788	-1,015713731	-2,0219029	6,78E-05	XP_022847201.1	Ethylene-responsive transcription factor-like protein At4g13040 = *Olea europaea var. Sylvestris*